

**DESIGN AND SYNTHESIS OF NITROGEN
CONTAINING HETEROCYCLIC FRAGMENTS VIA
ISOCYANIDE CHEMISTRY AND THEIR BIOLOGICAL
EVALUATION AS POTENTIAL INHIBITORS OF HIV-1
REPLICATION**

Thompho Jason Rashamuse

A thesis submitted to the Faculty of Science

University of the Witwatersrand

Johannesburg

In fulfilment for the requirements of the degree of Doctor of philosophy

March 2017



UNIVERSITY OF THE
WITWATERSRAND,
JOHANNESBURG

Declaration

I, Rashamuse Thompho Jason student number 750702, declare that the work presented in this thesis was carried out extensively by me under the supervision of Dr Moira L. Bode and Dr Elena C. Coyanis. It is being submitted for the degree of Doctoral philosophy of Science in the University of the Witwatersrand, Johannesburg. It has not been submitted before for any degree or examination in any other University.

Thompho Jason Rashamuse (Student number 750702)

June 2017 (Final Submission)

Abstract

Five membered nitrogen-containing heterocycles exhibit a wide range of biological activities. In this study we set out to demonstrate the utility of isocyanides in the synthesis of these heterocycles, and to identify hit scaffolds demonstrating the ability to disrupt important HIV-1-host protein-protein interactions. In this project study, isocyanide synthons were used to generate different libraries of five membered nitrogen-containing heterocycles. In the first part of the project (**Chapter 2**), *para*-toluenesulfonylmethyl isocyanide (TosMIC) was reacted with *N*-(arylidene)alkylamines (generated from aryl aldehydes and primary amines) under basic conditions using both a conventional and microwave-assisted van Leusen approach to generate a series of novel 5-aryl-1*H*-imidazole compounds. This family of 25 imidazole-based compounds were assessed for biological activity in an HIV-1 IN-LEDGF/p75 AlphaScreen assay and six compounds were found to be inhibitors of this interaction. In order to improve the potency of the hit fragments, a carboxylic acid functionality was introduced at the imidazole moiety of the hit compound to give novel 1,5-diaryl-1*H*-imidazole-4-carboxylic acid compounds as second generation of compounds. Biological evaluation of these carboxylic acid scaffolds in the HIV-1 IN-LEDGF/p75 AlphaScreen assay identified compounds exhibiting more than 50% inhibition, with four inhibitors surpassing the percentage inhibition of the hit scaffold.

In the second part of the thesis (**Chapter 3**), TosMIC was reacted with various aryl aldehydes under basic conditions *via* a microwave-assisted van Leusen reaction to afford a set of 5-aryl-1,3-oxazole derivatives. However, attempts to prepare similar scaffolds in acetonitrile afforded the oxazoline intermediates instead, which were easily converted into the corresponding 5-aryl-1,3-oxazoles in one additional step. This family of 12 compounds did not significantly inhibit the HIV-1 IN-LEDGF/p75 AlphaScreen assay and the binding of antiVpu to Vpu. To improve the percentage inhibition of the original scaffolds, insertion of an *N*-aryl-carboxamide at the 4-position of the oxazole moiety was carried out. Initial, attempts *via* formation of 2-isocyano-*N*-aryl-acetamide intermediates and oxidation of *N*,5-aryl-4,5-dihydrooxazole-4-carboxamide intermediates met with failure. However, this second generation of novel *N*,5-diaryl-4-carboxamide-1,3-oxazole derivatives were then synthesized successfully using benzoyl chloride and ethyl isocyanide as starting reagents. Evaluation of the desired 11 novel *N*,5-diaryl-4-carboxamide-1,3-oxazoles in the HIV-1 IN-LEDGF/p75 assay showed that at least two compounds with the *N*-aryl-4-carboxamide moiety showed increased inhibition potency at 100 μ M relative to the first generation of oxazoles.

In the third part of the study (**Chapter 4**), TosMIC was reacted with ethyl 2-(arylideneamino)acylate intermediates (generated from simple amino acids) under basic conditions *via* a van Leusen reaction to give a family of novel 5-aryl-1*H*-imidazolyl acylates. However, isolation of adducts derived from D-leucine proved to be impossible. A series of 5-aryl-1*H*-imidazolyl-acylates derived from glycine were further transformed into two novel sets of 5-aryl-1*H*-imidazolyl-acetic acid and 5-aryl-1*H*-imidazolyl-acetohydrazide compounds. This family of 25 novel 5-aryl-1*H*-imidazolyl-based compounds was screened for biological activity. In direct HIV-1 IN-LEDGF/p75 AlphaScreen assay, one compound was found to be active while seven compounds were identified as inhibitors of HIV-1 Vpu- host BST-2 interactions. To improve the percentage inhibition of these compounds in the HIV-1 IN-LEDGF/p75 AlphaScreen, *N'*-arylidene and carboxamide groups were introduced which resulted in the generation of two sets of novel (*E*)-*N'*-arylidene-2-(5-aryl-1*H*-imidazol-1-yl)acetohydrazides and, *N*,5-diaryl-2-(1*H*-imidazol-1-yl)acetamide compounds. From this library, at least three compounds with the 4-*tert*-butylphenyl motif were found to be a disruptor of HIV-1 IN and LEDGF/p75 interactions.

In the fourth part of the study (**Chapter 5**), aryl isocyanide synthons were reacted with 2-halo-arylethanone oximes to afford a series of 3-aryl-5-amino-isoxazole derivatives in poor yields. The poor yields were attributed to the low reactivity of the isocyanide and instability of the nitrosoalkene generated *in situ* from 2-halo-arylethanone oxime intermediates. Better yields of 3-aryl-5-amino-isoxazoles were obtained when methyl isocyanoacetate was used instead of aryl isocyanide. Additionally, treatment of 2-halo-arylethanone oxime intermediates with potassium cyanide in MeOH afforded 3-aryl-isoxazol-5-amine derivative in varying yields. From this library, 10 isoxazole-based compounds were biologically evaluated in an HIV-1 IN – LEDGF/p75 interaction assay at 100 μ M and, with the exception of two compounds, all the compounds displayed marginal activities.

All compounds showing significant inhibitory activity in one of the protein-protein interaction assays were tested for activity in a cell based anti-HIV-1 assay. Unfortunately, none of the compounds was found to be active in this cell based assay.

Lastly in **Chapter 6**, the synthesized libraries of the five membered nitrogen containing heterocyclic compounds were assessed for their antimicrobial activity using MIC methods. At least four compounds exhibited moderate antimicrobial activity against gram positive bacterial strains and a yeast strain.

Acknowledgement

I would like to express my gratitude to my supervisors, Dr M. L. Bode (University of Witwatersrand) and Dr E. M. Coyanis (Mintek), for their guidance, irreplaceable assistance, valuable ideas, and excellent support during the course of this PhD study. It was a privilege and I feel honoured to have worked under their supervisions. I have gained much invaluable experience through this study, their guidance and support has been appreciated.

I wish to express my appreciation to Professor Sandy van Vuuren from the Department of Pharmacy and Pharmacology at the University of the Witwatersrand for her guidance and assistance during assessment of my compounds for antimicrobial study. To Professor Yasien Sayed and Alisson William from the School of Molecular and Cell Biology at the University of the Witwatersrand thank you so much for their valuable input and help during isothermal titration calorimetry study

To members Centre of Metal Drug Discovery research group (Advanced Material Division, Mintek) Angela Harrison, Shaakira Abrahams, Zikhona Njekele and Dr Denise Le Noury thanks so much for purification of proteins and screening my compounds in the HIV-1 biological screening assays. My appreciation goes to Dr. Salerwe Mosebi and Dr Raymond Hewer for their sincere suggestions which were invaluable to me during the course of my studies. Furthermore, I would like to thank Dr Telisha Traut for helping with molecular modelling studies.

To my parents, sisters, bothers, my sister in law, my aunt and my late grandma (vho-Thivhafuni Rashamuse) thanks you so much for emotional, financial support, encouragement, and inspiration throughout my studies.

To my wife, Nomampondo Magwa, thank you very much for your love, patience, encouragement and moral support through my entire studies.

Lastly, I would like to acknowledge the School of chemistry at the University of the Witwatersrand, the National Research Foundation, and the Centre for Metal-based Drug Discovery and Mintek for the financial support during my course of this PhD studies.

I dedicate my life to God almighty

List of abbreviations

AlphaScreen	Amplified Luminescent Proximity Homogeneous assay
BST-2	Bone marrow stromal cell antigen 2
Compds	Compounds
CCD	Catalytic core domain
CC ₅₀	50% cytotoxic concentration
CDCl ₃	Deuterated chloroform
CTD	C-terminal DNA-binding domain
d	day(s)
DMSO- <i>d</i> ₆	Deuterated dimethyl sulfoxide
DBU	1,8-Diazabicyclo[5.4.0]undec-7-ene
DCM	Dichloromethane
ESI	Electrospray ionization
ER	Endoplasmic reticulum
EtOAc	Ethyl acetate
Et ₃ N	Triethylamine
ESI-LCMS	Electrospray ionization liquid chromatography mass spectrometry
ELISA	Enzyme-linked Immunosorbent Assay
ee	Enantiomeric excess
FBDD	Fragment based drug discovery
FTIR	Fourier transform infrared spectroscopy
HRMS	High resolution mass spectrometry
HIV-1	Human immunodeficiency Virus type-1
h	hour(s)
IC ₅₀	50% inhibitory concentration
IN	Integrase enzyme
INT	Iodonitrotetrazolium
INSTIs	Strand transfer inhibitors
K ₂ CO ₃	Potassium carbonate
KBr	Potassium bromide
LTR	long terminal repeat strands
LEDGF/p75	Lens epithelium-derived growth factor, or transcriptional coactivator
MT-4	Metallothionein 4 cell line

MeCN	Acetonitrile
MeOH	Methanol
MIC	Minimum inhibitory concentration
min	minute(s)
MW	Microwave irradiation
NMR	Nuclear magnetic resonance
NTD	N-terminal zinc finger domain
POCl ₃	Phosphoryl chloride
Rf	Retention factor
Rac	Racemic mixture
SOCl ₂	Thionyl chloride
SAR	Structure activity relationships
TFA	Trifluoroacetic acid
TosMIC	<i>p</i> -Toluenesulfonylmethyl isocyanide
^t BuOK	Potassium <i>tert</i> -butoxide
THF	Tetrahydrofuran
TLC	Thin layer chromatography
Vpu	Viral protein U
WHO	World Health Organization
Wits	University of the Witwatersrand

Table of contents

Declaration	ii
Abstract.....	iii
Acknowledgement	v
List of abbreviations	vi
Table of contents	viii
CHAPTER 1: Literature Review	1
1. INTRODUCTION.....	1
1.1. The Targets: Human immunodeficiency Virus (HIV-1).....	1
1.1.1 HIV-1 integrase.....	3
1.1.2. Co-factor LEDGF/p75- HIV-1 IN proteins interaction	4
1.1.3. Viral protein U	5
1.1.4. Bone marrow stromal cell antigen 2 (BST-2)	5
1.1.5. The interaction between BST-2 and viral Vpu protein	6
1.1.6. Therapeutic intervention on HIV-1 IN	7
1.1.7. Therapeutic intervention on HIV-1 Vpu BST-2 interaction	10
1.2. The Method: Fragment Based Approach to Drug Discovery	11
1.2.1 Saturated Transfer Difference Nuclear Magnetic Resonance (STD NMR) Spectroscopy	12
1.2.2. Isothermal Titration Calorimetry (ITC).....	13
1.2.2.3. Amplified Luminescent Proximity Homogeneous assay (AlphaScreen)	13
1.3. The Chemistry: TosMIC Synthon.....	14
1.3.1. Preparation of TosMIC and its analogues	14
1.3.2. Synthesis of five membered ring systems	17
1.3.2.1. Imidazole	17
1.3.3.2. Oxazoles	22
1.3.3.3. Pyrroles	23
1.3.3. Synthesis of six membered rings.....	24
1.3.4. TosMIC and Baylis-Hillman adducts.....	26
1.3.5. TosMIC in multicomponent reactions.....	27
1.4. The Chemistry: Aryl isocyanides	28
1.4.1. Preparation of aryl isocyanides.....	28
1.4.1.1. Dehydration of aryl formamide.....	28

1.4.1.2. Hoffmann carbylamine reaction.....	29
1.4.1.3. Deprotonation of aryl imidates	29
1.4.2. Isoxazoles	30
2. Project strategy and Aims	32
Application of TosMIC towards the synthesis of a small library of imidazole-based compounds and biological evaluation as possible inhibitors of HIV-1 protein- protein interactions	36
2.1. Introduction.....	36
2.2. Synthesis of 1-substituted-5-aryl-1 <i>H</i> -imidazole derivatives using a van Leusen reaction.....	36
2.2.1. Synthesis of the key <i>N</i> -(arylidene)alkylamine intermediates	37
2.2.2. The van Leusen approach towards the synthesis of 1-substituted-5-aryl-1 <i>H</i> - imidazoles	39
2.2.2.1. Stepwise cycloaddition of TosMIC to <i>N</i> -(arylidene)alkylamines.....	39
2.2.2.1.1. Synthesis of 1-substituted-5-aryl-1 <i>H</i> -imidazoles using conventional van Leusen reaction	39
2.2.2.1.2. Microwave-assisted synthesis of 1-substituted-5-aryl-1 <i>H</i> -imidazoles using van Leusen reaction.....	40
2.2.2.2. Synthesis of 1-substituted-5-aryl-1 <i>H</i> -imidazoles using three component van Leusen approach (3-cvL)	42
2.2.2.2.1. 3-CvL Synthesis in MeCN	42
2.2.2.2.2. 3-CvL Synthesis in MeOH.....	43
2.2.2.3. Effect of the aryl ring substituents on the reaction yield	46
2.2.2.4. Structure elucidation of the van Leusen products 79-83 by FTIR, NMR and HRMS techniques.....	46
2.2.3. Biological evaluation of library of 1-substituted-5-aryl-1 <i>H</i> -imidazole derivatives ..	48
2.2.3.1. Direct HIV- 1 integrase (IN)-LEDGF AlphaScreen assay	48
2.2.3.2. Direct Viral protein u (Vpu) binding ELISA assay.....	52
2.3. Synthesis of 1,5-diaryl-1 <i>H</i> -imidazole-4-carboxylic acid analogues as second generation compounds	53
2.3.1. Retrosynthesis of target compounds.....	54
2.3.2. Synthesis of the ethyl 1,5-diaryl-1 <i>H</i> -imidazole-4-carboxylic acid derivatives	55
2.3.2.1. Synthesis of <i>N</i> -aryl-benzamide chlorides.....	55
2.3.2.2. Synthesis of ethyl 1,5-diaryl-1 <i>H</i> -imidazole-4-carboxylates	59

2.3.2.2.1 Mechanism for the formation of ethyl 1,5-diaryl-1H-imidazole-4-carboxylates	88.
.....	60
2.3.2.3. Hydrolysis of 1-(4-bromophenyl)-5-aryl-1 <i>H</i> -imidazole-4-carboxylates	62
2.3.2.3.1. Structure elucidation of 1-(4-bromophenyl)-5-aryl-1H-imidazole-4- carboxylic acids 87a-e	64
2.3.3. Biological evaluation of 1-(4-bromophenyl)-5-(4-fluorophenyl)-1 <i>H</i> -imidazole analogues	65
2.3.3.1. Direct Integrase-LEDGF/p75 AlphaScreen Assay	65
2.3.3.2. Assessment through ADME parameters of the synthesized compounds 87a-e	67
2.3.4. Molecular modeling of the synthesized 1-(4-bromophenyl)-5-aryl-1 <i>H</i> -imidazole-4-carboxylic acid derivatives 87a -e	68
2.3.5. Preliminary Isothermal Calorimetry Titration (ITC) Study	74
2.4. Conclusions	78
2.5. Future work	80
CHAPTER 3	81
Synthesis of 5-aryl-1,3-oxazole compounds by means of microwave assisted van Leusen reaction and their biological evolution as possible HIV-1 inhibitors	81
3.1. Introduction	81
3.2. Synthesis of 5-aryl-1,3-oxazoles	81
3.2.1. Using MeOH as solvent	81
3.2.2. Using MeCN as solvent	83
3.2.3. Mechanism for the formation of oxazoles 96 and oxazolines 97	84
3.2.4. NMR Spectra of 5-aryl-1,3-oxazole and (4 <i>R</i> ,5 <i>R</i>)/(4 <i>S</i> ,5 <i>S</i>)-5-aryl-4-tosyl-4,5-dihydro-1,3-oxazole fragments	85
3.2.5. Mass spectral analysis of 5-aryl-1,3-oxazoles	86
3.2.6. Biological Evaluation of a series of 5-aryl-1,3-oxazoles and 5-aryl-4-tosyl-4,5-dihydrooxazoles	87
3.2.6.1 Biochemical target assays	88
3.2.6.1.1. HIV-1 IN -LEDGF/p75 assay	88
3.2.6.1.2. HIV-1 Vpu binding assay	88
3.2.6.2. Cell based assay	88
3.3. Synthesis of <i>N</i> ,5-diaryl-1-3-oxazole-4-carboxamides as second generation compounds	88
3.3.1. First retrosynthetic approach to target compounds	90

3.3.1.1. Synthesis of the 2-isocyano- <i>N</i> -aryl-acetamide	91
3.3.1.2. Reaction of 101b with benzoyl chlorides	92
3.3.1.3. Reaction of compound 101b with benzaldehydes	93
3.3.1.4. Attempted oxidation of 5-aryl-4,5-dihydro- <i>N</i> -(3,5-dimethoxyphenyl)-1,3-oxazole-4-carboxamides	95
3.3.2. Second retrosynthetic approach to the target compounds	96
3.3.2.1. Synthesis of 5-aryl-1,3-oxazole-4-carboxylic acids (108).....	96
3.3.2.2. Mechanism for the formation of ethyl 5-aryl-1,3-oxazole-4-carboxylates 109.....	97
3.3.2.3. Anilidation of 5-aryloxazole-4-carboxylic acid derivatives	99
3.3.2.5. FTIR and NMR spectroscopic analysis of <i>N</i> ,5-diaryl-1,3-oxazole-4-carboxamides 100	100
3.3.2.6. Mass analysis of <i>N</i> ,5-diaryl-1,3-oxazole-4-carboxamides 100.....	101
3.3.2.6.1. MS/MS fragmentation.....	102
3.3.3. Biological evaluation in LEDGF/p75-IN inhibition assay.....	105
3.3.4. The prediction of ADME parameters of the synthesized compounds.....	107
3.3.5 Molecular modelling of the synthesized <i>N</i> ,5-diaryl-1,3-oxazole-4-carboxamide derivatives.....	107
3.3.6. Conclusion.....	110
3.4. Future work.....	112
CHAPTER 4.....	113
Synthesis of a family of 5-aryl-imidazol-1-yl acyl-based compounds as potential inhibitors of HIV-1 protein-host protein interactions using a van Leusen approach.....	113
4.1. Introduction.....	113
4.2. Synthesis of 5-aryl-1 <i>H</i> -imidazol-1-yl acyl derivatives using van Leusen reaction.....	113
4.2.1. Synthesis of free amino ethyl ester derivatives.....	114
4.2.2. Condensation of amino ethyl ester derivatives with various benzaldehydes	116
4.2.3. Optimization of conditions towards cycloaddition of TosMIC to the prepared ethyl 2-(arylideneamino)acylate.....	118
4.2.4. Van Leusen reaction for the preparation of the ethyl 5-aryl-1 <i>H</i> -imidazol-1-yl acyls	121
4.2.4.1. Structure elucidation of newly synthesized 2-(5-aryl-1 <i>H</i> -imidazol-1-yl)acyls by NMR and FTIR spectroscopy	123
4.2.4.2. Structure elucidation of newly synthesized ethyl 5-aryl-1 <i>H</i> -imidazol-1-yl acyls by mass spectrometry	123

4.2.4.2.1. Mass fragmentation of ethyl 2-[5-(4-fluorophenyl)-1H-imidazolyl]acetate 120a	125
4.2.4.2.2. Mass fragmentation of ethyl 2-[5-(3,4-dimethoxyphenyl)-1H-imidazolyl]acetate 120d	127
4.2.5. Synthesis of novel 2-(5-aryl-1 <i>H</i> -imidazol-1-yl) acetic acids 123	129
4.2.6. Synthesis of novel 2-(5-aryl-1 <i>H</i> -imidazol-1-yl)acetohydrazide scaffolds 125	132
4.2.7. Biological evaluation of synthesized 1 <i>H</i> -imidazol-1-yl- based compounds	137
4.2.7.1. Direct IN-LEDGF/p75 AlphaScreen assay	137
4.2.7.2. Direct Vpu-BST-2 ELISA assay	139
4.2.8. <i>In silico</i> ADME profiling of novel 5-aryl-1 <i>H</i> -imidazolyl- based compounds	142
4.2.9. Molecular modelling of compound 123g at the IN dimer interface	143
4.3. The expansion on the 2-(5-aryl-1 <i>H</i> -imidazolyl) acyl fragments to produce second generation compounds	145
4.3.1. Synthesis of <i>N</i> '-arylidene-2-(5-aryl-1 <i>H</i> -imidazol-1-yl)acetohydrazide and <i>N</i> ,5-diaryl-2-(1 <i>H</i> -imidazol-1-yl)acetamide derivatives	146
4.3.1.1. Structure elucidation of <i>N</i> '-arylidene-2-(5-aryl-1 <i>H</i> -imidazol-1-yl)acetohydrazide 127a-o	147
4.3.2. Synthesis of <i>N</i> ,5-diaryl-2-(1 <i>H</i> -imidazol-1-yl)acetamide derivatives	148
4.3.2.1. Structure elucidation of the <i>N</i> ,5-diaryl-2-(1 <i>H</i> -imidazol-1-yl)acetamides 128	149
4.3.3. Biological evaluation of the synthesized (<i>E</i>)- <i>N</i> '-arylidene-2-(5-aryl-1 <i>H</i> -imidazol-1-yl)acetohydrazides 127a-o and <i>N</i> ,5-diaryl-2-(1 <i>H</i> -imidazol-1-yl)acetamides 128a-b	150
4.3.4. <i>In silico</i> ADME studies of novel (<i>E</i>)- <i>N</i> '-arylidene-2-(5-aryl-1 <i>H</i> -imidazol-1-yl)acetohydrazide compounds	151
4.3.5. Molecular modelling of the synthesized (<i>E</i>)- <i>N</i> '-arylidene-2-(5-aryl-1 <i>H</i> -imidazol-1-yl)acetohydrazides 127j and 127n-o at the HIV-1 IN dimer interface	153
4.4. Conclusion	156
4.5. Future Work	159
CHAPTER 5	160
Synthesis of 3-aryl- <i>N</i> -arylisoxazol-5-amine scaffolds using aryl isocyanides and their usefulness as for possible inhibitors of HIV-1 protein- host protein interactions	160
5.1 Introduction	160
5.2. Synthesis of 3-aryl- <i>N</i> -arylisoxazol-5-amine based compounds	160
5.2.1. Synthesis of key 2-halo-1-arylketoneoxime intermediates	161
5.2.1.1. Synthesis of the 2,2,2-trichloro-1-aryl-ethanol	161

5.2.1.2. Oxidation of 2,2,2-trichloro-1-aryl-ethanol derivatives.....	163
5.2.1.3. Synthesis of 2-chloro-1-aryl-ethanone oxime intermediates	165
5.2.2. Synthesis of aryl isocyanide derivatives	167
5.2.3. Synthesis of 3-aryl- <i>N</i> -isoxazol-5-amine derivatives.....	169
5.2.3.1. Control experiment between 2-chloro-1-aryl-ethanone oxime and aryl isocyanides	170
5.2.3.2. Determination of the effects of substituents and isocyanide reactivity on the reaction	171
5.2.3.3. Plausible mechanism for the formation of 5-amino-3-arylisoxazole	172
5.2.4. Synthesis of 3-aryl- <i>N</i> -isoxazol-5-amine derivatives.....	173
5.2.5. Structure elucidation of isoxazole-based compounds	174
5.3. Biological evaluation of isoxazole based compounds	175
5.3.1. Direct HIV-1 –LEDGF/p5 assay	175
5.4. Conclusion	176
5.5. Future work.....	177
CHAPTER 6.....	178
Antimicrobial activities of synthesized compounds	178
6.1 Introduction.....	178
6.2. Antimicrobial activities of the synthesized libraries of five membered nitrogen containing heterocyclic compounds	179
6.2.1. Antimicrobial activities of synthesized 5-aryl-1 <i>H</i> -imidazole-based compounds ...	180
6.2.2. Antimicrobial activities of synthesized 5-aryl-oxazole based compounds.....	183
6.2.3. Antimicrobial activities of synthesized 5-aryl-1 <i>H</i> -imidazol-1-yl based compounds	185
6.2.4. Antimicrobial activities of synthesized 3-aryl-isoxazole based compounds	188
6.3. Conclusion	189
CHAPTER 7.....	190
General Conclusion	190
7.1. Synthesis of small families of five-membered nitrogen containing heterocycles. First generation.....	190
7.2. Biological evaluation and hit identification.....	194
7.3. Synthesis of Second Generation Compounds and their Biological Evaluation	195
7.4. Modelling Results	199
7.5. Final Remarks	202

EXPERIMENTAL PROCEDURES	203
8.1 General Experimental Procedures	203
8.1.1. Purification of solvents and reagents	203
8.1.2. Chromatography.....	203
8.1.3. Spectroscopic and physical data	203
8.1.3. Nomenclature and Compound Numbering	204
8.1.4. Biological Evaluation Experiments	204
8.1.4.1. HIV-1 IN-LEDGF/p75 AlphaScreen Assay.....	204
8.1.4.2. HIV-1 Vpu binding Assay.....	204
8.1.4.3. HIV-1 Vpu- BST-2 ELISA Assay.....	205
8.1.4.4. Antiviral for HIV-1 LEDGF/p75 interatcion	205
8.1.4.5. Cellular Toxicity assay.....	206
8.1.4.6. Minimum inhibitory concentration using p-iodonitrotetrazolium (INT) chloride method	206
8.1.4.6.1. Preparation of stock solution for antimicrobial testing.....	207
8.1.4.6.2 Screening of synthesized compounds against pathogens.....	207
8.1.5. Computer Modeling	208
8.1.5.1. Ligand preparation	208
8.1.5.2. Preparation of HIV IN-1 protein.....	208
8.1.5.3 Docking of selected compound into HIV IN binding cavity	208
8.1.5.4. ADME properties	208
8.1.6. Isothermal titration calorimetry	209
8.1.6.1. Buffer exchange	209
8.1.6.2. Compound preparation	209
8.1.6.3. ITC experiment settings.....	209
8.2. Chapter 2 experimental procedure.....	210
8.2.1. Synthesis of <i>N</i> -arylidene alkylamines	210
8.2.1.1. Synthetic Procedure A: Conventional Method	210
8.2.1.2. Synthetic Procedure B: Microwave Irradiation.....	210
8.2.1.3. (<i>E</i>)- <i>N</i> -(4-Fluorobenzylidene)butan-1-amine 75a	210
8.2.1.4. (<i>E</i>)- <i>N</i> -(2-Chlorobenzylidene)butan-1-amine 75b.....	211
8.2.1.5. (<i>E</i>)- <i>N</i> -(3-Methoxybenzylidene)butan-1-amine 75c.....	211
8.2.1.6. (<i>E</i>)- <i>N</i> -(2,4-Dimethoxybenzylidene)butan-1-amine 75d.....	212
8.2.1.7. (<i>E</i>)- <i>N</i> -(Benzo[<i>d</i>][1,3]dioxol-5-ylmethylene)butan-1-amine 75e	212

8.2.1.8. (<i>E</i>)- <i>N</i> -(4- <i>tert</i> -butylbenzylidene)butan-1-amine 75f	213
8.2.1.8. (<i>E</i>)- <i>N</i> -(2,3-Dihydrobenzo[<i>b</i>][1,4]dioxin-6-yl)methylene)butan-1-amine 75g.....	213
8.2.1.9. (<i>E</i>)- <i>N</i> -(2-Nitrobenzylidene)butan-1-amine 75h.....	214
8.2.1.9. (<i>E</i>)- <i>N</i> -(4-Nitrobenzylidene)butan-1-amine 75i.....	214
8.2.1.11. (<i>E</i>)- <i>N</i> -(4-Fluorobenzylidene)cyclohexanamine 76a	214
8.2.1.12. (<i>E</i>)- <i>N</i> -(2-Chlorobenzylidene)cyclohexanamine 76b	215
8.2.1.13. (<i>E</i>)- <i>N</i> -(3-Methoxybenzylidene)cyclohexanamine 76c	215
8.2.1.14. (<i>E</i>)- <i>N</i> -(2,4-Dimethoxybenzylidene)cyclohexanamine 76d	216
8.2.1.15. (<i>E</i>)- <i>N</i> -(Benzo[<i>d</i>][1,3]dioxol-5-ylmethylene)cyclohexanamine 76e.....	216
8.2.1.16. (<i>E</i>)- <i>N</i> -(4- <i>tert</i> -Butylbenzylidene)cyclohexanamine 76f.....	217
8.2.1.17. (<i>E</i>)- <i>N</i> -(2-Nitrobenzylidene)cyclohexanamine 76h.....	217
8.2.1.17. (<i>E</i>)- <i>N</i> -(4-Nitrobenzylidene)cyclohexanamine 76i.....	218
8.2.1.19. (<i>E</i>)- <i>N</i> -(4-Fluorobenzylidene)cyclopropanamine 77a	218
8.2.1.20. (<i>E</i>)- <i>N</i> -(3-Methoxybenzylidene)cyclopropanamine 77c	219
8.2.1.21. (<i>E</i>)- <i>N</i> -(2,4-Dimethoxybenzylidene)cyclopropanamine 77d.....	219
8.2.1.22. (<i>E</i>)- <i>N</i> -(4-Fluorobenzylidene)-1-phenylmethanamine 78a	220
8.2.1.23. (<i>E</i>)- <i>N</i> -(2-Chlorobenzylidene)-1-phenylmethanamine 78b.....	220
8.2.1.24. (<i>E</i>)- <i>N</i> -(3-Methoxybenzylidene)-1-phenylmethanamine 78c.....	220
8.2.1.25. (<i>E</i>)- <i>N</i> -(2,4-Dimethoxybenzylidene)-1-phenylmethanamine 78d.....	221
8.2.1.26. (<i>E</i>)- <i>N</i> -(Benzo[<i>d</i>][1,3]dioxol-5-ylmethylene)-1-phenylmethanamine 78e	221
8.2.2. Synthesis of 1-substituted-5-aryl-1 <i>H</i> -imidazole.....	222
8.2.2.1. Stepwise van Leusen general synthetic procedure C	222
8.2.2.2. Microwave assisted van Leusen general synthetic procedure D	222
8.2.2.3. Three -component van Leusen reaction general synthetic procedure E	222
8.2.2.4. Three -component van Leusen reaction general synthetic procedure F.....	223
8.2.2.5. 1-Butyl-5-(4-fluorophenyl)-1 <i>H</i> -imidazole 79a	223
8.2.2.6. 1-Butyl-5-(2-chlorophenyl)-1 <i>H</i> -imidazole 79b	224
8.2.2.7. 1-Butyl-5-(3-methoxyphenyl)-1 <i>H</i> -imidazole 79c.....	224
8.2.2.8. 1-Butyl-5-(2,4-dimethoxyphenyl)-1 <i>H</i> -imidazole 79d	225
8.2.2.9. 5-(Benzo[<i>d</i>][1,3]dioxol-5-yl)-1-butyl-1 <i>H</i> -imidazole 79e.....	226
8.2.2.10. 1-Butyl-5-(4- <i>tert</i> -butylphenyl)-1 <i>H</i> -imidazole 79f.....	226
8.2.2.11. 1-Butyl-5-(2,3-dihydro-1,4-benzodioxin-6-yl)-1 <i>H</i> -imidazole 79g.....	227
8.2.2.12. 1-Butyl-5-(2-nitrophenyl)-1 <i>H</i> -imidazole 79h	228
8.2.2.13. 1-Butyl-5-(4-nitrophenyl)-1 <i>H</i> -imidazole 79i	228

8.2.2.14. 1-Cyclohexyl-5-(4-fluorophenyl)-1 <i>H</i> -imidazole 80a.....	229
8.2.2.15. 1-Cyclohexyl-5-(2-chlorophenyl)-1 <i>H</i> -imidazole 80b.....	229
8.2.2.16. 1-Cyclohexyl-5-(3-methoxyphenyl)-1 <i>H</i> -imidazole 80c	230
8.2.2.17. 1-Cyclohexyl-5-(2,4-dimethoxyphenyl)-1 <i>H</i> -imidazole 80d.....	231
8.2.2.18. 5-(Benzo[<i>d</i>][1,3]dioxol-5-yl)-1-cyclohexyl-1 <i>H</i> -imidazole 80e	231
8.2.2.19. 1-Cyclohexyl-5-(4- <i>tert</i> -butylphenyl)-1 <i>H</i> -imidazole 80f.....	232
8.2.2.22. 1-Cyclohexyl-5-(2-nitrophenyl)-1 <i>H</i> -imidazole 80h.....	233
8.2.2.23. 1-Butyl-5-(4-nitrophenyl)-1 <i>H</i> -imidazole 80i	233
8.2.2.24. 1-Cyclopropyl-5-(4-fluorophenyl)-1 <i>H</i> -imidazole 81a.....	234
8.2.2.25. 1-Cyclopropyl-5-(3-methoxyphenyl)-1 <i>H</i> -imidazole 81c	234
8.2.2.26. 1-Cyclopropyl-5-(2,4-dimethoxyphenyl)-1 <i>H</i> -imidazole 81d	235
8.2.2.27. 1-Benzyl-5-(4-fluorophenyl)-1 <i>H</i> -imidazole 82a	235
8.2.2.28. 1-Benzyl-5-(3-methoxyphenyl)-1 <i>H</i> -imidazole 82c	236
8.2.2.29. 1-Benzyl-5-(2,4-dimethoxyphenyl)-1 <i>H</i> -imidazole 82d	236
8.2.2.30. 5-(Benzo[<i>d</i>][1,3]dioxol-5-yl)-1-benzyl-1 <i>H</i> -imidazole 82e	237
8.2.2.31. 1-(4-Bromophenyl)-5-(4-fluorophenyl)-1 <i>H</i> -imidazole 83a	237
8.2.2.32. 1-(4-Bromophenyl)-5-(2,4-dimethoxyphenyl)-1 <i>H</i> -imidazole 83d	238
8.2.2.33. 5-(Benzo[<i>d</i>][1,3]dioxol-5-yl)-1-(4-bromophenyl)-1 <i>H</i> -imidazole 83e.....	238
8.2.3. Synthesis of <i>N</i> -aryl benzamide derivatives	239
8.2.3.1. General synthetic procedure.....	239
8.2.3.2. <i>N</i> -(4-Bromophenyl)-4-fluorobenzamide 91a.....	239
8.2.3.3. <i>N</i> -(4-Bromophenyl)-3-fluorobenzamide 91b	240
8.2.3.4. <i>N</i> -(4-Bromophenyl)-3-methoxybenzamide 91c	240
8.2.3.5. <i>N</i> -(4-Bromophenyl)-3-methylbenzamide 91d.....	241
8.2.3.7. <i>N</i> -(2,4-Dimethoxyphenyl)-4-fluorobenzamide 91f.....	241
8.2.3.8. <i>N</i> -(2,4-Dimethylphenyl)-4-fluorobenzamide 91g.....	242
8.2.3.9. <i>N</i> -(2,4-Dimethylphenyl)-3-methoxy-benzamide 91h.....	242
8.2.3.10. <i>N</i> -(2,4-Dichlorophenyl)-4-fluorobenzamide 91i	243
8.2.3.11. <i>N</i> -(2,4-Dichlorophenyl)-3-methoxybenzamide 91j.....	243
8.2.4. Synthesis of <i>N</i> -aryl benzimidoyl chloride intermediates	244
8.2.4.1. General Procedure	244
8.2.4.2. (<i>E</i>)- <i>N</i> -(4-Bromophenyl)-4-fluorobenzimidoyl chloride 90a	244
8.2.4.3. (<i>E</i>)- <i>N</i> -(4-Bromophenyl)-4-fluorobenzimidoyl chloride 90b	245
8.2.4.4. (<i>E</i>)- <i>N</i> -(4-Bromophenyl)-3-methoxybenzimidoyl chloride 90c.....	245

8.2.4.5. (<i>E</i>)- <i>N</i> -(4-Bromophenyl)-3-methylbenzimidoyl chloride 90d	246
8.2.4.6. (<i>E</i>)- <i>N</i> -(4-Bromophenyl)benzimidoyl chloride 90e	246
8.2.4.7. (<i>E</i>)- <i>N</i> -(2,4-Dimethoxyphenyl)-4-fluorobenzimidoyl chloride 90f	247
8.2.4.8. (<i>E</i>)- <i>N</i> -(2,4-Dimethylphenyl)-4-fluorobenzimidoyl chloride 90g	247
8.2.4.9. (<i>E</i>)- <i>N</i> -(2,4-Dimethylphenyl)-3-methoxybenzimidoyl chloride 90h.....	248
8.2.5. Synthesis of ethyl 1,5-diaryl-1 <i>H</i> -imidazole-4-carboxylates	248
8.2.5.1. General synthetic procedure A	248
8.2.5.2. General synthetic procedure B	248
8.2.5.3. Ethyl 1-(4-bromophenyl)-5-(4-fluorophenyl)-1 <i>H</i> -imidazole-4-carboxylate 88a...	249
8.2.5.4. Ethyl 1-(4-bromophenyl)-5-(3-fluorophenyl)-1 <i>H</i> -imidazole-4-carboxylate 88b ..	249
8.2.5.5. Ethyl 1-(4-bromophenyl)-5-(3-methoxyphenyl)-1 <i>H</i> -imidazole-4-carboxylate 88c ...	250
8.2.5.6. Ethyl 1-(4-bromophenyl)-5-(3-methylphenyl)-1 <i>H</i> -imidazole-4-carboxylate 88d.	251
8.2.5.7. Ethyl 1-(4-bromophenyl)-5-phenyl-1 <i>H</i> -imidazole-4-carboxylate 88e	251
8.2.6. Hydrolysis of ethyl 1,5-diaryl-1 <i>H</i> -imidazole-4-carboxylates	252
8.2.6.1. General synthetic procedure.....	252
8.2.6.2. 1-(4-Bromophenyl)-5-(4-fluorophenyl)-1 <i>H</i> -imidazole-4-carboxylic acid 87a	252
8.2.6.3. 1-(4-Bromophenyl)-5-(3-fluorophenyl)-1 <i>H</i> -imidazole-4-carboxylic acid 87b	253
8.2.6.4. 1-(4-Bromophenyl)-5-(3-methoxyphenyl)-1 <i>H</i> -imidazole-4-carboxylic acid 87c..	253
8.2.6.5. 1-(4-Bromophenyl)-5-(3-methylphenyl)-1 <i>H</i> -imidazole-4-carboxylic acid 87d	254
8.2.6.6. 1-(4-Bromophenyl)-5-phenyl-1 <i>H</i> -imidazole-4-carboxylic acid 87e	255
8.3. Chapter 3 experimental procedures	256
8.3.1. . Synthesis of 5-aryl-1,3-oxazole	256
8.3.1.1. Microwave assisted van Leusen general synthetic procedure A	256
8.3.1.2. Microwave assisted van Leusen general synthetic procedure B	256
8.3.1.3. Aromatization general synthetic procedure C.....	256
8.3.1.4. 5-(4-Fluorophenyl)-1,3-oxazole 96a	257
8.3.1.5. 5-(2-Chlorophenyl)-1,3-oxazole 96b.....	257
8.3.1.6. 5-(3-Methoxyphenyl)-1,3-oxazole 96c.....	257
8.3.1.7. 5-(2,4-Dimethoxyphenyl)-1,3-oxazole 96d.....	258
8.3.1.8. 5-(Benzo[<i>d</i>][1,3]dioxol-5-yl)-1,3-oxazole 96e	258
8.3.1.9. 5-(4- <i>tert</i> -Butylphenyl)-1,3-oxazole 96f	259
8.3.1.10. 5-(4-Nitrophenyl)-1,3-oxazole 96g	259
8.3.1.11. 5-(2-Nitrophenyl)-1,3-oxazole 96h.....	260

8.3.1.12. 5-Phenyl-1,3-oxazole 96i.....	260
8.3.1.13. (4 <i>R</i> ,5 <i>R</i>)/(4 <i>S</i> ,5 <i>S</i>)-5-(Benzo[<i>d</i>][1,3]dioxol-5-yl)-4-tosyl-4,5-dihydrooxazole 97e	261
8.3.1.14. (4 <i>R</i> ,5 <i>R</i>)/(4 <i>S</i> ,5 <i>S</i>)-5-(2-Nitrophenyl)-4-tosyl-4,5-dihydrooxazole 97h	261
8.3.1.15. (4 <i>R</i> ,5 <i>R</i>)/(4 <i>S</i> ,5 <i>S</i>)-5-Phenyl-4-tosyl-4,5-dihydrooxazole 97i.....	262
8.3.2. Synthesis of ethyl 2-formamidoacetate 104	262
8.3.3. Synthesis of <i>N</i> -(2-hydrazinyl-2-oxoethyl)formamide 103	263
8.3.4. Synthesis of <i>N</i> -aryl-2-formamidoacetamide	263
8.3.4.1. General synthetic procedure.....	263
8.3.4.2. <i>N</i> -(4-Bromophenyl)-2-formamidoacetamide 102a.....	263
8.3.4.2. <i>N</i> -(2,4-Dimethoxyphenyl)-2-formamidoacetamides 102b	264
8.3.5. Synthesis of 2-isocyano- <i>N</i> -arylacetamide 101	264
8.3.5.1. General procedure	264
8.3.5.2. Synthesis of 2-isocyano- <i>N</i> -(4-bromophenyl)acetamide 101a.....	264
8.3.5.4. Synthesis of 2-isocyano- <i>N</i> -(2,4-dimethoxyphenyl)acetamide 101b	265
8.3.6. Attempted reaction of <i>N</i> -aryl-2-isocyanoacetamide with benzoyl chloride and benzaldehydes	265
8.3.6.1. General procedure A.....	265
8.3.6.2. General procedure B.....	265
8.3.7. Reaction of <i>N</i> -aryl-2-isocyanoacetamide with benzaldehydes	266
8.3.7.1. General procedure.....	266
8.3.7.2. (4 <i>R</i> ,5 <i>R</i> /4 <i>S</i> ,5 <i>S</i>)- <i>N</i> -(2,4-Dimethoxyphenyl)-5-(4-fluorophenyl)-4,5-dihydrooxazole- 4-carboxamide 107a.....	266
8.3.7.3. (4 <i>R</i> ,5 <i>R</i> /4 <i>S</i> ,5 <i>S</i>)- <i>N</i> -(2,4-Dimethoxyphenyl)-5-(2-chlorophenyl)-4,5-dihydrooxazole- 4-carboxamide 107b.....	267
8.3.7.4. (4 <i>R</i> ,5 <i>R</i> ,4 <i>S</i> ,5 <i>S</i>)- <i>N</i> -(2,4-Dimethoxyphenyl)-5-(3,4-dimethoxyphenyl)-4,5- dihydrooxazole-4-carboxamide 107c.....	267
8.3.7.5. (4 <i>R</i> ,5 <i>R</i> /4 <i>S</i> ,5 <i>S</i>)- <i>N</i> -(2,4-Dimethoxyphenyl)-5-phenyl-4,5-dihydrooxazole-4- carboxamide 107d.....	268
8.3.8. Attempted oxidation of 4,5-aryl-4,5-dihydro- <i>N</i> -(3,5-dimethoxyphenyl)oxazole- 4-carboxamides	269
8.3.9. Synthesis of ethyl-5-aryl-1,3-oxazole-4-carboxylates	269
8.3.9.1. General procedure	269
8.3.9.2. Ethyl 5-(4-fluorophenyl)oxazole-4-carboxylate 109a	269
8.3.9.3. Ethyl 5-(3-methoxyphenyl)oxazole-4-carboxylate 109c.....	270

8.3.10. Hydrolysis of ethyl 1,5-diaryl-oxazole-4-carboxylates	270
8.3.10.1. General synthetic procedure	270
8.3.10.2. 5-(4-Fluorophenyl)oxazole-4-carboxylic acid 108a	270
8.3.10.3. 5-(3-Methoxyphenyl)oxazole-4-carboxylic acid 108c	271
8.3.11. Preparation of 5-aryloxazole-4-carbonyl chloride	271
8.3.11.1 General synthetic procedure	271
8.3.11.2. 5-(4-Fluorophenyl)oxazole-4-carbonyl chloride 112a	272
8.3.11.3. 5-(3-Methoxyphenyl)oxazole-4-carbonyl chloride 112c	272
8.3.12. Synthesis of <i>N</i> ,5-diaryl-4-carboxamide-1,3-oxazole	272
8.3.12.1 General synthetic procedure	272
8.3.12.2. 5-(4-Fluorophenyl)- <i>N</i> -(2-hydroxyphenyl)oxazole-4-carboxamide 100a	273
8.3.12.3. 5-(4-Fluorophenyl)- <i>N</i> -(2,4-dimethoxyphenyl)oxazole-4-carboxamide 100b	273
8.3.12.3. 5-(4-Fluorophenyl)- <i>N</i> -(4-bromophenyl)oxazole-4-carboxamide 100c.	274
8.3.12.4. 5-(4-Fluorophenyl)- <i>N</i> -(2,4-dimethylphenyl)oxazole-4-carboxamide 100d	275
8.3.12.5. (2,4-Dichlorophenyl)-5-(4-fluorophenyl)oxazole-4-carboxamide 100e	275
282-(5-(4-Fluorophenyl)oxazole-4-carboxamido)benzoic acid 100f.....	276
8.3.12.6. 5-(3-Methoxyphenyl)- <i>N</i> -(2-hydroxyphenyl)oxazole-4-carboxamide 100g	277
8.3.12.7. 5-(3-Methoxyphenyl)- <i>N</i> -(2,4-dimethoxyphenyl)oxazole-4-carboxamide 100h	277
8.3.12.8. 5-(3-Methoxyphenyl)- <i>N</i> -(4-bromophenyl)oxazole-4-carboxamide 100i...	278
8.3.12.9. 2-(5-(3-Methoxyphenyl)oxazole-4-carboxamido)benzoic acid 100j	278
8.3.12.10. 2-(5-(4-Methoxyphenyl)oxazole-4-carboxamido)-4-fluorobenzoic acid 100k	279
8.4. Chapter 4 experimental procedures	280
8.4.1. Synthesis of ethyl 2-amino hydrochloride salts	280
8.4.1.1. General synthetic procedure	280
8.4.1.2. Ethyl glycinate hydrochloride 105a	280
8.4.1.3. L-Ethyl 2-aminopropanoate hydrochloride 105b	280
8.4.1.4. D-Ethyl 2-amino-4-methylpentanoate hydrochloride 105c	281
8.4.2. Synthesis of ethyl 2-aminoacylates.....	281

8.4.2.1. General synthetic procedure	281
8.4.2.2. Ethyl 2-aminoacetate 115a	282
8.4.2.3. <i>L</i> -Alanine ethyl ester 115b.....	282
8.4.2.4. D-leucine ethyl ester 115c	282
8.4.3. Preparation of ethyl 2-arylideneamino acyl intermediates	283
8.4.3.1. General procedure	283
8.4.3.2. (<i>E</i>)-Ethyl 2-(4-fluorobenzylideneamino)acetate 116a	283
8.4.3.3. (<i>E</i>)-Ethyl 2-(2-chlorobenzylideneamino)acetate 116b	283
8.4.3.4. (<i>E</i>)-Ethyl 2-(3-methoxybenzylideneamino)acetate 116c	284
8.4.3.5. (<i>E</i>)-Ethyl 2-(3,4-dimethoxybenzylideneamino)acetate 116d	284
8.4.3.6. (<i>E</i>)-Ethyl 2-((benzo[<i>d</i>][1,3]dioxol-6-yl)methyleneamino)acetate 116e.....	285
8.4.3.7. (<i>E</i>)-Ethyl 2-(4- <i>tert</i> -butylbenzylideneamino)acetate 116f.....	285
8.4.3.8. (<i>E</i>)-Ethyl 2-(3-hydroxy-4-methoxybenzylideneamino)acetate 116g	286
8.4.3.9. (<i>E</i>)-Ethyl 2-(benzylideneamino)acetate 116h	286
8.4.3.10. (<i>S, E</i>)-Ethyl 2-(4-fluorobenzylideneamino)propanoate 117a	287
8.4.3.11. (<i>S, E</i>)-Ethyl 2-(3-methoxybenzylideneamino)propanoate 117b	287
8.4.3.12. (<i>S, E</i>)-Ethyl 2-(3,4-dimethoxybenzylideneamino)propanoate 117c	288
8.4.3.13. (<i>R, E</i>)-Ethyl-5-(4-Fluorobenzylideneamino)-7-methyloctan-4-one 118a	288
8.4.3.14 (<i>R, E</i>)-Ethyl 2-(3,4-dimethoxybenzylideneamino)-4-methylpentanoate 117c	289
8.4.3.15. (<i>R, E</i>)-Ethyl 2-(benzylideneamino)-4-methylpentanoate 118c.....	289
8.4.4. Synthesis of ethyl 2-(5-aryl-1 <i>H</i> -imidazol-1-yl)acyl derivatives.....	290
8.4.4.1. Synthesis of ethyl 2-[5-(3,4-dimethoxyphenyl)-4-tosyl-4,5-dihydro-1 <i>H</i> -imidazol-1-yl]acetate	290
8.4.4.2. Synthesis of ethyl 2-[5-(3,4-dimethoxyphenyl)-1 <i>H</i> -imidazol-1-yl]acetate	290
8.4.4.3. Synthetic procedure.....	291
8.4.4.4. Ethyl 2-[5-(4-fluorophenyl)-1 <i>H</i> -imidazol-1-yl]acetate 120a	291
8.4.4.5. Ethyl 2-(5-(2-chlorophenyl)-1 <i>H</i> -imidazol-1-yl)acetate 120b	292
8.4.4.6. Ethyl 2-[5-(3-methoxyphenyl)-1 <i>H</i> -imidazol-1-yl]acetate 120c.....	292
8.4.4.7. Ethyl 2-[5-(3,4-dimethoxyphenyl)-1 <i>H</i> -imidazol-1-yl]acetate 120d	293
8.4.4.8. Ethyl 2-(5-(benzo[<i>d</i>][1,3]dioxol-6-yl)-1 <i>H</i> -imidazol-1-yl)acetate 120e.....	294
8.4.4.9. Ethyl 2-(5-(4- <i>tert</i> -butylphenyl)-1 <i>H</i> -imidazol-1-yl)acetate 120f.....	294
8.4.4.10. Ethyl 2-(5-(3-hydroxy-4-methoxyphenyl)-1 <i>H</i> -imidazol-1-yl)acetate 120g.....	295
8.4.4.11. Ethyl 2-[(5-phenyl)-1 <i>H</i> -imidazol-1-yl]acetate 120h	295
8.4.4.12. (<i>R</i>)-Ethyl 2-(5-(4-fluorophenyl)-1 <i>H</i> -imidazol-1-yl)propanoate 121a	296

8.4.4.13. (<i>R</i>)-Ethyl 2-(5-(3,4-dimethoxyphenyl)-1 <i>H</i> -imidazol-1-yl)propanoate 121b.....	297
8.4.4.14. (<i>R</i>)-Ethyl 2-(5-phenyl-1 <i>H</i> -imidazol-1-yl)propanoate 121d.....	297
8.4.5. Synthesis of 2-(5-aryl)-1 <i>H</i> -imidazol-1-yl)acetic acid derivatives	298
8.4.5.1 Synthetic procedure A.....	298
8.4.5.2. Synthetic procedure B	298
8.4.5.3. 2-[5-(4-Fluorophenyl)-1 <i>H</i> -imidazol-1-yl]acetic acid 123a.....	298
8.4.5.4. 2-[5-(3-Methoxyphenyl)-1 <i>H</i> -imidazol-1-yl]acetic acid 123c	299
8.4.5.5. 2-[5-(3,4-Dimethoxyphenyl)-1 <i>H</i> -imidazol-1-yl]acetic acid 123d	299
8.4.5.6. 2-(5-(Benzo [<i>d</i>] [1,3]dioxol-6-yl)-1 <i>H</i> -imidazol-1-yl)acetic acid 123e	300
8.4.5.7. 2-(5-(4- <i>tert</i> -Butylphenyl)-1 <i>H</i> -imidazol-1-yl)acetic acid 123f.....	300
8.4.5.8. 2-(5-(3-Hydroxy-4-methoxyphenyl)-1 <i>H</i> -imidazol-1-yl)acetic acid 123g.....	301
8.4.5.9. 2-(5-Phenyl-1 <i>H</i> -imidazol-1-yl)acetic acid 123h	301
8.4.6. Synthesis of 2-(5-aryl-1 <i>H</i> -imidazol-1-yl)acetohydrazide.....	302
8.4.6.1. General synthetic procedure A	302
8.4.6.2. General synthetic procedure B	302
8.4.6.3. 2-[5-(4-Fluorophenyl)-1 <i>H</i> -imidazol-1-yl]acetohydrazide 125a.....	302
8.4.6.4. 2-[5-(3-Methoxyphenyl)-1 <i>H</i> -imidazol-1-yl]acetohydrazide 125c	303
8.4.6.5. 2-(5-(Benzo [<i>d</i>] [1,3]dioxol-6-yl)-1 <i>H</i> -imidazol-1-yl)acetohydrazide 125e	304
8.4.6.7. 2-[5-(4- <i>tert</i> -Butylphenyl)-1 <i>H</i> -imidazol-1-yl]acetohydrazide 125f.....	305
8.4.6.8. 2-(5-(3-Hydroxy-4-methoxyphenyl)-1 <i>H</i> -imidazol-1-yl)acetohydrazide 125g	305
8.4.6.9. 2-(5-Phenyl-1 <i>H</i> -imidazol-1-yl)acetohydrazide 125h.....	306
8.4.7. Synthesis of (<i>E</i>)- <i>N</i> '-arylidene-2-(5-aryl-1 <i>H</i> -imidazol-1-yl)acetohydrazide	307
8.4.7.1. General synthetic procedure.....	307
8.4.7.3. (<i>E</i>)- <i>N</i> '-(2-Chlorobenzylidene)-2-(5-(3-hydroxy-4-methoxyphenyl)-1 <i>H</i> -imidazol-1-yl)acetohydrazide 127b.....	308
8.4.7.4. (<i>E</i>)- <i>N</i> '-(3,4-Dimethoxybenzylidene)-2-(5-(3-hydroxy-4-methoxyphenyl)-1 <i>H</i> -imidazol-1-yl)acetohydrazide 127c	309
8.4.7.5. (<i>E</i>)- <i>N</i> '-(4- <i>tert</i> -Butylbenzylidene)-2-(5-(3-hydroxy-4-methoxyphenyl)-1 <i>H</i> -imidazol-1-yl)acetohydrazide 127d.....	309
8.4.7.6. (<i>E</i>)- <i>N</i> '-(3-Hydroxy-4-methoxybenzylidene)-2-(5-(3-hydroxy-4-methoxyphenyl)-1 <i>H</i> -imidazol-1-yl)acetohydrazide 127e.....	310
8.4.7.7. (<i>E</i>)- <i>N</i> '-Benzylidene-2-(5-(3-hydroxy-4-methoxyphenyl)-1 <i>H</i> -imidazol-1-yl)acetohydrazide 127f.....	311
8.4.7.8. (<i>E</i>)- <i>N</i> '-(4-Fluorobenzylidene)-2-(5-(4-fluorophenyl)-1 <i>H</i> -imidazol-1-yl)acetohydrazide 127g.....	311

yl)acetohydrazide 127g	311
7.4.7.9. (<i>E</i>)- <i>N'</i> -(2-Chlorobenzylidene)-2-(5-(4-fluorophenyl)-1 <i>H</i> -imidazol-1-yl)acetohydrazide 127h	312
8.4.7.10. (<i>E</i>)- <i>N'</i> -(3,4-Dimethoxybenzylidene)-2-(5-(4-fluorophenyl)-1 <i>H</i> -imidazol-1-yl)acetohydrazide 127i	313
8.4.7.11. (<i>E</i>)- <i>N'</i> -(4- <i>tert</i> -Butylbenzylidene)-2-(5-(4-fluorophenyl)-1 <i>H</i> -imidazol-1-yl)acetohydrazide 127j.....	313
8.4.7.12. (<i>E</i>)- <i>N'</i> -(3-Hydroxy-4-methoxybenzylidene)-2-(5-(4-fluorophenyl)-1 <i>H</i> -imidazol-1-yl)acetohydrazide 128k	314
8.4.7.13. (<i>E</i>)- <i>N'</i> -Benzylidene-2-(5-(4-fluorophenyl)-1 <i>H</i> -imidazol-1-yl)acetohydrazide 127l.....	315
8.4.7.14. (<i>E</i>)- <i>N'</i> -(4-Fluorobenzylidene)-2-(5-(3,4-dimethoxyphenyl)-1 <i>H</i> -imidazol-1-yl)acetohydrazide 127m	315
8.4.7.15. (<i>E</i>)- <i>N'</i> -(4- <i>tert</i> -Butylbenzylidene)-2-(5-(3,4-dimethoxyphenyl)-1 <i>H</i> -imidazol-1-yl)acetohydrazide 127n	316
8.4.7.16. (<i>E</i>)-2-(5-(4- <i>tert</i> -Butylphenyl)-1 <i>H</i> -imidazol-1-yl)- <i>N'</i> -benzylideneacetohydrazide 4.12o	317
8.4.8. Synthesis of <i>N</i> -aryl-2-(5-aryl-1 <i>H</i> -imidazol-1-yl)acetamide	317
8.4.8.1. General synthetic procedure	317
8.4.8.2. 2-(5-(4-Fluorophenyl)-1 <i>H</i> -imidazol-1-yl)- <i>N</i> -(2,4-dimethoxyphenyl)acetamide 128a	318
8.4.8.3. 2-(5-(4-Fluorophenyl)-1 <i>H</i> -imidazol-1-yl)- <i>N</i> -(2,4-dimethylphenyl)acetamide 128b.....	318
8.5. Chapter 5 experimental procedures	320
8.5.1. Synthesis of 2,2,2-trichloro-1-arylethanol	320
8.5.1.1. General synthetic procedure	320
8.5.1.2. 2,2,2-Trichloro-1-(4-fluorophenyl)ethanol 132a	320
8.5.1.3. 2,2,2-Trichloro-1-(4-chlorophenyl)ethanol 132b	320
8.5.1.4. 2,2,2-Trichloro-1-phenylethanol 132c.....	321
8.5.1.5. 1-(Benzo[<i>d</i>][1,3]dioxol-6-yl)-2,2,2-trichloroethanol 132d	321
8.5.2. Synthesis of 2-chloro-1-arylethanone by oxidation	321
8.5.2.1. General synthetic procedure	321
8.5.2.2. 2-Chloro-1-(4-fluorophenyl)ethanone 133a.....	322
8.5.2.3. 2-Chloro-1-(4-chlorophenyl)ethanone 133b.....	322

8.5.2.4. 2-Chloro-1-phenylethanone 133c	323
8.5.2.5. 1-(Benzo[<i>d</i>][1,3]dioxol-6-yl)-2-chloroethanone 133d	323
8.5.3. Synthesis of 2-chloro-1-arylethanone oxime	323
8.5.3.1. General synthetic procedure	323
8.5.3.2. (<i>E/Z</i>)-2-Chloro-1-(4-fluorophenyl)ethanone oxime 129a	324
8.5.3.3. (<i>E/Z</i>)-2-Chloro-1-(4-chlorophenyl)ethanone oxime 129b	324
8.5.3.4. (<i>E/Z</i>)-2-Chloro-1-phenylethanone oxime 129c	325
8.5.3.5. (<i>E/Z</i>)-1-(Benzo[<i>d</i>][1,3]dioxol-6-yl)-2-chloroethanone oxime 129d	325
8.5.4. Synthesis of <i>N</i> -aryl formamide	325
8.5.4.1. General synthetic procedure	325
8.5.4.3. <i>N</i> -(2,4-Dimethylphenyl)formamide 139b	326
8.5.4.4. <i>N</i> -(2,4-Dimethoxyphenyl)formamide 139c	327
8.5.4.5. <i>N</i> -(2,4-Dichlorophenyl)formamide 139d	327
8.5.5. Dehydration of <i>N</i> -arylformamide	327
8.5.5.1. General synthetic procedure	327
8.5.5.2. 1-Isocyano-4-bromobenzene 130a	328
8.5.5.3. 1-Isocyano-2,4-dimethylbenzene 130b	328
8.5.5.4. 1-Isocyano-2,4-dimethoxybenzene 130c	329
8.5.5.5. 1-Isocyano-2,4-dichlorobenzene 130d	329
8.5.6. Synthesis of 3-aryl- <i>N</i> -substituted-isoxazol-5-amine derivatives	329
8.5.6.1. General synthetic procedure: method A	329
8.5.6.2. General synthetic procedure: method B	330
8.5.6.3. General synthetic procedure: method C	330
8.5.6.4. General synthetic procedure: method D	330
8.5.6.5. General synthetic procedure: method E	330
8.5.6.6. General synthetic procedure: method F	331
8.5.6.7. <i>N</i> -(2,4-Dimethoxyphenyl)-3-phenylisoxazol-5-amine 131a	331
8.5.6.8. <i>N</i> -(2,4-Dimethylphenyl)-3-phenylisoxazol-5-amine 131b	332
8.5.6.9. 3-(4-Fluorophenyl)- <i>N</i> -(2,4-dimethylphenyl)isoxazol-5-amine 131c	332
8.5.6.10. <i>N</i> -(4-Bromophenyl)-3-phenylisoxazol-5-amine 131d	333
8.5.6.11. <i>N</i> -(4-Bromophenyl)-3-(4-fluorophenyl)isoxazol-5-amine 131e	333
8.5.6.12. Methyl 2-(3-(4-fluorophenyl)isoxazol-5-ylamino)acetate 141a	334
8.5.6.13. Methyl 2-(3-(4-chlorophenyl)isoxazol-5-ylamino)acetate 141b	334
8.5.7. Synthesis of 3-aryl-isoxazol-5-amine derivatives	335

8.5.7.1 General synthetic procedure.....	335
8.5.7.2. 3-(4-Fluorophenyl)isoxazol-5-amine 144a.....	335
8.5.7.3. 3-(4-Chlorophenyl)isoxazol-5-amine 144b	336
8.5.7.4. 3-Phenylisoxazol-5-amine 144c	336
APPENDIX: A: Virtual screening of pepMMsMIMIC 3-dimensinal database using BST- 2-Vpu interaction	337
APPENDIX B: Selected spectra	340
References.....	354

CHAPTER 1: Literature Review

1. INTRODUCTION

The drug discovery process has positively produced a great number of treatments that can suppress, stop or reverse the effects of viral and bacterial infections, resulting in the improvement of the quality and extension of lives. However, the emergence of new viral strains and the high mutation rate in several pathogens has led to multi-drug resistance. This has prompted the search for new effective and innovative therapeutic treatments. One path that holds great potential is to design new small molecular entities, which are selective, safe and can battle the new strains.

For the development of small molecules, identification of and insight into potential targets are of paramount importance to act as a guide for researchers. In addition, setting up usable protocols for testing activity at the target is important before commencing the actual design of drug candidates. Once the target is established, chemical libraries of compounds obtained from commercial vendors or through in-house synthetic efforts are screened using relevant approaches. Once the active molecules (hits) are identified, they can further undergo structural modifications to afford analogues called leads, with increased affinity and selectivity. The lead compounds additionally undergo structural alteration to optimise their physicochemical properties until being developed into potential drug candidates. These drug candidates are then subjected to different phases of pre-clinical trials to determine parameters such as pharmacokinetics, pharmacodynamics and bioavailability until they are accepted by relevant approval agencies and marketed for a specific disease.^{1,2}

This chapter provides an overview of the relatively newly exploited binding cavities on the HIV-1 lifecycle as a potential target for the development of a novel class of antiretroviral inhibitors. The second section of this chapter explores the fragment-based screening method as an alternative new drug discovery approach towards the identification of hit compounds to turn into leads. Heterocyclic compounds often possess interesting biological activities; therefore, the review also explores the importance of the *para*-toluenesulfonylmethyl isocyanide and aryl isocyanide synthons in the preparation of five membered nitrogen containing heterocycles.

1.1. The Targets: Human immunodeficiency Virus (HIV-1)

The infectious disease recognized as Acquired Immunodeficiency Syndrome (AIDS) initiated by the Human Immunodeficiency Virus type 1 (HIV-1) remains life-threatening to public health

worldwide, especially in low- and middle-income nations. According to the World Health Organization (WHO) in 2015, an estimated 16 million people worldwide were under antiretroviral treatment and roughly 36.9 million people globally were living with HIV-1.³ The financial toll of HIV/AIDS is tremendous and it is projected that South Africa alone spent approximately \$1 billion in 2014 on HIV/AIDS treatment and awareness programmes.⁴ Since the identification of HIV as the causative agent of AIDS, research scientists have tried to find an effective vaccine for the disease. Although attempts at discovering a cure have thus far been unsuccessful, therapeutic treatments that can sufficiently suppress the viral load to below detection levels have been developed.⁵ This has resulted in a significant decrease in the mortality rate and extends the lifespan of infected individuals worldwide. HIV-1 progression is managed through the process of using mixtures of more than one drug called highly active antiretroviral therapy (HAART).^{6,7} Although current HIV-1 treatments have much improved the clinical outcome, the high mutation rate of the virus has led to the development of drug resistance in many viral strains, thereby emphasizing necessity to develop novel anti-HIV-1 drugs that target relative newly exploited HIV-1 integrase (IN) - host lens epithelium-derived growth factor (LEDGF/p75) and HIV-1 viral protein U (Vpu) - host bone marrow stromal cell antigen 2 (BST-2) interactions.

The replication cycle of HIV-1 (*Figure 1.1*) begins with the contact of the viral glycoprotein 120 (gp120) with the CD4⁺ receptor and the co-receptor CCR5 or CXCR4 on a susceptible cell, which subsequently allows fusion of the viral envelope with the cell membrane.^{8,9,10,11,12} Upon fusion, the viral capsid is released and disassembled to allow the viral genome into the host cell.^{13,14,15} The viral genome codes for the necessary proteins and enzymes to complete the life cycle. Inside the host cell, the viral reverse transcriptase enzyme transcribes the single-stranded RNA genome into a double-stranded DNA, which is then introduced into the host nucleus by the viral enzyme integrase (IN).^{16,17}

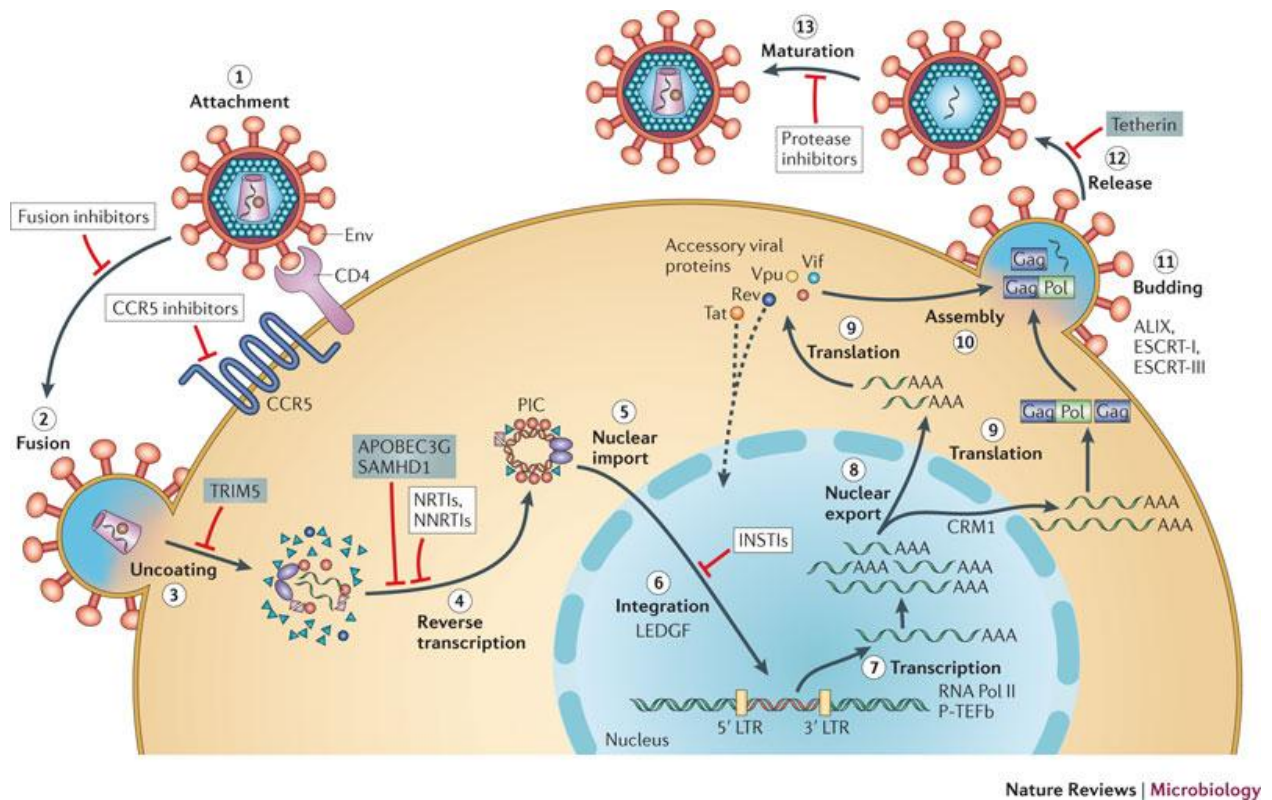


Figure 1.1: Schematic representation of the HIV-1 replication cycle (Figure taken from Engelman et al.)¹⁸

1.1.1 HIV-1 integrase

The 32 kDa monomeric form of IN is made up of 288 amino acids and comprises of three structural domains, the N-terminal zinc finger domain (NTD), a catalytic core domain (CCD) and the C-terminal DNA-binding domain (CTD).¹⁹ IN enzyme plays two essential enzymatic roles during the HIV-1 replication life cycle, namely: the 3'-processing and DNA strand transfer. During the 3'-processing, the IN displaces two conserved dinucleotides by attaching itself to the ends of long terminal repeat strands (LTR) of proviral complementary DNA.^{20,21} The resulting cleaved DNA is then used as a template for the strand transfer that involves the transesterification of 3'-OH viral ends leading to the proper insertion of viral DNA into the host cell chromatin. This DNA insertion has been presented as one of the targets for antiviral drug discovery and development. The molecules that inhibit insertion of the pre-integration complex (PIC) into the DNA of the host cell are known as strand transfer inhibitors (INSTIs).^{22,23,24}

1.1.2. Co-factor LEDGF/p75- HIV-1 IN proteins interaction

HIV-IN relies on cellular co-factors for the tethering and correct insertion of the viral genome into the host cell chromatin (*Figure 1.2*).^{25,26} It is evident that IN efficiently integrates the DNA by using its catalytic domain catalytic core (IN-CCD) and N-terminal domains. This critical step is successfully accomplished through interaction with the C-integrase domain of the host lens epithelium-derived growth factor, or transcriptional coactivator p75 (LEDGF/p75).²⁵⁻²⁶ As a result the LEDGF/p75 - IN interaction has been recognised as one of the new essential targets for development of a novel generation of HIV-1 inhibitors. In addition, mutagenesis analysis established that the Lys364, Ile365, Asp366, Phe406, Val408 residues of the LEDGF/p75 binds to the Ala128, His171, Thr174, Trp131, Trp132, Gln168 residues of an IN dimer.

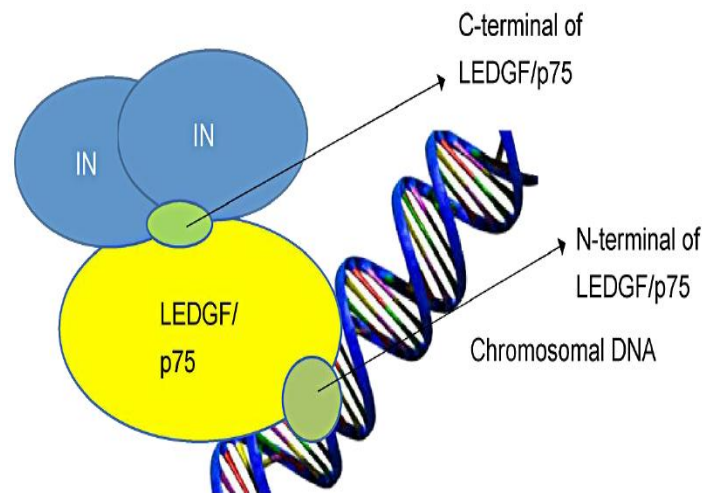


Figure 1.2: Interaction between LEDGF/p75-HIV-1 IN. (Figure taken from Harrison, A. T. Master's thesis)²⁷

Once the DNA is properly inserted inside the nucleus, it is then converted into messenger RNA by the cellular machinery, which is then translated into long polyproteins. The viral long polyproteins are cleaved by viral protease to afford functional proteins and viral components are packaged into newly formed virions. The newly formed virions sustain the downregulation of CD4 in the endoplasmic reticulum (ER), enable budding and enhance release of new virions from the plasma membrane, thus promoting the spread of infection.^{28,29,30,31}

1.1.3. Viral protein U

The degradation of CD4 and enhancement of extracellular viral particle release by HIV-1 relies on the viral protein U (Vpu), a type I integral protein of 81 amino acids, which is one of four accessory genes encoded in HIV-1.^{32,33,34} Vpu consists of a hydrophobic N-terminal domain in the transmembrane region, which has a well-defined α -helix structure, and a hydrophilic C-terminal domain (*Figure 1.3*).^{35,36} The C-terminal domain in the cytoplasmic region consists of two α -helix domains, which are linked together by two phosphorylated serine residues. The phosphorylation of the two serine residues in Vpu is mediated by casein kinase II enzyme.

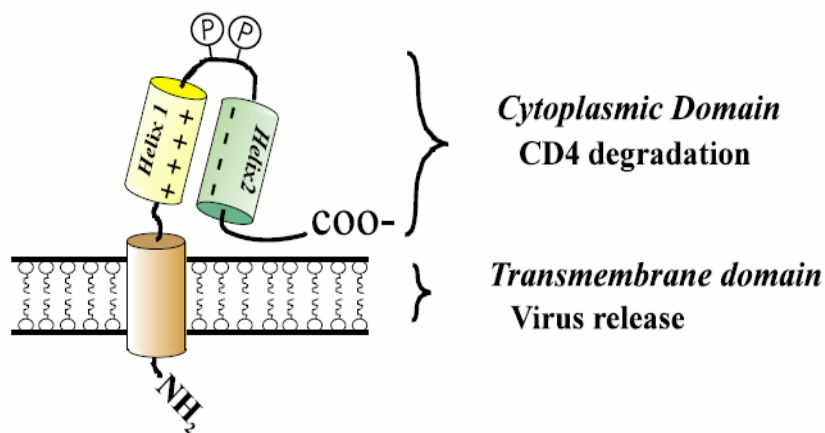


Figure 1.3: Structural domain of Vpu with two helices of the cytoplasmic domain oriented parallel to each other. (Figure taken from Strebel).³⁵

1.1.4. Bone marrow stromal cell antigen 2 (BST-2)

BST-2, also known as tetherin, CD317 or HM1.24, is a type II transmembrane protein of 180 amino acids. This interferon inducible (α -IFN) host restriction factor bears a short cytoplasmic N-terminal tail region (CT) of 21 amino acids, an α -helical transmembrane domain (TM) of 21 amino acids, a central coil-coiled extracellular domain (EC) of 116 amino acids and a C-terminal glycosylphosphatidylinositol (GPI) domain (*Figure 1.4*). The TM α -helical structure serves as an anchor of the molecule to the plasma membrane while GPI, which forms part of the C-terminal domain, acts as a secondary anchor connecting the BST-2 back to the cell membrane. Both TM and GPI anchors of BST-2 are critical for restriction of virus release. The EC domain provides dimer stability through formation of a disulfide bond between cysteine residues, which is necessary for retention of antiviral activity.^{37, 38,39}

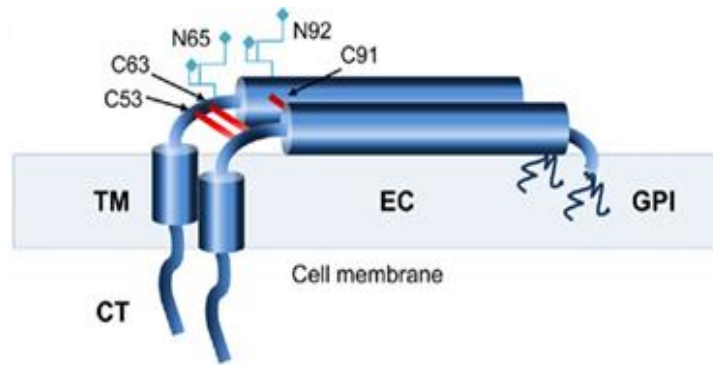


Figure 1.4: Representation of the structure of the BST-2 domain. (Figure taken from Arias *et al.*³⁷)

1.1.5. The interaction between BST-2 and viral Vpu protein

Evidence suggests that interaction of Vpu with BST-2 is of critical importance in HIV-1 replication.^{40,41,42} Although BST-2 inhibits the release of viral particles from the infected cell, Vpu manages to mediate the removal of the BST-2 from the cell membrane through a mechanistic pathway which is still under debate. Several reports suggest that downregulation of BST-2 by Vpu occurs as a result of several possible mechanistic actions, which include lysosome-dependent degradation of BST-2 *via* recruitment of a cellular co-factor called beta-transducing repeat-containing protein (β -TrCP) or proteasomal degradation.^{36,43} Arias *et al.* suggested that Vpu antagonises BST-2 by interfering with biosynthetic/secretory pathways, which reduces the supply of newly formed BST-2 to the cell membrane.⁴⁴ Regardless of the mechanistic pathway, the ability of Vpu to interact with BST-2 is of crucial importance in the downregulation of BST-2. Biological assays, computational and NMR spectroscopic studies confirmed that Vpu counteracts BST-2 *via* interaction through their α -helical transmembrane domains (*Figure 1.5*).^{44,45,46,47} Mutation analysis revealed that critical interacting residues on Vpu are Ala10, Ala14, Ala18 and Trp22, which are spaced at four residue intervals. Analysis of mutations on BST-2 revealed that Val30, Ile33, Ile34, leu37, Leu41 and Thr45 are the residues involved in the interaction. These residues are on the same side of the helix in proteins.⁴⁰⁻⁴⁸

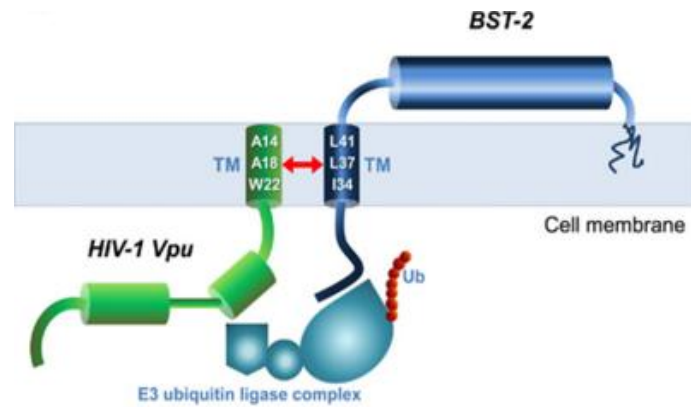


Figure 1.5: Representation of the interaction of HIV-1 Vpu and BST-2 through their transmembrane domains (Arias *et al.*).⁴⁴

1.1.6. Therapeutic intervention on HIV-1 IN

Since recognition of HIV-1 IN as a target, the Food and Drug Administration (FDA) has approved three clinical HIV-1 integrase strand transfer inhibitors (INSTIs) which are currently on the market; namely: elvitegravir,⁴⁹ dolutegravir,⁵⁰ and raltegravir^{51,52} (Figure 1.6). These INSTIs selectively target strand transfer through a unique mode of action, which involves the chelating of active site divalent metal ions, thereby preventing the insertion of the proviral DNA into the host DNA. Although these inhibitors have managed to suppress HIV-1 as part of highly active antiretroviral therapy (HAART), the emergence of new viral strains has resulted in development of resistance which has led to cytotoxicity and restricted the long-term prescription of these inhibitors. Therefore, the search for novel effective inhibitors to balance existing treatment approaches remains one of the key objectives in HIV drug discovery.

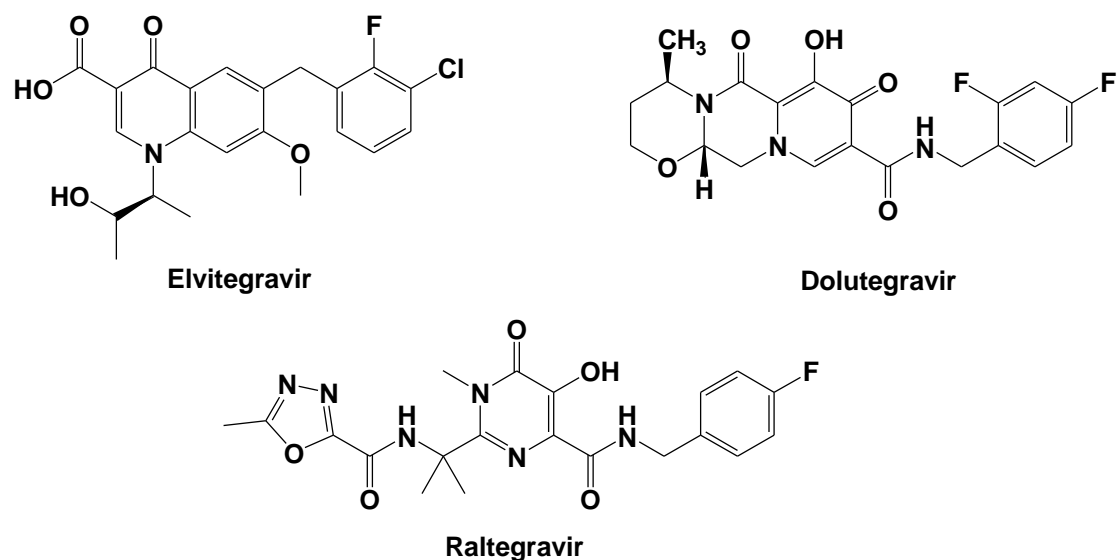


Figure 1.6: FDA approved IN inhibitors.

During the past decade, a lot of attention has been devoted to the development of inhibitors that can disrupt the formation of the HIV-1-IN and cofactor LEDGF/p75 complex, which led to the discovery of the small molecules listed in *Figure 1.7*.^{53,54,55} These small molecules have been identified by various approaches such as *in silico* virtual screening of compound libraries, fragment based drug discovery (FBDD) and structure-based *de novo* design.^{54,56,57} Some of these compounds contain carboxylic acid functionalities embedded within their chemical structures which proved to be significant to their binding properties. For instance, Du and co-workers⁵⁵ have identified a carboxylic acid containing compound, D77 as an inhibitor of IN-LEDGF interactions through molecular docking, site-directed mutagenesis analysis and surface plasmon resonance (SPR); while De Luca and colleagues⁵⁷ identified a class of indole molecules (CHIBA 3053 is one example, *Figure 1.7*), through AlphaScreen assay and computational studies, which has the ability to interrupt the catalytic activity of IN. An AlphaScreen assay, *in silico* docking and cell based assay study of libraries of compounds conducted by Christ and co-workers⁵³⁻⁵⁴ resulted in the discovery of the class of acetic acid scaffolds such as CX14442, BI-224436 and ALLIN (*Figure 1.7*) that inhibit interaction between the IN binding domain (IBD) of LEDGF/p75 and the catalytic core domain (CCD) of the HIV-1 IN proteins. BI-224436 was found to have significant antiretroviral activity and was further advanced into Phase I clinical development but was later withdrawn from clinicals without any reasons offered. Moreover, a virtual screening, docking studies, molecular dynamics and synthetic approach adopted by Ferro and co-workers⁵⁸ has led to the development of a rhodamine based family of compounds (*Figure 1.7*) which exhibited inhibitory effects by preventing the HIV-1 IN interaction with its cellular cofactor

LEDGF/p75 at micromolar concentration. Recently, a virtual screening of natural compounds and synthetic efforts conducted by Agharbaoui *et al.*⁵⁹ led to the identification of a set of lavendustin B derivatives (Figure 1.7) which exhibited IN-LEDGF/p75 inhibitory activity as well as decreased HIV-1 IN activity *via* an allosteric mechanistic pathway. These types of compounds are categorized as allosteric HIV-1 inhibitors and are a promising next generation of antiretroviral drugs.

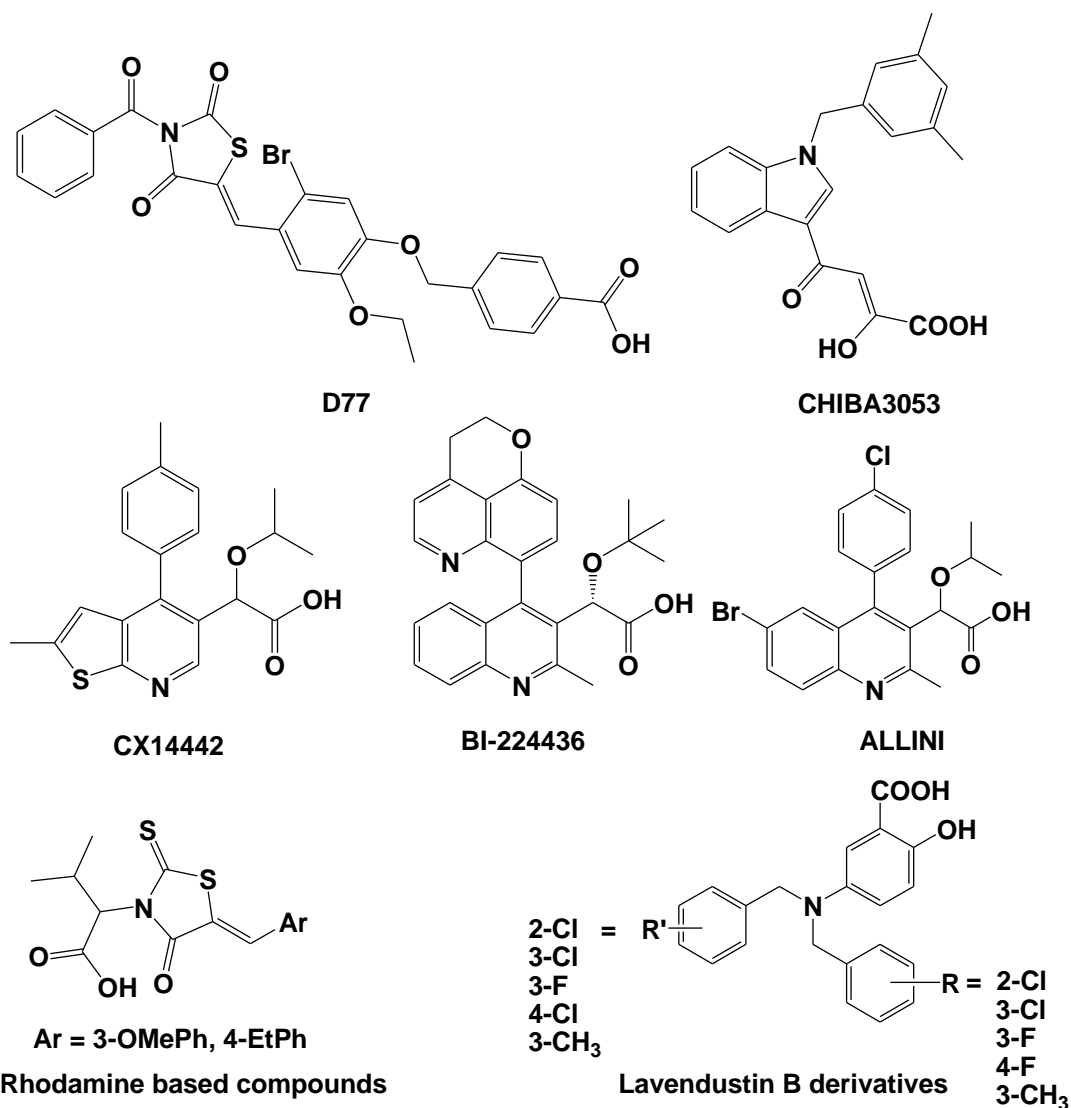


Figure 1.7: Examples of reported small molecule inhibitors of LEDGF/p75-IN interaction.

Furthermore, Sharma *et al.* modified ALLINI and designed a new class of pyridine-based compounds, KF115 and KF116 (Figure 1.8). Interestingly, these pyridine based compounds were found to promote the HIV-1 IN multimerization in virus particles but did not detectably disrupt

IN-LEDGF/p75 binding. Thus these compounds are classified as a new class of novel multimerization selective IN inhibitors.⁶⁰ In addition, a combination of different computational techniques and AlphaScreen-based IN dimerization assays conducted by Tintori and co-workers⁶¹ resulted in the discovery of hydrazine based compounds as promising HIV-1 IN dimerization inhibitors.

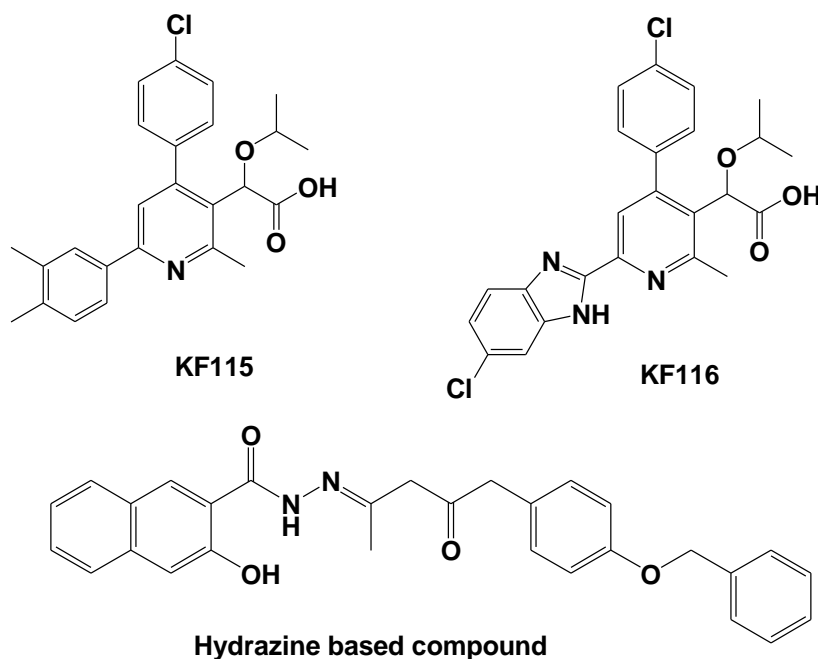


Figure 1.8: Novel class of multimerization selective IN inhibitors.

1.1.7. Therapeutic intervention on HIV-1 Vpu BST-2 interaction

Targeting HIV-1 Vpu and the host protein BST-2 interactions has attracted attention as a valuable approach to developing novel anti-HIV-1 inhibitors. To date, no antiretroviral drugs that target the HIV-1 Vpu - BST-2 complex formation have been approved in the market, which makes this target really interesting. However, in recent years, literature has reported three small molecules that can restrict the role of HIV-1 Vpu protein, therefore permitting the operation of the host BST-2 (*Figure 1.9*).^{62,63,64} For instance, BIT 225 has been reported as a potential inhibitor of Vpu ion channels, thereby preventing the assembly of the newly formed virions within the host cells.⁶² Recently, the use of an ELISA cell-based assay led to the discovery of two small molecules, IMB-LA and 2-thio-6-azauridine which were reported to specifically inhibit down-regulation of BST-2 mediated by HIV-1 Vpu.⁶³⁻⁶⁴ These molecules have been found to restrict the function of Vpu protein through diminished localization of BST-2 to lysosomes, but do not necessarily prevent the binding of BST-2 to Vpu.⁶³⁻⁶⁴ Although these compounds do not

necessarily disrupt the interaction between BST-2 and Vpu proteins; they offer the proof of concept that small molecules could be developed to block the release of new virions.

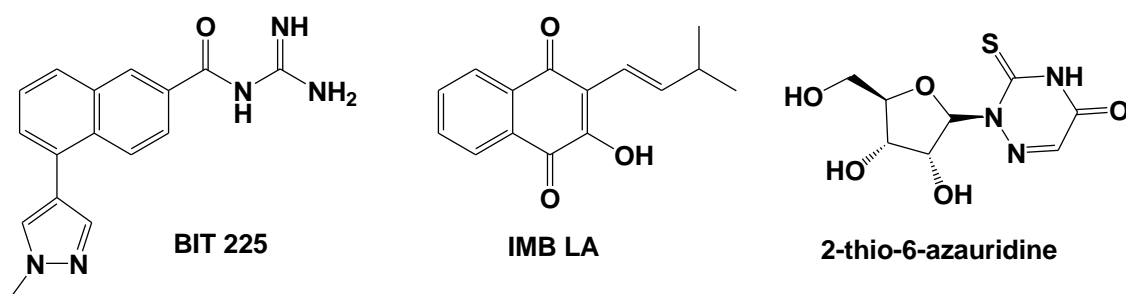


Figure 1.9: Structure of small molecules that inhibit Vpu mediated BST-2 degradation.

1.2. The Method: Fragment Based Approach to Drug Discovery

The fragment based approach to drug discovery has emerged as an interesting starting point for identification of high-affinity ‘hit’ molecules against targets of interest.^{65,66,67,68,69,70,71,72,73} This protocol involves screening of libraries of very small molecules called fragments with typically less than 350 Da mass, to search for affinities to their targets.⁶⁵⁻⁷³ The idea of fragment screening was first initiated by Verlinde *et al.* in 1990⁷¹ and later proposed by Shuker and co-workers⁷² in 1996.^{74,75} Since then it has been employed by various research laboratories, and resulted in some of the compounds in clinical trials.⁷⁶ For example, vemurafenib for the treatment of late-stage melanoma was designed through fragment screening methodology and approved by the FDA in 2011.⁷⁶ There are several potential benefits of using fragment screening as a starting point for identification of ‘hit’ molecules as compared to primary strategies such as conventional high-throughput screening (HTS),^{77,78} structure based-drug design⁷⁹ and analogue-based drug design⁸⁰. One of the advantages is that the structure activity relationships (SAR) of ‘hit’ molecules can be established at an early stage because various analogues can be synthesized without difficulty or acquired from commercially available sources due to their simplicity and low molecular weight.⁷³ Another advantage is that the low molecular weight fragments can optimally bind to the target because they are less selective, which allows exploration of the chemical space.^{81,82} Moreover, the fragment screening approach can identify lead compounds for previously undruggable proteins due to their relatively small size.^{83,84} Furthermore, screening of small libraries of fragments comprising 500-2000 compounds is usually carried out, in comparison to HTS where compound libraries consist of 100,000 to 1,000,000 compounds,

typically with a molecular mass between 350 -500 Da.⁸⁵ The scaffolds within a fragment library are usually governed by the so-called “rule of three”⁶⁹ in comparison to Lipinski’s⁸⁶ rule of five used for classification of drug like compounds. The rule of three (Ro3) states that fragments should ideally have: molecular weight < 300 g/mol, a number of hydrogen bond donors and acceptors ≤ 3 , XlogP ≤ 3 , a number of freely rotatable bonds ≤ 3 and polar surface area $\leq 60 \text{ \AA}^2$.

Lower molecular weight fragments have lower affinity for their targeted proteins. Therefore, arrays of physical screening protocols that are sensitive and robust have been developed to detect low binding affinity between fragments and their target of interest. These include Saturated Transfer Difference Nuclear Magnetic Resonance spectroscopy (STD-NMR),^{73,87,88,89} Isothermal Titration Calorimetry (ITC),^{90,91} and AlphaScreening Assay,^{92,93,94,95} to mention a few and which will be discussed in more detailed below.

1.2.1 Saturated Transfer Difference Nuclear Magnetic Resonance (STD NMR) Spectroscopy

STD NMR spectroscopy has emerged as one of the essential approaches to studying the interaction between fragments and the protein of interest.^{73,87} It measures the difference between two proton NMR spectra obtained with (on resonance) and without (off resonance) saturated receptor protein. The first step in STD NMR spectroscopy involves the recording of an off-resonance spectrum of a reference protein after sample irradiation at a frequency region far from both receptor and ligand resonances. In parallel, the on-resonance spectrum is registered by irradiation of the protons of the receptor protein (in the presence of ligand) in the selected region by a selective radio frequency pulse towards the proton NMR spectrum of the ligand. The irradiation causes magnetisation transfer through intra-molecular proton-proton cross-relaxation pathways from the protein to the small molecule, which results in the saturation of its proton NMR spectroscopic signals. Upon dissociation, the intensity of the NMR spectroscopic signals of the saturated molecule are reduced, leaving the signals of non-binding molecules unaffected. The difference between the on- and off-resonance spectra results in the saturation difference spectrum, with only the signals from ligands that are bound to the protein being present.

1.2.2. Isothermal Titration Calorimetry (ITC)

ITC is a consistent and precise screening tool for understanding not only the binding of protein to protein, but also the interactions between small molecules and receptor proteins.⁹⁰⁻⁹¹ This protocol measures the heat evolved or absorbed upon binding of two molecules. The heat exchange is determined through thermodynamic parameters, which are characterised using the binding constant, stoichiometry and enthalpy of binding. During binding evaluation by the ITC approach, a ligand is injected into the reaction cell containing the protein, which causes heat exchange proportional to the amount of small molecule interacting with the protein. The heat evolved by each injection is calculated based on the area under the peak produced.

1.2.2.3. Amplified Luminescent Proximity Homogeneous assay (AlphaScreen)

AlphaScreen technology is a biochemical analytical technique which allows the study of the interactions between small molecules and receptor proteins, but it's also an essential tool when looking at protein-protein interactions.⁹²⁻⁹⁵ This approach is based on donor and acceptor bead chemistry. The donor bead consists of photosynthesized phthalocyanine, which can be illuminated at 680 nm to excite ambient oxygen to the singlet oxygen state. The acceptor beads consist of thioxene, anthracene and rubrene chemical dyes that produce a luminescent response at 520-620 nm. A typical AlphaScreen experiment for determining the prevention of interaction between protein-protein by a ligand is carried out by attaching one protein to a donor bead and the other protein and a small molecule to the acceptor bead. During irradiation of the donor bead, the singlet oxygen generated reacts with the acceptor bead to emit energy in the form of light. However, if the small molecule prevents binding between two proteins, there will be no reaction between the donor bead and acceptor bead resulting in no light emission. If the ligand slightly prevents the interaction, the intensity of light produced is then reduced. The luminescent energy produced is then determined in terms of percentage; the higher the percentage the better the inhibition. One of the drawbacks possessed by the AlphaScreen is that compounds such as reactive compounds or chelators can still interfere by directly quenching the signal or reacting with the singlet oxygen. However, this drawback has been overcome by subjecting positive hits through the TruHit AlphaScreen assay. This assay is intended to eliminate false positives interfering with the AlphaScreen signal.⁹⁶ This kit contains streptavidin donor and biotinylated acceptor beads, which interact with each other to produce an AlphaScreen signal. Any compounds which are colour quenchers, singlet oxygen quenchers, light scatterers, and biotin mimetics interfering with the AlphaScreen signal are thus identified as false positives.

1.3. The Chemistry: TosMIC Synthons

Synthetic building blocks that can be manipulated by varying reaction conditions resulting in diverse nitrogen containing molecules are of utmost importance in medicinal organic synthesis and *para*-toluenesulfonylmethyl isocyanide TosMIC **1** has been proven to be such an entity. TosMIC **1** (Figure 1.10) has received great interest due to its 1,3-dipolar characteristics under basic conditions.^{97,98,99,100} It was first described by professor Daan van Leusen and co-workers in 1977⁹⁹ It is stable, non-volatile and unscented at room temperature, and it is also commercially available (CAS Number 36635-61-7).¹⁰¹

The sulfonyl substituent of TosMIC plays a prominent role as it enriches the acidity of α -protons as well as acting as a leaving group, while the isocyano group can undergo α - addition to produce α -adducts.⁹⁹⁻¹⁰⁰

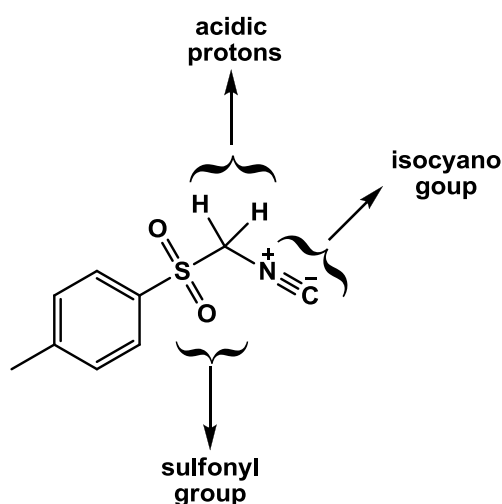
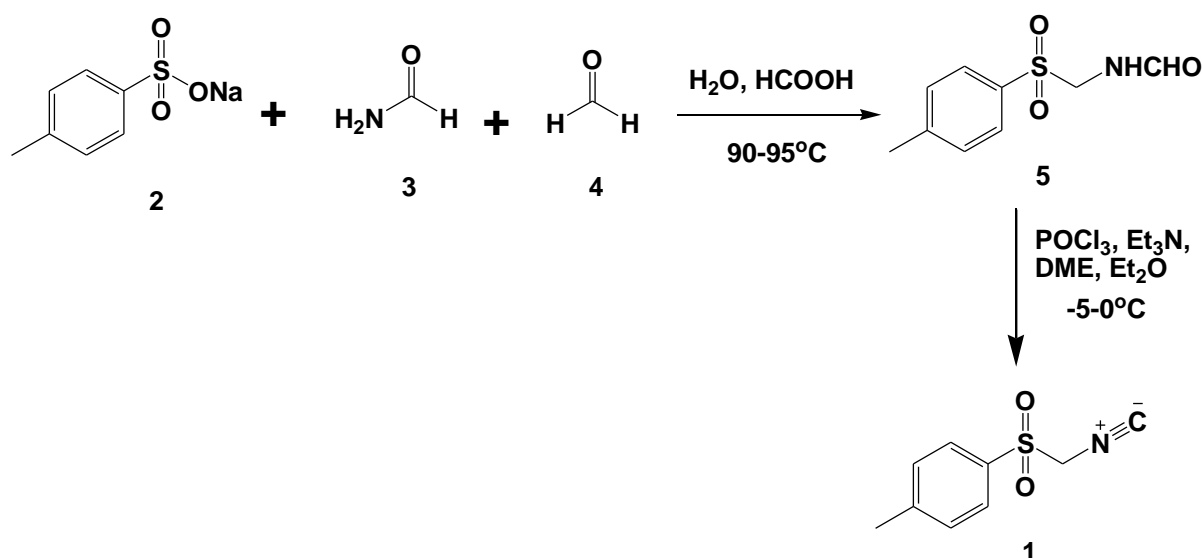


Figure 1.10: Structure of TosMIC (1).

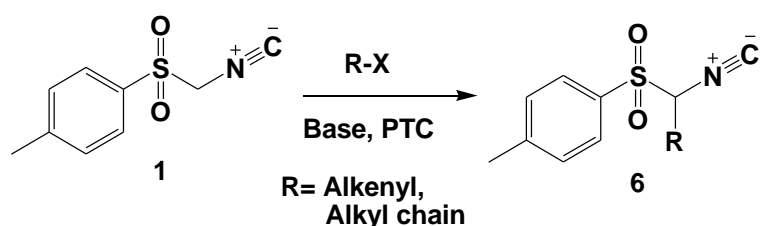
1.3.1. Preparation of TosMIC and its analogues

TosMIC **1** can be easily accessed in two stepwise processes. The initial stage involves a Mannich-type condensation, in which sodium 4-methylbenzenesulfonate **2** reacts with formamide **3** and formaldehyde **4** in water (H₂O) and formic acid (HCOOH) at 90-95°C to produce *N*-(*p*-tolylsulfonylmethyl)formamide **5**. The formamide **5** is then dehydrated with phosphoryl chloride (POCl₃) in the presence of triethylamine (Et₃N) using dimethoxyethane (DME) and diethyl ether (Et₂O) as solvents to afford TosMIC **1** in reasonable yield (**Scheme 1.1**).^{102, 103,104}



Scheme 1.1: Synthesis of TosMIC 1.

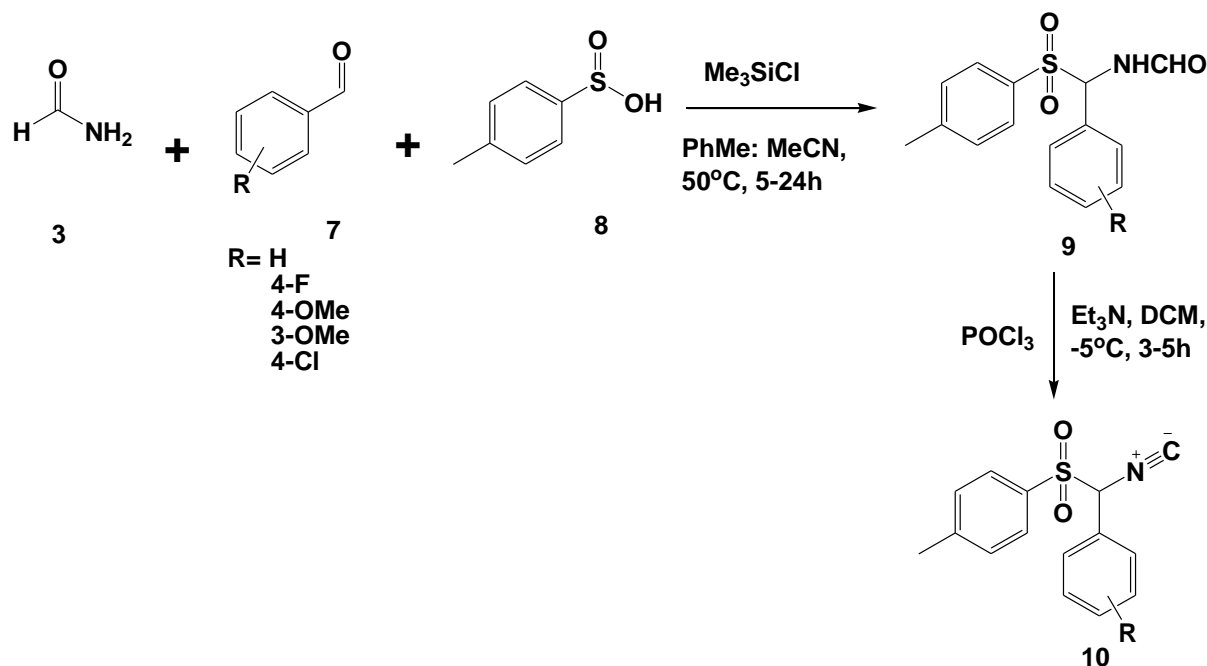
Analogues of TosMIC **1** have also been prepared by various groups.^{105,106,107,108} One of the approaches to access such scaffolds was also documented by van Leusen and co-workers.¹⁰⁵ In their approach, the α -acidic proton on the carbon adjacent to the isocyanide group is deprotonated under phase transfer catalyst (PTC) conditions, followed by alkylation to afford the desired TosMIC derivatives **6** (**Scheme 1.2**). Furthermore, monosubstituted-alkenyl and long chain alkyl groups have also been introduced at the α -acidic centre of TosMIC **1** under similar PTC conditions.¹⁰⁶⁻¹⁰⁷



Scheme 1.2: Synthesis of derivatised TosMIC *via* PTC.

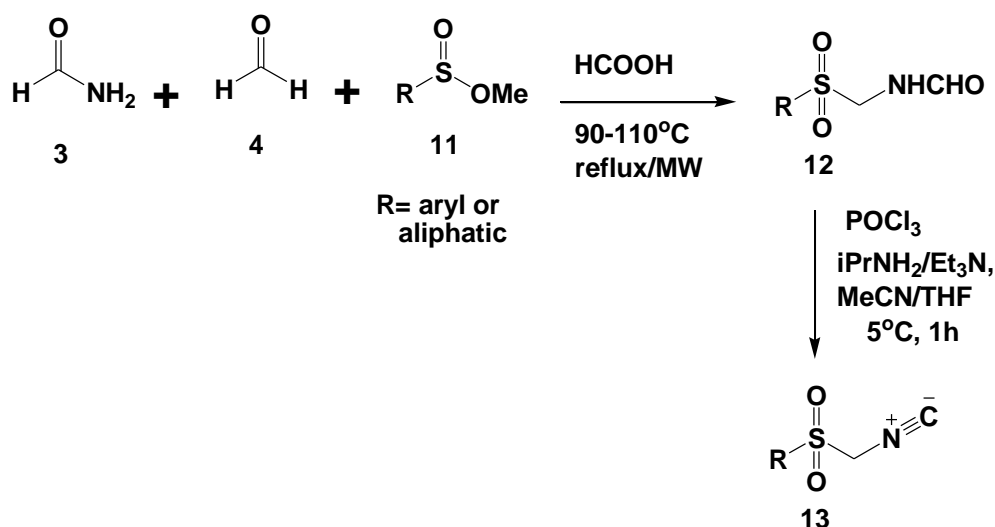
In another contribution, Sisko and co-workers¹⁰⁸ have described a method which introduces aryl groups at the α -methylene proton of TosMIC. In their protocol, formamide **3** was reacted with benzaldehydes **7** and *p*-toluenesulfonic acid **8** in the presence of chlorotrimethylsilane (TMSCl) using a 1:1 mixture of acetonitrile (MeCN) and toluene (PhMe) as solvents at 50°C to generate α -(*p*-toluenesulfonyl)-4-benzylformamide derivatives **9** in reasonable yields (**Scheme 1.3**). These

benzylformamide derivatives **9** were then subjected to a dehydration reaction with POCl₃ using Et₃N as a base in tetrahydrofuran (THF) to afford the aryl-substituted TosMIC analogues **10**. The derivatised TosMIC **10** has been found to be more reactive than TosMIC **1** itself, which is attributed to the further enhancement of the acidity of the α-proton by the substituents at the methylene group.



Scheme 1.3: Synthesis of derivatised TosMIC **10** as described by Sisko and co-workers.

Furthermore, a variety of synthetic analogues of TosMIC with substitution at the sulfonyl group by different aliphatic and aromatic rings have recently been exploited by Lujan-Montelongo and co-workers.¹⁰³ In this method, formamide **3** was treated under Mannich-type condensation with formaldehyde **4** and methyl aliphatic-substituted-benzoates/carboxylates **11** in the presence of HCOOH using both conventional and microwave heating at 90-110°C to afford the *N*-(aryl/aliphatic-sulfonylmethyl)formamide derivatives **12**, which further undergo dehydration with POCl₃ in the presence of isopropylamine (*i*PrNH₂) to furnish the desired aryl/aliphatic methyl isocyanide derivatives **13** in good yields (**Scheme 1.4**). The presence of the different substituents on the aromatic ring had little effect on the product yields.



Scheme 1.4: Synthesis of aryl/aliphatic methyl isocyanide derivatives.

TosMIC and its analogues are very reactive synthons and their reputation is credited to their ability to act as nucleophile and electrophile as well as radical depending on the reaction conditions.⁹⁷⁻¹⁰⁰ They have been found to be valuable reagents and their greatest principal function has been in the preparation of five-membered nitrogen containing heterocycles such as imidazoles,^{109,110,111,112,113} oxazoles^{114,115} and pyrroles.^{116,117,118} However, in recent years TosMIC has been used to generate six membered heterocyclic ring systems,^{119,120,121} and also react with Baylis-Hillman products to generate ethyl 2-[(tosylmethylcarbamoyl)methyl]-3-phenylacrylate and 3-phenyl-2-(tosylmethyl)acrylonitrile derivatives,^{106,122} as well as in multi-component reactions to produce diverse mandelamide products.¹²³

1.3.2. Synthesis of five membered ring systems

1.3.2.1. Imidazole

Imidazoles **14** are an important class of aromatic compound. This planar five membered-ring heterocycle contains two nitrogen atoms in its structure (*Figure 1.11*). Compounds incorporating the imidazole moiety have been shown to exhibit a variety of biological activities such as anti-fungal,^{124,125} anti-HIV,^{126,127} anti-microbial,^{128, 129} and anti-cancer activity.^{130,131}

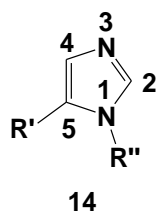
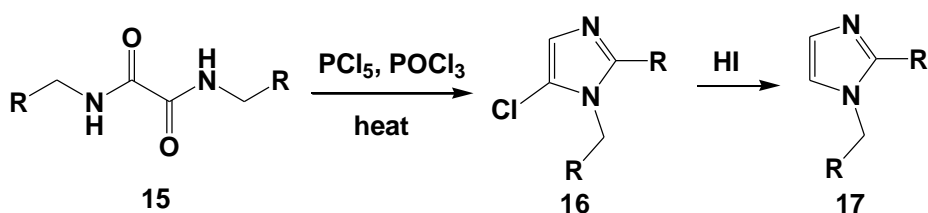


Figure 1.11: Structure of substituted-1-R''-imidazoles.

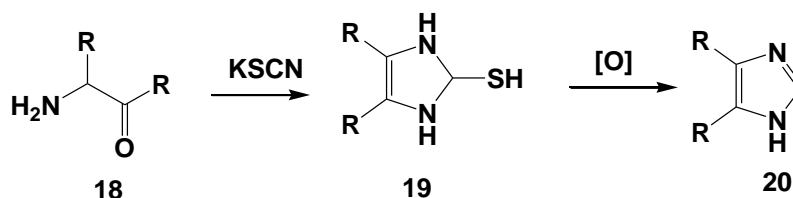
Because of their diverse pharmacological activities, the synthesis of compounds containing the imidazole core is of great importance in medicinal chemistry.²⁻⁹ A number of divergent approaches have been applied for imidazole synthesis such as Wallach Synthesis,¹³² Markwald synthesis,¹³³ Debus imidazole synthesis¹³⁴ and van Leusen imidazole synthesis.¹⁰⁹⁻¹¹³

In Wallach imidazole synthesis, the *N,N*-dimethyloxamide **15** is heated in the presence of phosphorus pentachloride (PCl₅) to give a chlorinated *N*-methyl-imidazole **16**, which then undergoes reduction using hydroiodic acid (HI) to afford *N*-methyl-imidazole **17** (**Scheme 1.5**).



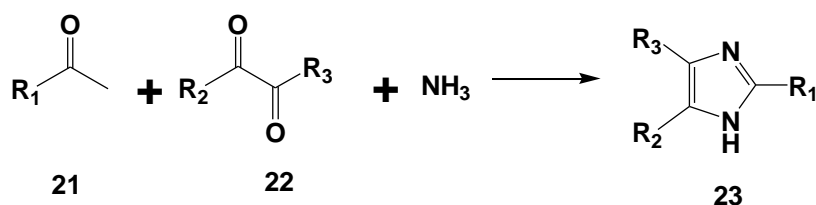
Scheme 1.5: Wallach imidazole synthesis

In Markwald synthesis,¹³⁵ an α -amino ketone or aldehyde **18** is treated with potassium thiocyanate to give 2-thiol-substituted-imidazoles **19**, followed by removal of sulfur under oxidative conditions to yield the desired imidazoles **20** as shown in **Scheme 1.6**.



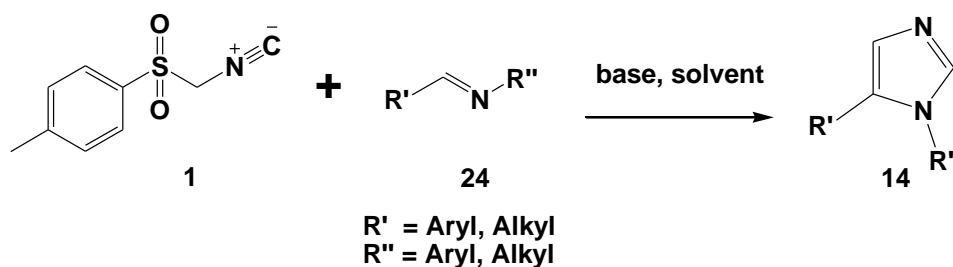
Scheme 1.6: Markwald imidazole synthesis.

In Debus imidazole reaction,¹³⁴ formaldehyde **21** is reacted with glyoxal; 1,2-diketones or ketoaldehydes **22** in ammonia to afford imidazole derivatives **23** as illustrated in **Scheme 1.7**. Even though this reaction is still employed towards generation of the C-substituted imidazoles, the relatively low yield of the products is a major drawback.



Scheme 1.7: Debus imidazole synthesis

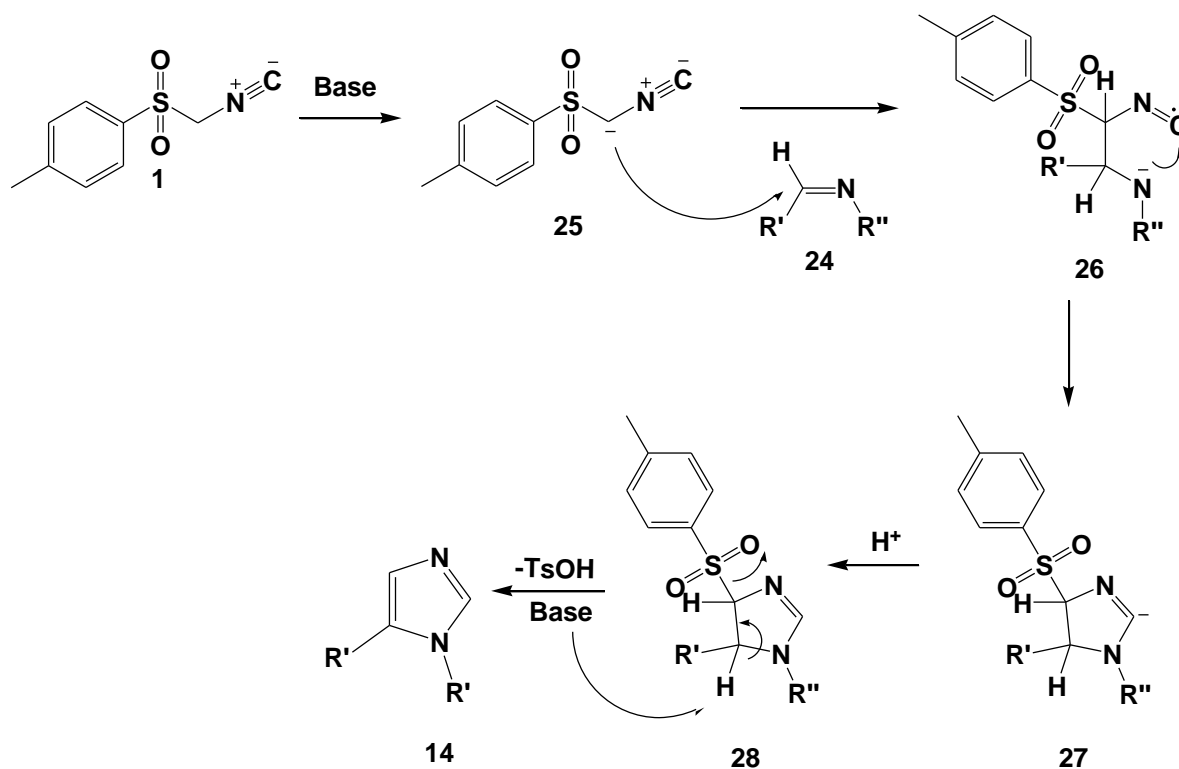
TosMIC **1** has been used as a synthon to generate mono-di and/or tri-substituted 1*H*-imidazoles. A typical method that employs TosMIC **1** as a starting building block is known as the van Leusen imidazole synthesis.¹¹⁰ In this protocol, TosMIC **1** reacts with aldimines or Schiff base **24** using catalytic base such as potassium carbonate (K₂CO₃), potassium *tert*-butoxide (*t*BuOK) or sodium hydride (NaH) in the presence of aprotic solvent to furnish 1,5-disubstituted-1*H*-imidazoles **14** (**Scheme 1.8**). This reaction was later expanded to the 3-component van Leusen reaction (3-CvL), in which an aldimine or Schiff base **24** is generated *in situ*, followed by addition of TosMIC to afford the desired 1,5-disubstituted-1*H*-imidazole derivatives **14**.⁹⁹ As a result of the reagents reacting in a stepwise manner; the 3-CvL reaction is not a true multicomponent reaction.



Scheme 1.8: van Leusen imidazole synthesis.

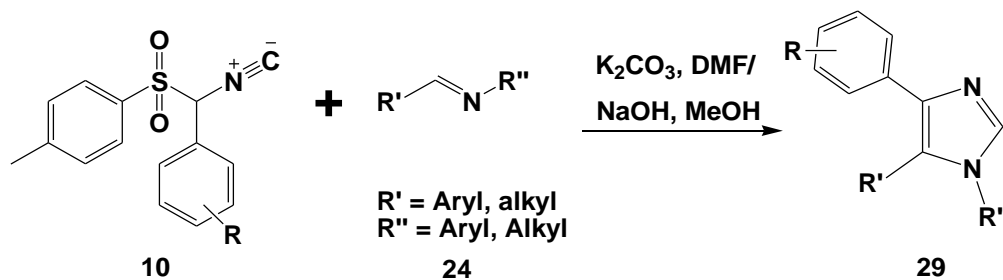
A possible mechanistic pathway for the above mentioned reaction is illustrated in **Scheme 1.9**. Initially, a base catalyzed deprotonation of one of the α -acidic protons of TosMIC **1** occurs to generate an α -carbanion **25**. The carbanion **25** is then involved in the nucleophilic attack on the

polarised carbon-nitrogen double bond ($-C=N$) of the aldimine or Schiff base moiety **24**, followed by cyclisation to afford a five membered ring (**26** and **27**), and protonation to form the imidazoline intermediate **28**. Elimination of *p*-toluenesulfonic acid provides the desired disubstituted-1*H*-imidazole products **14**.



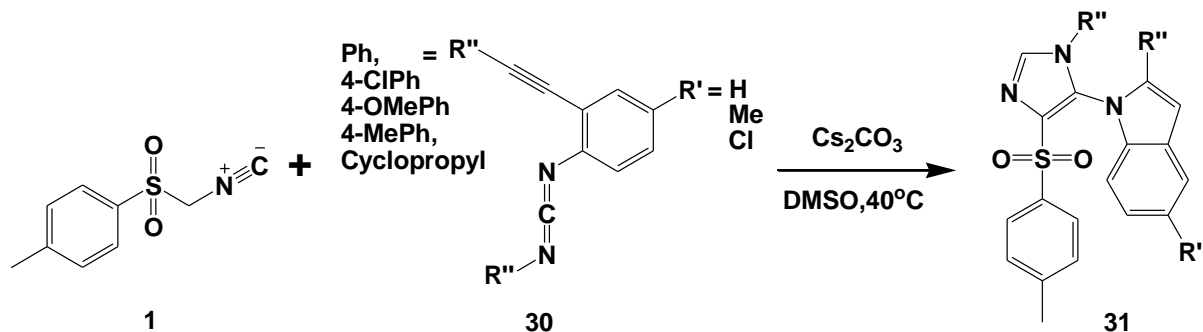
Scheme 1.9: Mechanism of the van Leusen imidazole synthesis.

In the past decade, aryl-substituted TosMIC analogues **10** have been described to react in a single pot with polyfunctional imines **24** (generated *in situ* from aldehyde and primary amine) in the presence of K_2CO_3 in dimethyl formamide (DMF) or aqueous methanol (MeOH) containing sodium hydroxide (NaOH) to furnish 1,4,5-trisubstituted-1*H*-imidazoles **29** (**Scheme 1.10**).¹¹¹



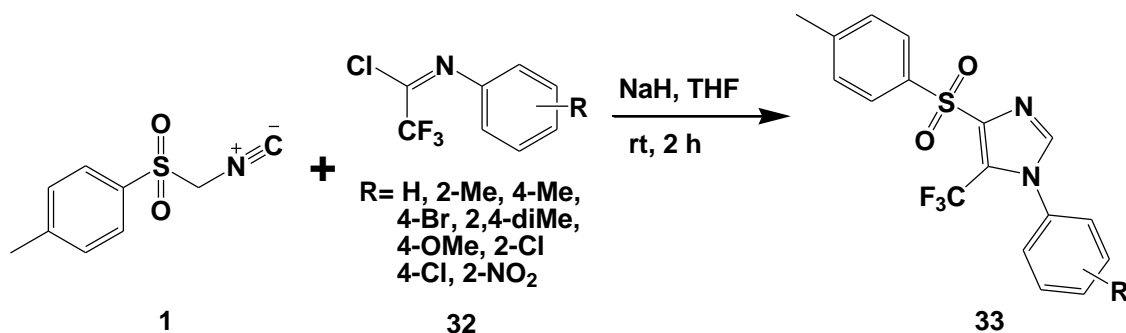
Scheme 1.10: Synthesis of 1,4,5-trisubstituted-1*H*-imidazoles **29**.

Moreover, TosMIC **1** has been found to undergo [3+2] cyclo-addition reaction with *N*-[2-(1-alkynyl)phenyl]carbodiimides **30** in the presence of cesium carbonate (Cs_2CO_3) in dimethyl sulfoxide (DMSO) to achieve the indolyl imidazole scaffolds **31** in good yields (**Scheme 1.11**).¹¹²



Scheme 1.11: Indolyl imidazoles synthesis **22**.

Furthermore, TosMIC **1** reacts with substituted-trifluoroacetimidoyl chlorides **32** in the presence of sodium hydride in THF at room temperature to access 5-(trifluoromethyl)-1-(substituted-phenyl)-4-tosyl-1*H*-imidazole derivatives **33** in good yields. The advantage of this protocol is the ability to accommodate both electron donating and withdrawing groups (**Scheme 1.12**).¹¹³



Scheme 1.12: Synthesis of imidazole derivatives.

1.3.3.2. Oxazoles

Oxazole **34** is a five membered heterocycle containing both an oxygen and a nitrogen atom at the 1- and 3-positions of the ring (*Figure 1.12*). This scaffold has been associated with a variety of pharmacological activities such as antifungal,^{136,137} antimicrobial,^{138,139,140} anti-HIV¹⁴¹, and anti-inflammatory activity.¹⁴² Numerous classic methodologies have been reported towards synthesis of oxazole and its derivatives; these include the Robinson-Gabriel synthesis,^{143,144,145} the Fischer oxazole synthesis,^{146,147} and the Van Leusen oxazole reaction.^{98,108,114-115}

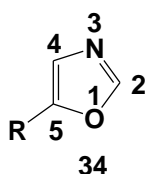
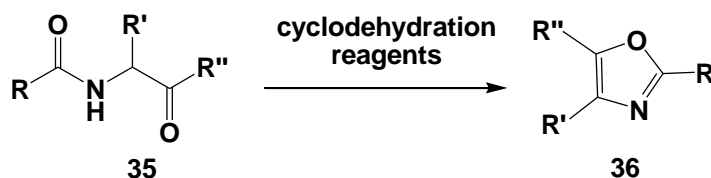


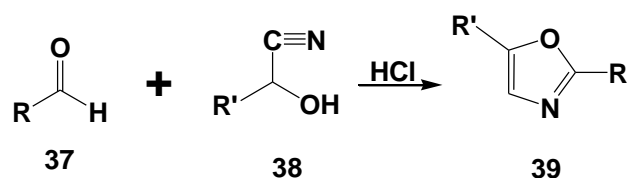
Figure 1.12: Structure of 5-substituted-1,3-oxazole.

In the Robinson-Gabriel synthesis, 2-acylaminoketones **35** undergo an intramolecular reaction promoted by cyclodehydration reagents (such as concentrated H₂SO₄, PCl₅, POCl₃, SOCl₂, and anhydrous HF), followed by the removal of water to yield 2,5-di- and 2,4,5-trialkyl, aryl- and heteroaryl-oxazoles **36** in various yields (*Scheme 1.13*).



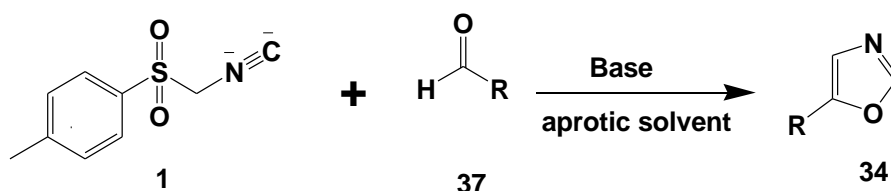
Scheme 1.13: Robinson-Gabriel oxazole synthesis.

In the Fischer oxazole synthesis, an aldehyde **37** reacts with cyanohydrins **38** in the presence of dry HCl using anhydrous ether as a solvent to give 2,5-disubstituted-1,3-oxazoles **39** as depicted in *Scheme 1.14*. The major drawback in this protocol is the formation of 2,5-diaryl-4-oxazolidones and oxazolid-4-ones as side products especially when an aliphatic aldehyde is used as a synthon. This problem may be overcome by using thionyl chloride in the reaction mixture.



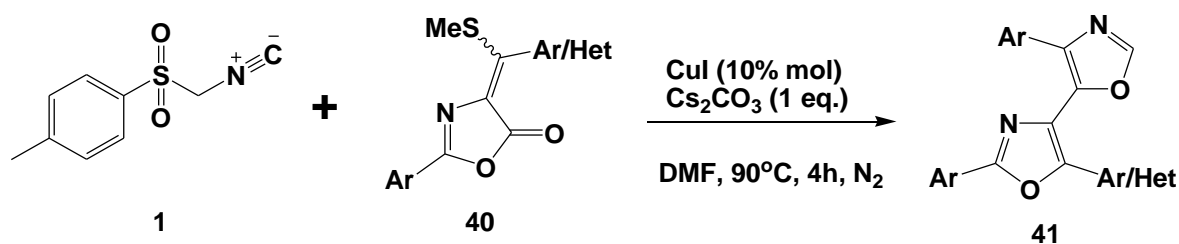
Scheme 1.14: Fischer oxazole synthesis.

In the so-called van Leusen oxazole reaction, TosMIC **1** undergoes a cyclo-addition reaction to an aldehyde **37** under basic conditions to furnish 5-monosubstituted-1,3-oxazoles **34** (*Scheme 1.15*).^{98,108, 114-115}



Scheme 1.15: Synthesis of 5-monosubstituted-1,3-oxazoles.

TosMIC **1** has been reported to react with aryl/heteroaryl substituted-oxazolone scaffolds **40** catalyzed by copper (I) iodide in the presence of Cs_2CO_3 in DMF under inert atmospheric conditions to give 2,5,4'-trisubstituted-4,5-bisoxazoles **41** (*Scheme 1.16*).¹¹⁴



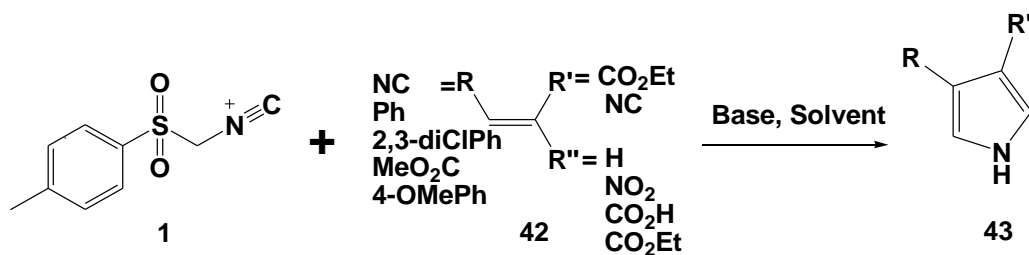
Scheme 1.16: Synthesis of bisoxazoles.

1.3.3.3. Pyrroles

Pyrrole is a five membered hetero-aromatic compound containing one nitrogen atom. It is an essential moiety in organic chemistry due its wide variety of biological properties.^{148,149,150,151,152}

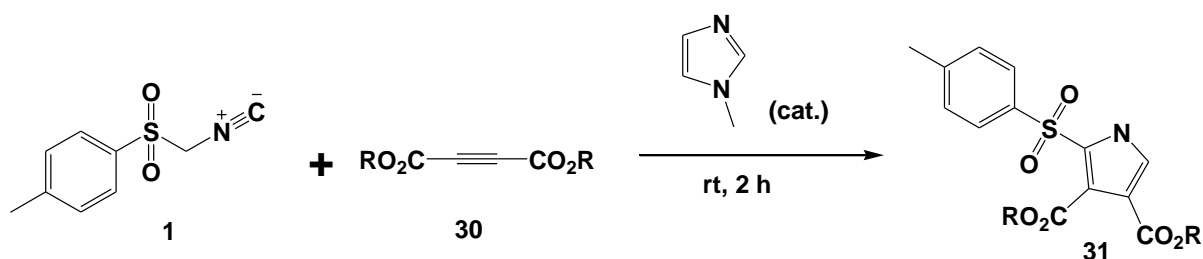
An efficient approach for the construction of substituted pyrroles was developed using TosMIC **1** as a building block. In the protocol, TosMIC undergoes a Michael addition reaction under

basic conditions to the acceptor substituted alkenes **42**, followed by ring closure between the isocyano group and enolate carbon and then aromatisation *via* elimination of the tosyl group to afford the pyrroles **43** in reasonable yields (**Scheme 1.17**).¹¹⁶⁻¹¹⁸ This transformation is carried out in the presence of a base such as DBU, NaOH, NaH or *t*BuOK using solvents such as ethanol (EtOH), THF, isopropyl alcohol (*i*PrOH) or DMF.



Scheme 1.17: Reaction of TosMIC with Michael acceptor alkenes.

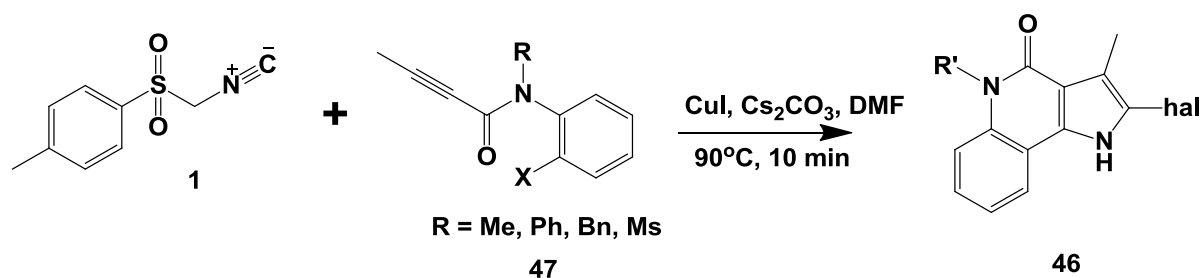
In addition, TosMIC **1** also has been described to react with Michael acceptor alkynes **44** in the presence of base to afford 2-tosylpyrrole derivatives **45** (**Scheme 1.18**).¹⁵³



Scheme 1.18: Reaction of TosMIC with Michael acceptor alkynes.

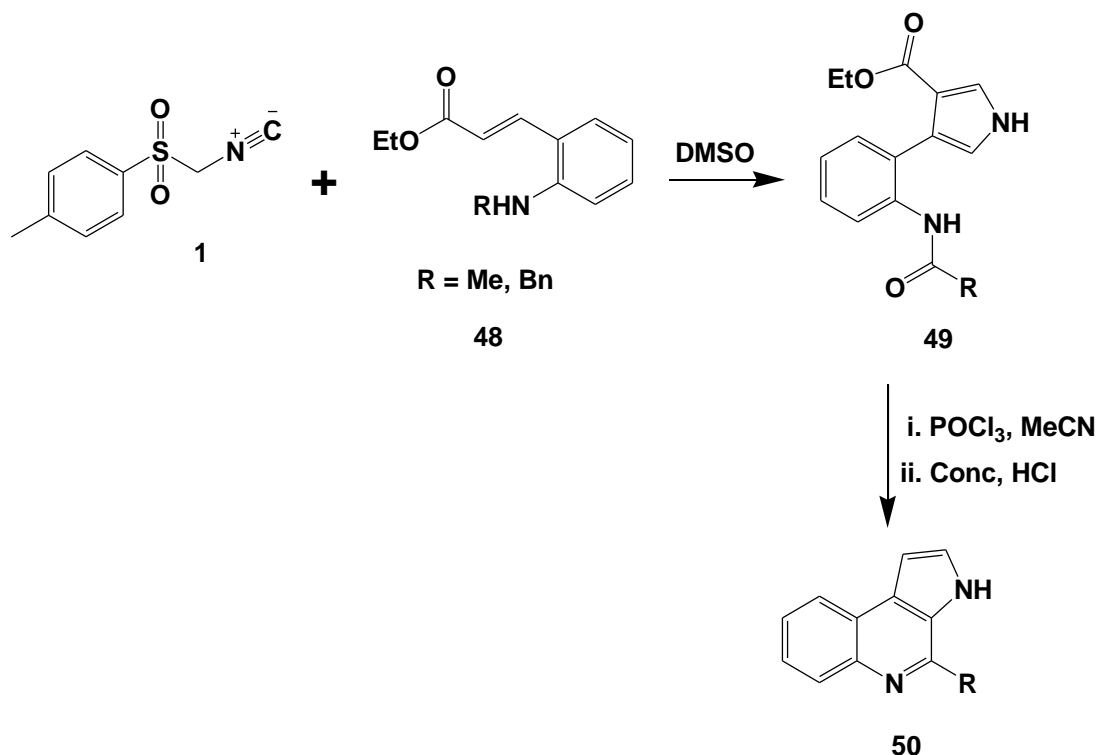
1.3.3. Synthesis of six membered rings

In recent years, TosMIC **1** has been used in the preparation of six-membered nitrogen-containing heterocycles. For instance, Zhou and co-workers¹¹⁹ have described the preparation of functionalised quinolinones **46** through tandem cyclo-addition of TosMIC **1** to *N*-(2-haloaryl)propionamide **47** under copper (I) iodide catalyzed reaction conditions using Cs₂CO₃ in DMF as illustrated in **Scheme 1.19**.



Scheme 1.19: Synthesis of quinolinone derivatives using TosMIC.

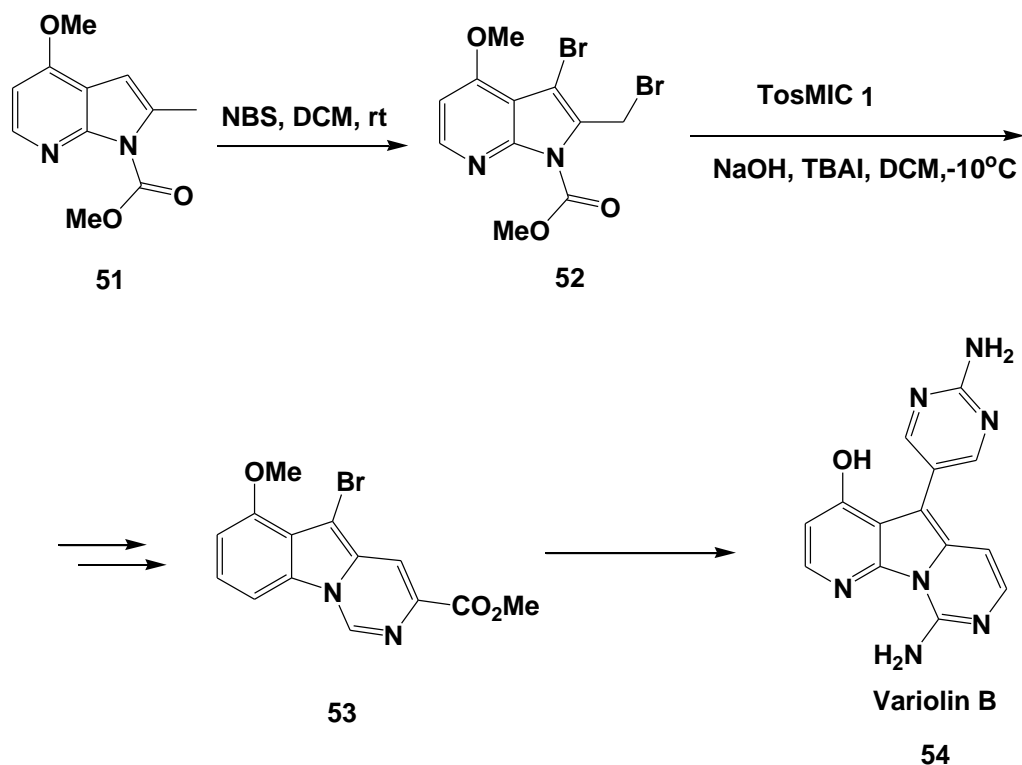
Ni and co-workers¹²⁰ have illustrated the construction of six membered anti-malarial marinoquinolines using TosMIC **1** as the starting synthon. In their protocol, the α -acidic carbon of TosMIC **1** reacts with the α,β -unsaturated ester acrylate derivatives **48** under basic conditions to form ethyl 4-(2-acetamidoaryl)-1*H*-pyrrole-3-carboxylate intermediates **49**, which are then subsequently cyclized upon treatment with POCl₃ in MeCN to afford the desired marinoquinoline **50** (*Scheme 1.20*).



Scheme 1.20: Synthesis of marinoquinoline **50** from TosMIC.

Coppola and co-workers have also detailed the involvement of the α -acidity of TosMIC towards construction of the anti-proliferative natural alkaloid variolin B. In their reaction, methyl 4-

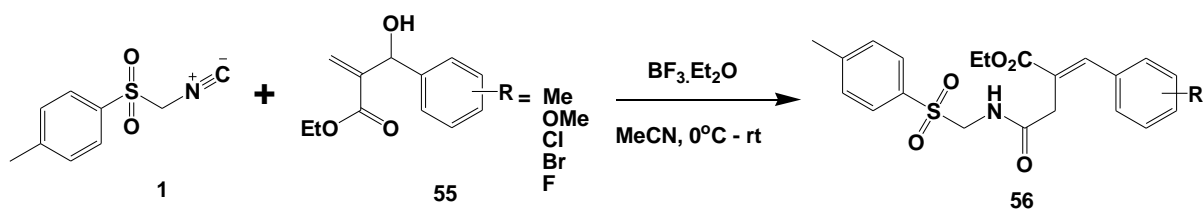
methoxy-2-methyl-1*H*-pyrrolo[2,3-*b*]pyridine-1-carboxylate **51** reacts with *N*-bromosuccinimide (NBS) in DCM to give 3-bromo-2-(bromomethyl)-4-methoxypyrrolo[2,3-*b*]pyridine **52**, which when treated with TosMIC under basic conditions generated 7-carboxylated-pyrido [2,3,4,5]pyrrolo[1,2-*c*]pyrimidine derivatives **53** (*Scheme 1.21*).¹²¹



Scheme 1.21: Involvement of TosMIC towards synthesis of Variolin B.

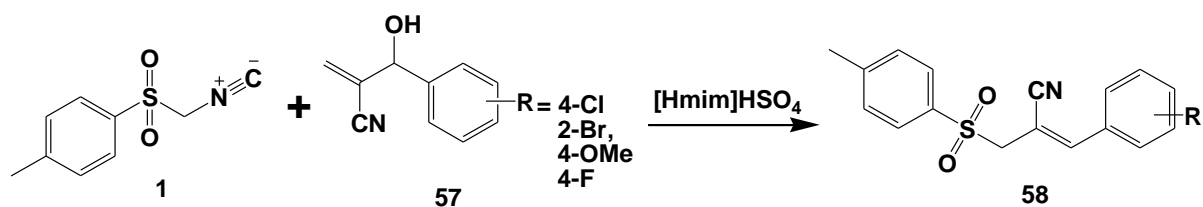
1.3.4. TosMIC and Baylis-Hillman adducts

Over the past decade, the reaction of TosMIC with Baylis-Hillman adducts has been explored. In 2010, Yadav and co-workers described the reaction of TosMIC **1** with Morita-Baylis-Hillman acetates **55** through S_N2 allylic nucleophilic substitution catalysed by $\text{BF}_3 \cdot \text{OEt}$ under mild conditions to provide ethyl 2-[(tosylmethylcarbamoyl)methyl]-3-phenylacrylate derivatives **56** in high yields (*Scheme 1.22*).¹⁰⁶ This protocol has been found to furnish the products as a mixture of isomers with high *E*-selectivity.



Scheme 1.22: Reaction of TosMIC with Morita-Baylis-Hillman acetates.

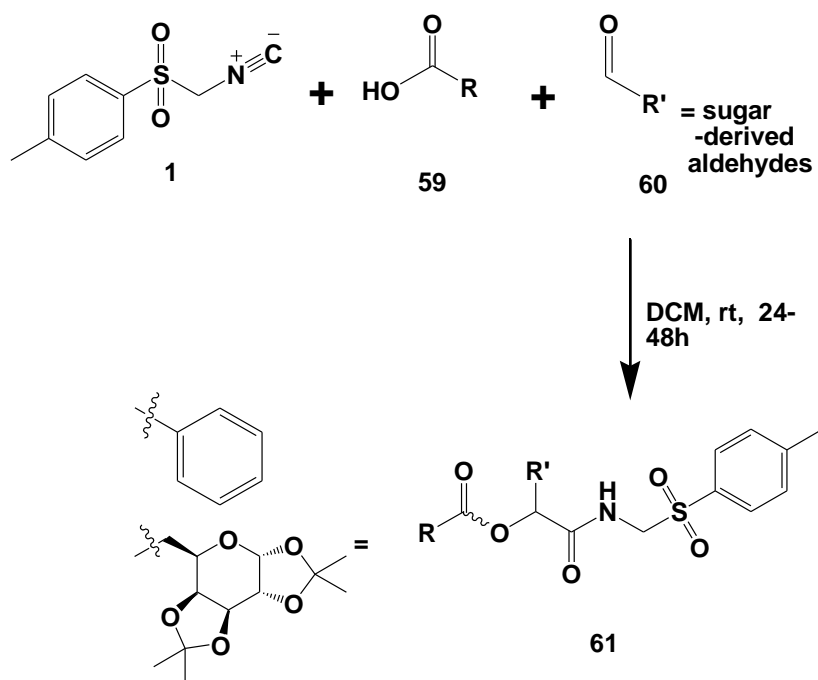
Garima *et al.* in 2011 reported an expansion of the methodology developed by Yadav described above. In their approach, TosMIC directly sulfonated Baylis-Hillman alcohols **57** using a Brønsted acidic ionic liquid, 1-butyl-3-methylimidazolium hydrogen sulfate {[Hmim]HSO₄} as a promoter of reaction to give the corresponding 3-phenyl-2-(tosylmethyl)acrylonitrile products **58** in good yields (**Scheme 1.23**).¹²²



Scheme 1.23: Reaction of TosMIC with Baylis-Hillman alcohol.

1.3.5. TosMIC in multicomponent reactions

TosMIC has also been exploited in multi-component reaction strategies. For example, Krishna and co-workers reported the contribution of TosMIC in 3-component diastereoselective Passerini reactions. In this protocol, TosMIC **1** is reacted with organic acids **59** (such as benzoic acid, 1,2,3,4-di-O-isopropylidene- α -D-galacturonic acids) and sugar-derived aldehydes **60** in the presence of DCM to afford diverse mandelamide products **61** in moderate to good yields (**Scheme 1.24**).¹²³



Scheme 1.24: TosMIC in 3-component diastereoselective Passerini reactions.

1.4. The Chemistry: Aryl isocyanides

Aryl isocyanide is one of the building blocks reported to be valuable in the construction of nitrogen-containing compounds in organic chemistry.^{154,155} Subsequently, aryl isocyanides have also attracted interest in coordination and organometallic chemistry, owing to the probability of partial delocalization of electron density into the aromatic rings.¹⁵⁶ Unlike TosMIC, aryl isocyanides lack the hydrocarbon substituent adjacent to the isocyanide group, which affects their stability under ambient conditions.^{157,158}

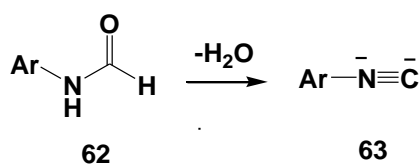
1.4.1. Preparation of aryl isocyanides

There are numerous synthetic methodologies that have been established for the preparation of aryl isocyanides. These include protocols such as dehydration of aryl formamide,¹⁵⁹ Hoffmann carbylamine reaction¹⁶⁰ and deprotonation of aryl imidates,¹⁶¹ just to mention a few.

1.4.1.1. Dehydration of aryl formamide

Dehydration of aryl formamide is a most useful method for preparing the aryl isocyanide. In this approach, aryl formamide **62** reacts with a dehydrating agent in the presence of a base in organic solvent to give aryl isocyanides **63** (**Scheme 1.25**).¹⁵⁹ The most commonly employed combination of dehydration agent and base for the formation of isocyanide is POCl₃ and triethylamine.

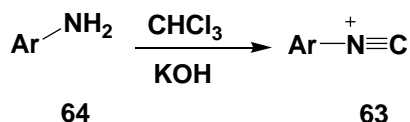
Another combination such as secondary amine with PCl_5 , P_2O_3 or PPh_3 and $\text{PPh}_3/\text{CCl}_4/\text{Et}_3\text{N}$ has also been reported.¹⁶²



Scheme 1.25: Dehydration of aryl formamide.

1.4.1.2. Hoffmann carbylamine reaction

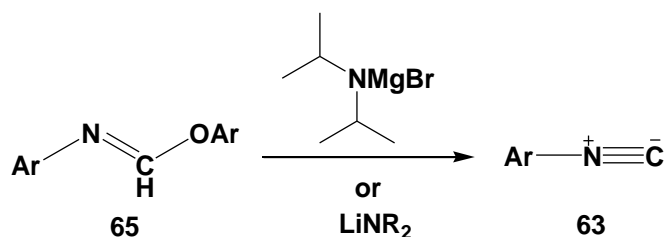
In the Hoffmann carbylamine reaction, the primary aryl amine **64** is treated with an aqueous solution of potassium hydroxide/chloroform (KOH/CHCl_3) to afford the corresponding aryl isocyanide **63** in moderate yields (*Scheme 1.26*).¹⁶³



Scheme 1.26: The Hoffmann carbylamine synthesis of aryl isocyanide.

1.4.1.3. Deprotonation of aryl imidates

The preparation of aryl isocyanides has also been reported by Pornet and Miginiac.¹⁶¹ In their protocol, aryl imidate ethers **65** are treated with magnesium diisopropylamide to give the corresponding aryl isocyanides **63** in reasonable yields (*Scheme 1.27*). In the extension of this method, disubstituted aryl imidate ethers are reacted with lithium dialkylamides to furnish the corresponding disubstituted aryl isocyanide in excellent yields.



Scheme 1.27: The Hoffmann carbylamines synthesis of aryl isocyanide.

The aryl isocyanides are very reactive and their utility as valuable reagents has been demonstrated in several synthetic transformations such as synthesis of isoxazoles and benzimidazoles.¹⁶⁴

1.4.2. Isoxazoles

Isoxazole is a five-membered heterocyclic compound containing an oxygen atom adjacent to the nitrogen atom. Compounds containing the isoxazole moiety have been found to possess a broad range of properties including anti-inflammatory,^{165,166,167} anticancer^{168,169} and antibacterial activities.^{170,171,172,173} A few approved drugs (like valdecoxib, dicloxacillin and flucloxacillin) and natural drugs (such as ibotenic acid) with the isoxazole motif are given in *Figure 1.13*.¹⁷⁴

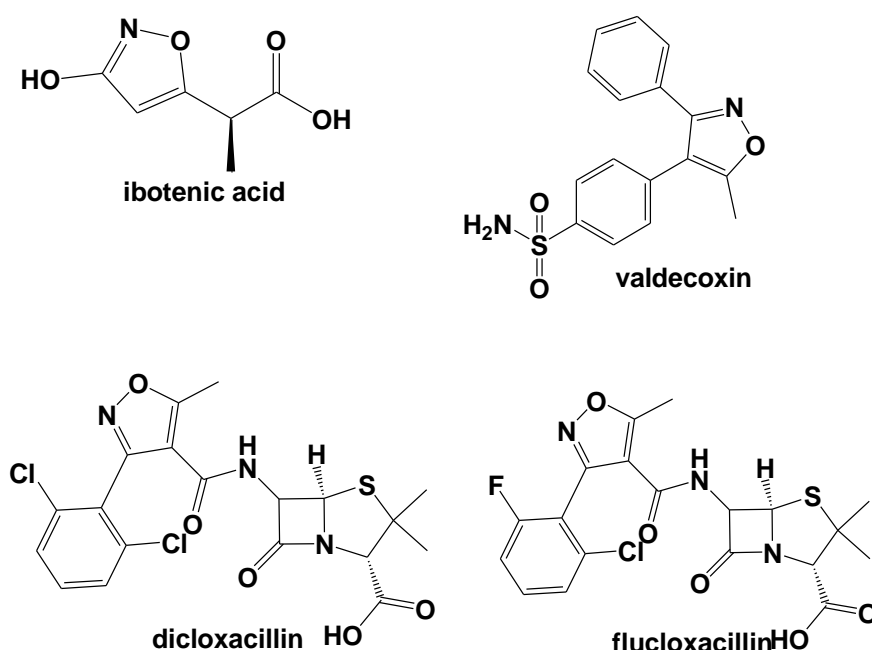
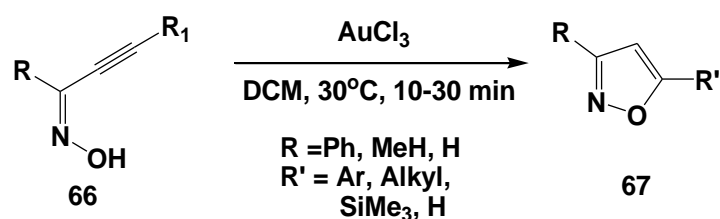


Figure 1.13: Structure of compounds containing isoxazole.

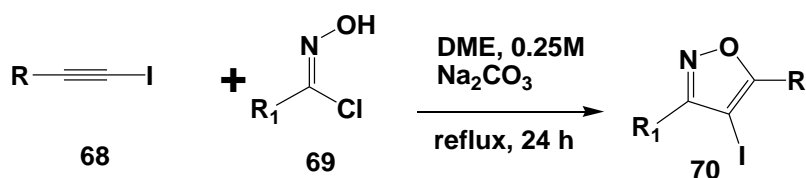
In view of the emerging importance of the isoxazole ring system, several synthetic protocols have been established to access this privileged scaffold. These methods include cyclo-isomerization of α,β -acetylenic oximes catalysed by AuCl_3 ,¹⁷⁵ an alkynyl iodide cycloaddition strategy¹⁷⁶ and reaction of the 2-haloacetophenone oxime with aryl isocyanide¹⁶⁴ to mention a few.

Praveen *et al.* synthesized 3-substituted, 5-substituted or 3,5-disubstituted-isoxazoles **67** in very good yields by the cyclo-isomerization of α,β -acetylenic oximes **66** in the presence of AuCl_3 catalyst in DCM under moderate reaction conditions (*Scheme 1.28*).¹⁷⁵



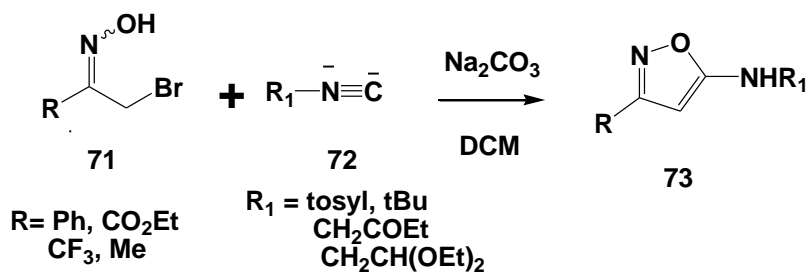
Scheme 1.28: Synthesis of isoxazole using AuCl_3 catalyst.

Crossley and Browne¹⁷⁶ described a regio-selective synthesis of iodoisoxazoles **70** in excellent yields through cycloaddition of alkyne iodide **68** to nitrile oxides **69** in the presence of 0.25 M aq. Na_2CO_3 using DME as solvent under heating for 24 hours as shown in **Scheme 1.29**.



Scheme 1.29: Synthesis of iodoisoxazoles using an alkyne iodide cycloaddition strategy.

Buron and co-workers¹⁶⁴ reported the synthesis of 5-amino-3-isoxazole derivatives **73** from reaction of isocyanide **72** with 2-bromo-ketone oximes **71** in the presence of sodium carbonate in DCM under mild conditions (**Scheme 1.30**). Reasonable yields were obtained when the electron deficient ketone oximes such as ethyl bromo-pyruvate oxime and trifluoromethyl-substituted oxime were used.



Scheme 1.30: Synthesis of 5-amino-3-substituted isoxazole from isocyanides.

2. Project strategy and Aims

The five-membered nitrogen-containing heterocycles have attracted a great deal of interest over the years as useful building blocks for drug discovery platforms. Their aromatic character contributes to their wide variety of biological properties and as a result they have functioned as a privileged core of several compounds inhibiting various stages of the HIV-1 replication cycle (*Figure 1.14*). For example; capravirine¹⁷⁷ (*Figure 1.14*) which contains the imidazole scaffold has been described as a non-nucleoside HIV-1 reverse transcriptase inhibitor with a unique resistance mode of action, while a series of 2-methyl-5-nitroimidazole-based analogues (DAMNI)^{178,179} with the imidazole motif are known to inhibit the HIV-1 reverse transcriptase (RT) enzyme at submicromolar concentrations.

Furthermore, another set of imidazole containing compounds known as 5-carbonyl-1*H*-imidazole-4-carboxamide derivatives¹⁸⁰ were established as a class of potential inhibitors that could disrupt the formation of the HIV-1 integrase-LEDGF/p75 interaction complex. Ritonavir,¹⁸¹ which contains a thiazole moiety, is an HIV-1 protease inhibitor that is now used clinically as a pharmacokinetic inhibitor to constrain cytochrome P540 metabolism of other HIV-1 protease inhibitors. Moreover, a class of isoxazole sulfonamide derivatives¹⁸² has been found to inhibit HIV-1 infection in human CD4⁺ lymphocytic T cells.

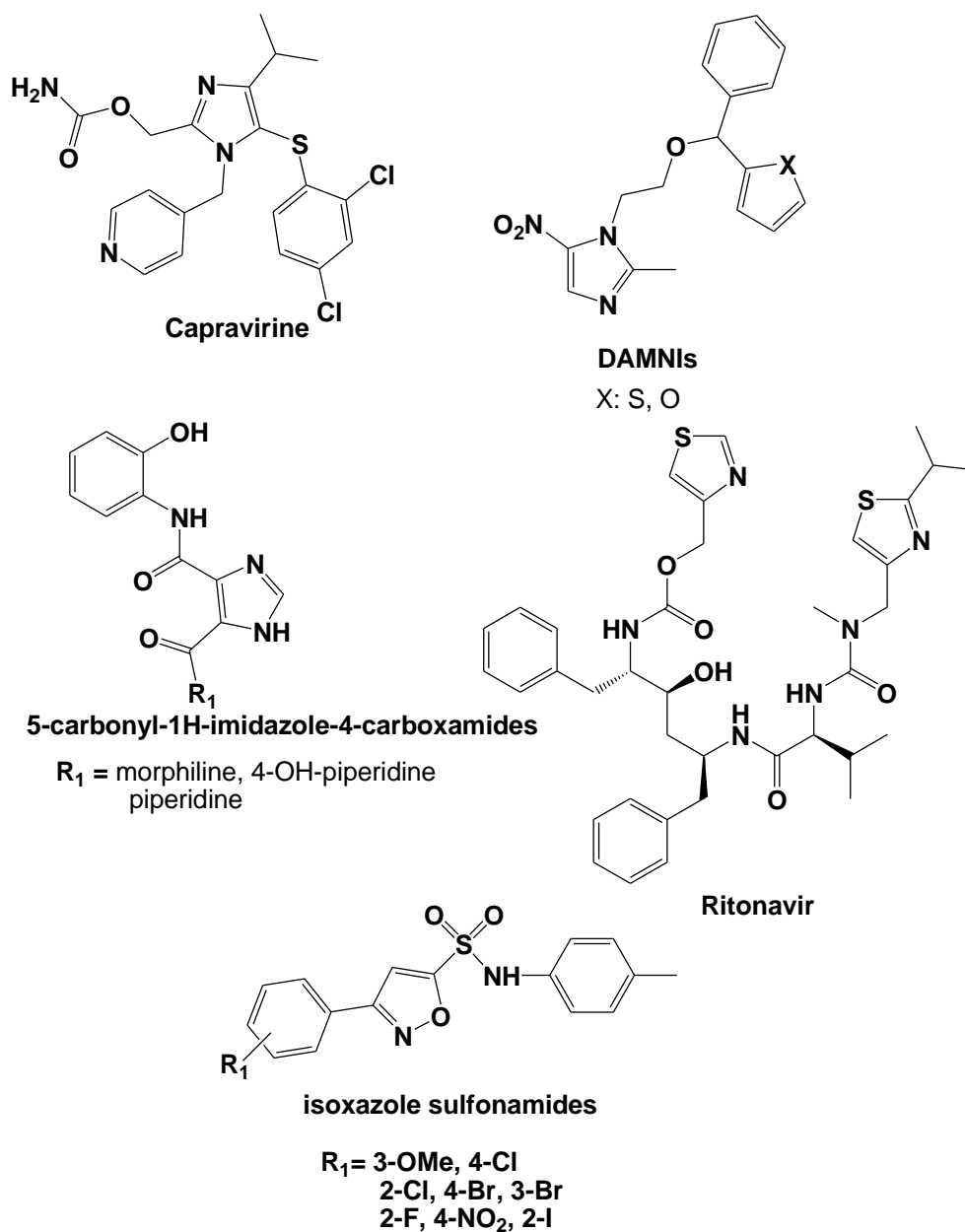


Figure 1.14: Structural formulae of some clinically used compounds containing five-membered nitrogen heterocycles.

The fragment screening approach has emerged as an important approach in drug discovery, where it is used as a starting point to identify valuable hits against a new target. The screening of small fragment collections with low molecular weight presented medicinal chemists with an effective starting point for synthetic optimization of hit candidates. Our laboratory has focused its research activities on the synthesis and screening of five membered nitrogen-containing heterocyclic fragments, in order to identify hits that exhibit the ability to interrupt the HIV-1-host protein-protein interactions. Virtual screening is a useful tool to identify promising scaffolds as the starting point for designing and synthesizing potentially active compounds for a

specific target. The huge number of possible compounds is reduced using a computerized system to a more convenient number of compounds for synthesis and screening in a biochemical assay against the relevant biological targets, which could lead to possible drug contenders.^{183,184} Thus, we undertook preliminary virtual screening of the pepMMsMIMIC database using a BST-2 template (PDB code: 2LK9) for querying purposes and identified candidate molecules containing heterocyclic systems such as benzimidazole and benzoxazole scaffolds (*Figure 1.15*, see **Appendix A**).¹⁸⁵ This prompted us to commence our research efforts by exploring the synthesis of 5-aryl-imidazoles and 5-aryl-oxazoles as simplified versions of these benzimidazole and benzoxazole scaffolds (*Figure 1.15*). The introduction of structural diversity at several positions on these heterocyclic systems could allow for the possible development of a new series of compound displaying interesting biological activity.

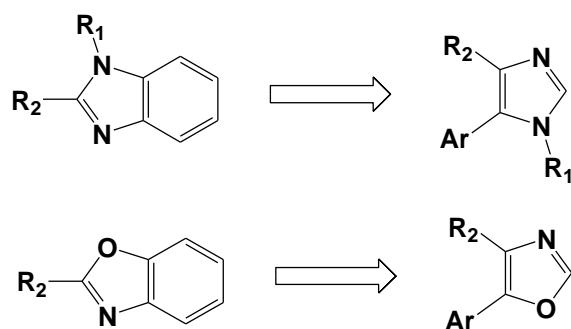


Figure 1.15: Nitrogen heterocyclic scaffolds of interest.

The established versatility and great potential of isocyanide chemistry led us to consider employing in the synthesis of five membered nitrogen-containing heterocyclic fragments. We hypothesized that isocyanide synthons such as TosMIC and aryl isocyanides could be used to synthesise small libraries of five membered nitrogen-containing heterocyclic compounds. These compounds could then be assessed as possible inhibitors of HIV-1 protein -protein interactions. Biological assays of these libraries could identify templates to design and synthesise the second generation of compounds. The current research project was achieved through the accomplishment of the following specific objectives:

1. Application of TosMIC towards the generation of a small library of 1-substituted-5-aryl-1*H*-imidazole compounds and biological evaluation as possible HIV-1 inhibitors.
2. Synthesis of aryl-1,3-oxazole derivatives by means of microwave assisted van Leusen reaction and their biological evaluation as possible HIV-1 inhibitors.

3. Incorporation of simple amino acids into the imidazole scaffold using the van Leusen reaction to generate a library of imidazo-1-yl-based derivatives and their elaboration as possible HIV-1 agents.
4. Synthesis of 3-aryl-*N*-arylisoxazol-5-amine scaffolds using aryl isocyanides and their usefulness as building blocks for possible inhibitors of HIV-1 protein- host protein interactions.
5. Evaluation of the antimicrobial effects of the synthesized five membered nitrogen heterocycle containing libraries of compounds.

CHAPTER 2

Application of TosMIC towards the synthesis of a small library of imidazole-based compounds and biological evaluation as possible inhibitors of HIV-1 protein-protein interactions

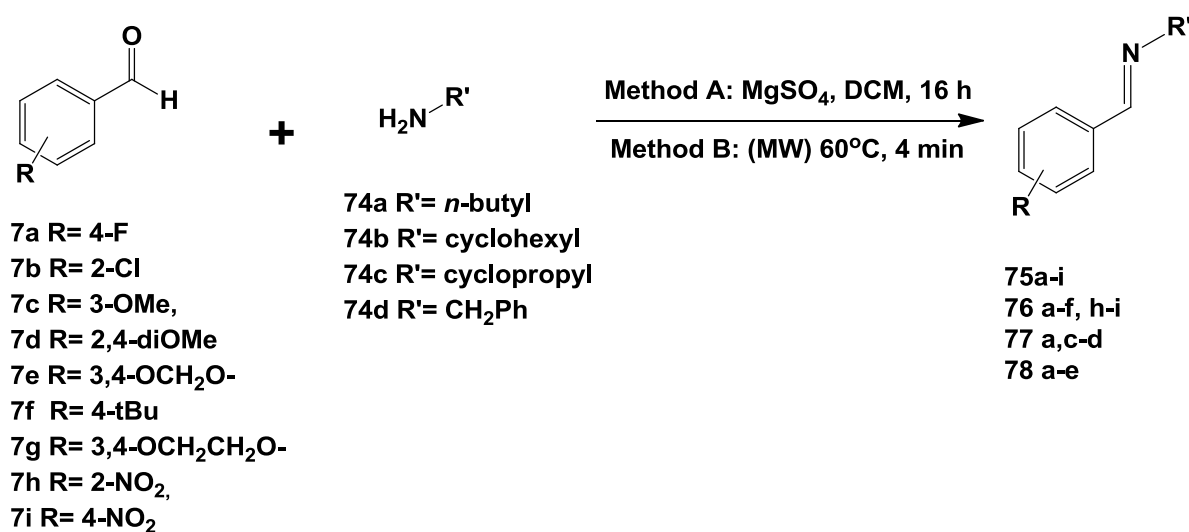
2.1. Introduction

In line with our project objectives defined in Chapter 1, the synthesis of a small library of substituted-imidazoles using isocyanide chemistry was undertaken with the intention of producing viable hits that could be used as templates to design drug-like molecules to target protein-protein interactions. Thus the current chapter is concerned with the preparation of a small library of 1-substituted-5-aryl-1*H*-imidazole scaffolds using TosMIC, and their assessment as potential disruptors of the interactions between the HIV-1 IN and host LEDGF/p75 proteins. Synthetic hurdles, isolation, characterization, yields and plausible mechanisms are described.

2.2. Synthesis of 1-substituted-5-aryl-1*H*-imidazole derivatives using a van Leusen reaction

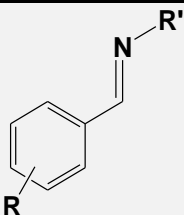
The van Leusen imidazole reaction is well-documented.^{99,186} It involves the cycloaddition of the α -acidic centre of TosMIC **1** to the imine double bond motif **24** to afford 1,5-disubstituted-1*H*-imidazoles **14**, promoted by a catalytic base (*see Scheme 1.8*, Chapter 1). In this study, the initial challenge was to synthesize imine building blocks as van Leusen intermediates. Imines contain the moiety R-C=N-R', with the nitrogen atom linked to either an aryl (Schiff bases) or alkyl moiety.¹⁸⁷ These carbon-nitrogen double bond containing scaffolds are routinely prepared by condensation of a primary amine with an aldehyde or ketone in a given solvent and/or with a drying agent (to drive the reaction), generating aldimines or ketimines respectively.^{188,189,190} The synthesis began by making use of readily available benzaldehydes **7a-g** and primary amines **74a-c** to produce *N*-(arylidene)alkylamine building blocks (azomethines) as van Leusen intermediates.

2.2.1. Synthesis of the key *N*-(arylidene)alkylamine intermediates



Scheme 2.1: Synthesis of *N*-(arylidene)alkylamines.

A series of benzaldehydes **7a-g** was reacted with primary amines **74a-c** (*n*-butyl-, cyclohexyl- and cyclopropyl- amines) in the presence of MgSO₄ in dichloromethane at room temperature for 16 hours affording *N*-(arylidene)alkylamine products **75-78** as outlined in **Scheme 2.1** (Method A).^{190,191} The product yields were obtained in a 72- 96% range (*Table 2.1*), and were comparable to values reported in literature.^{192,193,194,195} The products did not require further chromatographic purification. The use of microwave irradiation in organic synthesis has proven to significantly decrease reaction times and increase yields.^{196,197,198} Therefore, selected benzaldehydes **7a-i** and primary amines **74a-b** and **d** were microwave irradiated neat, at a set temperature of 60°C (**Scheme 2.1**, method B). Remarkably, the desired *N*-(arylidene)alkylamine products **75a-f**, **75h-i**, **76a-f**, **76h-i**, and **78a-e** were obtained in just 4 minutes in yields ranging from 73-100% (*Table 2.1*). Therefore, method B constitutes an improvement over published procedures,^{192,193} the use of microwave irradiation not only increases the reaction rate but also improves the already good yields obtained (*Table 2.1*).

Table 2.1: Comparative yields of the synthesized *N*-(arylidene)alkylamines.


Compound Entry	R	R'	Conventional Yield (%)	Microwave Yield
75a	4-F	<i>n</i> -butyl	87	98
75b	2-Cl	<i>n</i> -butyl	94	99
75c	3-OMe	<i>n</i> -butyl	-	97
75d	2,4-diOMe	<i>n</i> -butyl	84	98
75e	3,4-OCH ₂ O-	<i>n</i> -butyl	96	100
75f	4- <i>tert</i> -butyl	<i>n</i> -butyl	84	93
75g	3,4-OCH ₂ CH ₂ O	<i>n</i> -butyl	84	-
75h	2-NO ₂	<i>n</i> -butyl	-	73
75i	4-NO ₂	<i>n</i> -butyl	-	91
76a	4-F	cyclohexyl	85	88
76b	2-Cl	cyclohexyl	86	89
76c	3-OMe	cyclohexyl	71	88
76d	2,4-diOMe	cyclohexyl	81	99
76e	3,4-OCH ₂ O	cyclohexyl	90	97
76f	4- <i>tert</i> -butyl	cyclohexyl	93	99
76h	2-NO ₂	cyclohexyl	-	95
76i	4-NO ₂	cyclohexyl	-	91
77a	4-F	cyclopropyl	77	-
77c	3-OMe	cyclopropyl	92	-
77d	2,4-diOMe	cyclopropyl	87	
78a	4-F	benzyl	-	92
78b	2-Cl	benzyl		93
78c	3-OMe	benzyl	-	98
78d	2,4-diOMe	benzyl	-	90
78e	3,4-OCH ₂ O	benzyl	-	95

- = reaction not performed

The identity of *N*-(arylidene)alkylamine products **75-78** was confirmed by NMR spectroscopic analysis and the data was consistent with that of the expected chemical structures as described in the literature.^{195,199,200,201,202,203} The key changes are mainly observed in the chemical shifts of the substituents attached to the nitrogen atom and the aryl ring. A unique feature in the ¹H NMR spectra of these products **75-78** was the presence of a methine proton double bonded to a nitrogen atom which resonates as a singlet in the region of δ 8.0 ppm to 8.9 ppm while their ¹³C NMR spectra showed the methine carbon atom double bonded to a nitrogen atom in the region of δ 154-161 ppm.

The ¹³C NMR spectra of the fluorinated *N*-(arylidene)alkylamines **75a**, **76a**, **77a** and **78a** show the corresponding aryl signal splitting due to fluorine coupling, i.e. for compound **75a**, the *para*-C of the phenyl ring resonates at *ca.* δ 164.1 ppm with a ¹*J*_{FC} coupling constant of 250 Hz, whilst the carbon atom at position-1 on the aryl ring appears at δ 132.6 ppm with a ⁴*J*_{FC} value of 3 Hz. The *ortho*-carbon resonates at δ 129.8 ppm with a ³*J*_{FC} of 9 Hz, whereas the *meta*-carbon atom at δ 115.5 ppm splits with a ²*J*_{FC} coupling constant of 22 Hz.

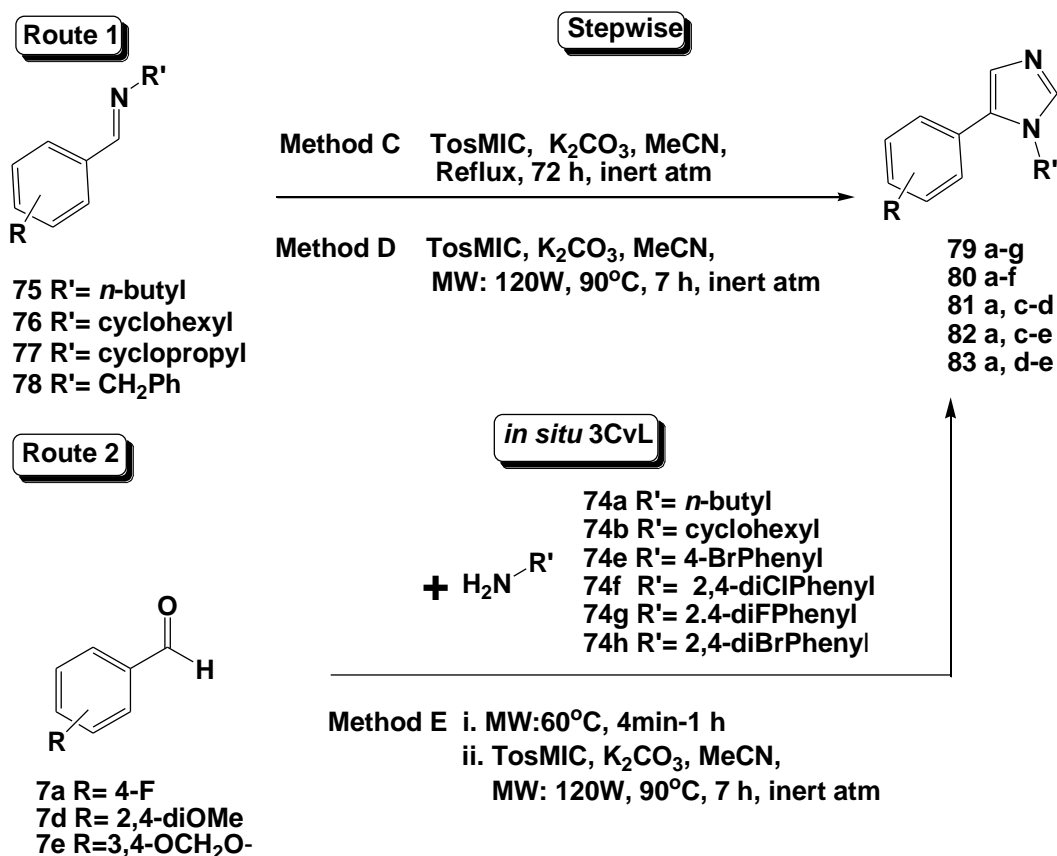
2.2.2. The van Leusen approach towards the synthesis of 1-substituted-5-aryl-1*H*-imidazoles

The cycloaddition of TosMIC **1** to synthesized *N*-(arylidene)alkylamines was then carried out using both conventional, stepwise microwave-assisted van Leusen reaction, as well as the so-called 3-component van Leusen reaction (3-CvL) under microwave irradiation. The reactions were monitored by thin layer chromatography (TLC).

2.2.2.1. Stepwise cycloaddition of TosMIC to *N*-(arylidene)alkylamines

2.2.2.1.1. Synthesis of 1-substituted-5-aryl-1*H*-imidazoles using conventional van Leusen reaction

Initially efforts were directed towards the use of the van Leusen imidazole synthesis using conventional methods. A series of selected *N*-(arylidene)alkylamines **75a-g**, **76a-f**, **77a**, **77c-d** and **78a**, **78c-e**, with TosMIC **1** in the presence of K₂CO₃ were refluxed in dry acetonitrile under inert conditions for 72 hours as shown in **Scheme 2.2** (Route 1, method C). Work up and purification of the crude brown materials by column chromatography afforded the corresponding pure 1-substituted-5-aryl-1*H*-imidazoles **79a-g**; **80a-f**, **81a**; **81c-d**; **82a** and **82c-e** in yields ranging from 20-80% (*see Table 2.2*).

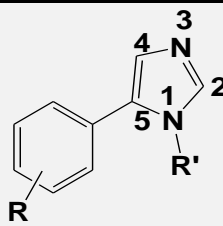


Scheme 2.2: Synthesis of 1-substituted-5-aryl-1*H*-imidazoles by the van Leusen approach.

Although the desired imidazole products were successfully obtained, the major drawbacks for the method are the long reaction times and low yields obtained for some of the imidazole derivatives.

2.2.2.1.2. Microwave-assisted synthesis of 1-substituted-5-aryl-1*H*-imidazoles using van Leusen reaction

Aiming to improve the reaction times for their synthesis, the synthesis of these scaffolds under microwave irradiation was investigated. TosMIC **1**, *N*-(arylidene)alkylamines (**75a-f**, **76a-f**, **77a, c-d** and **78a, c-e**) and K₂CO₃ in dry acetonitrile under inert conditions were microwave irradiated at 90°C and 120 Watts for 7 hours (**Scheme 2.2**, Route 1, method D). Work up and separation by column chromatography successfully afforded the corresponding imidazole products **79a-f**, **80a-f**, **81a, c-d** and **82a, c-e** in yields ranging from 23% to 87% (see **Table 2.2**). Although yields did not dramatically improve, reaction times were shortened 10-fold.

Table 2.2: Isolated yields (%) of the 1-substituted-5-aryl-1*H*-imidazole derivatives.

Substrate	R	R'	Method C yields (%)	Method D Yields (%)
79a	4-F	<i>n</i> -Butyl	38	55
79b	2-Cl	<i>n</i> -Butyl	20	26
79c	3-OMe	<i>n</i> -Butyl	-	60
79d	2,4-diOMe	<i>n</i> -Butyl	80	87
79e	3,4-OCH ₂ O-	<i>n</i> -Butyl	43	48
79f	4- <i>t</i> -Butyl	<i>n</i> -Butyl	44	52
79g	3,4-OCH ₂ CH ₂ O-	<i>n</i> -Butyl	54	-
80a	4-F	Cyclohexyl	46	51
80b	2-Cl	Cyclohexyl	23	29
80c	3-OMe	Cyclohexyl	47	53
80d	2,4-diOMe	Cyclohexyl	64	74
80e	3,4-OCH ₂ O-	Cyclohexyl	35	54
80f	4- <i>t</i> -Butyl	Cyclohexyl	29	50
81a	4-F	Cyclopropyl	-	23
81c	3-OMe	Cyclopropyl	-	40
81d	2,4-diOMe	Cyclopropyl	-	68
82a	4-F	CH ₂ Ph	-	26
82c	3-OMe	CH ₂ Ph	-	24
82d	2,4-diOMe	CH ₂ Ph	-	74
82e	3,4-OCH ₂ O-	CH ₂ Ph	-	22

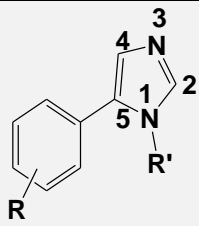
2.2.2.2. Synthesis of 1-substituted-5-aryl-1*H*-imidazoles using three component van Leusen approach (3-cvL)

2.2.2.2.1. 3-CvL Synthesis in MeCN

The synthesis of 1-substituted-5-aryl-1*H*-imidazole derivatives was also carried out using the so-called three component van Leusen approach (3-CvL). A series of selected benzaldehydes **7d-e** and aliphatic amines **74a** and **74b** were reacted neat using microwave irradiation (for 4 minutes at 60°C), followed by the addition of TosMIC **1**, K₂CO₃ and MeCN to further irradiate at a set power of 120 Watts and a temperature of 90°C for 7 hours under inert conditions (**Scheme 2.2**, Route 2, method E). Work up and chromatographic purification on silica gel gave rise to the desired 1-substituted-5-aryl-1*H*-imidazoles **79d-e**, and **80d-e** in yields similar to those obtained in the stepwise manner, therefore rendering the isolation of *N*-(arylidene)alkylamine intermediates unnecessary (**Table 2.3**).

Imidazoles derived from aryl amines were also readily prepared in a two-step one pot reaction by neat irradiation of substituted benzaldehydes **7a**, **d-e** and 4-bromoaniline **74e**, followed by addition of TosMIC **1**, K₂CO₃ and acetonitrile (**Scheme 2.2**, Route 2, method E). The crude reaction mixtures were then subjected to the microwave conditions described above to give the corresponding 1*H*-imidazole derivatives **83a**, **d-e** in yields ranging from 38-68% (*see Table 2.3*). In comparison with the *N*-aliphatic 4-fluorophenyl derivatives **79a**, **80a**, **81a** and **82a**, the *N*-aromatic imidazole **83a** was obtained in higher yield (68%), whilst the 1-(4-bromophenyl)-5-(2,4-dimethoxyphenyl)-1*H*-imidazole **83d** gave the lowest yield (38%). Any attempts to synthesize 1*H*-imidazoles derived from anilines with dihalide substituents at the *ortho*- and *para*-positions (**74f**, **74g** and **74h**) of the aryl ring were unsuccessful. Only reaction of the monosubstituted-aniline **74e** proceeded smoothly under the conditions described. This can be attributed to the fact that the two electron-withdrawing halides cause a decrease in the nucleophilicity of the aniline NH₂.

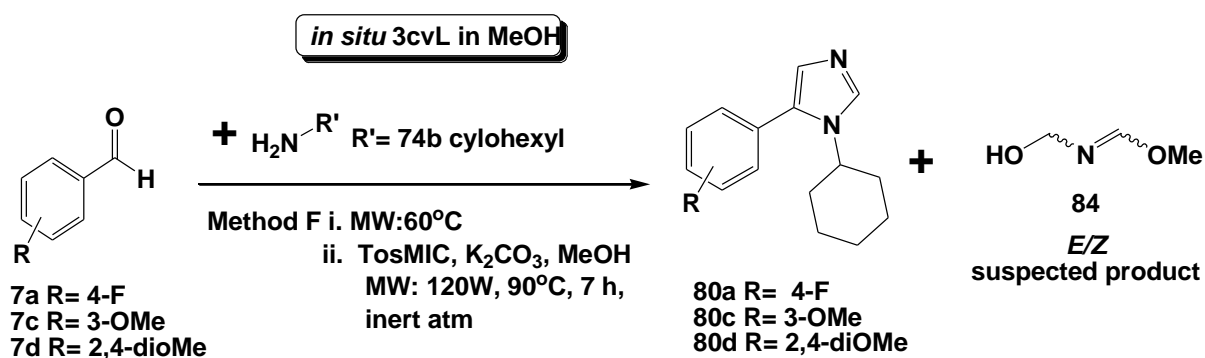
Table 2.3: Isolated yields (%) of the 1-substituted-5-aryl-1*H*-imidazole products obtained from 3-CvL in MeCN.



Substrate	R	R'	Method E
			Yields (%)
79d	2,4-diOMe	<i>n</i> -Butyl	81
79e	3,4-OCH ₂ O-	<i>n</i> -Butyl	55
80d	2,4-diOMe	Cyclohexyl	73
80e	3,4-OCH ₂ O-	Cyclohexyl	50
83a	4-F	4-BrPhenyl	68
83d	2,4-diOMe	4-BrPhenyl	38
83e	3,4-OCH ₂ O-	4-BrPhenyl	62

2.2.2.2.2. 3-CvL Synthesis in MeOH

Most of the conventional van Leusen imidazole reactions are reported to employ a protic solvent such as methanol.⁹⁹ We conducted the one pot 3-CvL reaction in methanol under microwave irradiation in order to assess the effect of solvent on the reaction yields, as per the conditions illustrated in *Scheme 2.3*.



Scheme 2.3: The 3-cvL imidazole synthesis in MeOH under MW irradiation.

According to NMR spectroscopic analysis, two additional unknown compounds were observed in the reactions giving 1-substituted-5-aryl-1*H*-imidazoles **80a**, **80d** and **80e**. These compounds

were UV inactive (at 254 nm) but co-eluted with the products during purification. The ^1H NMR spectrum in *Figure 2.1* of the mixture of compound **80d** with the unknown compounds revealed the presence of two singlets at 3.30 and 3.34 ppm which could be later assigned to two methoxy groups, while two doublets at 4.58 ppm (with $J = 6.8$ Hz) and 4.70 ppm (with 7.2 Hz) were assigned to methylene protons, and signals {a doublet ($J = 11.6$ Hz) and a singlet} at 8.17 and 8.30 ppm were assigned to N=CH groups, suggesting the presence of possible geometric isomers (*E*- and *Z*-) of $\text{OH-CH}_2\text{-N=CH(OMe)}$ **84**. The isomer ratio obtained varies with the substitution on the reacting aldehyde aryl group. For example for 1*H*-imidazoles **80a**, **80c** and **80d** ^1H NMR spectra show ratios of isomers to imidazole (isomer 1: isomer 2: product) of 1:1.7:1; 1:1.7:1.6 and 1:1.5:11 respectively. Further attempts to separate the mixture by chromatographic elution with different solvents in different ratios, aided by visualization of TLC plates under different revealing reagents was unsuccessful.

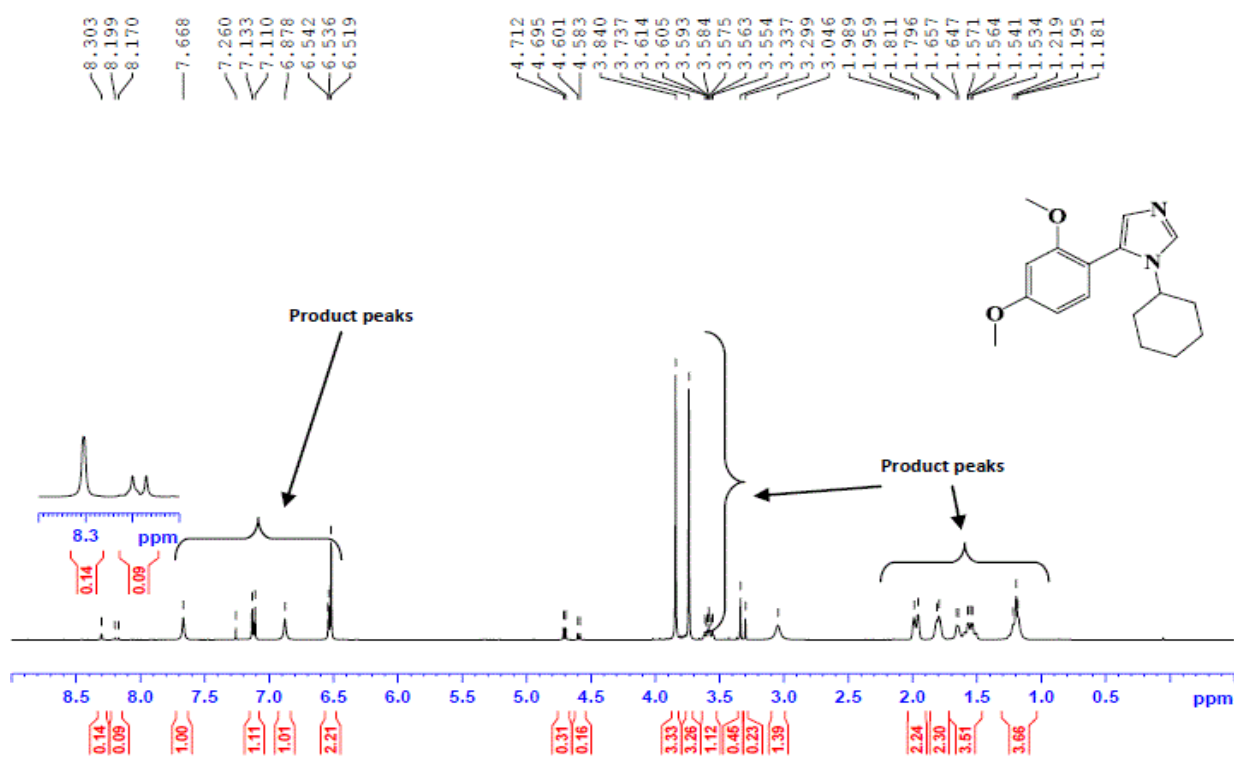
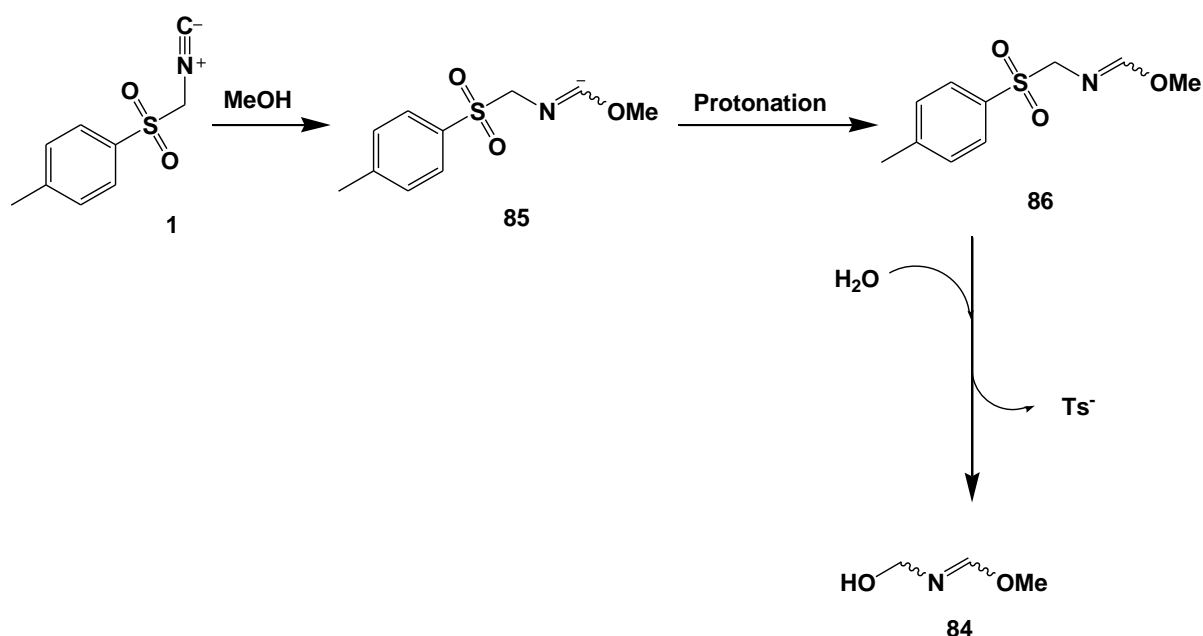


Figure 2.1: ^1H NMR spectrum with trace of **80d** and suspected (*E*- and *Z*-) $\text{HOCH}_2\text{N=CH(OMe)}$ in CDCl_3 .

The unexpected isomeric compounds **84** obtained when the reaction is conducted in MeOH may be attributed to the partial decomposition of TosMIC **1** in the presence of the solvent and the

base. van Leusen *et al.*⁹⁹ isolated three products, one of them $\text{MeOCH}_2\text{N}=\text{CH}(\text{OMe})$, from the reaction between TosMIC **1** and MeOH only in the presence of K_2CO_3 as catalyst (at room temperature for 20 hours).

A probable mechanism shown in **Scheme 2.4**, which is similar to the one proposed by van Leusen and co-workers,⁹⁹ could be offered as an explanation for the formation of compounds **84**. The initial step is believed to involve the nucleophilic attack by MeO^- on the isocyanato carbon of TosMIC **1** to afford **85**, followed by protonation to provide **86**. The water generated as a by-product of the van Leusen reaction then displaces the tosyl group through an addition-elimination reaction to give **84**. These results discourage the use of MeOH as solvent in the van Leusen synthesis of imidazoles under microwave irradiation, in favour of the use of MeCN as the solvent of choice.



Scheme 2.4: Suggested mechanism of the decomposition of TosMIC in MeOH.⁹⁹

Sisko and co-workers¹¹¹ described the preparation of imidazoles *via* 3-CvL reaction using derivatised TosMIC reagents and surprisingly reported that neither TosMIC nor its alkyl derivatives were reactive under the mild conditions in protic solvents using *t*-BuNH₂ or K_2CO_3 as a base. In our hands TosMIC has proved to be equally effective under microwave irradiation in acetonitrile, in both stepwise and in one pot procedures. A plausible mechanistic pathway of the formation of the 1-substituted-5-aryl-1*H*-imidazole products has been discussed in Chapter 1 (**Scheme 1.9**).

2.2.2.3. Effect of the aryl ring substituents on the reaction yield

The 1-substituted-5-aryl-1*H*-imidazole fragments were isolated in different yields according to the nature of the functional groups present on the aryl aldehyde. The highest yields of the series (independent of the energy source applied), were obtained when both the *ortho*- and *para*-positions of the aryl ring were occupied by the electron donating methoxy groups (**79d**, **80d** and **81d**), while on the other hand, the presence of an electron withdrawing bulky chlorine atom in the *ortho*-position gave the lowest yields in the series (**79b** and **80b**). To determine the influence of the substituents on the yield obtained, *N*-(arylidene)alkylamine intermediates **75h-i** and **76h-i** bearing an electron-withdrawing NO₂ group were subjected to the conditions described in **Scheme 2.2** (Route 1, method D) and afforded 1-substituted-nitrophenyl-1*H*-imidazoles **79h-i** and **80h-i** in even lower yields than their chlorine counterparts **79b** and **80b** (10-15%). The poor overall yields for the imidazoles could then be attributed to the electron-withdrawing effect of the nitro and chlorine substituents, confirming that the van Leusen reaction does not perform well in the presence of these groups on the benzaldehyde ring.

2.2.2.4. Structure elucidation of the van Leusen products 79-83 by FTIR, NMR and HRMS techniques

Examination of FTIR, 1-D and 2-D NMR spectra of the pure products was used to characterize and confirm the structures of obtained compounds **79-83**. The FTIR spectra of these products showed the C-H adsorption bands in the 2860 cm⁻¹ to 3130 cm⁻¹ regions, whilst the C=C stretching band appears at a range of 1614 cm⁻¹ to 1675 cm⁻¹. The absorption bands in the 1434 - 1489 cm⁻¹ region were assigned to C-N stretching modes of the imidazole motif. The ¹H NMR spectra of compounds **79-83** exhibited two singlet signals in the region of δ 7.4-7.7 ppm and δ 6.8-7.2 ppm corresponding to the two methine protons of the imidazole moiety. In the ¹³C NMR spectra, the methine carbon atoms of the imidazole motif displayed two characteristics signals at δ 134-138 ppm and δ 127-128 ppm.

Electrospray-ionisation Liquid Chromatography Mass Spectrometry (ESI-LCMS) was used to confirm preparation of the scaffolds **79-83**. Chromatograms exhibited a single peak corresponding to their protonated parent molecular ion [M+1]⁺ (a UV-vis detector was used in parallel with the mass detection). By way of example, compounds **79d**, **80b**, **80d**, **81d** with molecular formulae C₁₅H₂₁N₂O₂, C₁₅H₁₈ClN₂, C₁₇H₂₃N₂O₂ and C₁₄H₁₇N₂O₂, respectively, showed parent molecular ion peaks [M+1]⁺ at *m/z* 261.1587, 261.1155, 287.1770 and 245.1290, which correspond well with the theoretical calculated values for their formulae (Table 2.4). More

importantly, these compounds showed an acceptable tolerance of isotopic pattern fit factor (mSigma) lower than 20 (the lower the mSigma value the better the match) as shown in *Table 2.4*.

Table 2.4: HRMS results of the 1-substituted-5-aryl-1*H*-imidazoles compounds and their mSigma values.

Compds	Measured (m/z)	Formula [M+1] ⁺	Theoretical (m/z)	Err [mDa]	Err [ppm]	mSigma
79a	219.1294	C ₁₃ H ₁₆ FN ₂	219.1292	-0.2	-0.9	0.8
79b	235.1002	C ₁₃ H ₁₆ ClN ₂	235.0995	-0.7	-2.5	19.4
79c	231.1498	C ₁₄ H ₁₉ N ₂ O	231.1492	-0.6	-2.4	3.3
79d	261.1587	C ₁₅ H ₂₁ N ₂ O ₂	261.1598	1.1	3.9	1.4
79e	245.1276	C ₁₄ H ₁₇ N ₂ O ₂	235.1285	0.9	3.5	5.3
79f	257.2008	C ₁₇ H ₂₅ N ₂	257.2012	0.4	1.6	5.2
79g	259.1434	C ₁₅ H ₁₉ N ₂ O ₂	259.1441	0.7	2.7	4.7
79h	246.1240	C ₁₃ H ₁₆ N ₃ O ₃	246.1237	-0.3	-0.2	7.5
78i	246.1238	C ₁₃ H ₁₆ N ₃ O ₃	246.1237	-0.1	-3.0	7.2
80a	245.1475	C ₁₅ H ₁₈ FN ₂	245.1449	-2.7	-10.8	19.3
80b	261.1155	C ₁₅ H ₁₈ ClN ₂	261.1153	-0.8	-0.2	3.1
80c	257.1668	C ₁₆ H ₂₁ N ₂ O	257.1648	-1.9	-7.4	10.4
80d	287.1770	C ₁₇ H ₂₃ N ₂ O ₂	287.1754	-1.6	-5.4	2.1
80e	271.1464	C ₁₆ H ₁₉ N ₂ O ₂	271.1481	1.8	6.5	6.5
80f	283.2190	C ₁₉ H ₂₇ N ₂	283.2162	-2.1	-7.5	17.2
80h	272.1393	C ₁₅ H ₁₈ N ₃ O ₂	272.1394	1.1	4.2	13.8
80i	272.1382	C ₁₅ H ₁₈ N ₃ O ₂	272.1394	1.2	0.2	13.8
81a	203.0974	C ₁₂ H ₁₂ FN ₂	203.0979	0.5	2.4	2.8
81c	215.1188	C ₁₃ H ₁₅ N ₂ O	215.1179	-0.9	-4.3	7.5
81d	245.1290	C ₁₄ H ₁₇ N ₂ O ₂	245.1285	-0.5	-2.3	3.3
82a	253.1138	C ₁₆ H ₁₄ FN ₂	253.1136	-0.3	-1.1	17.2
82c	265.1329	C ₁₇ H ₁₇ N ₂ O	265.1335	0.6	2.3	8.6
82d	295.1408	C ₁₈ H ₁₉ N ₂ O ₂	295.1441	3.3	11.1	3.9
82e	279.1143	C ₁₇ H ₁₅ N ₂ O ₂	279.1128	-1.5	-5.4	13.2
83a	317.0115	C ₁₅ H ₁₁ ⁷⁹ BrFN ₂	317.0090	-2.5	-7.9	4.9
83d	359.0394	C ₁₇ H ₁₆ ⁷⁹ BrN ₂ O ₂	359.0395	0.1	0.2	4.8
83e	343.0099	C ₁₆ H ₁₂ ⁷⁹ BrN ₂ O ₂	343.0082	-1.7	-5.2	10.5

Overall, a total of twenty seven 1-substituted-5-aryl-1*H*-imidazole compounds were synthesized from the van Leusen imidazole reaction described above and 26 compounds are, to the best of

our knowledge, novel (only **82e** was previously reported but it was prepared using sodium cyanide in aprotic solvent under heating at 137°C for 16 h).²⁰⁴ The synthesized imidazole based compounds **79-83** were submitted for biological evaluation.

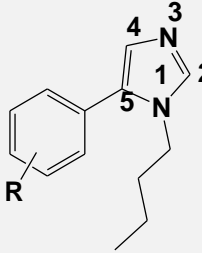
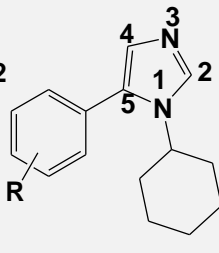
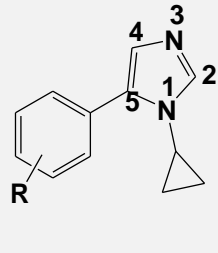
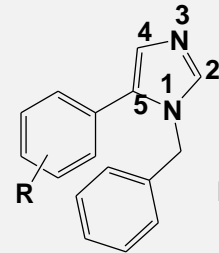
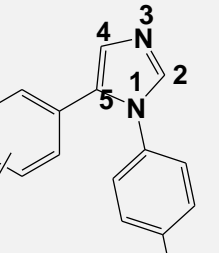
2.2.3. Biological evaluation of library of 1-substituted-5-aryl-1*H*-imidazole derivatives

The compounds **79-83** were assessed for their biological activity using two HIV-1 protein inhibition assays; namely HIV-1 IN - LEDGF/p75 inhibition, and the HIV-1 Vpu binding assays, in the hope of identifying viable hits which could be further developed. The compounds were also intended for targeting the interaction between HIV-1 Viral protein U (Vpu) and the host Bone Marrow Stroma-antigen-2 (BST-2) protein; however, tests capable of biologically evaluating the compounds as HIV-1 Vpu/ BST-2 inhibitors were unavailable at the time of the completion of the synthetic work. As a result, this imidazole based family of compounds were only assessed using the two HIV-1 inhibition assays mentioned above. The screening of compounds was conducted by the Centre of Metal Drug Discovery group (CMDD), Advanced Material Division, Mintek (Randburg, South Africa). Only compounds which exceeded the 50% inhibition benchmark were considered for further determination in a dose-response assay for determining their half maximum inhibitory concentration (IC₅₀), cellular cytotoxicity (CC₅₀) and antiviral activities.

2.2.3.1. Direct HIV- 1 integrase (IN)-LEDGF AlphaScreen assay

Initially, a set of twenty seven fragments belonging to a family of 1-substituted-5-aryl-1*H*-imidazoles were tested using the AlphaScreen[®] assay²⁰⁵ to determine the percentage inhibition of the interactions between the HIV integrase (IN)-LEDGF/p75 proteins at a concentration of 10 μM. The experiments were carried out in triplicate and average results are presented in *Table 2.5*.

Table 2.5: The HIV-1 IN-LEDGF/p75 inhibition activities of the 1-substituted-5-aryl-1*H*-imidazole compounds **79-83**.

Compounds Entry	Biochemical target assays		Cell-based assays (MT-4 cells)
	HIV-1 IN – LEDGF (%) inhibition @ 10 μ M (AlphaScreen)	HIV-1 IN – LEDGF	
		inhibition IC ₅₀ (AlphaScreen) (μ M)	CC ₅₀ (μ M)
			
79			
			
80			
			
81			
			
82			
			
83 Br			
79a	29.89 \pm 2.96		
79b	36.62 \pm 1.87		
79c	51.10 \pm 0.98	30.35 \pm 4.92	29.59 \pm 10.94
79d	25.88 \pm 2.73		
79e	34.72 \pm 2.73		
79f	55.68 \pm 0.85	22.40 \pm 1.46	23.93 \pm 2.36
79g	20.72 \pm 2.44		
79h	29.72 \pm 2.39		
79i	26.59 \pm 1.67		
80a	44.65 \pm 1.84		
80b	31.33 \pm 1.46		
80c	55.01 \pm 2.43	21.94 \pm 0.489	27.72 \pm 5.44
80d	39.68 \pm 2.14		
80e	37.79 \pm 7.70		
80f	61.79 \pm 0.53	14.58 \pm 0.24	21.77 \pm 2.84
81a	30.86 \pm 2.18		
81b	34.82 \pm 3.35		
81c	40.22 \pm 0.36		

	HIV-1 IN – LEDGF (%) inhibition @ 10 μ M (AlphaScreen)	HIV-1 IN – LEDGF inhibition IC ₅₀ (AlphaScreen) (μ M)	CC ₅₀ (μ M)
81d	27.66 \pm 2.78		
82a	24.68 \pm 2.43		
82c	20.82 \pm 2.06		
82d	17.03 \pm 3.99		
82e	43.20 \pm 1.91		
83a	52.41 \pm 1.67	25.07 \pm 2.47	48.00 \pm 12.58
83c	47.94 \pm 4.04		
83d	52.08 \pm 0.99	6.99 \pm 1.49	55.47 \pm 16.25
CX05168	91.37 \pm 0.85	1.38 \pm 0.29	
HIV-1 IN and LEDGF/p75	0		

* IC₅₀ - concentration of compound required to inhibit 50% of the specific biological process

*CC₅₀ – concentration of compounds that causes 50% reduction of cell growth

Of the twenty six imidazole-based compounds screened, six compounds showed more than 50% inhibition at a dose concentration of 10 μ M (Figure 2.2). The best inhibitor in the series with 62% inhibition and an IC₅₀ value of 15 μ M was compound **80f**, which contained a cyclohexyl moiety at the 1-position of the imidazole core. The replacement of the cyclohexyl group by an *n*-butyl moiety, (compound **79f**) gave rise to a compound with lower inhibitory activity of 56% and an IC₅₀ value of 22 μ M. Both **79f** and **80f** contained a *tert*-butyl substituent at the *para*-position of the benzene ring attached at the 5-position of the imidazole moiety. The *tert*-butyl group is likely to occupy the hydrophobic pocket of the target protein. Compound **80c**, an analogue of **80f**, containing a methoxy substituent at the *meta*-position inhibited the protein-protein-interaction by 55% with an IC₅₀ value of 22 μ M, whilst two compounds, **83a** and **83d**, both with a 4-bromophenyl group at the 1-position of the imidazole moiety prevented IN-LEDGF/p75 interaction by 52% inhibition each. In dose response assays, **83d** with the methoxy substituents at the *ortho*- and *para*-positions on the 5-aryl ring displayed the best IC₅₀ value (7 μ M) in the series, while its counterpart with a fluorine atom at the *para*-position **83a** produced an IC₅₀ value of 25 μ M. The lower IC₅₀ value of compound **83d** could be attributed to the methoxy group which can provide the possibility of hydrogen-bonding interactions with some of the amino acid residues

within the binding site, leading to higher binding affinity. Amongst the best six compounds with 51% inhibitory activity is an analogue of **79f**, compound **79c**, containing a *meta*-methoxy substituent and with an IC_{50} value of 30 μM in a dose response assay. Interestingly, another analogue of **83a** and **83d**, compound **83c** displayed 48% inhibition. The data suggest that the presence of the 4-bromophenyl at the 1-position of the imidazole motif might be of significance for the binding ability of these scaffolds. Attempts to synthesise imidazole derivatives from analogue **74f-h** were unsuccessful. Other compounds in this family of imidazole-based derivatives exhibited only marginal inhibitory activities towards IN - LEDGF/p75 interaction, ranging from 17% to 44%.

To eliminate the possibility of false positive results arising from the compound signal interfering with the AlphaScreen assay, the best six compounds, **79c**, **79f**, **80c**, **80f**, **83a** and **83d** (Figure 2.2) were subjected to the TruHit counter assay with all six showing true inhibition ability of the interaction between the HIV-1 integrase and LEDGF/P75 proteins.

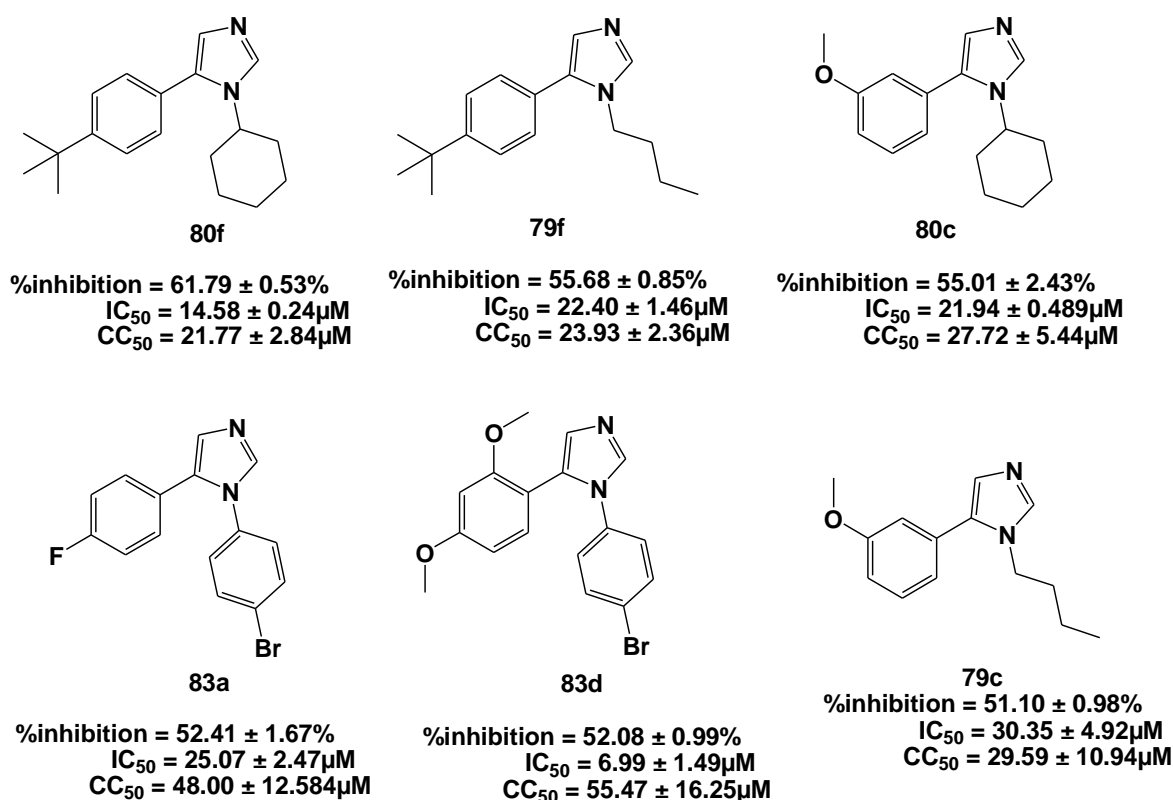


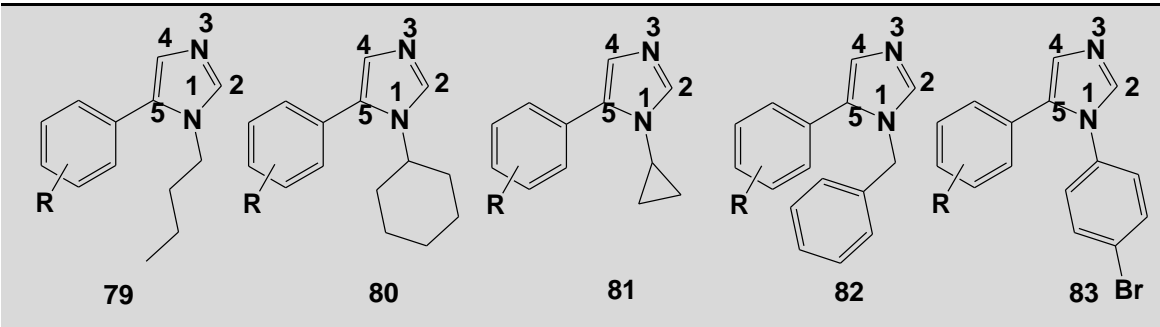
Figure 2.2: Six fragments exceeding 50% inhibition for the HIV-1 IN - LEDGF/p75 assays ranked according to their percentage inhibition with the cell based MT-4 assay data included.

The best six imidazole-based compounds (**79c**, **79f**, **80c**, **80f**, **83a** and **83d**) were further assessed for their cytotoxicity and antiviral activity in the metallothionein type 4 cell line (MT4). In a dose range cytotoxicity assay these scaffolds produced CC₅₀ values ranging from 55.47 to 21.77 μ M. Unfortunately, none of the best six compounds displayed any viral inhibition at 10 μ M within the MT-4 cell line. The lack of antiviral activity suggests either an inability of these compounds to reach the target or possibly point to poor compound solubility. Another crucial fact is that they lack the functionality that could make crucial hydrogen bonds with important residues at the binding sites. It is apparent that the best six fragments may be considered as templates for further development as inhibitors of IN-LEDGF/p75 interactions. Based on this, one of the best six fragments, **83a**, was chosen for further development in order to understand the SAR involved, as well as add extra functionalities which could lead to improved inhibitory performance against the target interaction.

2.2.3.2. Direct Viral protein u (Vpu) binding ELISA assay

To further test the biological activity of the synthesized compounds, twenty six imidazole-based compounds **79-83** were also submitted for screening in a second biochemical assay for their ability to inhibit the binding of the antibody (anti-Vpu) to Vpu at 10 μ M concentration using an ELISA assay. The binding site is the same region where Vpu binds to CD74 and to CD4. The biological data of the assessed compounds is recorded in *Table 2.6*.

Table 2.6: HIV-1 Vpu inhibition activities of 1-substituted-5-aryl-1*H*-imidazoles.

	
Compounds Entry	HIV-1 Vpu – binding (% inhibition) @ 10 μ M using ELISA
79a	0
79b	0
79c	35.25
79d	8.51
79e	8.42

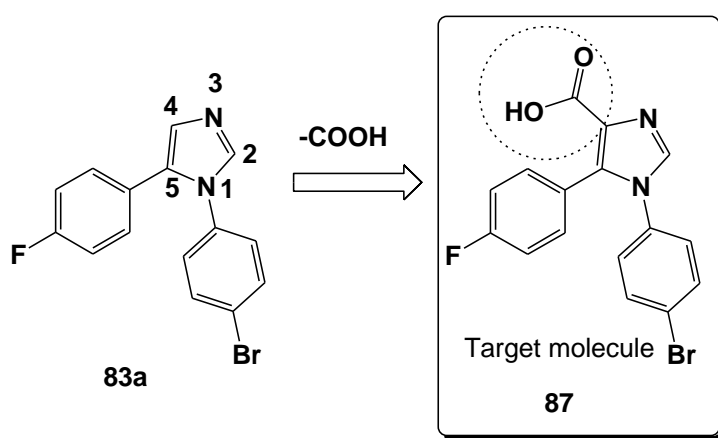
Compounds Entry	HIV-1 Vpu – binding (% inhibition) @ 10 μ M using ELISA
79f	0
79g	7.93
79h	0
79i	9.21
80a	0
80b	0
80c	0
80d	0
80e	2.17
80f	0
81a	0
81b	0
81c	23.41
81d	37.06
82a	6.76
82c	17.86
82d	0
82e	0
83a	4.04
83d	6.79

These scaffolds **79-83** were found to be well below the 50% benchmark to be considered further as promising candidate inhibitors of Vpu. It is likely; however, that these fragments cannot sufficiently block any interaction, as the protein binding site is rather large. Compound **81d** showed the highest inhibition (37%) of binding of the anti-Vpu to Vpu protein. These compounds were not deemed suitable to be pursued further for development as Vpu inhibitors.

2.3. Synthesis of 1,5-diaryl-1*H*-imidazole-4-carboxylic acid analogues as second generation compounds

Encouraged by the interesting biological data, the modification of one of the best six fragments was pursued as an ideal starting point for fragment growth into possibly more potent inhibitors of the LEDGF/p75-IN interaction. Examination of the best six compounds shows the absence

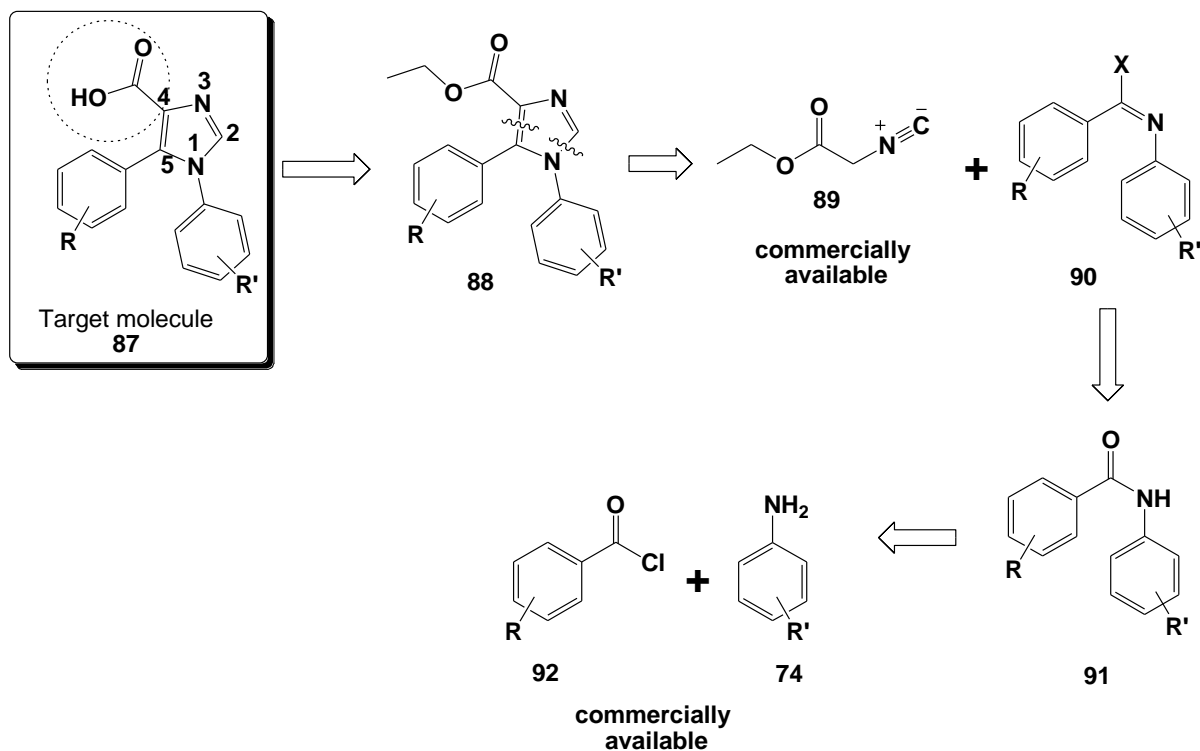
of key structural features that have been shown to enhance the disruption of the LEDGF/p75-IN interaction. A review of molecules reported as inhibitors of the LEDGF/p75-IN interaction indicate that some of them contain a carboxylic acid functionality which could be significant to their binding properties.^{53,206,207,208,209} Based on these observations, the introduction of a carboxylic acid functionality might improve the potency of the active fragments. Of the best six compounds, 1-(4-bromophenyl)-5-(4-fluorophenyl)-1*H*-imidazole **83a** was chosen as a suitable template (hit) for further modification because of the simplicity of its chemical structure and *in vitro* potency ($IC_{50} = 25.07 \pm 2.47 \mu\text{M}$). Therefore, a series of analogues of **83a**, namely 1-(4-bromophenyl)-5-(4-fluorophenyl)-1*H*-imidazole-4-carboxylic acid were envisaged (**Scheme 2.5**).



Scheme 2.5: Integration of -COOH group on the 1-(4-bromophenyl)-5-(4-fluorophenyl)-1*H*-imidazole fragment **83a**.

2.3.1. Retrosynthesis of target compounds

The first step was to design a plausible synthetic route towards the desired 1-(4-bromophenyl)-5-(4-fluorophenyl)-1*H*-imidazole-4-carboxylic acid **87**. The *retrosynthesis* idea was primarily initiated by 1990 Nobel Prize winner in chemistry, Prof E. J. Corey.²¹⁰ Since then it has been frequently exercised by organic chemists to map and develop synthetic pathways. By definition, retrosynthesis is the breaking down of a target molecule into simple and easily accessible commercially available synthons as starting points for a *synthesis*.²¹⁰



Scheme 2.6: Retrosynthesis of target compound **87**.

As depicted in **Scheme 2.6**, the retrosynthesis of target compound **87** can be attained in four stepwise reactions. Compound **87** can be obtained by hydrolysis of the ester group of carboxylate scaffold **88**. Further disconnection of bonds on the chemical structure **88** as shown in **Scheme 2.6** can lead to a commercially available ethyl isocyanoacetate **89** and intermediate **90** (where X is a leaving group). The presence of the leaving group could facilitate the C=C double bond formation at the 4- and 5-positions of the imidazole ring. Intermediate **90** can be obtained from the *N*-aryl benzamide **91**, which in turn can be easily produced from two commercially available synthons, aniline **74** and benzoyl chloride derivatives **92**.

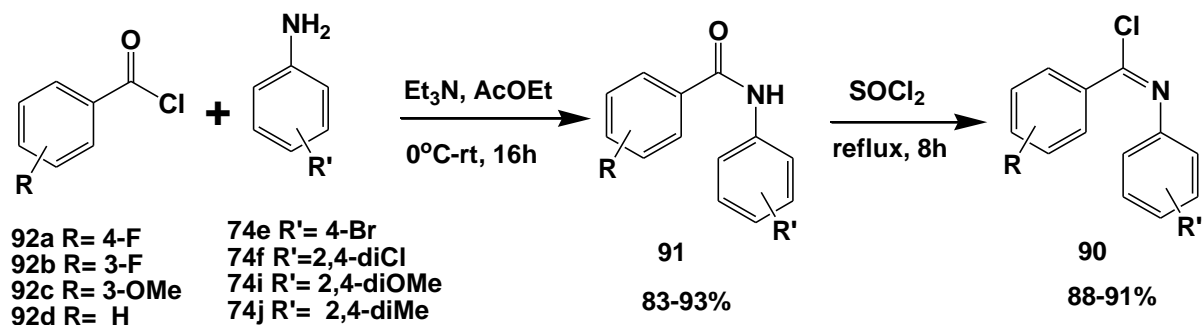
2.3.2. Synthesis of the ethyl 1,5-diaryl-1*H*-imidazole-4-carboxylic acid derivatives

With the planned synthetic pathway in hand, the synthesis of the family of ethyl 1,5-diaryl-1*H*-imidazole-4-carboxylic acid derivatives was pursued, starting with the synthesis of the iminochlorides **90** through their diarylamide intermediates **91**.

2.3.2.1. Synthesis of *N*-aryl-benzamide chlorides

To better understand the SAR between the compounds and the targets under investigation, various readily available benzoyl chlorides and aniline derivatives were employed. Initially, the

essential intermediates, *N*-aryl benzimidoyl chlorides **90** were prepared in two steps in accordance with reported methods as illustrated in **Scheme 2.7**.^{211,212} Thus benzoic chlorides **92a-d** were reacted with aniline scaffolds **74e-f** and **74i-j** in the presence of triethylamine and using ethyl acetate as solvent at room temperature for 16 hours.²¹¹ Work-up afforded *N*-aryl-benzamide products **91a-j** in yields ranging from 83-93% as recorded in *Table 2.7*.



Scheme 2.7: Synthesis of *N*-aryl-benzimidoyl chloride intermediates **90**.

Table 2.7: Isolated yields (%) of the *N*-aryl-benzamide products **91a-j**.

Compound Entry			Yields (%)
	R	R'	
91a	4-F	4-Br	91
91b	3-F	4-Br	91
91c	3-OMe	4-Br	90
91d	3-Me	4-Br	89
91e	H	4-Br	86
91f	4-F	2,4-diOMe	83
91g	4-F	2,4-diMe	88
91h	3-OMe	2,4-diMe	90
91i	4-F	2,4-diCl	93
91j	3-F	2,4-diCl	90

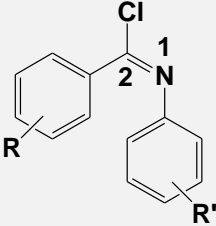
NMR spectroscopic analysis confirmed the structures and correlated with previously reported data in the literature.^{213,214,215,216} These scaffolds were therefore used in the next step without further purification. The products **91a-j** were all characterised by the clear presence of an N-H signal in the region of δ 7.8-10.6 ppm in the ¹H NMR spectra and a carbonyl carbon atom in the region of δ 163-170 ppm in their ¹³C NMR spectra. The presence of an N-H group was also evident in their FTIR spectra, where this band appears between 3226 and 3369 cm⁻¹ whilst a strong absorption band around 1642-1783 cm⁻¹ corresponds to the carbonyl group of the amide, as shown in *Table 2.8*.

Table 2.8: FTIR spectroscopic data of *N*-aryl-benzamide products **91a-j** showing N-H and C=O absorption bands.

Compds	91a	91b	91c	91d	91e	91f	91g	91h	91i	91j
$\nu_{\text{NH}} (\text{cm}^{-1})$	3345	3315	3329	3329	3332	3286	3286	3226	3386	3369
$\nu_{\text{C=O}} (\text{cm}^{-1})$	1642	1656	1658	1658	1656	1650	1652	1648	1783	1660

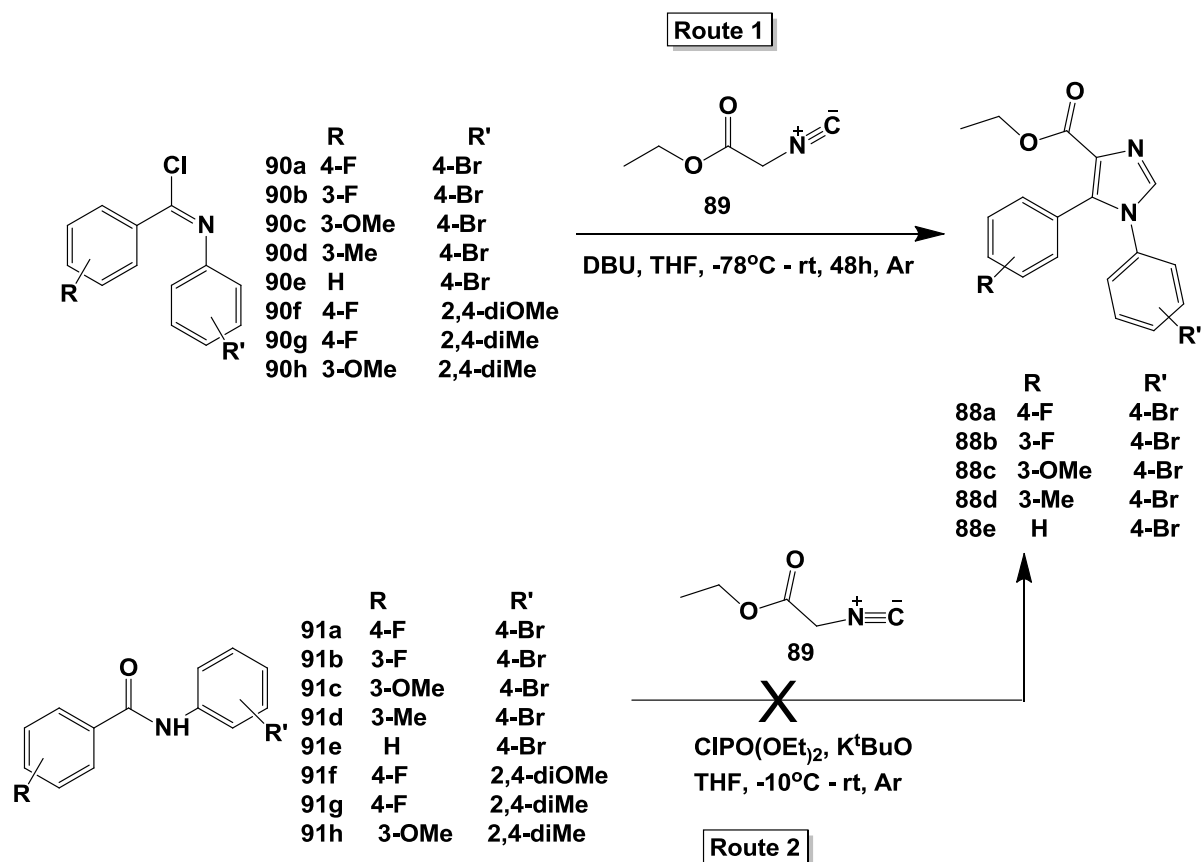
A series of *N*-aryl-benzamide scaffolds **91a-j** were then heated neat with thionyl chloride (SOCl₂) for 16 hours as shown in *Scheme 2.7*.²¹² Upon completion, the excess thionyl chloride was removed by co-evaporation with toluene, affording most of the *N*-arylbenzimidoyl chloride products **90a-h** in excellent yields (see *Table 2.9*). However, when the aniline ring was occupied by chlorine substituents at the *para*- and *ortho*-positions (**91i-j**) only trace amounts of products were observed (NMR spectroscopy). This may be due to the electron-withdrawing effects of the two chlorine atoms which may influence the stability of these products **90** at room temperature. The obtained products **90a-h** were immediately subjected to the next reaction step.

Table 2.9: Isolated yields (%) of the *N*-aryl-benzimidoyl chloride products **90a-h**.

Compound Entry			
	R	R'	Yields (%)
90a	4-F	4-Br	96
90b	3-F	4-Br	95
90c	3-OMe	4-Br	98
90d	3-Me	4-Br	98
90e	H	4-Br	96
90f	4-F	2,4-diOMe	95
90g	4-F	2,4-diMe	98
90h	3-OMe	2,4-diMe	96

In spite of the instability of compounds **90a-h**, 1D and 2D NMR spectra were used to confirm their structures. In solution, the ^1H NMR spectra in each case revealed that these compounds are isolated as a single geometrical isomer (likely *E*-isomer), which agrees with the reported literature.^{217,218} The ^1H NMR spectra of **90a-h** showed the disappearance of the secondary imide proton, while their ^{13}C NMR spectra showed the disappearance of the carbonyl signal and the appearance of a new signal at δ 143 ppm, assigned to the carbon atom directly attached to the chlorine atom.

2.3.2.2. Synthesis of ethyl 1,5-diaryl-1*H*-imidazole-4-carboxylates



Scheme 2.8: Synthesis of ethyl 1,5-diaryl-1*H*-imidazole-4-carboxylate derivatives **88**.

Ethyl isocyanoacetate **89** was then subjected to a cycloaddition reaction with *N*-aryl-benzimidoyl chloride derivatives **90a-h** as depicted in *Scheme 2.8* (Route 1). *N*-aryl-benzimidoyl chloride **90a-h** was added to a mixture of ethyl isocyanoacetate **89** and DBU in dry THF under argon at -78°C . The resulting reaction mixtures were then allowed to warm to room temperature and were stirred for 48 hours (monitored by TLC). Work up and column chromatography afforded novel ethyl 1,5-diaryl-1*H*-imidazole-4-carboxylate derivatives **88a-e** bearing a 4-bromophenyl substituent at the 1- position of the imidazole moiety. These products **88a-e** were isolated in yields ranging from 18% to 64% (*Table 2.10*). The highest yields were obtained when the aryl ring attached at the 5-position of the imidazole core contained fluorine atoms (**88a-b**). On the other hand, compounds **90f-h** failed to convert to the desired products; this may be attributable to the electron donating effects of the methoxy and methyl groups, which tend to disfavour cycloaddition.

With low yields of some of the products and failed conversions of some of the *N*-aryl-benzimidoyl chlorides **90f-h**, an attempt was made to directly synthesise the desired heterocyclic products **88** from *N*-aryl-benzamides **91** using a previously reported procedure^{219,220} as illustrated in **Scheme 2.8** (Route 2). Therefore, *N*-aryl-benzamides **91a-h** were treated with diethyl chlorophosphate in the presence of catalytic base, ^tBuOK in anhydrous THF under argon at -10°C, with the intention of generating unstable iminophosphates *in situ*, followed by subsequent addition of ethyl isocyanoacetate **89** and ^tBuOK with further stirring for 4 hours. Unfortunately, none of the desired products **88** could be detected (TLC); even extending the reaction time to 48 hours didn't have any effect on the formation of the products. The challenging nature of the reaction may be attributed to the instability of the iminophosphates which were generated *in situ*.

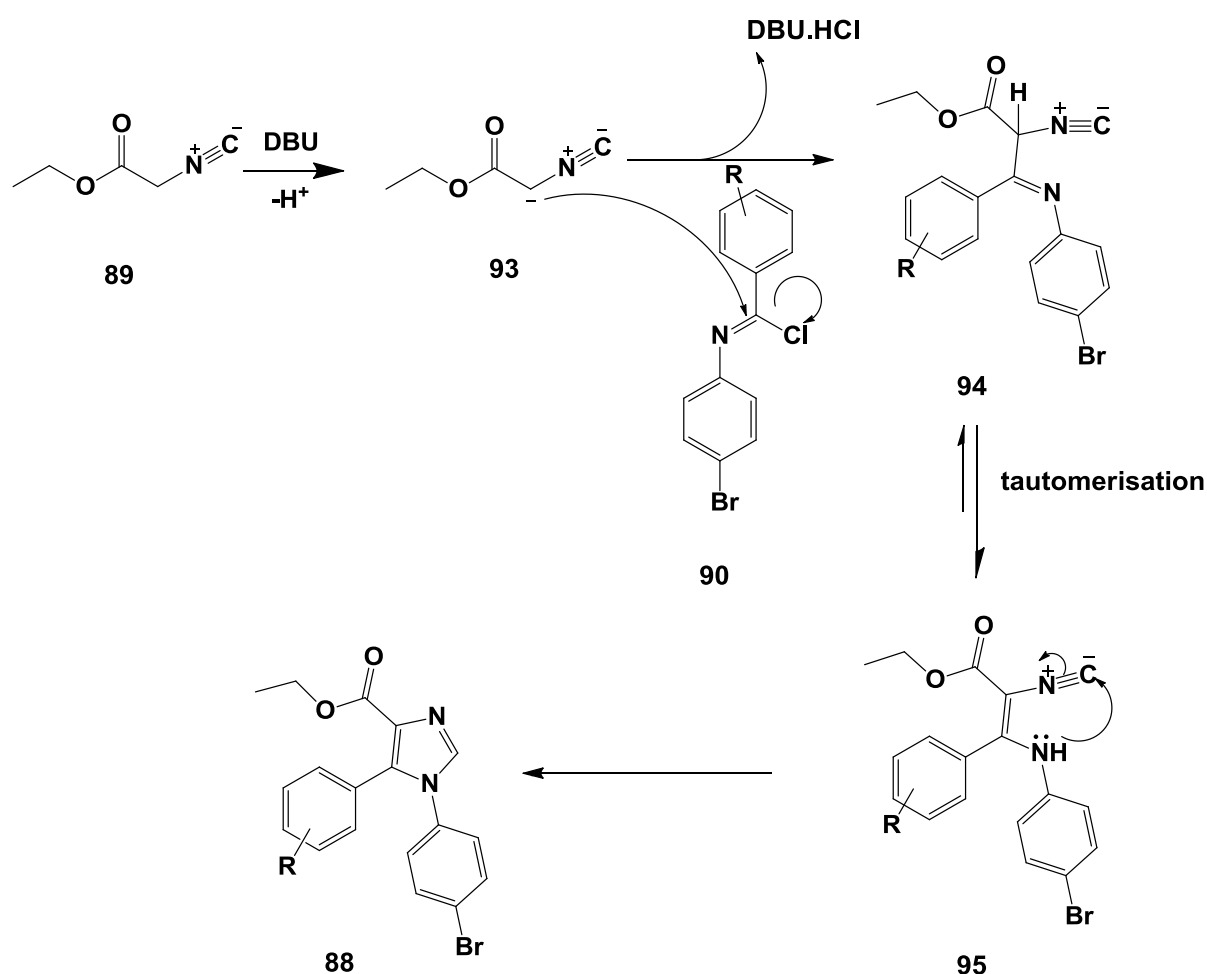
Table 2.10: Isolated yield (%) of compounds **88a-e**.

Compound Entry	R	Yields (%)
88a	4-F	64
88b	3-F	58
88c	3-OMe	18
88d	3-Me	30
88e	H	22

2.3.2.2.1 Mechanism for the formation of ethyl 1,5-diaryl-1*H*-imidazole-4-carboxylates **88**

A plausible mechanistic pathway for the formation of ethyl 1-(4-bromophenyl)-5-aryl-1*H*-imidazole-4-carboxylates **88a-e** is illustrated in **Scheme 2.9**. The initial step is thought to involve an activation of ethyl isocyanoacetate **89** by DBU to generate anion **93**. This intermediate **93** is then involved in a nucleophilic attack on the C=N double bond of *N*-phenyl-benzimidoyl chloride **90** to afford intermediate **94**, with elimination of a Cl atom as the DBU hydrochloride

salt. Intermediate **94** tautomerises to give **95**, which then undergoes *in situ* cyclisation and proton transfer to give the desired products **88**.



Scheme 2.9: Plausible mechanism for the formation of ethyl 1-(4-bromophenyl)-5-aryl-1H-imidazole-4-carboxylates **88**.

The newly synthesized compounds **88a-e** were characterised by FTIR as well as NMR spectroscopy, with the data obtained being in agreement with the expected structures. The FTIR spectra showed a strong absorption band assigned to the C=O stretching of the ester functionality at 1708-1716 cm^{-1} , whilst the bands between 1562-1587 cm^{-1} were assigned to C=N of the imidazole moiety. Other frequencies between 1449 and 1497 cm^{-1} were attributed to C-N stretching of the imidazole motif (see *Table 2.11*).

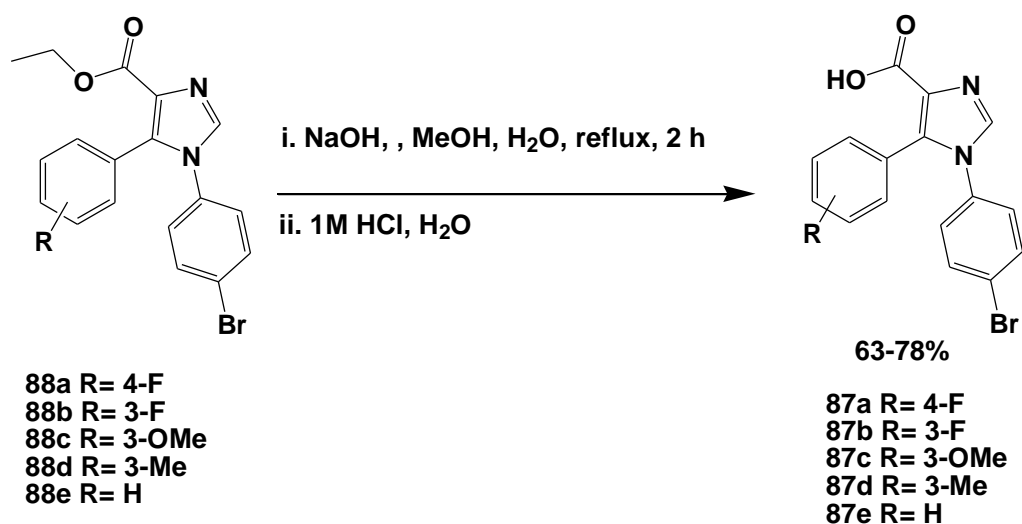
Table 2.11: FTIR spectroscopic data for ethyl 1-(4-bromophenyl)-5-aryl-1*H*-imidazole-4-carboxylates **88** showing the C=O, C=N, and C-N stretch signals.

Compound	88a	88b	88c	88d	88e
$\nu_{\text{C=O}}$ (cm ⁻¹)	1716	1708	1715	1713	1709
$\nu_{\text{C=N}}$ (cm ⁻¹)	1560	1582	1587	1552	1556
$\nu_{\text{C-N}}$ (cm ⁻¹)	1375	1372	1374	1372	1373

NMR spectra of compound **88c** will be discussed in detail below, being representative of this compound class. The ¹H NMR spectrum of compound **88c** shows the following characteristic features: a singlet corresponding to the methine proton of the imidazole ring at δ 7.61 ppm; the signals in the region of δ 6.70-7.37 ppm confirming the presence of two aryl rings; a quartet at δ 4.19 ppm with a coupling constant of 7.2 Hz assigned to the protons of the methylene group (ethyl moiety); an upfield triplet at δ 1.18 ppm ($J = 7.0$ Hz) corresponding to the methyl protons of the ethyl group and a singlet at δ 3.63 ppm corresponding to the protons of the *ortho*-methoxy group. The ¹³C NMR spectrum of compound **88c** shows the carbonyl carbon atom resonating at 162.6 ppm, while the methine carbon atom of the imidazole motif resonates at 137.6 ppm. The *ortho*-methoxy carbon atom resonates at 55.1 ppm while the methylene and methyl carbon atoms of the ethyl group are observed at 60.4 and 14.1 ppm, respectively.

2.3.2.3. Hydrolysis of 1-(4-bromophenyl)-5-aryl-1*H*-imidazole-4-carboxylates

The ester group of the ethyl 1-(4-bromophenyl)-5-aryl-1*H*-imidazole-4-carboxylates **88a-e** were then hydrolysed under reflux in the presence of NaOH in methanol and water for 2 hours, followed by acidification (**Scheme 2.10**). Work up afforded the novel 1-(4-bromophenyl)-5-aryl-1*H*-imidazole-4-carboxylic acid derivatives **87a-e** in yields of up to 78% (**Table 2.12**).



Scheme 2.10: Hydrolysis of ethyl 1-(4-bromophenyl)-5-aryl-1*H*-imidazole-4-carboxylates

Table 2.12: Isolated yields (%) of the 1-(4-bromophenyl)-5-aryl-1*H*-imidazole-4-carboxylic acids 87a-e

Compound Entry	R	Yields (%)
87a	4-F	68
87b	3-F	72
87c	3-OMe	78
87d	3-Me	75
87e	H	63

2.3.2.3.1. Structure elucidation of 1-(4-bromophenyl)-5-aryl-1*H*-imidazole-4- carboxylic acids **87a-e**

The title compound structures were confirmed by NMR spectroscopic analysis, FTIR spectroscopy and LCMS. Complete hydrolysis to yield products **87a-e** was confirmed by the disappearance of signals due to the ethyl group and emergence of the broad downfield signal at *ca.* δ 12 ppm corresponding to the acid proton in their ^1H NMR spectra. The disappearance of the ethyl group was also evident in their ^{13}C NMR spectra, while the FTIR spectra exhibited a decrease in C-H stretch signals due to the loss of the ethyl group and appearance of a slightly broad signal in the region of 2470-2565 cm^{-1} attributed to the OH group of the carboxylic acids. ESI-LCMS provided additional proof that the hydrolysis of the ester had occurred as it confirms the presence of the required molecular ion in all cases. For example, compounds **87b** and **87d**, with molecular formulae $\text{C}_{16}\text{H}_{11}^{79}\text{BrFN}_2\text{O}_2^+$ and $\text{C}_{17}\text{H}_{14}^{79}\text{BrN}_2\text{O}_2^+$ showed protonated molecular ion peaks $[\text{M}+\text{H}^+]$ at 360.9987 and 357.0244, respectively, which differ from the ester derivatives with molecular ions of 389.0301 (**88b**, $\text{C}_{18}\text{H}_{15}^{79}\text{BrFN}_2\text{O}_2^+$) and 385.0557 (**88d**, $\text{C}_{19}\text{H}_{18}^{79}\text{BrN}_2\text{O}_2^+$). Molecular ion peaks are all within acceptable SigmaFitTM values (below 20) (Table 2.13).

Table 2.13: HRMS results of compounds **87a-e** and **88a-e** with their mSigma values.

Compds	Measured (m/z)	Formula [M+1] ⁺	Theoretica l (m/z)	Err [mDa]	Err [ppm]	mSigma
87a	360.9991	$\text{C}_{16}\text{H}_{11}^{79}\text{BrFN}_2\text{O}_2^+$	360.9982	-0.8	-2.3	3.2
87b	360.9987	$\text{C}_{16}\text{H}_{11}^{79}\text{BrFN}_2\text{O}_2^+$	360.9982	-0.7	-1.9	8.7
87c	373.0201	$\text{C}_{17}\text{H}_{14}^{79}\text{BrN}_2\text{O}_3^+$	373.0182	-1.8	-4.9	6.0
87d	357.0244	$\text{C}_{17}\text{H}_{14}^{79}\text{BrN}_2\text{O}_2^+$	357.0233	-1.7	-4.9	6.6
87e	343.0089	$\text{C}_{16}\text{H}_{12}^{79}\text{BrN}_2\text{O}_2^+$	343.0077	-1.3	-3.7	8.1
88a	389.0301	$\text{C}_{18}\text{H}_{15}^{79}\text{BrFN}_2\text{O}_2^+$	389.0295	-0.6	-1.5	10.4
88b	389.0301	$\text{C}_{18}\text{H}_{15}^{79}\text{BrFN}_2\text{O}_2^+$	389.0295	-0.5	-1.4	7.6
88c	401.0487	$\text{C}_{19}\text{H}_{18}^{79}\text{BrN}_2\text{O}_3^+$	401.0495	0.8	2.0	19.0
88d	385.0557	$\text{C}_{19}\text{H}_{18}^{79}\text{BrN}_2\text{O}_2^+$	385.0546	-1.1	-2.8	18.3
88e	371.0398	$\text{C}_{16}\text{H}_{16}^{79}\text{BrN}_2\text{O}_2^+$	371.0390	-0.8	-2.2	12.5

Overall, the carboxylic acid moiety was incorporated at the 4-position of the imidazole ring using isocyanide chemistry. Five new 1-(4-bromophenyl)-5-aryl-1*H*-imidazole-4-carboxylic acids **87a-e** were obtained, which together with their ester intermediates **88a-e**, were submitted for biological evaluation in the IN-LEDGF/p75 binding assay.

2.3.3. Biological evaluation of 1-(4-bromophenyl)-5-(4-fluorophenyl)-1*H*-imidazole analogues

2.3.3.1. Direct Integrase-LEDGF/p75 AlphaScreen Assay

Because of weak binding affinity of small molecules for the protein target and the poor sensitivity of some biochemical assays, it is recommended to screen small fragments at concentrations between 100 and 200 μM .^{221,222,223,224,225} Therefore, compounds **87a-e** and **88a-e** were assessed and hit compound **83a** was re-assessed at 100 μM for their ability to interrupt HIV-1IN-LEDGF/p75 interactions using the AlphaScreen assay. All biological evaluations were carried out in duplicate and the average results are recorded in *Table 2.14*.

Table 2.14: The HIV-1 IN-LEDGF/p75 inhibition activities of the compounds **83a**, **87a-e** and **88a-e** at 100 μM .

Compounds Entry	Biochemical target assays	
	HIV-1 IN – LEDGF	HIV-1 IN – LEDGF inhibition
	(%)inhibition @ 100 μM (AlphaScreen)	IC ₅₀ (AlphaScreen) μM
83a	61 \pm 3.96	
87a	57 \pm 6.24	33.4 \pm 1.34
87b	79 \pm 2.24	37.3 \pm 3.24
87c	100 \pm 11.18	38.9 \pm 4.54
87d	100 \pm 6.76	302.0 \pm 1.34
87e	75 \pm 3.13	50.6 \pm 23.90
88a	13 \pm 1.21	
88b	17 \pm 1.89	
88c	48 \pm 4.98	
88d	13 \pm 7.37	
88e	68 \pm 5.23	
CX05168	91.37 \pm 0.85	1.38 \pm 0.29
HIV-1 IN and LEDGF with DMSO	0	

At a single dose concentration of 100 μM , hit compound **83a** exhibited 61% inhibition compared to the previously obtained 52% inhibition at 10 μM (see *Table 2.14*). Insertion of a carboxylate ester group at the 4-position of the imidazole core produced carboxylate derivatives **88a-d** which were found to be 1 to 5 times less potent than **83a**. The only ester showing significant inhibitory activity was **88e** (68%), which may be attributed to the absence of substituents on the 5-aryl ring which might allow the compound to adopt a geometry that favours the binding interaction.

However, after hydrolysis all five free acid derivatives **87a-e** exhibited more than 50% inhibition, with four compounds surpassing the inhibition of hit compound **83a**. Compound **87c** with a methoxy substituent at the *meta*-position of the 5-aryl ring exhibited 100% inhibition in the AlphaScreen assay. Similarly, when a methyl substituent was present at the *meta*-position (**87d**) there was also comparable inhibition. Moreover, replacing the electron-donating group at the *meta*-position in **87c** by a fluorine atom (**87b**) showed a decrease to 81% inhibition. In compound **87e** where there is no substituent on the 5-aryl ring, 75% inhibition was still shown. Lastly, the analogue with a 4-fluorine atom (**87a**) showed inhibition of 57%. Compounds **87a-e** were further evaluated *via* the Truhit kit assay to determine whether there were colour quenchers, light scatterers, singlet oxygen quenchers and biotin mimetics meddling with the signal of the AlphaScreen test. The compounds, however, were confirmed as true hits (not false positives).

Although the number of compounds tested was small, the following information can be abstracted from their biological data: (i) the presence of *meta*-substituents on the 5-aryl ring seems to have a significant impact in the inhibition ability, and (ii) the presence of the carboxylic acid group plays a major role in preventing the interaction between the HIV-1 IN and host LEDGF/p75 proteins as previously reported.^{226,227}

In a dose range assay, these compounds **87a-e** produced IC_{50} values ranging from $33.4 \pm 1.34 \mu\text{M}$ to $302.0 \pm 1.34 \mu\text{M}$ as recorded in *Table 2.14*. These IC_{50} values were much higher than the IC_{50} value of the hit compound **83a** ($25.07 \pm 2.47 \mu\text{M}$). The IC_{50} values of compounds **87a-e** appeared to be high, but these values may not be reliable because the compounds were found to have poor aqueous solubility. The best five compounds **87a-e** were subsequently assessed for their preliminary *in vitro* cytotoxicity and antiviral activity. The cytotoxicity study showed that the best five compounds **87a-e** did not reduce the viability of the MT-4 cell line. In the antiviral assay, no activity was seen for any of the compounds tested, which may be due to poor solubility or an inability of the compounds to reach the target due to their poor permeability. This is not of instant concern given the fact that most of the compounds described to be inhibitors of LEDGFp75 and IN interactions display a deficiency in antiviral activity in the cell based assay.²²⁸

2.3.3.2. Assessment through ADME parameters of the synthesized compounds 87a-e

Since a lack of solubility was suspected to be the possible reason for the higher IC₅₀ values obtained, it was of interest to calculate *in silico* their ADME (Absorption, Distribution, Metabolism and Excretion) properties so as to determine the compliance of compounds **87a-e** using BIOVIA Discovery Studio version 4.0. Applying an ADME descriptors algorithm, distinct pharmacokinetic parameters like human intestinal absorption, aqueous solubility, blood brain barrier (BBB) penetration and cytochrome P450 (CYP2D6) inhibition can be mathematically estimated. Standard values of ADME parameters are listed in *Table 2.15*.

Table 2.15: Standard level information of ADME descriptors from Discovery Studio version 4.0.

Aqueous Solubility		Blood Brain Barrier Penetration		Human Intestinal Absorption		CYP2D6	
level	intensity	level	Intensity	level	intensity	level	intensity
0	Extremely low	0	Very high	0	Good	0	Non inhibitor
1	slight	1	High	1	Moderate	1	Inhibitor
2	low	2	Medium	2	Poor		
3	good	3	Low	3	Very poor		
4	optimal	4	Undefined				
5	too soluble						

The well-known FDA approved integrase inhibitor, raltegravir, was used as a positive control and the results of ADME predictions are recorded in *Table 2.16*. Predicted aqueous solubility (expressed as logSw as conducted in water at 25°C) for compounds **87a-e** indicate they may be slightly soluble in water (level 2) whereas for raltegravir the prediction was good (level 3). The low solubility predicted for **87a-e** could be seen as a possible indication that low solubility may have had some effect on their (higher) IC₅₀ values. Furthermore, the predicted ADME AlogP98 results (associated with lipophilicity) indicate that these compounds could be poorly absorbed by the intestine (compared to raltegravir). The ADME BBB (Blood Brain Barrier) predicted levels were medium to high (level 2 to 1) suggesting that these scaffolds may pass through the blood brain barrier. These compounds were predicted to be non-inhibitors of cytochrome P450 (CYP2D6), which could indicate that they might well be processed in phase I metabolism.

Besides the low aqueous solubility and human intestinal absorption, prediction results are encouraging.

Table 2.16: ADME prediction for the synthesized compounds **87a-e** obtained from Discovery Studio version 4.0.

Compounds	ADMET Solubility values	ADMET Solubility Level	Human Intestinal Absorption (ADMET_AlogP98)	Blood-Brain Barrier (ADMET_BBB level)	CYPD2D6 inhibition
87a	-4.052	2	2.847	2	No
87b	-4.563	2	2.847	1	No
87c	-4.318	2	2.625	2	No
87d	-4.061	2	3.128	2	No
87e	-4.311	2	2.642	2	No
Raltegravir	-2.198	3	-0.994	4	No

2.3.4. Molecular modeling of the synthesized 1-(4-bromophenyl)-5-aryl-1*H*-imidazole-4-carboxylic acid derivatives **87a -e**

Molecular modelling has become a critical process in drug design, offering an insight into the specific chemical features involved in the possible interactions between the modelled docked compounds and the protein of interest. Five compounds **87a-e** (i.e. scaffolds with more than 50% inhibition in the AlphaScreen assay) were modelled to predict their binding mode by docking into the HIV-1 allosteric site at the IN-LEDGF/ p75 interface. The X-ray structure of the HIV-1 IN in complex with the LEDGF/p75 (PDB code: 2B4J) was retrieved from the protein databank, followed by removal of the LEDGF/p75 from the complex, preparing the HIV-1 IN, pinpointing the binding pocket at the IN monomers interface and then defining them as spheres (*Figure 2.3*) using the BIOVIA Discovery Studio™ version 4.0 package.²²⁹ Before docking, compounds were minimized to their lowest energy and all possible 3D structures of molecules were created using the prepare ligand procedure. The scaffolds were then primarily positioned in the same site where LEDGF/p75 binds to the HIV-1 IN dimer using the LibDock protocol, resulting in the generation of hundreds of poses for each compound. These poses were exposed to Jain, PLP2 and LibDock scoring protocols, and then analysed, and further optimised

by *in-situ*-energy-minimisation and flexible docking. The binding energies of the best poses generated from *flexible docking* were then calculated and the results are shown in *Table 2.15*.

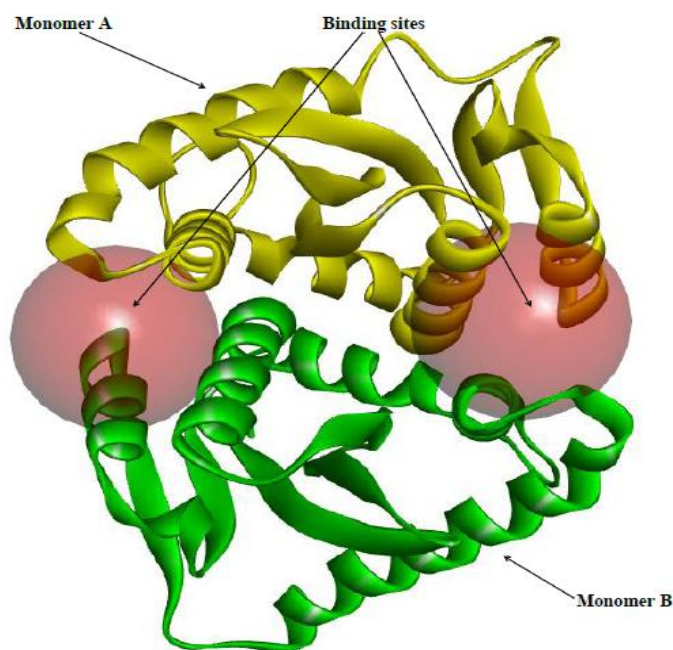


Figure 2.3: The dimeric structure of HIV-1 IN with monomer A in yellow and monomer B in green.

The predicted models of the docked compounds **87a-e** were analysed based on the interaction of four structural features, namely: carboxylic acid group, imidazole moiety, substituted-aryl ring and 4-bromophenyl group. The docking results predicted that compound **87c** was most favourable with the lowest calculated binding energy (-102.6620 kcal/mol) followed by other scaffolds in binding energy order of **87d** < **87b** < **87e** < **87a** (*Table 2.17*). The lower the binding energy the tighter the compound binds to the target. The order predicted by the binding energies correlates with the percentage inhibition data obtained from the AlphaScreen assay. Molecular docking further suggested that compounds **87a-e** were interacting with amino acid residues of the HIV-1 IN at the interface in a manner similar to that of the LEDGF/p75 protein. Models also suggested that the carboxylic acid group and the various substituents on the 5-aryl group have some impact on the binding of these compounds.

Table 2.17: A list of *in silico* interactions of compounds **87a-e** and binding site amino acids according to order of -PLP2 scoring function and their binding energy.

Comps.	Binding energy Kcal/mol	Amino acids interactions	(-)PLP2 scoring function	Jain scoring function	LibDocked Scoring functions
87c	-102.6620	Gln95, Tyr99, Ala98, Leu102, Ala128, Ala129, Ala169, Trp131	72.44	5.09	39.9524
87d	-75.9690	Gln95, Ala98, Leu102, Ala128, Glu170, His171, Trp131	71.29	1.32	52.7142
87b	-75.7536	Gln95, Ala98, Ala169, Glu170, His171, Trp131, Trp132	64.62	1.90	53.0888
87e	-33.6241	Gln95, Ala98, Glu170, His171, Trp131	62.97	1.92	28.3279
87a	-13.2486	Gln95, Ala98, Ala169, Glu170, His171, Trp131, Trp132	61.74	1.70	49.3002

A detailed examination of the predicted model for **87c** (Figure 2.4) at the HIV-1 IN interface reveals its carboxylic acid group formed two hydrogen bonds with the Gln95 and the Tyr99 residues whilst its *meta*-methoxy group was projected to make a hydrogen bond with the Ala169 residue. Furthermore, the 5-aryl group and the imidazole moiety exhibited a hydrophobic contact with the Gln95, Leu102 and Ala129 residues. Additionally, the 4-bromophenyl group and its bromine atom were predicted to occupy the hydrophobic pockets formed by the residues Ala128 and Trp131.

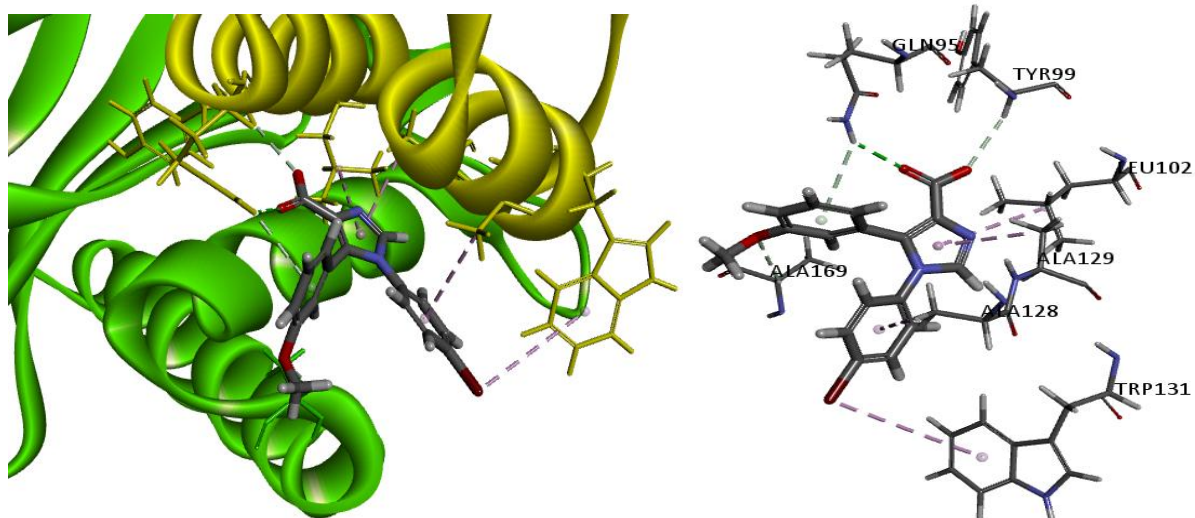


Figure 2.4: Predicted binding models of **87c** in grey, red and blue stick docked onto IN (yellow and green on the left and right side indicate the zoomed binding residues) at the LEDGF/p75 binding interface

For the carboxylic acid group of compound **87d** (Figure 2.5) two hydrogen bond interactions with backbone His171 of monomer B and one hydrogen bond to the Gln95 of monomer A were observed, whilst the imidazole moiety was projected towards the hydrophobic pockets formed by the Glu170 residue of monomer B. Additionally, the *meta*-methyl group was observed to be packed into hydrophobic pockets of the Ala98 and the Leu102 residues whereas its aryl ring formed hydrophobic interactions with the Ala98 and the Ala128 of monomer A. Finally, the bromine atom was projected to interact *via* a hydrophobic contact with Trp131 of monomer A.

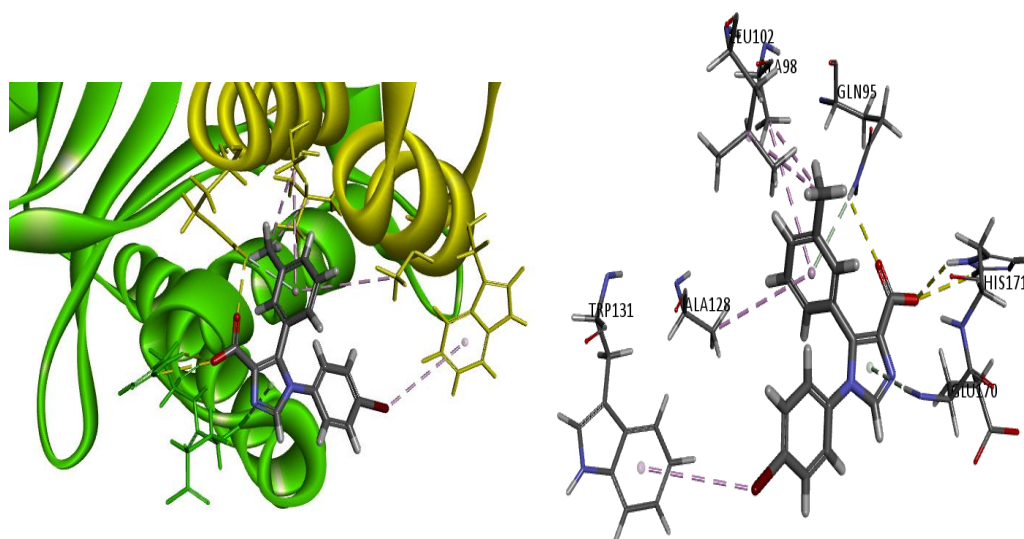


Figure 2.5: Predicted binding models of **87d** in grey, red and blue stick docked onto IN (yellow and green on the left and right side indicate the zoomed binding residues) at the LEDGF/p75 binding interface.

The binding model of **87b** (Figure 2.6) predicted that the carboxylic acid group formed one less hydrogen bond to the His171 residue of subunit B and the imidazole moiety made similar interactions to those in the model of compound **87d**, while a *meta*-fluorine atom formed an interaction with the Ala98 residue and its aryl group was projected to be packed into the hydrophobic pockets formed by IN residues Ala98 and Gln95 of monomer A. The bromine atom is shown to make hydrophobic interactions with both Trp131 and Trp132 of subunit A.

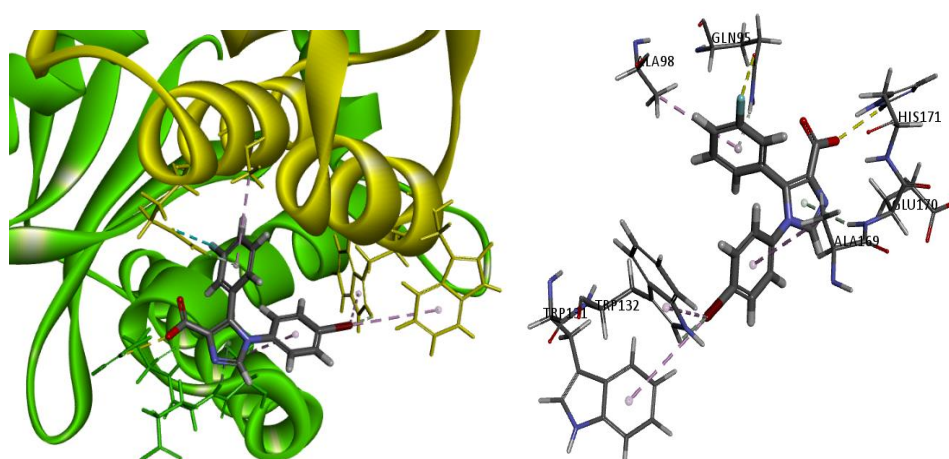


Figure 2.6: Predicted binding models of **87b** in grey, red and blue stick docked onto IN (yellow and green on the left and right side indicate the zoomed binding residues) at the LEDGF/p75 binding interface

Inspection of the binding model of compound **87e** (Figure 2.7) revealed that its carboxylic acid group and unsubstituted aryl ring formed similar interactions observed in the predicted binding model of compound **87b**, whilst the imidazole core formed similar hydrophobic interactions to those observed in both compounds **87b** and **87d**. The bromine atom showed a similar binding mode to that exhibited by compounds **87b**, **87c** and **87d**.

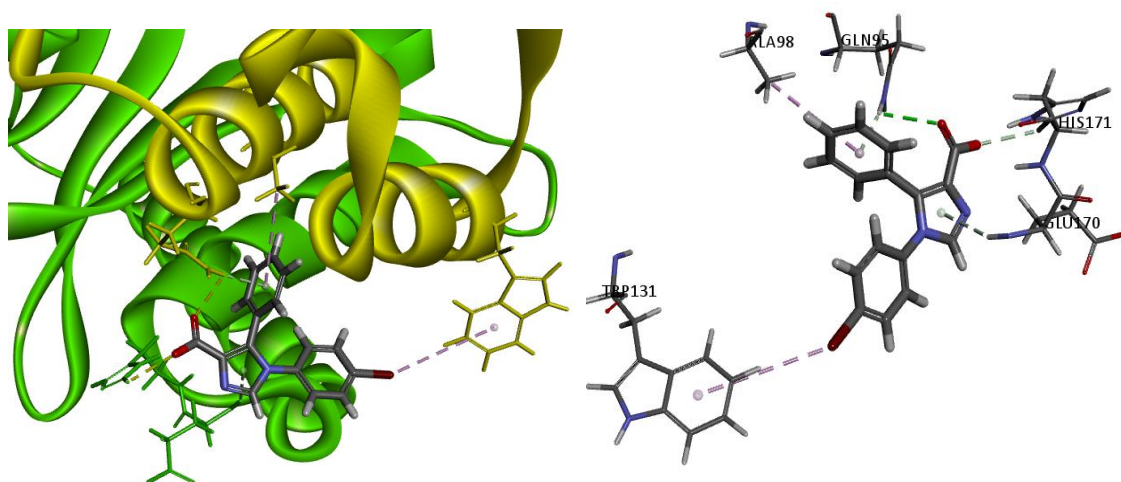


Figure 2.7: Predicted binding models of **87e** in grey, red and blue stick docked onto IN (yellow and green on the left and right side indicate the zoomed binding residues) at the LEDGF/p75 binding interface.

The model of compound **87a** (Figure 2.8) is predicted to have a similar binding mode to **87b** and **87d** whilst its *para*-fluorine atom interacts with the Gln95 residue of monomer A. However, this compound further showed that the aryl ring of the bromophenyl group was involved in hydrophobic interactions with the Ala169 amino acid of monomer B, while its bromine atom displays similar hydrophobic interactions exhibited by compound **87b**.

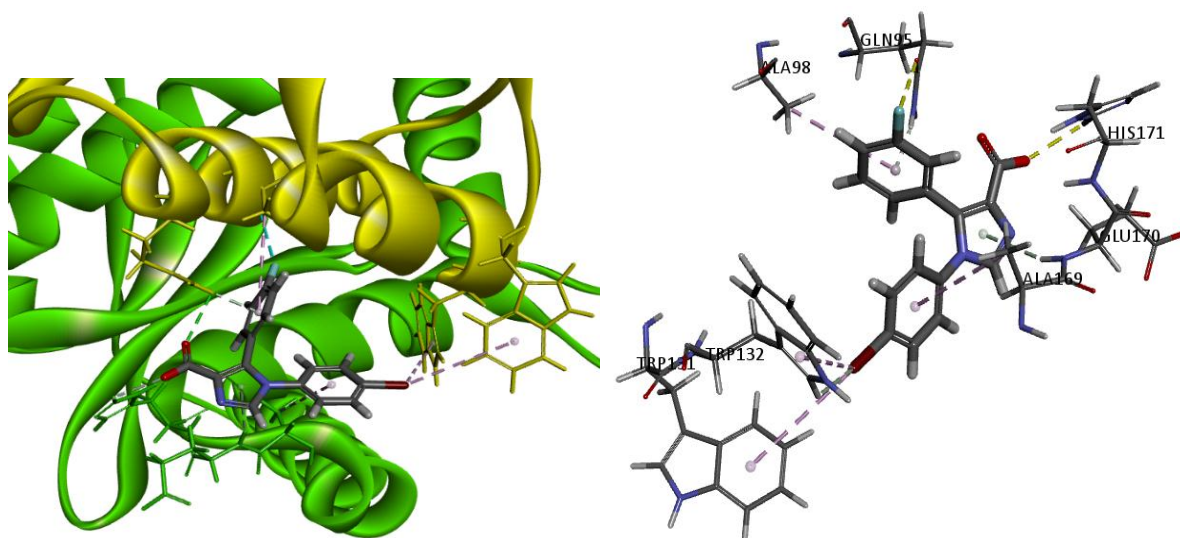


Figure 2.8: Predicted binding models of **87a** in grey, red and blue stick docked onto IN (yellow and green on the left and right side indicate the zoomed binding residues) at the LEDGF/p75 binding interface.

In brief, the results suggest that the presence of a *meta*-substituent on the 5-aryl group could be associated with better potency. The methoxy group was most favourable due to the presence of an electronegative group which could form a hydrogen bond with Ala169. Possible binding modes for compounds **87a-e** to HIV-1 IN were predicted using molecular modeling and it was found that these scaffolds were making some hydrogen bonds and hydrophobic interactions with essential amino acid residues significant for IN-LEDGF/p75 interactions.

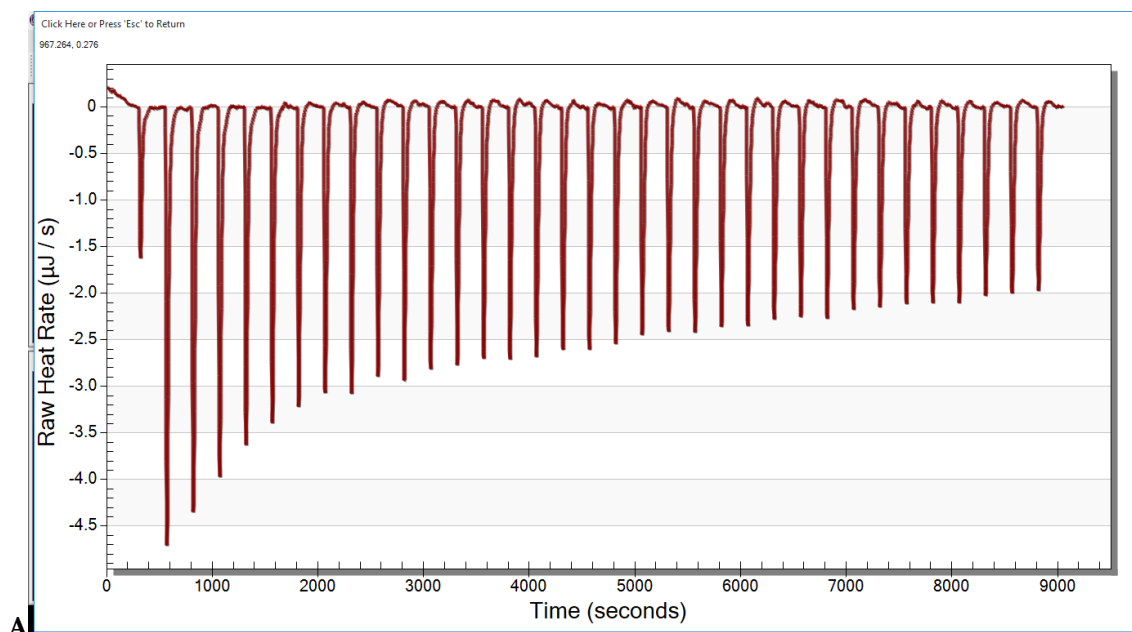
2.3.5. Preliminary Isothermal Calorimetry Titration (ITC) Study

We attempted to determine the thermodynamic parameters of 1,5-diaryl-1*H*-imidazole-4-carboxylic acid based HIV-1 IN-LEDGF/p75 inhibitors **87a-e** alongside CX05168 as a control compound (a compound known to inhibit HIV-1 IN-LEDGF/p75 interactions)⁵³ using a VP-ITC MicroCalorimeter™. The ITC studies were conducted at the University of the Witwatersrand, Department of Protein Structure-Function Research Unit in the School of Molecular and Cell Biology under guidance of Professor Yasien Sayed.

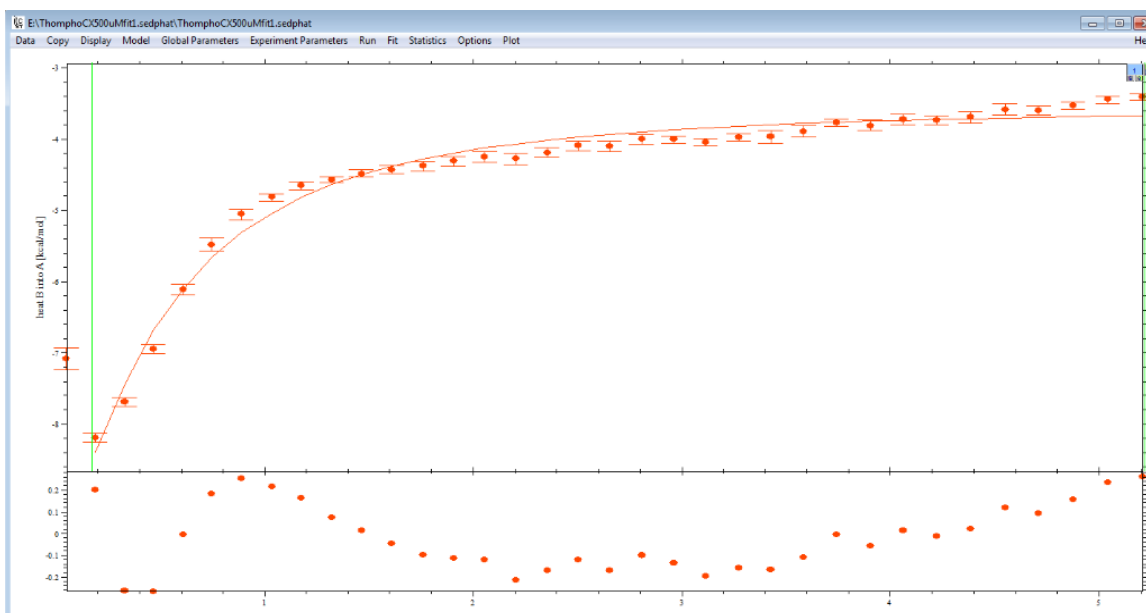
The ITC experiments were conducted by titrating the compound into the ITC cell containing HIV-1 IN. Initially the intention was to establish the proper protocol which can demonstrate the thermodynamic parameters of compound CX05168 binding to the HIV-1 IN protein as a control experiment. The ITC experiment was designed to initially inject 500 μM concentration of control compound into an ITC cell containing 25 μM of HIV -1 IN. The first injection

produced a small peak, which can be attributed to diffusion of titrant into titrate during equilibration. The preliminary ITC data (*Figure 2.9 A and B*) showed that the titration of control compound into HIV-1 IN displayed an exothermic titration reaction. As the titration continues, heat released gradually decreases but saturation could not be reached at a compound concentration of 500 μM . The integration and normalization of the exothermic peaks produced a hyperbolic curve relating to the amount of control compound added. The hyperbolic curve obtained was missing a pre-transition state region. However, increasing the concentration of the control compound to 1000 μM allowed for saturation to be successfully attained but the pre-transition was still deficient (*Figure 2.10 C and D*). The non-existence of the pre-transitions in the hyperbolic curve make it difficult to obtain the correct thermodynamic parameters such as enthalpy change (ΔH) for the experiment, which means that the free binding energy (ΔG) of the experiment could not be properly determined. Hence the binding affinity (K_D) of the control compound which is directly related to ΔG , could not be properly established.

The ITC experiment was also conducted using compound **87b** which was identified as a potential inhibitor of HIV-1 -IN LEDGF/p75 interaction through AlphaScreening. The preliminary ITC experiment results showed that titration at 500 μM concentration of the compound **87b** into an ITC cell containing HIV-1 IN was an exothermic reaction. However, as the titration continued, saturation could not be reached. Even further optimization by varying the concentration of compound **87b** between 1000 μM to 20 mM (*Figure 2.11*), did not allow saturation to be reached. The results suggest that compound **87b** could be weakly binding to the HIV-1 IN protein. The inability of this compound **87b** to reach saturation could also be attributed to the fact that the part of the scaffold also binds to the LEDGF/p75 protein, which is not present in the titration. Although the preliminary ITC data of compound **87b** thus far shows that the scaffold did not reach saturation, the data obtained offers proof that the compound is truly binding to HIV-1 IN. Further investigations into proper protocols to establish the binding constants (K_D) and other thermodynamic parameters of both synthesized compounds and the control compound to the HIV-1 IN protein are ongoing, but due to time constraints no further results could be included here.

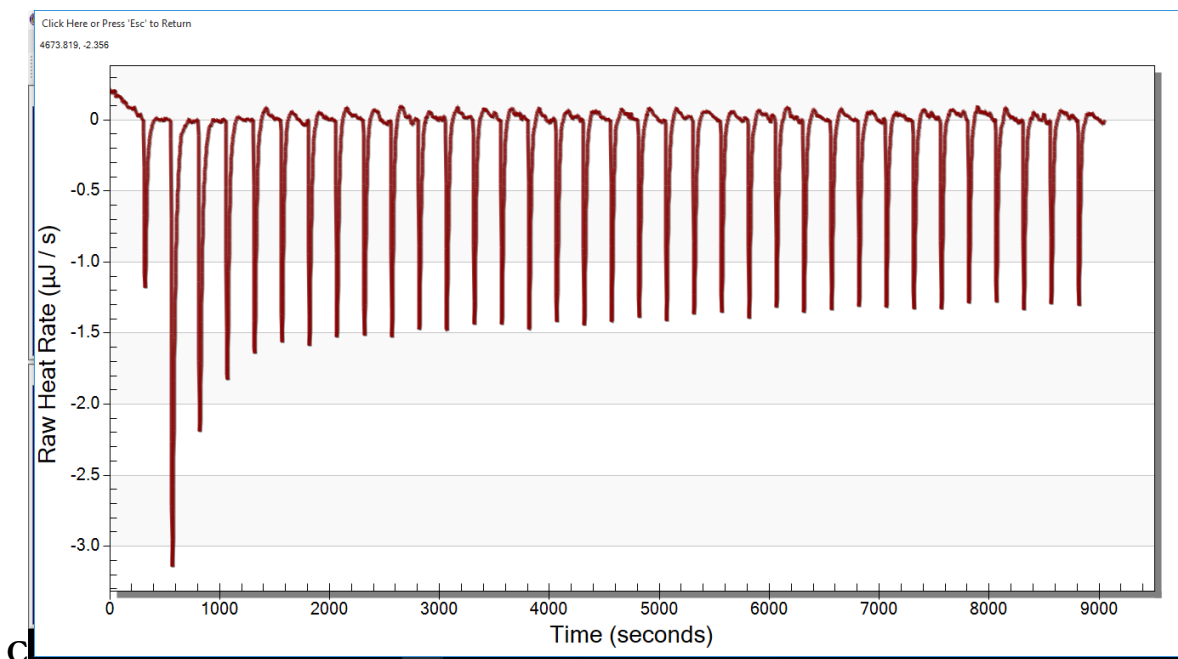


A

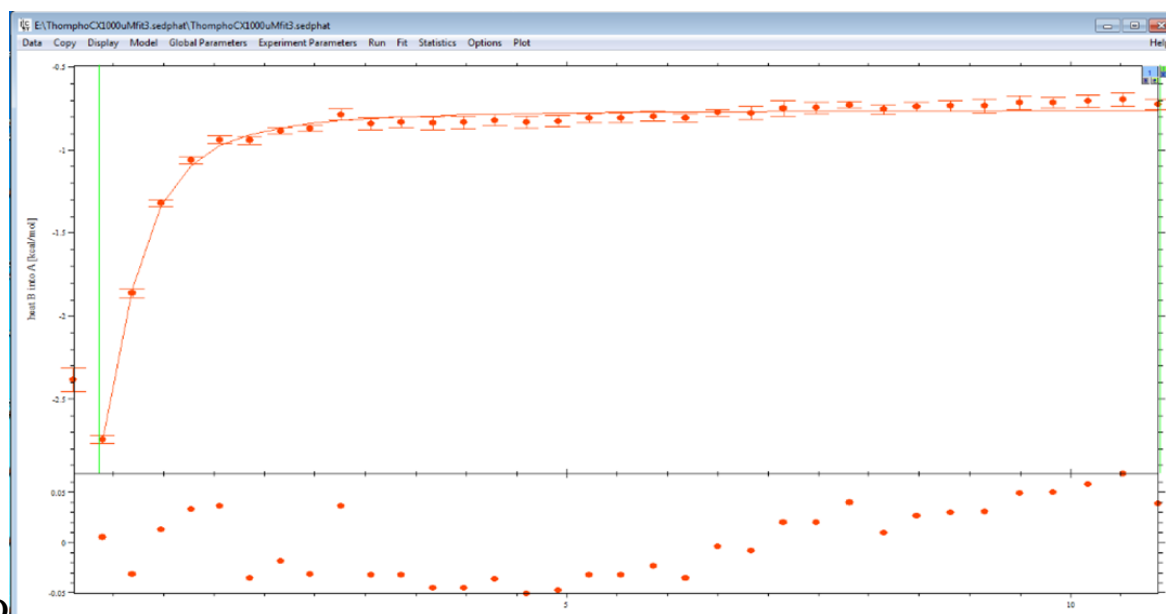


B

Figure 2.9: **A)** Raw titration data of CX05168 compound (500 µM) with HIV-1 IN (25 µM) measured in µJ/s. Each peak corresponds to a single injection of compound solution into the HIV-1 suspension; **B)** The fitted titration data to the injection of 500 µM of control compound into 20 µM of HIV-1 IN.



C



D

Figure 2.10: C) Raw titration data of CX05168 compound (1000 μM) with HIV-1 IN (25 μM) measured in $\mu\text{J}/\text{s}$. Each peak corresponds to a single injection of compound solution into the HIV-1 suspension; D) The fitted titration data to the injection of 500 μM of control compound into 20 μM of HIV-1 IN.

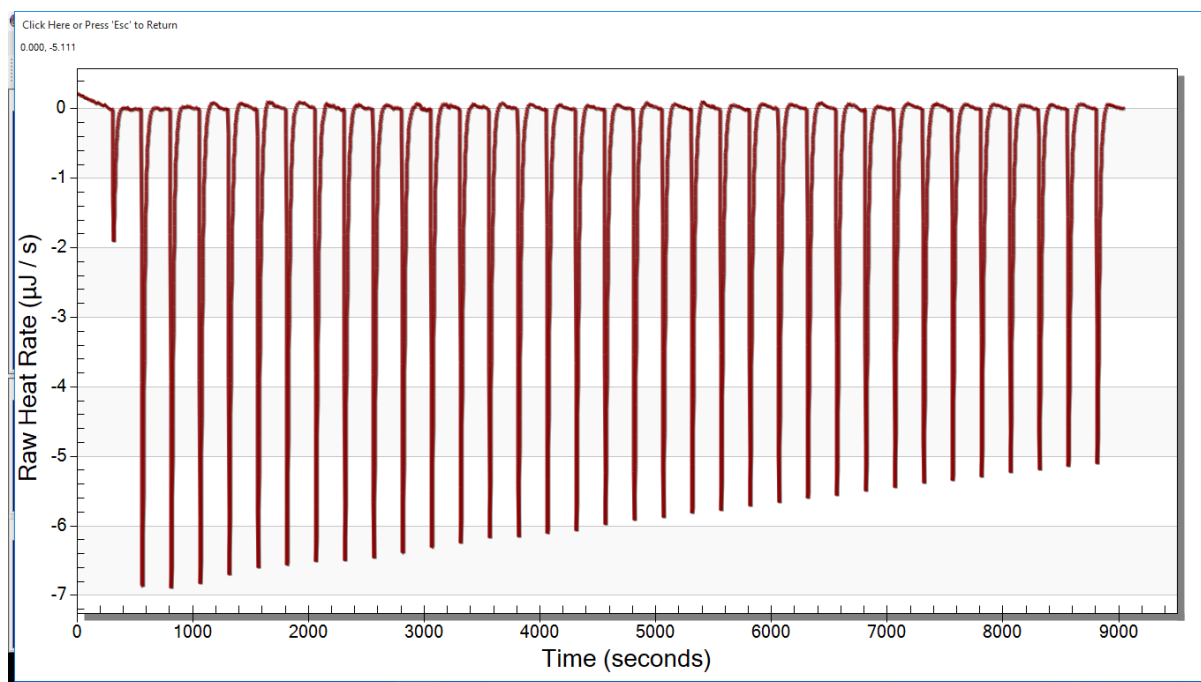


Figure 2.11: Raw titration data of compound **87b** (20 mM) with HIV-1 IN (25 μ M) measured in μ J/s. Each peak corresponds to a single injection of compound solution into the HIV-1 suspension.

2.4. Conclusions

With the aim of producing small heterocyclic fragments from which to identify viable hits to be developed into drug like compounds, a small library of imidazole-based fragments was successfully synthesized *via* the van Leusen reaction. Intermediate *N*-(arylidene)alkylamines were obtained in excellent yields by reacting benzaldehydes and primary amine derivatives using both conventional and microwave heating, with microwave irradiation resulting in an increase in the reaction rates. Further treatment of *N*-(arylidene)alkylamines with TosMIC and K_2CO_3 in dry MeCN, by both conventional and microwave assisted methods, gave a series of 1-substituted-5-aryl-1*H*-imidazole derivatives in yields ranging from poor (for those with electron-withdrawing substituents at the *ortho*-position of the phenyl ring) to high (for those with electron-donating groups in both *para* and *ortho* positions). The 1-substituted-5-aryl-1*H*-imidazole derivatives were also obtained in a one pot synthesis by *in situ* generation of the *N*-(arylidene)alkylamines by irradiation of a mixture of aryl aldehydes and aliphatic amines; followed by addition of TosMIC and K_2CO_3 in MeCN, with yields similar to those obtained in a stepwise manner. The preparation of imidazoles in MeOH proved to be more challenging due to the inherent preference of TosMIC to react with MeOH to afford products such as *E* and *Z*-

HOCH₂N=CH(OMe). Out of the twenty six prepared 1-substituted-5-aryl-1*H*-imidazole derivatives, twenty five are new and only one has been reported previously. Biological screening of compounds was performed in an HIV-1 IN-LEDGF/p75 assay and a Vpu binding assay.

Six fragments exhibited more than 50% inhibition of the HIV-1 IN- LEDGF/p75 interaction. These compounds produced IC₅₀ values of 7-30 μM and were not toxic to MT-4 cells, with CC₅₀ values between 21.77 - 55.47 μM. None of the compounds showed activity in the Vpu binding assay.

As part of the efforts to improve the potency of the hit compounds in the HIV-1 IN-LEDGF/p75 assay, hit analogues were designed and synthesized by introducing a carboxylic functionality at the 4-position of the imidazole moiety. This was successfully achieved by first react various anilines with benzoic chlorides using Et₃N in ethyl acetate at room temperature, affording *N*-aryl-benzamides in good yields. These *N*-aryl-benzamides were then treated with SOCl₂ to give *N*-aryl-benzimidoyl chlorides **90** in excellent yields. However, when the aniline ring was occupied by chlorine substituents at the *para*-and *ortho*-positions only traces of the desired chlorides were observed (¹H NMR spectroscopy). The *N*-aryl-benzimidoyl chlorides obtained were further reacted with ethyl isocyanide catalyzed by DBU in THF at -78°C to room temperature for 48 hours, affording a series of new ethyl 1,5-diaryl-1*H*-imidazole-4-carboxylates bearing 4-bromophenyl substituted at the 1-position of the imidazole moiety in low to moderate yields. Attempts to improve the low yields and failed conversion for some of the *N*-aryl-benzimidoyl chlorides by direct conversion of benzamides into ethyl 1,5-diaryl-1*H*-imidazole-4-carboxylates using diethyl chlorophosphate in the presence of catalytic ^tBuOK in THF at low temperature were unsuccessful. These carboxylate derivatives obtained were then hydrolysed into the corresponding 1,5-diaryl-1*H*-imidazole-4-carboxylic acids in excellent yields.

All newly synthesized compounds including the carboxylate derivatives and chosen hit compound **83a** were evaluated as potential inhibitors of the HIV-1 IN- LEDGF/p75 interaction in an AlphaScreen Assay at 100 μM. The introduction of the ester group in ethyl 1,5-diaryl-1*H*-imidazole-4-carboxylate derivatives resulted in 1 to 5 times lower percentage inhibition than the original hit. However, after hydrolysis all five 1,5-diaryl-1*H*-imidazole-4-carboxylic acid derivatives exhibited more than 50% inhibition in the AlphaScreen assay, with four compounds surpassing that of the hit. These 1,5-diaryl-1*H*-imidazole-4-carboxylic acids were confirmed as true hits (not false positives) *via* the Truhit kit assay. However, in dose range assays these compounds produced higher IC₅₀ values than the original hit compound which could be due to their insolubility. *In silico* docking studies predicted favourable interaction of 1,5-diaryl-1*H*-

imidazole-4-carboxylic acids with critical amino acids in a similar way to how the LEDGF/p75 protein binds to HIV-1 IN, while their binding energies are in accordance with the % inhibition activity emerging from AlphaScreen data. It was apparent that the introduction of a carboxylic acid group and the presence of *meta*-substituents on the 5-aryl ring have a significant impact on the binding capability of the scaffolds. Although these compounds did not reduce the viability of the MT-4 cell line, they also did not display antiviral effects in cell based assays, which may be due to poor permeability or even poor compound solubility.

Overall: Novel 1,5-diaryl-1*H*-imidazole-4-carboxylic acid derivatives were designed and synthesized as a second generation of 1,5-diaryl-1*H*-imidazoles. Four compounds showed better inhibition of the HIV-1 IN -LEDGF/p75 interaction in a direct single dose assay at 100 μ M than their non-carboxylated 1,5-diaryl-1*H*-imidazole predecessors. The newly synthesized compounds described in this chapter have not been used previously reported nor have they used been evaluated for targeting the interaction between LEDGF/p75-HIV-1 IN proteins.

2.5. Future work

The structural modification of substituents at the 1- and 5-positions of the imidazole ring, as well as extension of the chain along the carboxylic acid moiety, will be conducted with the potential to improve the direct inhibition values and ADME properties (such as better solubility and permeability) towards more effective inhibitors of HIV-1 viral replication (*Figure 2.12*).

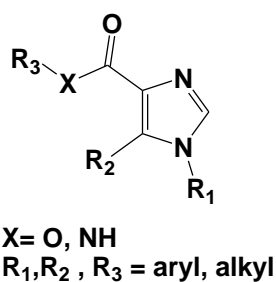


Figure 2.12: Possible structural modification of the imidazole motif.

CHAPTER 3

Synthesis of 5-aryl-1,3-oxazole compounds by means of microwave assisted van Leusen reaction and their biological evolution as possible HIV-1 inhibitors

3.1. Introduction

Synthesis of a library of 5-aryl-1,3-oxazole fragments was undertaken in the hope that the screening of these oxazoles might also provide a starting point for synthetic optimization of identified hits that could demonstrate the capability to disrupt the interactions between HIV-1 protein and host protein. In line with our objectives described in Chapter 1, we wished to explore the preparation of the 5-aryl-1,3-oxazole scaffolds *via* the van Leusen approach using microwave irradiation (MW) as a source of reaction energy. This chapter addresses the synthesis, characterization, mechanistic pathways and biological data of the synthesized oxazole compounds.

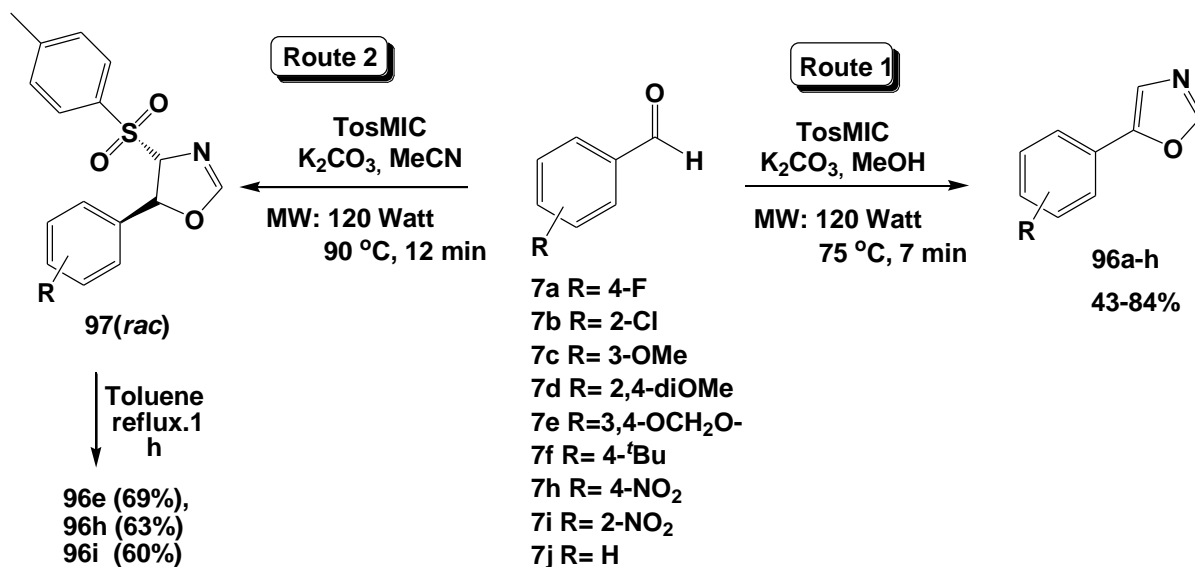
3.2. Synthesis of 5-aryl-1,3-oxazoles

The approach that utilizes TosMIC **1** as a synthon, in the preparation of oxazole heterocyclic compounds is commonly known as the van Leusen oxazole reaction.²³⁰ In this synthetic protocol, TosMIC **1** undergoes cyclo-addition to the carbonyl compounds **37** in the presence of catalytic base using aprotic solvents to provide 5-substituted-oxazole derivatives **34** (*see Scheme 1.15*, Chapter 1). In many instances, microwave irradiation has been shown to decrease significantly reaction time and increase reaction yields.¹⁹⁶⁻¹⁹⁹ In chapter 2, application of microwave irradiation to the van Leusen imidazole reaction was indeed shown to reduce the reaction time. With this in mind, and considering our interest in finding a more convenient preparation to build heterocyclic rings, we then focused our synthetic efforts on exploring the use of TosMIC **1** as a starting material under microwave irradiation to produce oxazoles in methanol or acetonitrile as solvents. Reaction progress was monitored by Thin Layer Chromatography (TLC).

3.2.1. Using MeOH as solvent

The synthesis of the desired heterocycles was first carried out in methanol as depicted in *Scheme 3.1* (Route 1). Precisely, a mixture of TosMIC **1**, benzaldehyde **7a-h** and a catalytic amount of K₂CO₃ in dry MeOH was microwave irradiated in a pressurized vessel, at a set temperature of 75°C and 120 Watts under inert conditions. Remarkably, TLC analysis indicated

that the reaction reached completion after just 7 minutes of irradiation. Isolation and purification of the crude materials using column chromatography afforded the corresponding 5-aryl-1,3-oxazoles **96a-h** in yields ranging from 43 % to 84 % (see Table 3.1).



Scheme 3.1: Synthesis of 5-aryl-1,3-oxazole **96** and (4*R*,5*R*)/(4*S*,5*S*)-5-aryl-4-tosyl-4,5-dihydro-1,3-oxazoles **97** under MW.

Table 3.1: Isolated yields (%) of the 5-aryl-1,3-oxazoles **96a-h** by route 1.

Compounds	R	Yields (%)
96a	4-F	84
96b	2-Cl	74
96c	3-OMe	60
96d	2,4-diOMe	44
96e	3,4-OCH ₂ O-	43
96f	4- ^t Bu	59
96g	4-NO ₂	73
96h	2-NO ₂	68

3.2.2. Using MeCN as solvent

In order to investigate the effect of other solvents on the reaction, three aldehydes with different electron donor substituents on the ring (**7e**, **7h** and **7i**) were chosen to react under the above described conditions, but using dry acetonitrile as solvent as shown in **Scheme 3.1** (Route 2). After 12 minutes TLC analysis showed the consumption of the starting materials, however the isolation of the products showed that the elimination of the *para*-toluenesulfonyl group had not occurred, affording instead the 5-aryl-4-tosyl-2,4-dihydro-1,3-oxazole intermediates **97e**, **97h**, and **97i** each as a racemic mixture in yields ranging from 65-80% (**Table 3.2**). We assume the geometry of these products to be *trans*, corresponding to the (4*R*, 5*R*) / (4*S*, 5*S*)-isomers, which matches the NMR spectroscopic data, including coupling constants, reported in the literature.²³¹ These (4*R*,5*R*)/(4*S*,5*S*)-5-aryl-4-tosyl-2,4-dihydro-1,3-oxazoles **97e**, **97h** and **97i** were then refluxed in toluene for 1 hour in accordance with the reported literature to afford the corresponding 5-aryl-1,3-oxazoles **96e**, **96h** and **96i** after column chromatography.²³² The overall yields of these three compounds *via* the acetonitrile reaction were higher than their corresponding yields in MeOH.

A possible explanation for non-aromatization of compounds **97** in MeCN could be attributed to a decrease in acidity of the proton at the 5-position of the five-membered ring, which allows the reaction to stop at the oxazoline intermediate. An alternative explanation could be that the nucleophilic protic solvent MeOH may assist in the elimination of the tosyl group.

Table 3.2: Isolated yields (%) of (4*R*,5*R*)/(4*S*,5*S*)-5-aryl-4-tosyl-4,5-dihydro-1,3-oxazoles **97**.

Compounds	R	Yields (%)
97e	3,4-OCH ₂ O-	80
97h	2-NO ₂	65
97i	H	76

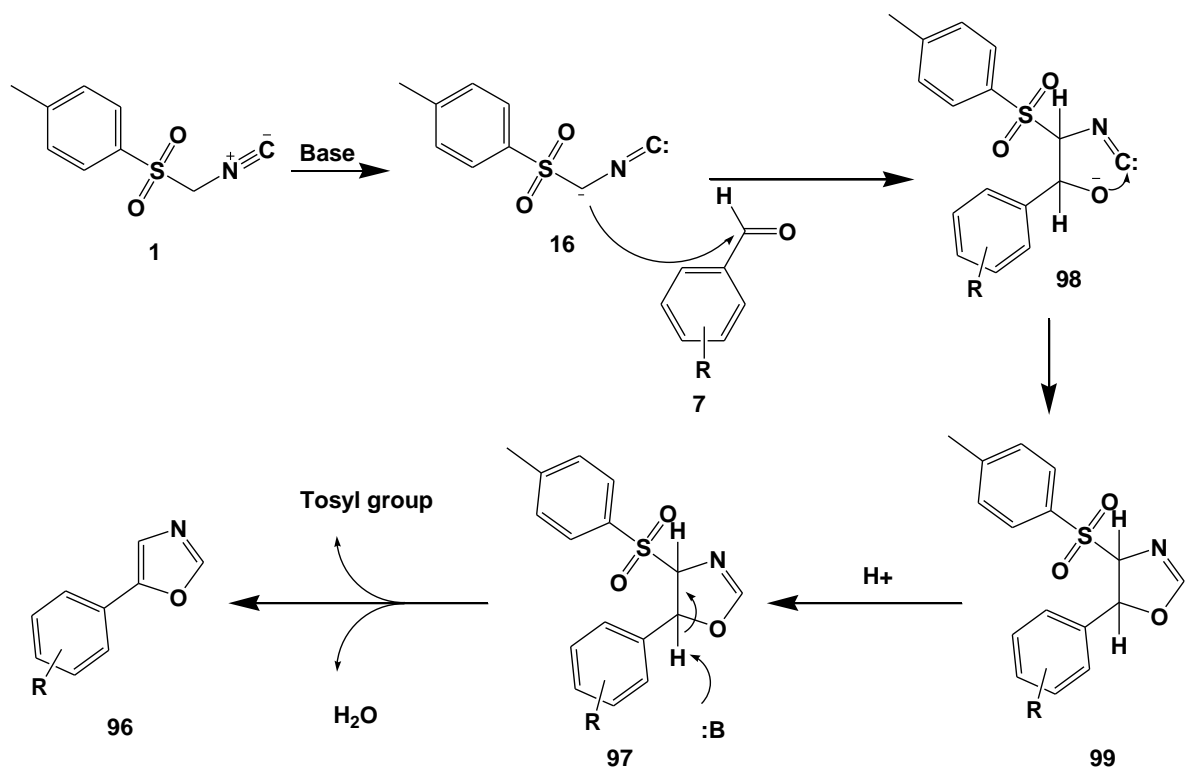
Table 3.3 below shows a comparative summary between literatures reported conventional methods, and the microwave methods developed here.

Table 3.3: Conventional vs microwave assisted reaction times for the preparation of oxazoles **96b** and **96h** and oxazolines **97e** and **97i** under similar conditions.

Compound		Reference	Solvent	Base	Temp.	Time	Yields (%)
Oxazoles	96b	Flegeau <i>et al.</i> ²³³	MeOH	K ₂ CO ₃	Reflux	14 h	84
		MW	”	”	75°C	7 min	74
	96h	Mayuko <i>et al.</i> ²³⁴	MeOH	K ₂ CO ₃	70°C	7 h	67
		MW	”	”	75°C	7 min	68
Oxazolines	97e	Companyó <i>et al.</i> ²³²	MeOH	Et ₃ N	r.t	16 h	80
		MW	ACN	K ₂ CO ₃	90°C	12 min	68
	97i	van Leusen <i>et al.</i> ²³¹	MeOH	”	r.t	2 h	94
		MW	ACN	”	90°C	12 min	76

3.2.3. Mechanism for the formation of oxazoles **96** and oxazolines **97**

The formation of the products **96** and **97** can be explained by the mechanistic pathway illustrated in **Scheme 3.2**. The first step involves the deprotonation of one of the α -methylene protons of the TosMIC by catalytic base to generate anion **16**.²³⁰ This anion **16** then attacks the aldehyde **7** to give an intermediate **98**, which then undergoes cyclization through the bond formation between the oxygen atom and the isocyno group to give the five membered ring system **99**. The protonation of **99** affords the oxazoline intermediate **97**, followed by aromatization by displacement of the tosyl group to afford the desired 5-aryl-1,3-oxazoles **96**.



Scheme 3.2: Mechanism for the formation of the 5-aryl-1,3-oxazoles **96**.

Although further investigation on the effect of reaction conditions under microwave irradiation on these oxazole derivatives might be undertaken, the microwave-assisted preparation of 5-aryl-1,3-oxazoles and (4*R*,5*R*)/(4*S*,5*S*)-5-aryl-4-tosyl-2,4-dihydrooxazoles, when compared to conventional methods, clearly results in a reduction in the reaction times from several hours to a few minutes. Furthermore, these 5-aryl-1,3-oxazoles **96a-h** and (4*R*,5*R*)/(4*S*,5*S*)-5-aryl-4-tosyl-2,4-dihydro-1,3-oxazole intermediates (**97e**, **97h**, and **97i**) have previously been reported, but the use of microwave irradiation to the best of our knowledge is a new synthetic approach. In total twelve (12) compounds were obtained from the microwave assisted-van Leusen reaction.

3.2.4. NMR Spectra of 5-aryl-1,3-oxazole and (4*R*,5*R*)/(4*S*,5*S*)-5-aryl-4-tosyl-4,5-dihydro-1,3-oxazole fragments

In depth NMR spectroscopic analysis of synthesized oxazole **96d** and oxazoline **97e** will be described below as examples representing these compound classes. Other related 5-aryl-1,3-oxazoles **96** and (4*R*,5*R*)/(4*S*,5*S*)-5-aryl-4-tosyl-4,5-dihydro-1,3-oxazole compounds **97** show similar spectra (changes are mainly observed in chemical shifts of the substituents of the phenyl ring).

The unique feature in the ^1H NMR spectrum of compound **96d** was the presence of two singlets at δ 7.85 and 7.42 ppm, corresponding to the two methine protons of the oxazole motif while in the ^{13}C NMR spectrum, the two methine carbon atoms of the oxazole ring appear at δ 148.9 ppm and 123.5 ppm.

On the other hand, the ^1H NMR spectrum for compound **97e** was characterized by a doublet at δ 7.18 ppm ($J = 1.2$ Hz) corresponding to the 2-methine proton of the oxazoline motif. This splitting pattern observed is due to long range coupling with the 4-methine proton at 4.99 ppm, which resonates as a doublet of doublets with coupling constants of 4.4 Hz and 1.6 Hz (due to further coupling with the 5-methine proton). Furthermore, the 5-methine proton resonates at δ 5.94 ppm as a doublet with a J value of 6.0 Hz. Meanwhile, the ^{13}C NMR spectrum for compound **97e** showed the 2-methine carbon atom at δ 159.3 ppm, whilst the 4- and 5-methine carbon atoms resonated at δ 94.2 ppm and 79.4 ppm.

3.2.5. Mass spectral analysis of 5-aryl-1,3-oxazoles

The obtained products were further analyzed using electrospray ionization mass spectrometry (ESI-MS), providing accurate identification of the compounds. In order to determine the accurate formula of the compounds obtained, the results were analyzed using the Bruker SmartFormula3D[®], with a mass accuracy of 5 ppm (5 mDa). All compounds showed an acceptable tolerance of isotopic pattern fit factor (mSigma) lower than 20 (the lower the mSigma value the better the match) and their mass correlated with expected values (*Table 3.4*).

Table 3.4: HRMS results of compounds **96** and their mSigma values.

Compds	Calculated m/z	Chemical formula [M+1]	Measured m/z	Err (mDa)	Err (ppm)	mSigma value
96a	164.0506	C ₉ H ₇ FNO	164.0508	-0.2	-1.2	3.0
96b	180.0211	C ₉ H ₇ ClNO	180.0245	-0.3	-8.9	12.2
96c	176.0706	C ₁₀ H ₁₀ NO ₂	176.0736	-3.0	-7.2	2.6
96d	206.0812	C ₁₁ H ₁₂ NO ₃	206.0839	-2.8	-3.4	6.1
96e	190.0499	C ₁₀ H ₈ NO ₃	190.0528	-2.9	-5.2	5.6
96f	202.1242	C ₁₃ H ₁₆ NO	202.1234	-2.8	-7.6	2.3
96g	191.0451	C ₉ H ₇ N ₂ O ₃	191.0458	-0.7	-3.6	2.7
96h	191.0451	C ₉ H ₇ N ₂ O ₃	191.0475	1.6	8.6	3.8

3.2.6. Biological Evaluation of a series of 5-aryl-1,3-oxazoles and 5-aryl-4-tosyl-4,5-dihydrooxazoles

A total of 12 compounds were submitted to be evaluated in two biochemical assays and cell-based assays. The tests were conducted in triplicate and the findings are summarized in *Table 3.5*.

Table 3.5: The biological activities of the 5-aryl-1,3-oxazole **96** and (4*R*,5*R*/4*S*,5*S*)-5-aryl-4-tosyl-4,5-dihydro-1,3-oxazole derivatives **97**.

Compound	Biochemical target assays		Cell-based assays (MT-4 cells)
	HIV-1 IN – LEDGF/p75 (%) inhibition assay @ 10 μM (AlphaScreen)	HIV-1 Vpu – binding assay @ 10 μM (% inhibition) (ELISA)	Viability @ 10 μM (Absorbance value ± STD DEV)
96a	23.37±3.44	3.99	1.26 ±0.18
96b	33.35± 0.97	0.92	1.32± 0.25
96c	32.98±0.60	0	1.29±0.187
96d	41.55±1.59	17.63	1.20±0.12
96e	34.64±1.56	14.30	1.21±0.22
96f	35.34±3.76	9.70	1.23±0.26
96g	29.48±2.03	25.66	1.34±0.11
96h	32.58±3.96	0	1.20±0.13
96i	30.57 ± 1.79	15.97	1.26 ± 0.28
97e	32.90 ± 4.92	15.76	1.43 ± 0.26
97h	38.00 ± 0.60	10.24	1.34 ± 0.21
97i	33.85 ± 1.72	11.67	1.33± 0.17
CX05168	91.37+/-0.85 at 100 μM		
HIV-1 IN and LEDGF with DMSO	0		

3.2.6.1 Biochemical target assays

The compounds were assessed using two biochemical assays; namely the HIV-1 IN-LEDGF/p75 inhibition assay and the HIV-1 Vpu binding assay.

3.2.6.1.1. HIV-1 IN -LEDGF/p75 assay

The compounds were initially evaluated at 10 μ M to determine percentage disruption of the HIV-1 IN-LEDGF/p75 interaction using AlphaScreen technology. Unfortunately, the scaffolds showed marginal activity on the disruption of IN-LEDGF/p75 interactions. Compound **96d** exhibited the highest inhibitory activity of 42% at 10 μ M for the 5-aryl-1,3-oxazole group of compounds while compound **97h** was highest for the (4*R*,5*R*)/(4*S*,5*S*)-5-aryl 4-tosyl-2,4-dihydro-1,3-oxazole derivatives, with 38% inhibition against LEDGF/p75-IN interaction. This value is, however, below our pre-defined cut off value of 50%.

3.2.6.1.2. HIV-1 Vpu binding assay

In the second biochemical assay, the compounds were tested for their ability to inhibit the binding of the antibody (anti-Vpu) to Vpu using an ELISA method. None of the tested compounds showed inhibition of the antigen-antibody interaction. It is likely, however, that small molecules cannot sufficiently block this interaction as the binding site is rather large.

3.2.6.2. Cell based assay

Each compound was evaluated for toxicity in the MT-4 cell line at 10 μ M. At this initial concentration, none of the compounds reduced the viability of the cells as determined by MT-2 lymphocyte cell line; therefore the compounds are regarded as not overly toxic.

3.3. Synthesis of *N*,5-diaryl-1-3-oxazole-4-carboxamides as second generation compounds

Based on the disappointing biological results obtained from the first fragment library, we wished to explore possible second generation compounds. Examination of the original scaffolds shows the absence of key structural characteristics that could disrupt protein-protein interactions. In recent years, compounds containing *N*-aryl-4-carboxamide cores have been developed as potential inhibitors of the interaction between LEDGF/p75 and IN proteins. For instance, Cavalluzzo and co-workers²³⁵ have designed, through pharmacophore modelling, and synthesized the 3-(1*H*-indol-3-ylthio)-*N*-(2-isopropoxy-6-methoxypyridin-3-yl)benzamide derivatives (known as **CAB** compounds) containing *N*-aryl-4-carboxamide moieties (framed in *Figure 3.1*) as potential inhibitors of the HIV-1 IN and host LEDGF/p75 co-factor interactions. These

particular compounds have also been established to prevent the binding of LEDGF/p75 to its natural protein JPO2, the same site at which IN binds. The data proved that the **CAB** compounds selectively bind to the cellular cofactor LEDGF/p75. Furthermore, Serroa *et al.*¹⁸⁰ have also reported the design, *via* molecular docking, and synthesis of another class of compounds bearing *N*-aryl-4-carboxamide cores as inhibitors that targeted the LEDGF/p75-IN interaction. These compounds were found to be non-toxic and exhibited submicromolar IC₅₀ values.

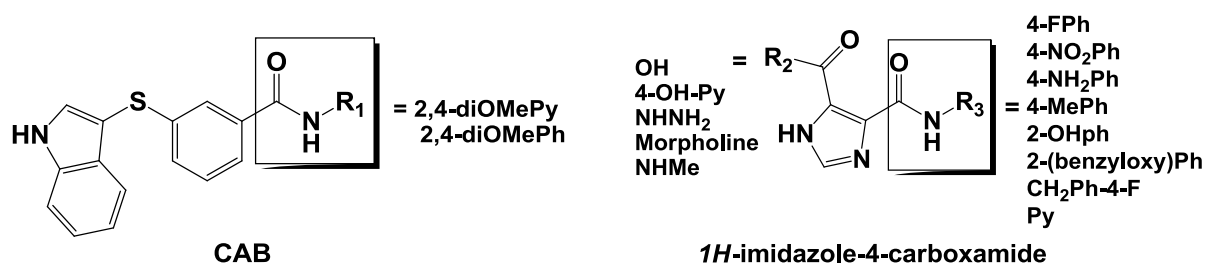
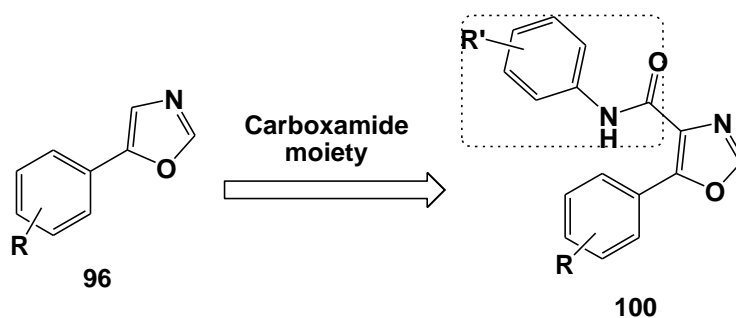


Figure 3.1: Structure of compounds containing *N*-aryl-4-carboxamide moieties.

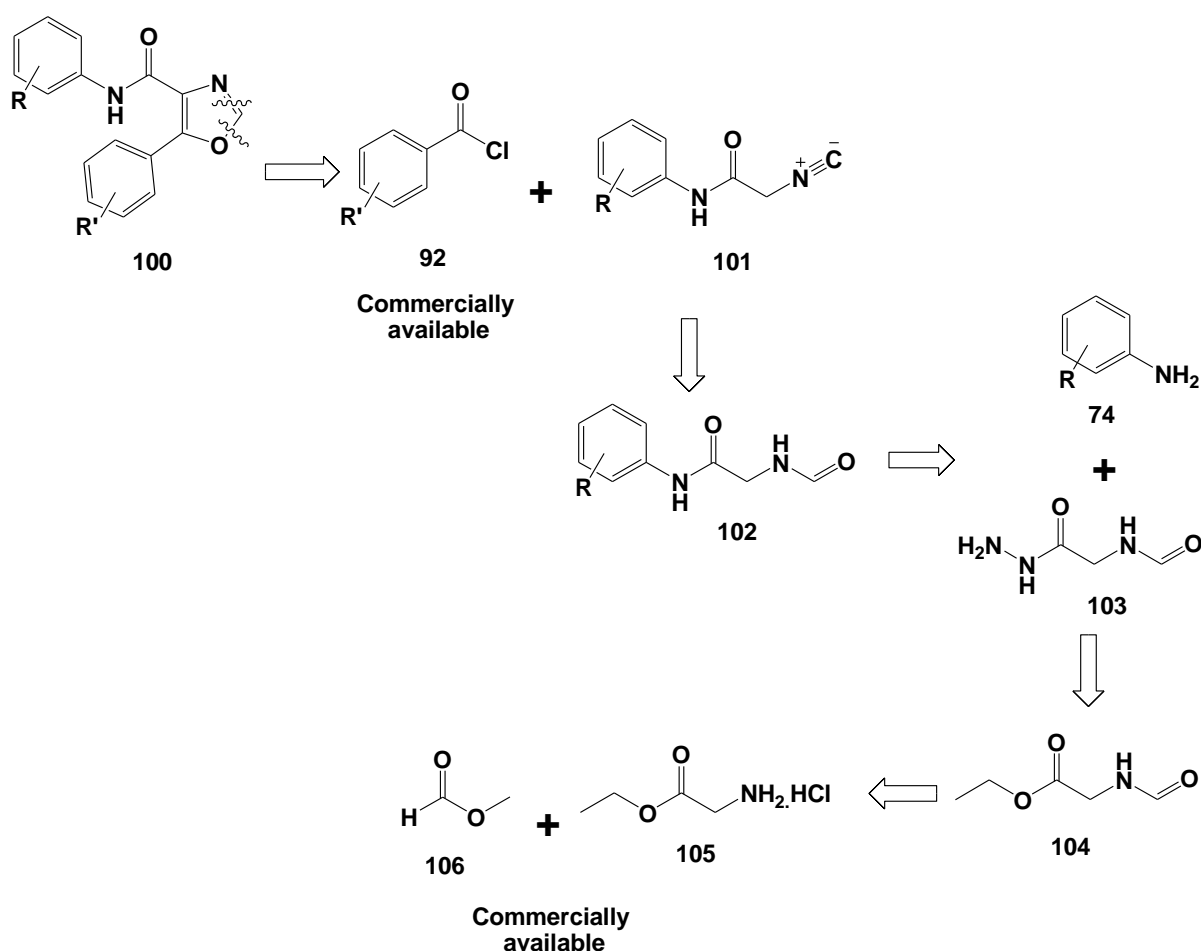
On the basis of the above and our interest in the development of new potential anti-HIV-1 drugs, attention was focused on exploring the effect of chemical structure variation by incorporating the *N*-aryl-4-carboxamide framework at the 4-position of the 5-aryl-1,3-oxazole scaffolds **96** (**Scheme 3.3**). Our *hypothesis* was that this modification would increase the inhibition effect of this scaffold as well as providing insight into the structure activity relationships (SAR) for these types of compounds. Therefore, the work described here was aimed at integration of *N*-aryl-4-carboxamide cores at the 4-position of 5-aryl-1,3-oxazole derivatives **96** to obtain a set of *N*,5-diaryloxazole-4-carboxamides **100** as a second generation library.



Scheme 3.3: Integration of carboxamide moiety on the 5-aryl-1,3-oxazole fragments.

3.3.1. First retrosynthetic approach to target compounds

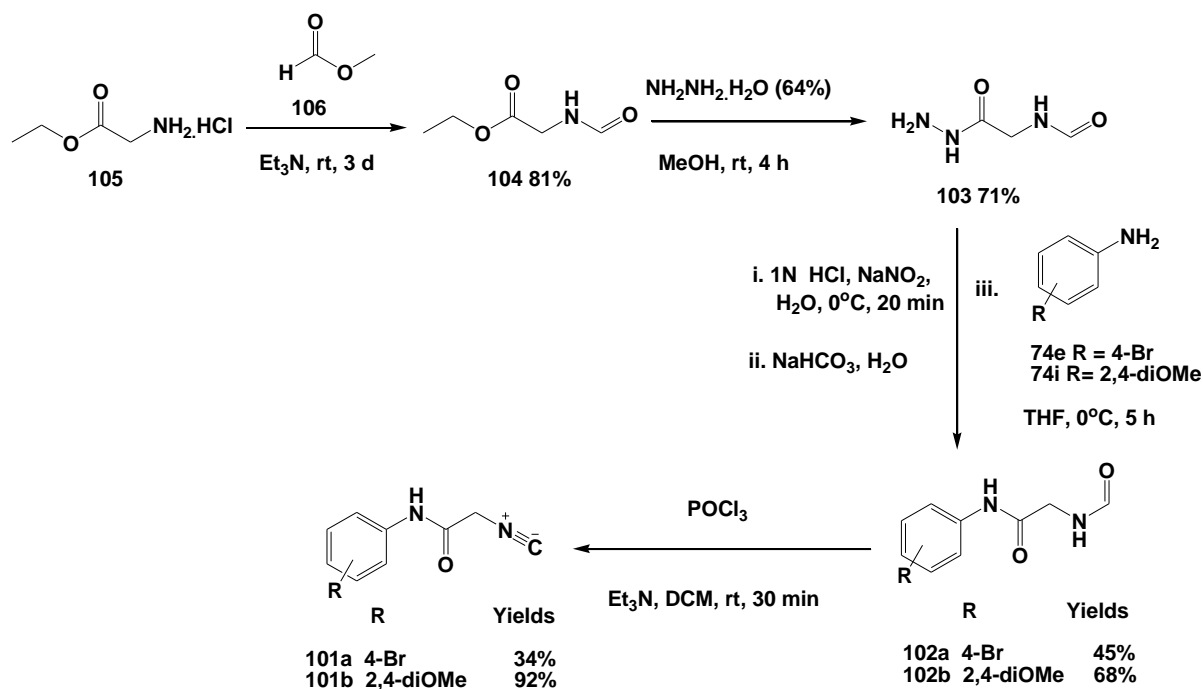
The retrosynthetic analysis of the target *N*,5-diaryl-1,3-oxazole-4-carboxamides **100** is shown in **Scheme 3.4**. It was envisaged that the 1,3-oxazole ring system of the target scaffold **100** could be constructed through cycloaddition of commercially available benzoyl chloride **92** to 2-isocyano-*N*-arylacetamide **101**. The key intermediate **101** in turn could be obtained through a well-established protocol which could involve the dehydration of *N*-aryl-2-formamidoacetamide precursor **102**, which could be derived by coupling of the aniline scaffold **74** with hydrazinyl formamide **103**. The precursor **103** could be obtained from previously reported literature *via* a nucleophilic substitution reaction of *N*-formyl glycine methyl ester **104** with hydrazine monohydrate. The scaffold **104** could be obtained from two possible commercially available synthons; amino acid ester hydrochloride salts **105** and methyl formate **106**.



Scheme 3.4: First retrosynthetic approach to the target compounds **100**.

3.3.1.1. Synthesis of the 2-isocyano-*N*-aryl-acetamide

The construction of the desired *N*,5-diaryl-1,3-oxazole-4-carboxamide derivatives **100** was then pursued and the key synthetic building blocks, 2-isocyano-*N*-arylacetamides **101**, were first synthesized over 4 steps as illustrated in **Scheme 3.5**.



Scheme 3.5: Synthesis of 2-isocyano-*N*-arylacetamides intermediates **101**.

Thus, the commercially available glycine ester hydrochloride **105** was reacted with excess methyl formate **106** in the presence of triethylamine catalyst at room temperature for 3 days. Work-up furnished the desired ethyl 2-formamidoacetate **104** in a yield of 81%. The yield and NMR spectrum of the product **104** were comparable to those reported in literature.^{236,237,238,239} The *N*-formyl glycine ethyl ester **104** was then subjected to a nucleophilic substitution reaction with hydrazine monohydrate in methanol at room temperature.²³⁸ After 4 hours, the resulting precipitate was then isolated by filtration and dried under high vacuum to afford pure *N*-(2-hydrazinyl-2-oxoethyl)formamide **103** in a yield of 71%. The identity of **103** was confirmed by the ¹H NMR spectrum which showed the disappearance of the signals due to the ethyl protons and the appearance of an NH proton at 8.25 ppm, as well as the NH₂ group at 4.26 ppm, while the ¹³C NMR spectrum further supported the loss of the carbon atoms of the ethyl group. The *N*-(2-hydrazinyl-2-oxoethyl)formamide **103** was then treated with 1N HCl and NaNO₂, followed by addition of a solution of aniline **74** in THF at 0°C for 5 hours. Work up and

purification by column chromatography on silica afforded novel *N*-aryl-2-formamidoacetamide **102a** and **102b** in yields of 45 and 68%. The ¹H NMR spectrum of compound **102b** confirmed the chemical structure of the *N*-aryl-2-formamidoacetamide products by exhibiting three downfield singlets at δ 9.09, 8.38 and 8.16 ppm, assigned to the two NH and 2-methine protons, while the signals in the aromatic region of δ 6.65-7.75 ppm correspond to the methine protons of the aryl ring.

The *N*-aryl-2-formamidoacetamides **102a** and **102b** were then subjected to dehydration conditions by stirring with phosphoryl chloride and triethylamine in DCM at room temperature for 30 minutes.²³⁸ Work up and isolation by short column chromatography furnished the desired novel *N*-aryl-2-isocyanoacetamide intermediates **101a** and **101b** in yields of 34% and 92%, respectively. The identity of the product in each case was established by the disappearance of the *N*-formamide protons (NHCHO) in the ¹H NMR spectrum for compound **101b** and the formation of a new signal at δ 159.4 ppm in the ¹³C NMR spectrum, which corresponds to the divalent carbon ($\text{R}-\overset{+}{\text{N}}\equiv\overset{-}{\text{C}}$) of the isocyano group. The FTIR spectroscopic data supported the formation of the *N*-aryl-2-isocyanoacetamides by exhibiting unique bands at 2157 cm⁻¹ (for **101b**) assigned to the isocyano group while the bands in the regions of 3291 and 1728 cm⁻¹ were assigned to the NH and carboxyl groups (*Table 3.6*).

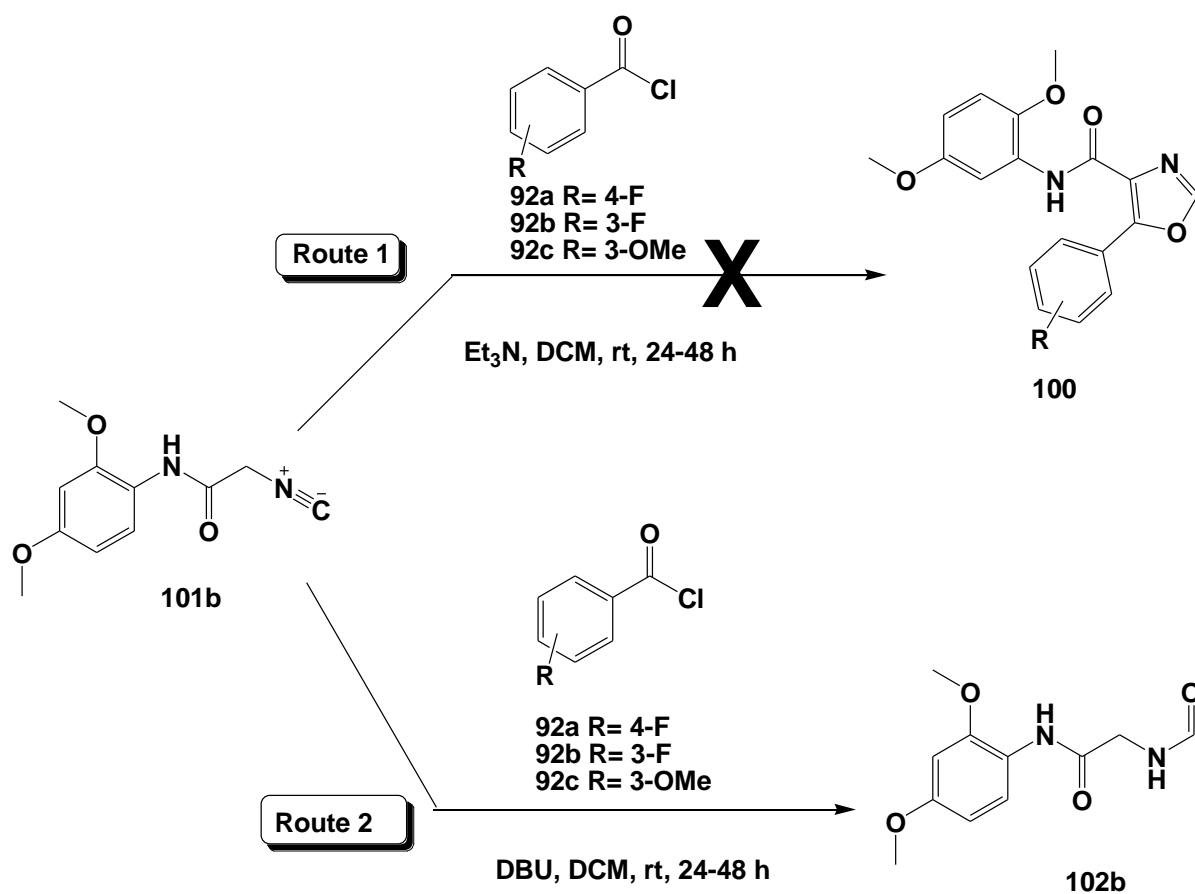
Table 3.6: FTIR spectroscopic data of *N*-aryl-2-isocyanoacetamide intermediates **101a-b** showing the N, C=O and isocyano bands.

Compounds	$\nu_{\text{NH}}(\text{cm}^{-1})$	$\nu_{\text{C=O}}(\text{cm}^{-1})$	$\nu_{\text{isocyano group}}(\text{cm}^{-1})$
101a	3291	1728	2157
101b	3250	1702	2160

3.3.1.2. Reaction of **101b** with benzoyl chlorides

As the final step in the synthesis of the target compounds, a set of benzoyl chlorides **92a-c** were then reacted with *N*-aryl-2-isocyanoacetamide **101b** in the presence of triethylamine in DCM at room temperature (*Scheme 3.6*, Route 1), but product formation could not be observed by TLC, even after prolonged stirring for 48 hours. A change of solvent (THF for DCM) only afforded the recovery of starting material **101**. However, when the reaction was conducted in the presence of DBU instead of Et₃N as catalyst (*Scheme 3.6*, Route 2), the hydration product

previously synthesized, *N*-(2,4-dimethoxyphenyl)-2-formamidoacetamide **102b**, was obtained after 48 hours of stirring at room temperature in a yield of 85%. It became clear then that the reactions between isocyanacetamides bearing a secondary amide (such as **101b**) with benzoyl chlorides do not proceed as expected. A possible explanation for lack of reactivity of isocyanacetamides might be the presence of an amide group, which tends to lower the acidity of the α -methylene protons adjacent to the isocyan group. Giustiniano and co-workers reported the lack of reactivity between acyl chloride and α -isocyanacetamide containing a secondary amide, which is in agreement with the findings of this study.²⁴⁰

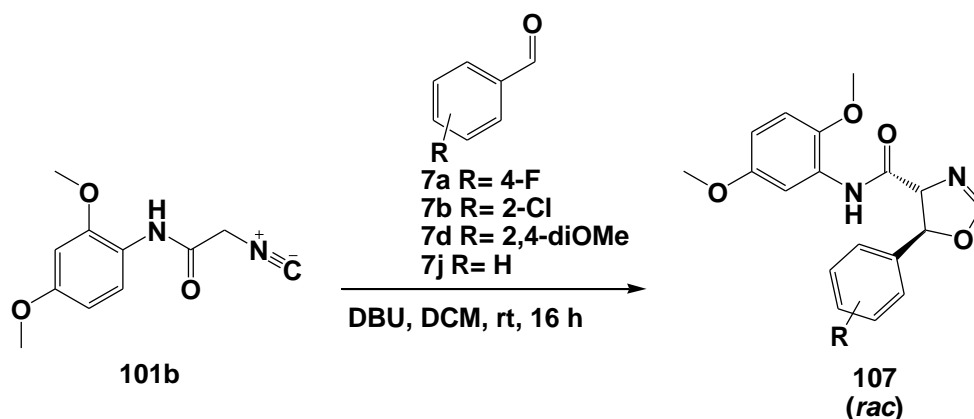


Scheme 3.6: Attempted synthesis of *N*,5-diaryl-1,3-oxazole-4-carboxamides.

3.3.1.3. Reaction of compound **101b** with benzaldehydes

With the failure of the last step of the planned reaction path towards the target **100**, an alternative route was envisaged and attention was turned to the reaction of benzaldehydes **7** with isocyanide **101b** (**Scheme 3.7**) and subsequent oxidation of the resulting 4,5-dihydro-*N*,5-diaryl-

1,3-oxazole-4-carboxamides **107** into target **100**. Thus the benzaldehydes **7a-c** and **7i** were reacted with *N*-(2,4-dimethoxyphenyl)-2-isocyanoacetamide scaffold **101b** in the presence of DBU in DCM at room temperature. TLC indicated the formation of a new spot and work up and purification using column chromatography gave (4*R*,5*R*)/(4*S*,5*S*)-4,5-dihydro-*N*,5-diaryl-1,3-oxazole-4-carboxamide scaffolds **107** as a racemic mixture in good yield (Table 3.7).



Scheme 3.7: Synthesis of the (4*R*,5*R*)/(4*S*,5*S*)-4,5-dihydro-*N*,5-diaryl-1,3-oxazole-4-carboxamides **107**.

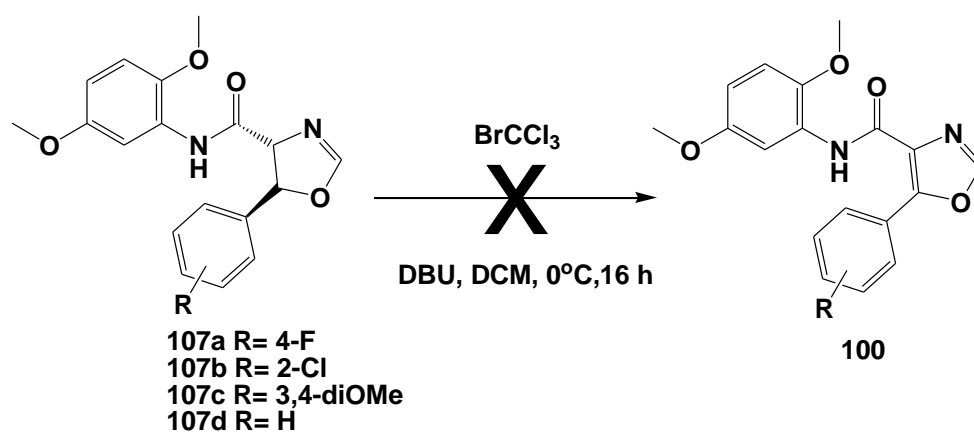
Table 3.7: Yields isolated (%) of (4*R*,5*R*)/(4*S*,5*S*)-4,5-dihydro-*N*,5-diaryl-1,3-oxazole-4-carboxamide scaffolds **107**.

 (rac)		
Compd	R	Yields (%)
107a	4-F	70
107b	2-Cl	60
107c	3,4-diOMe	55
107d	H	70

The synthesis of the (4*R*,5*R*)/(4*S*,5*S*)-4,5-dihydro-*N*,5-diaryl-1,3-oxazole-4-carboxamide scaffolds was confirmed by NMR spectroscopy and the geometry reported here resembles that discussed in section 3.2.2. The ¹H-NMR spectrum of compound **107a** in deuterated chloroform (CDCl₃) exhibited a singlet at 8.72 ppm, corresponding to the imine (NH) group, while another singlet at δ 7.18 ppm corresponds to the 2-methine proton of the 4,5-dihydro-1,3-oxazole ring. The two set of doublets at δ 5.72 and 4.62 ppm with *J* values of 7.6 Hz each correspond to the 5- and 4-methine protons of the 4,5-dihydro-1,3-oxazole ring which are in vicinal coupling to each other. This splitting between 5- and 4- methine protons has been reported the (4*R*, 5*R*) / (4*S*, 5*S*) isomers.²⁴¹ Furthermore, two singlets at δ 3.87 and 3.80 ppm were assigned to the six protons of two methoxy groups.

3.3.1.4. Attempted oxidation of 5-aryl-4,5-dihydro-*N*-(3,5-dimethoxyphenyl)-1,3-oxazole-4-carboxamides

Encouraged by a reported approach where the oxidation of 2-aryl-4,5-dihydrooxazole-4-carboxylates was accomplished using bromotrichloromethane (BrCCl₃) and DBU under mild conditions,²⁴² we explored the oxidation of our dihydro-carboxamides **107** using this reported protocol in DCM at 0°C. Unfortunately, even after 48 hours none of the desired *N*,5-diaryl-4-carboxamide-1,3-oxazole analogues **100** were obtained (**Scheme 3.8**).

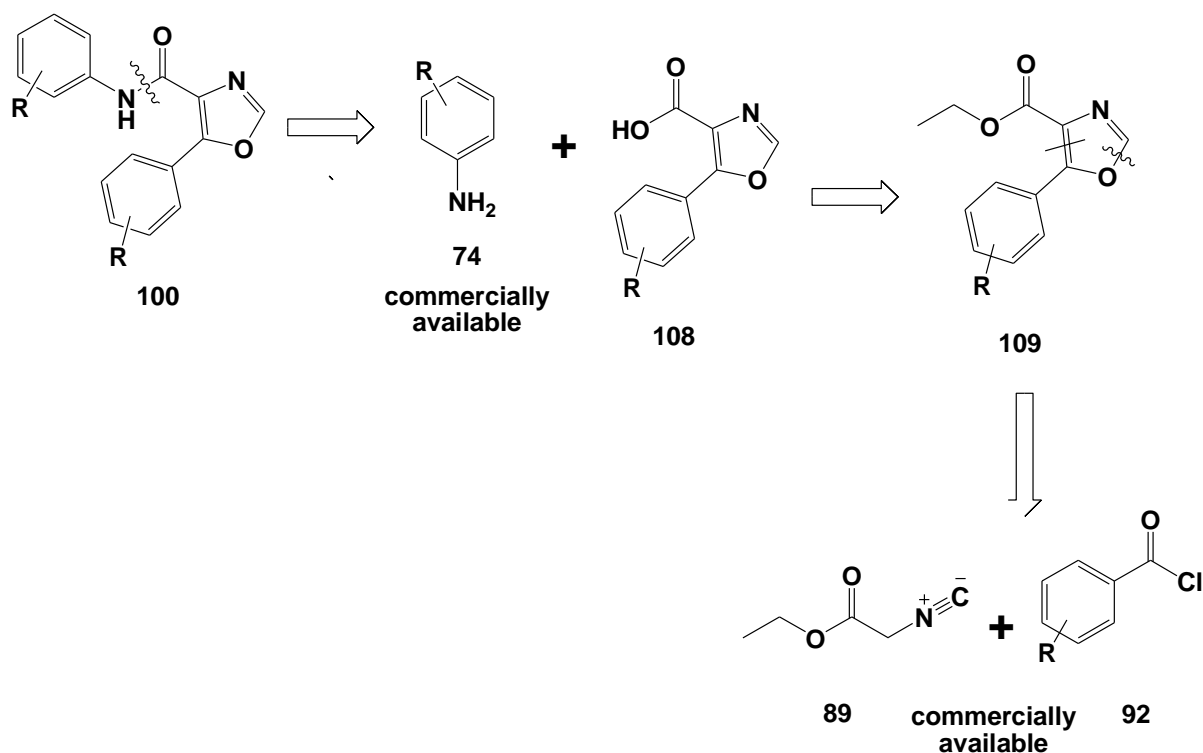


Scheme 3.8: Attempted oxidation of 5-aryl-4,5-dihydro-*N*-(3,5-dimethoxyphenyl)-1,3-oxazole-4-carboxamides.

Considering the number of steps required to synthesise the aryl-isocyanoacetamide synthetic intermediates and the failed final oxidation of 5-aryl-4,5-dihydro-*N*-(3,5-dimethoxyphenyl)oxazole-4-carboxamides, attention was concentrated on designing a new retrosynthetic route towards the *N*,5-diaryl-1,3-oxazole-4-carboxamides **100**.

3.3.2. Second retrosynthetic approach to the target compounds

A new retrosynthetic pathway for target **100** was then proposed (*Scheme 3.9*). The desired targeted **100** could be obtained from the coupling between aniline derivatives **74** and 5-aryl-1,3-oxazole-4-carboxylic acids **108**. Scaffold **108** could arise from hydrolysis of ethyl 5-aryl-1,3-oxazole-4-carboxylates **109**, which in turn could be obtained from the condensation of commercially available reagents benzoyl chloride **92** and ethyl isocyanoacetate **89**.

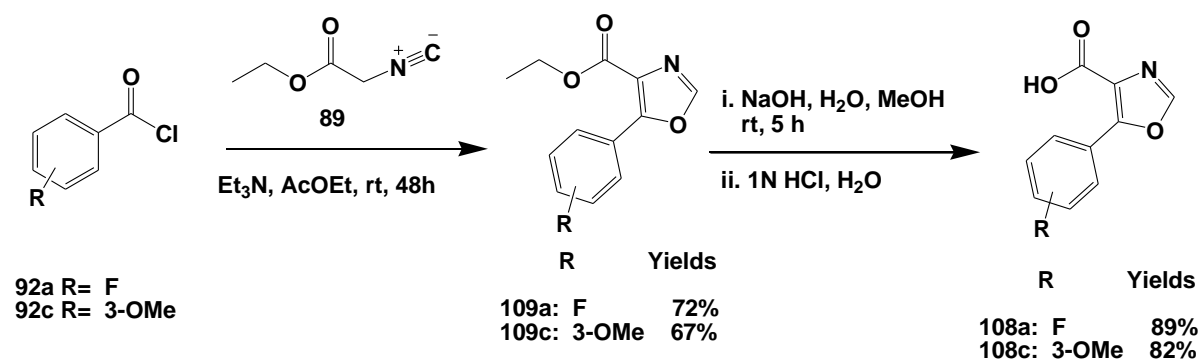


Scheme 3.9: Second retrosynthetic approach to the target compounds.

3.3.2.1. Synthesis of 5-aryl-1,3-oxazole-4-carboxylic acids (**108**)

As proposed in *Scheme 3.10*, the synthesis of 5-aryl-1,3-oxazole-4-carboxylic acids **108** was then pursued as a necessary step towards the target compounds **100**. Benzoyl chloride derivatives **92a** and **92c** were reacted with ethyl isocyanoacetate **89** in the presence of Et₃N as a catalytic base using ethyl acetate solvent for 48 hours (*Scheme 3.10*).^{243,244,245} Work up and separation by

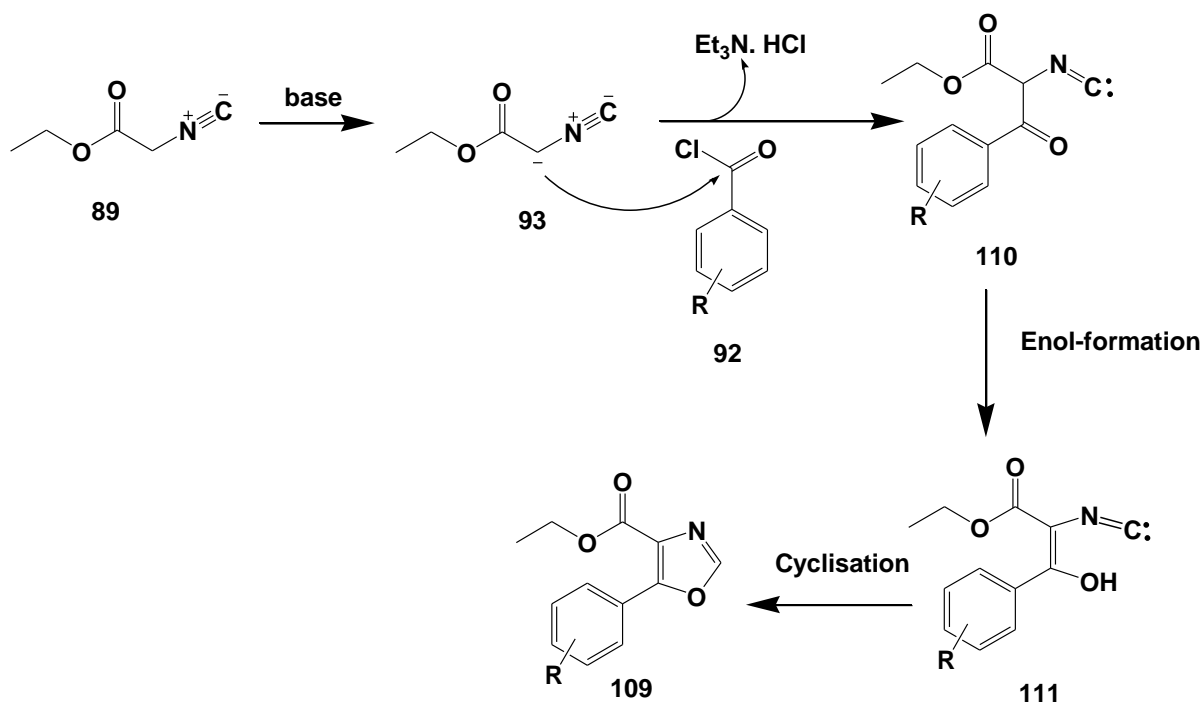
column chromatography on silica gel afforded the desired ethyl 5-aryl-1,3-oxazole-4-carboxylate derivatives **109a** and **109c** in good yields. The better reactivity of ethyl isocyanoacetate **89** in comparison to the earlier scaffold, *N*-aryl-isocyanoacetamide **101**, could be accredited to the presence of the ester group (R-CO₂-), which tends to enhance the reactivity of the α-acidic protons adjacent to the carbonyl, while acidity of the methylene protons of *N*-aryl-isocyanoacetamide **101** was reduced by the presence of the secondary amide.



Scheme 3.10: Synthesis of 5-aryl-1,3-oxazole-4-carboxylic acids.

3.3.2.2. Mechanism for the formation of ethyl 5-aryl-1,3-oxazole-4-carboxylates **109**

A possible mechanism (*Scheme 3.11*) for formation of the ethyl 5-aryl-1,3-oxazole-4-carboxylates **109** is believed to proceed *via* the deprotonation of the α-acidic proton of ethyl isocyanoacetate **89** by a catalytic base to generate a highly reactive nucleophile **93**, which then attacks the benzoyl chloride **92**, to give the alpha isocyano carbonyl intermediates **110**, with displacement of the chlorine atom as the triethylamine hydrochloride salt.²⁴³ The intermediate **110**, under basic conditions, exists in a dynamic equilibrium with α-isocyanoenolate **111**, which then undergoes a ring closure upon work up to afford the desired ethyl 5-aryl-1,3-oxazole-4-carboxylates **109**.

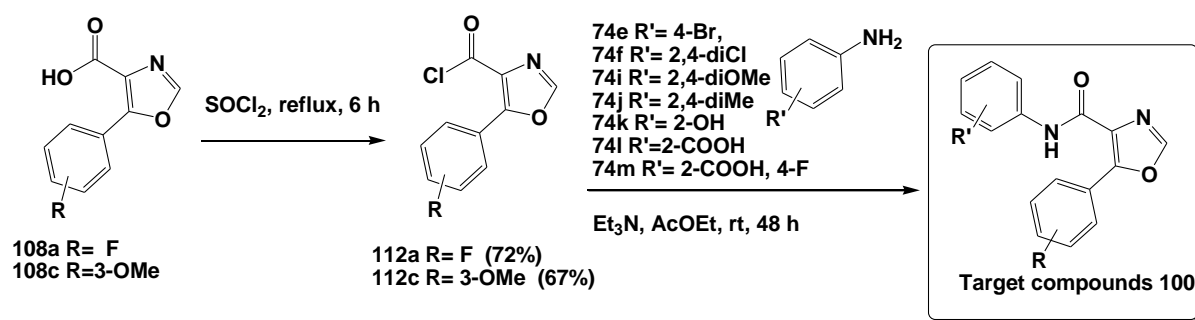


Scheme 3.11: Mechanism of the formation of ethyl 5-aryl-1,3-oxazole-4-carboxylates.

The formation of the products **109** was confirmed by NMR spectroscopic analysis. The ¹H NMR spectrum of compound **109a** showed a singlet signal at 7.90 ppm corresponding to the methine proton of the oxazole moiety; while the ¹³C NMR spectrum revealed the methine carbon atom at 148.8 ppm. Additionally, the ¹³C NMR further displays two signals at 161.9 and 154.7 ppm corresponding to the carbonyl carbon atom and the 5-carbon atom of the oxazole motif.

The ethyl 5-aryl-1,3-oxazole-4-carboxylates **109a** and **109c** were then subjected to hydrolysis by refluxing in a mixture containing NaOH, methanol and water for 6 hours, followed by acidifying with HCl.^{246,247} Work up afforded the desired free carboxylic acid derivatives **108a** and **108c** in excellent yields of 82% and 89%. The identity of the products was confirmed by means of 1D- and 2-D NMR spectroscopy. The ¹H NMR spectrum of compound **108a** was characterised by the loss of the signals arising from protons belonging to the ethyl group and the presence of a new signal downfield at 13.2 ppm corresponding to the proton of the carboxylic acid group. The loss of the ethyl group was also observed in the ¹³C NMR spectrum of the compound. In addition, the hydrolysis of the ester group was also evident in the FTIR spectra of 5-aryl-1,3-oxazole-4-carboxylic acids **108**, which displayed a broad signal at 2461 cm⁻¹ (for **108a**) and 2569 cm⁻¹ (for **108c**) corresponding to the hydroxyl group, whilst the bands of the carbonyl (C=O) and the C=N group were observed in the region of 1709-1727 cm⁻¹ and 1506-1596 cm⁻¹.

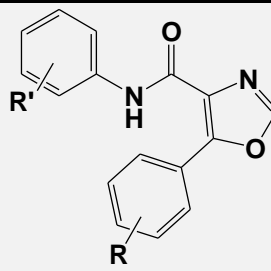
3.3.2.3. Anilidation of 5-aryloxazole-4-carboxylic acid derivatives



Scheme 3.12: Synthesis of the target compounds **100**.

The 5-aryl-1,3-oxazole-4-carboxylic acids **108a** and **108c** were first converted to the more reactive 5-aryl-1,3-oxazole-4-carbonyl chloride intermediates **112a** and **112c** using SOCl₂ under reflux for 8 hours (**Scheme 3.12**).^{248,249} These compounds are characterized by the absence of the hydroxyl group in the ¹H NMR spectra.

The final synthetic step was the nucleophilic attack of aniline derivatives **74** on the carbonyl chlorides **112a** and **112c** in the presence Et₃N using ethyl acetate as a solvent for 48 hours.^{250,251} Target compounds *N*,5-diaryl-4-carboxamide-1,3-oxazoles **100a-e** and **100g-i** were obtained after column chromatography, while the products **100f** and **100j-k** (with carboxylic substituent) were obtained as precipitates from DCM in good yields (*Table 3.8*). Moreover, this transformation of the 5-aryl-1,3-oxazole-4-carboxylic acid scaffolds into the corresponding *N*,5-diaryl-1,3-oxazole-4-carboxamide derivatives led to a total number of eleven novel compounds **100a-k**. Spectral analysis of the corresponding products with FTIR, 1D and 2D NMR, and LCMS confirmed the structures of the desired final products.

Table 3.8: Isolated yields (%) of the *N*,5-diaryl-1,3-oxazole-4-carboxamides **100a-k**.

The chemical structure shows a 1,3-oxazole ring with a carbonyl group at position 4. The nitrogen at position 1 is bonded to an NH group, which is further attached to an aryl ring with substituent R'. The carbon at position 5 of the oxazole ring is bonded to another aryl ring with substituent R.

Compound	R	R'	Yields (%)
100a	4-F	2-OH	84
100b	4-F	2,4-diOMe	68
100c	4-F	4-Br	73
100d	4-F	2,4-diMe	70
100e	4-F	2,4-diCl	72
100f	4-F	2-COOH	64
100g	3-OMe	2-OH	78
100h	3-OMe	2,4-diOMe	72
100i	3-OMe	4-Br	84
100j	3-OMe	2-COOH	52
100k	3-OMe	2-COOH,4-F	60

3.3.2.5. FTIR and NMR spectroscopic analysis of *N*,5-diaryl-1,3-oxazole-4-carboxamides **100**

The ^1H NMR spectrum of *N*-(4-bromophenyl)-5-(3-methoxyphenyl)-1,3-oxazole-4-carboxamide **100i** is used as a representative of this compound class. This compound exhibited two singlets at 9.12 and 8.00 ppm corresponding to the secondary amide group (NH) and the methine proton of the oxazole core. The eight methine protons of the two benzene ring systems resonate in the aromatic region of 7.00 ppm to 7.89 ppm, while the singlet signal at 3.90 ppm accounting for three protons corresponds to the methoxy group. The ^{13}C NMR spectrum of compound **100i** confirms the expected presence of 15 unique carbon environments with the carbonyl carbon atom resonating at 159.5 ppm, while the signals at 153.6 and 147.7 correspond to the 5-carbon and methine carbon atoms of the oxazole moiety, respectively. The FTIR spectra of target

compounds showed intense peaks in the region of 3200-3397 cm^{-1} corresponding to the NH stretch while the bands in the regions of 1660-1730 cm^{-1} and 1525-1591 cm^{-1} correspond to the amide carbonyl group and C=N of the oxazole motif.

3.3.2.6. Mass analysis of *N*,5-diaryl-1,3-oxazole-4-carboxamides **100**

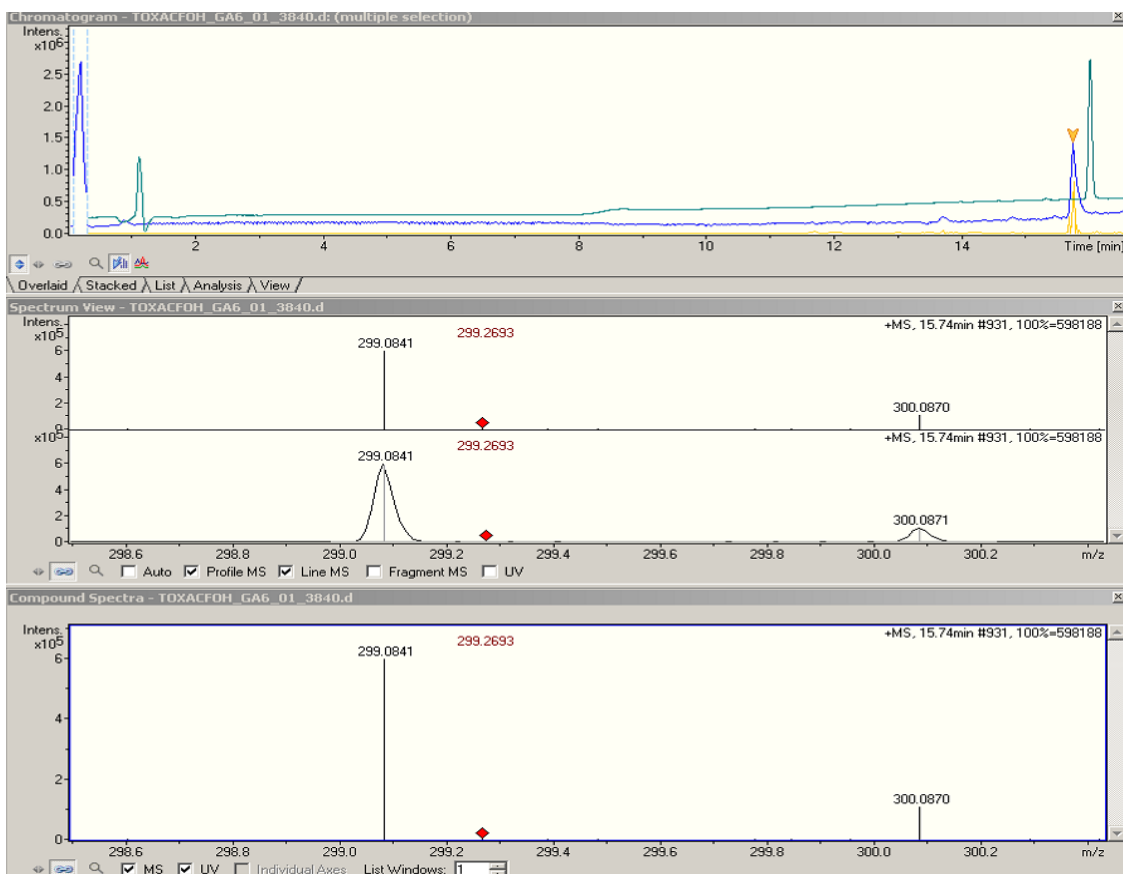
Analysis of the compounds **100** by high-resolution mass spectrometry was done using an LC-MS system with an ESI (electrospray ionisation) probe. Calculated and experimental m/z values for the molecular ions of the parent compounds and their mSigma values are displayed in *Table 3.9*. Accurate formulae for the compounds were calculated using the Bruker SmartFormula3D® algorithm that associates within 5 mDa calculated isotopic patterns to the parent compound ion masses and their fragments (acceptable mSigma values ≤ 20).

Table 3.9: HRMS results of the *N*,5-diaryl-1,3-oxazole-4-carboxamides **100a-k** and their mSigma values.

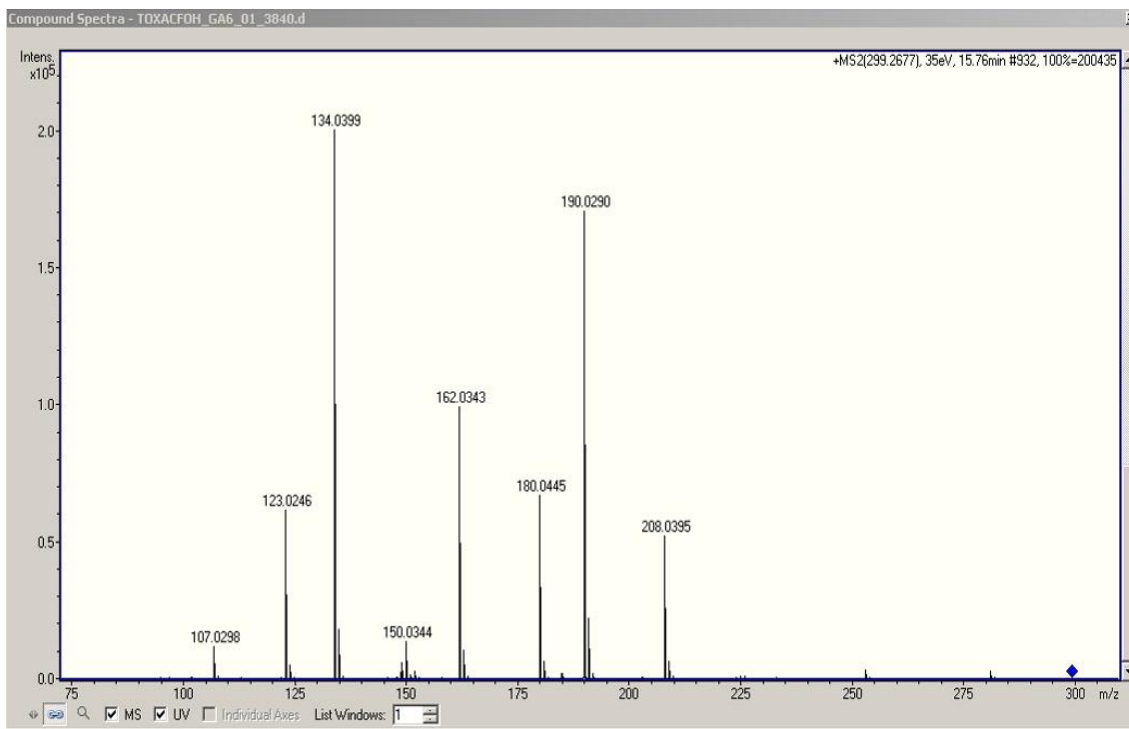
Compds	Calculated m/z	Chemical formula [M+1]	Measured m/z	Err ppm	Err mDa	mSigma values
100a	299.0826	C ₁₆ H ₁₂ FN ₂ O ₃	299.0841	-1.5	-2.9	0.6
100b	343.1094	C ₁₆ H ₁₆ FN ₂ O ₄	343.1116	-2.2	-6.3	1.2
100c	360.9982	C ₁₆ H ₁₁ ⁷⁹ BrFN ₂ O ₂	361.0004	-2.2	-6.1	3.6
100d	311.1190	C ₁₈ H ₁₆ FN ₂ O ₄	311.1186	-0.4	-2.3	1.5
100e	351.0098	C ₁₆ H ₁₀ Cl ₂ FN ₂ O ₂	351.0095	-0.3	-4.3	7.5
100f	327.0781	C ₁₇ H ₁₂ FN ₂ O ₄	327.0795	-1.9	-4.2	0.6
100g	311.1026	C ₁₉ H ₁₅ N ₂ O ₄	311.1036	-1.0	-1.3	9.4
100h	355.1288	C ₁₉ H ₁₉ N ₂ O ₅	355.1309	-2.1	-4.2	7.7
100i	373.0182	C ₁₇ H ₁₄ ⁷⁹ BrN ₂ O ₃	373.0200	-1.8	-4.9	6.3
100j	399.0975	C ₁₈ H ₁₅ N ₂ O ₅	39.0977	-0.2	-0.6	8.8
100k	357.0881	C ₁₈ H ₁₄ FN ₂ O ₅	357.0906	-2.5	-6.9	3.2

3.3.2.6.1. MS/MS fragmentation

Compound *N*-(2-hydroxyphenyl)-5-(4-fluorophenyl)-1,3-oxazole-4-carboxamide **100a** was chosen as the model to discuss in detail the mass fragmentation patterns. As illustrated in *Figure 3.2*, analysis of compound **100a** by ESI-MS revealed a molecular ion peak at m/z 299.0841 corresponding to the protonated parent ion, with a molecular formula $C_{16}H_{12}FN_2O_3^+$. The MS/MS spectrum of *N*-(2-hydroxyphenyl)-5-(4-fluorophenyl)-1,3-oxazole-4-carboxamide **100a** at m/z 299.08 with the molecular formula $C_{16}H_{12}FN_2O_3^+$ exhibited a possible fragmentation pattern as depicted in *Figure 3.3*. The parent molecular ion decomposes by losing a neutral C_6H_5N group to give a fragment ion $C_{10}H_7FNO_3^+$ at m/z 208.04. This ion further undergoes breakdown to provide two possible pathways: the first arises as a result of the loss of a water molecule to furnish a fragment ion at m/z 190.03 with chemical formula $C_{10}H_5FNO_2^+$. This fragment then loses carbon monoxide (-CO) to provide the cation with formula $C_9H_5FNO^+$ at m/z 162.04, followed by further loss of another carbon monoxide (-CO) to afford a base peak at m/z 134.04 with chemical formula $C_8H_5FN^+$. This base peak may undergo the loss of hydrogen cyanide (-HCN) to form the fragment ion at m/z 107.03 with the formula $C_7H_4F^+$. The second pathway involves the loss of carbon monoxide (-CO) to provide $C_9H_7FNO_2^+$ at m/z 180.05, followed by further decomposition through loss of a neutral formaldehyde (-HCOH) to yield a fragment ion at m/z 150.04 with the formula $C_8H_5FNO^+$. This ion then undergoes decomposition by losing hydrogen cyanide (-HCN) to give m/z 123.02 with the chemical formula $C_7H_4FO^+$.



a)



b)

Figure 3.2: Recorded spectra for compound **100a**: (a) MS and b) MS/MS (col. energy 35 eV)

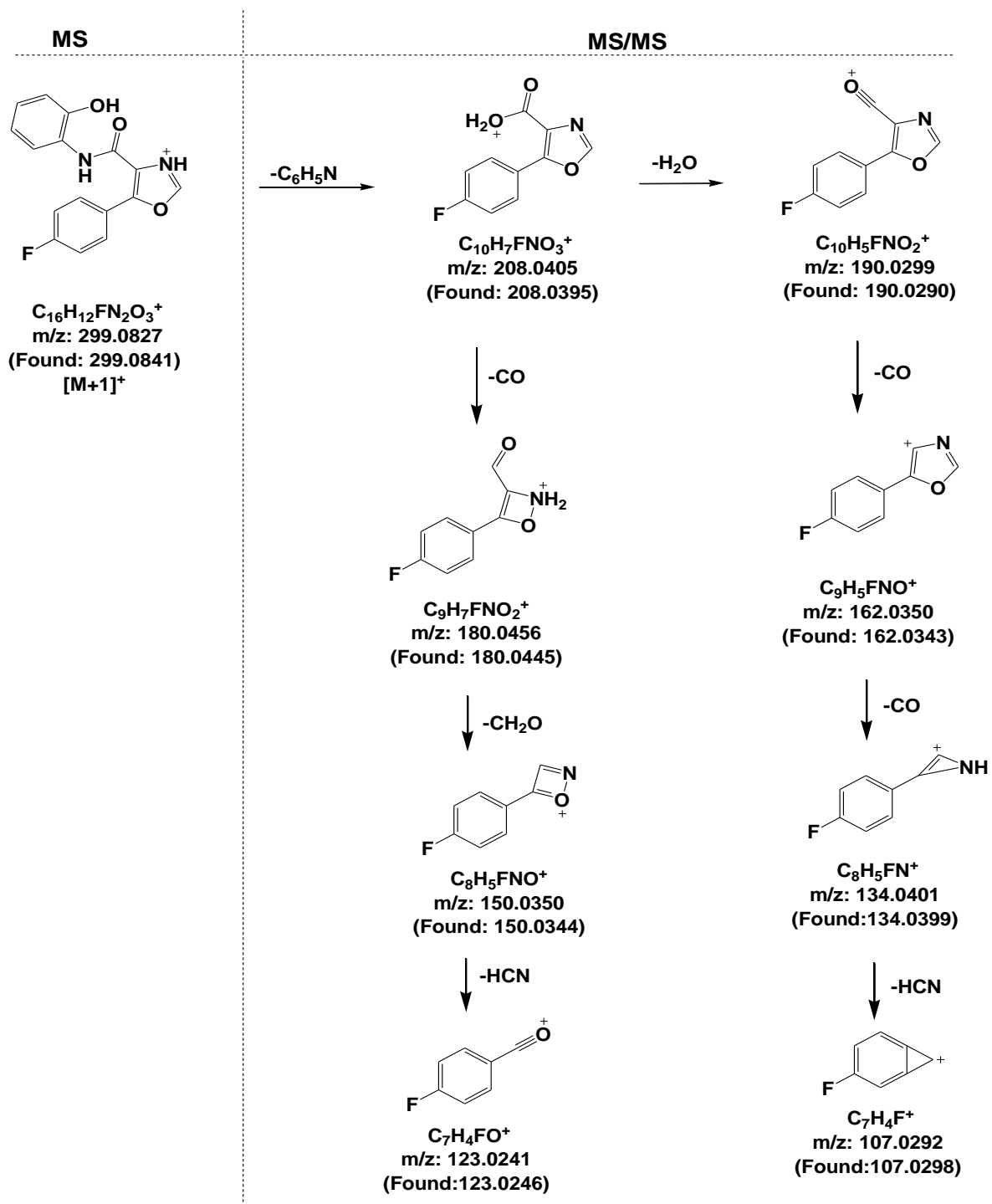


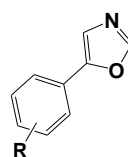
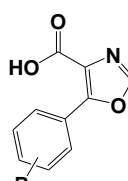
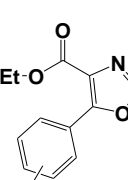
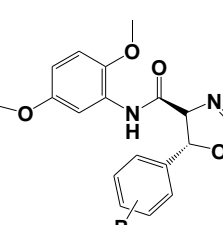
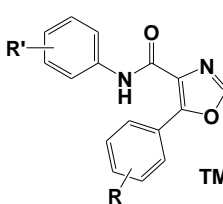
Figure 3.3: Fragmentation pathway of compound 100a

3.3.3. Biological evaluation in LEDGF/p75-IN inhibition assay

A series of compounds containing a 5-aryl-1,3-oxazole core, were tested in an *in vitro* AlphaScreen assay to determine the percentage inhibition of the interaction between the host co-factor LEDGF/p75 and HIV1 IN proteins. Due to the success seen in Chapter 2, and suggestions from the literature review regarding the screening of fragment libraries at higher concentration, we therefore wished to conduct the assessment of the second generation of oxazole-based compounds at 100 μM .^{252,253,254,255} The experiments were run in triplicate and results are recorded in *Table 3.10*. Re-evaluation of compounds **96a** and **96d** at a single dose of 100 μM displayed lower percentage inhibition than at 10 μM concentration, which is attributed to the poor solubility of these compounds at higher concentration. Further evaluation of compounds containing a carboxylate ester group at the 4-position of the 5-aryl-1,3-oxazole ring showed these compounds displayed poor activity [**109a** (0%) and **109c** (3%)]. However, the hydrolysis of these ethyl carboxylates into their corresponding free carboxylic acids slightly improved their percentage inhibition to 23% (**108a**) and 29% (**108c**). These results point to the fact that the carboxylic acid functionality at the 4-position of the five-membered ring has some capacity to disrupt the interaction between LEDGF/p75 and IN proteins. In the set of target compounds, at least two compounds (**100b** and **100h**) exceeded the pre-defined minimum cut-off of 50%. The compound bearing the electron withdrawing fluorine substituent at the *para*-position of the phenyl ring directly linked to the oxazole moiety (compound **100b**) exhibited the highest average percentage inhibition of 58% for the disruption of the LEDGF/p75-IN interaction, while the compound with the electron donating methoxy group at the *meta*-position of the benzene ring attached to the oxazole system (compound **100h**) displayed an average percentage inhibition of 56%. It is interesting to note that both of these compounds **100b** and **100h** have electron-donating methoxy groups at the *ortho*- and *para*-positions of the aniline rings. The presence of the two methoxy groups may be significant due to their ability to participate in hydrogen bonding to the target protein. Comparing compounds **100b** and **100h** versus **100a** and **100g** (with the *ortho*-hydroxyl group), it is shown that the presence of a second electron-donating group at the *para*-position of the *N*-aryl ring is critical to accomplish better inhibition. However, the presence of an electron withdrawing chlorine atom at the *ortho*- and *para*-positions in compound **100e** displayed lower inhibition (43%) compared to the percentage inhibition of compounds **100b** and **100h**, which could be attributed to the loss of the hydrogen bond of the methoxy group. Furthermore, the presence of the electron withdrawing bromine atom at the *para*-position in scaffolds **100c** and **100i**, as well as the presence of carboxylic substituents at the *ortho*-position didn't have major effects on the binding of the scaffolds. Further SAR revealed

that a large group occupying the *ortho*- and *para*-position of the aniline ring is favoured while the substitution of the other phenyl ring plays little role in inhibition. It is also noteworthy to mention that compounds **100b** and **100h**, showing the highest inhibition, contain similar 2,4-dimethoxyaniline subunits in their structures to that found in the reported **CAB** compounds, which were active in disrupting the LEDGF/p75-IN interaction (see *Figure 3.1*).²³⁵

Table 3.10: The HIV-1 IN-LEDGF/p75 inhibition activities of compounds **96a-d**, **100a-k**, **107a-d**, **108a-b** and **109a-b** at 100 μ M.

COMPOUND ENTRY	HIV-1 IN – LEDGF (%) inhibition @ 100 μ M (AlphaScreen)	
96a	4.04 \pm 1.08	 <p>96a: R 4-F 96b: R 3-OMe</p>
96d	3.63 \pm 3.03	
100a	22.07 \pm 1.57	
100b	58.04\pm8.70	
100c	3.44 \pm 1.77	 <p>108a: R 4-F 108b: R 3-OMe</p>
100e	42.92 \pm 2.35	
100f	34.02 \pm 3.99	
100g	7.45 \pm 2.93	
100h	55.74\pm2.28	 <p>109a: R 4-F 109b: R 3-OMe</p>
100i	23.56 \pm 2.80	
100j	29.42 \pm 7.22	
100k	28.07 \pm 5.31	
107a	2.48. \pm 7.28	 <p>107a: R 4-F 107b: R 2-Cl 107c: R 3,4-diOMe 107d: R H</p>
107b	0	
107c	2.53 \pm 5.26	
107d	4.13 \pm 10.36	
108a	22.84 \pm 1.20	 <p>100a: R 4-F, R' 2-OH 100b: R 4-F, R' 2,4-diOMe 100c: R 4-F, R' 4-Br 100d: R 4-F, R' 2,4-diOMe 100e: R 4-F, R' 2,4-diCl 100f: R 4-F, R' 2-COOH 100g: R 3-OMe, R' 2-OH 100h: R 3-OMe, R'2,4-diOMe 100i: R 3-OMe, R' 4-Br 100j: R 3-OMe, R' 2-COOH 100k: R 3-OMe, R' 2-COOH,4F</p>
108c	28.71 \pm 7.29	
109a	0	
109c	3.37 \pm 3.31	
CX05168	91.37 \pm 0.85	
HIV-1 IN and LEDGF with DMSO	0	

Analogues of the desired *N*,5-diaryl-4-carboxamide-1,3-oxazole products, the (4*R*,5*R*/4*S*,5*R*)-4,5-dihydro-*N*-5-diaryl-1,3-oxazole-4 carboxylate derivatives **107**, with no double bond between the 4- and 5-carbons of the oxazole ring, were inactive in the LEDGF/p75-IN assay. This may be due to the lack of planarity resulting from the missing double bond in the oxazoline moiety.

3.3.4. The prediction of ADME parameters of the synthesized compounds

The ADME properties of the best two compounds were predicted using Discovery Studio™ and results are recorded in *Table 3.11*.

Table 3.11: The ADME prediction for the synthesized compounds **100b** and **100h** obtained from Discovery Studio version 4.0.

Compounds	Aqueous Solubility	Blood Brain Barrier Penetration	Human Intestinal Absorption	CYP2D6 Inhibition
100b	2	3	2	No
100h	3	3	3	No

The ADME prediction of compound **100h** showed a good solubility level of 3 while the compound **100b** had a low solubility level of 2. Furthermore, both compounds were predicted to be absorbed very poorly in the human intestine and were also found to be non-inhibitors of cytochrome p4502D6. Moreover, compound **100b** was shown to be a medium penetrator of the BBB, while compound **100h** exhibited a BBB penetration level of 3, representing low penetration. These results indicate the compounds warrant further modification to improve their ADME properties.

3.3.5 Molecular modelling of the synthesized *N*,5-diaryl-1,3-oxazole-4-carboxamide derivatives

Compounds **100b** and **100h** which displayed acceptable IN-LEDGF/p75 inhibition were subjected to a docking protocol in order to obtain details on the SARs and also to gain understanding of the binding patterns. The two best compounds were then docked into the same cavity where LEDGF/p75 binds to the HIV-1 IN dimer of the 2B4J crystal structure using the previously described LibDock method in Section 2.3.4. The poses generated from LibDock were further subjected to scoring functions, analysed, *in-situ* energy minimized and then re-docked

using CDocker and flexible docking. Finally the binding energies of the flexible poses were then calculated and the results are recorded in *Table 3.12*. The predicted binding model indicated that the two compounds were binding at the interface between subunits A and B of the HIV-1 IN with compound **100b** displaying the lowest binding energy of -66.956 Kcal/mol whilst compound **100h** exhibited a binding energy of -53.8902Kcal/mol.

Table 3.12: A list of *in silico* interactions of compounds **100b** and **100h** and binding site amino acids according to order of their binding energy.

Compounds	Binding energy Kcal/mol	Amino acids interactions	LibDocked Scoring functions
100b	-66.956	Gln95, Ala128, THR124, Ala169, Glu170	20.731
100h	-53.8902	Gln95, Gln98, Ala169,	23.336

The predicted model for **100b** (*Figure 3.4, A and B*) displayed the *para*-methoxy group of the aniline ring making a hydrogen bond to the Gln95 residue, while the fluorine atom and its phenyl ring occupy the hydrophobic pockets formed by the residues Thr124 and Ala128 of monomer A. Furthermore, the carbonyl oxygen atom was shown to make two hydrogen bonds with the Ala169 and Glu170 residues of subunit B of the HIV-1 IN.

The projected binding model of compound **100h** (*Table 3.4, C and D*) shows the *para*-methoxy of the aniline ring making two hydrogen bonds with the backbone Gln95 residue of monomer A whilst the *meta*-methoxy of the phenyl ring at the 5-position of the oxazole motif exhibited hydrogen bonding to the Glu170 of subunit B. Moreover, the phenyl at the 5-position of the oxazole ring is shown to occupy the hydrophobic pocket formed by the Ala169 amino acid residue while the NH adjacent to the carbonyl group shows a hydrogen bond to the oxygen of Gln98 residue.

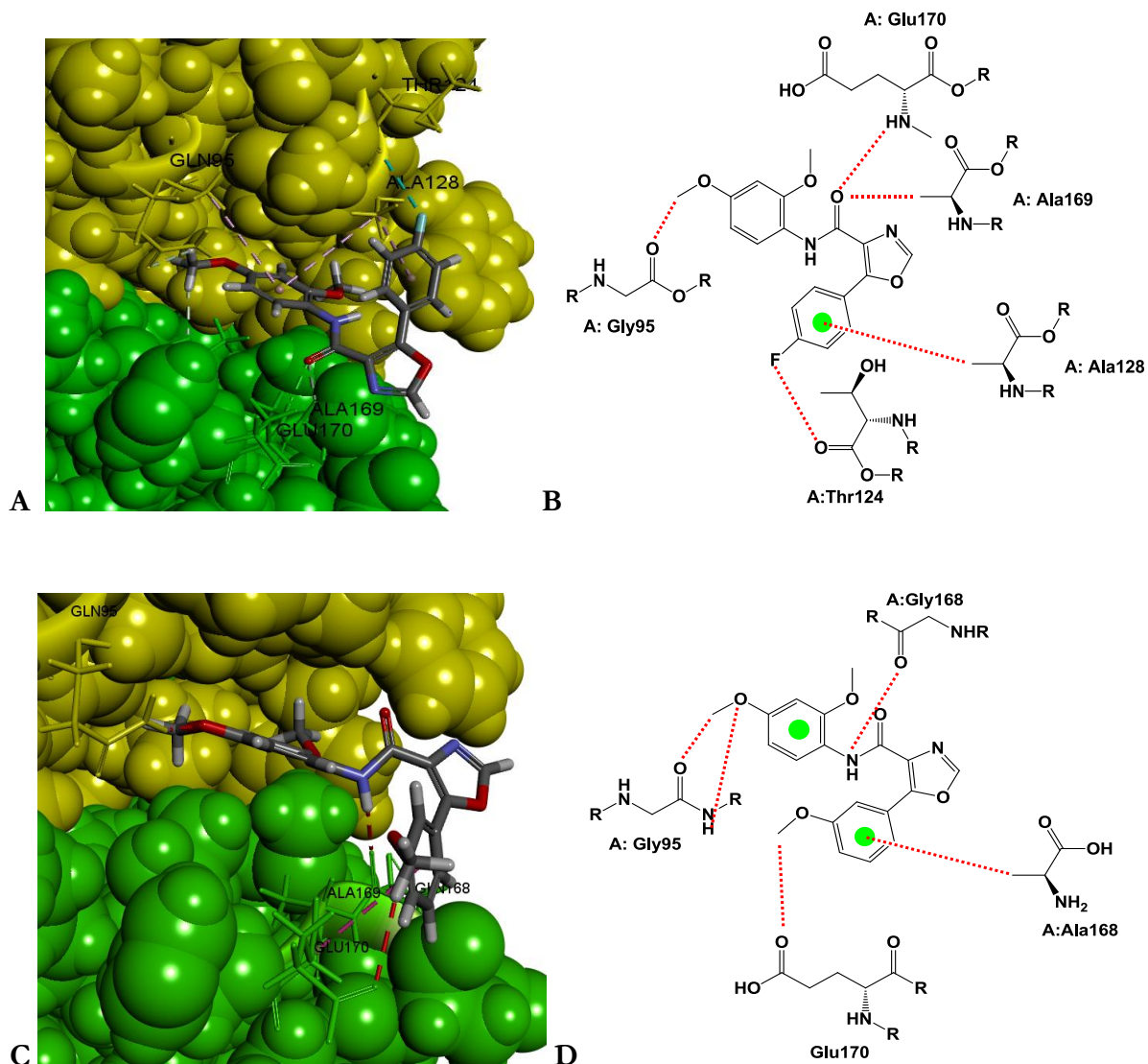


Figure 3.4: Predicted binding models of compounds **100b** (A and B), and **100h** (C and D) docked in the LEDGF/p75 binding cavity at the HIV-1 IN dimer interface (with yellow CPK display sphere sized representing monomer A and green CPK display sphere sized for monomer B).

The modelling results revealed that the *para*-methoxy group of the aniline is highly favoured through making a hydrogen bond with the Gln95 residue (as shown in *Figures 3.4* and *3.5*). Furthermore, compounds **100a** and **100h** were interacting with what are reported to be critical residues in the binding of the LEDGF/p75 protein.

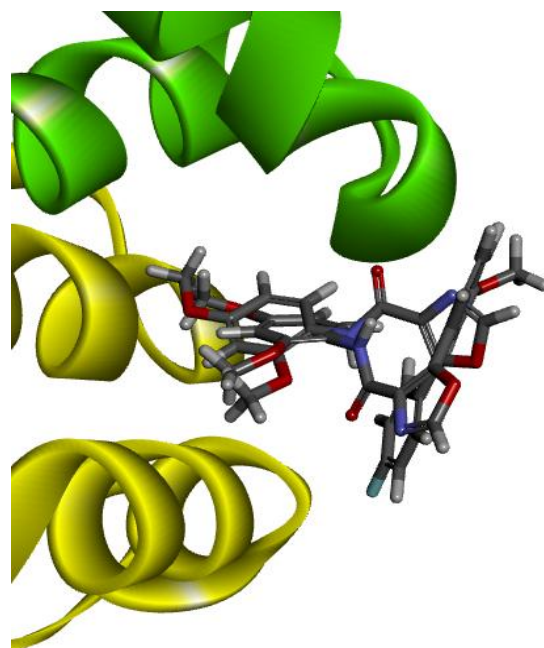


Figure 3.5: Overlaying projection model of compound **100b** and **100h** in the LEDGF/p75 binding cavity at the HIV-1 IN dimer interface

3.3.6. Conclusion

A series of 5-aryl-1,3-oxazoles were successfully synthesized *via* the van Leusen approach by reacting TosMIC and substituted benzaldehydes in the presence of catalytic K_2CO_3 in MeOH in just 7 minutes under microwave conditions. The 5-aryl-1,3-oxazole products were obtained in good to high yields. However, attempts to prepare 5-aryl-1,3-oxazole scaffolds under the same microwave conditions in MeCN afforded instead the intermediates 5-aryl-4-tosyl-4,5-dihydro-1,3-oxazoles, which were also obtained in high yields and could be converted easily to their respective oxazoles though an elimination step. The microwave assisted van Leusen approach used resulted in a time efficient method towards the preparation of both 5-aryl-1,3-oxazoles and 5-aryl-4-tosyl-4,5-dihydro-1,3-oxazole scaffolds.

Further investigations into the effect of reaction conditions on this synthesis under microwave irradiation may be interesting but time constraints did not allow this. The present fragment library, although not overly toxic to cells, showed no significant inhibitory activity on the LEDGF-IN interaction assay, nor on the Vpu binding assay, which may be attributed to their relatively small size.

Based on the disappointing biological results obtained from the first fragment library, a second generation of compounds were prepared. Initial attempts were made to synthesise the *N*,5-diaryl-1,3-oxazole-4-carboxamide derivatives *via* formation of *N*-aryl-2-isocyanoacetamide

intermediates. These key intermediates were successfully obtained by first converting the glycine ester hydrochloride with methyl formate into *N*-formyl glycine ethyl ester in good yield. This was followed by reaction with hydrazine monohydrate to afford the corresponding *N*-(2-hydrazinyl-2-oxoethyl)formamide in excellent yield. Further treatment of the compound with 1M HCl and aqueous NaNO₂ in water, followed by treatment with anilines in THF furnished the *N*-aryl-2-formamidoacetamides in yields ranging from moderate to good. The *N*-aryl-2-formamidoacetamides were then dehydrated using POCl₃, Et₃N in DCM to provide the corresponding *N*-aryl-2-isocyanoacetamide intermediates in yields of 84 and 92%. Attempts to synthesize *N*,5-diaryl-1,3-oxazole-4-carboxamide derivatives by treatment of benzoyl chloride derivatives with these *N*-aryl-2-isocyanoacetamide intermediates using Et₃N in DCM at room temperature for 24-48 hours were unsuccessful. Attempts to use DBU as a base didn't yield any desired products but instead resulted in an addition reaction to give the previously prepared *N*-aryl-2-formamidoacetamide in 85% yield. Reaction of benzaldehydes with the *N*-aryl-2-isocyanoacetamide intermediate in the presence of DBU afforded the corresponding 4,5-dihydro-*N*,5-diaryl-1,3-oxazole-4-carboxamide scaffolds in good yields. Attempts to oxidize these (4*R*,5*R*/4*S*,5*R*)-4,5-dihydro-*N*,5-diaryl-1,3-oxazole-4-carboxamide scaffolds with BrCCl₃ in DCM were unsuccessful. This prompted the search for a simple and effective route towards *N*,5-aryl-1,3-oxazole-4-carboxamide derivatives.

The *N*,5-aryl-1,3-oxazole-4-carboxamide derivatives were successfully constructed over three steps. Initial reaction of benzoyl chloride analogues with ethyl isocyanoacetate in the presence of DBU as base in THF afforded the ethyl 5-phenyl-1,3-oxazole-4-carboxylate products in good yields. These scaffolds were subjected to hydrolysis conditions with NaOH in water and MeOH, followed by acidification with 1M HCl to furnish the 5-phenyl-1,3-oxazole-4-carboxylic acid derivatives in high yields. Further treatment of 5-phenyl-1,3-oxazole-4-carboxylic acid compounds with thionyl chloride gave the more reactive 5-phenyl-1,3-oxazole-4-carbonyl chloride analogues, which were then reacted with aniline derivatives in the presence of Et₃N at room temperature for 24 hours to obtain a series of novel *N*,5-aryloxazole-4-carboxamide derivatives in yields ranging from moderate to excellent.

The synthesized novel *N*,5-aryl-1,3-oxazole-4-carboxamide derivatives, 5-aryloxazole-4-carboxylic acids and the ethyl 5-phenyloxazole-4-carboxylate compounds were assessed for their ability to disrupt the interaction between HIV-1 IN and LEDGF/p75 proteins. In the IN-LEDGF/p75 biochemical assay, inhibition by two compounds exceeded the pre-defined cut-off value of 50%. These compounds contain electron donating methoxy groups at the *ortho*- and

para-positions of the aniline core that are similar to the **CAB** compounds described in the literature that exhibited inhibitory activity above 50%. These results indicate that the presence of electron donating methoxy substituents at the *ortho*- and *para*-positions of the aniline ring is highly favoured in compounds for disruption of the interaction between LEDGF/p75 and HIV-1 IN proteins.

From the ADME studies, compound **100b** exhibited low solubility while compound **100h** displayed a good solubility level. Both scaffolds were non-inhibitors of cytochrome enzymes and were found to be poorly absorbed in the human intestine. The ligand-protein docking study showed that both compounds **100b** and **100h** interact with some of critical residues within the HIV-1 IN dimer site. Furthermore, the *para*-methoxy group on the aniline ring was shown to be significant in the binding of these scaffolds. Their binding energies correlate with the percentage inhibition from AlphaScreen assay.

Thus it appears that compounds containing the *N*-(2,4-dimethoxyphenyl)acetamide moiety can serve as templates for further modification to design more potent biologically active compounds that can specifically target the LEDGF/p75-IN interaction.

3.4. Future work

Further modification by varying the substituents on the phenyl group at the 5-position of the oxazole ring and their biological assessment as possible inhibitors of HIV-1 IN-LEDGF/p75 interaction will form part of future work (*Figure 3.6*). Furthermore, screening of the oxazole-based library in the HIV-1 Vpu-BST-2 ELISA assay, with the aim of possibly identifying hits to further modify and generate a next generation of compounds will be conducted in future.

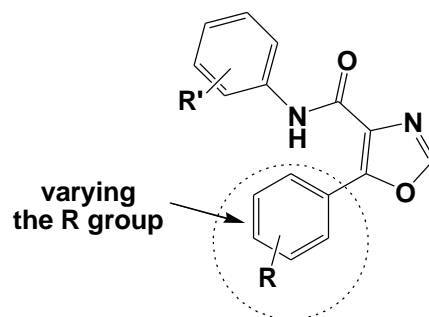


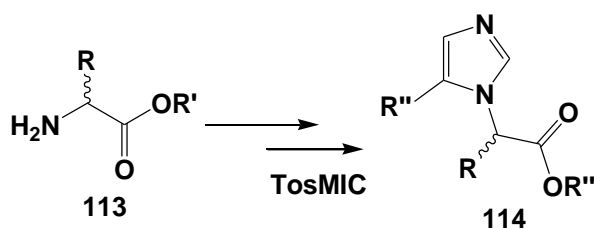
Figure 3.6: Possible structural modifications of the oxazole based compounds.

CHAPTER 4

Synthesis of a family of 5-aryl-imidazol-1-yl acyl-based compounds as potential inhibitors of HIV-1 protein-host protein interactions using a van Leusen approach

4.1. Introduction

Amino acids play a significant role in many biological processes, hence they are often used as building blocks for designing new pharmacologically active compounds.^{256,257,258} Compounds with an amino acid backbone have displayed interesting biological activities like anti-HIV-1 and antimicrobial activities.^{259,260,261} On the basis of the above and aligned with our objectives defined in Chapter 1, we set out to incorporate a simple amino acid framework into the imidazole nucleus *via* the van Leusen reaction, anticipating the generation of a small family of 5-aryl-1*H*-imidazol-1-yl acyl compounds **114** (*Scheme 4.1*). We hoped that the screening of 5-aryl-1*H*-imidazol-1-yl-based compounds could also provide viable hits that could be used as a template to design a second generation of compounds that could act as possible inhibitors of the HIV-1 IN-host LEDGF/p75 and/or HIV-1 Vpu-Host BST-2 interactions. This chapter will address synthetic challenges encountered in the incorporation of amino acids into the imidazole motif as well as the characterization of the synthesized compounds. Biological evaluation of the synthesized compounds in AlphaScreen and ELISA assays will also be discussed.



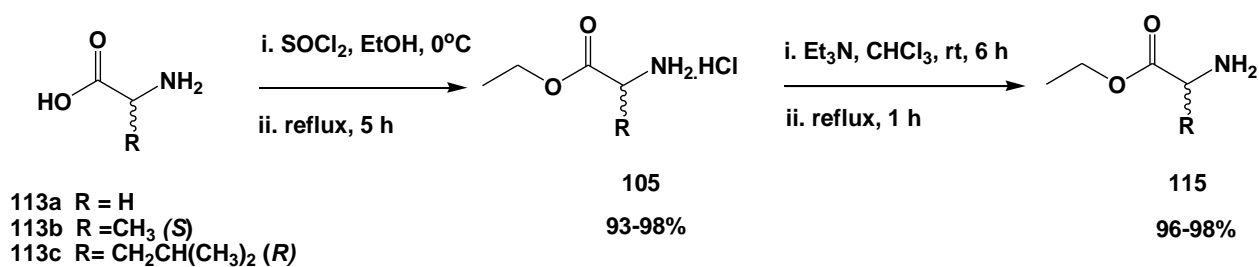
Scheme 4.1: The integration of an amino acid into the imidazole motif using the van Leusen reaction.

4.2. Synthesis of 5-aryl-1*H*-imidazol-1-yl acyl derivatives using van Leusen reaction

The key intermediates required for the van Leusen imidazole reaction were imines, prepared from amines and aldehydes. The amine components we required were derived from amino acids, while commercially available aldehydes were used.

4.2.1. Synthesis of free amino ethyl ester derivatives

In order to generate van Leusen precursors from amino acids, the carboxylic acid groups required protection before conducting the condensation reactions with an aldehyde. The carboxylic group is usually protected by converting the amino acid into the corresponding amino acid ester hydrochloride salt. Convenient procedures for preparing the ester hydrochloride salts involve the addition of hydrochloric acid (HCl),²⁶² thionyl chloride (SOCl₂)^{263,264} or acetyl chloride (AcCl)²⁶⁵ to a solution of the amino acid in a protic solvent such as methanol or ethanol. Although, the ester hydrochloride salts can be obtained commercially, it was ideal to utilise the commercially available amino acids which were readily accessible in our laboratory. Therefore, the approach employing thionyl chloride was adopted and commercially available glycine **113a**, L-alanine **113b** and D-leucine **113c** were chosen as synthons for the synthesis of van Leusen intermediates.

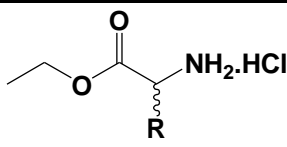


Scheme 4.2: Synthesis of free amino acid ester **115**.

The synthesis commenced with the addition of SOCl₂ to a mixture containing commercially available amino acids **113a-c** in ethanol at 0°C, followed by refluxing for 5 hours as shown in **Scheme 4.2**. Work up afforded the corresponding amino ester hydrochloride salts **105a-c** in excellent yields. The yields obtained were comparable to those values reported using a HCl/EtOH system (*Table 4.1*).^{266,267,268,269} The NMR spectra of the corresponding salts were in agreement with the data reported in literature while melting points of 144-147°C for compound **105a** and 76-78°C for compound **105b** were comparable to the reported literature values.^{263,}

^{269, 270, 271}

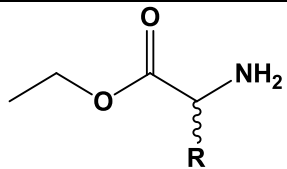
Table 4.1: Isolated yields (%) of the amino ester hydrochloride salt **105**.



Compounds	R	Yields (%)
105a	H	90
105b	CH ₃ (<i>S</i>)	99
105c	CH ₂ CH(CH ₃) ₂ (<i>R</i>)	95

The esterified amino acid salts **105a-c** were then treated with Et₃N using CHCl₃ as solvent at room temperature for 6 hours, followed by heating under reflux for 1 hour (**Scheme 4.2**).^{272,273} Work up furnished the free amino ethyl esters **115a-c** in yields ranging from 96-98% (**Table 4.2**).

Table 4.2: Isolated yields (%) of the free amino esters **115**.

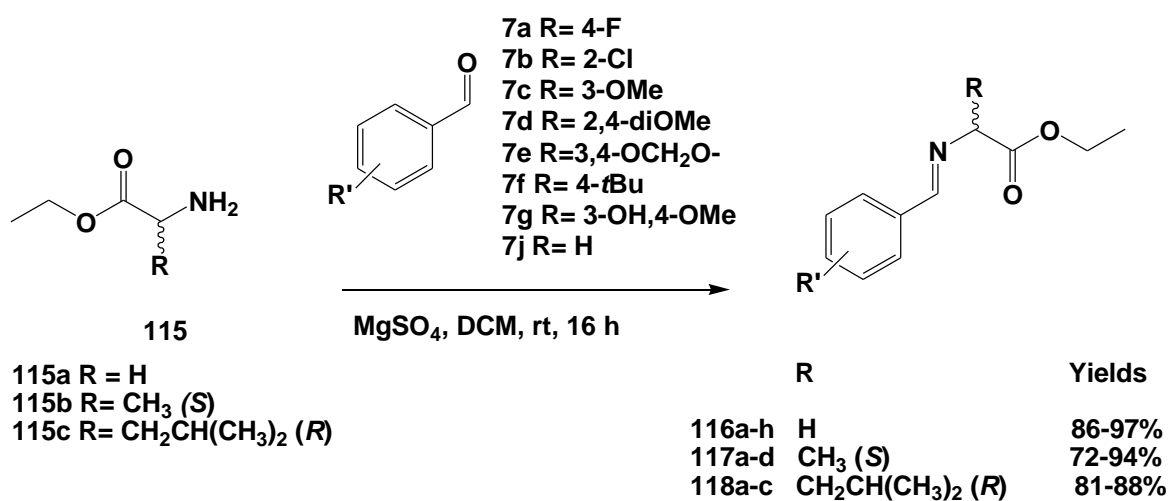


Compounds	R	Yields (%)
115a	H	96
115b	CH ₃ (<i>S</i>)	98
115c	CH ₂ CH(CH ₃) ₂ (<i>R</i>)	98

The chemical structures of free amino esters **115a-c** were supported by NMR spectroscopic analysis and were consistent with reported literature.^{274,275,276,277,278} The NMR spectra of L-alanine ethyl ester **115b** will be discussed in detail as an illustration representing this compounds class. A distinguishing feature of compound **115b** in the ¹H NMR spectrum was the presence of two quartets: one at 4.01 ppm for the methylene protons of the ethyl group and one at 3.43 ppm for the methine proton at a chiral centre, with each having a coupling constant value of 7.2 Hz. Furthermore, a singlet corresponding to the two protons of the NH₂ group appears at 1.59 ppm, whereas a doublet at 1.19 ppm with a *J* value of 7.4 Hz corresponds to the protons of the methyl group attached to the chiral centre. The upfield triplet at 1.13 ppm (*J* = 7.2 Hz) is assigned to the

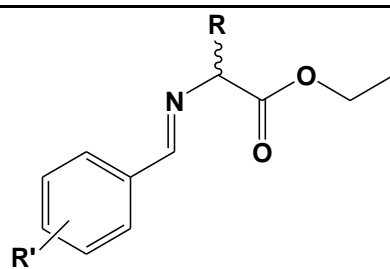
protons of the methyl group, which are coupled with the methylene group (ethyl moiety). The ^{13}C NMR spectrum of compound **115b** confirmed the presence of all five carbon atoms, with the carbonyl carbon atom signal appearing at 176.3 ppm, and signals at 60.5 and 49.8 ppm belonging to the methylene carbon atom of the ethyl group and methine carbon atom at a chiral centre. Furthermore, the signal at 20.4 ppm corresponds to the methyl carbon atom at a chiral centre, while the methyl carbon atom of the ethyl group resonates at 13.9 ppm.

4.2.2. Condensation of amino ethyl ester derivatives with various benzaldehydes



Scheme 4.3: Synthesis of ethyl 2-(arylideneamino)acyl intermediates.

Walton *et al.* described the reaction of various aldehydes with esterified amino acid salts using Et₃N as a base in the presence of MgSO₄ in DCM at room temperature to afford the corresponding ethyl (*E*)-2-{(arylidene)amino}acetates in quantitative yields.²⁷⁹ Inspired by this protocol, our free amino ethyl esters **115a-c** were then exposed to the condensation reaction conditions by reacting with various benzaldehydes **7a-h** in the presence of MgSO₄ using DCM as solvent at room temperature for 16 hours (*see Table 4.3*). Work up furnished the desired ethyl 2-(arylideneamino)acyl intermediates (**116a-h**, **117a-d** and **118a-c**) in yields of up to 96%. The yields of the products obtained (96% for **116h** and 92% for **117d**) were considerable improvements over those reported by López-Pérez *et al.* (81% for **116h** and 87% for **117d**).²⁸⁰ Compounds **116a-h**, **117a-d** and **118a-c** were used in the next stage without further purification.

Table 4.3: Isolated yields (%) of the ethyl 2-(arylideneamino)acyl intermediates.

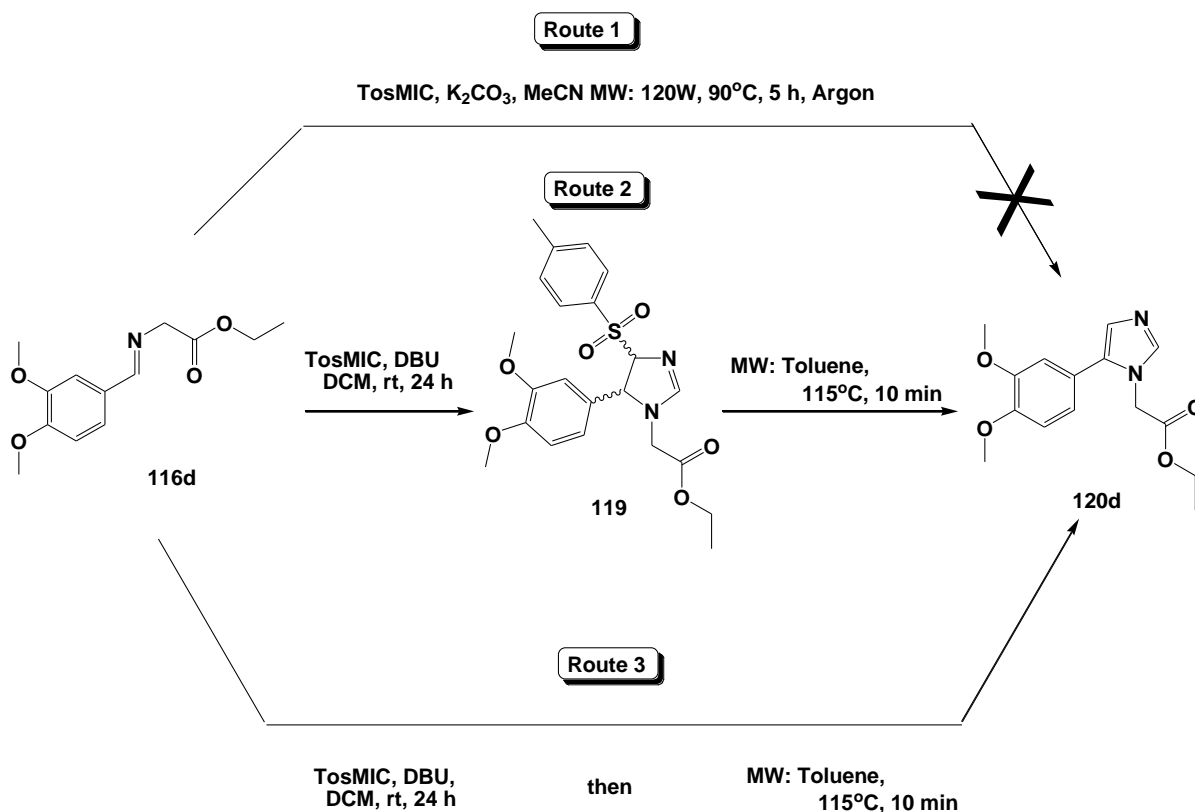
Compound	R	R'	Yields (%)
116a	H	4-F	91
116b	H	2-Cl	87
116c	H	3-OMe	90
116d	H	3,4-diOMe	93
116e	H	3,4-OCH ₂ O	91
116f	H	4- <i>t</i> Bu	88
116g	H	3-OH,4-OMe	86
116h	H	H	96
117a	CH ₃ (<i>S</i>)	4-F	91
117b	CH ₃ (<i>S</i>)	3-OMe	72
117c	CH ₃ (<i>S</i>)	3,4-diOMe	83
117d	CH ₃ (<i>S</i>)	H	92
118a	CH ₂ CH(CH ₃) ₂ (<i>R</i>)	4-F	88
118b	CH ₂ CH(CH ₃) ₂ (<i>R</i>)	3,4-diOMe	86
118c	CH ₂ CH(CH ₃) ₂ (<i>R</i>)	H	81

The product structures were elucidated by NMR and FTIR spectroscopy, which verified that the compounds obtained were the desired ethyl 2-(arylideneamino)acyl intermediates **116**, **117** and **118**. In solution, NMR spectroscopy indicates that compounds **116**, **117** and **118** are present in each case as only one geometrical isomer, which by comparison with data reported in the literature is most likely the *E*- isomer^{279,280,281}. All ¹H NMR spectra of the van Leusen intermediates **116**, **117** and **118** showed a characteristic azomethine (N=CH) singlet in the region of δ 8.1-8.2 ppm, whilst the ¹³C NMR spectra for the same compounds exhibited the azomethine and carbonyl carbon atoms in the region of δ 163-165 and 170-171 ppm, respectively. The ¹H NMR spectra of compounds **116a-h** with no substituents at the carbon atom adjacent to the nitrogen atom and carbonyl group showed a singlet in the region of δ 4.3 to 4.4 ppm

corresponding to the methylene protons. Signals from the methine protons at the chiral centre of the van Leusen intermediates **117a-d** derived from L-alanine, can be observed as multiplets in the region of δ 4.0-4.2 ppm, due to overlapping with the quartet due to the 5-methylene protons of the ethyl group. Furthermore a doublet at 1.4 ppm ($J = 7.2$ Hz) and triplet at 1.2 ppm ($J = 7.2$ Hz) correspond to the protons of the methyl group at the chiral centre and the methyl protons of the ethyl group, respectively.

4.2.3. Optimization of conditions towards cycloaddition of TosMIC to the prepared ethyl 2-(arylideneamino)acrylate

The cycloaddition of TosMIC **1** to the ethyl 2-(arylideneamino)acryls was initially attempted using our previously reported procedure described in Chapter 2. The (*E*)-ethyl-2-(3,4-dimethoxybenzylideneamino)acetate **116d** was then chosen as a precursor for the investigation. A mixture of ethyl-2-(3,4-dimethoxybenzylideneamino)acetate **116d** and TosMIC **1** in MeCN using K_2CO_3 as a Lewis base was microwave-irradiated at a set temperature of 90°C and a power of 120 Watts under inert conditions, as depicted in **Scheme 4.4** (Route 1). TLC indicated full consumption of **116d** and little presence of TosMIC **1** after 5 hours. However, no new development of spots could be observed by TLC. To further determine whether there was any product formed or not, the solvent was evaporated *in vacuo* and dried to afford a crude brown oil material. The crude product was then analysed by NMR spectroscopy, however, 1H NMR revealed a complicated spectrum with none of the signals corresponding to the desired product present. A possible explanation for the failed conversion may be attributed to decomposition of the intermediate **116d** under microwave irradiation, which implied that milder reaction conditions might be required in order to successfully afford the product.



Scheme 4.4: Effects of the reaction conditions on the formation of the desired products **120**.

With the failure of the above described reaction, an alternative route was envisaged and effort was then shifted to using 1,8-diazabicyclo[5.4.0]undec-7-ene (DBU) as a catalytic base towards the preparation of the van Leusen products. We assumed that using a strong base under mild conditions, might promote the cycloaddition of TosMIC **1** to the ethyl 2-(5-aryl-1*H*-imidazol-1-yl)acrylates, which could afford the desired van Leusen adducts. The reaction was then pursued by reacting ethyl 2-(3,4-dimethoxybenzylideneamino)acetate **116d** and TosMIC **1**, in the presence of DBU using DCM as a solvent of choice at room temperature as illustrated in **Scheme 4.4** (Route 2). After 24 hours, TLC indicated complete consumption of TosMIC **1** and the formation of a new spot, suspected to be product. Isolation and purification of a newly formed spot by column chromatography afforded a pale yellow solid. However, analysis of the obtained product by ¹H NMR spectroscopy (*Figure 4.1*) revealed that instead of the expected desired product, the ethyl 2-[5-(3,4-dimethoxyphenyl)-4-tosyl-4,5-dihydro-1*H*-imidazol-1-yl]acetate **119d** was obtained as a racemic mixture of 2 diastereomers in 55% yield. This kind of product arises due to the unsuccessful elimination of the *para*-toluenesulfonyl group under certain reaction conditions. Further examination of the ¹H NMR spectrum in *Figure 4.1* revealed a 2:1 diastereomeric ratio (for *trans*-ethyl 2-[5-(3,4-dimethoxyphenyl)-4-tosyl-4,5-dihydro-1*H*-imidazol-1-yl]acetate **A** to *cis*-

ethyl 2-[5-(3,4-dimethoxyphenyl)-4-tosyl-4,5-dihydro-1*H*-imidazol-1-yl]acetate **B**. The *trans*-1*H*-imidazoline **A** was characterised by the presence of two doublets at 5.05 and 5.25 ppm with a coupling constant of 6.4 Hz corresponding to the two methine protons at the 4- and 5-positions of the oxazoline motif, while the two methine protons of *cis*-1*H*-imidazoline **B** resonate as a singlet at 4.77 ppm. Furthermore, the methyl group of the imidazoline **A** resonates as a singlet at 2.42 ppm, while for the imidazoline **B** the singlet appears at 2.04 ppm. The two doublets at the 4- and 5-positions of the oxazoline ring arise as a result of the *trans*- geometry. These findings are supported by reported literature.²⁸²

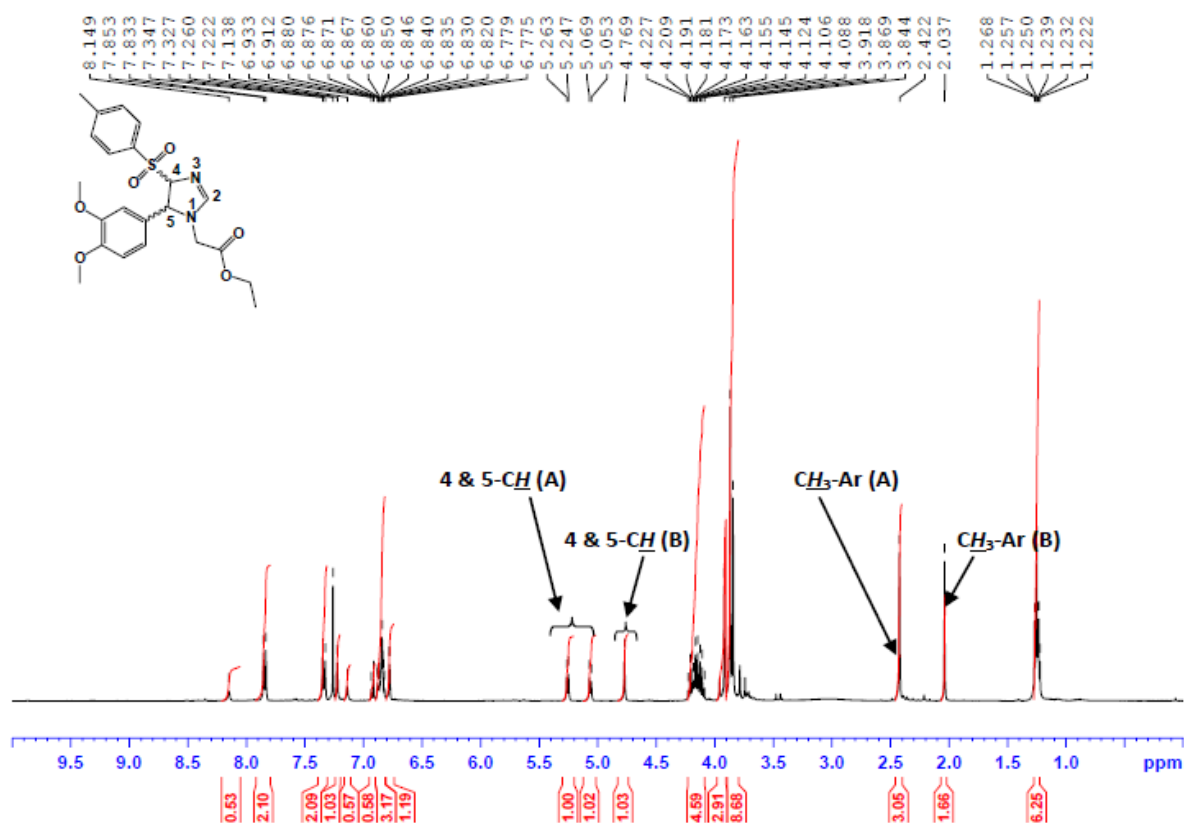
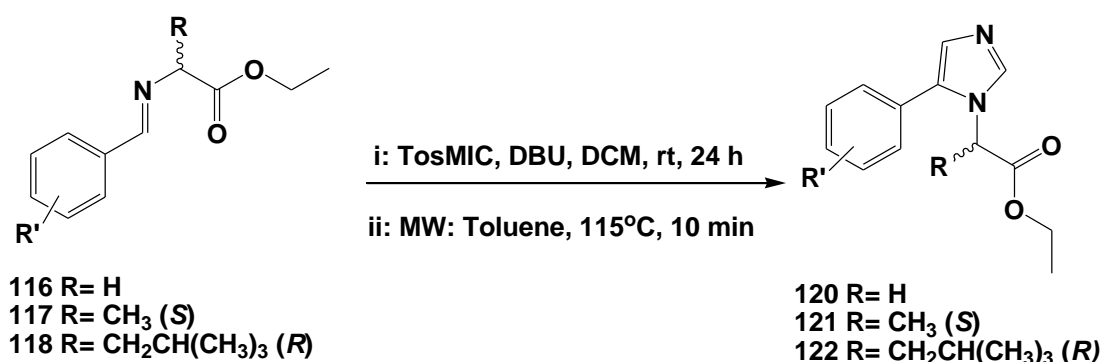


Figure 4.1: 400 MHz ¹H NMR spectrum of mixture of *trans*-ethyl 2-[5-(3,4-dimethoxyphenyl)-4-tosyl-4,5-dihydro-1*H*-imidazol-1-yl]acetate (**A**) and *cis*- ethyl 2-[5-(3,4-dimethoxyphenyl)-4-tosyl-4,5-dihydro-1*H*-imidazol-1-yl]acetate imidazoline (**B**) as diastereomeric mixture.

Inspired by our experience with the oxazole synthesis in section 3.2.2 and a reported protocol where the elimination of the *para*-toluenesulfonyl group was accomplished in toluene, we explored removal of this group in toluene under microwave irradiation.²³² Thus, compound **119d** was dissolved in toluene and subjected to microwave irradiation at a set temperature of 115°C for 10 minutes (observed by TLC). Work up and isolation by silica gel column chromatography

furnished the desired ethyl 2-[5-(3,4-dimethoxyphenyl)-1*H*-imidazol-1-yl]acetate **120d** in a yield of 60%. The synthesis of ethyl 2-[5-(3,4-dimethoxyphenyl)-1*H*-imidazol-1-yl]acetate **120d** was also investigated without purification of compound **119d** as illustrated in **Scheme 4.4** (Route 3). The reaction mixture was initially stirred under the conditions described for Route 2, followed by the removal of DCM *in vacuo* to obtain a crude brown product. The crude material was then re-dissolved in toluene, microwaved under the conditions described above, and remarkably afforded ethyl 2-[5-(3,4-dimethoxyphenyl)-1*H*-imidazol-1-yl]acetate **120d** in 74% yield after column chromatography, suggesting that the separation of intermediates is not necessary. Furthermore, the yield of formation of **120d** without separation of intermediate **119d** was better than the overall yield of the product in two steps *via* formation of **119d**.

4.2.4. Van Leusen reaction for the preparation of the ethyl 5-aryl-1*H*-imidazol-1-yl acyls

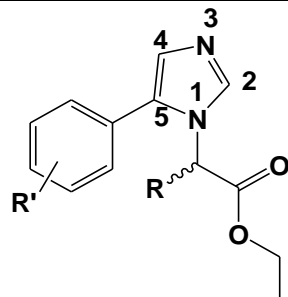


Scheme 4.5: Synthesis of 2-(5-aryl-1*H*-imidazol-1-yl)acyls using optimized conditions.

Under these optimized conditions, the generality and restrictions of the van Leusen reaction were investigated using other synthesized ethyl 2-(arylideneamino)acetate intermediates (**Scheme 4.5**). Firstly, the ethyl 2-(arylideneamino)acetates **116a-h** derived from glycine were used and successfully transformed into the corresponding novel ethyl 2-(5-aryl-1*H*-imidazol-1-yl)acetates **120a-h** in yields of between 26-74% (**Scheme 4.5** and *Table 4.4*). The product yields were strongly influenced by the presence of substituents on the 5-aryl ring. However, attempted conversion of the other remaining intermediates **117a, c-d** and **118a-c** under similar conditions only afforded the corresponding novel (5-aryl-1*H*-imidazol-1-yl)acyls (**121a**, and **121c-d**) derived from L-alanine **117a, c-d** in yields ranging from 11 to 23% (*Table 4.4*). Products **122** derived from D-leucine **118a-c** were, however, not obtained. From the observed results it is clear that the

yields of the products are strongly influenced by the substituents at the chiral centre and on the aryl ring.

Table 4.4: Isolated yields (%) of the novel ethyl 2-(5-aryl-1*H*-imidazol-1-yl)acryls **120** and **121**.



Compounds	R	R'	Yields (%)
120a	H	4-F	52
120b	H	2-Cl	26
120c	H	3-OMe	38
120d	H	3,4-diOMe	74
120e	H	3,4-OCH ₂ O	45
120f	H	4- <i>t</i> Bu	35
120g	H	3-OH,4-OMe	51
120h	H	H	33
121a	CH ₃ (<i>S</i>)	4-F	11
121c	CH ₃ (<i>S</i>)	3,4-diOMe	23
121d	CH ₃ (<i>S</i>)	H	20

In summary, we successfully incorporated simple amino acids into the imidazole nucleus *via* van Leusen reactions under mild conditions. A total of eleven new ethyl 2-(5-aryl-1*H*-imidazol-1-yl)acryl derivatives **120** and **121** were obtained using our novel van Leusen protocol described above. A mechanistic rationale for the formation of compounds **120** and **121** can be based on a similar mechanism to that outlined in Chapter 1, **Scheme 1.6**. However, in this case the elimination of the *para*-toluenesulfonyl group was accomplished by microwave irradiation in toluene.

4.2.4.1. Structure elucidation of newly synthesized 2-(5-aryl-1*H*-imidazol-1-yl)acyls by NMR and FTIR spectroscopy

The characterization of these novel compounds **120** and **121** was assisted by ¹H-NMR, ¹³C-NMR and FTIR spectral data. Compound **120d** was chosen as the prototype representing this compound class. The presence of two singlets at δ 7.56 ppm and 7.03 ppm for the 2- and 4-methine protons of the imidazole motif in the ¹H NMR spectrum of compound **120d** clearly indicate that the van Leusen product had been formed. Further evidence for the formation of compound **120d** was a singlet at 4.61 ppm integrating for two protons corresponding to the methylene group adjacent to the carbonyl group. A quartet and a triplet at δ 4.13 ppm and 1.18 ppm with *J* values of 7.2 Hz each, correspond to the methylene and methyl protons of the ethyl group, coupling with each other, while the six protons of the two methoxy groups appear at 3.87 and 3.83 ppm as two singlets. In the ¹³C NMR spectrum of compound **120d**, the carbonyl carbon atom resonates as a signal at 167.8 ppm while the 2- and 4-methine carbon atoms emerge at 138.5 ppm and 121.5 ppm. The methylene carbon atom next to the carbonyl group appears as a signal at 46.3 ppm, whereas the methylene and methyl carbon atoms of the ethyl group resonate at 61.9 and 13.9 ppm. The two methoxy carbon atoms at the *para*- and *meta*-positions give rise to signals at 55.81 and 55.78 ppm. The FTIR spectra of novel ethyl 2-(5-aryl-1*H*-imidazol-1-yl)acyls **120** and **121** showed the carbonyl (C=O) bands in the region of 1745-1755 cm⁻¹, whilst the bands in the region of 1306 cm⁻¹ to 1380 cm⁻¹ were assigned to the C-N group of the imidazole core (Table 4.5).

Table 4.5: FTIR spectroscopic data of ethyl 2-(5-aryl-1*H*-imidazol-1-yl)acyl products showing the C=O and C=N bands.

Compnds	120a	120b	120c	120d	120e	120f	120g	120h	121a	121c
ν_{C=O}(cm⁻¹)	1747	1748	1745	1748	1741	1755	1748	1736	1748	1750
ν_{C-N}(cm⁻¹)	1380	1356	1379	1356	1336	1363	1334	1376	1306	1324

4.2.4.2. Structure elucidation of newly synthesized ethyl 5-aryl-1*H*-imidazol-1-yl acyls by mass spectrometry

Evidence of the successful incorporation of amino acids into the imidazole moiety was further provided by ESI-LCMS, which provides accurate identification of the compounds. The calculated and experimental molecular ions (*m/z*) of these novel scaffolds **120** and **121** as well as

their mSigma values are displayed in *Table 4.6*. The accurate formula of the compounds was calculated using Bruker SmartFormula3D[®], with a mass accuracy within 5 ppm (5 mDa). The Bruker SmartFormula algorithm is used to associate the theoretical isotopic pattern of each potential accurate mass formula with the experimentally determined pattern. Detailed elucidations of the fragments were carried out in positive ion mode and the parent molecular ions are presented as [M+H]⁺. All eluted products from LC into mass spectrometry showed one peak on both detectors (UV before reaching the mass spectrometer and MS detector afterwards). The mass chromatograms single peak corresponds to the protonated molecular ion.

Table 4.6: HRMS results of the ethyl 2-(5-aryl-1*H*-imidazol-1-yl)aclys (**120** and **121**) and their mSigma values.

Compds	Chemical formula [M+1]	Calculated m/z	Measured m/z	Err (mDa)	Err (ppm)	mSigma value
120a	C ₁₃ H ₁₄ FN ₂ O ₂ ⁺	249.1034	249.1027	-0.7	10.8	2.0
120b	C ₁₃ H ₁₄ N ₂ O ₂ Cl ⁺	265.0738	265.0738	0.0	0.0	3.8
120c	C ₁₄ H ₁₇ N ₂ O ₃ ⁺	261.1234	261.1232	0.2	0.6	5.1
120d	C ₁₅ H ₂₁ N ₂ O ₄ ⁺	291.1339	291.1332	-0.7	-2.2	6.4
120e	C ₁₃ H ₁₃ N ₂ O ₄ ⁺	261.1183	261.1186	0.3	0.3	5.9
120f	C ₁₅ H ₁₉ N ₂ O ₂ ⁺	287.1754	287.1764	-1.0	-3.7	7.5
120g	C ₁₂ H ₁₃ N ₂ O ₄ ⁺	277.1183	277.1184	-0.1	-0.4	2.3
120h	C ₁₃ H ₁₅ N ₂ O ₂ ⁺	231.1128	231.1126	0.2	0.9	1.1
121a	C ₁₄ H ₁₆ FN ₂ O ₂ ⁺	263.1173	263.1190	-0.3	-1.1	4.4
121c	C ₁₆ H ₂₁ N ₂ O ₄ ⁺	305.1476	305.1503	-0.7	-2.4	3.1
121d	C ₁₄ H ₁₇ N ₂ O ₂ ⁺	245.1258	245.1279	-2.1	-1.1	5.0

It was interesting to observe that variation on the 5-aryl ring had a significant influence on the fragmentation pattern of these ethyl 5-aryl-1*H*-imidazol-1-yl acyl scaffolds. These findings were observed in the MS/MS analysis supported by SmartFormula, which confirms possible formula for the fragment ions. Compounds **120a** and **120d** were chosen as the models to discuss in detail the mass fragmentation patterns further.

4.2.4.2.1. Mass fragmentation of ethyl 2-[5-(4-fluorophenyl)-1*H*-imidazolyl]acetate **120a**

The mass spectrum in *Figure 4.2 (a)* of compound **120a** revealed an intense molecular ion peak at m/z 249.1027, which was confirmed by SmartFormula as having the molecular formula $C_{13}H_{14}FN_2O_2[M + H]^+$, consistent with the parent ion.

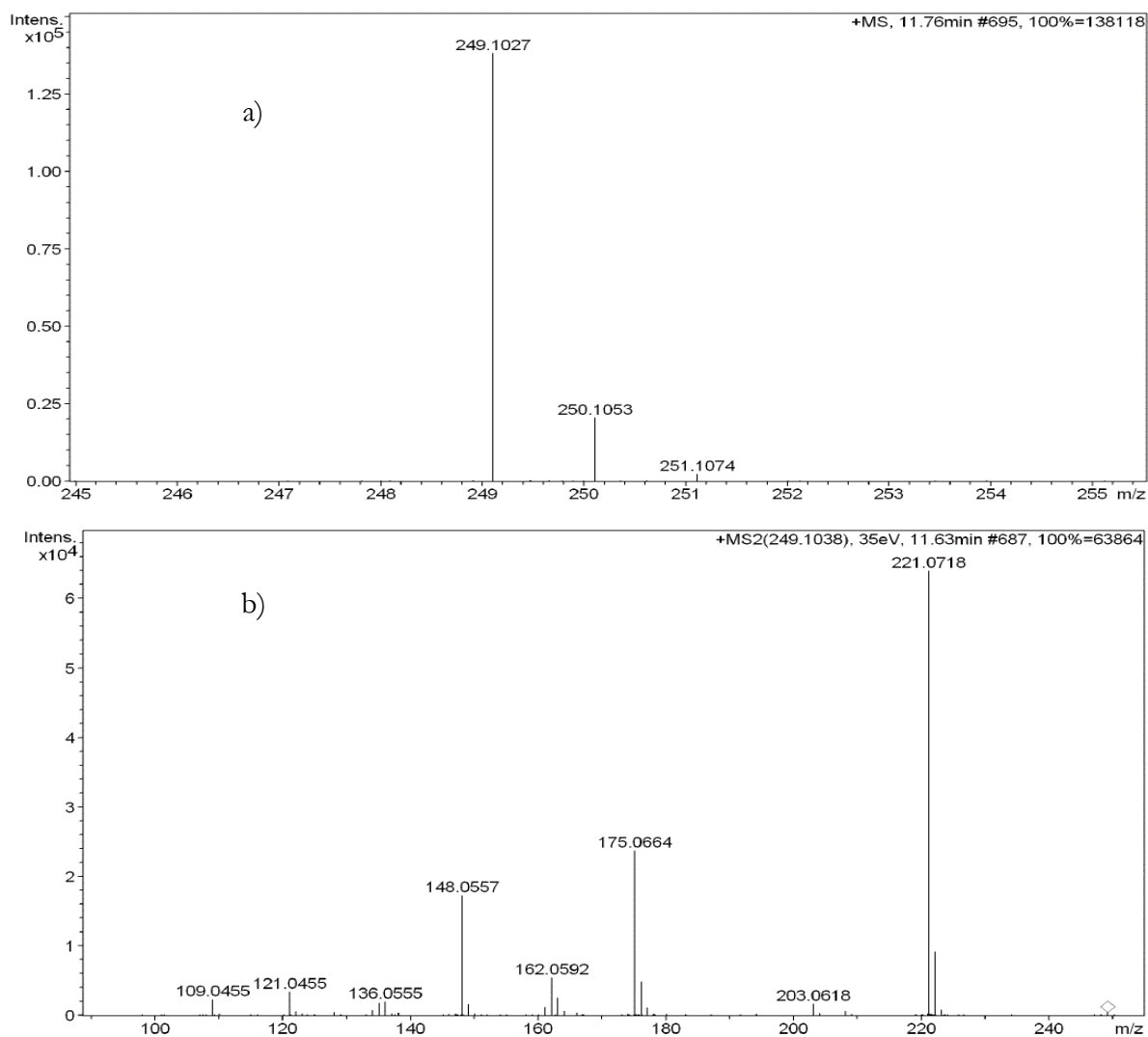


Figure 4.2: Recorded spectra for compound **120a**: (a) MS of $[M+H]^+$ and b) MS/MS (collision energy of 35 eV).

MS/MS fragmentation with 35 eV N_2 collision energy produced the spectrum depicted in *Figure 4.2 (b)* of compound **120a**, $[M+H]^+$ peak m/z 249.10. A possible fragmentation pathway (*Figure 4.3*) shows the compound undergoing disintegration to produce a base peak at m/z 221.07 with formula $C_{11}H_{10}FN_2O_2^+$ corresponding to the loss of a neutral ethene ($CH_2=CH_2$). The ion, $C_{11}H_{10}FN_2O_2^+$ then endures further fragmentation to give a peak at m/z 203.06 with a formula of

$C_{11}H_8FN_2O^+$ relating to the loss of a H_2O molecule, which defragments further and produces two fragmentation pathways. The first pathway involves a loss of carbon monoxide (CO) to form an ion at m/z 175.06 with formula $C_{10}H_8FNO^+$. Further breakdown of $C_{10}H_8FNO^+$ affords a peak at m/z 148.06 with formula $C_9H_7FN^+$ corresponding to the loss of hydrogen cyanide (CHN) through a ring opening of the imidazole moiety, followed by another loss of CHN to generate the ion at m/z 121 of formula $C_8H_6FN^+$. The second pathway from m/z 203.06 shows the loss of cyanic acid (HOCN) through ring opening of the imidazole moiety to afford $C_{10}H_9FN^+$ at m/z 162.07, which further loses a neutral ethylene molecule to give m/z at 136.06 with formula $C_8H_7FN^+$. The molecular ion at 136.06 then loses an HCN molecule to yield a low fragment ion at m/z 109 with molecular formula $C_7H_6F^+$.

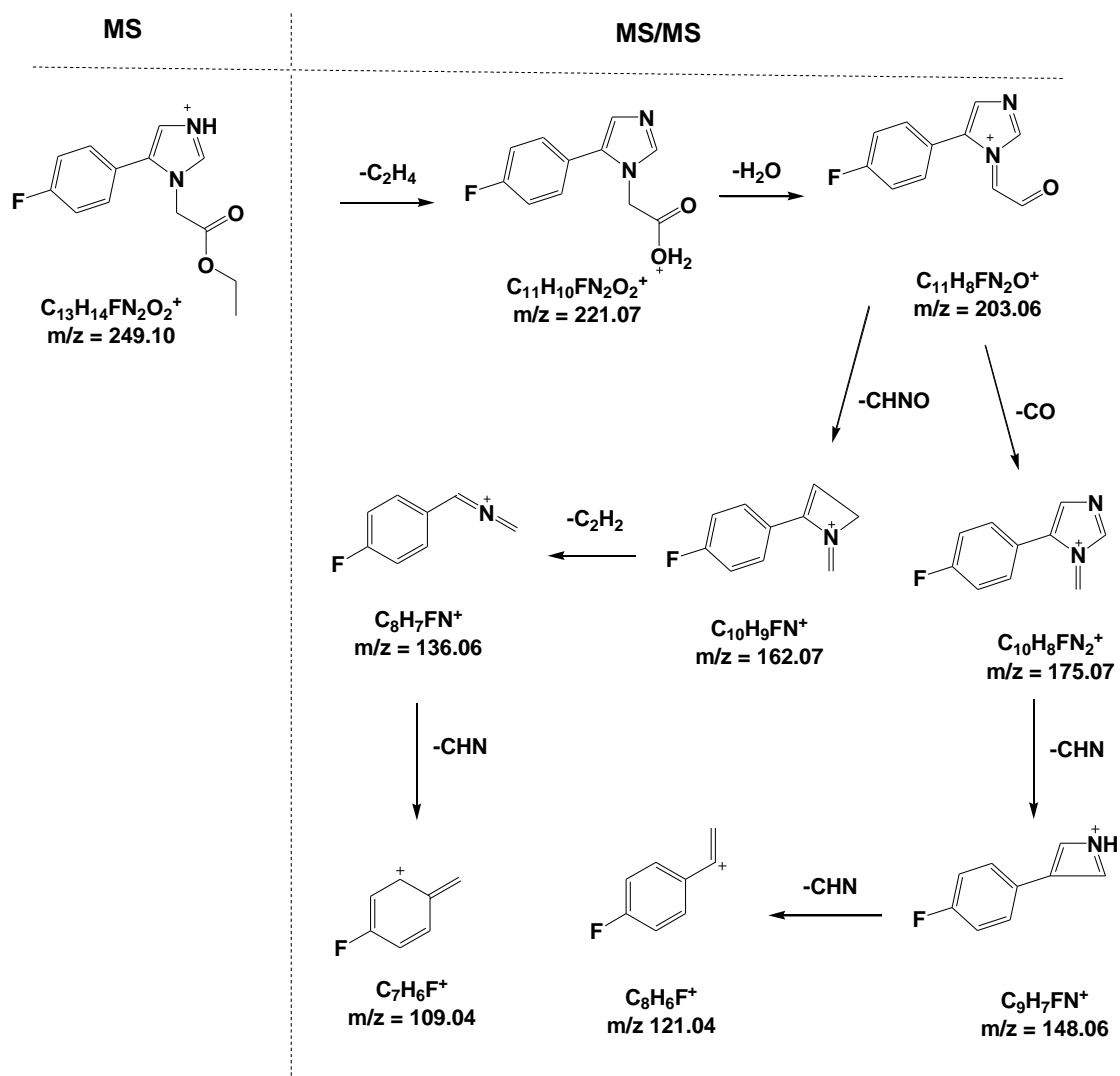


Figure 4.3: Possible fragmentation pathways of compound 120a.

4.2.4.2.2. Mass fragmentation of ethyl 2-[5-(3,4-dimethoxyphenyl)-1*H*-imidazolyl]acetate **120d**

The measured spectrum of compound **120d** (Figure 4.4 a) exhibited a peak at m/z 291.1332, which corresponds to the parent compound $[M+H]^+$, with molecular formula $C_{15}H_{19}N_2O_4$.

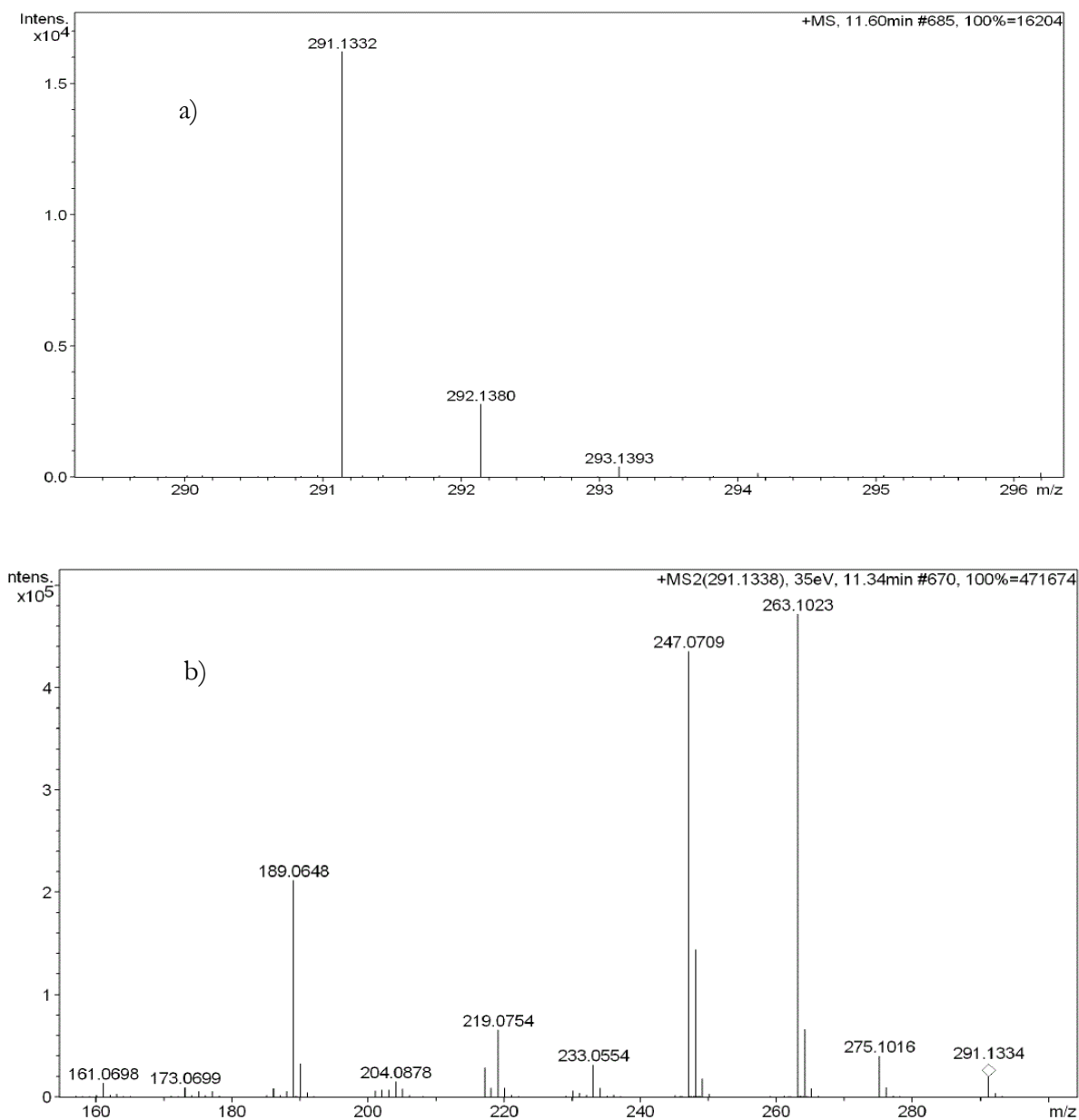


Figure 4.4: Recorded spectra for compound **120d**: (a) MS and b) MS/MS (col. energy 35eV).

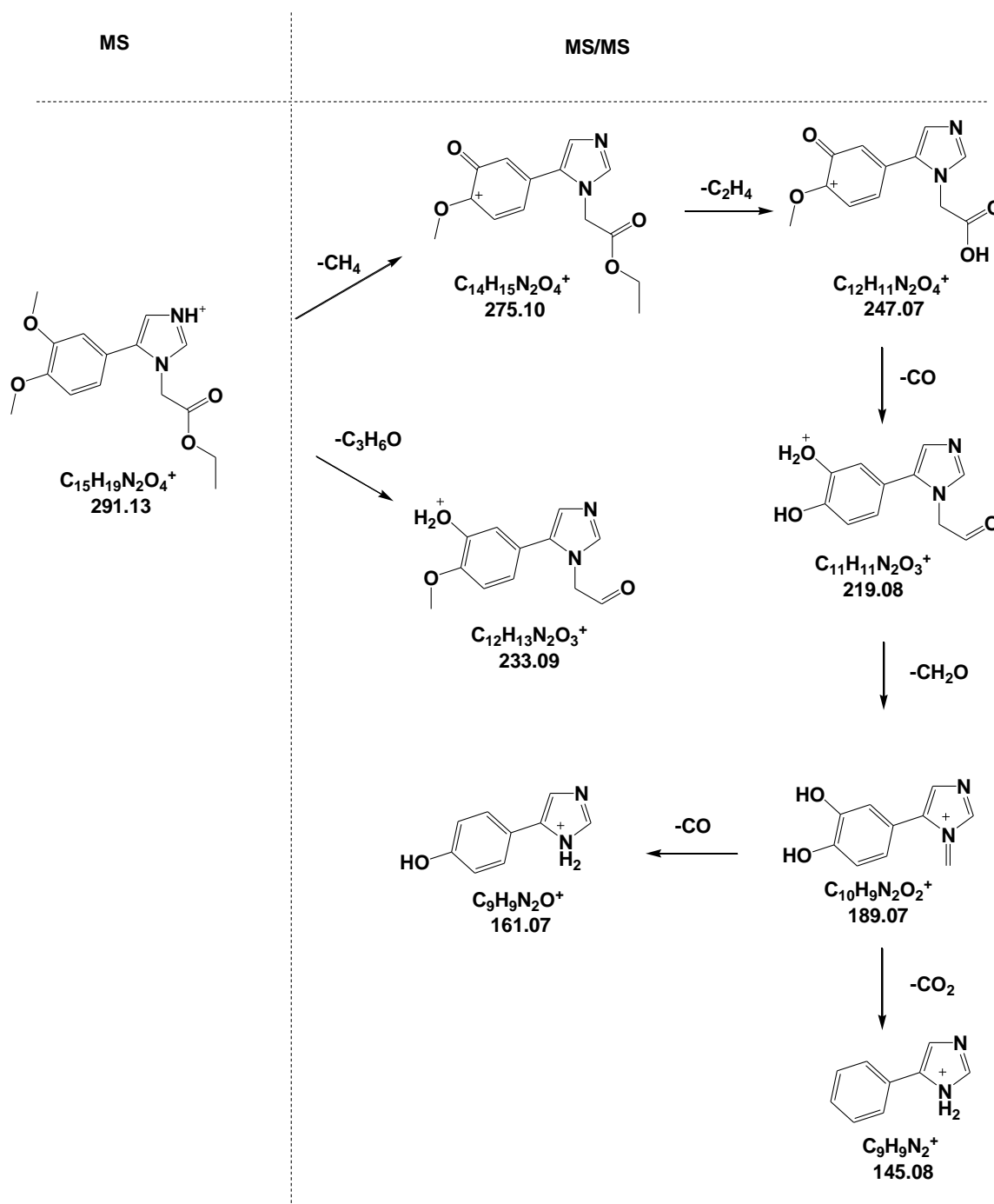


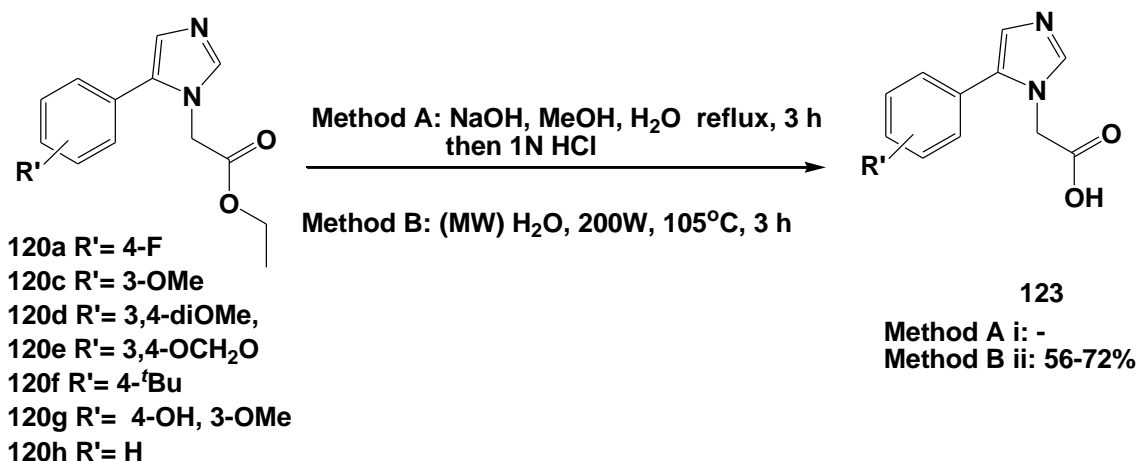
Figure 4.5: Possible fragmentation pathways for compound 120d.

The MS/MS spectrum (Figure 4.4b) shows a parent molecular ion exhibiting two fragmentation pathways as depicted Figure 4.5. The first route shows the formation of a fragment ion at m/z 275.10 with formula $\text{C}_{14}\text{H}_{15}\text{N}_2\text{O}_4^+$ due to a neutral loss of methane ($-\text{CH}_4$); followed by a loss of ethene (C_2H_4) to provide molecular ion $\text{C}_{12}\text{H}_{11}\text{N}_2\text{O}_4^+$ at m/z 247.07. A further loss of carbon monoxide ($-\text{CO}$) from $\text{C}_{12}\text{H}_{11}\text{N}_2\text{O}_4^+$ gives rise to an ion at m/z 219.08 with formula $\text{C}_{11}\text{H}_{11}\text{N}_2\text{O}_3^+$, which further endures the loss of formaldehyde (HCOH) to produce fragment ion

$C_{10}H_9N_2O_2^+$ at m/z equal to 189.07. The ion at 189.07 then decomposes further to give two molecular ions at m/z 161.07 having formula $C_9H_9N_2O^+$ attributed to the loss of carbon monoxide (-CO) and at m/z 145.0 with chemical formula $C_9H_9N_2^+$, which arises due to loss of carbon dioxide (CO_2). The second pathway involves a neutral loss of propan-2-one (C_3H_6O) to give a molecular ion at m/z 233.09 with formula $C_{12}H_{13}N_2O_3^+$.

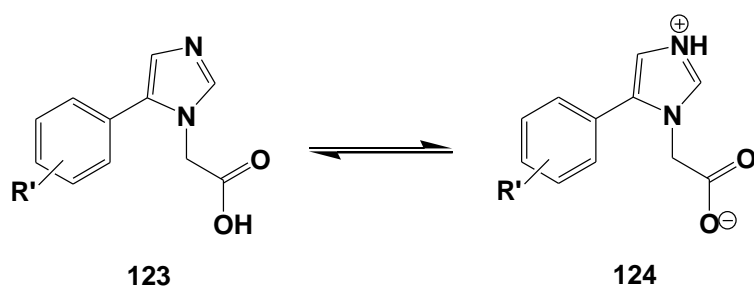
Having successfully established the structure of the novel ethyl 2-(5-aryl-1*H*-imidazol-1-yl) acyl derivatives **120** using FTIR and NMR spectroscopy and mass spectrometry, we thus wished to expand the existing library of imidazol-1-yl-based compounds by further transforming esters **120** into two sets of compounds: 2-(5-aryl-1*H*-imidazol-1-yl)acetic acids and 2-(5-aryl-1*H*-imidazol-1-yl)acetohydrazide derivatives.

4.2.5. Synthesis of novel 2-(5-aryl-1*H*-imidazol-1-yl) acetic acids **123**



Scheme 4.6: Hydrolysis of ethyl 5-aryl-1*H*-imidazol-1-yl acylates.

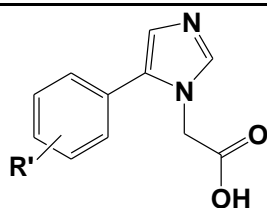
Initially, the hydrolysis of ethyl 5-aryl-1*H*-imidazolyl acylates **120a** and **120c-h** was carried out under reflux in the presence of NaOH using water and MeOH for 3 hours, followed by acidification with 1N HCl as illustrated in **Scheme 4.6** (Method A).²⁸³ However, the isolation of the desired products from the water layer was challenging, which may be due to the existence of the desired products in zwitterionic form as indicated in **Scheme 4.7**. This may be attributed to the presence of both the basic imidazole ring and the carboxylic acid, which can tautomerise *via* internal hydrogen transfer from the carboxylic acid group to the nitrogen of the imidazole ring, resulting in compound **124** having both acidic and basic functionalities.²⁸⁴



Scheme 4.7: Zwitterionic form of 2-(5-aryl-1*H*-imidazol-1-yl) acetic acids: neutral **123** and ionized form **124**.

Having failed to isolate the desired products, an alternative approach to hydrolysing the ethyl 2-(5-aryl-1*H*-imidazol-1-yl)acetates using microwave irradiation was pursued. This was inspired by the fact that microwaves can enable water to act like a pseudo-organic solvent, thus speeding up the reactions in an aqueous medium.²⁸⁵ Therefore, a mixture of 2-(5-aryl-1*H*-imidazol-1-yl)acetates **120a** and **120c-h** in water was microwave irradiated at a set power of 200 Watts and temperature of 105°C for 3 hours as indicated in **Scheme 4.6** (Method B). Work up by washing with DCM and evaporating the water layer *in vacuo* afforded pure novel 2-(5-aryl-1*H*-imidazol-1-yl) acetic acids **123** in yields ranging from 56 to 72% (*Table 4.7*). This method was better than the procedure described by Zhou *et al.*,²⁸³ because no removal of the acid or base catalyst at the end of the reaction was necessary.

Table 4.7: Isolated yields (%) of the novel 2-(5-aryl-1*H*-imidazol-1-yl) acetic acids **123** *via* MW irradiation.



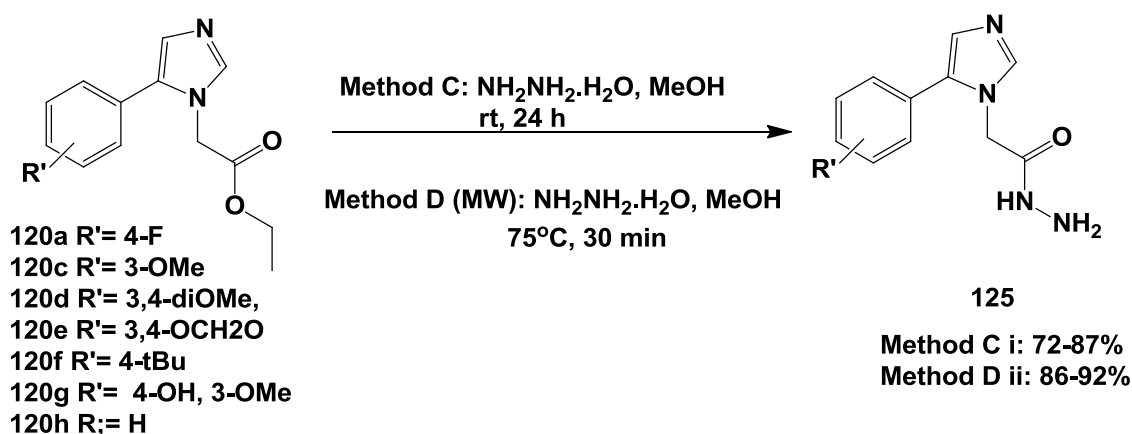
Compounds	R'	Yields (%)
123a	4-F	72
123c	3-OMe	56
123d	3,4-diOMe	71
123e	3,4-OCH ₂ O	68
123f	4- <i>t</i> Bu	56
123g	3-OH,4-OMe	58
123h	H	68

The formation of acetic acid products **123** was easily confirmed by the disappearance of signals due to the ethyl protons in their ^1H NMR spectrum and the appearance of a quaternary ammonium proton due to the zwitterionic form (see *Scheme 4.7*) as a broad signal at 6.01 ppm for compound **123d**, whilst the ^{13}C NMR spectrum further confirmed the loss of the ethyl group. The FTIR spectra of 2-(5-aryl-1*H*-imidazol-1-yl) acetic acids **123a** and **123c-h** showed an absorption band in the region of 2434 to 2604 cm^{-1} that can be attributed to the NH^+ of the zwitterionic form, which agrees with the observed ^1H NMR spectroscopy. More evidence for the formation of the products **123** was found from their mass spectra, which confirmed the loss of an ethyl group with an acceptable tolerance of isotopic pattern fit factor (mSigma) lower than 20 as recorded in *Table 4.8*. For example, compounds **123a** and **123f** with molecular formulae $\text{C}_{11}\text{H}_{10}\text{FN}_2\text{O}_2^+$ and $\text{C}_{15}\text{H}_{19}\text{N}_2\text{O}_2^+$ respectively, display the parent molecular ion peaks $(\text{M}+1)^+$ at m/z 221.0720, and 259.1440, while their ester analogues **120a** and **120f** (see *Table 4.6*) with molecular formulae $\text{C}_{13}\text{H}_{14}\text{FN}_2\text{O}_2^+$ and $\text{C}_{15}\text{H}_{19}\text{N}_2\text{O}_2^+$ exhibited the parent molecular ion peaks at m/z 249.1034 and 287.1764, respectively. The calculated difference of m/z 28.034 between the parent molecular ions of compounds **120** and **123** provides the proof that indeed the ethyl group was lost.

Table 4.8: HRMS results of the 2-(5-aryl-1*H*-imidazol-1-yl) acetic acids **123** and their mSigma values.

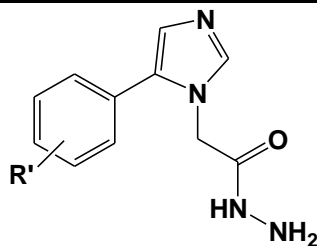
Compds	Calculated m/z	Chemical formula [M+1]	Measured m/z	Err (mDa)	Err (ppm)	mSigma value
123a	221.0721	$\text{C}_{11}\text{H}_{10}\text{FN}_2\text{O}_2^+$	221.0720	0.1	0.5	2.3
123c	233.0921	$\text{C}_{12}\text{H}_{13}\text{N}_2\text{O}_3^+$	233.0922	-0.1	-0.6	1.6
123d	263.1040	$\text{C}_{13}\text{H}_{15}\text{N}_2\text{O}_4^+$	263.1017	2.3	8.5	4.3
123e	247.0713	$\text{C}_{12}\text{H}_{11}\text{N}_2\text{O}_4^+$	247.0702	1.1	4.5	0.6
123f	259.1441	$\text{C}_{15}\text{H}_{19}\text{N}_2\text{O}_2^+$	259.1440	0.3	1.2	1.0
123g	249.2421	$\text{C}_{12}\text{H}_{13}\text{N}_2\text{O}_4^+$	263.2438	-1.7	11.1	8.4
123h	203.0815	$\text{C}_{11}\text{H}_{11}\text{N}_2\text{O}_2^+$	203.0807	0.8	3.9	4.1

4.2.6. Synthesis of novel 2-(5-aryl-1*H*-imidazol-1-yl)acetohydrazide scaffolds **125**



Scheme 4.8: Synthesis of 2-(5-aryl-1*H*-imidazol-1-yl)acetohydrazide scaffolds **125**.

The selected ethyl 5-aryl-1*H*-imidazol-1-yl acyl derivatives **120** were also subjected to nucleophilic attack by hydrazine monohydrate in MeOH at room temperature for 24 hours (**Scheme 4.8**, Method C). Work up gave pure 2-(5-aryl-1*H*-imidazol-1-yl)acetohydrazide derivatives **125a** and **125c-h** in good yields (*Table 4.9*). It was interesting to observe that the same scaffolds **125a** and **125c-h** were successfully obtained in excellent yields under microwave irradiation at a set temperature of 75°C in just 30 minutes as depicted in **Scheme 4.8**, method D (see *Table 4.9* for the isolated yield). The microwave method has once again been shown to be a better synthetic option, with an increase in the reaction rate of 48-fold.

Table 4.9: Isolated yields (%) of the novel 2-(5-aryl-1*H*-imidazol-1-yl)acetic acids **125**.

Compounds	R'	Conventional heating Yields (%)	Microwave Yields (%)
125a	4-F	86	92
125c	3-OMe	72	86
125d	3,4-diOMe	87	94
125e	3,4-OCH ₂ O	86	90
125f	4- <i>t</i> Bu	80	93
125g	3-OH,4-OMe	-	94
125h	H	74	90

The formation of the desired products **125** was confirmed by means of FTIR and 1-D and 2D NMR spectroscopic analysis. The FTIR spectra of these acetohydrazide derivatives **125** showed absorption bands in the region of 3104-3565 cm⁻¹ corresponding to the NH₂ of hydrazine while the bands in the region of 3026-3220 cm⁻¹ were assigned to the NH group. Furthermore, the stretching bands of the amide carbonyl (C=O) group were found in the area of 1613-1747 cm⁻¹ (Table 4.10). This was a clear indication that the nucleophilic substitution reaction had occurred.

Table 4.10: FTIR spectroscopic data of the 2-(5-aryl-1*H*-imidazol-1-yl)acetohydrazides **125**: showing the NH₂, NH and C=O bands.

Compounds	125a	125c	125d	125e	125f	125g	125h
ν_{NH₂} (cm⁻¹)	3104	3320	3565	3317	3335	3146	3321
ν_{NH} (cm⁻¹)	3026	3198	3209	3104	3220	3120	3197
ν_{C=O} (cm⁻¹)	1747	1677	1693	1655	1663	1613	1675

The NMR spectra of the synthesized 2-(5-aryl-1*H*-imidazol-1-yl)acetohydrazide scaffolds **125** further validate the formation of the products. The ¹H NMR spectrum of compound **125f** (Figure 4.6) reveals a singlet peak at δ 4.46 ppm integrating for two protons corresponding to an NH₂ group while an imine proton (NH) resonates as a singlet signal downfield at δ 9.28 ppm.

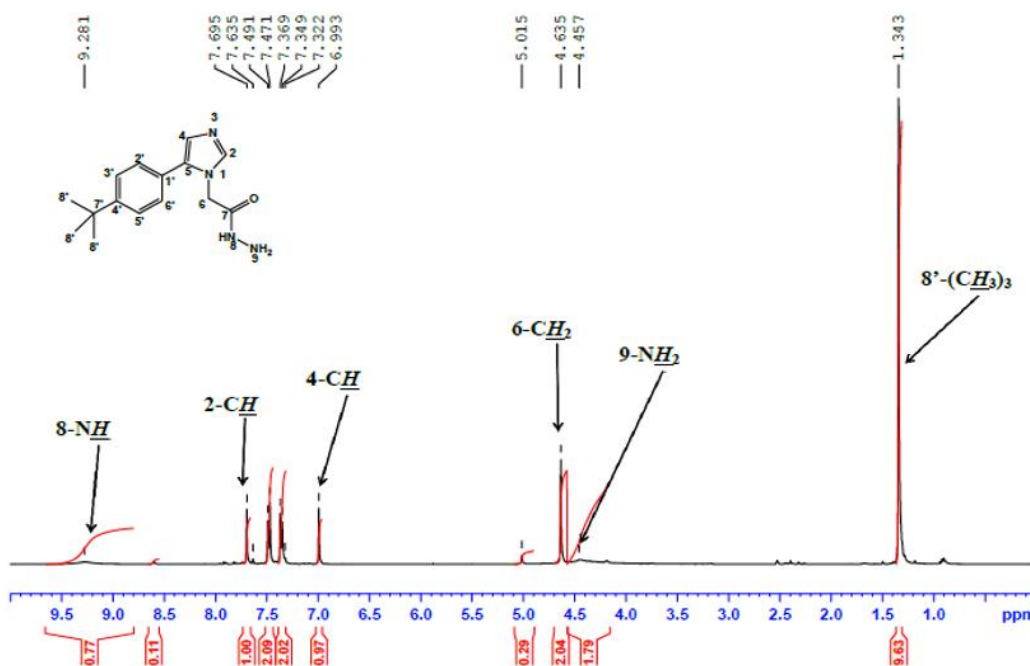
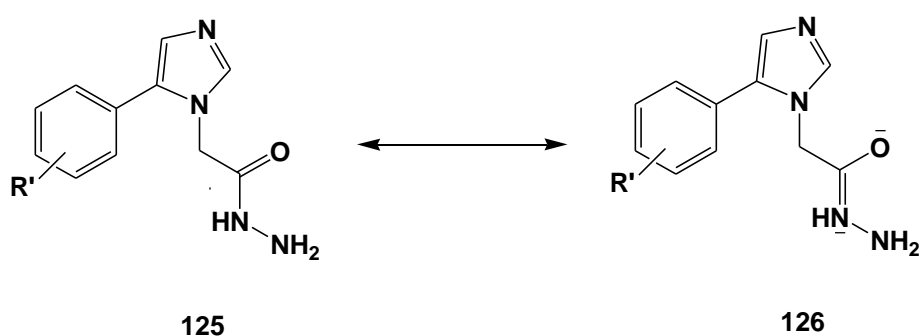


Figure 4.6: ¹H NMR spectrum of ethyl 2-[5-(4-*tert*-butylphenyl)-1*H*-imidazol-1-yl]acetohydrazide **4.10f** in DMSO-*d*₆ at 30°C citing major rotamer.

Extra signals were observed on NMR spectroscopic analysis which could be the result of rotamers. Rotamers arise due to hindered rotation around the amide C-N bond caused by delocalization (**Scheme 4.9**).^{286,287}



Scheme 4.9: Resonance of partial double bond in amide system.

To establish whether indeed the extra signals observed corresponded to rotamers, compound **125f** was studied at different temperatures by analysing the signals around the aromatic region in the ^1H NMR spectrum. At 30°C , the ^1H NMR spectrum in $\text{DMSO}-d_6$ of **125f** (Figure 4.7) reveals that the relative ratio of the major and minor rotamers is 8:1. When the temperature is increased to 70°C , the signals for the two rotamers begin to move closer to each other, but can still be observed. Finally, at a temperature of 90°C , the two signals had coalesced into a single peak, this can be attributed to the fact that at these higher temperatures the rotation barrier between rotamers can be easily overcome, and the interconversion is fast enough when compared to the NMR spectroscopic time-scale.

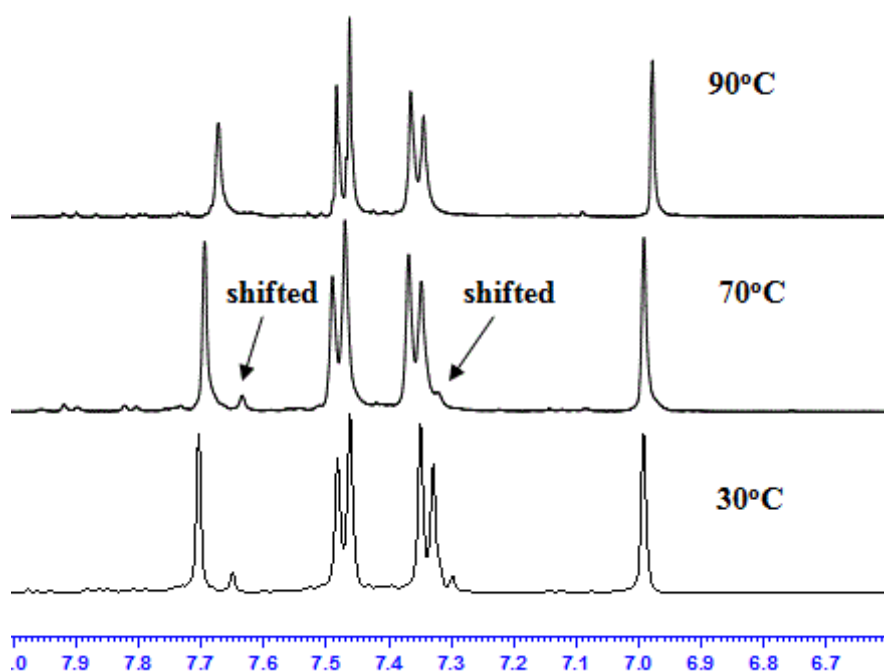


Figure 4.7: Effect of temperature on the aromatic signal markers in the ^1H -NMR spectrum of ethyl 2-[5-(4-*tert*-butylphenyl)-1*H*-imidazol-1-yl]acetohydrazide **125f** in $\text{DMSO}-d_6$.

The ^{13}C NMR spectrum (Figure 4.8 and 4.9) of compound **125f** also showed the existence of rotamers. Changes in the spectrum around aromatic signals and the carbonyl carbon atom were also observed at different temperatures. At lower temperature, the carbonyl carbon atom of the major rotamer resonates at δ 166.6 ppm, while the minor rotamer emerges at δ 170.9 ppm. The signals of the minor rotamer broaden and then coalesce at temperatures of 70°C and 90°C .

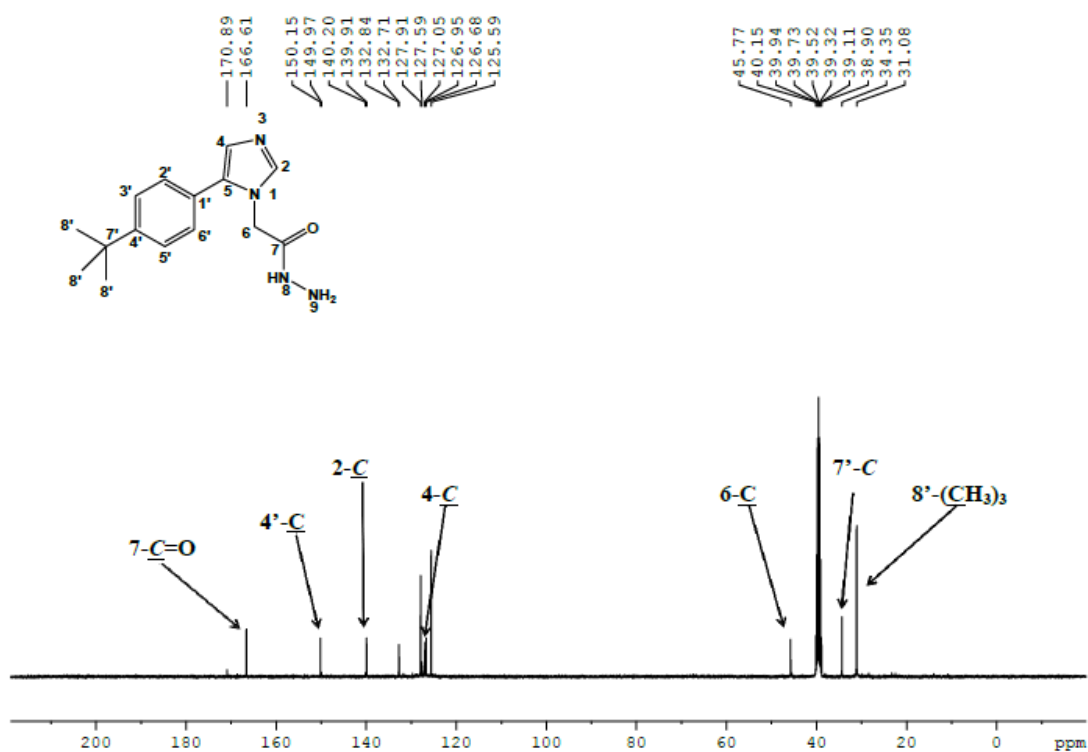


Figure 4.8: ^{13}C NMR spectrum of 2-[5-(4-*tert*-butylphenyl)-1*H*-imidazol-1-yl]acetohydrazide **125f** in $\text{DMSO-}d_6$ citing major rotamer.

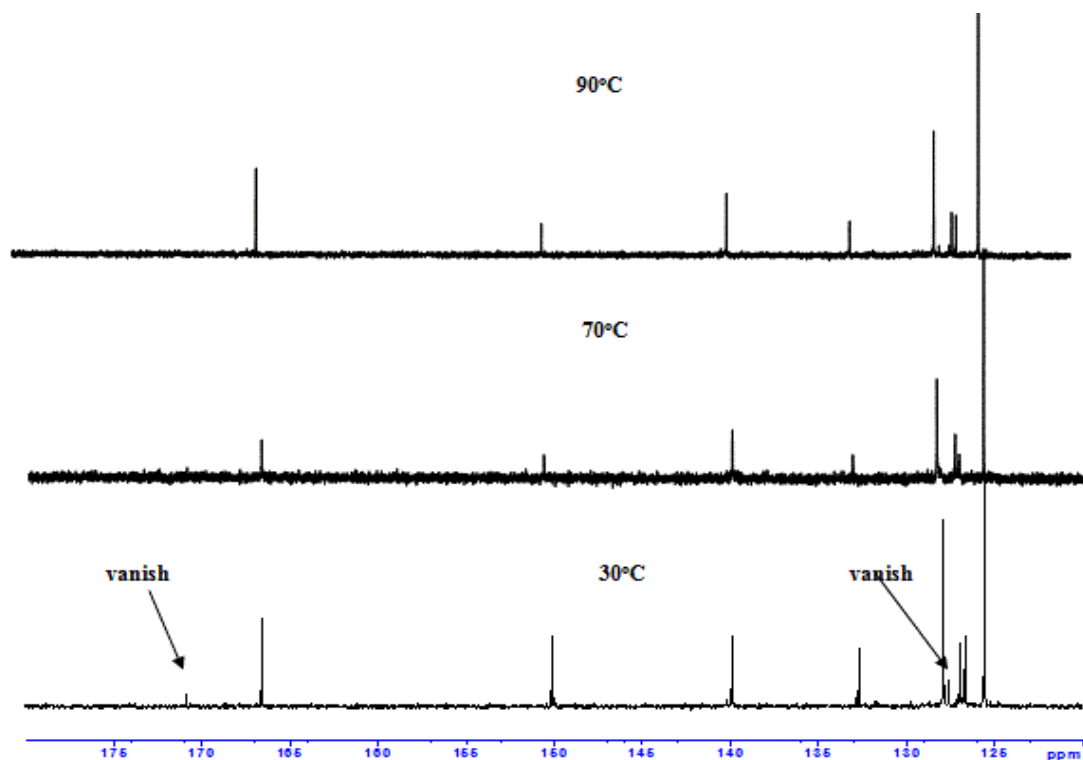


Figure 4.9: Effect of temperature on the aromatic signals markers in the ^{13}C -NMR spectrum of ethyl 2-[5-(4-*tert*-butylphenyl)-1*H*-imidazol-1-yl]acetohydrazide **125f** in $\text{DMSO-}d_6$.

In summary, a total of 25 novel compounds belonging to ethyl 2-(5-aryl-1*H*-imidazol-1-yl)acrylate (**120** and **121**), 2-(5-aryl-1*H*-imidazol-1-yl) acetic acid **123** and 2-(5-aryl-1*H*-imidazol-1-yl)acetohydrazide **125** scaffolds were obtained from the above chemistry. These novel imidazol-1-yl scaffolds were submitted for biological evaluation (direct assays).

4.2.7. Biological evaluation of synthesized 1*H*-imidazol-1-yl- based compounds

A total of 25 compounds were submitted for testing in the IN-LEDGF/p75 AlphaScreen and the BST-2-Vpu ELISA assays for their ability to disrupt protein-protein interactions of interest: a) IN - LEDGF/p75 and b) BST-2 -Vpu. All biological assays were conducted in house, at the Centre of Metal-based Drug Discovery laboratories, Advanced Material Division, Mintek (Randburg, South Africa). Compounds with the highest inhibition (more than 50%) were further evaluated in a dose range assay for their IC₅₀ values and in cell-based assay for their CC₅₀ values.

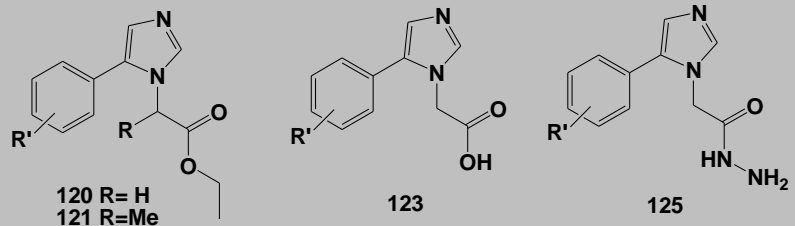
4.2.7.1. Direct IN-LEDGF/p75 AlphaScreen assay

Initially, 25 novel compounds were tested in an AlphaScreening assay to determine the percentage inhibition of disruption of the LEDGF-IN interaction at 100 μM. The tests were carried out in triplicate and average results are displayed in *Table 4.11*.

Initial testing was carried out for 1*H*-imidazol-1-yl-based compounds (**120** and **121**). All ester derivatives, excluding compounds **120b** and **121c** exhibited a marginal ability of preventing LEDGF/p75-IN interaction. Compound **120h** with no substituent on the 5-aryl ring was found to exhibit the highest inhibitory activity in this series (of only 26%). Furthermore, variation on the 5-aryl ring and at the stereogenic centre did not have a significant effect on the inhibition activities of these scaffolds.

However, hydrolysis of ester derivatives **120** to the corresponding acetic acids **123** revealed one compound, **123g** exceeding the 50% inhibition benchmark. This best inhibitor **123g**, with a hydroxyl group and the methoxy group at the *meta*- and *para*-positions, exhibited 82% inhibition of the formation of the HIV-1 IN - LEDGF/p75 complex, and in a dose range assay produced an IC₅₀ value of 19 μM. Instead of the *meta*-OH group found in compound **123g**, compound **123d** has a *meta*-methoxy group and shows a 10-fold reduced percentage inhibition activity, which implies that the presence of both OH and carboxylic acid (COOH) groups might be significant for the binding activity of the scaffold. In addition, the variation on the 5-aryl ring of the acetic acid derivatives **123** displayed a minimal inhibition activity ranging from 5-20%.

Table 4.11: The HIV-1 IN-LEDGF/p75 inhibition activities of the 5-aryl-1*H*-imidazol-1-yl compounds **120**, **121**, **123** and **125** at 100 μ M.

		
Compounds Entry	R'	Biochemical target assays
		HIV-1 IN – LEDGF (%) inhibition @ 100 μ M (AlphaScreen)
120a	4-F	19 \pm 2.13
120b	2-Cl	0
120c	3-OMe	14 \pm 4.91
120d	3,4-diOMe	7 \pm 3.94
120e	3,4-OCH ₂ O-	9 \pm 4.15
120f	4- <i>t</i> Bu	8 \pm 3.55
120g	3-OH,4-OMe	11 \pm 3.84
120h	H	26 \pm 2.13
121a	4-F	21 \pm 5.12
121c	3-OMe	0
121d	3,4-diOMe	21 \pm 3.02
123a	4-F	26 \pm 1.67
123c	3-OMe	5 \pm 4.18
123d	3,4-diOMe	8 \pm 1.89
123e	3,4-OCH ₂ O-	30 \pm 6.67
123f	4- <i>t</i> Bu	0
123g	3-OH,4-OMe	82 \pm 2.41
123h	H	31 \pm 3.42
125a	4-F	40 \pm 5.02
125c	3-OMe	23 \pm 4.52
125d	3,4-diOMe	34 \pm 4.41
125e	3,4-OCH ₂ O-	33 \pm 8.46
125f	4- <i>t</i> Bu	40 \pm 4.62
125g	3-OH,4-OMe	6 \pm 8.39
125h	H	10 \pm 3.96
CX05168		91.37 \pm 0.85
HIV-1 IN and LEDGF with DMSO		0

Transforming the ester derivatives **120** to the corresponding acetohydrazide scaffolds **125** also showed inhibition lower than the pre-defined 50% minimum benchmark. But their percentage inhibition values were slightly improved in comparison to the ester derivatives. For instance, compound **125a** with no substituent on the 5-aryl ring and compound **125f** with 4-*tert*-butyl group at the *para*-position of the 5-aryl ring exhibited 40% inhibition each, higher than that of the corresponding analogues **125a** and **125f**, which showed only 26% and 7% inhibition, respectively. The rest of the compounds in the acetohydrazide set displayed marginal inhibition (ranging from 6% to 33%) of the formation of the IN-LEDGF/p75 complex.

The best inhibitor **123g** was further evaluated in an AlphaScreen TruHit counter assay to determine if it could have interfered with the interaction of the FLAG peptide with the anti-FLAG acceptor beads. The compounds found to prevent the interactions of beads are regarded as false positives meaning that they are not disrupting the protein-protein interaction, but instead are absorbing the energy at the emission frequency, hence significantly diminishing the output signal for accurate reading. The best compound **123g** was not a false positive.

The cytotoxic effect of the best compound **123g** was evaluated in the MT4-cell line at 100 μ M concentration and was shown not to reduce the viability of the cell, hence it is considered as non-toxic. The antiviral activity was also carried out; however compound **123g** did not inhibit HIV replication in cell culture. This is not of immediate concern given the fact that most of the compounds reported to be inhibitors of LEDGFp75 and IN interactions show lack of antiviral activity in cell based assays.²⁸⁸ Furthermore, lack of antiviral activity may also be attributed to an inability of the compound to penetrate the cell or to not reaching the target. Besides the lack of antiviral activity, compound **123g** can be considered a viable hit and warrants further investigation.

4.2.7.2. Direct Vpu-BST-2 ELISA assay

At the time of completion of the synthesis of the 5-aryl-1*H*-imidazolyl fragments, Mintek biochemists had finished developing and validating a BST-2-Vpu ELISA assay, which was then ready to screen a small batch of 25 compounds, namely: ethyl 5-aryl-1*H*-imidazol-1-yl acyls (**120** and **121**), 2-(5-aryl-1*H*-imidazol-1-yl) acetic acids (**123**) and 2-(5-aryl-1*H*-imidazol-1-yl)acetohydrazide scaffolds (**125**), alongside 6-aza-2-thiouridine (a compound that has previously been shown to inhibit Vpu mediated BST-2 degradation).²⁸⁸ The assay was carried out at 100 μ M concentration (fragment screening) and the respective inhibition percentages were calculated; results are shown in *Table 4.12*.

Table 4.12: HIV-1 Vpu-BST- inhibition activities of the 5-aryl-1*H*-imidazol-1-yl compounds **120**, **121**, **123** and **125** at 100 μ M.

Compound	Biochemical target assays		Cell-based assays (MT-4 cells)
	HIV-1 Vpu – BST-2 (%) inhibition @ 100 μ M (ELISA)	HIV-1 Vpu– BST-2 inhibition IC ₅₀ (ELISA) (μ M)	CC ₅₀ (μ M)
	120a	54	-
120b	13	-	-
120c	51	-	> 200
120d	58	-	194 \pm 0.6
120e	33	-	-
120f	17	-	-
120g	30	-	-
120h	82	12	161 \pm 0.8
121a	63	-	103 \pm 0.5
121c	20	-	-
121d	22	-	-
123a	11	-	-
123c	30	-	-
123d	25	-	-
123e	9	-	-
123f	2	-	-
123g	0	-	-
123h	0	-	-
125a	48	-	-
125c	69	-	> 200
125d	28	-	-
125e	22	-	-
125f	45	-	-
125g	72	23	> 200
125h	39	-	-
6-aza-2-thiouridine	54	-	-

From the family of ester derivatives **120** and **121**, five compounds showed more than 50% activity of disrupting the interactions between the HIV-1 Vpu and host BST-2 transmembrane domains at 100 μ M. Compound **120h**, with no substituent on the benzene ring, exhibited the highest percentage of 82%, followed by compound **121a** (63% inhibition) with an electron-withdrawing fluorine atom at the *para*-position on the 5-aryl ring and a methyl group at the chiral centre. Compound **120d** with the methoxy substituents at the *para*- and *meta*-positions and no chiral centre exhibited 58% inhibition of the Vpu- BST-2 interactions. The absence of the *para*-methoxy substituent in scaffold **120c** resulted in this compound showing 50% inhibitory activity. It was interesting to observe compound **120a**, an analogue of **121a**, with no chiral centre, also exhibited 54% inhibition in this ELISA assay. These data suggest that the presence of the *para*-fluorine atom in scaffolds **120a** and **121a** as well as the presence of the methoxy substituent at the *meta*-position for **120c** and **120d** may be significant in preventing the interactions between HIV-1 Vpu and the host BST-2 protein.

However, the potency observed for the five compounds belonging to ester series **120** was lost after hydrolysis into the corresponding acetic acids **123**. These acetic acid scaffolds exhibited minimal inhibition activity (2-30%) with the exception of compounds **123g** and **123h** which were completely inactive. The results suggest that the family of 2-(5-aryl-1*H*-imidazol-1-yl) free acetic acids is not a suitable template for the design of potential inhibitors of the Vpu-BST-2 interaction.

The conversion of ester **120** into the corresponding acetohydrazide scaffolds **125** gave rise to two compounds, **125c** and **125g**, with more than 50% inhibition. Compound **125g** with an OH and the methoxy group at the *meta*- and *para*-positions of the aryl ring displayed the highest inhibition percentage in this series (72%), whilst compound **125c** with a methoxy substituent at the *meta*-position showed 69% inhibition. Furthermore, it was interesting to note that both compounds **125c** and **125g** showed improved percentage inhibition in comparison with their ester analogues **120c** and **120g**. By contrast, an analogue of **120h** (82%), compound **125h** was 2-times less potent. The results suggest that the presence of the electron donating groups at the *meta*- and *para*-positions of the 5-aryl ring are significant for the inhibition of these scaffolds. Additionally, compound **125a**, a close analogue of **120a** and **121a**, exhibited 48% inhibition. Other compounds in the series of acetohydrazides displayed between 21-44% inhibitions.

In summary, seven compounds from 25 screened imidazol-1-yl based compounds exceeded the pre-defined cut-off of 50%, and amongst them six surpassed the percentage inhibition of the standard 6-aza-2-thiouridine control compound in our BST-2-Vpu ELISA assay. It is

worthwhile to mention that the 6-aza-2-thiouridine does not directly disrupt the formation of Vpu-BST-2 complex, but it has been reported to act on the ion channel of the HIV-1 Vpu protein instead.²⁸⁸The results suggest that these best seven compounds may be unique Vpu-BST inhibitors acting exclusively on the prevention of the Vpu-BST-2 complex formation. Compounds **120h** and **125g**, with the highest percentage inhibition were subjected to a dose response test and produced IC₅₀ values of 12.42 and 23.36 μ M, respectively (*Table 4.12*).

In addition, the antiviral activity and cytotoxicity effects of the 7 best test compounds were determined in parallel using the MT-4 cell line. For the cytotoxicity assay the seven compounds were shown not to be overly toxic to the MT-4 cells and produced cytotoxic concentration (CC₅₀) values ranging from 103 μ M to greater than 200 μ M in a dose response assay (*Table 4.12*). The activity of the virus in the presence of the test compounds was determined by detecting the p24 expression in HIV infected MT-4 cells. The compounds were tested at 10 and 100 μ M doses; unfortunately none of the test compounds showed any significant inhibition at 10 and 100 μ M. The lack of antiviral activity could point to the fact that the compounds are not penetrating the cell or not reaching the desired target. These results indicate that a further modification in the structures of these compounds is necessary in order to improve their chemical and biological properties.

4.2.8. In *silico* ADME profiling of novel 5-aryl-1*H*-imidazolyl- based compounds

The ADME properties of the best seven compounds **120a**, **120c**, **120d**, **120h**, **121a**, **125c** and **125g** shown to exceed the 50% inhibition benchmark in the HIV-1 Vpu-BST-2 ELISA assay, and compound **123g** which showed 82% disruption of the interaction between the HIV-1 IN and LEDGF/p75 were simulated using Biovia Discovery Studio™ with the aim of timeously evaluating and discarding unfavourable compounds.^{289,290} The results are displayed in *Table 4.13*. All eight 2-(5-aryl-1*H*-imidazolyl) acyl derivative were predicted to have good or optimal aqueous solubility (level 3 and 4) and projected drug like properties with blood brain barrier (BBB) penetration levels medium to low, as shown in *Table 4.13*. By contrast, compounds, **120a**, **120c**, **120d**, **120h** and **121a**, from the ester family were predicted to have low intestinal absorption, while scaffolds **123g**, **125c** and **125g** were predicted to have good human intestinal absorption. All eight analogues were projected to be non-inhibitors of CYP2D6, which means that these scaffolds are not expected to inhibit the CYP2D6 enzyme during metabolism through cytochrome p450 (CYP). These predictions suggest that these compounds merit further exploration as templates for possible inhibitors of the Vpu-BST-2 interaction.

Table 4.13: Predicted ADME profiles of eight 2-(5-aryl-1*H*-imidazolyl) acyl derivative using Discovery studio 4.0.

comps	Aqueous Solubility & Drug likeness	Blood Brain Barrier Penetration	Human Intestinal Absorption	CYP2D6 Inhibition
120a	3	2	2	No
120c	3	2	2	No
120d	3	3	2	No
120h	3	2	2	No
121a	3	2	2	No
123g	4	3	0	No
125c	3	3	0	No
125g	4	3	0	No

4.2.9. Molecular modelling of compound 123g at the IN dimer interface

The potential binding modes of compound **123g** (which showed more than 50% inhibition in the AlphaScreen assay) to the binding cavity of the HIV-1 IN dimer interface was simulated using BIOVIA Discovery Studio, making use of the crystal structure of HIV-1 IN (PDB code: 2B4J). The best binding pose had a total binding energy of -150.388 kcal/mol. The carboxylic group (-COOH) in the best pose of compound **123g** (in *Figure 4.10 A* and *B*) made two hydrogen bonds with the main chain nitrogen atoms of the His171 residue of subunit B whilst the *para*-methoxy group is involved in a hydrogen bond with the Ala128 residue and its phenyl ring occupied the hydrophobic pocket of the same Ala128 amino side chain of monomer A. The *meta*-hydroxyl group exhibited three hydrogen bonds with the carbonyl group and a hydroxyl group as well as the hydrogen atom at a chiral centre of the Thr125 amino acid of subunit A. The docking results for compound **123g** with HIV-1 IN dimer resemble the mode of interaction exhibited by the LEDGF/p75 protein with the dimer.²⁹¹ The interactions between compound **123g** at the LEDGF/p75 binding site of the IN dimer interface were projected to be at relative distances of less than 3Å.

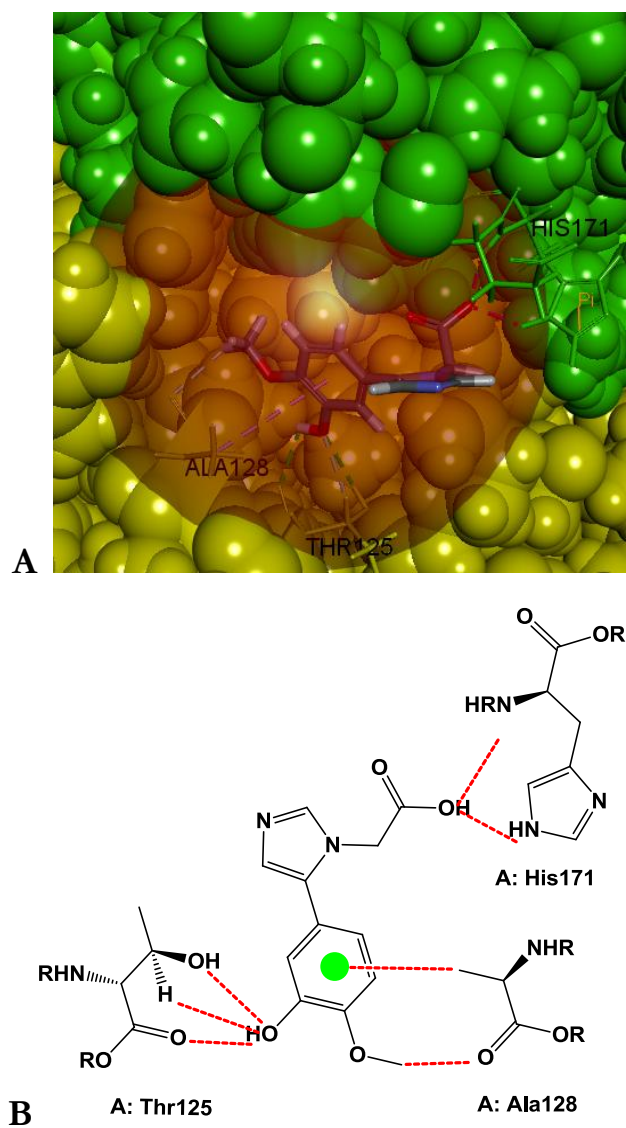


Figure 4.10: **A**) 3D representation of molecular docking of the best pose of compound **123g** in the LEDGF/p75 binding site at the IN dimer interface with hydrogen bonds provided in dashed lines at projected distances of less than 3Å; and **B**) 2D representation of compound **123g** with critical residues within LEDGF/p75 binding site at the IN dimer interface.

4.3. The expansion on the 2-(5-aryl-1*H*-imidazolyl) acyl fragments to produce second generation compounds

Encouraged by the biological results from the AlphaScreen assay, we wished to explore the second generation of compounds through a fragment growing method starting from the hit compound **123g**. A literature survey revealed several compounds containing the hydrazine framework as potential inhibitors that prevent the formation of the LEDGF/p75-IN complex (outlined in *Figure 4.11*).^{292,293} For example, Tintori and co-workers²⁹² identified a class of hydrazine compounds that prevent the binding of the LEDGF/p75 to the IN dimer interface through molecular docking while Sanchez *et al.* identified the hydrazine containing compounds through screening using LEDGF/p75 IBD-based pharmacophore models as potential inhibitors of the LEDGF/p75 – IN interaction (*Figure 4.11*).²⁹³

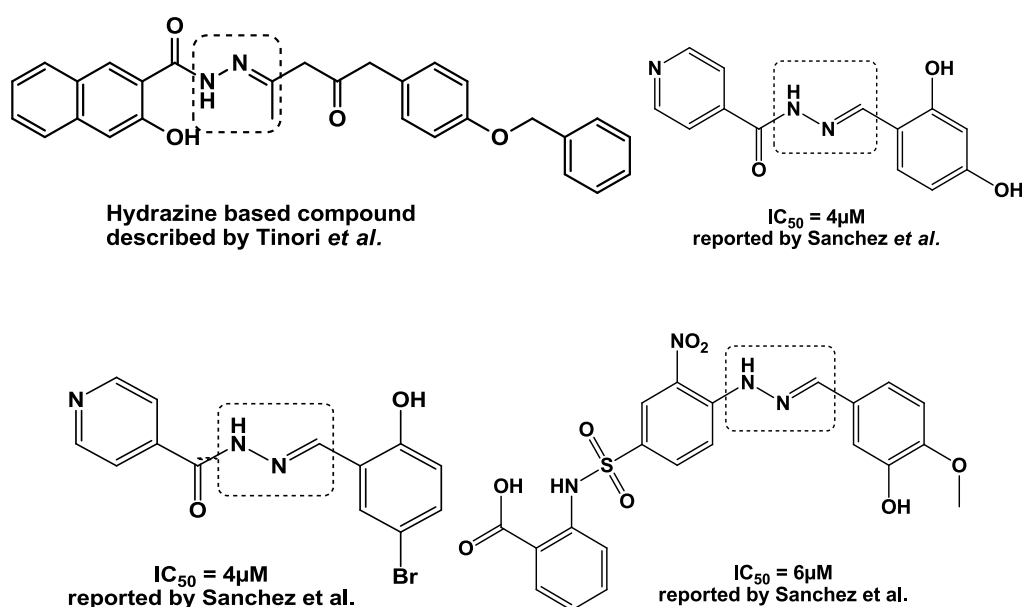


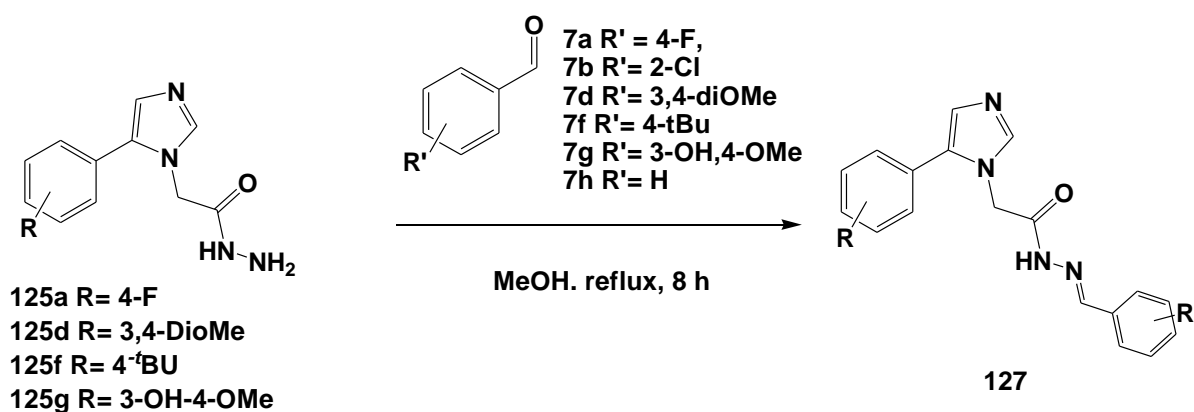
Figure 4.11: Examples of reported hydrazine-based compounds as potential inhibitors of LEDGF/p75-IN interaction.

On the basis of the above and our interest in the development of possible inhibitors that can prevent the formation of the HIV-1 IN and host LEDGF/p75 protein complex, attention was shifted to exploring the effects of structure variation by fragment expansion on the hit compound **123g** through incorporating the hydrazine framework. Our proposition was that the hydrazine incorporation would increase percentage inhibition of the scaffolds as well as probing the structure activity relationship of these types of compounds. Thus, the work described here

was aimed at insertion of a hydrazine motif through a fragment expansion method to give a set of *N'*-arylidene-based compounds as second generation of these compounds.

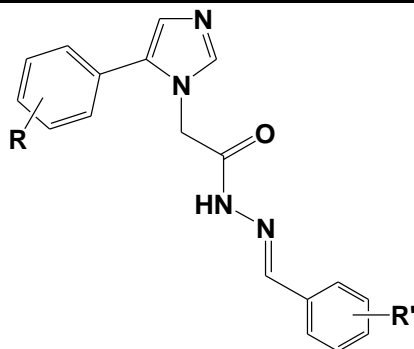
4.3.1. Synthesis of *N'*-arylidene-2-(5-aryl-1*H*-imidazol-1-yl)acetohydrazide and *N*,5-diaryl-2-(1*H*-imidazol-1-yl)acetamide derivatives

An analogue of identified hit compound **123g**, 2-(5-aryl-1*H*-imidazol-1-yl)acetohydrazide **125g** was used as the starting point, as it was readily available. In addition, other selected 2-(5-aryl-1*H*-imidazol-1-yl)acetohydrazide scaffolds were also included, which would assist in probing the SAR of the compounds. Therefore, 2-(5-aryl-1*H*-imidazol-1-yl)acetohydrazide scaffolds **125a**, **125d**, **125f** and **125g** were then heated under reflux in the presence of benzaldehydes **7a-f** using MeOH as solvent for about 8 hours as shown in **Scheme 4.10**.²⁹⁴ Work up furnished the desired fifteen novel *N'*-arylidene-2-(5-aryl-1*H*-imidazol-1-yl)acetohydrazide derivatives **127a-o**. The yields of the products obtained were in the range of 63 to 86% as recorded in **Table 4.14**.



Scheme 4.10: Synthesis of (*E*)-*N'*-arylidene-2-(5-aryl-1*H*-imidazol-1-yl)acetohydrazide **127**.

Table 4.14: Isolated yields (%) of the novel (*E*)-*N'*-arylidene-2-(5-aryl-1*H*-imidazol-1-yl)acetohydrazide **127a-o**.



Compounds	R	R'	Yield (%)
127a	3-OH, 4-OMe	4-F	73
127b	3-OH, 4-OMe	2-Cl	64
127c	3-OH, 4-OMe	3,4-diOMe	75
127d	3-OH, 4-OMe	4- <i>t</i> Bu	70
127e	3-OH, 4-OMe	3-OH, 4-OMe	76
127f	3-OH, 4-OMe	H	63
127g	4-F	4-F	54
127h	4-F	2-Cl	68
127i	4-F	3,4-diOMe	86
127j	4-F	4- <i>t</i> Bu	76
127k	4-F	3-OH, 4-OMe	81
127l	4-F	H	72
127m	3,4-diOMe	4-F	83
127n	3,4-diOMe	4- <i>t</i> BU	71
127o	4- <i>t</i> Bu	H	81

4.3.1.1. Structure elucidation of *N'*-arylidene-2-(5-aryl-1*H*-imidazol-1-yl)acetohydrazide **127a-o**

The formation of the desired *N'*-arylidene-2-(5-aryl-1*H*-imidazol-1-yl)acetohydrazide compounds **127a-o** were characterised by FTIR and NMR spectroscopy and ESI-MS. The FTIR spectra of *N'*-arylidene-2-(5-aryl-1*H*-imidazol-1-yl)acetohydrazides **127a-o** showed the disappearance of NH₂ bands while the NH band was still observed in the region of 3061 cm⁻¹ to 3216 cm⁻¹. Moreover, the hydrazide C=O stretching bands were observed in the region of 1672 cm⁻¹ to 1698 cm⁻¹, whilst the two bands in the region of 1503cm⁻¹ to 1564cm⁻¹ correspond to the N=CH stretch of the azomethine group and the imidazole moiety.

The NMR spectra of the compounds **127** determined in DMSO-*d*₆ confirmed the loss of NH₂ and the appearance of the azomethine proton (-N=CH) with signals in the region of 8.00-8.63 ppm, whilst the signals in the region of δ 11.57-11.89 ppm correspond to an NH proton. Both ¹H and ¹³C NMR spectra of compounds **127** presented additional signals due to the restricted rotation around the carbonyl amide bond. The ¹³C NMR spectra of the fluorinated compounds **127a, g-l** showed the corresponding fluorine splittings.

The parent molecular ion peaks in the ESI-MS spectra ([M+H]⁺) further validate their chemical structures (Table 4.15).

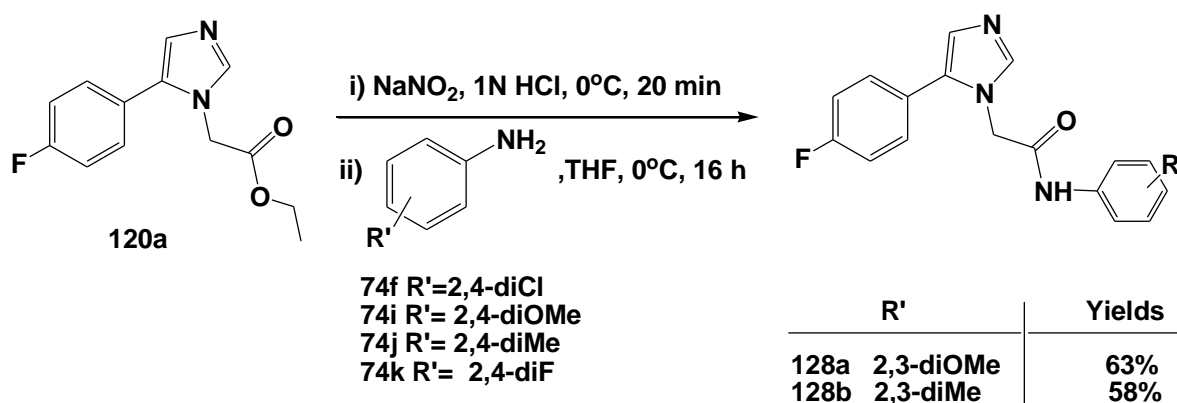
Table 4.15: HRMS results of the (*E*)-*N*¹-arylidene-2-(5-aryl-1*H*-imidazol-1-yl)acetohydrazide **127a-o** and their mSigma values.

Comps	Chemical formula [M+1]	Calculated m/z	Measured m/z	mSigma value	Err (mDa)	Err (ppm)
127a	C ₁₉ H ₁₈ FN ₄ O ₃ ⁺	369.1357	369.1366	-0.9	-2.4	1.8
127b	C ₁₉ H ₁₈ ClN ₄ O ₃ ⁺	385.1062	385.1062	-0.0	-0.0	0.8
127c	C ₂₃ H ₂₇ N ₄ O ₃ ⁺	407.2078	407.2083	-0.5	-1.2	0.4
127d	C ₂₁ H ₂₃ N ₄ O ₅ ⁺	411.1663	411.1674	-1.1	-2.7	4.3
127e	C ₂₀ H ₂₁ N ₄ O ₅ ⁺	397.1506	397.1510	-0.4	-2.7	5.2
127f	C ₁₉ H ₁₉ N ₄ O ₃ ⁺	351.1452	351.1455	-0.3	-0.8	3.6
127g	C ₁₈ H ₁₅ F ₂ N ₄ O ⁺	341.1208	341.1217	-0.8	-2.4	6.5
127h	C ₁₈ H ₁₅ FCIN ₄ O ⁺	357.0913	357.0918	-0.5	-1.5	7.0
127i	C ₂₀ H ₂₀ FN ₄ O ₃ ⁺	383.1514	383.1521	-0.7	-0.7	6.2
127j	C ₂₂ H ₂₄ FN ₄ O ⁺	379.1929	379.1933	-0.4	-1.1	4.4
127k	C ₁₉ H ₁₈ FN ₄ O ₃ ⁺	369.1357	359.1363	-0.5	-1.4	5.5
127l	C ₁₈ H ₁₆ FN ₄ O ⁺	323.1303	359.1304	-0.1	-0.6	1.6
127m	C ₂₀ H ₂₀ FN ₄ O ₃ ⁺	383.1514	383.1522	-0.8	-2.0	6.2
127n	C ₁₈ H ₁₆ FN ₄ O ⁺	421.2234	421.2238	0.4	1.2	5.4
127o	C ₂₂ H ₂₅ N ₄ O ⁺	361.2023	361.2025	-0.2	-0.7	9.1

4.3.2. Synthesis of *N*,5-diaryl-2-(1*H*-imidazol-1-yl)acetamide derivatives

It was of further interest to extend the existing library by converting the ethyl 2-(5-aryl-1*H*-imidazol-1-yl) acyl derivatives **120** into the corresponding *N*,5-diaryl-2-(1*H*-imidazol-1-

yl)acetamides **128** in accordance with the previously reported protocols.²³⁸ We were hoping that the inclusion of the carboxamide group in scaffolds **120** might increase the inhibition activities of the compounds. Due to time constraints, only ethyl 2-[5-(4-fluorophenyl)-1*H*-imidazol-1-yl]acetate **127a** was reacted with NaNO₂ in 1M HCl at 0°C, followed by addition of a solution of aniline derivatives **74** in THF and further stirring at the same temperature for 16 hours (**Scheme 4.11**). Work up and isolation by column chromatography afforded two novel *N*,5-diaryl-2-(1*H*-imidazol-1-yl)acetamide derivatives **128a-b** bearing electron-donating groups at the *N*-aryl ring in yields of 58 and 68%, respectively. However, when the *N*-aryl group contained dihalide groups at the *ortho*- and *para*-positions, no products were isolated under the tested reaction conditions. This may be attributed to the electron-withdrawing effects of the substituents at those positions reducing the nucleophilicity of the aniline nitrogen.



Scheme 4.11: Synthesis of *N*,5-diaryl-2-(5-aryl-1*H*-imidazol-1-yl)acetamide derivatives **128**.

4.3.2.1. Structure elucidation of the *N*,5-diaryl-2-(1*H*-imidazol-1-yl)acetamides **128**

In this section, by way of example, FTIR and NMR spectra of compound **128a** will be discussed in detail below as representative of this compound class. The FTIR spectrum of compound **128a** showed the absorption band at 3241 cm⁻¹ relating to an NH group whilst the band at 1742 cm⁻¹ corresponded to an amide carbonyl group.

A characteristic feature of compound **128a** in the proton NMR spectrum was the presence of an NH singlet at 8.01 ppm while another two singlets at 7.76 and 7.16 ppm correspond to the two methine protons of the imidazole motif. A singlet signal at 4.74 ppm was assigned to the methylene protons adjacent to the carbonyl group while two characteristic methoxy singlets resonate at 3.78 and 3.72 ppm. The ¹³C NMR spectrum for compound **128a** displayed signals at 164.2 ppm and 162.9 ppm which correspond to the carbonyl carbon atom and the carbon atom (¹J_{C,F}= 253 Hz) directly attached to the fluorine atom. Furthermore, the carbon signals of the aryl

ring directly attached to fluorine at the *para*-position appears as a doublet due to fluorine splitting.

4.3.3. Biological evaluation of the synthesized (*E*)-*N'*-arylidene-2-(5-aryl-1*H*-imidazol-1-yl)acetohydrazides **127a-o** and *N*,5-diaryl-2-(1*H*-imidazol-1-yl)acetamides **128a-b**

The newly synthesized seventeen compounds belonging to a families of novel (*E*)-*N'*-arylidene-2-(5-aryl-1*H*-imidazol-1-yl)acetohydrazides **127a-o** and *N*,5-diaryl-2-(1*H*-imidazol-1-yl)acetamides **128a-b** were submitted to be evaluated for inhibition of LEDGF/p75-IN interactions using the AlphaScreen assay at 100µM. The tests were carried out in triplicate and average results are recorded in *Table 4.16*.

Table 4.16: The HIV-1 IN-LEDGF/p75 inhibition activities of *N'*-arylidene-2-(5-aryl-1*H*-imidazol-1-yl)acetohydrazides **127** and *N*,5-diaryl-2-(1*H*-imidazol-1-yl)acetamides **128**.

Compounds entry	Biochemical target assays
	HIV-1 IN – LEDGF (%) inhibition @ 100 µM
	(AlphaScreen)
127a	0
127b	19 ± 3.31
127c	24 ± 9.03
127d	49 ± 6.06
127e	20 ± 2.53
127f	0
127g	37 ± 6.67
127h	48 ± 5.06
127i	19 ± 5.74
127j	75 ± 4.47
127k	13 ± 8.40
127l	13 ± 9.44
127m	6 ± 3.02
127n	64 ± 2.22
127o	83 ± 1.40
128a	31 ± 7.07
128b	0
CX05168	91.37±0.85
HIV-1 IN and LEDGF with DMSO	0

Of the seventeen screened compounds, at least three arylidene-based compounds (**127j**, **127n** and **127o**) exceeded the 50% benchmark at a single dose concentration of 100 μ M. These best three inhibitors of the IN-LEDGF/p75 interaction contained the 4-*tert*-butylphenyl group. Compound **127o** with no substituent on the aryl ring directly linked to the hydrazine motif exhibited the highest inhibition percentage of 83%, followed by compound **127j** with a *para*-fluorine atom on the 5-aryl ring with 75% inhibition. Compound **127n**, with the methoxy groups at the *meta*- and *para*-positions on the 5-aryl ring displayed 64% inhibition of the LEDGF/p75-IN interaction. It was interesting to observe that another compound **127d** with a 4-*tert*-butylphenyl group on the aryl ring linked to the hydrazine motif exhibited 49% inhibition, which proves further the significance of a *tert*-butyl moiety in the disrupting activity of the compounds. Compound **127h** with a chlorine atom at the *ortho*-position of the aryl ring linked to the hydrazine motif and fluorine atom at the *para*-position on the 5-aryl ring yielded inhibition activity of 48%, while a close analogue, compound **127b**, containing a hydroxyl and a methoxy group at the *meta*- and *para*-position showed a significant decrease in activity with an inhibition of 19%. Other hydrazine scaffolds exhibited minimal inhibition activity (6-37%) with the exception of compounds **127a** and **127f** which were entirely inactive. Amongst the acetamide family, compounds **128a** with two methoxy group at the *ortho*- and *para*-positions of the *N*-arylacetamide motif exhibited only 31% inhibition of the formation of the IN-LEDGF/p75 complex, while compound **128b** with two methyl group at the *ortho*- and *para*-positions of the *N*-arylacetamide moiety was inactive.

The best three compounds were further assessed in the TruHit assay and they were found not to be false positives. The two LEDGF/p75-IN inhibitors **127j** and **127o** showing highest inhibition were further evaluated in a dose range assay and they produced IC₅₀ values of 27 μ M and 32 μ M, respectively. In a cell based assay, these compounds were found not to reduce the viability of the MT-cell and no antiviral activities were observed for the best three compounds, which may point to poor solubility or that they are only disrupting the protein-protein interaction and not causing multimerization. The inhibition activity observed for the best three *N*-arylidene-based compounds reported here provides groundwork for further investigations.

4.3.4. *In silico* ADME studies of novel (*E*)-*N*-arylidene-2-(5-aryl-1*H*-imidazol-1-yl)acetohydrazide compounds

The ADME and Lipinski's "rule of five" or Veber's rule, of the best three compounds were determined in order to filter compounds which do not adhere with these properties using BIOVIA Discovery Studio^{TM 289,295}. The best three compounds were found to have less than 5

hydrogen donors, 5 to 7 hydrogen acceptors and their molecular weights were established to be less than 500 ($360.45 > MW < 420.20$), which falls within the Lipinski rule (*Table 4.17*). These compounds did not violate Lipinski's or Veber's rules, which indicate good drug-likeness properties whilst the polar surface area of the best four compounds were established to be below 140\AA displaying good lipophilicity.

Table 4.17: The predicted Lipinski properties of the best four (E)-N'-arylidene-2-(5-aryl-1H-imidazol-1-yl)acetohydrazides **127j** and **127n-o**.

Compounds	Molecular Weight (g/mol)	Lipinski's Number of hydrogen donor	Lipinski's Number of hydrogen acceptor	Number of rotational bond	Polar Surface Area (PSA_2D)
127j	378.443	1	5	6	58.043
127n	420.504	1	7	8	75.903
127o	360.452	1	5	6	58.043

Note: ideal ranges for druggability; Mw <500; H donors <5; H acceptors from 5-7; PSA <140.

ADME properties of the best three compounds **127j** and **127n-o** were also performed by means of Discovery StudioTM to determine their BBB penetration, aqueous solubility and human intestinal absorption, and cytochrome p450 2D6 protein inhibition (*Table 4.18*).^{289,290} The three compounds were predicted to have low solubility (level 2) which implies that the compounds slightly dissolve in water, and all were projected to have good absorption levels, which indicate that they can be absorbed very well by the human intestine after oral dosage. Compounds **127j** and **127o** were predicted to be high BBB penetrators indicating that they might cause central nervous system side effects, whilst compound **127n** was a medium penetrator which suggests that it might have low chances of causing side effects in the central nervous system. Furthermore, compound **127n** was predicted to be a non-inhibitor of the CYP2D6 enzymes, which are responsible for metabolism of many drugs in the human body.

Table 4.18: Predicted ADME profiles of four (E)-N'-arylidene-2-(5-aryl-1H-imidazol-1-yl)acetohydrazides **127j** and **127n-o**.

Compounds	Aqueous Solubility &	Blood Brain Barrier Penetration	Human Intestinal Absorption	CYP2D6 Inhibition
127j	2	1	0	Yes
127n	2	2	0	No
127o	2	1	0	Yes

4.3.5. Molecular modelling of the synthesized (E)-N'-arylidene-2-(5-aryl-1H-imidazol-1-yl)acetohydrazides **127j** and **127n-o** at the HIV-1 IN dimer interface

The best three N'-arylidene compounds which were found to be active by exhibiting more than 50% inhibition of the LEDGF/p75 -IN protein-protein interaction were docked in the LEDGF/p75 binding site of the HIV-IN dimer-dimer interface (PDB code: 2B4J). The docking studies were carried out using Discovery Studio software. The best three compounds were docked at the dimer cavity of the HIV-IN where the LEDGF/p75 binds using LibDock scoring, and following energy minimizations until achieving the lowest binding energy poses. The scoring results and their calculated binding energy are recorded in *Table 4.19*. The docking study showed that the best three compounds were binding in the LEDGF/p75 binding cavity of the IN dimer interface with compound **127n** displaying a total binding energy of -61.1730Kcal/mol (lowest binding energy), followed by **127j** with a total binding energy of -59.624 Kcal/mol whilst compound **127o** exhibited a total binding energy of -53.8902 Kcal/mol. The lowest binding energy exhibited by compound **127n** could be attributed to the methoxy group which could form a hydrogen bond with residues within the binding site causing the stabilisation of the interaction between HIV-1 IN and the compound.

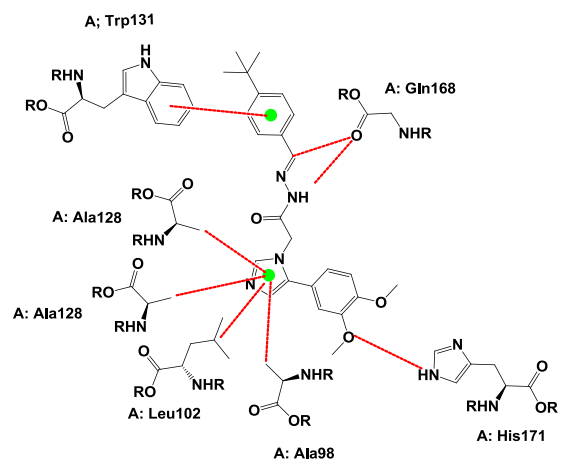
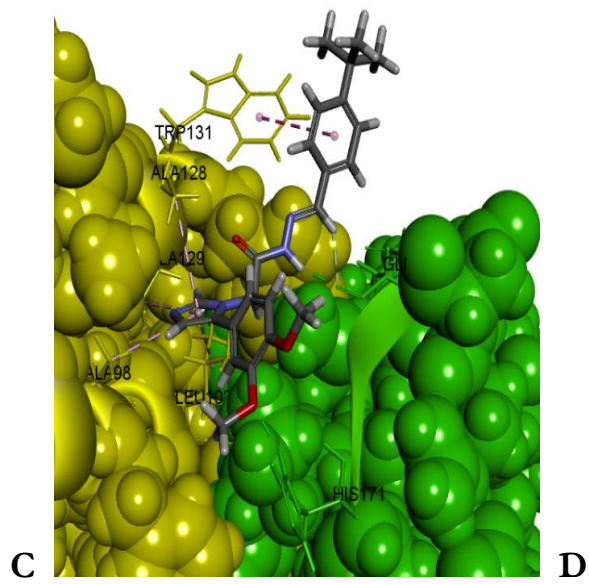
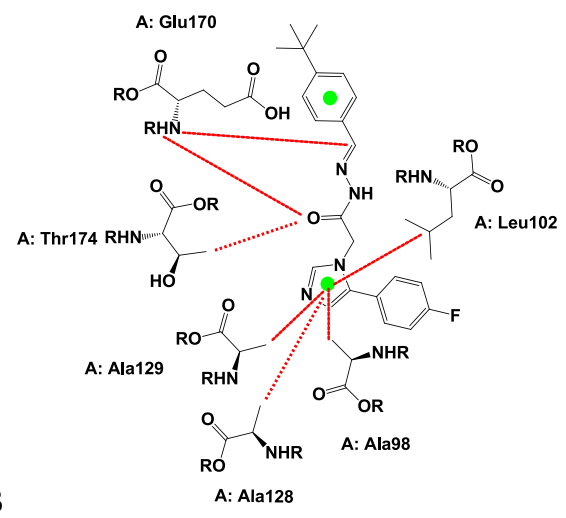
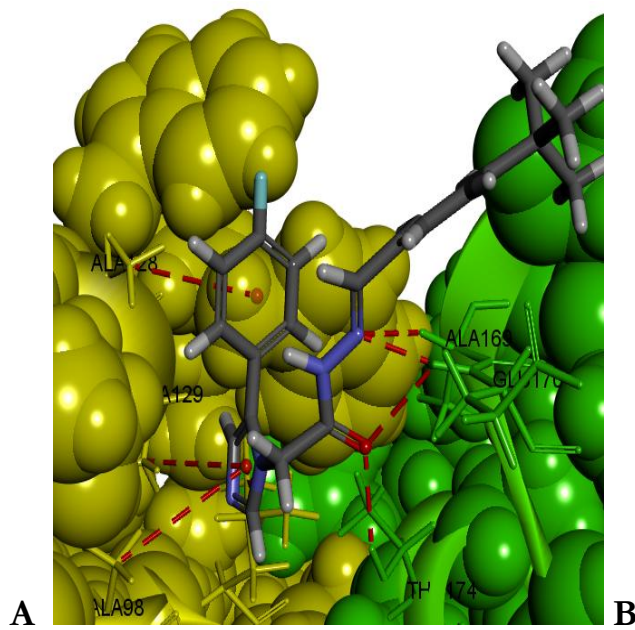
Table 4.19: A list of *in silico* interaction of compounds (**127j**, **127n** and **127o**) and their binding energy.

Compounds	Binding energy Kcal/mol	LibDock Score	Jain score	Amino acids interactions
127j	-53.8902	30.9486	3.52	Ala98, Leu102 Ala128, Ala129, Ala169, Glu170, Thr174
127n	-61.1730	36.8581	2.38	Ala98, Leu102 Ala128, Ala129, Gln168, Trp131, Glu170, His171
127o	-53.8902	44.8739	1.46	Ala98, Leu102 Ala128, Gln168, Glu170, His171

The predicted binding model of compound **127j** shown in *Figure 12 A* and *B* displayed the carbonyl oxygen forming two hydrogen bonds with an NH of Gln168 and Glu170 residues while the 4-*tert*-butylphenyl group at the 5-position of the imidazole motif occupies the hydrophobic pockets of the Ala98 residue. The phenyl ring directly attached to the hydrazine group is shown to pack in a hydrophobic cavity of His171, whilst the imidazole moiety falls in the hydrophobic cavity of Ala98 and Leu102 residues.

The *para*-methoxy group in **127n** (*Figure 4.12, C* and *D*) exhibited a hydrogen bond to the His171 residue, while its imidazole moiety interacts in a similar mode to compound **127j**. Moreover, the azomethine and an NH group of the hydrazine motif display two hydrogen bonds to the Gln168 residue while the 4-*tert*-butylphenyl ring is packed into the hydrophobic pockets of Trp131.

The model of compound **127o** (*Figure 4.12, E* and *F*) shows the imidazole core packed into hydrophobic pockets of the Ala98 and Leu102 residues while the 4-*tert*-butylphenyl ring is packed into the hydrophobic cavity of Ala128. Furthermore, the oxygen atoms of the carbonyl group display two hydrogen bonds to the Gln98 and Glu170 amino acids whilst the phenyl ring directly attached to the hydrazine group packs into the hydrophobic His171 residue.



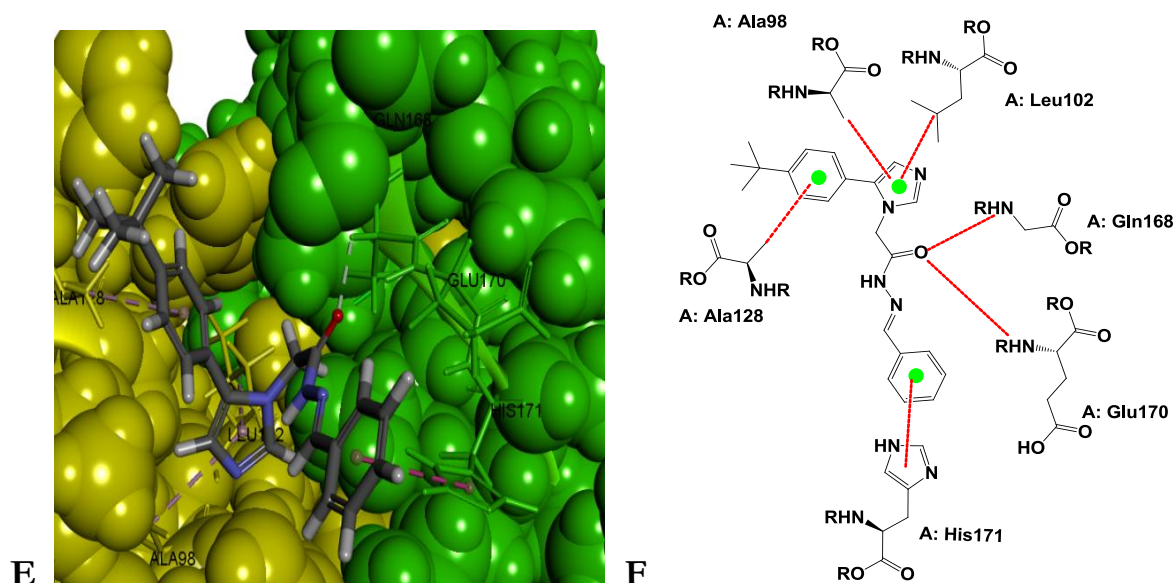


Figure 4.12: Predicted binding models of compounds **127j** (A and B), **127n** (C and D) and **127o** (E and F) docked in the LEDGF/p75 binding cavity at the HIV-1 IN dimer interface (with yellow CPK display sphere sized representing monomer A and green CPK display sphere sized for monomer B).

In summary, the binding model shows that the three compounds with the best activity in the AlphaScreen interact with the amino acids in the HIV-1 IN binding cavity, with compound **127n** exhibiting the lowest binding energy. The study reveals that the imidazole motif of the best compounds occupies the hydrophobic pockets of amino acid residues known to interact with LEDGF/p75. Furthermore, these compounds occupy the same binding cavity of the HIV-1 IN as occupied by LEDGF/p75.

4.4. Conclusion

A novel family of 5-aryl-imidazol-1-yl-based compounds were successfully synthesized by incorporation of simple amino acids *via* a van Leusen approach. Firstly, glycine, L-alanine and D-leucine were converted to the corresponding amino acid ethyl ester hydrochloride salts in excellent yields, followed by treatment with Et₃N in CHCl₃ to afford free amino esters in good yields. These free amino esters were further subjected to condensation reactions with various benzaldehydes to furnish the ethyl 2-(arylideneamino)acyl intermediates in excellent yields. An initial attempt to react TosMIC with ethyl 2-(arylideneamino)acyl intermediates using previously established protocols, under microwave irradiation was unsuccessful. This was attributed to possible decomposition of the intermediate under MW heating. However, the problem was

overcome by reacting TosMIC with ethyl 2-(arylideneamino)acyl intermediates induced by DBU in DCM at room temperature for 24 hours, followed by removal of DCM and further subjecting the crude material to microwave heating under toluene at a set temperature of 115°C for 10 minutes to afford the ethyl 2-(5-aryl-1*H*-imidazol-1-yl)acyls in poor to good yield. The yields of the products were strongly influenced by the substituents at the chiral centre and on the aryl ring. Initial attempts to isolate the hydrolysed 2-(5-aryl-1*H*-imidazol-1-yl) acetic acids from reaction of selected ethyl 2-(5-aryl-1*H*-imidazol-1-yl)acylates with NaOH in MeOH proved to be challenging, which may be due to the existence of these compounds in ionized form. However, the hydrolysis of ethyl 2-(5-aryl-1*H*-imidazol-1-yl)acylates to the corresponding 2-(5-aryl-1*H*-imidazol-1-yl) acetic acids was successfully achieved in good yield by microwave irradiation in water at a set power of 200 Watts and temperature of 105°C for 3 hours. Furthermore, selected ethyl 2-(5-aryl-1*H*-imidazol-1-yl)acylates were subjected to nucleophilic attack by hydrazine monohydrate using both conventional heating and microwave methods to afford 2-(5-aryl-1*H*-imidazol-1-yl)acetohydrazide scaffolds in various yields. A total of 26 novel 5-aryl-imidazol-1-yl-based scaffolds were obtained and submitted for biological evaluation.

IN-LEDGF/p75 AlphaScreen assay: The 26 novel 5-aryl-imidazol-1-yl-based compounds were screened for direct inhibition of HIV-1 IN-LEDGF/p75 interaction. Only compound **123g** from a family of 2-(5-aryl-1*H*-imidazol-1-yl)acetic acids displayed inhibition above 50% with an IC₅₀ value of 19 μM. The best scaffold was non-toxic to the MT-4 cell at 100 μM but unfortunately, it did not inhibit HIV-1 replication in the cell.

Compound **123g** was then modelled and subjected to docking simulations in order to understand the probable binding modes at molecular level. This scaffold was projected to have a good probability of interacting with important amino acids in the HIV-1 dimer interface in a comparable mode of action to the LEDGF/p75 protein. Furthermore, the best scaffold **123g** is predicted to have good ADME properties. The results indicated that compound **123g** has significant ability to prevent the formation of the LEDGF/p75-IN complex and is considered a promising hit to design the next generation of compounds.

Vpu-BST-2 ELISA assay: Seven out of 26 5-aryl-imidazol-1-yl-based compounds were found to exceed the 50% benchmark value at 100 μM. Compound **120h** exhibiting the highest percentage inhibition of 82% with an IC₅₀ of 12.42 μM, followed by compound **125g** with 72% inhibition and an IC₅₀ value of 23.36 μM for preventing the Vpu-BST-2 interaction. The seven best compounds were further evaluated in MT-4 cells in order to determine the CC₅₀ values and

produced CC_{50} values between 102 μ M to greater than 200 μ M. None of the compounds showed any antiviral activity in the cell-based assay. The best compounds could be used as viable hits to design compounds with improved inhibition and IC_{50} values.

The predicted ADME properties of the best seven inhibitors of the Vpu -BST-2 interactions showed good to optimal aqueous solubility with medium to low blood brain barrier (BBB) penetration levels. Furthermore, five compounds **120a**, **120c**, **120d**, **120h** and **121a** showed low predicted intestinal absorption while scaffolds **123g**, **125c** and **125g** were shown to have good human intestinal absorption. The best seven compounds were predicted to be non-inhibitors of the cytochrome P450 enzyme. These data reveal that these compounds merit further exploration as viable hits to design the next generation inhibitors of the Vpu-BST-2 interaction.

A series of new *N*'-arylidene-2-(5-aryl-1*H*-imidazol-1-yl)acetohydrazide compounds and *N*,5-diaryl-2-(1*H*-imidazol-1-yl)acetamide derivatives were designed and synthesized as second generation compounds. Initially, a small family of *N*'-arylidene-2-(5-aryl-1*H*-imidazol-1-yl)acetohydrazide derivatives was successfully synthesized by reacting acetohydrazide derivatives with various benzaldehydes in MeOH under reflux. The products were obtained in excellent yields as rotamers due to the restricted rotation around the amide bond.

To further increase the number of compounds in the existing library, ethyl 2-[5-(4-fluorophenyl)-1*H*-imidazol-1-yl]acrylate was then reacted with $NaNO_2$ in 1N HCl at 0°C, followed by addition of aniline derivatives in THF to afford the two novel *N*,5-diaryl-2-(1*H*-imidazol-1-yl)acetamide derivatives bearing electron-donating groups at the *N*-aryl ring in good yields. When aniline with dihalides at the *ortho*- and *para*-positions were used, none of the desired compounds were isolated, which could be attributed to the electron-withdrawing effects of the halides.

Having successfully synthesized the desired target compounds, seventeen novel compounds were sent for biological testing for their ability to disrupt LEDGF/p75-IN complex formation in an AlphaScreen assay. Three compounds showed inhibition that exceeded the 50% inhibition benchmark at 100 μ M concentration and both contained the 4-*tert*-butylphenyl group. The top two LEDGF/p75-IN inhibitors **127j** and **127o** with the highest percentage inhibition in the AlphaScreen assay produced IC_{50} values of 27 μ M and 32 μ M.

Molecular docking was performed to give the probable binding mode of the best three compounds at the binding cavity of the HIV-1 dimer. The best three compounds were binding in the HIV-1 dimer interface in a mode of action similar to the LEDGF/p75 protein. The imidazole moiety was found to be packed into the hydrophobic cavities of important residues

known to interact with LEDGF/p75. Furthermore, the ADME predictions conducted on the best three compounds (**127j**, **127n** and **127o**) indicate that these compounds have low solubility (level 2) but good absorption levels. However, only compound **127n** was predicted as a non-inhibitor of the CYP2D6 protein.

These results suggest that compound **127n** could be selected for further optimization for improvement in anti-HIV-1 activity and aqueous solubility. The studies described in the present chapter demonstrate the usefulness of TosMIC chemistry towards development of nitrogen containing heterocycles. It also provides credence to the belief that such progress can be accomplished in the academic domain. Furthermore, the compounds described have not been previously described for targeting the interaction between LEDGF/p75-HIV-1 IN proteins.

4.5. Future Work

Future work will involve insertion of a second aryl ring at the 4-position of the imidazole motif of the 2-(5-aryl-1*H*-imidazol-1-yl) acetic acids, hoping that the modification will increase the percentage inhibition as well as the IC₅₀ values of the compounds in the HIV-1 IN-LEDGF/p75 AlphaScreen assay (Figure 4.13). Evaluation of the *N*¹-arylidene-2-(5-aryl-1*H*-imidazol-1-yl)acetohydrazides and *N*,5-diaryl-2-(1*H*-imidazol-1-yl)acetamides in the HIV-1 Vpu-BST-2 assay will also form part of future work.

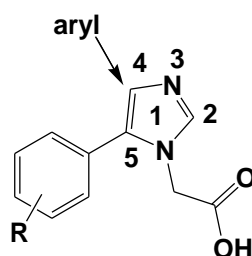


Figure 4.13: Possible structural modification of the 2-(5-aryl-1*H*-imidazol-1-yl) acetic acids.

CHAPTER 5

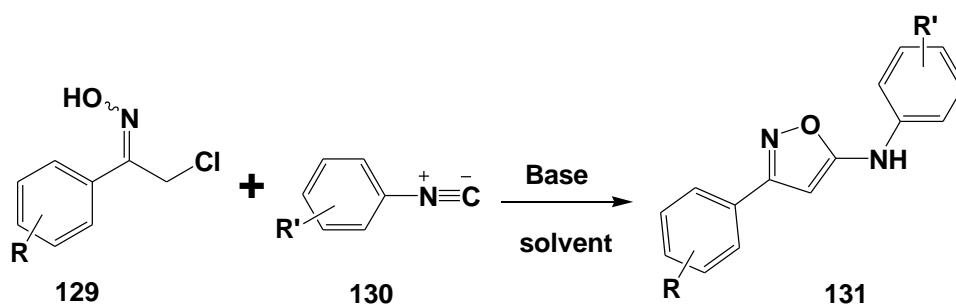
Synthesis of 3-aryl-*N*-arylisoxazol-5-amine scaffolds using aryl isocyanides and their usefulness as for possible inhibitors of HIV-1 protein- host protein interactions

5.1 Introduction

Compounds containing the isoxazole motif have been reported to possess significant biological activity.^{296,297,298,299,300,301} To date no compounds with the isoxazole moiety have been reported as potential inhibitors that could disrupt the HIV-1 IN- LEDGF/p75 interactions, which made this moiety more interesting for this project. Keeping this in mind and considering our interest in extending the existing library of aryl-linked five-membered nitrogen containing heterocyclic fragments, we pursued the synthesis of a series of 3-aryl-*N*-arylisoxazol-5-amine fragments by employing aryl isocyanide as a synthon. We hoped that evaluation of these compounds could also offer a starting point to design a second generation of compounds, which could have anti-HIV-1 activity through inhibiting the HIV-1 IN-LEDGF/p75 interactions.

5.2. Synthesis of 3-aryl-*N*-arylisoxazol-5-amine based compounds

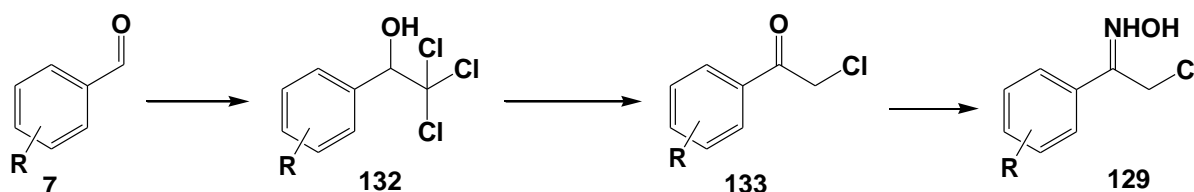
The synthesis of 3-aryl-*N*-arylisoxazol-5-amines **131** requires the preparation of two essential intermediates; namely: the 2-halo-1-arylketone oximes **129** and aryl isocyanides **130** (*Scheme 5.1*). The synthesis of these key intermediates was then pursued *en-route* to the final products. This chapter will discuss the synthetic challenges encountered in the preparation of isoxazoles, as well as characterization of compounds, reaction mechanisms and biological data of the isoxazole products.



Scheme 5.1: Synthetic strategy towards isoxazoles.

5.2.1. Synthesis of key 2-halo-1-arylketoneoxime intermediates

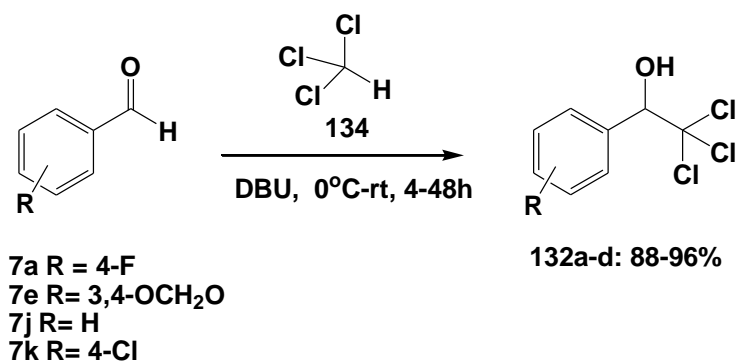
Our first efforts were towards the synthesis of the 2-halo-1-arylethanone oxime intermediates **129**, which were obtained over three steps *via* formation of 2-halo-1-arylethanone intermediate **133** starting from aldehyde **7** as proposed in *Scheme 5.2*.



Scheme 5.2: Proposed synthetic strategy for the formation of 2-halo-1-arylethanone oximes.

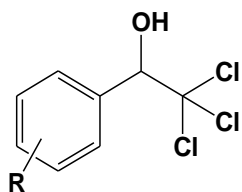
5.2.1.1. Synthesis of the 2,2,2-trichloro-1-aryl-ethanol

The starting point of the synthesis was conversion of the aldehyde into the corresponding trihalocarbiniols. These trihalocarbiniols are routinely prepared through a base promoted addition of chloroform to the carbonyl group of the aldehyde using relatively strong base at mild temperatures to avoid the Cannizzaro reaction.^{302,303} In addition, cyclic amidines such as 1,8-diazabicyclo[5.4.0]undec-7-ene (DBU), 1,5-diazabicyclo[4.3.0]non-5-ene (DBN) and guanidine have been described to stimulate the addition of chloroform to aldehyde under mild conditions.³⁰⁴ DBU was chosen as a catalytic base to induce the addition of chloroform to the aldehyde. Specifically, selected benzaldehydes **7** were reacted with dry chloroform **134** in the presence of DBU at room temperature under inert conditions for 4-48 hours as shown in *Scheme 5.3*. Work up furnished the desired 2,2,2-trichloro-1-aryl-ethanol products **132a-d** as racemates in yields of up to 96% (*Table 5.1*). The yield of products was comparable to those values described in literature.³⁰⁴



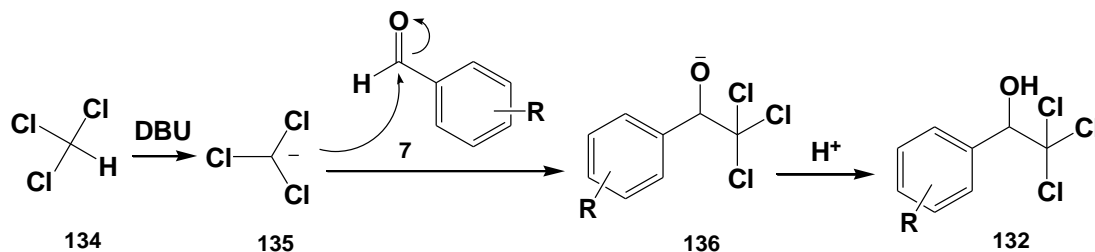
Scheme 5.3: Synthesis of 2,2,2-trichloro-1-aryl-ethanol derivatives **132**.

Table 5.1: Isolated yields (%) of the 2,2,2-trichloro-1-arylethanone products **132**.



Compd	R	Yields (%)
132a	4-F	94
132b	3,4-OCH ₂ O-	96
132c	H	93
132d	4-Cl	88

A probable mechanism for the formation of the 2,2,2-trichloro-1-arylethanol derivatives **132** is shown in *Scheme 5.4* and is thought to involve deprotonation of chloroform **134** by the catalytic DBU to generate a reactive chloroform carbanion **135**. This carbanion **135** then attacks the carbonyl carbon of aldehyde **7** to generate 2,2,2-trichloro-1-arylethan-1-olate intermediate **136**, followed by subsequent protonation to give 2,2,2-trichloro-1-arylethanol product **132**.³⁰⁴



Scheme 5.4: Mechanistic pathway for the formation of 2,2,2-trichloro-1-arylethanol **132**.

The structures of 2,2,2-trichloro-1-arylethanol derivatives **132** were confirmed by NMR and FTIR spectroscopic analysis and were consistent with reported values.³⁰⁴ Compounds **132a-d** were obtained as racemates.³⁰⁴ By way of example, compound **132c** is discussed in detail and the key features of the proton NMR spectrum for this compound was the presence of a signal for the hydroxyl group which resonates as a singlet at δ 3.45 ppm and the methine proton at the chiral centre resonating as a signal at δ 5.21 ppm. The signals in the aromatic region were integrated and correspond to the five methine protons of the benzene ring. The ¹³C NMR spectrum of compound **132c** exhibited all the expected carbon signals with the methine carbon

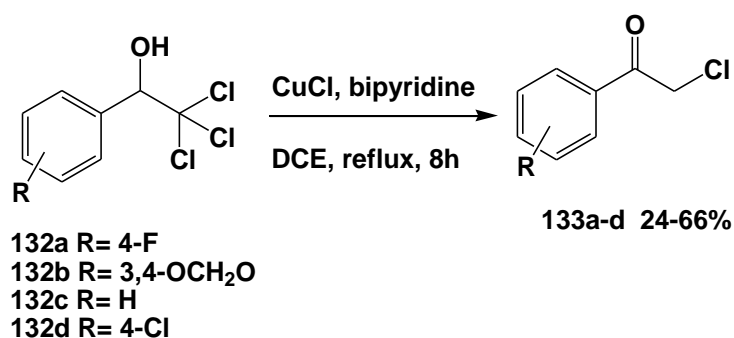
atom at the chiral centre resonating at δ 84.4 ppm whilst the carbon atom directly attached to the three chlorine atoms emerged at 103.0 ppm.

The FTIR spectra of the compounds **132a-d** confirmed the presence of an OH group as a broad signal appearing between 3326 and 3500 cm^{-1} as recorded in *Table 5.2*.

Table 5.2: FTIR spectroscopic data of 2,2,2-trichloro-1-arylethanol derivatives **132** showing the OH bands.

Compounds	132a	132b	132c	132d
$\nu_{\text{OH}} (\text{cm}^{-1})$	3447	3326	3426	3500

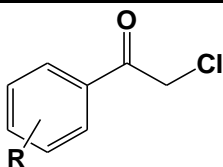
5.2.1.2. Oxidation of 2,2,2-trichloro-1-aryl-ethanol derivatives



Scheme 5.5: Synthesis of 2-chloro-1-aryl-ethanone derivatives **133**

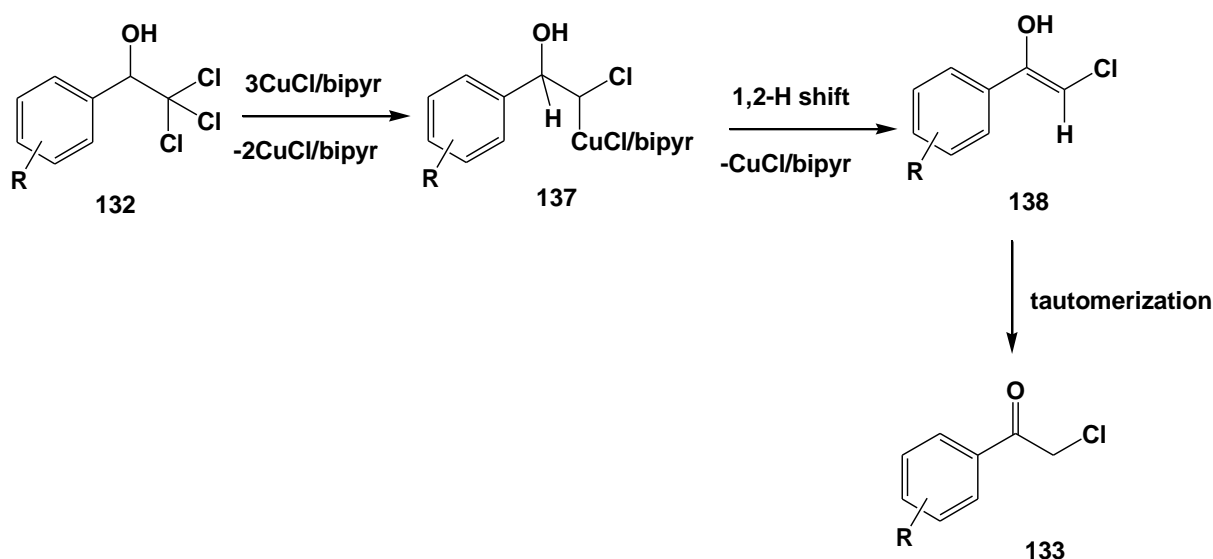
A series of 2,2,2-trichloro-1-arylethanol derivatives **132a-d** were then subjected to an oxidation reaction in accordance with a protocol reported in the literature.³⁰⁵ Thus, 2,2,2-trichloro-1-aryl-ethanol derivatives **133a-d** were heated under reflux in the presence of CuCl and bipyridine using 1,2-dichloroethane (DCE) as solvent under oxygen free conditions for 8 hours (*Scheme 5.5*). Separation by short column chromatography gave 2-chloro-1-aryl-ethanone scaffolds **133a-d** in yields ranging between 24 -66% (see *Table 5.3*). In our hands the yields of the products **133c** and **133d** obtained were significantly lower than yields previously reported by Ram and co-workers (i.e. 96% for **133c** and 90% for **133d**).³⁰⁵ Compound **133a** and **133b** were not reported in the study conducted by Ram *et al.*,³⁰⁵ but they have been previously prepared using different starting materials.

Table 5.3: Isolated yields (%) of the 2-chloro-1-aryl-ethanone products **133**.



Compound	R	Yields (%)
133a	4-F	66
133b	3,4-OCH ₂ O-	24
133c	H	54
133d	4-Cl	60

The proposed mechanistic pathway for the oxidation of 2,2,2-trichloro-1-arylethanols **132** by CuCl/bipyridine is depicted in **Scheme 5.6** and is similar to the previously reported by Ram *et al.*³⁰⁵ The initial step is considered to involve the reduction of one carbon-chlorine bond to generate copper-chlorocarbenoid intermediate **137**, followed by removal of the CuCl/bipyridine complex, to produce enol **138** *via* a hydride shift. This compound **138** tautomerises to give 2-chloro-1-aryl-ethanone **133**.³⁰⁵



Scheme 5.6: Proposed mechanism of formation of 2-chloro-1-aryl-ethanones **133**.³⁰⁵

The 2-chloro-1-aryl-ethanone products **133a-d** were characterized by FTIR, and 1D and 2D NMR spectroscopy, and were in agreement with reported literature values.³⁰⁵ The main characteristic in the ¹H NMR spectrum of compound **133b** was the presence of a singlet at δ 4.66 ppm integrating for two protons of the methylene group adjacent to the carbonyl group,

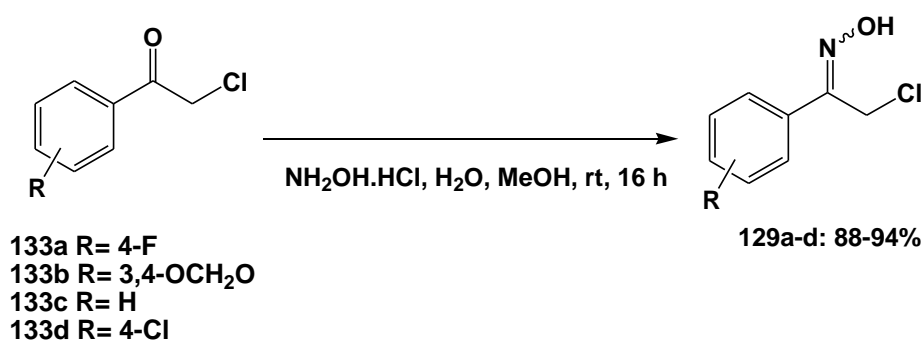
whilst the ^{13}C NMR spectrum revealed the presence of a carbonyl carbon atom at 189.0 ppm and a methylene carbon atom adjacent to the carbonyl group at 45.6 ppm. The existence of the methylene carbon atom was evident in the DEPT 135 spectrum, where it resonated as a negative signal. The FTIR spectra further confirmed the presence of the carbonyl group by showing stretch bands in the region of 1686-1701 cm^{-1} as shown in *Table 5.4*.

Table 5.4: FTIR spectroscopic data of 2-chloro-1-aryl-ethanone products **133** showing the C=O bands.

Compounds	133a	133b	133c	133d
$\nu_{\text{C=O}}$ (cm^{-1})	1706	1736	1701	1686

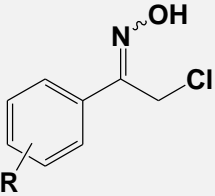
5.2.1.3. Synthesis of 2-chloro-1-aryl-ethanone oxime intermediates

Zhang *et al.* had earlier reported a synthetic procedure for 2-chloro-1-phenylethanone oxime.³⁰⁶ To explore this route to 2-chloro-1-aryl-ethanone oxime intermediates, compounds **133a-d** were subjected to condensation reaction conditions by reacting with hydroxylamine hydrochloride in the presence of water and MeOH as solvent at room temperature for 16 hours as indicated in *Scheme 5.7*. Work up by addition of more water, furnished the key 2-chloro-1-aryl-ethanone oxime intermediates **129a-d** as precipitates in excellent yields (*Table 5.5*). The yield of the product **129c** obtained was as good as that reported by Zhang (i.e. 83%).³⁰⁶



Scheme 5.7: Synthesis of 2-chloro-1-aryl-ethanone oxime intermediates.

Table 5.5: Isolated yields (%) of the 2-chloro-1-aryl-ethanone oxime products **129**.

		
Compound	R	Yields (%)
129a	4-F	94
129b	4-Cl	93
129c	H	88
129d	3,4-OCH ₂ O-	94

The structures of the products obtained were elucidated by NMR spectroscopy and values were in agreement with those found in the literature.^{306,307,314,315} NMR spectroscopic analysis revealed that the 2-chloro-1-aryl-ethanone oxime products **129** were obtained as a mixture of geometric isomers in a ratio of 8:1 and assignment of the NMR spectra was based on previously reported literature values.^{314,315} The ¹H NMR spectrum of compound **129b** in chloroform revealed two singlets at 4.59 and 4.44 ppm corresponding to the methylene proton adjacent to a chlorine atom of both isomers, while hydroxylic protons for the two isomers were registered at 9.41 and 9.11 ppm. However, the ¹H NMR spectrum of compound **129d** in DMSO-*d*₆ exhibited the OH groups of the two isomers as peaks at 11.9 and 11.8 ppm whilst the methine protons adjacent to the chlorine atom resonated as signals at 4.67 and 4.61 ppm, respectively. The ¹³C NMR spectrum of compound **129b** revealed the signal of the carbon atom double bonded to nitrogen of both isomers at 153.5 and 152.9 ppm while the methylene carbon atoms emerged at 44.5 and 32.1 ppm. The FTIR spectra of these scaffolds revealed the presence of an OH group in the frequency region between 3226 and 3369 cm⁻¹ whilst the C=N signal resonates in range of 1604-1701cm⁻¹ (*Table 5.6*). Furthermore, the frequencies in a region of 956 to 998 cm⁻¹ were assigned to the stretching vibration of the N-O group.

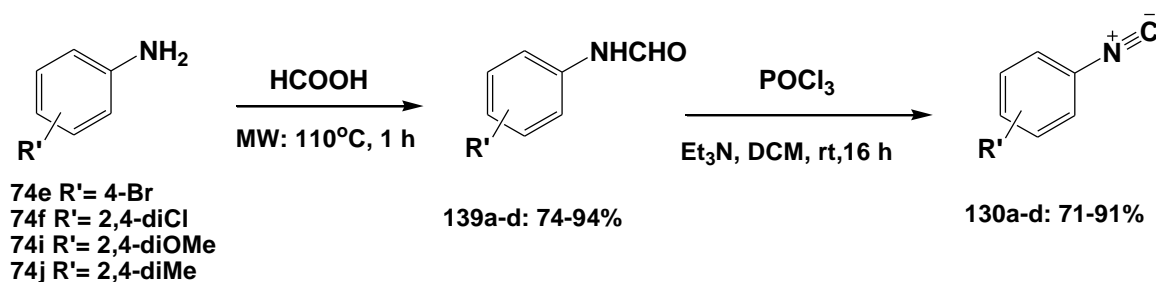
Table 5.6: FTIR spectroscopic data of 22-chloro-1-aryl-ethanone oxime products **129** showing the OH, C=N and N-O bands.

compounds	129a	129b	129c	129d
$\nu_{\text{OH}} (\text{cm}^{-1})$	3295	3360	3226	3269
$\nu_{\text{C=N}} (\text{cm}^{-1})$	1701	1686	1700	1717
$\nu_{\text{N-O}} (\text{cm}^{-1})$	836	833	960	953

With the 2-chloro-1-aryl-ethanone oxime intermediates in hand, the focus was then shifted to the preparation of aryl isocyanide intermediates, making use of readily commercially available anilines.

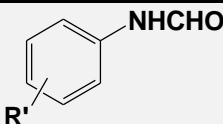
5.2.2. Synthesis of aryl isocyanide derivatives

N-formylated compounds are very valuable intermediates in the preparation of isocyanide compounds. They are readily generated by formylation of primary amines using various reagents such as acetic formic anhydride,^{308,309} silica sulfuric acid,³¹⁰ zinc oxide,³¹¹ formic acid,³¹² ammonium formate,³¹³ ethyl formate,³¹⁴ and other reagents. However, recently, a protocol involving the *N*-formylation of amines using ultrasound irradiation under solvent- and catalyst-free conditions at 110°C has been cited.³¹⁵ Encouraged by this observation, we pursued the synthesis of *N*-formylated anilines under microwave irradiation utilising the same temperatures reported for the ultrasound irradiation approach. Thus, a series of aniline derivatives **74e-f, i** and **j** were microwave irradiated neat with formic acid at a set temperature of 110°C for 1 hour (as monitored by TLC), as illustrated in **Scheme 5.8**. Work up afforded the corresponding *N*-aryl-formamide products **139a-d** in yields similar to those reported under ultrasound irradiation and acetic formic anhydride methods (*Table 5.7*).³¹²⁻³¹⁵



Scheme 5.8: Synthesis of aryl isocyanides **130a-d**.

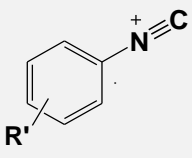
Table 5.7: Isolated yields (%) of the *N*-aryl-formamide products **139a-d**.

		
Compounds	R'	Yields (%)
139a	4-Br	92
139b	2,5-diCl	83
139c	2,4-diOMe	74
139d	2,4-diMe	79

The structures of the *N*-aryl-formamide products **139a-d** were confirmed by NMR spectroscopic analysis as rotamers which resulted due to the restricted rotation about the amide bond. By way of example the structure of *N*-(2,4-dimethylphenyl) formamide **139d** will be discussed in detail. The ^1H NMR spectrum of *N*-(2,4-dimethylphenyl) formamide **139d** showed a doublet at 8.54 ppm with a J value of 12 Hz, corresponding to the presence of the major rotamer while the minor rotamer appears as a singlet at 8.39 ppm. Furthermore, the NH proton of the major rotamer resonates as a signal at 7.96 ppm whilst the signal at 7.17 ppm corresponds to the existence of the NH proton of the minor rotamer. The ^{13}C NMR spectrum of compound **139d** showed the aldehyde carbon atom of the major rotamer at 163.5 ppm, while the aldehyde carbon atom of the minor rotamer emerged as a signal at 159.2 ppm.

The *N*-aryl-formamide derivatives **139a-d** were then subjected to dehydration conditions with POCl_3 in the presence of triethylamine in DCM at room temperature for 2 hours as depicted in **Scheme 5.6**.^{316,317,318} Work up and purification by column chromatography afforded the corresponding aryl isocyanides **130a-d** in good yields (*Table 5.8*). The aryl isocyanide products **130a-d** isolated had an extremely distressing odour, which is associated with the majority of members of the isocyanide class of compounds.³¹⁹

Table 5.8: Isolated yields (%) of the aryl-isocyanide products **130a-d**.

		
Compd	R	Yields (%)
130a	4-Br	71
130b	2,5-diCl	78
130c	2,4-diOMe	91
130d	2,4-diMe	75

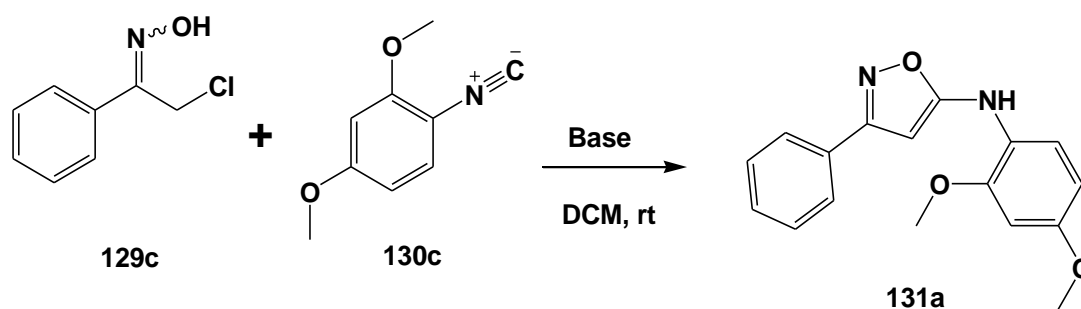
Due to their strong odour, the synthesized aryl isocyanides **130a-d** were only analysed by NMR spectroscopy and values were compared to those reported in literature.³¹⁹ The unique characteristics were observed in their ¹H NMR spectra which showed the loss of signals due to both amine and aldehyde protons. Further evidence was observed in the ¹³C NMR spectra which exhibited the disappearance of the signal for the aldehyde carbon atom and the appearance of a signal arising from an isocyano carbon atom. The isocyano carbon atom in compounds **130a** and **130c** was observed as a triplet with *J* values of 6 Hz each at 164.8 and 165.8 ppm, respectively, whilst compounds **130b** and **130d** displayed the same carbon atom as a singlet signal at 165.9 and 170.9 ppm, respectively. Furthermore, the carbon atom of the aryl ring directly linked to the isocyano group in compounds **130a** and **130c** resonated as triplets at 123.9 and 125.5 ppm with a coupling constant of 13 Hz each, whilst ¹³C NMR spectra of **130b** and **130d** showed the same carbon atoms as singlets at 129.4 and 109.5 ppm. The appearance of signals due to the isocyano carbon atom and the carbon atom of the aryl ring directly attached to isocyano group as triplets could be attributed to ¹³C-¹⁴N coupling.³²⁰

5.2.3. Synthesis of 3-aryl-*N*-isoxazol-5-amine derivatives

With all the necessary intermediates in hand, attention was concentrated on the synthesis of a series of 3-aryl-*N*-arylisoxazol-5-amine derivatives in accordance with the methodology described by Buron and co-workers.¹⁶⁴ However, only a few examples that involve reaction between the α -haloacetophenoneoxime with aryl isocyanide catalysed by Na₂CO₃ in DCM as solvent to produce the corresponding 3-aryl-*N*-arylisoxazol-5-amines have been reported thus far.

5.2.3.1. Control experiment between 2-chloro-1-aryl-ethanone oxime and aryl isocyanides

The reaction of 2-chloro-1-(2,4-dimethoxyphenyl)ethanone oxime **129c** and 1-isocyano-2,4-dimethoxybenzene **130c** was chosen as a model system to test the reaction conditions. Initial attempts were carried out without any base, thus 2-chloroacetophenoneoxime **129c** and 1-isocyano-2,4-dimethoxybenzene **130c** were reacted in DCM at room temperature as depicted in **Scheme 5.9** (*Table 5.9*, **entry 1**). After seven days TLC still indicated the presence of both starting materials with no formation of products. However, the addition of Na₂CO₃ to the above described reaction conditions showed that the 2-chloroacetophenoneoxime **129c** was fully consumed after 24 hours and showed the presence of a new spot, although the smell of isocyanide was still present (*Table 5.9*, **entry 2**). Work up and purification of the new spot by column chromatography afforded the *N*-(2,4-dimethoxyphenyl)-3-phenylisoxazol-5-amine product **131a** in a yield of 12%. Due to the low yield isolated, we decided to explore several other bases as shown in *Table 5.9* using conditions similar to those described above. When a similar reaction was conducted in the presence of NaOAc.3H₂O (**entry 3**), the yield of the desired product **131a** didn't improve even after 7 days, while the yield of the product was worse in the presence of K₂CO₃ (**entry 4**). Furthermore, the use of Cs₂CO₃ (**entry 5**) attained the desired product in just an hour with no improvement in terms of the product yields (11% yield obtained). Attempts to carry out the reaction at lower temperature didn't have any significant effect on the yields of the reaction (**entry 6**).



Scheme 5.9: Experimental control reaction.

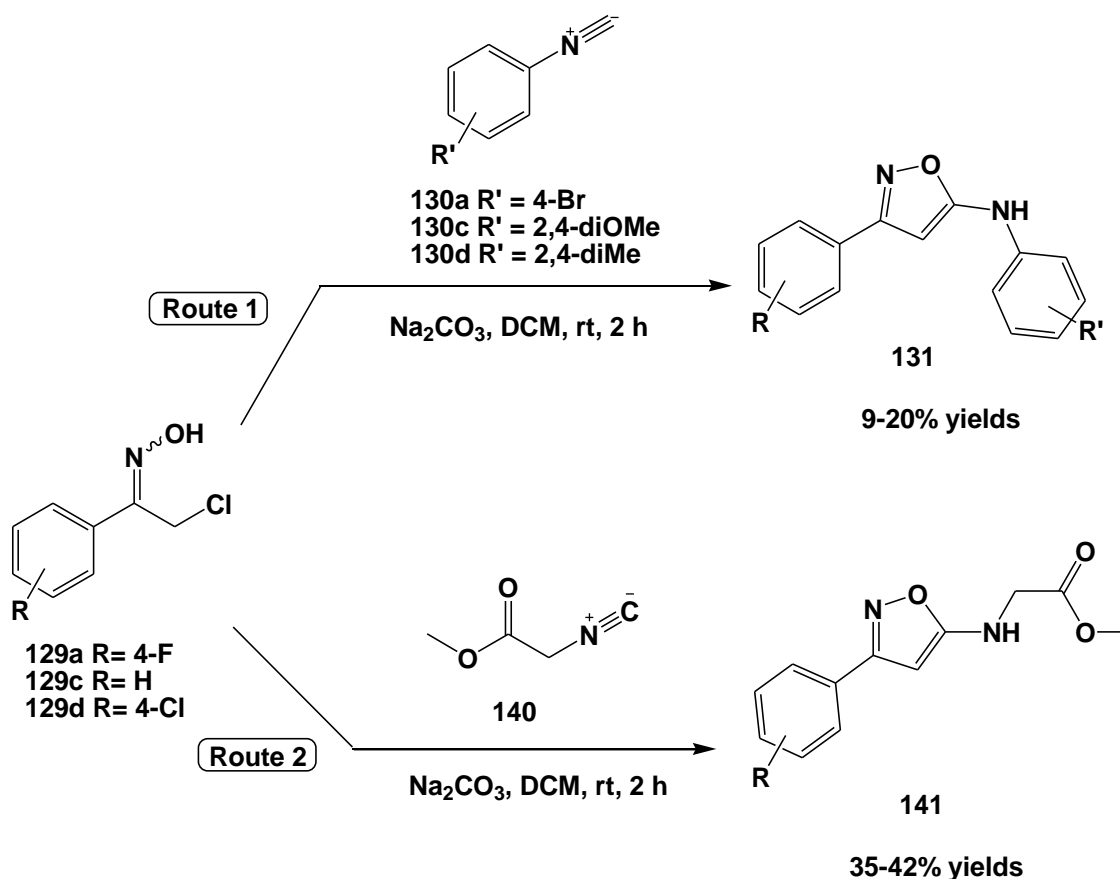
Table 5.9: Effects on the yield of different reaction conditions.

Entry	Base	Time	Yields (%)
1	-	7 d	No reaction
2	Na ₂ CO ₃	24 h	12
3	NaOAc.3H ₂ O	7 d	13

Entry	Base	Time	Yields (%)
4	K ₂ CO ₃	5 d	11
5	CS ₂ CO ₃	1 h	11
6	Na ₂ CO ₃ at -10°C	24 h	12

5.2.3.2. Determination of the effects of substituents and isocyanide reactivity on the reaction

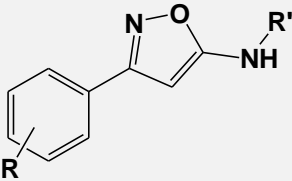
With the above reactions giving low yields of the title compound, attention was focused on exploring the reactivity of other synthesized aryl isocyanides **130a** and **130b** with 2-chloroacetophenone oximes **129a** and **129d** in order to determine the effects of the aryl substituents on the reaction, using Na₂CO₃ as catalytic base (*Scheme 5.10*).



Scheme 5.10: Reaction of 2-chloro-1-aryl-ethanone oxime with isocyanides.

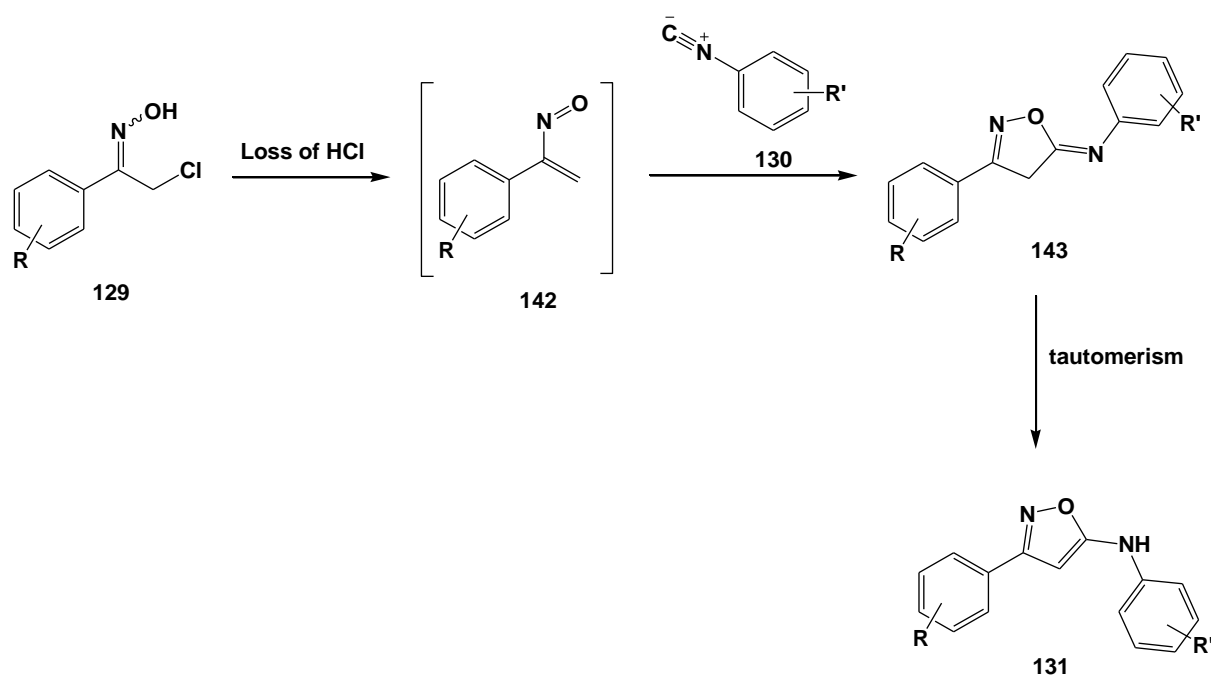
Therefore, 2-chloro-1-aryl-ethanone oximes **129a** and **129d** and aryl isocyanides **130a** and **130d** were reacted in the presence of Na_2CO_3 with DCM as solvent at room temperature, as shown in **Scheme 5.10** (Route 1). After 24 hours, TLC indicated complete consumption of 2-chloro-1-aryl-ethanone oximes **129a** and **129d** and two spots, one corresponding to aryl isocyanides and the other to suspected product. The suspected product spot was then isolated by column chromatography to afford the desired products, **131b-e** with yields ranging from 9-20% as indicated in *Table 5.10*. These results indicate that the substituents of both aryl rings didn't have much influence on the product yields. To determine certainly if the aryl isocyanide reactivity was the problem, a commercially available methyl isocyanide **140** was used under similar conditions (**Scheme 8**, Route 2). Work up and column chromatography gave the desired methyl 2-(3-phenylisoxazol-5-ylamino)acetate product **141a-b** in yields of 35 and 42%, respectively (*Table 5.10*). The yield was much improved as compared to the yields obtained when aryl isocyanide was used, which implies that the low yields of these products could be attributed to the low reactivity of aryl isocyanide and the short life span of the unstable nitrosoalkene species generated *in situ*.

Table 5.10: Isolated yields (%) of 5-amino-3-arylisoxazole **131b-g** and **141a-b**.

			
Compounds	R	R'	Yields (%)
131b	H	2,4-dimethylphenyl	20
131c	4-F	2,4-dimethylphenyl	9
131d	H	4-Brphenyl	11
131e	4-F	4-Brphenyl	9
141a	4-F	CH_2COOMe	35
141b	4-Cl	CH_2COOMe	42

5.2.3.3. Plausible mechanism for the formation of 5-amino-3-arylisoxazole

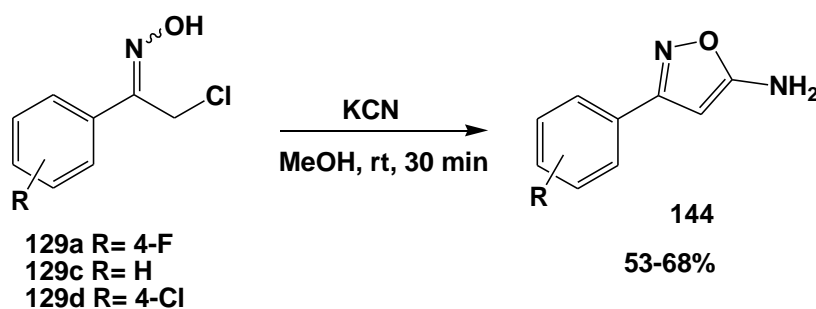
The suggested mechanism shown in **Scheme 5.11** involves a base induced removal of HCl from 2-chloro-1-aryl-ethanone oxime **129** to generate an unstable reactive nitroalkene species **142** *in situ*, which is followed by rapid attack by the isocyanide **130** resulting in the generation of **143**, which then tautomerises to give desired product **131**.¹⁶⁴



Scheme 5.11: Plausible mechanism for the formation of 5-amino-3-arylisoazole **131**.

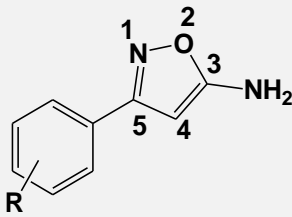
5.2.4. Synthesis of 3-aryl-*N*-isoxazol-5-amine derivatives

To increase the diversity of the synthesized series of 5-amino-3-arylisoazoles described above, it was decided to convert the 2-chloro-1-aryl-ethanone oxime derivatives **129** into the corresponding 5-amino-3-arylisoazole derivatives **144** with no substituent on the amine position in accordance with a previously described protocol by Kong *et al.*³²¹ Therefore, the scaffolds **129a-c** in MeOH were added slowly to a suspension of potassium cyanide in MeOH at room temperature, followed by stirring of the resulting mixture for 30 minutes as depicted in **Scheme 5.12**. Work up and separation by column chromatography furnished 3-arylisoazol-5-amine derivatives **144a-c** in reasonable yields similar to those obtained by Kong and co-workers (*Table 5.11*).³²¹



Scheme 5.12: Reaction between 2-chloroacetophenoneoximes with KCN.

Table 5.11: Isolated yields (%) of the 5-amino-3-arylisoxazole **144a-c** from KCN reaction.

		
Compounds	R	Yields (%)
144a	4-F	68
144b	4-Cl	63
144c	H	53

5.2.5. Structure elucidation of isoxazole-based compounds

The synthesized compounds were characterised by NMR spectroscopy and their data were in agreement with the expected chemical structures. The important aspects of the ^1H NMR spectrum for compound **131b** was a singlet signal at 6.56 ppm corresponding to an NH proton, whilst in compounds **141b**, an NH proton resonates as a triplet at 5.34 ppm with a J value of 5.0 Hz due to coupling with the adjacent two protons of the methylene group (which resonates at 4.00 ppm as a doublet with a J value of 5.5 Hz). On other hand, evidence of formation of compound **144c** in the ^1H NMR spectrum was a broad signal at 4.50 ppm corresponding to the NH_2 protons. Furthermore, more evidence for the formation of the desired compounds was the presence of the 4-methine of the isoxazole moiety, which emerges as a singlet at 5.83 ppm for **131b**, 5.28 ppm for **141a** and 5.42 ppm for **144c**. Additionally, ^{13}C NMR spectra of the compounds displayed signals of the 5-carbon atom at 167.1 ppm (for **131b**), 169.3 (for **141a**) and 168.9 ppm for **144c**; while the 3-carbon atom resonating at 163.6 ppm (for **131b**), 162.7 ppm (for **141a**) and 163.8 ppm for **144c**. The 4-methine carbon atom of an isoxazole moiety on these scaffolds resonates at 78.4 ppm (for **131b**), 77.3 for **141a** and 78.2 for **144c**. The FTIR spectra of the compounds **131a-e** and **141a-b** showed the presence of the NH stretching band between 3263-3407 cm^{-1} whilst the compounds **144a-c** show the presence of the NH_2 stretch in the region of 3321-3454 cm^{-1} (Table 5.12). Moreover, the FTIR spectra of compounds **141a-b** further exhibited an amide carbonyl signal at 1742-1743 cm^{-1} .

Table 5.12: FTIR spectroscopic data of of-arylisoxazol-5-amines showing the NH, C=O and NH₂ bands

Compound	131a	131b	131c	131d	131e	141a	141b	144a	144b	144c
$\nu_{\text{NH}} (\text{cm}^{-1})$	3314	3268	3267	3291	3281	3407	3381	-	-	-
$\nu_{\text{C=O}} (\text{cm}^{-1})$	-	-	-	-	-	1742	1743	-	-	-
$\nu_{\text{NH}_2} (\text{cm}^{-1})$	-	-	-	-	-	-	-	3454	3433	3433

In summary the reactivity of aryl isocyanides and the short life span of the *in situ* generated nitroalkene species were found to be major drawbacks towards generation 3-aryl-*N*-arylisoxazol-5-amine derivatives. Therefore, effective reaction conditions that can activate the aryl isocyanide **130** prior to reaction with 2-chloro-1-aryl-ethanone oximes **129** were required; however time constraints did not allow this study. Thus investigation into such reaction conditions will form part of future work. However, a total of 10 target 5-amino-3-arylisoxazole compounds were obtained from the above described chemistry and five of these (**131a-e**) were found to be novel compounds. These 10 compounds were submitted for biological testing.

5.3. Biological evaluation of isoxazole based compounds

5.3.1. Direct HIV-1 –LEDGF/p5 assay

The synthesized isoxazole based fragments **131**, **141** and **144** were sent for evaluation using a well-established AlphaScreen assay at a single concentration of 100 μM in order to determine the inhibitory percentage by interrupting the interaction between HIV-1 IN and host LEDGF/p75 proteins. The screening results were carried out in triplicate and the results are reported in *Table 5.14*.

Table 5.14: The HIV-1 IN-LEDGF/p75 inhibition activities of the 3-arylisoxazol-5-amines at 100 μ M.

Compounds Entry	Biochemical target assays	
	HIV-1 IN – LEDGF (%)	
	inhibition @ 100 μ M (AlphaScreen)	Standard Deviations
131a	27.83	\pm 1.24
131b	18.02	\pm 0.27
131c	26.65	\pm 2.57
131d	0	\pm 1.50
131e	29.60	\pm 1.78
141a	43.05	\pm 1.99
141b	15.03	\pm 4.17
144a	29.84	\pm 0.77
144b	0	\pm 2.46
144c	29.94	\pm 0.36
CX05168	91.37	+ -0.85
HIV-1 IN and LEDGF with DMSO	0	

The biological data obtained showed that the synthesized isoxazole-based fragments with the exception of **131d** and **144b** displayed low inhibitory activities at a single concentration of 100 μ M, with a percentages ranging from 15 to 43%. The compound **141a** exhibited the highest percentage in the series with 43%. Based on the results, it was decided that this library would not be pursued further.

5.4. Conclusion

The title isoxazole based-compounds were successfully synthesized. Initially, two essential intermediates; 2-halo-1-arylketone oximes and aryl isocyanides were prepared in accordance with literature reported protocols. The 2-halo-1-arylketone oximes were achieved over three steps; by firstly reacting a series of selected benzaldehydes with chloroform under inert atmosphere at room temperature for 4-48 hours to afford 2,2,2-trichloro-aryl-ethanols with excellent yields. These trihaloarylethanols were further subjected to oxidative conditions by treatment with CuCl and bipyridine in DCE to furnish 2-chloro-1-arylethanone derivative in lower yields in

comparison to the yield obtained in literature. The 2-chloro-1-arylethanone derivatives were treated with hydroxylamine hydrochloride in MeOH at room temperature to give 2-chloro-1-aryl-ethanone oximes as geometric isomers in good yields. The second intermediates were obtained over two steps by initial microwave irradiation of a mixture of anilines with formic acid to afford *N*-aryl-formamide, followed by dehydration with POCl₃ in the presence of triethylamine to afford aryl isocyanide scaffolds in excellent yields. The 2-halo-1-arylketone oximes and aryl isocyanides were reacted in the presence of Na₂CO₃ using DCM as solvent at room temperature to afford the desired 3-aryl-*N*-arylisoxazol-5-amine products in poor yields. Several other bases were also screened, however, none of the bases was able to exceed the initial result obtained with Na₂CO₃ even lowering the temperature to -10°C didn't have a significant effect on the formation of the products. These low yields were attributed to the low reactivity of aryl isocyanides and the short life span of the unstable reactive nitroalkene species, which is generated *in situ* through elimination of HCl. However, when commercially available methyl isocyanoacetate was used, the desired methyl 2-(3-phenylisoxazol-5-ylamino)acetate products were isolated in much improved yields. These data support the theory discussed above. In order to extend the library, 2-halo-1-arylketone oximes were then treated with KCN in MeOH to furnish 3-arylisoxazol-5-amine derivatives with a free amine group. Compounds **131**, **141** and **144** were submitted for biological evaluation in the HIV-1 IN-LEDGF/p75 AlphaScreen assay at 100 μM. Unfortunately, none of the fragments exceeded the 50% inhibition benchmark.

5.5. Future work

1. Investigate the effective reaction conditions that can activate the aryl isocyanides prior to reaction with 2-chloro-1-aryl-ethanone oximes.
2. Screening of isoxazole-based compounds in BST-2 Vpu ELISA assay to identify possible hits.

CHAPTER 6

Antimicrobial activities of synthesized compounds

6.1 Introduction

Infectious diseases caused by bacterial pathogens continue to be a major threat to public health in both developing and developed countries.^{322,323,324} Although many species of bacteria are beneficial, several harmful gram positive and gram negative bacteria are responsible for infectious diseases like pneumonia^{325,326} and tuberculosis (TB)^{327,328} to point out a few. Much therapeutic progress has been made to protect against infections caused by bacterial pathogens through the use of immunization and antimicrobial agents such as antibiotics. Natural isolated antibiotics like ampicillin,³²⁹ chlortetracycline,³³⁰ and demeclocycline^{331,332} (Figure 6.1) can act by either killing or preventing the growth of the bacterial pathogens. In addition, chemical synthesis also plays its role in the development of the antibacterial drugs such as ciprofloxacin,^{333,334} and cefamandole³³⁵ to mention a few (Figure 6.1).

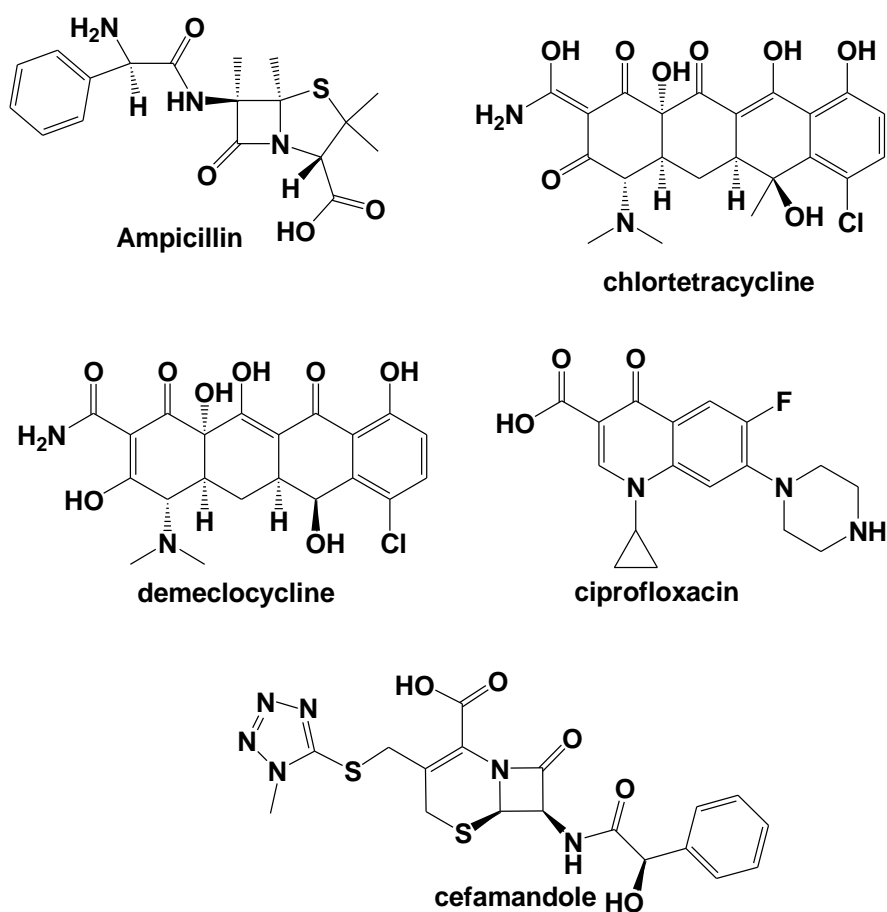


Figure 6.1: Representative examples of antibacterial agents.

Although the current antibiotics have managed to improve clinical outcomes over the past decades, evolving bacterial strains have hampered the treatment of bacterial infections, resulting in higher morbidity and mortality rates. The overuse and misuse of antibiotics in people and animals as well as genetic mutation of bacterial proteins are some factors which have contributed to an increase in antimicrobial resistance. According to WHO in 2016, an estimated 480 000 people worldwide had developed multi-drug resistance to the two most powerful anti-TB agents.³³⁶ Furthermore, the resistance to artemisinin-based combination therapies (ACTs), which are used for the treatment of *Plasmodium falciparum* malaria, has also been detected all over the world.^{337,338} The development of drug resistance has already posed many therapeutic challenges like affecting the battle against HIV and malaria as well as medical procedures such as diabetes management, cancer chemotherapy and organ transplantation. The efficacy of current antimicrobial agents is compromised because of the emergence of new drug resistance and as such the need for development of small molecules with novel modes of action is high.

This chapter therefore focuses on the antimicrobial assessment of the synthesized 5-aryl-1*H*-imidazole, 5-aryl-oxazole, 5-aryl-1*H*-imidazol-1-yl and 3-aryl-isoxazole based families of compounds. We hypothesised that screening of synthesized libraries of compounds may provide an important starting point for the development of the next generation of antimicrobial agents.

6.2. Antimicrobial activities of the synthesized libraries of five membered nitrogen containing heterocyclic compounds

The libraries of synthesized 5-aryl-1*H*-imidazole, 5-aryl-oxazole, 5-aryl-1*H*-imidazol-1-yl and 3-aryl-isoxazole based compounds were evaluated in the same way for their antimicrobial activities against two Gram-positive bacterial species (*Staphylococcus aureus* ATCC 25923 and *Bacillus cereus* ATCC 11779), two Gram negative bacterial species (*Escherichia coli* ATCC 8739 and *Pseudomonas aeruginosa* ATCC 27858) and one yeast (*Candida tropicalis* ATCC 750) using the Minimum Inhibitory Concentration (MIC) assay determined by the iodinitrotetrazolium (INT) chloride method. The MIC assay was conducted at the University of the Witwatersrand, Department of Pharmacy and Pharmacology in the School of Therapeutic Science under the guidance of Professor Sandy van Vuuren. Ciprofloxacin and nystatin were used as positive controls for bacteria and yeast, respectively. Compounds which exhibit an MIC value of 15.6 µg/ml are considered to be good antibacterials, while MIC values of 31.3, 65.5 and 125 µg/ml are considered to represent moderate, marginal and low/weak activity, respectively. The compounds were tested in duplicate and their results recorded.

6.2.1. Antimicrobial activities of synthesized 5-aryl-1*H*-imidazole-based compounds

The antimicrobial activities of the twenty three novel 5-aryl-1*H*-imidazole based compounds (Figure 6.1) were investigated and results are documented in Table 6.1. Antimicrobial testing (Table 6.1) revealed that some of the compounds exhibited significant antimicrobial activities against bacterial strains.

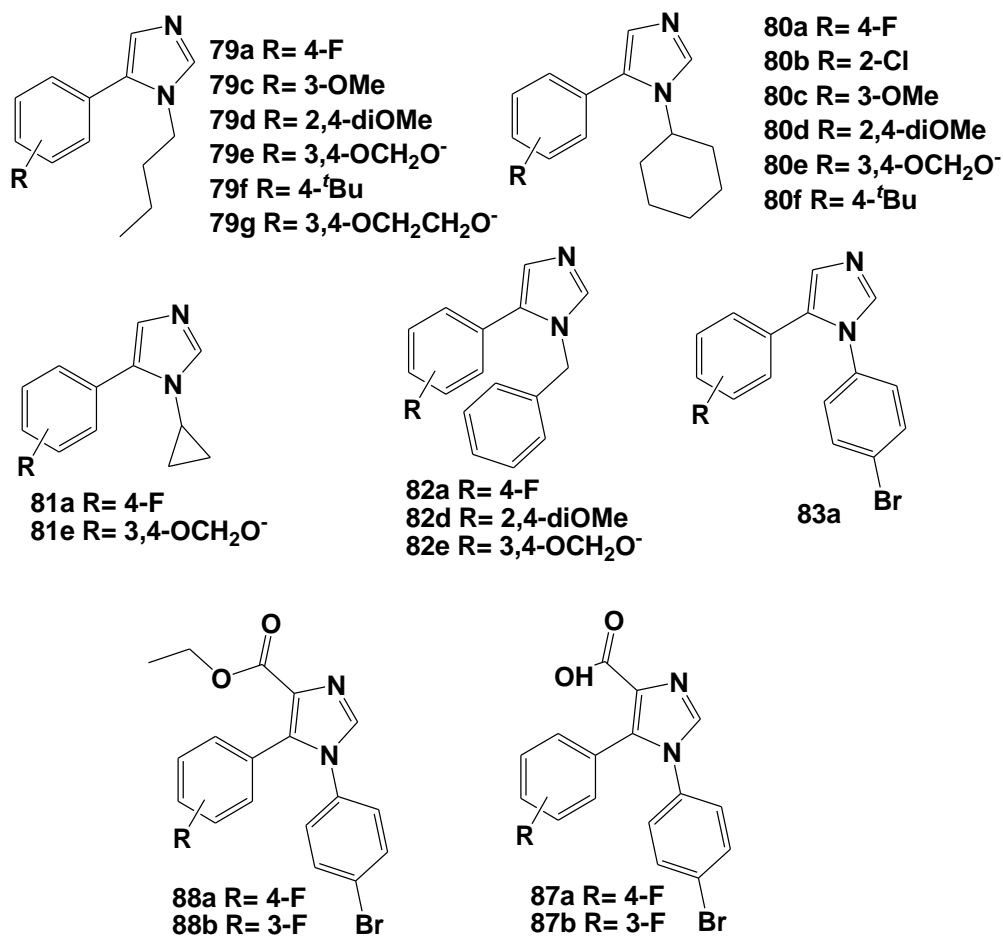


Figure 6.1: Representation of the 5-aryl-1*H*-imidazole based compounds as possible antimicrobial agents.

Table 6.1: Minimum inhibitory concentrations (MIC, $\mu\text{g/ml}$) of synthesized 5-aryl-1*H*-imidazole based compounds

Compounds	Gram positive bacteria		Gram negative bacteria		Yeast
	<i>S. aureus</i> ATCC 2592	<i>B. cereus</i> ATCC 11779	<i>E.coli</i> ATCC 8739	<i>P.aeruginosa</i> ATCC 27858	<i>C. tropicalis</i> ATCC 750
79a	125	125	250	205	125
79c	> 250	62.5	125	>250	62.5
79d	> 250	> 250	250	250	250
79e	-	31.3	>250	>250	-
79f	15.6	31.3	250	250	31.3
79g	250	250	250	250	125
80a	125	125	250	250	125
80b	250	250	>250	>250	250
80c	62.5	62.5	>250	>250	62.5
80d	62.5	250	>250	>250	125
80e	125	250	>250	>250	250
80f	62.5	15.6	>250	>250	31.3
81a	> 250	> 250	> 250	> 250	-
81d	250	250	250	250	125
82a	62.5	125	>250	>250	>250
82d	62.5	125	>250	>250	250
82e	250	250	125	250	> 250
83a	> 250	> 250	> 250	> 250	> 250
87a	> 250	> 250	> 250	> 250	31.3

Compounds	Gram positive bacteria		Gram negative bacteria		Yeast
	<i>S. aureus</i>	<i>B. cereus</i>	<i>E. coli</i>	<i>P. aeruginosa</i>	<i>C. tropicalis</i>
	ATCC 2592	ATCC 11779	ATCC 8739	ATCC 27858	ATCC 750
87b	> 250	> 250	> 250	> 250	> 250
88a	> 250	> 250	> 250	> 250	> 250
88b	> 250	> 250	> 250	> 250	> 250
Ciprofloxacin	1.25	0.156	0.313	0.313	-
Nystatin	-	-	-	-	0.156

The most potent compound **79f** with an *n*-butyl group attached to a nitrogen atom and the *tert*-butyl substituent at the *para*-position on the 5-aryl ring exhibited a remarkably good MIC value of 15.6 µg/ml against *S. aureus* and a moderate MIC value of 31.3 µg/ml against *B. cereus* and *C. tropicalis*. These values correspond to the 60 µM (i.e. against *S. aureus* and 112 µM (i.e. 122 µM against *B. cereus*) concentration for **79f**. Compound **80f**, with a cyclohexyl group instead of the *n*-butyl group of **79f**, showed a good MIC value of 15.6 µg/ml (i.e. 55 µM) against *B. cereus*, while against *C. tropicalis* it displayed a comparable MIC value to that of compound **79f**. Both compounds **79f** and **80f** were inactive against the two Gram negative bacterial strains. Introduction of an electron donating group (-OCH₂O-) at the *meta*- and *para*-positions in the 5-aryl ring in compound **79f** gave compound **80e**, which displayed a moderate MIC value of 31.3 µg/ml (i.e. 116 µM) against *B. cereus*, while against gram-negative strains no activity was observed. However, compound **79e** showed a weak MIC value of 125 µg/ml against *C. tropicalis* while no activity was observed against two gram-positive and negative strains. Furthermore, compound **80c** with the methoxy group at the *meta*-position exhibited a marginal MIC value of 62.5 µg/ml against *S. aureus*, *B. cereus* and *C. tropicalis*, while its analogue compound **79c** also showed a marginal MIC value of 62.5 µg/ml against *B. cereus* and *C. tropicalis*. Compound **80d** bearing two methoxy groups at the *meta*- and *para*-positions of the 5-aryl ring displayed a marginal MIC value of 62.5 µg/ml against *S. aureus*, while against *B. cereus*, *E. coli*, *P. aeruginosa* and *C. tropicalis* it was inactive. Furthermore, an analogue of **80d**, compound **79d** exhibited no activity against any of the four bacterial and one yeast strain. Compound **82a** and **82d**, with a benzyl group attached to

a nitrogen atom, both exhibited MIC values of 62.5 µg/ml against *S. aureus* and displayed a low MIC activity of 125 µg/ml against *B. cereus*. Compound **87a** with a *para*-fluorine atom on the 5 aryl ring and 4-bromophenyl group linked to the nitrogen atom exhibited a moderate MIC value of 31.3 µg/ml against *C. tropicalis*, while the rest of the compounds with a 4-bromophenyl group were inactive against all strains tested. The rest of the compounds did not exhibit any activity against any of the tested bacterial and yeast strains. Although some imidazole compounds exhibited good antimicrobial activities, their MIC values were much higher than those of the ciprofloxacin and nystatin positive controls. MIC values of the evaluated imidazole-based compounds indicated that they were more active against Gram-positive bacteria and yeast strains than against gram negative bacteria. The results suggest that compound **79f** and **80f** could be viable hits to design a next generation of antimicrobial agents targeting *S. aureus* and *B. cereus* strains.

6.2.2. Antimicrobial activities of synthesized 5-aryl-oxazole based compounds

Nineteen synthesized 5-aryl-oxazole- and oxazoline-based compounds (*Figure 6.2*) were assessed for their antimicrobial effects and results are detailed in *Table 6.2*. Analysis of the obtained results showed that compounds **108a-b** and **109a-b** were inactive against all four bacterial and the one yeast strain. However, compound **100e**, which contains a chlorine atom at the *ortho*- and *para*-positions on the 5-aryl ring showed moderate antibacterial activity against *S. aureus* and against yeast *C. tropicalis*, with MIC values of 31.3 µg/ml (89 µM), whereas against *B. cereus* it exhibited a marginal MIC value of 62.5µg/ml. Moreover, compound **100c** exhibited good antibacterial activity against *P.aeruginosa*, with an MIC value of 31.3 µg/ml (87 µM), and marginal antimicrobial activity against *S. aureus* and *B. cereus* with MIC values of 62.5 µg/ml. Compound **100j** displayed marginal antibacterial effects against *S. aureus* and *C. tropicalis*, with MIC values of 62.5 µg/ml, and against *B. cereus* with an MIC value of 125 µg/ml. Compound **100b** and **100k** only showed marginal antimicrobial activities against *B. cereus*, with MIC values of 62.5 µg/ml and 125 µg/ml, respectively. All these synthesized compounds exhibited marginal MIC values as compared to the bacterial positive control, ciprofloxacin with an MIC value of 1.25 µg/ml and yeast control, nystatin with an MIC of 0.156 µg/ml.

The 4,5-dihydro-*N*,5-diaryl-1,3-oxazole-4-carboxamide scaffolds **107** were shown to be inactive against all four bacterial and one yeast strain. Halogenated *N*-(2,4-dichlorophenyl)-5-(4-fluorophenyl)oxazole-4-carboxamide (**100e**) showed some antimicrobial activity and could be selected for further development at a later stage, if deemed necessary.

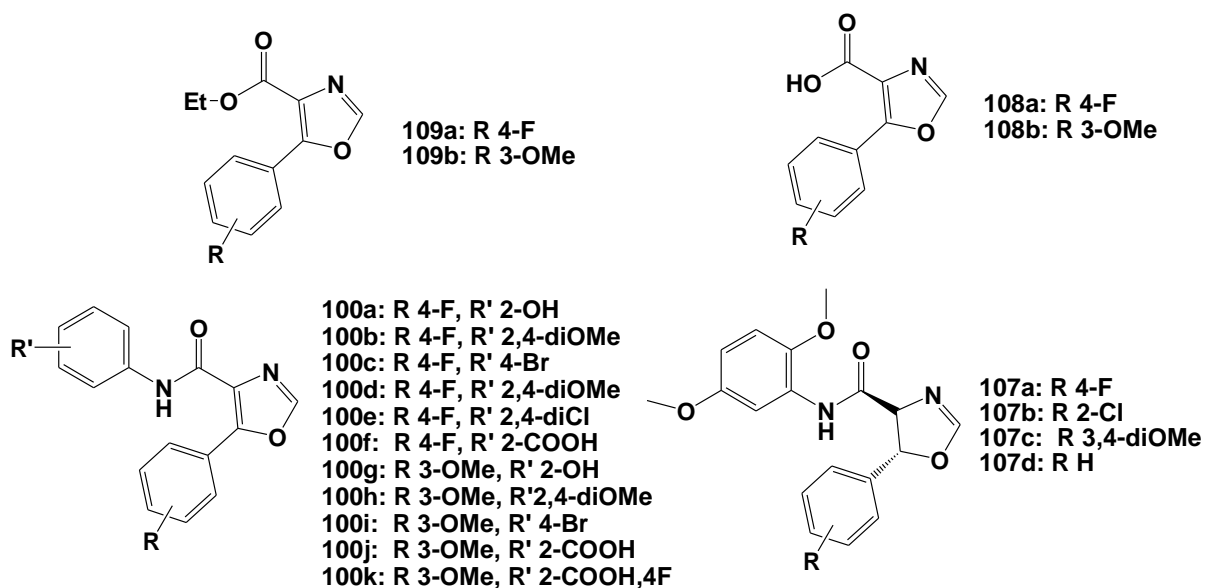


Figure 6.2: Representation of the 5-aryl-oxazole and oxazoline-based compounds as possible antimicrobial agents.

Table 6.2: Minimum inhibitory concentrations (MIC, $\mu\text{g/ml}$) of synthesized 5-aryl-oxazole-based compounds

Compounds	Gram positive bacteria		Gram negative bacteria		Yeast
	<i>S. aureus</i>	<i>B. cereus</i>	<i>E. coli</i>	<i>P. aeruginosa</i>	<i>C. tropicalis</i>
	ATCC 2592	ATCC 11779	ATCC 8739	ATCC 27858	ATCC 750
100a	> 250	> 250	>250	-	-
100b	> 250	62.5	>250	-	> 250
100c	62.5	62.5	>250	31.3	-
100d	> 250	> 250	>250	> 250	-
100e	31.3	62.5	250	> 250	31.3
100f	250	62.5	>250	-	125
100g	> 250	> 250	>250	> 250	-

Compounds	Gram positive bacteria		Gram negative bacteria		Yeast
	<i>S. aureus</i>	<i>B. cereus</i>	<i>E.coli</i>	<i>P.aeruginosa</i>	<i>C. tropicalis</i>
	ATCC 2592	ATCC 11779	ATCC 8739	ATCC 27858	ATCC 750
100h	> 250	> 250	>250	> 250	> 250
100i	> 250	> 250	>250	> 250	> 250
100j	62.5	125	>250	> 250	62.5
100k	250	125	>250	> 250	> 250
107a	> 250	> 250	>250	> 250	> 250
107b	> 250	> 250	>250	> 250	> 250
107c	> 250	> 250	>250	> 250	> 250
107d	> 250	> 250	>250	> 250	> 250
108a	> 250	> 250	>250	> 250	> 250
108b	> 250	> 250	>250	> 250	> 250
109a	> 250	> 250	>250	> 250	> 250
109b	> 250	> 250	>250	> 250	> 250
Ciprofloxacin	1.25	0.156	0.313	0.313	-
Nystatin	-	-	-	-	0.156

6.2.3. Antimicrobial activities of synthesized 5-aryl-1*H*-imidazol-1-yl based compounds

The antimicrobial activity of the twenty three novel 5-aryl-imidazol-1-yl compounds (*Figure 6.3*) was determined using the MIC assay and results are recorded in *Table 6.3*.

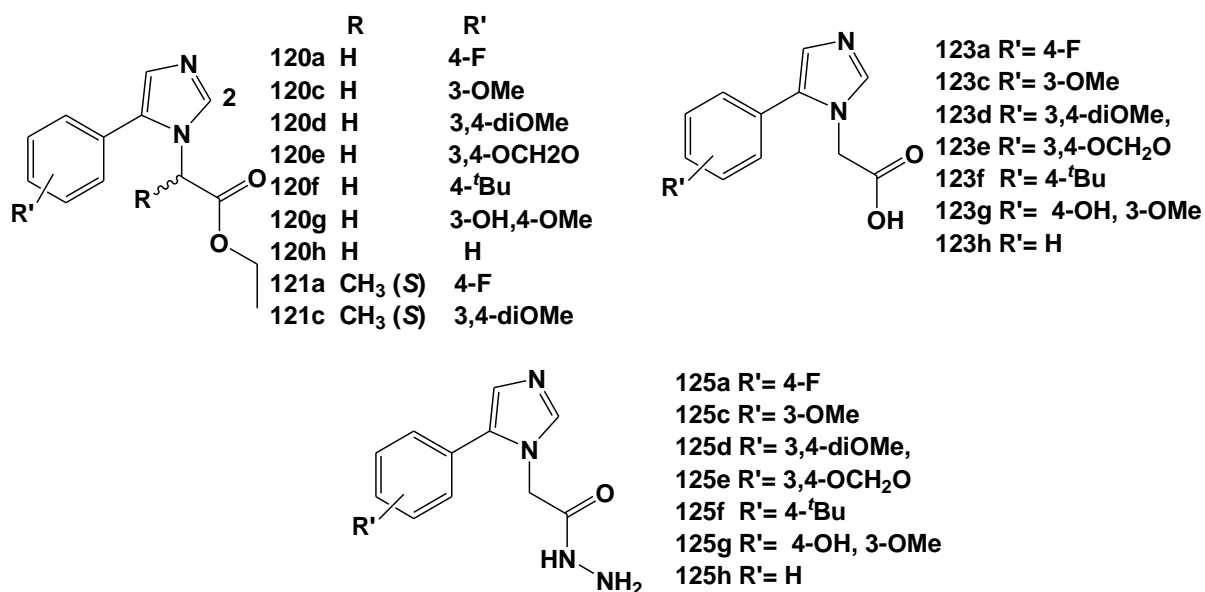


Figure 6.3: Representation of the 5-aryl-imidazol-1-yl compounds as possible antimicrobial agents.

Table 6.3: Minimum inhibitory concentrations (MIC, $\mu\text{g/ml}$) of synthesized imidazol-1-yl-based compounds

Compounds	Gram positive bacteria		Gram negative bacteria		Yeast
	<i>S. aureus</i>	<i>B. cereus</i>	<i>E.coli</i>	<i>P.aeruginosa</i>	<i>C. tropicalis</i>
	ATCC 2592	ATCC 11779	ATCC 8739	ATCC 27858	ATCC 750
120a	> 250	> 250	> 250	> 250	> 250
120c	> 250	> 250	> 250	> 250	> 250
120d	> 250	> 250	> 250	> 250	> 250
120e	> 250	> 250	> 250	> 250	> 250
120f	125	>250	> 250	> 250	> 250
120h	> 250	> 250	> 250	> 250	> 250
120g	> 250	> 250	> 250	> 250	> 250
121a	> 250	> 250	> 250	> 250	> 250
121c	> 250	> 250	> 250	> 250	> 250

Compounds	Gram positive bacteria		Gram negative bacteria		Yeast
	<i>S. aureus</i>	<i>B. cereus</i>	<i>E.coli</i>	<i>P.aeruginosa</i>	<i>C. tropicalis</i>
	ATCC 2592	ATCC 11779	ATCC 8739	ATCC 27858	ATCC 750
123a	> 250	> 250	> 250	> 250	> 250
123c	125	> 250	62.5	> 250	> 250
123d	> 250	> 250	> 250	> 250	> 250
123e	> 250	> 250	> 250	> 250	> 250
123f	> 250	> 250	> 250	> 250	> 250
123g	125	> 250	62.5	> 250	15.6
123h	> 250	> 250	> 250	> 250	> 250
125a	125	250	250	> 250	250
125c	> 250	250	250	> 250	250
125d	125	250	250	> 250	250
125e	> 250	> 250	> 250	> 250	> 250
125f	> 250	> 250	> 250	> 250	> 250
125g	250	> 250	> 250	> 250	> 250
125h	> 250	> 250	> 250	> 250	> 250
Ciprofloxacin	1.25	0.156	0.313	0.313	-
Nystatin	-	-	-	-	0.156

The results of antimicrobial testing indicated that only compound **120f** from a set of ester derivatives **120** exhibited a marginal antimicrobial activity at an MIC value of 125 µg/ml against the *S. aureus* strain, while the rest of the compounds in the series were found to be inactive against all four bacterial and one yeast strain.

The tested compound **123g** with a hydroxyl and methoxy group at the *meta*- and *para*-positions of the 5-aryl ring from the series of acetic acids scaffolds **123** exhibited the highest MIC activity

of 15.6 $\mu\text{g/ml}$ (63 μM) against the *C. tropicalis*, but moderate MIC activity against *E. coli* of 65.2 $\mu\text{g/ml}$, whereas against *S. aureus* strain it only showed an MIC value of 125 $\mu\text{g/ml}$. Furthermore, compound **123d** with the electron-donating methoxy group at the *meta*-position of the 5-aryl ring displayed weak antimicrobial activity against *S. aureus*, at an MIC value of 125 $\mu\text{g/ml}$, while an MIC value of 62.5 $\mu\text{g/ml}$ against *E. coli* was observed. The rest of the acetic acid derivatives did not show any activity against the four bacterial and one yeast strain.

Compounds **125a** (with the *para*-fluorine atom) and **125d** (with methoxy groups at the *meta*- and *para*-positions) exhibited a weak MIC value of 125 $\mu\text{g/ml}$ each against *S. aureus* while other scaffolds within the acetohydrazide series **125** were found to have no activity against any strains. Unfortunately, the active imidazol-1-yl compounds mentioned above demonstrated marginal MIC values as compared to positive controls for both bacterial and yeast strains. In general, results suggest that only compound **123g** could be used as a template to design next generation antimicrobial agents.

6.2.4. Antimicrobial activities of synthesized 3-aryl-isoxazole based compounds

The antimicrobial effects of the 10 synthesized isoxazole-based compounds (*Figure 6.4*) were investigated and results are detailed in *Table 6.4*. The results of antimicrobial testing indicated that none of the isoxazole based compounds were active against any of the four bacterial and yeast strains.

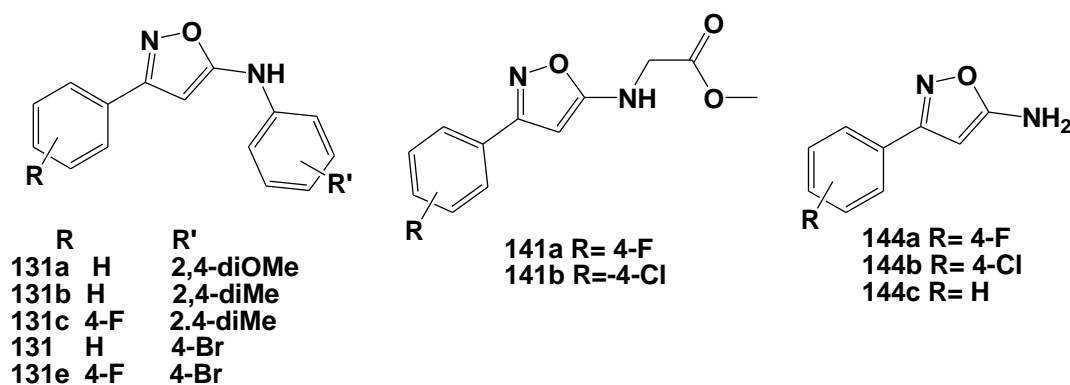


Figure 6.4: Representation of the isoxazole-based compounds as possible antimicrobial agents.

Table 6.4: Evaluation of *in vitro* antimicrobial activity of the synthesized isoxazole based compounds

Compounds Tested	Gram Positive bacteria		Gram Negative bacteria		Yeast
	<i>S. aureus</i>	<i>B. cereus</i>	<i>E. coli</i>	<i>P. aeruginosa</i>	<i>C. tropicalis</i>
	ATCC 2592	ATCC 11779	ATCC 8739	ATCC 27858	ATCC 750
131a	> 250	> 250	> 250	> 250	> 250
131b	> 250	> 250	> 250	> 250	> 250
131c	> 250	> 250	> 250	> 250	> 250
131d	> 250	> 250	> 250	> 250	> 250
131e	> 250	> 250	> 250	> 250	> 250
141a	> 250	> 250	> 250	> 250	> 250
141b	> 250	> 250	> 250	> 250	> 250
144a	> 250	> 250	> 250	> 250	> 250
144b	> 250	> 250	> 250	> 250	> 250
144c	> 250	> 250	> 250	> 250	> 250
Ciprofloxacin	1.25	0.156	0.313	0.313	-
Nystatin	-	-	-	-	0.156

6.3. Conclusion

The antimicrobial activities of the synthesized 5-aryl-1*H*-imidazole, 5-aryl-oxazole, 5-aryl-1*H*-imidazol-1-yl and 3-aryl-isoxazole based compounds were assessed in an MIC assay using the INT method against *Staphylococcus aureus* ATCC 25923 and *Bacillus cereus* ATCC 11779 (gram-positive bacteria strains) and *Escherichia coli* ATCC 8739 and *Pseudomonas aeruginosa* ATCC 27858 (gram negative bacteria strains) as well as against *Candida tropicalis* ATCC 750 (yeast strain). Although some of the synthesized compounds were found to display promising antimicrobial activities with good MIC values, their values were marginal compared to those of ciprofloxacin for bacteria and nystatin for yeast standard controls. Among the tested compounds **79f**, **80g**, **123g** and **100e** were found to be the most potent antibacterial hits and it can be concluded that these scaffolds could act as a framework for further development through synthetic modification to obtain more potent biologically active compounds.

CHAPTER 7

General Conclusion

Isocyanides have been widely applied in organic synthesis, due to the ease of manipulating different reaction conditions to provide different nitrogen-containing heterocyclic compounds. In this dissertation, we have explored the application of two isocyanide precursors, TosMIC and aryl isocyanide, to generate small diverse libraries of five membered nitrogen containing heterocycles and evaluated them for their ability to disrupt HIV-1 IN-LEDGF/p75 interactions; binding of Vpu to CD4/CD74; and/ or HIV-1 Vpu-BST-2 protein interactions. Hit compounds were identified from biological screening, and these were used in the design of second generation compounds which were synthesised with additional structural diversity at several positions. Second generation compounds were subsequently screened for their ability to inhibit HIV-1 protein-protein interactions.

7.1. Synthesis of small families of five-membered nitrogen containing heterocycles. First generation

In **Chapter 2**, the utility of TosMIC was successfully demonstrated in the synthesis of a small library of twenty six substituted imidazoles **79-83** using both conventional and microwave irradiation approaches (see *Figure 7.1*). The microwave strategy described represents a significant improvement over the conventional method using MeCN as solvent.

Yields of these 1*H*-imidazole based products were found to be influenced by two factors, namely:

- 1) The nature of the substituents on the 5-aryl ring (derived from an aldehyde) and the primary amine used. For example, when both the *ortho*- and *para*-positions of the 5-aryl ring were occupied by electron donating methoxy groups (**79d**, **80d** and **81d**) the highest yields were obtained, while the presence of electron-withdrawing substituents at the *ortho*- or *para*-position of the 5-aryl ring gave rise to low yields (i.e. 20% for **79b**, 38% for **79a**, and 23% for **80b**). When substituted anilines were used in the reaction, the 4-bromoaniline **74e** gave the best results, while anilines with halides at the *ortho*- and *para*-positions did not give rise to any desired product.
- 2) The choice of solvent; with the use of MeCN being favoured. The use of MeOH was less favourable because of the inherent preference of TosMIC to react with MeOH and afford products such as *E* and *Z*- HOCH₂N=CH(OMe).

Of the 27 imidazole-based compounds synthesised (**79-83**), 26 compounds were found to be new, with only **82e** having been previously reported, although it was obtained under different conditions using sodium cyanide in a protic solvent under heating using *t*BuNH₂ and K₂CO₃ as catalytic base.²⁰⁴

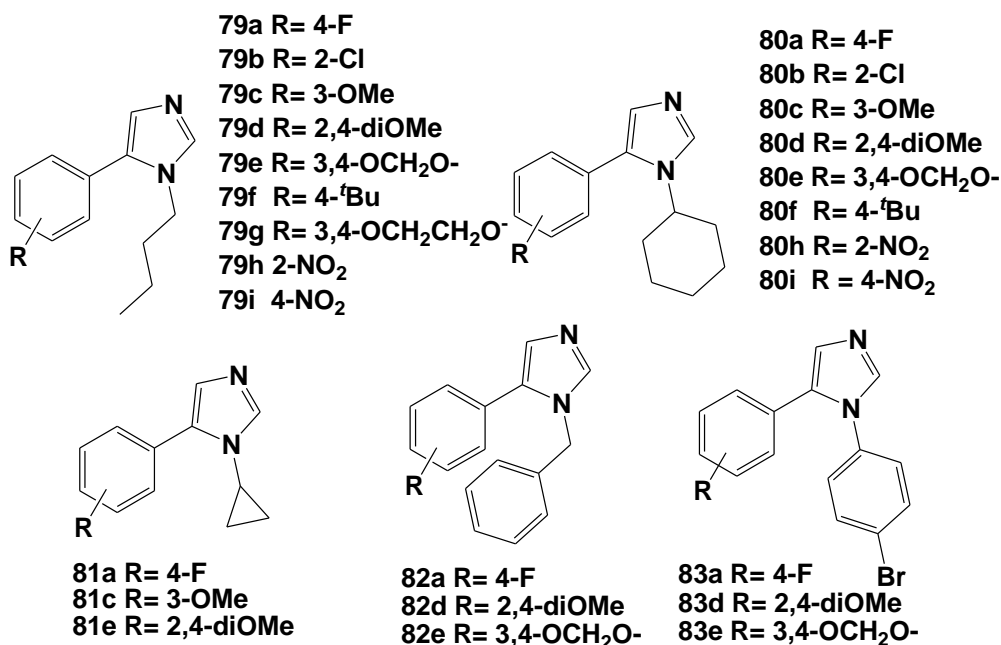


Figure 7.1: Representation of the first generation of synthesised imidazole based compounds

Having successfully established the usefulness of TosMIC under microwave irradiation conditions in **Chapter 2**, we then set out to expand the scope of the study towards the synthesis of 5-aryl-1,3-oxazoles **96** and 5-aryl-4-tosyl-2,4-dihydro-1,3-oxazoles **97** (*Figure 7.2*), which was successfully achieved (**Chapter 3**). Although the compounds obtained have previously been reported, the use of microwave irradiation was found to be a novel synthetic approach. The microwave assisted van Leusen approach used resulted in a time efficient method towards the preparation of both 5-aryl-1,3-oxazoles **96** and 5-aryl-4-tosyl-4,5-dihydro-1,3-oxazole **97** scaffolds. The substituents on the 5-aryl ring were shown to have little effect on the yield of the products, while the choice of the solvent had a marked influence on product formation. When MeOH was used, the desired 5-aryl-1,3-oxazoles **96a-h** were obtained, but in MeCN the intermediate 5-aryl-4-tosyl-4,5-dihydro-1,3-oxazoles **97** were obtained instead.

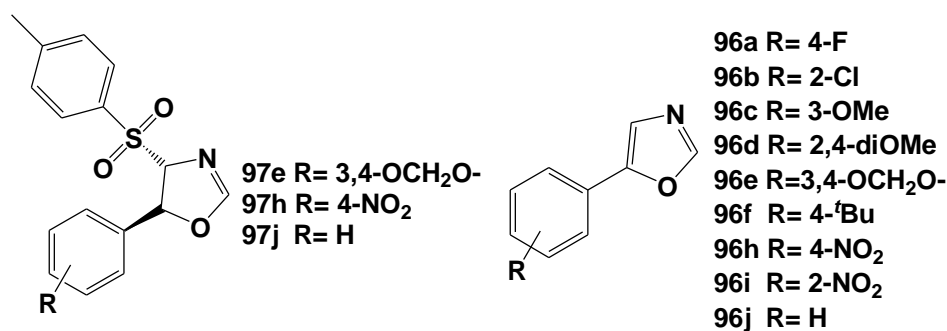


Figure 7.2: Representation of the first generation of synthesised oxazole and oxazoline-based compounds

The exciting success achieved using a microwave assisted van Leusen reaction to access the imidazole and oxazole derivatives, led to the third main objective of the project (**Chapter 4**). An attempt was made to achieve a direct route for the incorporation of simple amino acids to generate a library of novel 5-aryl-1*H*-imidazolyl acyl derivatives using a microwave assisted van Leusen reaction. Unfortunately we were unable to obtain ethyl 2-(5-aryl-1*H*-imidazol-1-yl)acetates **120**, which may be attributed to decomposition of the intermediates under microwave irradiation. An alternative approach using DBU as a catalytic base to promote the addition of TosMIC to ethyl 2-(arylideneamino)acetates intermediates **116** and **117** (derived from aldehydes and simple amino acids) under milder reaction conditions was developed. This method led to the isolation of the novel ethyl 2-(5-aryl-1*H*-imidazol-1-yl)acetates **120-121** (*Figure 7.3*) derived from glycine and L-alanine in various yields; while the products derived from D-leucine **118a-c** were, however, not obtained. From the observed results it was clear that the yields of the products were strongly influenced by the substituents at the chiral centre and on the aryl ring. For example, when a methyl group was present at the chiral centre and the electron-donating methoxy group was at the *meta*- and *para*-positions (compound **121c**), a 23% yield was obtained which is low when compared to that of compound **120c** (74 %) without a substituent at the chiral centre. These 5-aryl-1*H*-imidazolyl-acylate derivatives **120** were further transformed into two novel sets of 5-aryl-1*H*-imidazolyl-acetic acids **123** and 5-aryl-1*H*-imidazolyl-acetohydrazides **125**. In this way, a total of 25 novel compounds belonging to the 1*H*-imidazol-1-yl-based scaffold were obtained.

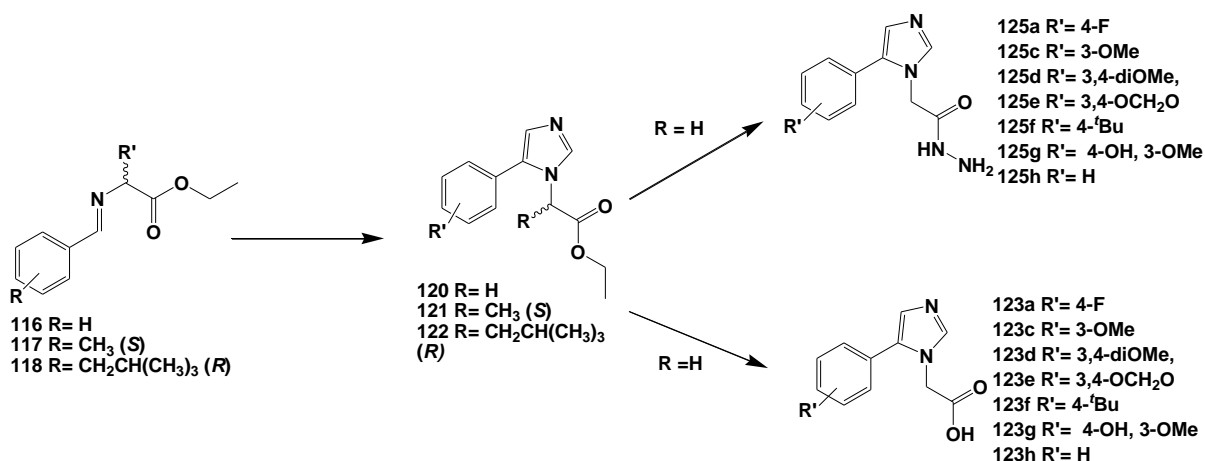


Figure 7.3: Representation of the first generation of synthesised imidazol-1-yl based compounds

Our final synthetic objective is described in Chapter 5, where we successfully synthesised 3-aryl-5-amino-isoxazole derivatives **131** (Figure 7.4) using aryl isocyanides **130**, although in poor yields. However, when commercially available methyl isocyanoacetate **140** was used, the desired methyl 2-(3-phenylisoxazol-5-ylamino)acetate products **141** were isolated in much improved yields. A total of 10 compounds were obtained, with five found to be new. The methodology employed in the synthesis of these scaffolds has been previously described, with a single example involving the reaction of an aryl isocyanide with an oxime being reported by Buron *et al.*¹⁶⁴

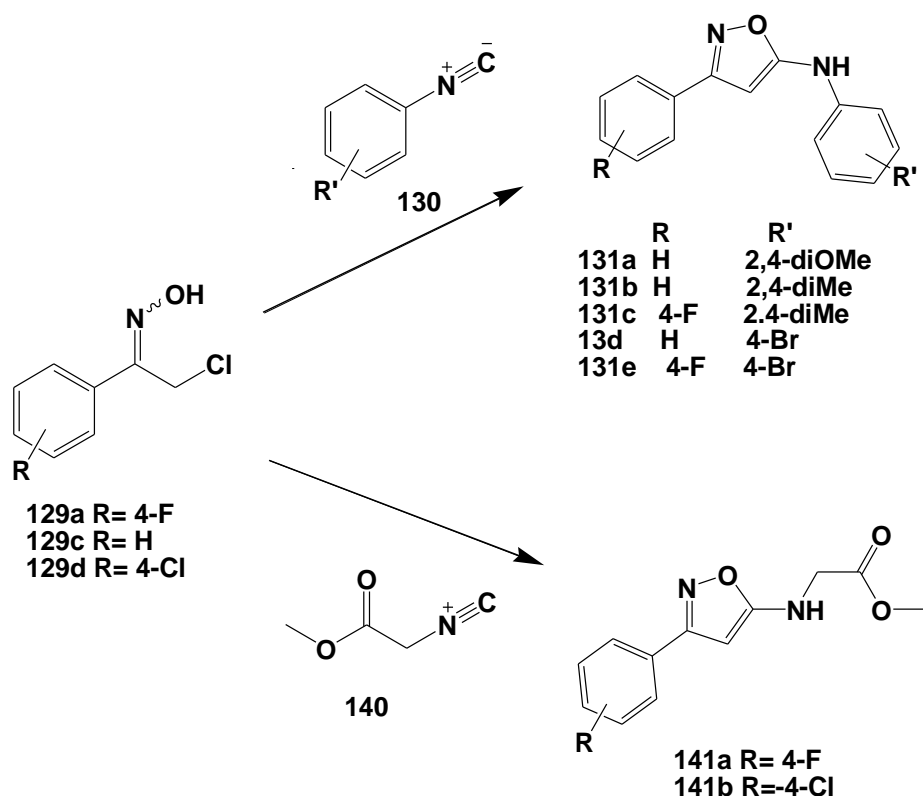


Figure 7.4: Representation of the synthesised isoxazole-based compounds **131** and **141**

From a synthetic point of view, it can be concluded that the success of the van Leusen reaction, independent of the energy source applied, was strongly influenced by the nature of the imine intermediates (mainly towards the imidazole moiety) and the choice of the solvent, while in case of aryl isocyanides, the formation of the products was affected by the low reactivity of aryl isocyanides and the short life span of the unstable reactive nitroalkene species, which is generated *in situ* through elimination of HCl. Undoubtedly, isocyanide chemistry, in particular the use of TosMIC, is an essential tool in the synthesis of five membered nitrogen containing fragments with distinctive properties for medicinal chemistry.

7.2. Biological evaluation and hit identification

The libraries of the synthesised diverse nitrogen containing heterocycles were then evaluated for their ability to disrupt HIV-1 IN-LEDGF/p75 interactions; binding of Vpu to CD4/CD74; and/ or HIV-1 Vpu-BST-2 protein interactions. Based on the assays conducted, the compounds tested did not effectively bind to HIV-1 Vpu and as a result, a decision was made not to pursue this avenue further. Several of the compounds, however, inhibited the HIV-1 IN-LEDGF/p75 and HIV-1 Vpu-BST-2 protein interactions at micromolar concentration. The compounds tested

were not overtly toxic in the MT-4 cell line. Despite having inhibitory activity within the biochemical assay, none of the compounds inhibited viral replication within their respective cell based assays. As the compounds display varying levels of toxicity, it is unlikely that the compounds have poor permeability. The results could suggest an inability of the compounds to reach the target or possibly point to poor compound solubility. Considering all possible factors, compound **83d** (52% inhibition and an IC_{50} value of 25 μ M) and **123g** (82% inhibition and an IC_{50} value of 19 μ M) were selected as suitable hits to produce a family of closely-related compounds, which specifically target interactions between HIV-1 IN and LEDGF/p75 proteins, while compound **125g** (72% inhibition and an IC_{50} value of 23 μ M) was identified as viable hit that could be used as a template to design the next generation of possible HIV-1 Vpu-BST-2 inhibitors.

7.3. Synthesis of Second Generation Compounds and their Biological Evaluation

Starting from the identified HIV-1 IN-LEDGF/p75 hits, sets of second generation compounds were designed and synthesized through introduction of structural diversity at several positions, with the hope of improving the potency of the original hits. Based on the chosen hit **83d**, a carboxylic group was inserted at the 4-position of the imidazole moiety to generate 1,5-diaryl-1*H*-imidazole-4-carboxylic acids **87** as second generation compounds (Figure 7.5)

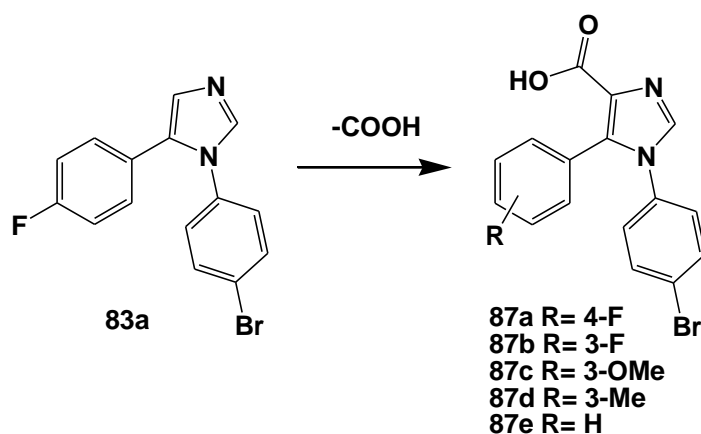


Figure 7.5: Integration of -COOH group on the hit **83a** to give 1,5-diaryl-1*H*-imidazole-4-carboxylic acids **87**.

N-arylidene and carboxamide groups were introduced onto the scaffold of hit compound **123g** and other selected compounds (**120a**, **125a**, **125d** and **125f**), which resulted in the generation of

two sets of novel (*E*)-*N*'-arylidene-2-(5-aryl-1*H*-imidazol-1-yl)acetohydrazides **127** and *N*,5-diaryl-2-(1*H*-imidazol-1-yl)acetamide compounds **128** (Figure 7.6).

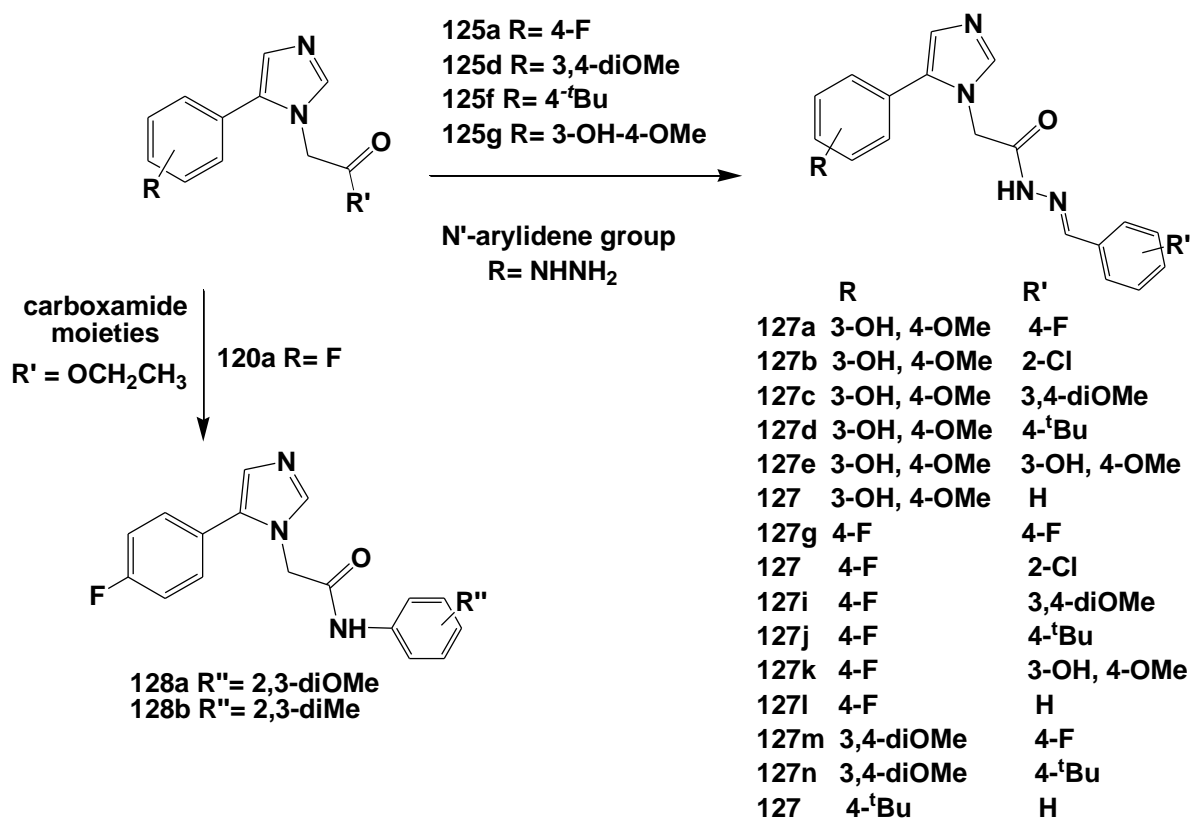


Figure 7.6: Integration of *N*'-arylidene and carboxamide groups on compound **120** and **125** to give (*E*)-*N*'-arylidene-2-(5-aryl-1*H*-imidazol-1-yl)acetohydrazides **127** and *N*,5-diaryl-2-(1*H*-imidazol-1-yl)acetamide compounds **128**.

For second generation oxazole derivatives, an *N*-aryl-carboxamide was inserted at the 4-position of the oxazole moiety, resulting in a series of novel *N*,5-diaryl-4-carboxamide-1,3-oxazoles **100** (Figure 7.7).

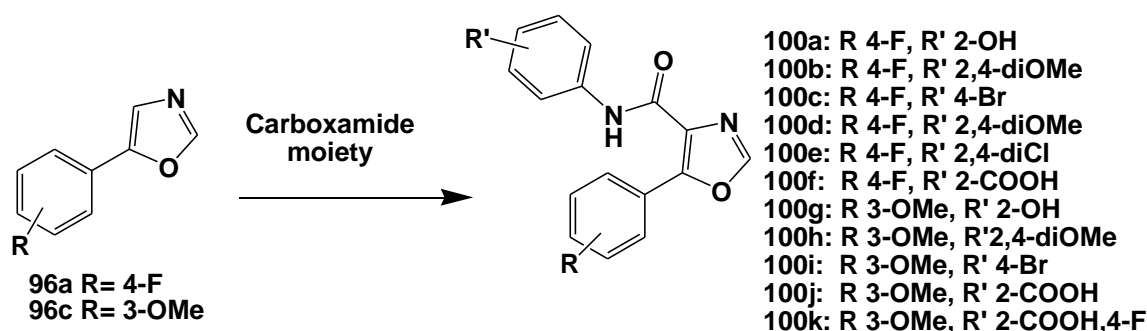


Figure 7.7: Integration of *N'*-arylidene and carboxamide groups on compound **96** to give *N*,5-diaryl-4-carboxamide-1,3-oxazoles **100**.

These second generation compounds were biologically evaluated in an HIV-1-LEDGF/p75 AlphaScreen assay. Biological assessment of the 1,5-diaryl-1*H*-imidazole-4-carboxylic acids **87a-e** identified four compounds surpassing the percentage inhibition of the original hit compound, **83d**, while at least two compounds from the *N*,5-diaryl-4-carboxamide-1,3-oxazoles scaffold **100** exhibited improved percentage inhibition of the LEDGF/p75-IN interactions (Figure 7.8). Furthermore, three compounds with the 4-*tert*-butylphenyl motif from the set of *N'*-arylidene derivatives **127** were found to be disruptors of HIV-1 IN and LEDGF/p75 interactions (Figure 7.8). In the dose response assay, the best inhibitors produced micromolar inhibition values but, unfortunately, these compounds did not effectively exhibit antiviral activity. This is not of immediate concern given the fact that most of the compounds reported to be inhibitors of LEDGF/p75 and IN interactions show lack of antiviral activity in cell based assays. It was interesting to observe that our active compounds **87a-e**, like most of the previously reported HIV-1-LEDGF inhibitors such as ALLINI (Figure 1.8), and CX05168 (Figure 8.1), have aryl rings substituted with a halide, while compounds **100b** and **100h**, like the CAB compounds (Figure 3.1), have electron donating methoxy groups at the *ortho*- and *para*-positions on the phenyl ring. Furthermore, the synthesized compounds **87a-e** also contain a carboxylic moiety, which is found in the HIV-1 IN-LEDGF inhibitors shown in Figure 1.7. These results seem to indicate that our synthesised compounds have certain essential core elements present in their structures, which play a role in preventing the HIV-1 IN-LEDGF/p75 interactions. Hence these compounds have potential for development into the next generation IN inhibitors.

A total of eleven inhibitors were identified that were able to inhibit the HIV-1 IN-LEDGF/p75 interaction (Figure 7.8).

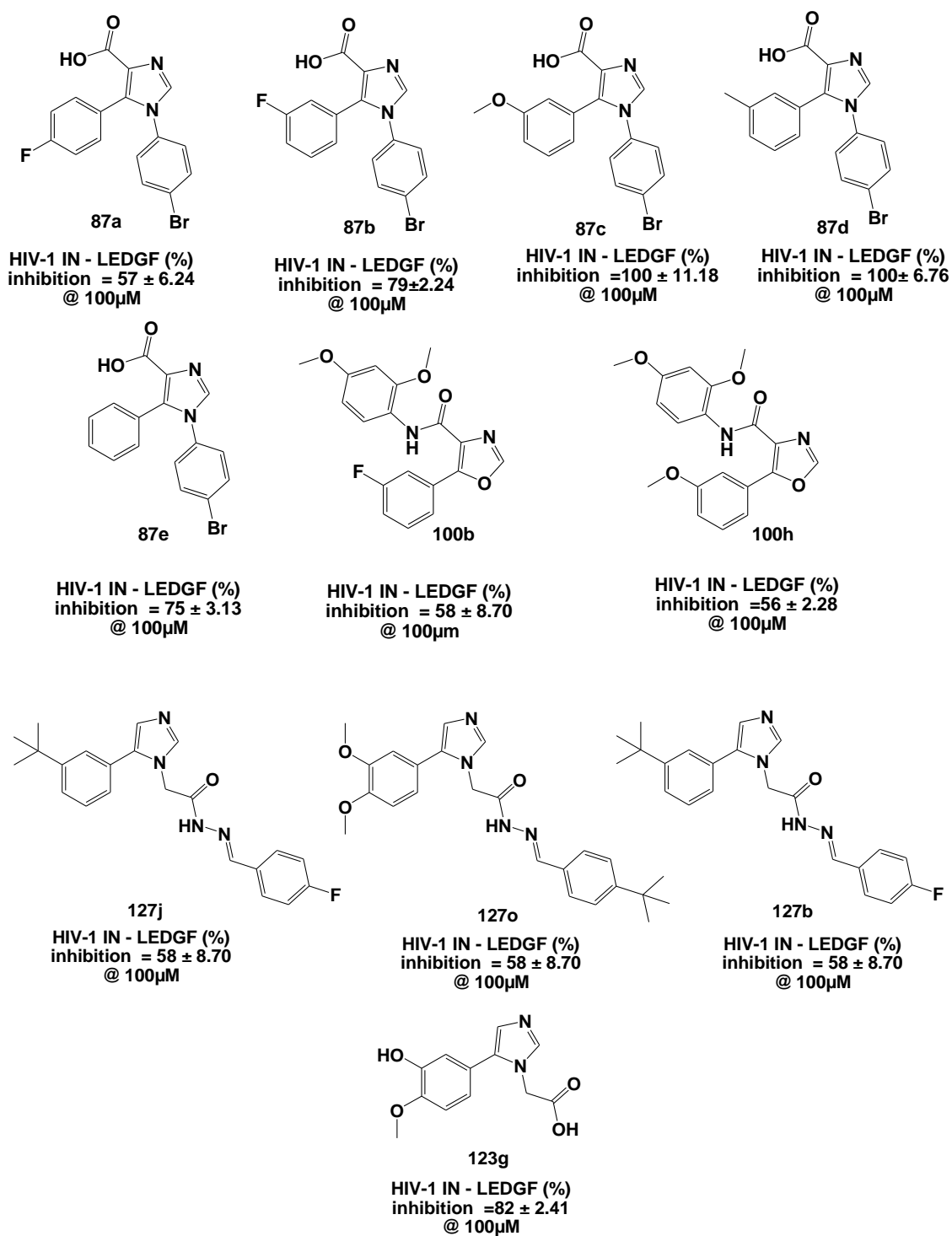


Figure 7.8: Representation of the eleven identified inhibitors of HIV-1 IN-LEDGF/p53 including their percentage inhibition at 100 μ M.

Seven compounds from the imidazolyl family (*Figure 7.9*) were identified as viable hits that could be further modified by introducing various groups to generate a possible second generation of HIV-1 Vpu-BST-2 inhibitors. None of these compounds have previously been synthesised nor have similar compounds been reported as inhibitors of this interaction.

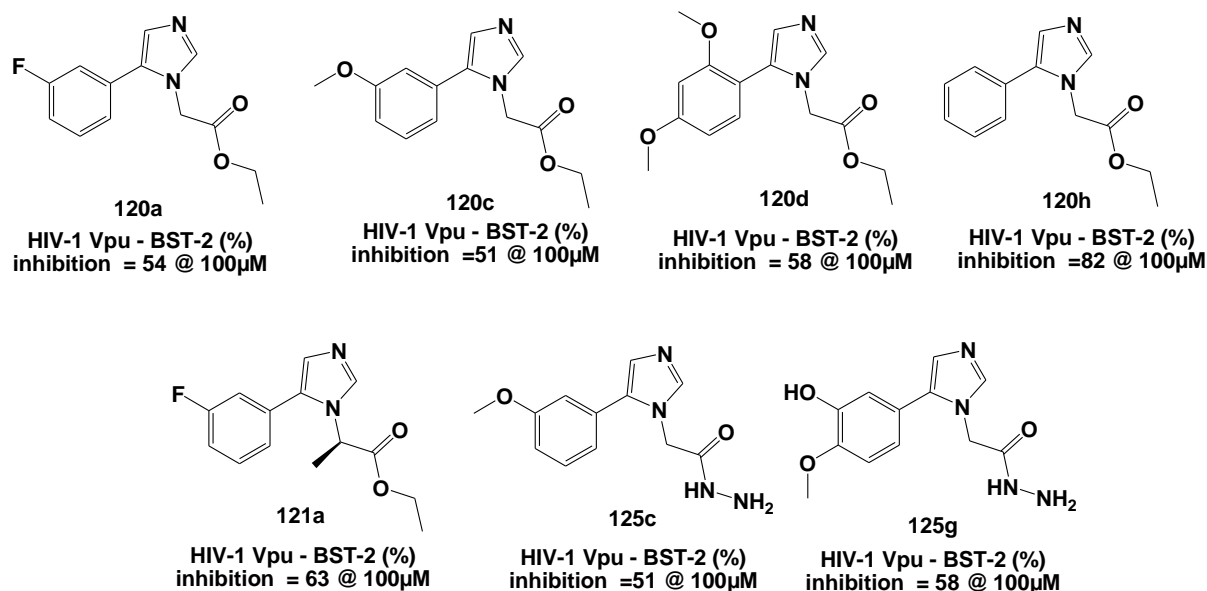


Figure 7.9: Representation of the seven identified inhibitors of HIV-1 Vpu-BST-2 interactions including their percentage inhibition at 100 μM.

The synthesized libraries of five membered nitrogen containing heterocycles were assessed for their antimicrobial activities using MIC methods (**Chapter 6**). At least four compounds **79f**, **80g**, **123g** and **100e** exhibited moderate antimicrobial activity in various concentrations ranging from 55 to 122 μM against gram positive bacterial strains and one yeast strain.

7.4. Modelling Results

The predicted binding model at the HIV-1 interface reveals that these active compounds in *Figure 7.8* are able to form several hydrogen bonds and hydrophobic interactions with important allosteric site amino acids residues, such as Gln95, Ala98, Leu102, Ala128, Trp132, Glu170, His171 and Thr174, consequently, preventing the HIV-1 IN-LEDGF/p75 interactions. These residues have been previously described to be critical to the binding of the LEDGF/p75 protein. In addition, compound **87c** was found to have the lowest binding energy among the active compounds. This implies that this compound might bind more strongly than the others at the HIV-1 IN binding cavity. An overlay of the modelled binding poses for compounds **87a**, **b**, **c**

and **d** and **127j** and **n** is shown in *Figure 7.9*. This shows that the imidazole moiety of compound **87c** in red, as well as that of compounds **127j** and **127n** in light blue falls in the hydrophobic cavity of Ala128 and Ala129, while for compounds **87a**, **87b**, **87d** and **87e** the imidazole moiety projects towards the hydrophobic pockets formed by the Glu170 residue. Overlaying of the acetic acid scaffolds **87** (*Figure 7.10*) shows that they interact *via* hydrogen bonding interactions with the backbone of His171. The exception to this compound **87c** which is shown to form hydrogen bonds with the Gln95 and the Tyr99 residues.

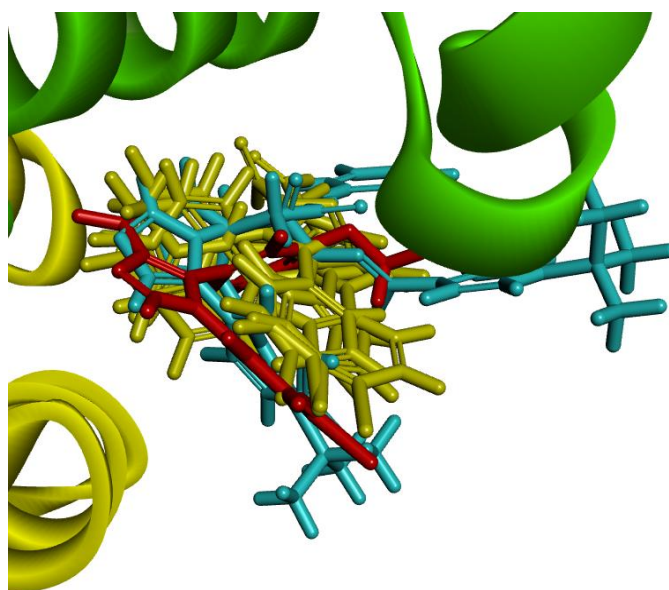


Figure 7.9: Overlaying projection model of compound **87c** (in red), **87a**, **87b**, **87d**, **87e** in yellow and **120j**, **120n** and **120o** in light blue in the LEDGF/p75 binding cavity at the HIV-1 IN dimer interface.

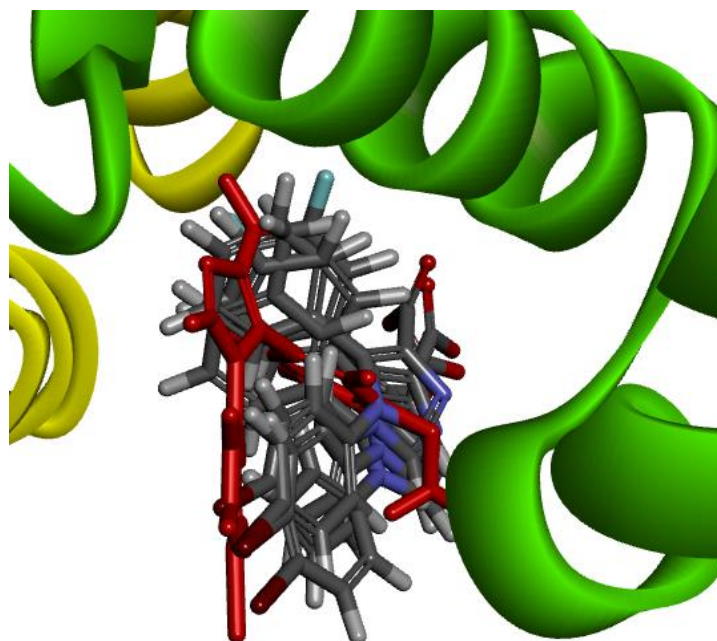


Figure 7.10: Overlaying projection model of compound **87c** (in red), **87a**, **87b**, **87d**, **87e** (in grey) in the LEDGF/p75 binding cavity at the HIV-1 IN dimer interface.

The eighteen identified inhibitors (*Figure 7.8*) exhibited different ADME properties, these parameters are essential factors in determining whether the compounds can be taken further for drug development. Amongst the active inhibitors, the following compounds exhibited an ADME solubility level of 2 (implying that the compounds have poor oral absorption), namely: 5-aryl-1*H*-imidazole-4-carboxylic **87a-e**, compounds **100b**, **127j**, **127n** and **127o**, while compounds **100h**, **120a**, **120c**, **120d**, **121a** and **125c** exhibited an ADME level of 3 (good oral absorption), which is comparable to the control raltegravir. Furthermore, compounds **123g** and **125g** are predicted to have optimal solubility, indicating that they might be completely absorbed by the human intestine after oral dosage. Of the eighteen identified active inhibitors, compounds **87b**, **127j** and **127o** were predicted to have a BBB level of 1, which indicates that they might be able to penetrate the blood brain barrier, hence the probability of central nervous system side effects is very high, while compounds **87a**, **87c**, **87d**, **87e**, **120a**, **120c**, **120h**, **121a** and **127n** are predicted to have level 2 BBB properties and compounds **100a**, **100b**, **120g**, **120c** and **120g** are predicted to have a small chance of causing side effects in the central nervous system. All eighteen active inhibitors, excluding compounds **127j** and **127n**, are predicted to have a false CYP2D6, which suggests these compounds do not inhibit CYP2D6 enzymes of the cytochrome p450 (CYP) enzyme system.

7.5. Final Remarks

Besides a lack of antiviral activity in a cell-based assay, the data acquired in this dissertation is very encouraging. The newly synthesised second generation of compounds have not been previously reported as targeting the interaction between host LEDGF/p75 and HIV-1 IN proteins. This provides new structures that could be potential leads in the development of HIV-1 IN-LEDGF/p75 inhibitors, which hold great promise for future therapy.

Of the eighteen active compounds, the most promising set appears to be the family of 1,5-diaryl-1*H*-imidazole-4-carboxylic acids **87** for the following reasons:

- 1) They possess the COOH functional group which is known to be critical to the binding of other reported HIV-1 IN LEDGF/p75 inhibitors.
- 2) These compounds can theoretically form the necessary hydrogen bonds and hydrophobic interactions with important allosteric site residues, such as Gln95, Ala128, Trp132, Glu170, His171 and Thr174.
- 3) Their ADME parameters could be easily improved because of their relatively small size.
- 4) Their chemical structure permits the introduction of structural diversity at the carboxylic acid group, which could enhance their biological properties.
- 5) The SAR at the 1-position of the imidazole ring can be further exploited by development of new synthetic methodology to allow other anilines to be incorporated.
- 6) They have not been previously reported and could be considered as lead compounds to be further developed as potential HIV-1 IN LEDGF/p75 inhibitors.

The success in the generation of diverse five membered nitrogen containing heterocycles in the present study was made possible by the versatility of the isocyanide synthons. The usefulness of TosMIC further allows for the exploration of structure activity relationships of closely related analogues, which is critical in the fragment drug discovery approach. The study presented further provides evidence that synthetic efforts and a fragment screening approach are complementary approaches in drug discovery that enable the identification of valuable hit compounds against new targets.

CHAPTER 8

EXPERIMENTAL PROCEDURES

8.1 General Experimental Procedures

8.1.1. Purification of solvents and reagents

All commercially available reagents were supplied by Sigma Aldrich and used without further purification. Dry solvents were used directly from an LC-Tech SP-1 Solvent Purification System stored under argon gas. The microwave-assisted reactions were performed in a CEM Discover reactor (Dynamic Temperature and Power set, with 250 psi maximum pressure allowed). All solvents used for chromatographic purposes were supplied by Sigma Aldrich and/or RadChem and were used without further distillation.

8.1.2. Chromatography

Column chromatography was performed using Merck Silica gel 60 [particle size 0.040-0.063 mm (230-400 mesh)] and MN Kieselgel 60 (particle size 0.063-0.200 mm) employing different types of solvents. TLC was performed on pre-coated Merck silica gel F254 plates and viewed under UV light (254 nm) or following exposure to iodine vapour.

8.1.3. Spectroscopic and physical data

NMR spectra were recorded on a 400 MHz Bruker Avance Spectrometer at 298 K equipped with a BBI 5 mm probe. Chemical shifts are reported in ppm, and are referenced internally to residual solvent resonances and calibrated using solvent signals [7.26 (CDCl₃) and 2.50 (DMSO-*d*₆) for ¹H NMR; 77.0 (CDCl₃) 39.52 (DMSO-*d*₆) for ¹³C NMR].

High-resolution mass spectra were obtained on an LC-MS system consisting of a Dionex Ultimate 3000 Rapid Separation LC system equipped with a C-18 pre-coated column and coupled to a MicrOTOF QII Bruker mass spectrometer fitted with an electrospray source and operating in positive mode. Sodium formate clusters were used as internal calibration. LC-MS grade acetonitrile and methanol were obtained from Sigma Aldrich and water from a Milli-Q integral system. The MicrOTOF QII source parameters source were as follows: ESI source type; autoMSMS mode; mass range: 50-3000 Da; on positive polarity; end plate offset -500 V; capillary voltage 4500 V; nebulizer N₂ 1.2 bar; dry heater 200°C; drying N₂ flow 8.0 l/min. The mass analyses were performed using DatAnalysis software (Bruker Daltonics, Germany).

Fast Fourier Infrared spectra (FTIR) were recorded using a Thermo Nicolet 5700 spectrometer, from 4000 to 400 cm⁻¹, with the following collecting parameters: Number of sample scans: 128;

Number of background scans: 64; Resolution: 4.000; Sample gain: 8.0; Mirror velocity: 0.1581; Aperture: 100.00; Detector: DTGS KBr; Beam splitter: XT-KBr. Samples were prepared in a mortar as KBr mixtures. All signals are reported on the wavenumber scale (ν/cm^{-1}).

All melting points were obtained using a Stuart SMP10 melting point apparatus and are uncorrected.

8.1.3. Nomenclature and Compound Numbering

The compound numbering system used for purposes of discussion are not meant to reflect the systematic numbering of these compounds. Nomenclature is based on the IUPAC system.

8.1.4. Biological Evaluation Experiments

The screening of compounds by means of HIV binding assays was conducted in-house within the Centre of Metal Drug Discovery group (CMDD), Advanced Material Division, Mintek, Randburg.

8.1.4.1. HIV-1 IN-LEDGF/p75 AlphaScreen Assay

For the HIV-1 IN-LEDGF/p75 AlphaScreen assay,²⁰⁶ HIV-1 IN was incubated with 10 μM /100 μM of each compound for 30 minutes at 26°C with slight shaking and subsequently 0.3 μM LEDGF/p75 was added and incubated for an hour. Nickel chelating acceptor beads (Perkin Elmer, USA) and Nickel chelating donor beads (Perkin Elmer, USA) were added to a final concentration of 10 $\mu\text{g}/\text{ml}$ and incubated at 30°C in the dark with gentle shaking. Once incubation was complete the plate was read between 520-620nm on the EnSpire® plate reader (Perkin Elmer, USA). Controls included: HIV-1 IN and LEDGF/p75 protein and CX05168; which is a known HIV-1 IN-LEDGF/p75 inhibitor was used as the control compound to validate the assay. Compounds displaying inhibition of above 50% were analyzed and were subsequently tested in ten serially diluted doses ranging from 0.39 μM to 200 μM to determine an IC_{50} for each compound. This was carried out in duplicate on the plate and in three separate experiments.

8.1.4.2. HIV-1 Vpu binding Assay

In the HIV-1 Vpu binding ELISA assay,^{339,340} the Vpu: GFP fusion protein (400 ng per well) was plated in coating buffer (0.05 M Na_2CO_3 [Sigma Aldrich, USA], 0.05 M NaHCO_3 [Saarchem, Merck Chemicals (Pty) Ltd, USA] and 0.1 % NaN_3 [Sigma Aldrich, USA], pH 9.6), and incubated overnight at 4 °C. After washing three times with 1 X tris-buffered saline (TBS) and blocking

with 5 % casein peptone (Conda Pronadisa Molecular Biology, Spain) for 2 hours at room temperature, plates were washed again and incubated with 1000 x diluted anti-Vpu antibody (NIH catalogue number 969) for 2 hours at room temperature. Plates were then washed three times with TBST (a mixture of tris-buffered TBS and Tween 20) and incubated with 2000 x diluted goat anti-rabbit IgG peroxidase labelled antibody (KPL, USA) for 90 minutes at room temperature before visualizing with the substrate, 3,3',5,5'-tetramethylbenzidine liquid (TMB; Life Technologies, USA). Controls were included in all plates.

8.1.4.3. HIV-1 Vpu- BST-2 ELISA Assay

For this assay, 5 ng/mL of Vpu was incubated with 100 μ M of each compound for 30 minutes at 37 °C with slight shaking; and BST-2, to a final concentration of 5 ng/mL, was coated on a 96-well polysorp plate that was pre-coated with an anti-BST-2 antibody. Following the incubation period, the BST-2 was aspirated and the wells were washed three times with wash buffer. The Vpu/compound complexes were introduced, and the plates were incubated at 37 °C for an hour, washed, and a biotin-conjugated anti-BST-2 antibody was added and incubated at 37 °C for another hour. Streptavidin conjugated to HRP was added and the plates were incubated at 37 °C for 30 minutes. HRP activity was detected using the TMB substrate, the enzyme-substrate reaction was terminated by addition of sulphuric acid, and the colour change was measured spectrophotometrically at 490 nm using the xMark microplate reader. A total of 24 compounds were tested alongside 6-aza-2-thiouridine, which has previously been shown to inhibit the Vpu/BST-2 interaction, and was thus used as a positive control.

8.1.4.4. Antiviral for HIV-1 LEDGF/p75 interaction

MT-4 cells (obtained through the NIH AIDS Reagent Program, Division of AIDS, NIAID, NIH: MT-4 catalogue number 120) were seeded the day before antiviral testing at 3×10^5 cells per ml. The following day the viability was checked and 2×10^5 cells per ml were placed into a 50 ml conical tube and HIV-1_{NL4.3} stock added. The cells were spinoculated (O'Doherty et al., 2000) at $3000 \times g$ for 90 minutes. Cells were subsequently washed four times with 0.01 M PBS to remove any unbound virus. A control set of cells were spinoculated without virus and washed four times with 0.01 M PBS to replicate the test cells. A total of 10 ml 10 % RPMI media was then added to the cells and 100 μ l of cells were added to each well of a Corning® Costar® 96-Well Cell Culture Plates (Sigma Aldrich, USA). The plate was placed into the 37°C, 5 % CO₂ incubator to equilibrate for one hour. During the incubation compounds were made up in RPMI media containing 10 % heat inactivated FCS. The compounds were serially diluted from 100 μ M

to 1.56 μM . A total of 100 μl of compound solution was added to the wells containing cells and mixed to ensure they were homogeneous. The plate was placed into a 37°C, 5 % CO_2 incubator for five days.

A Biomerieux Vironostika HIV-1 Ab/Ag micro ELISA system was used to test for p24. All buffers were prepared according to manufacturer's specifications and the manufacturer's protocol was followed. Briefly, 145 μl of disruption buffer was added to each well including control wells and incubated at 37°C for one hour. A total volume of 5 μl of each test specimen was added to the disruption buffer and control samples were added. The plate was then incubated at 37°C for 60 minutes and wells were then washed with 1x wash buffer for 30 seconds. Washing was repeated six times. Once washed 100 μl of 3,3',5,5'-tetramethylbenzidine (TMB) substrate mix (1:1 ratio of TMB substrate A and B) was added and incubated for 5-30 minutes in the dark until sufficient colour had developed. The reaction was stopped by the addition of 100 μl 1 M sulphuric acid. The plates were then read on a multiplate reader at 450nm (xMARK™, Bio-Rad, USA).

8.1.4.5. Cellular Toxicity assay

The day of cytotoxicity testing, cells were counted and seeded at 1×10^6 cells per ml. A total of 100 μl of cells were added to each well of a 96 well cell culture plate for testing. The plate was placed into the incubator to equilibrate to 37°C and 5 % CO_2 . During this time, test compounds were made up in 10% RPMI solution in a serial dilution from 100 μM to 1.56 μM . A total of 100 μl compound was added to wells containing cells and mixed to ensure the solution was homogeneous with the cells. The plate was placed into the 37°C incubator for 5 days. On the 5th day 10 μl of MTS was added and mixed. The plates were then incubated for a further four hours, and read at 490 nm (xMARK™, Bio-Rad, USA.) The data analysis was completed on Origin 8.1 with the log value of the concentration plotted against the absorbance level to determine a dose curve. From the curve, a half maximal cytotoxicity CC_{50} for compounds was determined. Controls used included auranofin, raltegravir and CX05168.

8.1.4.6. Minimum inhibitory concentration using *p*-iodonitrotetrazolium (INT) chloride method

The antimicrobial minimum inhibition concentration (MIC) using the *p*-iodonitrotetrazolium chloride method was conducted at the University of the Witwatersrand, Department of

Pharmacy and Pharmacology in the School of Therapeutic Science under guidance of Professor Sandy van Vuuren.

8.1.4.6.1. Preparation of stock solution for antimicrobial testing

The stock of solutions the synthesized compounds used for the minimum inhibitory concentration (MIC) assays were prepared by dissolving the sample in 10% dimethyl sulfoxide (DMSO), followed by dilution with sterile water in order to make a concentration of 1 mg/ml. In cases where the synthesized compounds were insoluble in 10% DMSO, 100% acetone was used to create the same concentration of 1mg/ml. The concentration of 0.01 mg/ml of ciprofloxacin and 0.01 mg/ml nystatin were also prepared and were used as positive controls for bacteria and yeast, respectively, while the 10% DMSO in water and 100% acetone were used as the negative controls. A solution of *p*-iodonitrotetrazolium (INT) chloride (0.08 g) in 200 ml of sterile water was prepared as the indicator.

8.1.4.6.2 Screening of synthesized compounds against pathogens

The synthesized compounds were assessed for their antimicrobial effects against two Gram-positive bacterial species (*Staphylococcus aureus* ATCC 25923 and *Bacillus cereus* ATCC 11779), two Gram-negative bacterial species (*Escherichia coli* ATCC 8739 and *Pseudomonas aeruginosa* ATCC 27858) and one yeast (*Candida tropicalis* ATCC 750) in tryptone soya broth using the MIC assay. Tryptone soya broth (100 µl) was added into each of the 96 well microtiter plates, followed by the addition 100 µl of each tested compound solution including positive and negative controls. Serial dilutions were performed by pipetting 100 µl into next well and the last 100 µl of dilution was discarded. The serial dilution provided the following nine concentrations: 250, 125, 62.5, 31.25, 15.6, 7.8, 3.91, 1.95, and 0.98 µg/ml. Prior to the addition of culture to the microtiter plates, 1 ml of each culture was sub-cultured in 100 µl tryptone soya broth to obtain a 0.5 McFarland standard. Sub-culture volume of 100 µl was then added to all wells of microtiter plates, which contained the compounds and broth. Each plate was sealed with a sterile adhesive sealing film to avoid evaporation of test samples, followed by incubation at 37°C for 24 hours for bacteria species and for 48 hours for the yeast. After incubation, 40 µl of *p*-iodonitrotetrazolium (INT) chloride was added to each well of the microtiter plates.^{341, 342} Each plate was read to determine the minimum inhibitory concentration. The wells with clear or no visible bacterial growth determined the lowest concentration. The assessments were carried out in duplicate.

8.1.5. Computer Modeling

8.1.5.1. Ligand preparation

Prior to docking, the selected compounds were energy minimized using a CHARMM based force field function under Small Molecules' Prepare and Filter Ligands function to generate all possible combinations of stereoisomers and conformers.

8.1.5.2. Preparation of HIV IN-1 protein

The HIV-1 IN protein used in the modeling was prepared by a previous member of the group, Dr Telisha Traut,³⁴³ using a BIOVIA Discovery Studio 4.0 package. The PDB code 2B4J model (IN-LEDGF/p75) was retrieved (<http://www.rcsb.org/pdb>) and LEDGF/p75 was removed from the HIV-1 IN-LEDGF/p75 complex and prepared by building missing loops, addition of hydrogen atoms, bond order assignment, and optimization of bond lengths, bond angles, torsion angles and non-bonded interactions. Known HIV-1 IN-LEDGF/p75 inhibitors (27) identified by Bruno Simoneau *et al.*³⁴⁴ consisting of known IC₅₀, EC₅₀, CC₅₀ and K_D values were used to train the model. The sphere had the following xyz coordinates: 7.175, -17.325, -17.502 and radius of 14Å.

8.1.5.3 Docking of selected compound into HIV IN binding cavity

Molecular docking studies were performed using the BIOVIA Discovery Studio software package, version 4.0 in the allosteric site (LEDGF/p75-binding site) of HIV-1 IN protein (PDB code: 2B4J). The selected compounds were primarily positioned in the same site where LEDGF/p75 binds to the HIV-1 IN dimer using the LibDock protocol, which resulted in the generation of hundreds for poses of each compound. These poses were exposed to Jain, PLP2 and LibDock scoring protocols, and then analysed, followed by the further optimised by *in-situ*-energy-minimisation and flexible docking. The binding energies of the best poses generated from flexible docking were then calculated.

8.1.5.4. ADME properties

The absorption, distribution, metabolism and excretion (ADME) of synthesized compounds was determined theoretically using the ADMET Descriptors application in the BIOVIA Discovery StudioTM, version 4.0. The ADME determinations were carried out in order to analyse solubility, intestinal absorption, blood-brain barrier (BBB) penetration and cytochrome P450 inhibition.

8.1.6. Isothermal titration calorimetry

The proteins was purified in house within the Centre of Metal Drug Discovery group (CMDD), Advanced Material Division, Mintek, Randburg. The ITC experiments were conducted at the University of the Witwatersrand, Department of Protein Structure-Function Research Unit in the School of Molecular and Cell Biology under guidance of Professor Yasien Sayed.

8.1.6.1. Buffer exchange

A total of 2.5 ml HIV-1 IN sub B protein with a final concentration of 25 μ M was loaded into a cellulose dialysis membrane with a 10 kDa cut-off. The dialysis membrane was submerged in dialysis buffer (1M NaCl, 20 mM Hepes pH 7.4 , 1 mM DTI, 2.5 mM β -mercaptoethanol, 5% glycerol) and buffer exchanged for 5 hours at 4°C. After 5 hours the buffer was changed to a fresh buffer and exchanged for a further 5 hours. A final change of buffer was performed overnight and the buffer kept for use in the ITC experiment.

8.1.6.2. Compound preparation

CX05168 (*Figure 8.1*) which is known to be a HIV-1 IN-LEDGF/p75 inhibitor was used as a control in an attempt to establish the ITC protocol.⁵³ Control compound was made up to a stock solution of 20 mg/ml in DMSO. For a final concentration of 1 mM CX05168 for use in the ITC experiment, 8.84 μ l of 20mg/ml CX05168 was added to 491.136 μ l of ITC buffer. Other concentrations were prepared in a similar manner.

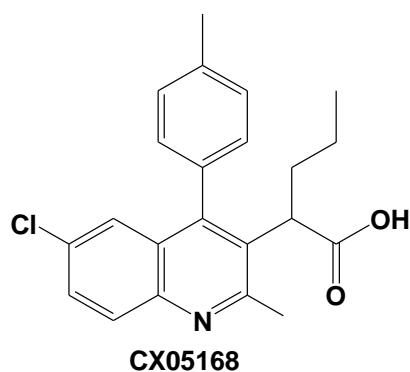


Figure 8.1: Structure of the control compound CX05168.

8.1.6.3. ITC experiment settings

ITC experiments were conducted using a VP-ITC MicroCalorimeter TM. The cell temperature was set at 20°C and experiments were programmed to run 35 injections at 300-second intervals with stirring speed of 750 revolutions per minute (rpm). The initial default volume of injection

was set at 3 μ l while other the 34 injections were 8 μ l. The preliminary ITC data fitting was carried out using NITPIC and ITCsy software.

8.2. Chapter 2 experimental procedure

8.2.1. Synthesis of *N*-arylidene alkylamines

The following general synthetic procedures for the preparation of *N*-arylidene alkylamines were performed and the yields obtained are indicated for each compound:

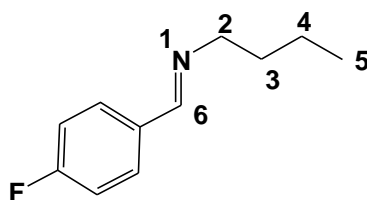
8.2.1.1. Synthetic Procedure A: Conventional Method

To a solution of aldehyde (1 molar equivalent) in DCM (5 ml) was added primary amine (1.2 molar equivalent) and MgSO_4 (0.14 mg). The resulting reaction mixture was then allowed to stir at room temperature for 16 hours (monitored by TLC). At the end of the reaction time, the solution was filtered to remove the MgSO_4 and washed with DCM (2 x 5 ml). The combined DCM fractions were then concentrated *in vacuo* and dried under high vacuum to give pure *N*-arylidene alkylamine.³⁴⁵

8.2.1.2. Synthetic Procedure B: Microwave Irradiation

A mixture of aldehyde (1 molar equivalent) and primary amine (1.2 molar equivalents) in a 10 ml microwave vessel was irradiated neat at 60°C for 4 minutes using the standard MW method (in the CEM microwave standard control method, the specified set temperature is held over a set time period, while the power applied is controlled by the instrument default settings). At the end of the reaction time (monitored by TLC), DCM was added and reaction mixture was transferred into round bottom flask and the vessel was then rinsed with DCM. The combined DCM fractions were then concentrated *in vacuo* to give pure *N*-arylidene alkylamine.

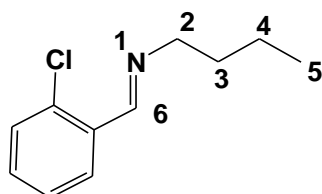
8.2.1.3. (*E*)-*N*-(4-Fluorobenzylidene)butan-1-amine 75a



(*E*)-*N*-(4-Fluorobenzylidene)butan-1-amine **75a** was successfully synthesized as described by synthetic procedure A {4-fluorobenzaldehyde (0.596 g, 4.80 mmol) and *n*-butylamine (421 mg, 5.76 mmol)} and synthetic procedure B {4-fluorobenzaldehyde (338 mg, 2.72 mmol) and *n*-butylamine (239 mg, 4.08 mmol)}; **Physical characteristics:** pale brown oil; **Yields:** 748 mg,

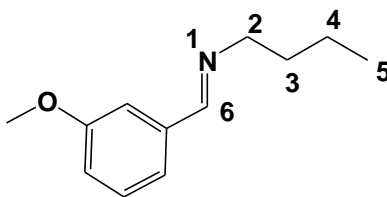
87% for synthetic procedure A and 478 mg, 98% for synthetic procedure B; $^1\text{H NMR}$ (400 MHz, CDCl_3) δ 8.21 (1H, s, $\text{N}=\text{CH}$), 7.12 (2H, m, Hz, ArH), 7.02 (2H, t, $J = 8.8$ Hz, ArH), 3.57 (2H, t, $J = 7.0$ Hz, 2- CH_2), 1.63-1.70 (2H, m, 3- CH_2), 1.33-1.42 (2H, m, 4- CH_2), 0.92 (3H t, $J = 7.4$ Hz, 5- CH_3); $^{13}\text{C NMR}$ (101 MHz, CDCl_3) δ 164.1 (d, $^1J_{\text{CF}} = 250$ Hz, *para*-CF), 159.1 (6-C) 132.6 (d, $^4J_{\text{CF}} = 3$ Hz, 1'-C), 129.8 (d, $^3J_{\text{CF}} = 9$ Hz, *ortho*-C), 115.5 (d, $^2J_{\text{CF}} = 22$ Hz, *meta*-C), 61.3 (2-C), 32.9 (3-C), 20.4 (4-C), 13.8 (5-C).

8.2.1.4. (*E*)-*N*-(2-Chlorobenzylidene)butan-1-amine 75b



(*E*)-*N*-(2-Chlorobenzylidene)butan-1-amine **75b** was successfully synthesized as described by synthetic procedure A {2-chlorobenzaldehyde (550 mg, 3.91 mmol) and *n*-butylamine (343 mg, 4.69 mmol)} and synthetic procedure B {2-chlorobenzaldehyde (351 mg, 2.50 mmol) and *n*-butylamine (219 mg, 3.00 mmol)}; **Physical characteristics:** colourless oil; **Yields:** 719 mg, 94% for synthetic procedure A and 484 mg, 99% for synthetic procedure B; $^1\text{H NMR}$ (400 MHz, CDCl_3) δ 8.61 (1H, s, $\text{N}=\text{CH}$), 7.92 (1H, d, $J = 8.4$ Hz, ArH), 7.17-7.28 (3H, m, ArH), 3.56 (2H, t, $J = 7.0$ Hz, 2- CH_2), 1.58-1.65 (2H, m, 3- CH_2), 1.29-1.34 (2H, m, 4- CH_2), 0.85 (3H, t, $J = 7.4$ Hz, 5- CH_3); $^{13}\text{C NMR}$ (101 MHz, CDCl_3) δ 157.4 ($\text{N}=\text{CH}$), 134.9, 133.3, 131.2, 129.7, 128.2, 126.9 (ArC), 61.5 (2-C), 32.8 (3-C), 20.4 (4-C), 13.8 (5-C).

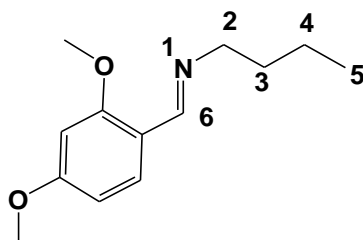
8.2.1.5. (*E*)-*N*-(3-Methoxybenzylidene)butan-1-amine 75c



(*E*)-*N*-(3-Methoxybenzylidene)butan-1-amine **75c** was successfully synthesized as described by synthetic procedure B using 3-methoxybenzaldehyde (313 mg, 2.30 mmol) and *n*-butylamine (202 mg, 2.76 mmol); **Physical characteristics:** colourless oil; **Yields:** 428 mg, 97% for synthetic procedure B; $^1\text{H NMR}$ (400 MHz, CDCl_3) δ 8.26 (1H, s, $\text{N}=\text{CH}$), 7.28-7.37 (3H, m, ArH), 6.98 (1H, d, $J = 8.4$ Hz, ArH), 3.87 (3H, s, ArOCH_3), 3.62 (2H, t, $J = 7.0$ Hz, 2- CH_2), 1.70-1.75 (2H, m, 3- CH_2), 1.39-1.50 (2H, m, 4- CH_2), 0.96 (3H, t, $J = 7.4$ Hz, 5- CH_3); $^{13}\text{C NMR}$ (101

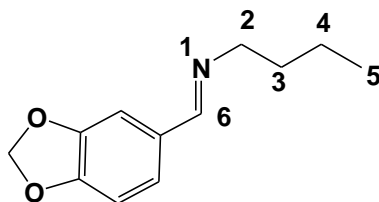
MHz, CDCl₃) δ 160.5 (ArCOCH₃), 159.8 (N=CH), 137.8, 129.4, 121.2, 117.1, 111.4 (ArC), 61.3 (2-C), 55.2 (ArCOCH₃), 32.9 (3-C), 20.4 (4-C), 13.8 (5-C).

8.2.1.6. (*E*)-*N*-(2,4-Dimethoxybenzylidene)butan-1-amine 75d



(*E*)-*N*-(2,4-Dimethoxybenzylidene)butan-1-amine **75d** was successfully synthesized as described by synthetic procedure A {2,4-dimethoxybenzaldehyde (1.01 g, 6.10 mmol) and *n*-butylamine (535 mg, 7.32 mmol) and synthetic procedure B {2,4-dimethoxybenzaldehyde (332 mg, 2.00 mmol) and *n*-butylamine (210 mg, .40 mmol)}; **Physical characteristics:** light brown oil; **Yields:** 1.13 g, 84% for synthetic procedure A and 434 mg, 98% for synthetic procedure B; **¹H NMR** (400 MHz, CDCl₃) δ 8.48 (1H, s, N=CH), 7.77 (1H, d, *J* = 8.8 Hz, ArH), 6.37 (1H, d, *J* = 8.8 Hz, ArH), 6.28 (1H, s, ArH), 3.66 and 3.68 (6H, 2 x s, 2 x ArOCH₃), 3.44 (2H, t, *J* = 7.0 Hz, 2-CH₂), 1.51-1.57 (2H, m, 3-CH₂), 1.24-1.30 (2H, m, 4-CH₂), 0.81 (3H, t, *J* = 7.4 Hz, 5-CH₃); **¹³C NMR** (101 MHz, CDCl₃) δ 162.5 and 159.6 (2 x ArCOCH₃), 155.8 (N=CH), 128.1, 117.9, 105.0, 97.6 (ArC), 61.4 (2-C), 55.0 and 54.9 (2 x ArCOCH₃), 33.0 (3-C), 20.2 (4-C), 13.7 (5-C).

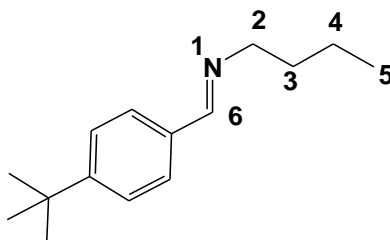
8.2.1.7. (*E*)-*N*-(Benzo[*d*][1,3]dioxol-5-ylmethylene)butan-1-amine 75e



(*E*)-*N*-(Benzo[*d*][1,3]dioxol-5-ylmethylene)butan-1-amine **75e** was successfully synthesized as described by synthetic procedure A {piperonal (2.07 g, 13.87 mmol) and *n*-butylamine (1.21 g, 16.55 mmol) and synthetic procedure B {piperonal (330 mg, 2.20 mmol) and *n*-butylamine (193 mg, 2.64 mmol)}; **Physical characteristics:** brown oil; **Yields:** 2.73 g, 96% for synthetic procedure A and 451 mg, 100% for synthetic procedure B; **¹H NMR** (400 MHz, CDCl₃) δ 8.11 (1H, s, N=CH), 7.32 (1H, s, ArH), 7.05 (1H, d, *J* = 7.6 Hz, ArH), 6.77 (1H, d, *J* = 8.0 Hz, ArH), 5.94 (2H, s, ArOCH₂O-), 3.52 (2H, t, *J* = 7.0 Hz, 2-CH₂), 1.60-1.67 (2H, m, 3-CH₂), 1.33-1.39

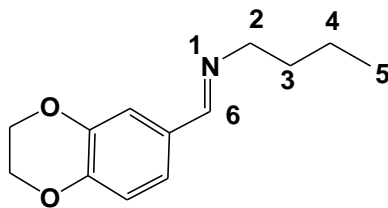
(2H, m, 4-CH₂), 0.90 (3H, t, *J* = 7.4 Hz, 5-CH₃); ¹³C NMR (101 MHz, CDCl₃) δ 159.6 (N=CH), 149.5, 148.1, 131.1, 123.9, 107.8, 106.4 (ArC), 101.2 (ArOCH₂O), 61.0 (2-C), 33.0 (3-C), 20.3 (4-C), 13.8 (5-C).

8.2.1.8. (*E*)-*N*-(4-*tert*-butylbenzylidene)butan-1-amine 75f



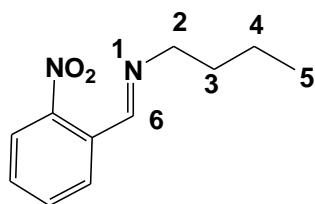
(*E*)-*N*-(4-*tert*-Butylbenzylidene)butan-1-amine **75f** was successfully synthesized as described by synthetic procedure A {4-*tert*-butylbenzaldehyde (600 mg, 3.70 mmol) and *n*-butylamine (325 mg, 4.44 mmol)} and synthetic procedure B {4-*tert*-butylbenzaldehyde (339 mg, 2.09 mmol) and *n*-butylamine (183 mg, 2.51 mmol)}; **Physical characteristics**: pale brown oil; **Yields**: 676 mg, 84% for synthetic procedure A and 423 mg, 93% for synthetic procedure B; ¹H NMR (400 MHz, CDCl₃) δ 8.30 (1H, s, N=CH), 7.65-7.68 (2H, m, ArH), 7.41-7.43 (2H, m, ArH), 3.15 (2H, t, *J* = 7.0 Hz, 2-CH₂), 1.60-1.77 (2H, m, 3-CH₂), 1.31-1.33 [11H, m, 4-CH₂ and ArC(CH₃)₃], 0.98 (3H, t, *J* = 7.4 Hz, 5-CH₃); ¹³C NMR (101 MHz, CDCl₃) δ 158.4 (N=CH), 153.7, 134.0, 127.9, 125.5 (ArC), 70.1 (2-C), 34.9 [ArCC(CH₃)₃], 33.0 (3-C), 20.3 (4-C), 13.8 (5-C), 25.4 [ArCC(CH₃)₃].

8.2.1.8. (*E*)-*N*-(2,3-Dihydrobenzo[*b*][1,4]dioxin-6-yl)methylene)butan-1-amine 75g



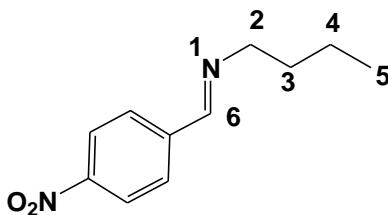
(*E*)-*N*-(2,3-Dihydrobenzo[*b*][1,4]dioxin-6-yl)methylene)butan-1-amine **75g** was successfully synthesized as described by synthetic procedure A using 1,4-benzodioxan-6-carboxaldehyde (506 mg, 3.08 mmol) and *n*-butylamine (271 mg, 3.70 mmol); **Physical characteristics**: pale brown oil; **Yield**: 567 mg, 84 %; ¹H NMR (400 MHz, CDCl₃) δ 8.03 (1H, s, N=CH), 7.18 (1H, s, ArH) 7.10 (1H, d, *J* = 8.4 Hz, ArH), 6.77 (1H, d, *J* = 8.0 Hz, ArH), 4.16 (4H, s, ArOCH₂CH₂O), 3.45-3.49 (2H, t, *J* = 7.0 Hz, 2-CH₂), 1.55-1.59 (2H, m, 3-CH₂), 1.26-1.31 (2H, m, 4-CH₂), 0.83 (3H, t, *J* = 7.4 Hz, 5-CH₃); ¹³C NMR (101 MHz, CDCl₃) δ 159.7 (N=CH), 145.5 and 143.5 (ArCOCH₂CH₂O), 130.1, 121.5, 117.2, 116.5 (ArC), 64.4 and 64.0 (ArCOCH₂CH₂O-), 61.3 (2-C), 32.9 (3-C), 20.3 (4-C), 13.8 (5-C).

8.2.1.9. (*E*)-*N*-(2-Nitrobenzylidene)butan-1-amine 75h



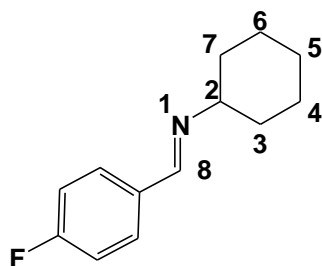
(*E*)-*N*-(2-Nitrobenzylidene)butan-1-amine **75h** was successfully synthesized as described by synthetic procedure B using 4-nitrobenzaldehyde (227 mg, 1.50 mmol) and *n*-butylamine (133 mg, 1.80 mmol); **Physical characteristics**: yellow oil; **Yield**: 226 mg, 73%; **¹H NMR** (400 MHz, CDCl₃): δ 8.66 (1H, s, N=CH), 7.97-8.03 (2H, m, ArH), 7.51-7.66 (2H, m, ArH), 3.65 (2H, t, *J* = 7.0 Hz, 2-CH₂), 1.66-1.73 (2H, m, 3-CH₂), 1.35-1.44 (2H, m, 4-CH₂), 0.92 (3H, t, *J* = 7.4 Hz, 5-CH₃); **¹³C NMR** (101 MHz, CDCl₃) δ 156.6 (N=CH), 148.7, 133.4, 131.3, 130.4, 129.6, 124.2 (ArC), 61.4 (2-C), 32.6 (3-C), 20.3(4-C), 13.8 (5-C).

8.2.1.9. (*E*)-*N*-(4-Nitrobenzylidene)butan-1-amine 75i



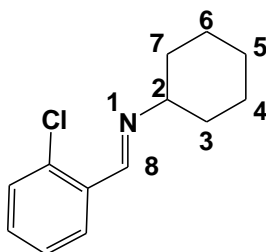
(*E*)-*N*-(4-Nitrobenzylidene)butan-1-amine **75i** was successfully synthesized as described by synthetic procedure B using 4-nitrobenzaldehyde (197 mg, 1.30 mmol) and *n*-butylamine (114 mg, .55 mmol); **Physical characteristics**: yellow oil; **Yield**: 244 mg, 91%; **¹H NMR** (400 MHz, CDCl₃) δ 8.34 (1H, s, N=CH), 8.22-8.25 (2H, m, ArH), 7.86-7.90 (2H, m, ArH), 3.64 (2H, t, *J* = 7.0 Hz, 2-CH₂), 1.65-1.73 (2H, m, 3-CH₂), 1.38-1.43 (2H, m, 4-CH₂), 0.92-0.96 (3H, t, *J* = 7.4 Hz, 5-CH₃); **¹³C NMR** (101 MHz, CDCl₃) δ 158.3 (N=CH), 148.8, 141.8, 128.6, 123.8 (ArC), 61.6 (2-C), 32.7 (3-C), 20.4 (4-C), 13.8 (5-C).

8.2.1.11. (*E*)-*N*-(4-Fluorobenzylidene)cyclohexanamine 76a



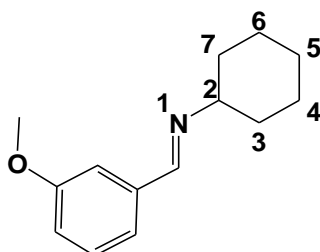
(*E*)-*N*-(4-Fluorobenzylidene)cyclohexanamine **76a** was successfully synthesized as described by synthetic procedure A {4-fluorobenzaldehyde (545 mg, 4.39 mmol) and cyclohexylamine (523 mg, 5.27 mmol)} and synthetic procedure B {4-fluorobenzaldehyde (347 mg, 2.80 mmol) and cyclohexylamine (333, mg, 3.36 mmol)}; **Physical characteristics**: pale yellow oil; **Yields**: 766 mg, 85% for synthetic procedure A and 506 mg, 88% for synthetic procedure B; **¹H NMR** (400 MHz, CDCl₃) δ 8.26 (1H, s, N=CH), 7.69 (2H, m, ArH), 7.04 (2H, t, *J* = 8.8 Hz, ArH), 3.14 (1H, m, 2-CH), 1.38-1.85 (10H, m, 3-, 4-, 5-, 6- & 7-CH₂); **¹³C NMR** (101 MHz, CDCl₃) δ 164.0 (d, ¹*J*_{C,F} = 249.6 Hz, *para*-CF), 157.0 (8-C), 132.9 (d, ⁴*J*_{C,F} = 3.0 Hz 1'-C), 129.8 (d, ³*J*_{C,F} = 8.1 Hz, *ortho*-C), 115.6 (d, ²*J*_{C,F} = 22.0 Hz, *meta*-C), 69.8 (2-C), 34.3 (3- & 7-C), 25.6 (4- & 6-C), 24.7 (5-C).

8.2.1.12. (*E*)-*N*-(2-Chlorobenzylidene)cyclohexanamine **76b**



(*E*)-*N*-(2-Chlorobenzylidene)cyclohexanamine **76b** was successfully synthesized as described by synthetic procedure A {2-chlorobenzaldehyde (593 mg, 4.23 mmol) and cyclohexylamine (504 mg, 5.08 mmol)} and synthetic procedure B {2-chlorobenzaldehyde (336 mg, 2.39 mmol) and cyclohexylamine (285 mg, 2.87 mmol)}; **Physical characteristics**: pale yellow solid; **Yields**: 807 mg, 86% for synthetic procedure A and 472 mg, 89% for synthetic procedure B; **¹H NMR** (400 MHz, CDCl₃) δ 8.71 (1H, s, N=CH), 7.99 (1H, d, *J* = 7.6 Hz, ArH), 7.23-7.34 (3H, m, ArH), 3.22-3.28 (1H, m, 2-CH), 1.38-1.83 (10H, m, 3-, 4-, 5-, 6- & 7-CH₂); **¹³C NMR** (101 MHz, CDCl₃) δ 155.4 (N=CH), 134.9, 133.6, 131.1, 129.6, 128.4, 126.9 (ArC), 70.0 (2-C), 34.3 (3- & 7-C), 25.6 (4- & 6-C), 24.7 (5-C).

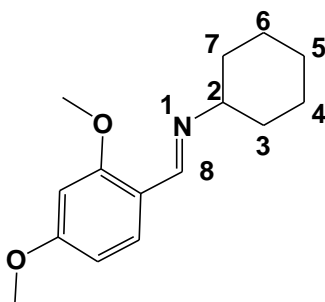
8.2.1.13. (*E*)-*N*-(3-Methoxybenzylidene)cyclohexanamine **76c**



(*E*)-*N*-(3-Methoxybenzylidene)cyclohexanamine **76c** was successfully synthesized as described by synthetic procedure A {3-methoxybenzaldehyde (515 mg, 3.78 mmol) and cyclohexylamine

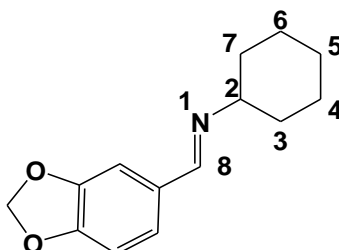
(450 mg, 4.54 mmol)} and synthetic procedure B {3-methoxybenzaldehyde (354 mg, 2.60 mmol) and cyclohexylamine (309 mg, 3.12 mmol)}; **Physical characteristics:** white solid; **Yields:** 591 mg, 72% for synthetic procedure A and 497 mg, 88% for synthetic procedure B; **Melting point:** 58-61°C; **¹H NMR** (400 MHz, CDCl₃) δ 8.30 (1H, s, N=CH), 7.28-7.34 (3H, m, ArH), 6.95 (1H, dd, *J* = 8.0 Hz, 1.2 Hz, ArH), 3.86 (3H, s, ArOCH₃), 3.17-3.25 (1H, m, 2-CH), 1.38-1.88 (10H, m, 3-, 4-, 5-, 6- & 7-CH₂); **¹³C NMR** (101 MHz, CDCl₃) δ 159.8 (ArCOCH₃), 158.4 (N=CH), 138.1, 129.4, 121.2, 116.9, 111.7 (ArC), 69.9 (2-C), 55.3 (ArCOCH₃), 34.2 (3- & 7-C), 25.6 (4- & 6-C), 24.8 (5-C).

8.2.1.14. (*E*)-*N*-(2,4-Dimethoxybenzylidene)cyclohexanamine 76d



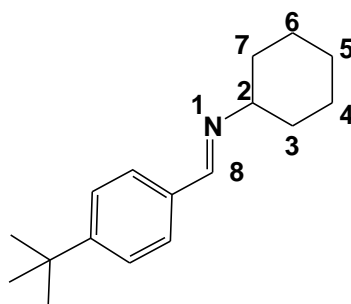
(*E*)-*N*-(2,4-Dimethoxybenzylidene)cyclohexanamine **76d** was successfully synthesized as described by synthetic procedure A {2,4-dimethoxybenzaldehyde (589 mg, 3.55 mmol) and cyclohexylamine (422 mg, 4.25 mmol)} and synthetic procedure B {2,4-dimethoxybenzaldehyde (330 mg, 1.99 mmol) and cyclohexylamine (236 mg, 2.38 mmol)}; **Physical characteristics:** pale yellow solid; **Yields:** 711 mg, 81% for synthetic procedure A and 487 mg, 99% for synthetic procedure B; **Melting point:** 55-58°C; **¹H NMR** (400 MHz, CDCl₃) δ 8.63 (1H, s, N=CH), 7.87 (1H, d, *J* = 8.8 Hz, ArH), 6.47 (1H, d, *J* = 6.8 Hz, ArH), 6.40 (1H, s, ArH), 3.81 (6H 2 x s, 2 x ArOCH₃), 3.11-3.80 (1H, m, 2-CH), 1.20-1.82 (10H, m, 3-, 4-, 5-, 6- & 7- CH₂); **¹³C NMR** (101 MHz, CDCl₃) δ 162.7 and 159.8 (2 x ArCOCH₃), 154.1 (N=CH), 127.5, 118.4, 105.2, 98.0 (ArC), 70.2 (2-C), 55.4 and 55.3 (2 x ArCOCH₃), 34.6 (3- & 7-C), 25.7 (2- & 6-C), 25.0 (5-C).

8.2.1.15. (*E*)-*N*-(Benzo[*d*][1,3]dioxol-5-ylmethylene)cyclohexanamine 76e



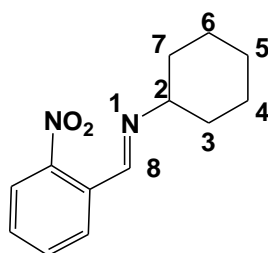
(*E*)-*N*-(Benzo[*d*][1,3]dioxol-5-ylmethylene)cyclohexanamine **76e** was successfully synthesized as described by synthetic procedure A {piperonal (583 mg, 3.88 mmol) and cyclohexylamine (462 mg, 4.66 mmol)} and synthetic procedure B {piperonal (339 mg, 2.26 mmol) and cyclohexylamine (269 mg, 2.71 mmol)}; **Physical characteristics**: pale yellow solid; **Yields**: 807 mg, 90% for synthetic procedure A and 507 mg, 97% for synthetic procedure B; **Melting point**: 64-67°C (lit^{346,347}); **¹H NMR** (400 MHz, CDCl₃) δ 8.18 (1H, s, N=CH), 7.34 (1H, s, ArH) 7.07 (1H, d, *J* = 6.8 Hz, ArH), 6.79 (1H, d, *J* = 8.0 Hz, ArH), 5.96 (2H, s, ArOCH₂O), 3.10-3.16 (1H, m, 2-CH), 1.36-1.84 (10H, m, 3-, 4-, 5-, 6- & 7- CH₂); **¹³C NMR** (101 MHz, CDCl₃) δ 157.6 (N=CH), 149.4 and 148.1 (ArCOCH₂O), 131.4, 123.9, 107.9 (ArC), 101.3 (ArCOCH₂O), 61.0 (2-C), 34.3 (3- & 7-C), 25.6 (4- & 6-C), 24.8 (5-C).

8.2.1.16. (*E*)-*N*-(4-*tert*-Butylbenzylidene)cyclohexanamine **76f**



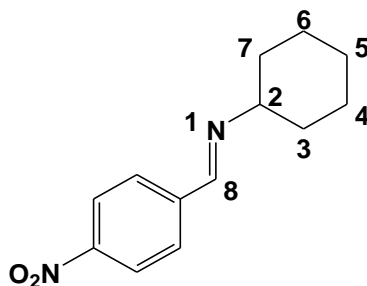
(*E*)-*N*-(4-*tert*-Butylbenzylidene)cyclohexanamine **76f** was successfully synthesized as described by synthetic procedure A {4-*tert*-butylbenzaldehyde (550 mg, 3.39 mmol) and cyclohexylamine (404 mg, 4.07 mmol)} and synthetic procedure B {4-*tert*-butylbenzaldehyde (357 mg, 2.20 mmol) and cyclohexylamine (2.64 mmol)}; **Physical characteristics**: white solid; **Yields**: 767 mg, 93% for synthetic procedure A and 530 mg, 99% for synthetic procedure B; **Melting point**: 45-48°C; **¹H NMR** (400 MHz, CDCl₃) δ 8.30 (1H, s, N=CH), 7.65 (2H, d, *J* = 8.4 Hz, ArH), 7.41 (2H, d, *J* = 8.4 Hz, ArH), 3.15-3.20 (1H, m, 2-CH), 1.33-1.86 [19H, m, 3-, 4-, 5-, 6- & 7- CH₂ and ArC(CH₃)₃]; **¹³C NMR** (101 MHz, CDCl₃) δ 158.4 (N=CH), 153.7 [ArCC(CH₃)₃], 134.0, 127.9, 125.5 (ArC), 70.1 (2-C), 34.9 [ArCC(CH₃)₃], 34.4 (3- & 7-C), 31.3 [ArCC(CH₃)₃], 25.7 (4- & 6-C) 24.9 (5-C).

8.2.1.17. (*E*)-*N*-(2-Nitrobenzylidene)cyclohexanamine **76h**



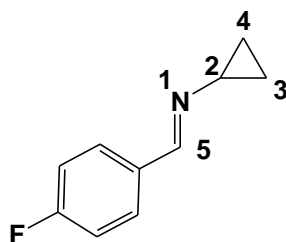
(*E*)-*N*-(2-Nitrobenzylidene)cyclohexanamine **76h** was successfully synthesized as described by synthetic procedure B using 2-nitrobenzaldehyde (190 mg, 1.26 mmol) and cyclohexylamine (1.51 mmol); **Physical characteristics:** yellow oil; **Yield:** 278 mg, 95%; **¹H NMR** (400 MHz, CDCl₃) δ 8.70 (1H, s, N=CH), 7.97-8.03 (2H, m, ArH), 7.61-7.65 (1H, m, ArH), 7.49 (1H, m, ArH), 3.28-3.33 (1H, m, 2-CH), 1.23-1.85 (10H, m, 3-, 4-, 5-, 6- & 7- CH₂); **¹³C NMR** (101 MHz, CDCl₃) δ 154.6 (N=CH), 148.7 (ArCNO₂), 133.4, 131.6, 130.3, 12.7, 124.1 (ArC), 70.0 (2-C), 34.0 (3- & 7-C), 25.5 (4- & 6-C), 24.5 (5-C).

8.2.1.17. (*E*)-*N*-(4-Nitrobenzylidene)cyclohexanamine **76i**



(*E*)-*N*-(4-Nitrobenzylidene)cyclohexanamine **76i** was successfully synthesized as described by synthetic procedure B using 4-nitrobenzaldehyde (230 mg, 1.52 mmol) and cyclohexylamine (181 mg, 1.82 mmol); **Physical characteristics:** yellow oil; **Yield:** 321 mg, 91%; **¹H NMR** (400 MHz, CDCl₃) δ 8.38 (1H, s, N=CH), 8.23-8.25 (2H, m, ArH), 7.86-7.89 (2H, m, ArH), 3.25-3.30 (1H, m, 2-CH), 1.25-1.87 (10H, m, 3-, 4-, 5-, 6- & 7- CH₂); **¹³C NMR** (101 MHz, CDCl₃) δ 156.2 (N=CH), 148.8 (ArCNO₂), 142.1, 128.7, 128.8 (ArC), 70.1 (2-C), 34.1 (3- & 7-C), 25.5 (4- & 6-C), 24.6 (5-C).

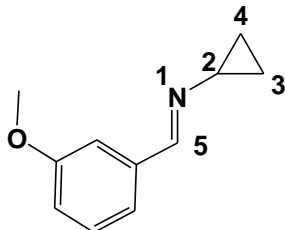
8.2.1.19. (*E*)-*N*-(4-Fluorobenzylidene)cyclopropanamine **77a**



(*E*)-*N*-(4-Fluorobenzylidene)cyclopropanamine **77a** was successfully synthesized as described by synthetic procedure A using 4-fluorobenzaldehyde (424 mg, 3.42 mmol) and cyclopropylamine (234 mg, 4.10 mmol); **Physical characteristics:** brown oil; **Yield:** 430 mg, 77%; **¹H NMR** (400 MHz, CDCl₃) δ 8.40 (1H, s, N=CH), 7.64 (2H, d, *J* = 8.6 Hz, ArH), 7.04 (2H, t, *J* = 8.6 Hz, ArH), 2.98-3.02 (1H, m, 2-CH), 0.89-0.99 (4H, m, 3- & 4-CH₂); **¹³C NMR** (101 MHz, CDCl₃) δ

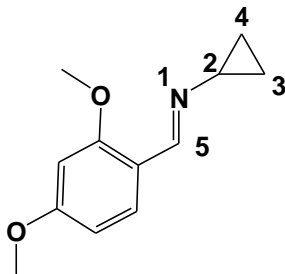
163.9 (d, $^1J_{\text{F,C}} = 249.6$ Hz, *para*-CF), 156.9 (N=CH), 132.8 (d, $^4J_{\text{F,C}} = 3.0$ Hz, 1'-C), 129.8 (d, $^3J_{\text{F,C}} = 8.1$ Hz, *ortho*-C), 115.5 (d, $^2J_{\text{F,C}} = 21.1$ Hz, *meta*-C), 41.8 (2-C), 8.70 (3- & 4-C)..

8.2.1.20. (*E*)-*N*-(3-Methoxybenzylidene)cyclopropanamine 77c



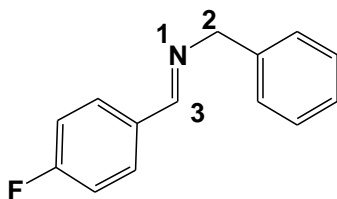
(*E*)-*N*-(3-Methoxybenzylidene)cyclopropanamine **77c** was successfully synthesized as described by synthetic procedure A using 3-methoxybenzaldehyde (483 mg, 3.55 mmol) and cyclopropylamine (243 mg, 4.26 mmol); **Physical characteristics:** brown oil; **Yield:** 572 mg, 92%; **$^1\text{H NMR}$** (400 MHz, CDCl_3) δ 8.47 (1H, s, N=CH), 7.28-7.37 (3H, m, ArH), 6.98 (1H, dd, $J = 3.5$ Hz, ArH), 3.89 (3H, s, ArOCH_3), 3.07-3.10 (1H, m, 2-CH), 0.98-1.05 (4H, m, 3- & 4- CH_2); **$^{13}\text{C NMR}$** (101 MHz, CDCl_3): δ 159.8 (ArCOCH_3), 158.2 (N=CH), 137.9, 129.5, 120.7, 116.6, 111.2 (ArC), 55.3 (ArCOCH_3), 41.8 (2-C), 8.77 (3- & 4-C).

8.2.1.21. (*E*)-*N*-(2,4-Dimethoxybenzylidene)cyclopropanamine 77d



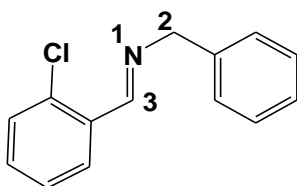
(*E*)-*N*-(2,4-dimethoxybenzylidene)cyclopropanamine **77d** was successfully synthesized as described by synthetic procedure A using 2,4-dimethoxybenzaldehyde (450 mg, 2.71 mmol) and cyclopropylamine (186 mg, 3.25 mmol); **Physical characteristics:** pale yellow solid; **Yield:** 484 mg, 87% for synthetic procedure A; **$^1\text{H NMR}$** (400 MHz, CDCl_3) δ 8.77 (1H, s, N=CH), 7.79 (1H, d, $J = 8.4$ Hz, ArH), 6.47 (1H, d, $J = 8.4$ Hz, ArH), 6.42 (1H, s, ArH), 3.81 and 3.84 (6H 2 x s, 2 x ArOCH_3), 2.99-3.02 (1H, m, 2-CH), 0.85-0.93 (4H, m, 3- & 4- CH_2); **$^{13}\text{C NMR}$** (101 MHz, CDCl_3): δ 162.7 and 159.8 (2 x ArCOCH_3), 158.6 (N=CH), 129.5, 116.6, 111.2, 98.0 (ArC), 55.4 and 55.3 (2 x ArCOCH_3), 41.8 (1-C), 8.77 (2- & 3-C).

8.2.1.22. (*E*)-*N*-(4-Fluorobenzylidene)-1-phenylmethanamine 78a



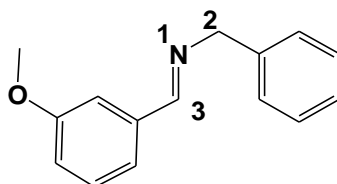
(*E*)-*N*-(4-Fluorobenzylidene)-1-phenylmethanamine **78a** was successfully synthesized as described by synthetic procedure B using 4-fluorobenzaldehyde (161 mg, 1.30 mmol) and benzylamine (167 mg, 1.55 mmol); **Physical characteristics:** orange solid; **Yield:** 255 mg, 92%; **¹H NMR** (400 MHz, CDCl₃) δ 8.37 (1H, s, CH=N), 7.78-7.82 (2H, m, ArH) 7.05 (7H, m, ArH), 4.83 (2H, s, CH=NCH₂); **¹³C NMR** (101 MHz, CDCl₃) δ 165.5 (d, ¹J_{C,F} = 250 Hz, *para*-CF), 160.4 (CH=N), 139.1 (ArC), 132.4 (d, ¹J_{C,F} = 3 Hz, 1'-C), 130.1, 130.0, 128.5 (d, ³J_{C,F} = 8 Hz, *ortho*-C) 127.9 (ArC), 115.6 (d, ¹J_{C,F} = 22 Hz, *meta*-C), 64.9 (CH=NCH₂).

8.2.1.23. (*E*)-*N*-(2-Chlorobenzylidene)-1-phenylmethanamine 78b



(*E*)-*N*-(2-chlorobenzylidene)-1-phenylmethanamine **78b** was successfully synthesized as described by synthetic procedure B using 2-chlorobenzaldehyde (163 mg, 1.16 mmol) and benzylamine (149 mg, 1.39 mmol); **Physical characteristics:** pale yellow oil; **Yield:** 248 mg, 93%; **¹H NMR** (400 MHz, CDCl₃) δ 8.86 (1H, s, CH=N), 8.01 (1H, dd, *J* = 6 Hz, 1.2 Hz, ArH) 7.05 (8H, m, ArH), 4.89 (2H, s, CH=NCH₂); **¹³C NMR** (101 MHz, CDCl₃) δ 158.7 (CH=N), 139.0, 135.2, 133.1, 131.6, 129.7, 128.6, 128.3, 128.0, 127.1, 127.0 (ArC); 65.3 (CH=NCH₂).

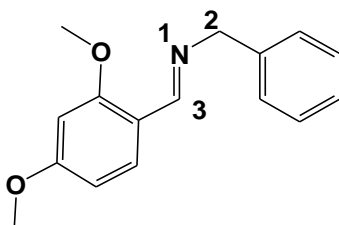
8.2.1.24. (*E*)-*N*-(3-Methoxybenzylidene)-1-phenylmethanamine 78c



(*E*)-*N*-(3-Methoxybenzylidene)-1-phenylmethanamine **78c** was successfully synthesized as described by synthetic procedure B using 3-methoxybenzaldehyde (127 mg, 0.93 mmol) and benzylamine (120 mg, 1.12 mmol); **Physical characteristics:** pale yellow oil; **Yield:** 205 mg,

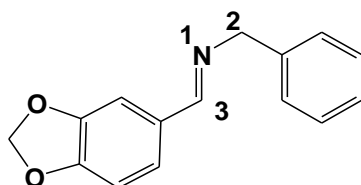
98%; $^1\text{H NMR}$ (400 MHz, CDCl_3) δ 8.29 (1H, s, $\text{CH}=\text{N}$), 7.31 (1H, d, $J = 8.4$ Hz, ArH), 6.91-7.29 (8H, m, ArH), 4.72 (2H, s, $\text{CH}=\text{NCH}_2$), 3.76 (3H, s, ArOCH_3); $^{13}\text{C NMR}$ (101 MHz, CDCl_3) δ 161.9 ($\text{CH}=\text{N}$), 159.8 (ArCOCH_3), 139.1, 137.5, 129.5, 128.4, 127.9, 126.9, 121.9, 117.5, 115.6 (ArC), 64.9 ($\text{C}=\text{NCH}_2$), 55.3 (ArCOCH_3).

8.2.1.25. (*E*)-*N*-(2,4-Dimethoxybenzylidene)-1-phenylmethanamine 78d



(*E*)-*N*-(2,4-Dimethoxybenzylidene)-1-phenylmethanamine **78d** was successfully synthesized as described by synthetic procedure B using 2,4-dimethoxybenzaldehyde (170 mg, 1.02 mmol) and benzylamine (132 mg, 1.23 mmol); **Physical characteristics**: yellow oil; **Yield**: 234 mg, 90%; $^1\text{H NMR}$ (400 MHz, CDCl_3) δ 8.89 (1H, s, $\text{CH}=\text{N}$), 8.11 (1H, d, $J = 8.4$ Hz, ArH), 7.36-7.47 (5H, m, ArH), 6.5-6.66 (2H, m, ArH), 4.97 (2H, s, $\text{CH}=\text{NCH}_2$), 3.95 and 3.97 (6H, 2 x s, 2 x ArOCH_3); $^{13}\text{C NMR}$ (101 MHz, CDCl_3) δ 163.0 and 160.1 (2 x ArCOCH_3), 157.4 ($\text{CH}=\text{N}$), 139.9, 128.6, 128.5, 128.3, 127.9, 117.9, 105.3, 98.0 (ArC), 65.5 ($\text{C}=\text{NCH}_2$), 55.4 and 55.3 (2 x ArCOCH_3).

8.2.1.26. (*E*)-*N*-(Benzo[*d*][1,3]dioxol-5-ylmethylene)-1-phenylmethanamine 78e



(*E*)-*N*-(Benzo[*d*][1,3]dioxol-5-ylmethylene)-1-phenylmethanamine **78e** was successfully synthesized as described by synthetic procedure B using piperonal (141 mg, 0.94 mmol) and benzylamine (121 mg, 1.13 mmol); **Physical characteristics**: white solid; **Yield**: 214 mg, 95%; **Melting point**: 64-70°C (lit.³⁴⁸); $^1\text{H NMR}$ (400 MHz, CDCl_3) δ 8.18 (1H, s, $\text{CH}=\text{N}$), 7.04-7.34 (8H, m, ArH), 6.73 (1H, d, $J = 8.8$ Hz, ArH), 5.90 (2H, s, ArOCH_2O), 4.96 (2H, s, $\text{C}=\text{NCH}_2$); $^{13}\text{C NMR}$ (101 MHz, CDCl_3) δ 161.0 ($\text{C}=\text{N}$), 149.9 and 148.2 (2 x ArCOCH_2O), 139.4, 131.0, 128.4, 127.9, 126.9, 124.5, 108.0, 106.7 (ArC), 101.4 (ArCOCH_2O), 64.7 ($\text{C}=\text{NCH}_2$).

8.2.2. Synthesis of 1-substituted-5-aryl-1*H*-imidazole

8.2.2.1. Stepwise van Leusen general synthetic procedure C

In a 100 ml three-necked flask equipped with a magnetic stirrer bar was introduced *N*-arylidene alkylamine (1 molar equivalent), TosMIC (1.5 molar equivalents) and K₂CO₃ (1.3 molar equivalents). An inert atmosphere was then created by degassing through evacuating and refilling with argon three times, followed by introduction of dry acetonitrile (5 ml). The resulting reaction mixture was then refluxed for 72 hours (monitored by TLC) under argon. Upon completion of the reaction, the solvent was evaporated *in vacuo* to afford brown oily crude material which was then purified by column chromatography [on silica; elution with hexane-EtOAc (1:2), followed by 100% ethyl acetate] to afford the desired pure 1-substituted-5-aryl-1*H*-imidazoles with R_f values of between 0.78-0.8

8.2.2.2. Microwave assisted van Leusen general synthetic procedure D

In a 10 ml microwave reaction vessel equipped with a magnetic stirrer bar was introduced *N*-arylidene alkylamine (1 molar equivalent), TosMIC (1.5 molar equivalents), K₂CO₃ (1.2 molar equivalents). An inert atmosphere was created by degassing through evacuating and refilling with argon three times, followed by addition of dry acetonitrile (5 ml). The resulting reaction mixture was then microwave irradiated at a set temperature of 90°C and a power of 120 Watts for 7 hours in a sealed vessel. The progress of the reaction was monitored by TLC. After cooling to room temperature, the solvent was concentrated *in vacuo* to give brown oily crude material which was then purified by column chromatography on silica gel as described in synthetic procedure C to furnish the desired 1-substituted-5-aryl-1*H*-imidazoles.

8.2.2.3. Three -component van Leusen reaction general synthetic procedure E

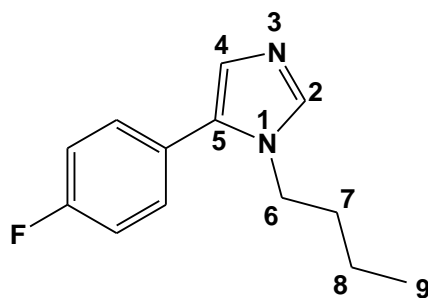
In order to generate the *N*-arylidene alkylamine *in situ*, aryl aldehyde (1 molar equivalent) and an aliphatic amine (1.1 molar equivalents) were introduced into a 10 ml microwave reaction vessel equipped with magnetic stirrer bar. The resulting reaction mixture was then microwave irradiated at a set temperature of 60°C using standard method for 4 minutes. After cooling to room temperature, TosMIC (1.5 molar equivalents) and K₂CO₃ (1.3 molar equivalent) were then added. An inert atmosphere was created by degassing through evacuating and refilling with argon three times, followed by addition of dry MeCN (5 ml). The resulting reaction mixture was then irradiated at a set temperature of 90°C and a power of 120 Watts for 7 hours in a sealed vessel. The progress of the reaction was monitored by TLC. After cooling to room temperature, the solvent was concentrated *in vacuo* to give a brown oily residue which was then purified by column

chromatography on silica gel as described in synthetic procedure C to furnish the desired 1-substituted-5-aryl-1*H*-imidazoles. (**N.B.**: in cases where aniline derivatives were used, the reaction mixture was irradiated for 1 hour prior to addition of TosMIC and K₂CO₃).

8.2.2.4. Three -component van Leusen reaction general synthetic procedure F

In order to generate the *N*-arylidene alkylamine *in situ* appropriate aryl aldehyde (1 molar equivalent) and an aliphatic amine (1.1 molar equivalents) were introduced into a 10 ml microwave reaction vessel equipped with a magnetic stirrer bar. The resulting reaction mixture was then microwave irradiated at a set temperature of 60°C using standard method for 4 minutes. After cooling to room temperature, K₂CO₃ (1.3 molar equivalent) and TosMIC (1.5 molar equivalent) were then introduced. An inert atmosphere was created by degassing through evacuating and refilling with argon three times, followed by introduction of anhydrous MeOH (5 ml). The resulting reaction mixture was then irradiated at set temperature of 90°C and a power of 120 Watts for 7 hours in a sealed vessel. The progress of the reaction was monitored by TLC. After cooling to room temperature, the solvent was concentrated *in vacuo* gave brown oily residue which was then purified by column chromatography on silica gel as described in synthetic procedure C.

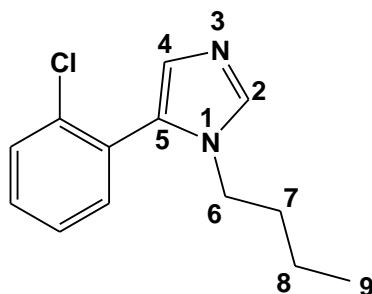
8.2.2.5. 1-Butyl-5-(4-fluorophenyl)-1*H*-imidazole 79a



1-Butyl-5-(4-fluorophenyl)-1*H*-imidazole **79a** was successfully synthesized according to procedure C {*N*-(4-fluorobenzylidene)butan-1-amine **75a** (345 mg, 1.93 mmol), TosMIC (565 mg, 2.89 mmol) and K₂CO₃ (346 mg, 2.51 mmol)} and synthetic procedure D {*N*-(4-fluorobenzylidene)butan-1-amine (317 mg, 1.77 mmol), TosMIC (518 mg, 2.66 mmol) and K₂CO₃ (318 mg, 2.30 mmol)}; **Physical characteristics**: brown oil; **Yields**: 160 mg, 38% for synthetic procedure C and 213 mg, 55% for synthetic procedure D; **¹H NMR** (400 MHz, CDCl₃) δ 7.55 (1H, s, 2-CH), 7.30-7.34 (2H, m, ArH), 7.10-7.14 (2H, m, ArH), 7.01 (1H, s, 4-CH) 3.89 (2H, t, *J* = 7.0 Hz, NCH₂), 1.56-1.60 (2H, m, 7-CH₂), 1.19-1.24 (2H, m, 8-CH₂), 0.81 (3H, t, *J* = 7.4 Hz, 9-CH₃); **¹³C NMR** (101 MHz, CDCl₃) δ 163.9 (d, *J*_{C,F} = 246.9 Hz, *para*-CF),

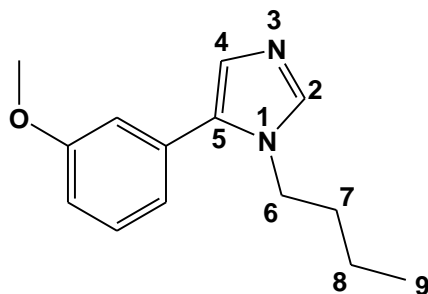
138.0 (2-CH), 130.7 (d, $^4J_{\text{FC}} = 3.0$ Hz, 1'-C), 130.6 (d, $^3J_{\text{FC}} = 8.1$ Hz, *ortho*-C), 128.0 (4-C), 115.9 (d, $^2J_{\text{FC}} = 21.1$ Hz, *meta*-C), 45.0 (6-C), 32.8 (7-C), 19.6 (8-C), 13.4 (9-C); **FTIR** $\nu_{\text{max}}/\text{cm}^{-1}$ (KBr): 3388, 3104, 2960, 2873, 1682, 1599, 1516, 1456, 1448, 1221, 1110, 1023, 915, 853, 755, 695, 658, 603, 537; **HRMS** (ESI-TOF) m/z : $[\text{M}+\text{H}]^+$ Calcd for $\text{C}_{13}\text{H}_{16}\text{FN}_2$ 219.1292, found 219.1294.

8.2.2.6. 1-Butyl-5-(2-chlorophenyl)-1*H*-imidazole 79b



1-Butyl-5-(2-chlorophenyl)-1*H*-imidazole **79b** was successfully synthesized according to procedure C {*N*-(2-chlorobenzylidene)butan-1-amine **75b** (313 mg, 1.60 mmol), TosMIC (469 mg, 2.40 mmol) and K_2CO_3 (288 mg, 208 mmol)} and synthetic procedure D {*N*-(2-chlorobenzylidene)butan-1-amine (266 mg, 1.36 mmol), TosMIC (398 mg, 2.04 mmol) and K_2CO_3 (244 mg, 1.77 mmol)}; **Physical characteristics**: brown oil; **Yields**: 75 mg, 20% for synthetic procedure C and 83 mg, 26% for synthetic procedure D; **^1H NMR** (400 MHz, CDCl_3) δ 7.58 (1H, s, 2-CH), 7.32-7.50 (4H, m, ArH), 7.02 (1H, s, 4-CH), 3.78 (2H, t, $J = 7.2$ Hz, NCH_2), 1.50-1.57 (2H, m, 7- CH_2), 1.15-1.22 (2H, m, 8- CH_2), 0.77 (3H, t, $J = 7.2$ Hz, 9- CH_3); **^{13}C NMR** (101 MHz, CDCl_3) δ 137.5 (2-CH), 135.0 (5-C), 132.8, 130.2, 129.8, 129.7, 129.3 (ArC), 128.9 (4-C), 115.6 (ArC), 45.1 (6-C), 32.7 (7-C), 19.5 (8-C), 13.4 (9-C); **FTIR** $\nu_{\text{max}}/\text{cm}^{-1}$ (KBr): 3401, 2959, 2873, 1727, 1633, 1557, 1458, 1367, 1285, 1220, 1145, 1114, 1035, 916, 767, 659, 537; **HRMS** (ESI-TOF) m/z : $[\text{M}+\text{H}]^+$ Calcd for $\text{C}_{13}\text{H}_{16}\text{ClN}_2$ 235.0995, found 235.1002.

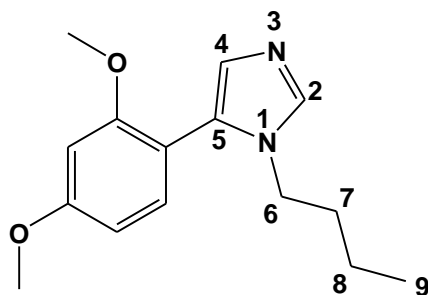
8.2.2.7. 1-Butyl-5-(3-methoxyphenyl)-1*H*-imidazole 79c



1-Butyl-5-(3-methoxyphenyl)-1*H*-imidazole **79c** was successfully synthesized according to procedure D using *N*-(3-methoxybenzylidene)butan-1-amine **75c** (176 mg, 0.92 mmol), TosMIC

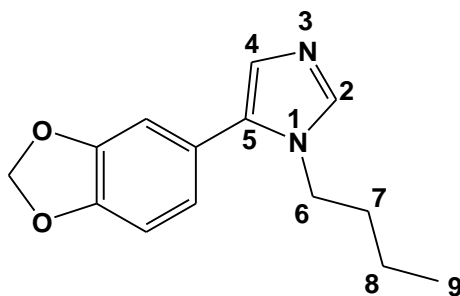
(407 mg, 1.38 mmol) and K_2CO_3 (171 mg, .24 mmol); **Physical characteristics:** yellow oil; **Yield:** 127 mg, 60%; **1H NMR** (400 MHz, $CDCl_3$) δ 7.54 (1H, s, 2-CH), 7.31 (1H, t, $J = 6.8$ Hz, ArH), 7.04 (1H, s, 4-CH), 6.89-6.94 (3H, m, ArH), 3.83 (2H, t, $J = 7.4$ Hz, NCH_2), 3.83 (3H, s, $ArOCH_3$), 1.57-1.65 (2H, m, 7- CH_2), 1.18-1.27 (2H, m, 8- CH_2), 0.81 (3H, t, $J = 7.4$ Hz, 9- CH_3); **^{13}C NMR** (101 MHz, $CDCl_3$) δ 159.7 ($ArCOCH_3$), 138.0 (2-C), 132.8 (5-C), 131.5, 129.7 (ArC), 128.1 (4-C), 121.1, 114.5, 113.3 (ArC), 55.3 ($ArCOCH_3$), 45.1 (6-C), 32.8 (7-C), 19.6 (8-C), 13.4 (9-C); **FTIR** ν_{max}/cm^{-1} (KBr): 3383, 2958, 2873, 1682, 1610, 1580, 1489, 1290, 1212, 1169, 1116, 1050, 1029, 919, 845, 785, 698, 656, 570; **HRMS** (ESI-TOF) m/z : $[M+H]^+$ Calcd for $C_{14}H_{19}N_2O$ 231.1492, found 231.1498.

8.2.2.8. 1-Butyl-5-(2,4-dimethoxyphenyl)-1*H*-imidazole 79d



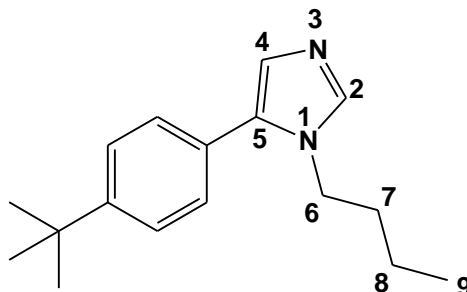
1-Butyl-5-(2,4-dimethoxyphenyl)-1*H*-imidazole **79d** was successfully synthesized according to procedure C {*N*-(2,4-dimethoxybenzylidene)butan-1-amine **75d** (107 mg, 0.55 mmol), TosMIC (245 mg, 0.83 mmol) and K_2CO_3 (100 mg, 0.72 mmol)}; synthetic procedure D {*N*-(2,4-dimethoxybenzylidene)butan-1-amine (137 mg, 0.71 mmol), TosMIC (209 mg, 1.07 mmol) and K_2CO_3 (127 mg, 0.92 mmol)} and synthetic procedure E {2,4-dimethoxybenzaldehyde (81 mg, 0.49 mmol) and *n*-butylamine (43 mg, 0.59 mmol) TosMIC (144 mg, 0.74 mmol) and K_2CO_3 (88 mg, 0.64 mmol)}; **Physical characteristics:** brown oil; **Yields:** 115 mg, 80 % for synthetic procedure C and 161 mg, 87% synthetic procedure D, 103 mg, 81% for synthetic procedure E; **1H NMR** (400 MHz, $CDCl_3$) δ 7.50 (1H, s, 2-CH), 7.09 (1H, d, $J=8.8$ Hz, ArH), 6.88 (1H, s, 4-CH), 6.52 (2H, d, $J = 7.6$ Hz, ArH), 3.84 and 3.75 (6H, 2 x s, 2 x $ArOCH_3$), 3.72 (2H, t, $J = 7.2$ Hz, NCH_2), 1.51-1.58 (2H, m, 7- CH_2), 1.15 (2H, m, 8- CH_2), 0.78 (3H, t, $J = 7.2$ Hz, 9- CH_3); **^{13}C NMR** (101 MHz, $CDCl_3$) δ 161.4 and 158.3 (2 x $ArCOCH_3$), 137.0 (4-CH), 132.8 (ArC), 129.5 (5-C), 128.0 (4-CH), 111.5, 104.4, 98.6 (Ar-C), 55.3 and 55.2 (2 x $ArCOCH_3$), 45.0 (6-C), 32.5 (7-C), 19.5 (8-C), 13.3 (9-C); **FTIR** ν_{max}/cm^{-1} (KBr): 3383, 2958, 2875, 1722, 1678, 1616, 1578, 1459, 1416, 1364, 1305, 1283, 1208, 1160, 1132, 1030, 92, 1030, 922, 834, 660, 618; **HRMS** (ESI-TOF) m/z : $[M+H]^+$ Calcd for $C_{15}H_{21}N_2O_2$ 261.1598, found 261.1587.

8.2.2.9. 5-(Benzo[*d*][1,3]dioxol-5-yl)-1-butyl-1*H*-imidazole 79e



5-(Benzo[*d*][1,3]dioxol-5-yl)-1-butyl-1*H*-imidazole **79e** was successfully synthesized according to procedure C {*N*-(benzo[*d*][1,3]dioxol-5-ylmethylene)butan-1-amine **75e** (320 mg, 1.56 mmol), TosMIC (459 mg, 2.34 mmol) and K₂CO₃ (281 mg, 2.03 mmol)}; synthetic procedure D {*N*-(benzo[*d*][1,3]dioxol-5-ylmethylene)butan-1-amine (372 mg, 1.81 mmol), TosMIC (531 mg, 2.72 mmol) and K₂CO₃ (325 mg, 2.35 mmol)} and synthetic procedure E {piperonal (96 mg, 0.63 mmol) and *n*-butylamine (55 mg, 0.76 mmol), TosMIC (186 mg, 0.95 mmol) and K₂CO₃ (113 mg, 0.82 mmol)}; **Physical characteristics:** brown oil; **Yields:** 164 mg, 43% synthetic procedure C, 212 mg, 48% for synthetic procedure D and 84 mg, 55% for synthetic procedure E; **¹H NMR** (400 MHz, CDCl₃) δ 7.48 (1H, s, 2-CH), 6.94 (1H, s, 4-CH), 6.77-6.84 (3H, m, ArH), 5.97 (2H, s, ArOCH₂O), 3.87 (2H, t, *J* = 7.2 Hz, NCH₂), 1.53-1.60 (2H, m, 7-CH₂), 1.15-1.24 (2H, m, 8-CH₂), 0.79 (3H, t, *J* = 7.2 Hz, 9-CH₃); **¹³C NMR** (101 MHz, CDCl₃) δ 147.7 and 147.4 (2 x ArCOCH₂O), 137.6 (2-C), 132.5 (5-C), 127.7 (4-C), 123.7, 122.6, 109.2, 108.4 (ArC), 101.2 (ArCOCH₂O), 44.8 (6-C), 32.7 (7-C), 19.5 (8-C), 13.3 (9-C); **FTIR** ν_{\max} /cm⁻¹ (KBr): 3378, 2959, 2931, 2873, 1721, 1683, 1609, 1558, 1478, 1379, 1331, 1237, 1113, 1038, 933, 879, 812, 660; **HRMS** (ESI-TOF) *m/z*: [M+H]⁺ Calcd for C₁₇H₂₅N₂O₂ 245.1285, found 245.1276.

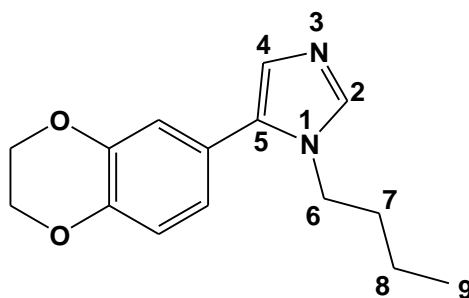
8.2.2.10. 1-Butyl-5-(4-*tert*-butylphenyl)-1*H*-imidazole 79f



1-Butyl-5-(4-*tert*-butylphenyl)-1*H*-imidazole **79f** was successfully synthesized according to procedure C {*N*-(4-*tert*-butylbenzylidene)butan-1-amine **75f** (322 mg, 1.48 mmol), TosMIC (433 mg, 2.22 mmol) and K₂CO₃ (265 mg, 1.92 mmol)} and synthetic procedure D {*N*-(4-*tert*-

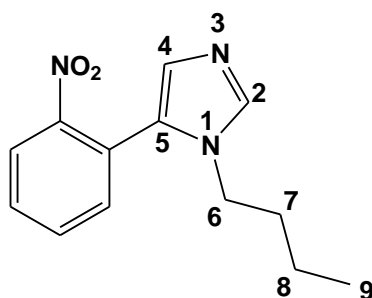
butylbenzylidene)butan-1-amine (382 mg, 1.76 mmol), TosMIC (515 mg, 2.64 mmol) and K_2CO_3 (317 mg, 2.29 mmol)}; **Physical characteristics:** brown oil; **Yields:** 167 mg, 44% for synthetic procedure C and 235 mg, 52% for synthetic procedure D; **1H NMR** (400 MHz, $CDCl_3$) δ 7.55 (1H, s, 4-CH), 7.43 (2H, $J = 8.4$ Hz, ArH), 7.28 (2H, $J = 8.4$ Hz, ArH), 7.03 (1H, s, 4-CH), 3.93 (2H, t, $J = 7.2$ Hz, NCH_2), 1.60-1.67 (2H, m, 7- CH_2), 1.35 [9H, s, $C(CH_3)_3$], 1.24-1.30 (2H, m, 8- CH_2), 0.83 (3H, t, $J = 7.4$ Hz, 9- CH_3); **^{13}C NMR** (101 MHz, $CDCl_3$) δ 151.0 [ArCC(CH_3) $_3$], 137.8 (2-C), 132.9 (5-C), 128.5 (ArC), 127.8 (4-C), 127.2, 125.9, 45.0 (6-C), 34.6 [ArCC(CH_3) $_3$], 32.9 (7-C), 31.6, [ArCC(CH_3) $_3$], 19.7 (8-C), 13.5 (9-C); **FTIR** ν_{max}/cm^{-1} (KBr): 3373, 2960, 2931, 2865, 1717, 1682, 1614, 1556, 1463, 1363, 1269, 1220, 1114, 1033, 916, 839, 659, 571; **HRMS** (ESI-TOF) m/z : $[M+H]^+$ Calcd for $C_{17}H_{25}N_2$ 257.2012, found 257.2008.

8.2.2.11. 1-Butyl-5-(2,3-dihydro-1,4-benzodioxin-6-yl)-1*H*-imidazole 79g



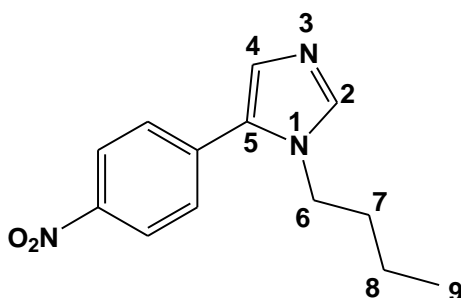
1-Butyl-5-(2,3-dihydro-1,4-benzodioxin-6-yl)-1*H*-imidazole **79g** was successfully synthesized according to procedure C using *N*-(2,3-dihydrobenzo[*b*][1,4]dioxin-6-yl)methylene)butan-1-amine **75g** (112 mg, 0.51 mmol), TosMIC (150 mg, 0.77mmol) and K_2CO_3 (91 mg, 0.66 mmol); **Physical characteristics:** brown oil; **Yield:** 71 mg, 54%; **1H NMR** (400 MHz, $CDCl_3$) δ 7.49 (1H, s, 2-CH), 6.96 (1H, s, 4-CH), 6.79-6.90 (3H, m, ArH), 4.27 (4H, s, $ArOCH_2CH_2O$), 3.89 (2H, t, $J = 7.2$ Hz, NCH_2), 1.55-1.63 (2H, m, 7- CH_2), 1.90-1.25 (2H, m, 8- CH_2), 0.81 (3H, t, $J = 7.2$ Hz, 9- CH_3); **^{13}C NMR** (101 MHz, $CDCl_3$) δ 143.5 and 143.4 ($ArCOCH_2CH_2O$), 137.6 (2-C), 132.4 (5-C), 127.7 (4-C), 123.3, 122.0, 117.7, 117.3 (ArC), 64.3 and 64.2 ($ArCOCH_2CH_2O$), 44.9 (6-C), 32.8 (7-C), 19.6 (8-C), 13.4 (9-C); **FTIR** ν_{max}/cm^{-1} (KBr): 3374, 2962, 2931, 2874, 1720, 1584, 1503, 1460, 1362, 1286, 1250, 1123, 1067, 921, 893, 815, 749, 658; **HRMS** (ESI-TOF) m/z : $[M+H]^+$ Calcd for $C_{15}H_{19}N_2O_2$ 259.1441, found 259.1434.

8.2.2.12. 1-Butyl-5-(2-nitrophenyl)-1*H*-imidazole 79h



1-Butyl-5-(2-nitrophenyl)-1*H*-imidazole **79h** was successfully synthesized according to the described general procedure D using *N*-(2-nitrobenzylidene)butan-1-amine **75h** (361 mg, 1.75 mmol), TosMIC (513 mg, 2.63 mmol) and K_2CO_3 (315 mg, 2.28 mmol); **Physical characteristics**: brown oil; **Yield**: 56 mg, 13%; **1H NMR** (400 MHz, $CDCl_3$) δ 8.01-8.03 (1H, m, ArH), 7.67 (1H, s, 2-CH), 7.41-7.69 (3H, m, ArH), 6.96 (1H, s, 4-CH), 3.71 (2H, t, $J=7.2$ Hz, NCH_2), 1.51-1.57 (2H, m, 7- CH_2), 1.15-1.23 (2H, m, 8- CH_2), 0.77 (3H, t, $J = 7.2$ Hz, 9- CH_3); **^{13}C NMR** (101 MHz, $CDCl_3$) δ 149.5 (ArCNO₂), 138.0 (2-C), 133.6 (5-C), 132.7, 130.4 (ArC), 129.9 (4-C), 128.6, 127.9, 124.6, 45.1 (6-C), 32.4 (7-C), 19.5 (8-C), 13.0 (9-C); **FTIR** ν_{max}/cm^{-1} (KBr): 3400, 3108, 2959, 2873, 1727, 1633, 1557, 1456, 1367, 1367, 1284, 1219, 1146, 1114, 1083, 1035, 916, 812, 768, 659, 537; **HRMS** (ESI-TOF) m/z : $[M+H]^+$ Calcd for $C_{13}H_{16}N_3O_2$ 246.1237, found 246.1240.

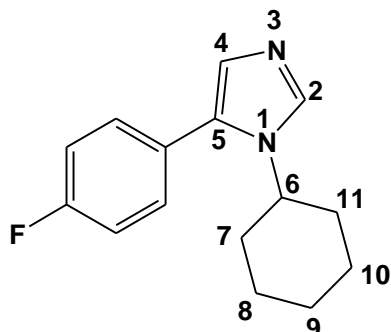
8.2.2.13. 1-Butyl-5-(4-nitrophenyl)-1*H*-imidazole 79i



1-Butyl-5-(4-nitrophenyl)-1*H*-imidazole **79i** was successfully synthesized according to the described general procedure D using *N*-(4-nitrobenzylidene)butan-1-amine **75i** (379 mg, 1.84 mmol), TosMIC (539 mg, 2.76 mmol) and K_2CO_3 (330 mg, 2.39 mmol); **Physical characteristics**: brown oil; **Yield**: 66 mg, 15%; **1H NMR** (400 MHz, $CDCl_3$) δ 8.28-8.31 (2H, m, ArH), 7.63 (1H, s, 2-CH), 7.26-7.56 (2H, m, ArH), 7.20 (1H, s, 4-CH), 4.01 (2H, t, $J=7.4$ Hz, 6- CH_2), 1.61-1.66 (2H, m, 7- CH_2), 1.21-1.29 (2H, m, 8- CH_2), 0.83 (3H, t, $J = 7.4$ Hz, 9- CH_3); **^{13}C NMR** (101 MHz, $CDCl_3$) δ 147.03 (ArCNO₂), 139.8 (2-C), 136.7 (5-C), 130.8, 130.2 (ArC), 128.6 (4-C), 126.8 (ArC), 45.6 (6-C), 32.8 (7-C), 19.6 (8-C), 13.4 (9-C); **FTIR** ν_{max}/cm^{-1} (KBr): 3388,

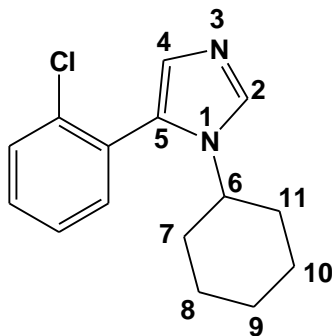
3103, 2960, 2873, 1682, 1599, 1516, 1456, 1368, 1221, 1110, 1023, 916, 854, 755, 696, 658, 536;
HRMS (ESI-TOF) m/z : $[M+H]^+$ Calcd for $C_{13}H_{16}N_3O_2$ 246.1237, found 246.1238.

8.2.2.14. 1-Cyclohexyl-5-(4-fluorophenyl)-1*H*-imidazole 80a



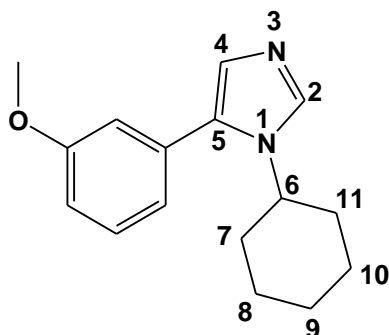
1-Cyclohexyl-5-(4-fluorophenyl)-1*H*-imidazole **80a** was successfully synthesized according to the described general procedure C {*N*-(4-fluorobenzylidene)cyclohexanamine **76a** (129 mg, 0.63 mmol), TosMIC (186 mg, 0.95 mmol) and K_2CO_3 (116 mg, 0.84 mmol)} and synthetic procedure D {*N*-(4-fluorobenzylidene)cyclohexanamine (172 mg, 0.84 mmol), TosMIC (246 mg, 1.26 mmol) and K_2CO_3 (140 mg, 1.01 mmol)}; **Physical characteristics**: pale yellow solid; **Yields**: 71 mg, 46% for synthetic procedure C, 105 mg, 51% for synthetic procedure D; **Melting point**: 111-114°C; **1H NMR** (400 MHz, $CDCl_3$) δ 7.64 (1H, s, 2-*CH*), 7.27-7.7.30 (2H, m, ArH), 7.01-7.13 (2H, m, ArH), 6.69 (1H, s, 4-*CH*) 3.79-3.87 (1H, m, NCH), 1.18-2.01 (10H, m, 7-, 8-, 9-, 10 and 11- CH_2); **^{13}C NMR** (101 MHz, $CDCl_3$) δ 163.7 (d, $^1J_{C,F}$ = 246.9 Hz, *para*-CF), 134.9 (2-C), 131.4 (5-C), 130.8 (d, $^4J_{F,C}$ = 3.0 Hz, 1'-C), 127.5 (4-C), 126.3 (d, $^3J_{F,C}$ = 8.1 Hz, *ortho*-C), 115.6 (d, $^2J_{F,C}$ = 21 Hz, *meta*-C), 54.5 (6-C), 34.7 (7- & 11-C), 25.6 (8- & 10-C), 25.0 (9-C); **FTIR** ν_{max}/cm^{-1} (KBr): 3109, 3091, 3070, 2942, 2857, 1665, 1630, 1609, 1557, 1491, 1470, 1455, 1357, 1265, 814, 664, 604, 565, 504; **HRMS** (ESI-TOF) m/z : $[M+H]^+$ Calcd for $C_{15}H_{18}FN_2$ 245.1449, found 245.1475.

8.2.2.15. 1-Cyclohexyl-5-(2-chlorophenyl)-1*H*-imidazole 80b



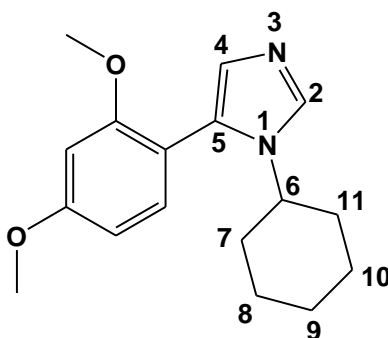
1-Cyclohexyl-5-(2-chlorophenyl)-1*H*-imidazole **80b** was successfully synthesized according to procedure C {*N*-(2-chlorobenzylidene)cyclohexanamine **76b** (337 mg, 1.52 mmol), TosMIC (445 mg, 2.28 mmol) and K₂CO₃ (274 mg, 1.98 mmol)} and synthetic procedure D {*N*-(2-chlorobenzylidene)cyclohexanamine (195 mg, 0.88 mmol), TosMIC (256 mg, 1.31 mmol) and K₂CO₃ (145 mg, 1.05 mmol)}; **Physical characteristics**: pale yellow solid; **Yields**: 91 mg, 23% for synthetic procedure C and 67 mg, 29% for procedure D; **Melting point**: 131-134°C; **¹H NMR** (400 MHz, CDCl₃) δ 7.70 (1H, s, 2-CH), 7.29-7.51 (4H, m, ArH), 6.99 (1H, s, 4-CH), 3.55-3.63 (1H, m, NCH), 1.18-2.03 (10H, m, 7-, 8-, 9-, 10- and 11-CH₂); **¹³C NMR** (101 MHz, CDCl₃) δ 135.2 (2-C), 134.7 (5-C), 133.0, 130.2, 129.8, 129.4, 129.3 (ArC), 128.1 (4-C), 126.8 (ArC), 55.2 (6-C), 34.5 (7 and 11-C), 25.7 (8- and 10-C), 25.2 (9-C); **FTIR** $\nu_{\max}/\text{cm}^{-1}$ (KBr): 3095, 2934, 2855, 1704, 1661, 1566, 1477, 1453, 1272, 1231, 1113, 1074, 1034, 923, 916, 830, 754, 666; **HRMS** (ESI-TOF) *m/z*: [M+H]⁺ Calcd for C₁₅H₁₈ClN₂ 261.1153, found 261.1155.

8.2.2.16. 1-Cyclohexyl-5-(3-methoxyphenyl)-1*H*-imidazole **80c**



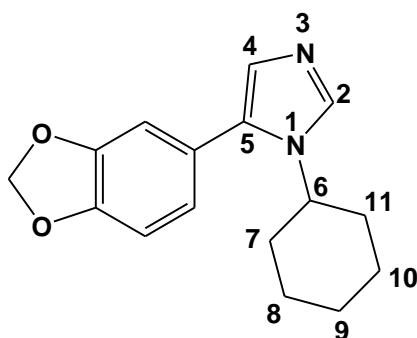
1-Cyclohexyl-5-(3-methoxyphenyl)-1*H*-imidazole **80c** was successfully synthesized according to procedure C {*N*-(3-methoxybenzylidene)cyclohexanamine **76c** (341 mg, 1.57 mmol), TosMIC (461 mg, 2.36 mmol) and K₂CO₃ (282 mg, 2.04 mmol)} and synthetic procedure D {*N*-(3-methoxybenzylidene)cyclohexanamine (380 mg, 1.75 mmol), TosMIC (514 mg, 2.63 mmol) and K₂CO₃ (315 mg, 2.28 mmol)}; **Physical characteristics**: pale yellow oil; **Yields**: 189 mg, 47% for synthetic procedure C, 238 mg, 53% for procedure D; **¹H NMR** (400 MHz, CDCl₃) δ 7.64 (1H, s, 2-CH), 7.29-7.34 (1H, m, ArH), 7.00 (1H, s, 4-CH), 6.86-6.89 (3H, m, ArH), 3.93-3.99 (1H, m, NCH), 3.78 (3H, s, ArOCH₃), 1.22-2.04 (10H, m, 7-, 8-, 9-, 10- and 11-CH₂); **¹³C NMR** (101 MHz, CDCl₃) δ 159.6 (ArCOCH₃), 135.0 (2-C), 132.4 (5-C), 131.6, 129.6, 127.5 (4-C), 121.3, 114.7, 113.3 (ArC), 55.2 (ArCOCH₃), 54.5 (6-C), 34.8 (7- and 11-C), 25.6 (8- and 10-C), 25.1 (9-C); **FTIR** $\nu_{\max}/\text{cm}^{-1}$ (KBr): 2934, 2856, 1679, 1605, 1580, 1482, 1450, 1352, 1318, 1225, 1117, 1168, 1087, 1052, 1036, 998, 860, 844, 814, 699, 659; **HRMS** (ESI-TOF) *m/z*: [M+H]⁺ Calcd for C₁₆H₂₁N₂O 257.1648, found 257.1668.

8.2.2.17. 1-Cyclohexyl-5-(2,4-dimethoxyphenyl)-1*H*-imidazole 80d



1-Cyclohexyl-5-(2,4-dimethoxyphenyl)-1*H*-imidazole **80d** was successfully synthesized according to procedure C {*N*-(2,4-dimethoxybenzylidene)cyclohexanamine **76d** (138 mg, 0.56 mmol), TosMIC (164 mg, 0.84 mmol) and K_2CO_3 (239 mg, 1.73 mmol)}; synthetic procedure D {*N*-(2,4-dimethoxybenzylidene)cyclohexanamine (151 mg, 0.61 mmol), TosMIC (180 mg, 0.92 mmol) and K_2CO_3 (101 mg, 0.73 mmol)} and synthetic procedure E {2,4-dimethoxybenzaldehyde (85 mg, 0.51 mmol) and cyclohexylamine (61 mg, 0.61 mmol), TosMIC (150 mg, 0.77 mmol) and K_2CO_3 (93 mg, 0.67 mmol)}; **Physical characteristics**: pale yellow solid; **Yields**: 103 mg, 64% for synthetic procedure C, 129 mg, 74% for procedure D and 107 mg, 73% for Procedure F; **Melting point**: 99-102°C; **1H NMR** (400 MHz, $CDCl_3$) δ 7.60 (1H, s, 2-CH), 7.09 (1H, d, $J = 8.8$ Hz, ArH), 6.84 (1H, s, 4-CH), 6.49-6.51 (2H, m, ArH), 3.80 and 3.70 (6H, 2 x s, 2 x $ArOCH_3$), 3.51-3.59 (1H, m, NCH), 1.15-1.99 (10H, m, 7-, 8-, 9-, 10- and 11- CH_2); **^{13}C NMR** (101 MHz, $CDCl_3$) δ 161.4 and 158.2 (2 x $ArCOCH_3$), 134.2 (2-C), 132.9 (5-C), 128.9 (ArC), 127.1 (4-C), 111.4, 104.4, 98.5 (ArC), 55.0 and 55.1 (2 x $ArCOCH_3$), 55.2 (6-CH), 34.6 (7- and 11-C), 25.7 (8- and 10-C), 25.1 (9-C); **FTIR** ν_{max}/cm^{-1} (KBr): 3096, 3002, 2957, 2932, 2857, 1614, 1581, 1553, 1495, 1435, 1307, 1289, 1265, 1211, 1161, 1136, 1055, 1028, 925, 817, 796; **HRMS** (ESI-TOF) m/z : $[M+H]^+$ Calcd for $C_{17}H_{23}N_2O_2$ 287.1754, found 287.1770.

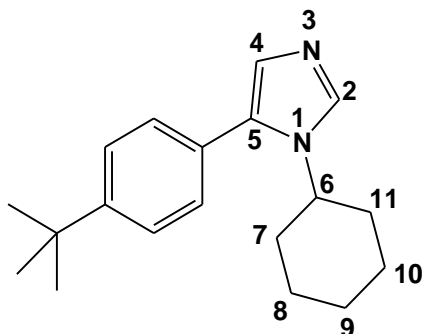
8.2.2.18. 5-(Benzo[*d*][1,3]dioxol-5-yl)-1-cyclohexyl-1*H*-imidazole 80e



5-(benzo[*d*][1,3]dioxol-5-yl)-1-cyclohexyl-1*H*-imidazole **80e** was successfully synthesized according to procedure C {*N*-(benzo[*d*][1,3]dioxol-5-ylmethylene)cyclohexanamine **76e** (206 mg,

0.89 mmol), TosMIC (262 mg, 1.34 mmol) and K_2CO_3 (216 mg, 1.56 mmol)}; synthetic procedure D {*N*-(benzo[*d*][1,3]dioxol-5-ylmethylene)cyclohexanamine (409 mg, 1.77 mmol), TosMIC (519 mg, 2.66 mmol) and K_2CO_3 (318 mg, 2.30 mmol)} and synthetic procedure E {piperonal (102 mg, 0.68 mmol) and cyclohexylamine (81 mg, 0.82 mmol), TosMIC (1.02 mmol) and K_2CO_3 (0.88 mmol)}; **Physical characteristics:** pale yellow solid; **Yields:** 84 mg, 35% for synthetic procedure C, 258 mg, 54% for synthetic procedure D and 92 mg, 50% for synthetic procedure E; **Melting point.:** 85-88°C; **1H NMR** (400 MHz, $CDCl_3$) δ 7.58 (1H, s, 2-CH), 6.90 (1H, s, 4-CH), 6.72-6.83 (3H, m, ArH), 5.96 (2H, s, $ArOCH_2O$), 3.81-3.87 (1H, m, NCH), 1.15-1.98 (6H, m, 7-, 8-, 9-, 10- and 11- CH_2); **^{13}C NMR** (101 MHz, $CDCl_3$) δ 147.6 and 147.4 ($ArCOCH_2O$), 134.6 (2-C), 132.0 (5-C), 127.2 (4-C), 123.8, 122.8, 109.5, 108.4 (ArC), 101.1 ($ArCOCH_2O$), 54.3 (6-C), 34.6 (7- and 11-C), 25.5 (8- and 10-C), 25.0 (9-C); **FTIR** ν_{max}/cm^{-1} (KBr): 3126, 3100, 3070, 2944, 2894, 2848, 2783, 1670, 1556, 1501, 1475, 1445, 1265, 1232, 1118, 1099, 1042, 943, 862, 878, 808, 659, 626; **HRMS** (ESI-TOF) m/z : $[M+H]^+$ Calcd for $C_{16}H_{19}N_2O_2$ 271.1481, found 271.1464.

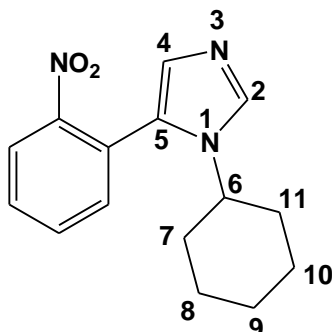
8.2.2.19. 1-Cyclohexyl-5-(4-*tert*-butylphenyl)-1*H*-imidazole 80f



1-Cyclohexyl-5-(4-*tert*-butylphenyl)-1*H*-imidazole **80f** was successfully synthesized according to procedure C {*N*-(4-*tert*-butylbenzylidene)cyclohexanamine **76f** (306 mg, 1.49 mmol), TosMIC (437 mg, 2.24 mmol) and K_2CO_3 (241 mg, 1.74 mmol)} and synthetic procedure D {*N*-(4-*tert*-butylbenzylidene)cyclohexanamine (339 mg, 1.65 mmol), TosMIC (484 mg, 2.48 mmol) and K_2CO_3 (297 mg, 2.15 mmol)}; **Physical characteristics:** pale orange solid; **Yields:** (122 mg, 29% for synthetic procedure C and 233 mg, 50% for synthetic procedure D); **Melting point:** 113-116°C; **1H NMR** (400 MHz, $CDCl_3$) δ 7.65 (1H, s, 2-CH), 7.44-7.46 (2H, m, ArH), 7.24-7.25 (2H, m, ArH), 6.99 (1H, s, 4-CH) 3.92-4.00 (2H, m, 6-CH), 1.20-2.07 [19H, m, 7-, 8-, 9-, 10-, 11- CH_2 and $C(CH_3)_3$]; **^{13}C NMR** (101 MHz, $CDCl_3$) δ 150.9 [$ArCC(CH_3)_3$], 134.9 (2-C), 132.5 (5-C), 128.7 (ArC), 127.3 (4-C), 125.6 (ArC), 54.4 (6-C), 34.9 (7- and 11-C), 34.6 [$ArCC(CH_3)_3$], 31.6 [$ArCC(CH_3)_3$], 25.7 (8- and 10-C), 25.2 (9-C); **FTIR** ν_{max}/cm^{-1} (KBr): 3130, 3065, 3035, 2931,

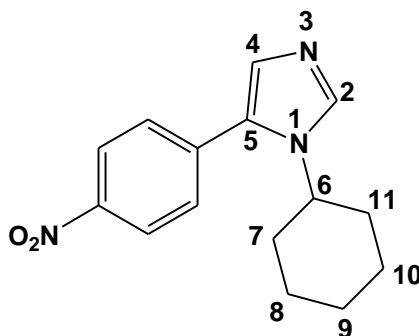
2860, 1669, 1613, 1548, 1474, 1463, 1454, 1403, 1360, 1268, 1218, 1117, 993, 917, 956, 817, 808, 665, 579; **HRMS** (ESI-TOF) m/z : $[M+H]^+$ Calcd for $C_{17}H_{27}N_2$ 283.2169, found 283.2190.

8.2.2.22. 1-Cyclohexyl-5-(2-nitrophenyl)-1*H*-imidazole 80h



1-Cyclohexyl-5-(2-nitrophenyl)-1*H*-imidazole **80h** was successfully synthesized according to procedure C using *N*-(2-nitrobenzylidene)cyclohexanamine **76h** (369 mg, 1.59 mmol), TosMIC (554 mg, 2.84 mmol) and K_2CO_3 (286 mg, 2.07 mmol) C; **Physical characteristics**: brown oil; **Yield**: 52 mg, 12%; **1H NMR** (400 MHz, $CDCl_3$) δ 7.74 (1H, s, 2-CH), 7.33-7.64 (4H, m, ArH), 7.03 (1H, s, 4-CH), 3.58-3.69 (1H, m, NCH), 1.21-1.21 (10H, m, 7-, 8-, 9-, 10 and 11- CH_2); **^{13}C NMR** (101 MHz, $CDCl_3$) δ 137.5 (2-C), 135.0 (5-C), 132.8, 130.2, 129.8, 129.3 (ArC), 128.9 (4-C), 115.6 (ArC), 45.1 (6-C), 32.7 (7- and 11-C), 19.5 (8- and 10-C), 13.4 (9-C); **HRMS** (ESI-TOF) m/z : $[M+H]^+$ Calcd for $C_{15}H_{18}N_3O_2$ 272.1394, found 272.1393.

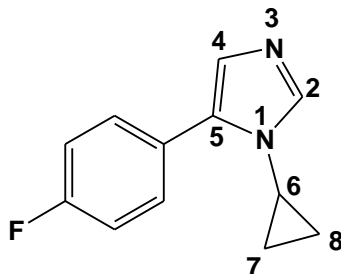
8.2.2.23. 1-Butyl-5-(4-nitrophenyl)-1*H*-imidazole 80i



1-Cyclohexyl-5-(4-nitrophenyl)-1*H*-imidazole **80h** was successfully synthesized according to procedure C using *N*-(4-nitrobenzylidene)cyclohexanamine **76i** (386 mg, 1.66 mmol), TosMIC (469 mg, 2.40 mmol) and K_2CO_3 (299 mg, 2.16 mmol); **Physical characteristics**: brown oil; **Yield**: 45 mg, 10%; **1H NMR** (400 MHz, $CDCl_3$) δ 8.30 (2H, d, $J=8.4$ Hz, ArH), 7.77 (1H, s, 2-CH), 7.49 (2H, 8.8 Hz, ArH), 7.15 (1H, s, 4-CH), 3.92-3.98 (1H, m, 6-CH), 1.63-2.07 (4H, m, 7- and 11- CH_2), 1.22-1.32 (6H, m, 8-, 9- and 10- CH_2); **^{13}C NMR** (101 MHz, $CDCl_3$) δ 147.2 (ArCNO₂), 136.7 (2-C), 136.6 (5-C), 130.6 (ArC), 129.1 (4-C), 126.3, 115.7 (ArC), 55.5 (6-C), 34.8

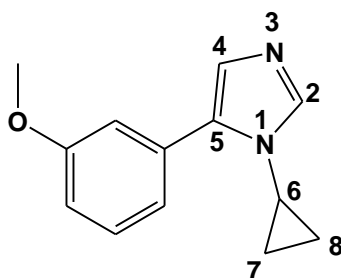
(7- and 11-C), 25.6 (8-, and 10-C), 25.0 (9-C); **HRMS** (ESI-TOF) m/z : $[M+H]^+$ Calcd for $C_{15}H_{18}N_3O_2$ 272.1394, found 272.1382.

8.2.2.24. 1-Cyclopropyl-5-(4-fluorophenyl)-1*H*-imidazole **81a**



1-Cyclopropyl-5-(4-fluorophenyl)-1*H*-imidazole **81a** was successfully synthesized according to procedure D using *N*-(4-fluorobenzylidene)cyclopropanamine **77a** (250 mg, 1.53 mmol), TosMIC (447 mg, 2.29 mmol) and K_2CO_3 (275 mg, 1.99 mmol); **Physical characteristics**: brown oil; **Yield**: 71 mg, 23 %; **1H NMR** (400 MHz, $CDCl_3$) δ 7.58 (1H, s, 2-CH), 7.46-7.50 (2H, m, ArH), 7.09-7.13 (2H, m, ArH), 7.03 (1H, s, 4-CH), 3.28-3.34 (H, m, 6-CH), 0.83-0.97 (4H, m, 7- and 8- CH_2); **^{13}C NMR** (101 MHz, $CDCl_3$) δ 162.4 ($^1J_{F,C}$ = 245.9 Hz, *para*-CF), 138.6 (2-C), 133.4 (5-C), 129.8 (d, $^4J_{F,C}$ = 3.0 Hz, 1'-C), 127.6 (4-C), 126.2 (d, $^3J_{F,C}$ = 8.1 Hz, *ortho*-C), 115.6 (d, $^2J_{F,C}$ = 21.1 Hz, *meta*-C), 27.3 (6-C), 7.48 (7- and 8-C); **HRMS** (ESI-TOF) m/z : $[M+H]^+$ Calcd for $C_{12}H_{12}FN_2$ 203.0974, found 203.0979.

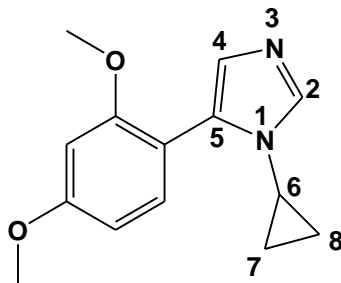
8.2.2.25. 1-Cyclopropyl-5-(3-methoxyphenyl)-1*H*-imidazole **81c**



1-Cyclopropyl-5-(3-methoxyphenyl)-1*H*-imidazole **81c** was successfully synthesized according to the described general procedure D using *N*-(3-methoxybenzylidene)cyclopropanamine **77c** (405 mg, 2.31 mmol), TosMIC (678 mg, 3.47 mmol) and K_2CO_3 (415 mg, 3.00 mmol); **Physical characteristics**: pale yellow oil; **Yield**: 198 mg, 40%; **1H NMR** (400 MHz, $CDCl_3$) δ 7.58 (1H, s, 2-CH), 7.31-7.35 (1H, m, ArH), 6.88-7.13 (5H, overlapping multiplets and singlet, ArH and 4-CH), 3.84 (3H, s, $ArOCH_3$), 3.33-3.39 (1H, m, 6-CH), 0.85-1.01 (4H, m, 7- and 8- CH_2); **^{13}C NMR** (101 MHz, $CDCl_3$) δ 159.5 ($ArCOCH_3$), 138.7 (2-C), 134.2 (5-C), 131.3, 129.5 (ArC),

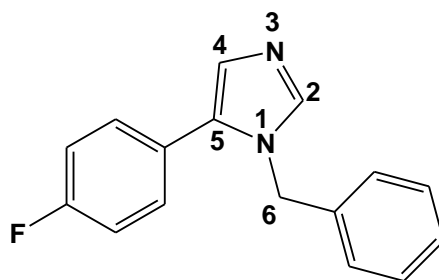
127.9 (4-C), 120.5, 113.8, 112.9 (ArC), 55.1 (ArCOCH₃), 27.5 (6-C), 7.56 (7-and 8-C); **HRMS** (ESI-TOF) m/z: [M+H]⁺ Calcd for C₁₃H₁₅N₂O 215.1179, found 215.1188.

8.2.2.26. 1-Cyclopropyl-5-(2,4-dimethoxyphenyl)-1*H*-imidazole **81d**



1-Cyclopropyl-5-(2,4-dimethoxyphenyl)-1*H*-imidazole **81d** was successfully synthesized according to procedure D using *N*-(2,4-dimethoxybenzylidene)cyclopropanamine **78d** (302 mg, 1.47 mmol), TosMIC (429 mg, 2.20 mmol) and K₂CO₃ (264 mg, 1.91 mmol); **Physical characteristics**: brown oil; **Yield**: 244 mg, 68%; **¹H NMR** (400 MHz, CDCl₃) δ 7.49 (1H, s, 2-CH), 7.10 (1H, d, *J* = 8.8 Hz, ArH), 6.87 (1H, s, 4-CH), 6.47 (2H, *J* = 6.8 Hz, ArH), 3.73 and 3.80 (6H, 2 x s, 2 x ArOCH₃), 3.18-3.22 (1H, m, NCH), 0.66-0.70 (4H, m, 7- and 8-CH₂); **¹³C NMR** (101 MHz, CDCl₃) δ 161.2 and 158.3 (2 x ArCOCH₃), 137.6 (2-C), 132.0 (5-C), 131.0 (ArC), 127.9 (4-C), 111.9, 104.1, 98.4 (ArC), 55.2 and 55.1 (2 x ArCOCH₃), 26.6 (6-C), 5.84 (7- and 8-C); **HRMS** (ESI-TOF) m/z: [M+H]⁺ Calcd for C₁₄H₁₇N₂O₂ 245.1285, found 245.1290.

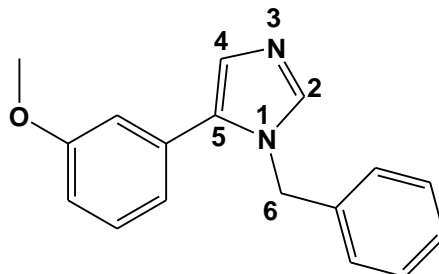
8.2.2.27. 1-Benzyl-5-(4-fluorophenyl)-1*H*-imidazole **82a**



1-Benzyl-5-(4-fluorophenyl)-1*H*-imidazole **82a** was successfully synthesized according to procedure D using *N*-(4-fluorobenzylidene)-1-phenylmethanamine **78a** (226 mg, 1.06 mmol), TosMIC (308 mg, 1.58 mmol) and K₂CO₃ (189 mg, 1.37 mmol); **Physical characteristics**: brown oil; **Yield**: 70 mg, 26%; **¹H NMR** (400 MHz, CDCl₃) δ 7.57 (1H, s, 2-CH), 7.20-7.32 (5H, m, ArH), 7.09 (1H, s, 4-CH), 6.97-7.05 (4H, m, ArH), 5.10 (2H, s, NCH₂); **¹³C NMR** (101 MHz, CDCl₃) δ 163.8 (d, ¹*J*_{C,F} = 247 Hz, *para*-CF), 138.6 (2-C), 136.5 (5-C), 132.4 130.8, 130.7 (ArC), 128.8 (d, ⁴*J*_{F,C} = 3.0 Hz, 1'-C), 128.2 (4-C) 128.0 (ArC), 126.5 (d, ³*J*_{F,C} = 8.1 Hz, *ortho*-C), 115.6 (d,

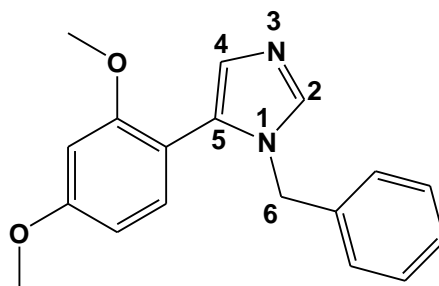
$^2J_{\text{F,C}} = 21.1$ Hz, *meta*-C), 48.6 (NCH₂); **HRMS** (ESI-TOF) *m/z*: [M+H]⁺ Calcd for C₁₆H₁₄FN₂ 253.1136, found 253.1138.

8.2.2.28. 1-Benzyl-5-(3-methoxyphenyl)-1*H*-imidazole **82c**



1-Benzyl-5-(3-methoxyphenyl)-1*H*-imidazole **82c** was successfully synthesized according to procedure D using *N*-(3-methoxybenzylidene)-1-phenylmethanamine **78c** (327 mg, 1.45 mmol), TosMIC (439 mg, 2.25 mmol) and K₂CO₃ (261 mg, 1.89 mmol); **Physical characteristics**: brown oil; **Yield**: 92 mg, 24 %; **¹H NMR** (400 MHz, CDCl₃) δ 7.58 (1H, s, 2-CH), 7.27-7.35 (4H, m, ArH), 6.87-7.15 (5H, m, ArH), 6.79 (1H, s, 4-CH), 5.17 (2H, s, NCH₂) 3.69 (3H, s, ArOCH₃); **¹³C NMR** (101 MHz, CDCl₃) δ 159.6 (ArCOCH₃), 138.7 (2-C), 136.8(5-C), 133.3, 130.8 (ArC), 129.7 (4-C), 128.9, 128.1, 127.9, 126.6, 121.2, 114.1, 113.9 (ArC), 55.1 (ArCOCH₃), 48.7 (NCH₂); **HRMS** (ESI-TOF) *m/z*: [M+H]⁺ Calcd for C₁₇H₁₇N₂O₂ 265.1335, Found 265.1329.

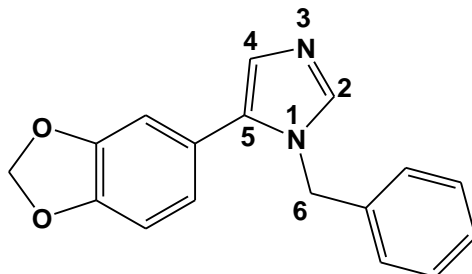
8.2.2.29. 1-Benzyl-5-(2,4-dimethoxyphenyl)-1*H*-imidazole **82d**



1-Benzyl-5-(2,4-dimethoxyphenyl)-1*H*-imidazole **82d** was successfully synthesized according to procedure D using *N*-(2,4-dimethoxybenzylidene)-1-phenylmethanamine **78d** (391 mg, 1.53 mmol), TosMIC (449 mg, 2.30 mmol) and K₂CO₃ (275 mg, 1.99 mmol); **Physical characteristics**: brown oil; **Yield**: 333 mg, 74%; **¹H NMR** (400 MHz, CDCl₃) δ 7.55 (1H, s, 2-CH), 7.28-7.31 (3H, m, ArH), 7.03-7.12 (4H, m, ArH and 4-CH), 6.50-6.53 (2H, m, ArH), 4.98 (2H, s, NCH₂), 3.86 and 3.71 (6H, 2 x s, 2 x ArOCH₃); **¹³C NMR** (101 MHz, CDCl₃) δ 161.5 and 158.3 (2 x ArCOCH₃), 137.6 (2-C), 136.7 (5-C), 133.0, 130.0 (ArC), 128.5 (4-C), 128.2, 127.6

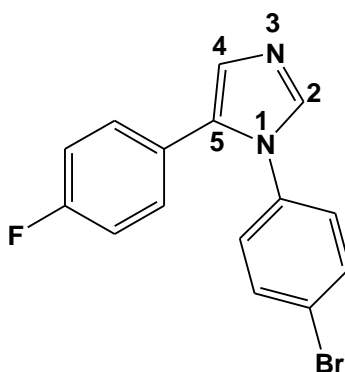
,127.2, 111.1, 104.4, 98.6 (ArC), 55.3 and 55.2 (2 x ArCOCH₃), 48.8 (NCH₂); **HRMS** (ESI-TOF) m/z: [M+H]⁺ Calcd for C₁₈H₁₉N₂O₂ 295.1441, found 295.1408.

8.2.2.30. 5-(Benzo[d][1,3]dioxol-5-yl)-1-benzyl-1*H*-imidazole **82e**



5-(Benzo[d][1,3]dioxol-5-yl)-1-benzyl-1*H*-imidazole **82e** was successfully synthesized according to procedure D using *N*-(benzo[d][1,3]dioxol-5-ylmethylene)-1-phenylmethanamine **78e** (122 mg, 0.51 mmol), TosMIC (149 mg, 0.77 mmol) and K₂CO₃ (91 mg, 0.66 mmol); **Physical characteristics**: pale yellow solid; **Yields**: 31 mg, 22%; **Melting point**: 84-87°C; **¹H NMR** (400 MHz, CDCl₃) δ 7.53 (1H, s, 2-CH), 7.29-7.33 (3H, m, ArH), 6.74-7.06 (5H, m, ArH), 6.72 (1H, s, 4-CH), 5.97 (2H, s, ArOCH₂O), 5.11 (2H, s, NCH₂); **¹³C NMR** (101 MHz, CDCl₃) δ 147.8 and 147.6 (ArCOCH₂O), 138.3 (2-C), 136.7 (5-C), 130.7, 133.1 (ArC), 127 (4-C) 123.2, 127.9, 126.6, 122.9, 109.4, 108.5 (ArC), 101.2 (ArCOCH₂O), 48.6 (NCH₂); **HRMS** (ESI-TOF) m/z: [M+H]⁺ Calcd for C₁₇H₁₅N₂O₂ 279.1128, found 279.1143.

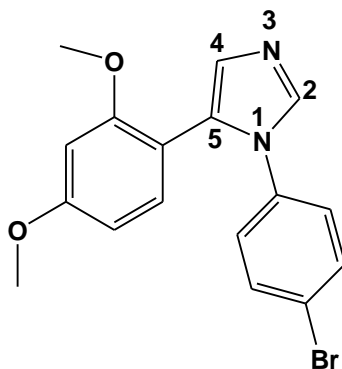
8.2.2.31. 1-(4-Bromophenyl)-5-(4-fluorophenyl)-1*H*-imidazole **83a**



1-(4-Bromophenyl)-5-(4-fluorophenyl)-1*H*-imidazole **83a** was successfully synthesized according to procedure E using 4-fluorobenzaldehyde (99 mg, 0.80 mmol), 4-bromoaniline (151 mg, 0.88 mmol), TosMIC (234 mg, 1.2 mmol) and K₂CO₃ (144 mg, 1.04 mmol); **Physical characteristics**: pale yellow solid; **Yield**: 173 mg, 68%; **Melting Point**: 130-133°C; **¹H NMR** (400 MHz, CDCl₃) δ 7.70 (1H, s, 2-CH), 7.51 (2H, m, ArH), 7.23 (1H, s, 4-CH), 6.69-7.11 (6H, m, ArH); **¹³C NMR** (101 MHz, CDCl₃) δ 161.1 (d, J_{C,F} = 247Hz, *para*-CF), 138.5 (2-C), 135.4 (5-

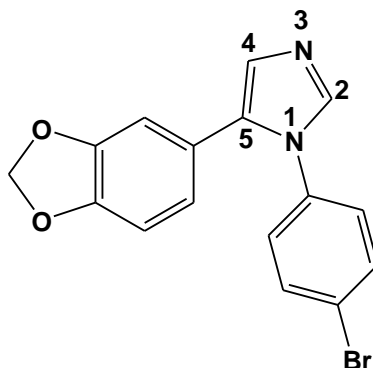
C), 132.8 136.1, 130.0, 128.8, (ArC), 127.0 (4-C), 122.1 (ArC), 125.0 (d, $^3J_{C,F} = 10$ Hz, *ortho*-C) 115.7 (d, $^2J_{F,C} = 21$ Hz, *meta*-C); **HRMS** (ESI-TOF) m/z : $[M+H]^+$ Calcd for $C_{15}H_{11}^{79}BrFN_2$ 317.0090, found 317.0115

8.2.2.32. 1-(4-Bromophenyl)-5-(2,4-dimethoxyphenyl)-1*H*-imidazole **83d**



1-(4-Bromophenyl)-5-(2,4-dimethoxyphenyl)-1*H*-imidazole **83d** was successfully synthesized according to procedure E using 2,4-dimethoxybenzaldehyde (143 mg, 0.86 mmol), 4-bromoaniline (163 mg, 0.95 mmol), TosMIC (252 mg, 1.29 mmol) and K_2CO_3 (155 mg, 1.12 mmol); **Physical characteristics**: pale yellow oil; **Yield**: 117 mg, 38%; **1H NMR** (400 MHz, $CDCl_3$) δ 7.62 (1H, s, 2-CH), 7.43-7.45 (2H, m, ArH), 7.13-7.18 (1H, d, $J = 12$ Hz, ArH), 7.12 (1H, s, 4-CH), 6.98-7.00 (2H, m, ArH), 6.31-6.50 (2H, m, ArH), 3.80 and 3.34 (3H, 2 x s, 2 x ArOCH₃); **^{13}C NMR** (101 MHz, $CDCl_3$) δ 161.5 and 157.5 (2 x ArCOCH₃), 137.2 (2-C), 136.8 (5-C), 134.5, 132.1, 132.0 (ArC), 129.8 (4-C), 125.6, 120.9, 111.0, 104.6, 98.7 (ArC), 55.3 and 54.7 (2 x ArCOCH₃); **HRMS** (ESI-TOF) m/z : $[M+H]^+$ Calcd for $C_{17}H_{16}^{79}BrN_2O_2$ 359.0395, found 359.0394.

8.2.2.33. 5-(Benzo[*d*][1,3]dioxol-5-yl)-1-(4-bromophenyl)-1*H*-imidazole **83e**



5-(Benzo[*d*][1,3]dioxol-5-yl)-1-(4-bromophenyl)-1*H*-imidazole **83e** was successfully synthesized according to procedure E using piperonal (110 mg, 0.73 mmol), 4-bromoaniline (139 mg, 0.81 mmol), TosMIC (215 mg, 1.10 mmol) and K_2CO_3 (130 mg, 0.94 mmol); **Physical**

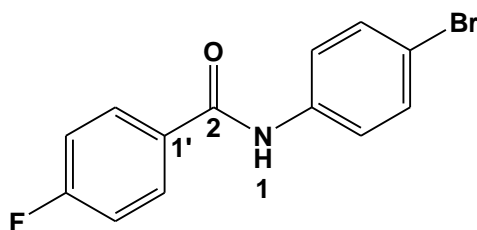
characteristics: pale yellow solid; **Yield:** 155 mg, 62%; **Melting point:** 115-118°C; **¹H NMR** (400 MHz, CDCl₃) δ 7.69 (1H, s, 2-CH), 7.2-7.54 (2H, m, ArH), 7.18 (4-CH), 7.051-7.07 (2H, m, ArH), 6.57-6.74 (3H, m, ArH), 5.92 (2H, s, ArOCH₂O); **¹³C NMR** (101 MHz, CDCl₃) δ 147.7 and 147.5 (ArCOCH₂O), 138.1 (2-C), 135.4 (5-C), 132.7 ArC), 128.3 (4-C), 127.0, 122.6, 122.4, 122.1, 108.7, 108.5, (ArC), 101.3 (ArCOCH₂O); **HRMS** (ESI-TOF) m/z: [M+H]⁺ Calcd for C₁₆H₁₂⁷⁹BrN₂O₂ 343.0082, found 343.0099.

8.2.3. Synthesis of *N*-aryl benzamide derivatives

8.2.3.1. General synthetic procedure

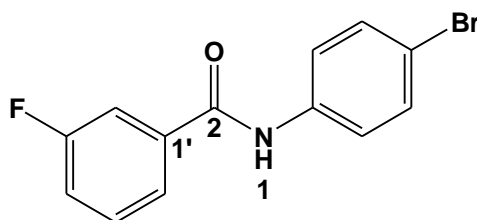
To a stirred solution containing aniline (1.0 molar equivalent), triethylamine (1.05 molar equivalents) in EtOAc (30 ml) was added benzoyl chloride (1.05 molar equivalents) at 0°C. After addition, the resulting reaction mixture was stirred at room temperature for 16 hours (monitored by TLC). Upon completion, EtOAc (20 ml) was then added, followed by washing with 1M HCl, saturated NaHCO₃ and water. The organic layer was dried over MgSO₄ and concentrated *in vacuo* to afford the pure *N*-aryl-benzamide derivatives.²¹¹

8.2.3.2. *N*-(4-Bromophenyl)-4-fluorobenzamide **91a**



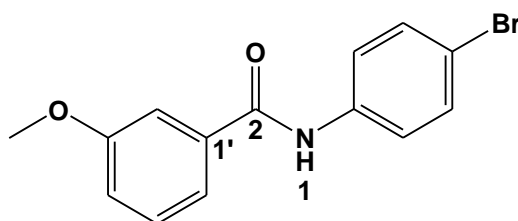
N-(4-Bromophenyl)-4-fluorobenzamide **91a** was successfully synthesized according to general procedure using 4-fluorobenzoyl chloride (2.39 g, 15.1 mmol) and 4-bromoaniline (2.6 g, 14.4 mmol); **Physical characteristics:** pale yellow solids; **Yield:** 3.85 g, 91%; **Melting point:** 167-169 °C (lit³⁴⁹); **¹H NMR** (400 MHz, DMSO-*d*₆) δ 10.4 (1H, s, NH), 8.01-8.06 (2H, m, ArH), 7.75 (2H, m, ArH), 7.51 (2H, d, *J* = 8.0 Hz, ArH), 7.34 (2H, d, *J* = 8.0 Hz, ArH); **¹³C NMR** (101 MHz, DMSO-*d*₆) δ 164.2 (d, ¹*J*_{C,F} = 248 Hz, *para*-CF), 164.5 (C=O), 138.5 (ArC), 131.2 (d, ⁴*J*_{C,F} = 3 Hz, 1'-C), 130.5 (d, ³*J*_{C,F} = 9 Hz, *ortho*-C), 122.26 (ArC), 115.5 (d, ⁴*J*_{C,F} = 21 Hz, *meta*-C), 115.4 (ArCBr); **FTIR** ν_{max} /cm⁻¹ (KBr): 3345, 3089, 3070, 1904, 1713, 1642, 1591, 1525, 1505, 1395, 1316, 1299, 1236, 1106, 1098, 1076, 1013, 901, 858, 821, 762, 659, 625, 516, 501.

8.2.3.3. *N*-(4-Bromophenyl)-3-fluorobenzamide **91b**



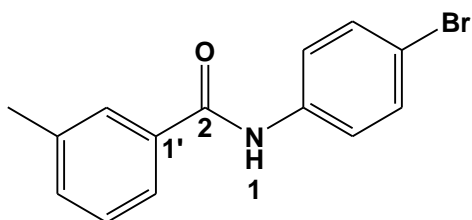
N-(4-Bromophenyl)-3-fluorobenzamide **91b** was successfully synthesized according to general procedure using 3-fluorobenzoyl chloride (3.30 g, 20.8 mmol) and 4-bromoaniline (3.41 g, 19.8 mmol); **Physical characteristics**: pale yellow solid; **Yield**: 5.30 g, 91%; **Melting point**: 169-171°C; **¹H NMR** (400 MHz, DMSO-*d*₆) δ 10.5 (1H, s, NH), 7.79-7.86 (4H, m, ArH), 7.56-7.65 (3H, m, ArH) 7.46-7.51 (1H, m, ArH); **¹³C NMR** (101 MHz, DMSO-*d*₆) δ 164.3 (C=O), 162.0 (d, ¹*J*_{C,F} = 247 Hz, 3'-CF), 136.9 (d, ⁴*J*_{C,F} = 4 Hz, 6'-C), 135.6, 131.5 (ArC), 130.6 (d, ³*J*_{C,F} = 8 Hz, 1'-C), 123.9 (d, ³*J*_{C,F} = 3 Hz, 5'-C), 122.3 (ArC), 118.5 (d, ²*J*_{C,F} = 24 Hz, 4'-C), 115.7 (ArCBr); 114.6 (d, ²*J*_{C,F} = 22.1 Hz, 2'-C); **FTIR** $\nu_{\max}/\text{cm}^{-1}$ (KBr): 3315, 3178, 3100, 3065, 1900, 1656, 1585, 1517, 1491, 1435, 1397, 1313, 1267, 1198, 1083, 1007, 948, 885, 823, 802, 750, 678, 504.

8.2.3.4. *N*-(4-Bromophenyl)-3-methoxybenzamide **91c**



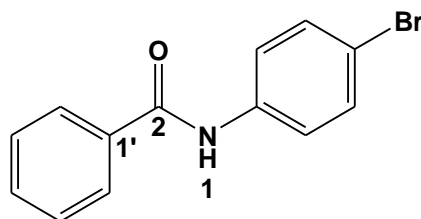
N-(4-Bromophenyl)-3-methoxybenzamide **91c** was successfully synthesized according to general procedure using 3-methoxybenzoyl chloride (2.08 g, 12.2 mmol) and 4-bromoaniline (2.00 g, 11.6 mmol); **Physical characteristics**: pale yellow solid; **Yield**: 3.20 g, 90%; **Melting point**: 161-163°C; **¹H NMR** (400 MHz, DMSO-*d*₆) δ 10.6 (1H, s, NH), 7.41-7.52 (5H, m, ArH), 7.33 (1H, d, *J* = 6.8 Hz, ArH), 7.03 (2H, d, *J* = 6.8 Hz, ArH), 3.88 (3H, s, ArOCH₃); **¹³C NMR** (101 MHz, DMSO-*d*₆) δ 164.3 (C=O), 157.6 (ArCOCH₃), 136.5, 133.5, 131.9, 129.4, 122.2, 122.1, 118.7, 118.3 (ArCBr), 113.9 (ArC), 55.5 (ArCOCH₃); **FTIR** $\nu_{\max}/\text{cm}^{-1}$ (KBr): 3329, 3100, 3057, 3028, 1896, 1658, 1591, 1513, 1491, 1393, 1312, 1235, 1078, 1007, 920, 909, 883, 745, 688, 661, 509.

8.2.3.5. *N*-(4-Bromophenyl)-3-methylbenzamide 91d



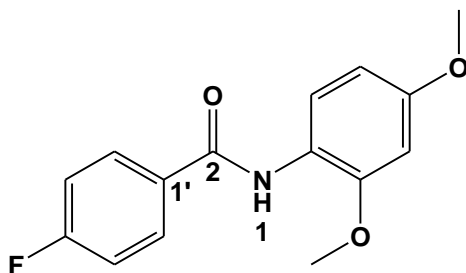
N-(4-Bromophenyl)-3-methylbenzamide **91d** was successfully synthesized according to the general procedure using 3-methylbenzoyl chloride (1.78 g, 11.5 mmol) and 4-bromoaniline (1.88 g, 10.9 mmol); **Physical characteristics:** pale yellow solid; **Yield:** 2.81 g, 89%; **Melting point:** 161-163°C; $^1\text{H NMR}$ (400 MHz, $\text{DMSO-}d_6$) δ 10.5 (1H, s, NH), 7.53-7.76 (4H, m, ArH), 7.31-7.45 (4H, m, ArH), 2.23 (3H, s, ArCH_3); $^{13}\text{C NMR}$ (101 MHz, $\text{DMSO-}d_6$) δ 164.4 (C=O), 134.6, 134.2, 131.1, 129.9, 129.1, 128.4, 126.0, 124.8, 121.3 (ArC), 24.1 (ArCCH_3); **FTIR** $\nu_{\text{max}}/\text{cm}^{-1}$ (KBr): 3329, 3174, 3096, 3061, 1948, 1900, 1658, 1587, 1512, 1491, 1393, 1357, 1312, 1291, 1244, 1183, 1074, 1012, 8200, 809, 744, 701, 688, 669, 502.

8.2.3.6. *N*-(4-Bromophenyl)benzamide 91e



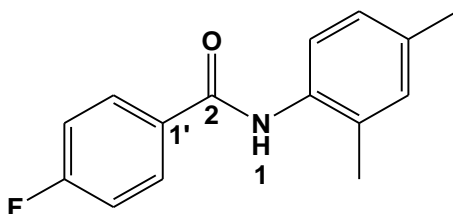
N-(4-Bromophenyl)benzamide **91e** was successfully synthesized according to general procedure using benzoyl chloride (2.09 mg, 14.9 mmol) and 4-bromoaniline (2.44 g, 14.2 mmol); **Physical characteristics:** pale yellow solid; **Yield:** 3.37 g, 86%; **Melting point:** 203-205°C (lit³⁵⁰); $^1\text{H NMR}$ (400 MHz, $\text{DMSO-}d_6$) δ 10.4 (1H, s, 1-NH), 7.94 (2H d, $J=6.8$ Hz) ArH), 7.76 (2H, d, $J=7.6$ Hz, ArH), 7.48-7.64 (5H, m, ArH); $^{13}\text{C NMR}$ (101 MHz, $\text{DMSO-}d_6$) δ 172.7 (C=O), 138.4, 137.1, 136.8, 134.7, 134.0, 133.8, 133.1, 127.6 (ArC); **FTIR** $\nu_{\text{max}}/\text{cm}^{-1}$ (KBr): 3332, 3174, 3096, 3055, 1656, 1540, 1512, 1452, 1346, 1322, 1440, 1096, 989, 845, 760, 512.

8.2.3.7. *N*-(2,4-Dimethoxyphenyl)-4-fluorobenzamide 91f



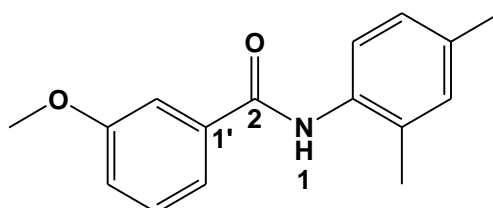
N-(2,4-Dimethoxyphenyl)-4-fluorobenzamide **91f** was successfully synthesized according to the general procedure using 4-fluorobenzoyl chloride (1.68 g, 10.6 mmol) and 2,4-dimethoxyaniline (1.55 g, 10.1 mmol); **Physical characteristics:** grey solid; **Yield:** 2.31 g, 83%; **Melting point:** 172-175 °C; **¹H NMR** (400 MHz, DMSO-*d*₆) δ 9.57 (1H, s, NH), 7.63-7.82 (3H, m, ArH), 7.46-7.62 (4H, m, ArH), 3.87 and 3.90 (6H, 2 x s, ArOCH₃); **¹³C NMR** (101 MHz, DMSO-*d*₆) δ 163.8 (C=O), 162.1 (d, ¹J_{C,F} = 245 Hz, *para*-FC), 158.2 and 153.8 (2 x ArCOCH₃), 137.0 (d, ⁴J_{C,F} = 3 Hz, 1'-C), 130.6 (d, ³J_{C,F} = 8 Hz, *ortho*-C), 126.2, 123.7 (ArC), 118.3 (d, ²J_{C,F} = 23 Hz, *meta*-C), 114.2, 99.0 (ArC), 55.7 and 55.4 (2 x ArCOCH₃); **FTIR** ν_{\max} /cm⁻¹ (KBr): 3286, 2660, 2922, 2839, 1900, 1650, 1602, 1497, 1394, 1313, 1224, 1158, 1025, 853, 822, 765, 679, 694, 606, 507.

8.2.3.8. *N*-(2,4-Dimethylphenyl)-4-fluorobenzamide **91g**



N-(2,4-dimethylphenyl)-4-fluorobenzamide **91g** was successfully synthesized according to the general procedure using 4-fluorobenzoyl chloride (2.25 g, 14.2 mmol) and 2,4 dimethylaniline (1.64 g, 13.5 mmol); **Physical characteristics:** light grey solid; **Yield:** 2.89 g, 88%; **Melting point:** 179-181 °C; **¹H NMR** (400 MHz, DMSO-*d*₆) δ 9.93 (1H, s, NH), 8.09-8.13 (2H, dd, *J* = 5.6 Hz, 3.2 Hz, ArH), 7.32 (2H, t, *J* = 8.8 Hz, ArH), 7.21 (1H, d, *J* = 7.6 Hz, ArH), 7.06 (1H, s, ArH), 7.00 (1H, d, *J* = 7.6 Hz, ArH), 2.22 and 2.28 (6H, 2 x s, 2 x ArCH₃); **¹³C NMR** (101 MHz, DMSO-*d*₆) δ 164.4 (C=O), 164.2 (d, ¹J_{C,F} = 249 Hz, *para*-CF), 135.2 and 133.0 (2 x ArCCH₃), 131.1 (d, ⁴J_{C,F} = 3.0 Hz, 1'-C), 130.9 (d, ³J_{C,F} = 9 Hz, *ortho*-C), 126.7, 115.4 (ArC), 115.2 (d, ²J_{C,F} = 21 Hz, *meta*-C), 20.6 and 17.9 (2 x ArCCH₃); **FTIR** ν_{\max} /cm⁻¹ (KBr): 3286, 3078, 3017, 2922, 1896, 1652, 1602, 1522, 1497, 1313, 1297, 1223, 1276, 1158, 1091, 1013, 855, 809, 765, 606, 539, 506.

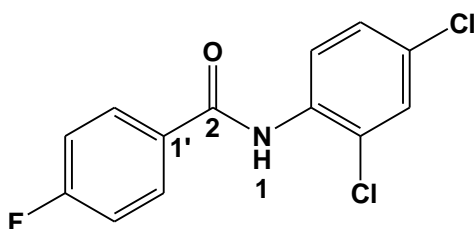
8.2.3.9. *N*-(2,4-Dimethylphenyl)-3-methoxy-benzamide **91h**



N-(2,4-Dimethylphenyl)-3-methoxybenzamide **91h** was successfully synthesized according to the general procedure using 3-methoxybenzoyl chloride (1.98 g, 12.8 mmol) and 2,4 dimethylaniline

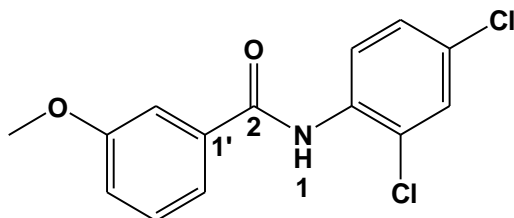
(1.48 g, 12.2 mmol); **Physical characteristics:** light grey solid; **Yield:** 2.80 g, 90%; **Melting point:** 156-159°C; **¹H NMR** (400 MHz, CDCl₃) δ 7.80 (1H, s, NH), 7.62 (1H, d, *J* = 7.6 Hz, ArH), 7.39 (1H, s, ArH), 7.32-7.38 (2H, m, ArH), 7.01-7.08 (3H, m, ArH), 3.83 (3H, s, ArOCH₃), 2.31 and 2.25 (6H, 2 x s, 2 x ArCH₃); **¹³C NMR** (101 MHz, CDCl₃) δ 165.6 (C=O), 159.8 (ArCOCH₃), 153.8 and 136.3 (2 x ArCCH₃), 135.2, 132.9, 131.1, 130.1, 129.6, 123.7, 118.7, 117.7, 112.5 (ArC), 55.3 (ArCOCH₃) 20.8 and 17.7 (2 x ArCCH₃); **FTIR** $\nu_{\max}/\text{cm}^{-1}$ (KBr): 3226, 3013, 2965, 1934, 1752, 1648, 1586, 1512, 1311, 1253, 1239, 1219, 1188, 1129, 1033, 986, 878, 822, 761, 688, 607, 506.

8.2.3.10. *N*-(2,4-Dichlorophenyl)-4-fluorobenzamide **91i**



N-(2,4-Dichlorophenyl)-4-fluorobenzamide **91i** was successfully synthesized according to the described general procedure using 4-fluorobenzoyl chloride (2.55 g, 16.1 mmol) and 2,4-dichloroaniline (2.48 g, 15.3 mmol); **Physical characteristics:** white solid; **Yield:** 4.04 g, 93%; **Melting point:** 134-136°C (lit.³⁵¹); **¹H NMR** (400 MHz, DMSO-*d*₆) δ 10.2 (1H, s, NH), 8.07-8.11 (2H, m, ArH), 7.68 (1H, s, ArH), 7.62 (1H, d, *J* = 8.8 Hz, ArH), 7.34 -7.47 (3H, m, ArH); **¹³C NMR** (100 MHz, DMSO-*d*₆) δ 164.4 (d, ¹*J*_{C,F} = 250 Hz, *para*-CF), 164.4 (C=O), 134.2, 133.2, 130.9, 130.6 (d, ³*J*_{C,F} = 9 Hz, *ortho*-C), 130.5 (d, ⁴*J*_{C,F} = 3 Hz, 1'-C) 129.5, 129.1, 127.6 (ArC), 115.5 (d, ²*J*_{C,F} = 22 Hz, *meta*-C); **FTIR** $\nu_{\max}/\text{cm}^{-1}$ (KBr): 3369, 3282, 3060, 1909, 1783, 1696, 1660, 1581, 1507, 1406, 1292, 1275, 1440, 1096, 989, 849, 807, 652, 626, 608, 556, 507.

8.2.3.11. *N*-(2,4-Dichlorophenyl)-3-methoxybenzamide **91j**



N-(2,4-Dichlorophenyl)-3-methoxybenzamide **91j** was successfully synthesized according to the general procedure using 3-methoxybenzyl chloride (2.12 g, 12.4 mmol) and 2,4-dichloroaniline (1.91 g, 11.8 mmol); **Physical characteristics:** white solid; **Yield:** 3.15 g, 90%; **Melting point:**

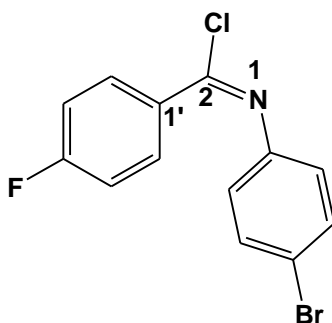
177-180 °C; $^1\text{H NMR}$ (400 MHz, DMSO- d_6) δ 10.4 (1H, s, NH), 7.71 (2H, d, $J = 7.6$ Hz, ArH), 7.49 (1H, s, ArH), 7.31-7.33 (3H, m, ArH), 7.23 (1H, d, $J = 7.6$ Hz, ArH), 3.87 (3H, s, ArOCH $_3$); $^{13}\text{C NMR}$ (101 MHz, DMSO- d_6) δ 164.3 (C=O), 157.8 (ArCOCH $_3$), 145.2, 144.8, 132.0, 130.6, 129.6, 128.2, 128.1, 126.0, 124.9, 122.6, 120.9, (ArC), 55.8 (ArCOCH $_3$); **FTIR** $\nu_{\text{max}}/\text{cm}^{-1}$ (KBr): 3369, 3438, 2154, 1660, 1601, 1539, 1499, 1438, 1328, 1220, 1016, 691, 667.

8.2.4. Synthesis of N-aryl benzimidoyl chloride intermediates

8.2.4.1. General Procedure

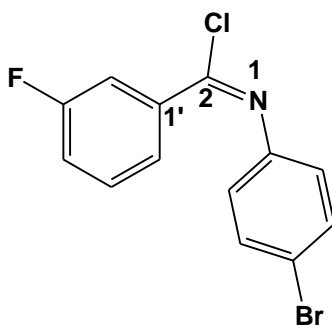
A mixture *N*-Aryl-benzamide (1.0 molar equivalent) and thionyl chloride (6.0 molar equivalents) was refluxed for 16 hours (monitored by TLC). Upon reaction completion, excess of thionyl chloride was removed by co-evaporation with toluene under rotavapour to afford (*E*)-*N*-aryl-benzimidoyl chloride after drying under high vacuum.²¹²

8.2.4.2. (*E*)-*N*-(4-Bromophenyl)-4-fluorobenzimidoyl chloride **90a**



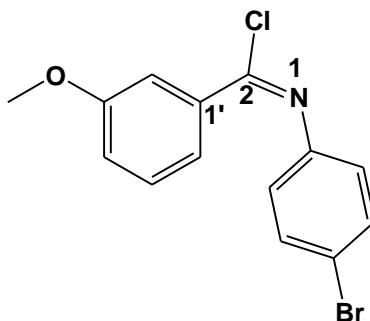
(*E*)-*N*-(4-Bromophenyl)-4-fluorobenzimidoyl chloride **90a** was successfully synthesized according to the general procedure using *N*-(4-bromophenyl)-4-fluorobenzamide **90a** (2.08 g, 7.07 mmol) and SOCl $_2$ (5.04 g, 42.4 mmol); **Physical characteristics**: pale yellow solid; **Yield**: 2.01 g, 96%; $^1\text{H NMR}$ (400 MHz, CDCl $_3$) δ 8.15-8.19 (2H, m, ArH), 7.52 (2H, d, $J = 7.6$ Hz, ArH), 7.14 (2H, d, $J = 7.6$ Hz, ArH), 6.89 (2H, d, $J = 5.6$ Hz, ArH); $^{13}\text{C NMR}$ (101 MHz, CDCl $_3$) δ 164.8 (d, $^1J_{\text{C,F}} = 252$ Hz, *para*-CF), 146.3 (ArCCCl), 142.7, 131.9 (ArC), 131.7 (d, $^3J_{\text{C,F}} = 9$ Hz, *ortho*-C), 130.2 (d, $^4J_{\text{C,F}} = 3$ Hz, 1'-C), 122.3 (ArC), 118.4 (ArCBr), 115.5 (d, $^2J_{\text{C,F}} = 22$ Hz, *meta*-C).

8.2.4.3. (*E*)-*N*-(4-Bromophenyl)-4-fluorobenzimidoyl chloride **90b**



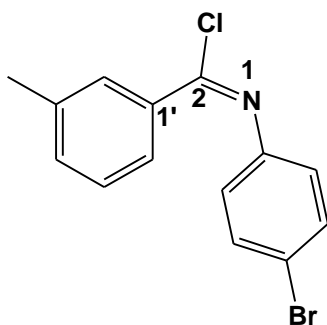
(*E*)-*N*-(4-Bromophenyl)-3-fluorobenzimidoyl chloride **90b** was successfully synthesized according to the general procedure using *N*-(4-bromophenyl)-3-fluorobenzamide **90b** (1.93g, 6.55 mmol) and SOCl_2 (4.68 g, 39.3 mmol); **Physical characteristics**: pale yellow solid; **Yield**: 1.84 g, 95%; **$^1\text{H NMR}$** (400 MHz, CDCl_3) δ 7.75-7.87 (2H, m, ArH), 7.42-7.45 (2H, m, ArH), 7.32-7.39 (2H, m, ArH), 6.80-6.84 (2H, m, ArH); **$^{13}\text{C NMR}$** (101 MHz, CDCl_3) δ 162.5 (d, $^1J_{\text{C,F}} = 247.4$ Hz, 3'-CF), 146.1 (ArCCl), 142.2 (d, $^4J_{\text{C,F}} = 4$ Hz, 6'-C), 137.2 (d, $^3J_{\text{C,F}} = 8$ Hz, 1'-C), 132.0 (ArC), 130.5, 129.93 (ArC), 125.1 (d, $^3J_{\text{C,F}} = 3$ Hz, 5'-C), 122.3 (ArC), 119.2 (d, $^2J_{\text{C,F}} = 22$ Hz, 2'-C), 116.3 (d, $^2J_{\text{C,F}} = 24$ Hz, 4'-C).

8.2.4.4. (*E*)-*N*-(4-Bromophenyl)-3-methoxybenzimidoyl chloride **90c**



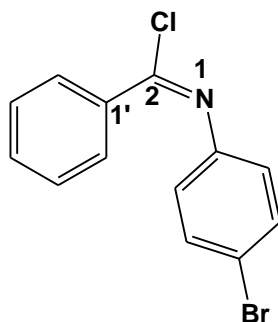
(*E*)-*N*-(4-Bromophenyl)-3-methoxybenzimidoyl chloride **90c** was successfully synthesized according to the general procedure using *N*-(4-bromophenyl)-3-methoxybenzamide **90c** (3.12 g, 10.2 mmol) and SOCl_2 (7.28 g, 61.2 mmol); **Physical characteristics**: pale yellow solid; **Yield**: 3.24 g, 98%; **$^1\text{H NMR}$** (400 MHz, CDCl_3) δ 7.74 (1H, d, $J = 7.6$ Hz, ArH), 7.68 (1H, s, ArH), 7.52 (2H, d, $J = 7.6$ Hz, ArH), 6.80 (1H, t, $J = 8.2$ Hz, ArH), 7.11 (1H, d, $J = 7.6$ Hz, ArH), 6.89 (2H, d, $J = 7.6$ Hz, ArH), 3.88 (3H, s, ArOCH_3); **$^{13}\text{C NMR}$** (101 MHz, CDCl_3) δ 159.6 (ArCOCH₃), 146.5 (ArCCl), 143.9, 136.5, 131.9, 129.4, 122.2, 122.1, 118.7, 118.3 (ArCBr), 113.9 (ArC), 55.5 (ArCOCH₃).

8.2.4.5. (*E*)-*N*-(4-Bromophenyl)-3-methylbenzimidoyl chloride **90d**



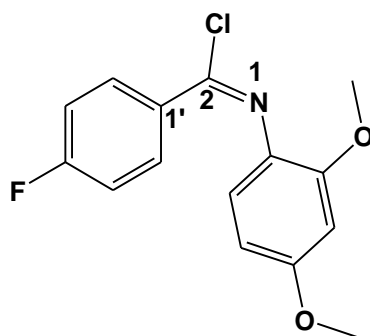
(*E*)-*N*-(4-Bromophenyl)-3-methylbenzimidoyl chloride **90d** was successfully synthesized according to the general procedure using *N*-(4-bromophenyl)-3-methylbenzamide **91d** (2.56 g, 8.85 mmol) and SOCl_2 (6.32 g, 53.1 mmol); **Physical characteristics:** pale yellow solid; **Yield:** 2.68 g, 98%; **$^1\text{H NMR}$** (400 MHz, CDCl_3) δ 7.74 (2H, d, $J = 7.6$ Hz, ArH), 7.01-7.56 (4H, m, ArH), 6.89 (2H, d, $J = 7.6$ Hz, ArH), 2.22 (3H, s, ArCH_3); **$^{13}\text{C NMR}$** (101 MHz, CDCl_3) δ 154.3, 146.5 (ArCCl), 138.6, 133.2, 131.1, 129.9, 129.1, 128.4, 126.0, 124.8 (ArC), 121.3 (ArCBr), 24.1 (ArCCH₃).

8.2.4.6. (*E*)-*N*-(4-Bromophenyl)benzimidoyl chloride **90e**



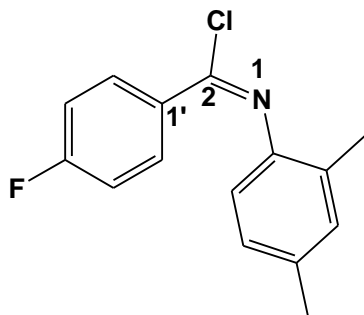
(*E*)-*N*-(4-Bromophenyl)benzimidoyl chloride **90e** was successfully synthesized according to the described general procedure using *N*-(4-bromophenyl)benzamide **91e** (2.50 g, 9.05 mmol) and SOCl_2 (6.46 g, 54.3 mmol); **Physical characteristics:** pale yellow solid; **Yield:** 2.56 g, 96%; **$^1\text{H NMR}$** (400 MHz, CDCl_3) δ 8.20 (2H, d, $J = 7.6$ Hz, ArH), 7.51-7.62 (5H, m, ArH), 6.95 (2H, d, $J = 8.8$ Hz, ArH); **$^{13}\text{C NMR}$** (101 MHz, CDCl_3) δ 146.5 (ArCCl), 144.0, 135.2, 132.0, 131.9, 129.4, 128.5, 122.3, 118.3 (ArC).

8.2.4.7. (*E*)-*N*-(2,4-Dimethoxyphenyl)-4-fluorobenzimidoyl chloride **90f**



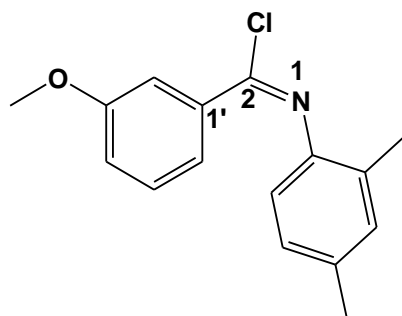
(*E*)-*N*-(2,4-Dimethoxyphenyl)-4-fluorobenzimidoyl chloride **90f** was successfully synthesized according to the general procedure using 4-fluoro-*N*-(2,4-dimethoxyphenyl)benzamide **91f** (2.14 g, 7.66 mmol) with SOCl_2 (5.47 g, 46.0 mmol); **Physical characteristics:** grey solid; **Yield:** 2.14 g, 95%; **$^1\text{H NMR}$** (400 MHz, CDCl_3) δ 7.74-7.76 (2H, m, ArH), 7.51 (2H, t, $J = 7.6$ Hz, ArH), 6.90-7.42 (3H, m, ArH), 3.88 and 3.92 (6H, 2 x s, ArOCH_3); **$^{13}\text{C NMR}$** (101 MHz, CDCl_3) δ 162.1 (d, $^1J_{\text{C,F}} = 245$ Hz, *para*-CF), 158.2 and 153.8 (2 x ArCOCH₃), 143.5 (ArCCl), 137.0 (d, $^4J_{\text{C,F}} = 6$ Hz, 1'-C), 130.6 (d, $^3J_{\text{C,F}} = 8$ Hz, *meta*-C), 126.2, 123.7, 119.4 (ArC), 118.3 (d, $^2J_{\text{C,F}} = 23$ Hz, *meta*-C), 114.2 and 99.0 (ArC), 55.7 and 55.4 (2 x ArCOCH₃).

8.2.4.8. (*E*)-*N*-(2,4-Dimethylphenyl)-4-fluorobenzimidoyl chloride **90g**



(*E*)-*N*-(2,4-Dimethylphenyl)-4-fluorobenzimidoyl chloride **90g** was successfully synthesized according to the general procedure using 4-fluoro-*N*-(2,4-dimethylphenyl)benzamide **91g** (1.77 g, 7.26 mmol) and SOCl_2 (5.19 g, 43.6 mmol); **Physical characteristics:** pale grey solid; **Yield:** 1.86 g, 98%; **$^1\text{H NMR}$** (400 MHz, CDCl_3) δ 8.21-8.24 (2H, m, ArH), 7.10-7.20 (4H, m, ArH), 6.8 (1H, d, $J = 8.2$ Hz, ArH), 2.37 and 2.20 (2 x ArCCH₃); **$^{13}\text{C NMR}$** (101 MHz, CDCl_3) δ 164.2 (d, $^1J_{\text{C,F}} = 253$ Hz, *para*-CF), 143.9 (ArCCl), 141.6, 134.7, 131.7 (d, $^3J_{\text{C,F}} = 9$ Hz, *ortho*-C), 131.1, 128.4, 126.8, 119.2 9 (ArC), 115.9 (d, $^2J_{\text{C,F}} = 22$ Hz, *meta*-C), 20.9 and 17.8 (2 x ArCCH₃).

8.2.4.9. (*E*)-*N*-(2,4-Dimethylphenyl)-3-methoxybenzimidoyl chloride **90h**



(*E*)-*N*-(2,4-Dimethylphenyl)-3-methoxybenzimidoyl chloride **90h** was successfully synthesized according to the described general procedure using *N*-(2,4-dimethylphenyl)-3-methoxybenzamide **91h** (2.18 g, 8.53 mmol) with SOCl_2 (6.09 g, 51.2 mmol); **Physical characteristics**: white solid; **Yield**: 2.24 g, 96%; **$^1\text{H NMR}$** (400 MHz, CDCl_3) δ 7.80 (1H, d, $J = 8.2$ Hz, ArH), 7.76 (1H, t, $J = 5.6$ Hz, ArH), 7.39 (1H, t, $J = 5.6$ Hz, ArH), 7.07-7.14 (3H, m, ArH), 6.82 (1H, d, $J = 7.6$ Hz, ArH), 3.91 (3H, s, ArOCH_3), 2.37 and 2.20 (6H, 2 x s, 2 x ArCH_3); **$^{13}\text{C NMR}$** (101 MHz): δ 159.6 (ArCOCH_3), 143.9 (ArCCl), 143.0 and 136.6 (ArCCH_3), 134.6, 131.0, 129.3, 128.3, 126.8, 122.0, 119.2, 118.3, 114.0, 55.4 (ArCOCH_3), 20.9 and 17.7 (2 x ArCCH_3).

8.2.5. Synthesis of ethyl 1,5-diaryl-1*H*-imidazole carboxylates

8.2.5.1. General synthetic procedure A

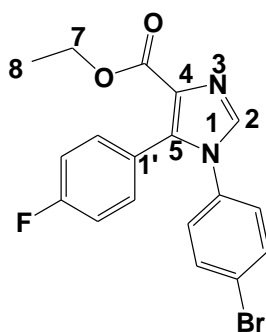
A mixture of ethyl isocyanoacetate (1 molar equivalent) and DBU (1.0 molar equivalent) in anhydrous THF was cooled to -78°C under a continuous flow of argon. *N*-aryl benzimidoyl chloride (1.0 molar equivalent) was then added. The resulting reaction mixture was allowed to warm to room temperature and was stirred for 48 hours (monitored by TLC) under inert atmosphere. Upon completion, the solvent was concentrated *in vacuo* to give a brown oily residue which was then purified by column chromatography on silica gel [eluting first with EtOAc/Hexane (1:4), followed by 100% EtOAc] to afford the desired ethyl 1,5-diaryl-1*H*-imidazole carboxylate.

8.2.5.2. General synthetic procedure B

Potassium *t*-butoxide (1.1 molar equivalent) was added to a solution of the *N*-aryl-benzamide (1.0 molar equivalent) in anhydrous THF (20 ml) at 0°C under argon. After stirring the mixture at 0°C for 20 min, the reaction mixture was again cooled to -35°C and diethylchlorophosphate (1.3 molar equivalents) was added slowly. After stirring this mixture at 0°C for 30 min, the

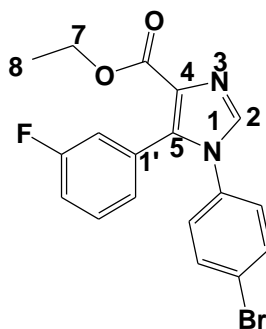
reaction flask was cooled to -35 °C and ethyl isocyanoacetate (1.1 molar equivalent) was added, followed by potassium *t* butoxide (1.1 molar equivalent). The mixture was stirred at room temperature for 8-16 hours with TLC monitoring. Unfortunately no formation of products was observed.

8.2.5.3. Ethyl 1-(4-bromophenyl)-5-(4-fluorophenyl)-1*H*-imidazole-4-carboxylate **88a**



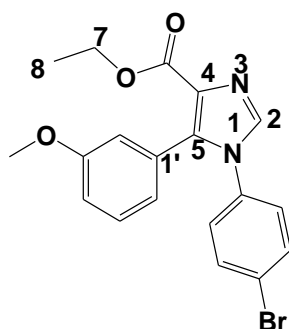
Ethyl 1-(4-bromophenyl)-5-(4-fluorophenyl)-1*H*-imidazole-4-carboxylate **88a** was successfully synthesized according to procedure A using *N*-(4-bromophenyl)-4-fluorobenzimidoyl chloride **90a** (592 mg, 2.00 mmol), ethyl isocyanoacetate (226 mg, 2.00 mmol) and DBU (305 mg, 2.00 mmol) in anhydrous THF (20 ml); **Physical characteristics**: pale yellow solid; **Yield**: 497 mg, 64%; **Melting point**: 145-147°C; **¹H NMR** (400 MHz, CDCl₃) δ 7.70 (1H, s, 2-CH), 7.46 (2H, d, *J* = 8.4 Hz, ArH), 7.19 (2H, m, ArH), 6.93-7.02 (4H, m, ArH), 4.26 (2H, q, *J* = 7.2 Hz, OCH₂CH₃), 1.26 (3H, t, *J* = 7.2 Hz, OCH₂CH₃); **¹³C NMR** (101 MHz, CDCl₃) δ 162.9 (d, ¹*J*_{C,F} = 251 Hz, *para*-CF), 162.6 (C=O), 137.3 (2-C), 136.9, 134.4, 132.7 (d, ⁴*J*_{C,F} = 3 Hz, 1'-C), 132.6, 127.2, 125.3, 123.8 (d, ³*J*_{C,F} = 8 Hz, *ortho*-C), 122.8 (ArCBr), 115.2 (d, ²*J*_{C,F} = 22.1 Hz, *meta*-C), 60.5 (7-C), 14.2 (8-C); **FTIR** ν_{\max} /cm⁻¹ (KBr): 3104, 3096, 2987, 1904, 1716, 1609, 1591, 1560, 1497, 1375, 1348, 1279, 1256, 1185, 1090, 1070, 1028, 963, 845, 830, 665, 617, 515; **HRMS** (ESI-TOF) *m/z*: [M+H]⁺ Calcd for C₁₈H₁₅⁷⁹BrFN₂O₂ 389.0295, found 389.0301.

8.2.5.4. Ethyl 1-(4-bromophenyl)-5-(3-fluorophenyl)-1*H*-imidazole-4-carboxylate **88b**



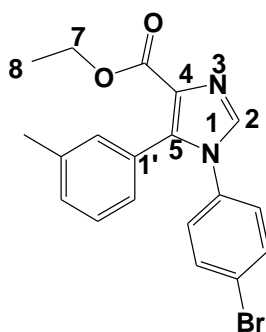
Ethyl 1-(4-bromophenyl)-5-(3-fluorophenyl)-1*H*-imidazole-4-carboxylate **88b** was successfully synthesized according to general procedure A using *N*-(4-bromophenyl)-3-fluorobenzimidoyl chloride **90b** (625 mg, 2.11 mmol), ethyl isocynoacetate (239 mg, 2.11 mmol) and DBU (321 mg, 2.11 mmol) in anhydrous THF (20 ml); **Physical characteristics**: yellow solid; **Yield**: 475 mg, 58%; **Melting point**: 129-131°C; **¹H NMR** (400 MHz, CDCl₃) δ 7.74 (1H, s, 2-CH), 7.48 (2H, d, *J* = 8.2 Hz, ArH), 7.27-7.32 (1H, m, ArH), 6.96-7.08 (5H, m, ArH), 4.28 (2H, q, *J* = 7.2 Hz, OCH₂CH₃), 1.28 (3H, t, *J* = 7.2 Hz, OCH₂CH₃); **¹³C NMR** (101 MHz, CDCl₃) δ 162.1 (d, ¹*J*_{C,F} = 247 Hz, *meta*-CF), 162.4 (C=O), 137.6 (C-2), 136.4, 132.8, 131.0 (ArC), 129.9 (d, ³*J*_{C,F} = 8 Hz, 1'-C), 127.1 (ArC), 126.5 (d, ⁴*J*_{C,F} = 3 Hz, 6'-C), 122.8 (ArCBr), 117.8 (d, ²*J*_{C,F} = 22 Hz, 2'-C), 116.1 (d, ²*J*_{C,F} = 21 Hz, 4'-C), 60.7 (7-C), 14.1 (8-C); **FTIR** ν_{\max} /cm⁻¹ (KBr): 3093, 2991, 2978, 1900, 1708, 1617, 1582, 1561, 1498, 1372, 1343, 1297, 1259, 1236, 1192, 1178, 1092, 1073, 1032, 964, 830, 799, 601, 517; **HRMS** (ESI-TOF) *m/z*: [M+H]⁺ Calcd for C₁₈H₁₅⁷⁹BrFN₂O₂ 389.0295, found 389.0301.

8.2.5.5. Ethyl 1-(4-bromophenyl)-5-(3-methoxyphenyl)-1*H*-imidazole-4-carboxylate **88c**



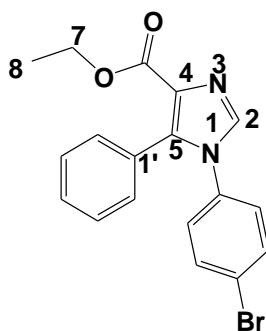
Ethyl 1-(4-bromophenyl)-5-(3-methoxyphenyl)-1*H*-imidazole-4-carboxylate **88c** was successfully synthesized according to procedure A using *N*-(4-bromophenyl)-3-methoxybenzimidoyl chloride **90c** (1.88 g, 5.79 mmol), ethyl isocynoacetate (655 mg, 5.79 mmol) and DBU (882 mg, 5.79 mmol) in anhydrous THF (20 ml); **Physical characteristics**: yellow solid; **Yield**: 418 mg, 18%; **¹H NMR** (400 MHz, CDCl₃) δ 7.61 (1H, s, 2-CH), 7.37 (2H, d, *J* = 8.4 Hz, ArH), 7.10 (1H, t, *J* = 8.0 Hz, ArH), 6.88 (2H, d, *J* = 8.4 Hz, ArH), 6.70-6.80 (3H, m, ArH), 4.19 (2H, q, *J* = 7.2 Hz, OCH₂CH₃), 3.63 (3H, s, ArOCH₃), 1.18 (3H, t, *J* = 7.0 Hz, OCH₂CH₃); **¹³C NMR** (101 MHz, CDCl₃) δ 162.6 (C=O), 159.0 (ArCOCH₃), 137.6 (2-C), 137.2, 134.7, 132.6, 130.9, 129.1, 127.1, 123.1, 122.5, 119.3, 116.5, 114.5 (ArC), 60.4 (7-C), 55.1 (ArCOCH₃), 14.1 (8-C); **FTIR** ν_{\max} /cm⁻¹ (KBr): 3097, 3000, 2978, 2930, 1891, 1715, 1587, 1552, 1496, 1449, 1374, 1344, 1321, 1261, 1207, 1187, 1097, 1070, 1042, 1029, 961, 829, 661, 569, 517; **HRMS** (ESI-TOF) *m/z*: [M+H]⁺ Calcd. for C₁₉H₁₈⁷⁹BrN₂O₃ 401.0495, found 401.0487.

8.2.5.6. Ethyl 1-(4-bromophenyl)-5-(3-methylphenyl)-1*H*-imidazole-4-carboxylate **88d**



Ethyl 1-(4-bromophenyl)-5-(3-methylphenyl)-1*H*-imidazole-4-carboxylate **88d** was successfully synthesized according to general procedure A using *N*-(4-bromophenyl)-3-methylbenzimidoyl chloride **90d** (1.93 g, 6.25 mmol), ethyl isocynoacetate (707 mg, 6.25 mmol) and DBU (952 mg, 6.25 mmol) in anhydrous THF (20 ml); **Physical characteristics**: white solid; **Yield**: 722 mg 30%; **Melting point**: 185-187°C; **¹H NMR** (400 MHz, CDCl₃) δ 7.69 (1H, s, 2-CH), 7.43 (2H, d, *J* = 8.4 Hz, ArH), 7.13-7.19 (2H, m, ArH), 7.05 (1H, s, ArH), 6.93-6.98 (3H, m, ArH), 4.25 (2H, q, *J* = 7.2 Hz, OCH₂CH₃), 2.27 (3H, s, ArCH₃), 1.24 (3H, t, *J* = 7 Hz, OCH₂CH₃); **¹³C NMR** (101 MHz, CDCl₃) δ 162.6 (C=O), 138.0, 137.6 (2-C), 137.2, 134.6, 132.5, 131.3, 130.7, 129.7, 127.8, 127.1, 122.4 (ArC), 60.4 (7-C), 21.3 (ArCCH₃), 14.1 (8-C); **FTIR** ν_{max} /cm⁻¹ (KBr): 3100, 2987, 1896, 1713, 1591, 1552, 1497, 1372, 1279, 1258, 1194, 1177, 1101, 1070, 1039, 962, 830, 819, 652, 621, 522; **HRMS** (ESI-TOF) *m/z*: [M+H]⁺ Calcd for C₁₉H₁₈⁷⁹BrN₂O₂ 385.0546, found 385.0557.

8.2.5.7. Ethyl 1-(4-bromophenyl)-5-phenyl-1*H*-imidazole-4-carboxylate **88e**



Ethyl 1-(4-bromophenyl)-5-phenyl-1*H*-imidazole-4-carboxylate **88e** was successfully synthesized according to procedure A using *N*-(4-bromophenyl)-benzimidoyl chloride **90e** (1.48 g, 5.03 mmol), ethyl isocynoacetate (569 mg, 5.03 mmol) and DBU (766 mg, 5.03 mmol) in anhydrous THF (20 ml); **Physical characteristics**: white solid; **Yield**: 411 mg, 22%; **Melting point**: 138-140°C; **¹H NMR** (400 MHz, CDCl₃) δ 7.70 (1H, s, 2-CH), 7.44 (2H, d, *J* = 8.4 Hz, ArH), 7.28-7.33 (3H, m, ArH), 7.21-7.22 (2H, m, ArH), 6.93 (2H, d, *J* = 8.4 Hz, ArH), 4.26 (2H, q, *J* = 7.2

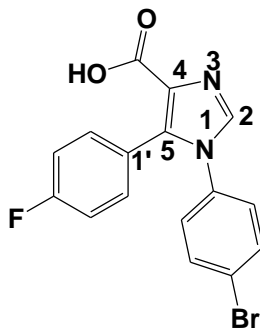
Hz, OCH₂CH₃), 1.25 (3H, t, *J* = 7.2 Hz, OCH₂CH₃); ¹³C NMR (101 MHz, CDCl₃) δ 162.7 (C=O), 137.9 (2-C), 137.3, 134.6, 132.6, 130.8, 129.0, 128.0, 127.8, 127.2, 125.3, 122.5 (ArC), 60.5 (7-C), 14.2 (8-C); FTIR ν_{\max} /cm⁻¹ (KBr): 3096, 2974, 1900, 1709, 1604, 1586, 1556, 1498, 1373, 1295, 1280, 1181, 1091, 1073, 993, 828, 765, 661, 517; HRMS (ESI-TOF) *m/z*: [M+H]⁺ Calcd for C₁₆H₁₆⁷⁹BrN₂O₂ 371.0390, found 371.0398.

8.2.6. Hydrolysis of ethyl 1,5-diaryl-1*H*-imidazole-4-carboxylates

8.2.6.1. General synthetic procedure

NaOH (2 molar equivalent) was added to a solution of ethyl 1,5-diaryl-1*H*-imidazolyl carboxylate (1 molar equivalent) in MeOH (5 ml) and H₂O (5 ml). The resulting reaction mixture was refluxed until disappearance of the starting material (monitored by TLC). MeOH solvent was then removed *in vacuo* and the remaining aqueous crude material was slowly neutralized with 1M HCl, followed by extraction with EtOAc (2 x 20 ml). The organic layer was then washed with brine, dried over MgSO₄, and the solvent was removed *in vacuo* to produce the desired novel 1,5-diaryl-1*H*-imidazole-4-carboxylic acids.

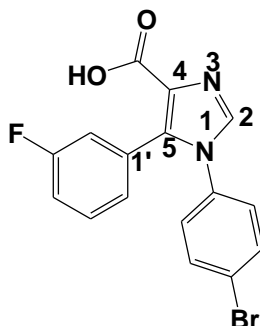
8.2.6.2. 1-(4-Bromophenyl)-5-(4-fluorophenyl)-1*H*-imidazole-4-carboxylic acid **87a**



1-(4-Bromophenyl)-5-(4-fluorophenyl)-1*H*-imidazole-4-carboxylic acid **87a** was successfully synthesized according to the general procedure using ethyl 1-(4-bromophenyl)-5-(4-fluorophenyl)-1*H*-imidazole-4-carboxylate **88a** (404 mg, 1.04 mmol) and NaOH (83 mg, 2.08 mmol) in MeOH (5 ml) and water (5 ml); **Physical characteristics**: pale yellow solid; **Yield**: 255 mg, 68%; **Melting point**: 189-192°C; ¹H NMR (400 MHz, DMSO-*d*₆) δ 12.4 (1H, br, COOH), 8.06 (1H, s, 2-CH), 7.59 (2H, d, *J* = 8.4 Hz, ArH), 7.13-7.32 (6H, m, ArH); ¹³C NMR (100 MHz, DMSO-*d*₆) δ 163.7 (C=O), 161.3 (d, ¹*J*_{C,F} = 246.1 Hz, *para*-CF), 138.2 (2-C), 136.2, 134.5 (ArC), 133.1 (d, ³*J*_{C,F} = 8.0 Hz, *ortho*-C), 132.3 128.4 (ArC), 125.0 (d, ⁴*J*_{C,F} = 3.1 Hz, 1'-C); 121.7 (ArCBr), 114.8 (d, ²*J*_{C,F} = 22.1 Hz, *meta*-C); FTIR ν_{\max} /cm⁻¹ (KBr): 3124, 2831, 2511 (OH), 1697, 1603,

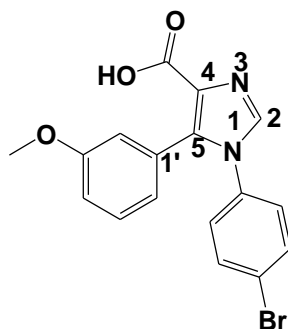
1594, 1503, 1351, 1292, 1258, 1227, 1195, 1186, 1160, 1070, 1001, 974, 840, 817, 769, 730, 577, 501; **HRMS** (ESI-TOF) m/z : $[M+H]^+$ Calcd, for $C_{16}H_{11}^{79}BrFN_2O_2$ 360.9982, found 360.9991.

8.2.6.3. 1-(4-Bromophenyl)-5-(3-fluorophenyl)-1*H*-imidazole-4-carboxylic acid **87b**



1-(4-Bromophenyl)-5-(3-fluorophenyl)-1*H*-imidazole-4-carboxylic acid **87b** was successfully synthesized according to the general procedure using ethyl 1-(4-bromophenyl)-5-(3-fluorophenyl)-1*H*-imidazole-4-carboxylate **88b** (342 mg, 0.88 mmol) and NaOH (70 mg, 1.76 mmol) in MeOH (5 ml) and water (5 ml); **Physical characteristics**: pale yellow solid; **Yield**: 229 mg, 72%; **¹H NMR** (400 MHz, DMSO- d_6): δ 12.3 (1H, br, COOH), 8.08 (1H, s, 2-CH), 7.60 (2H, d, $J = 8.8$ Hz, ArH), 7.31 (1H, d, $J = 6.8$ Hz, ArH), 7.15-7.22 (4H, t, $J = 10.4$ ArH), 7.01 (1H, d, $J = 7.6$ Hz, ArH); **¹³C NMR** (101 MHz, DMSO- d_6) δ 163.7 (C=O), 161.2 (d, $^1J_{C,F} = 244$ Hz, *meta*-FC), 138.4 (2-C), 135.7, 134.6, 131.6 (d, $^3J_{C,F} = 3$ Hz, 1'-C), 130.8 (d, $^3J_{C,F} = 9$ Hz, 6'-C), 129.7 (d, $^4J_{C,F} = 8$ Hz, 5'-C), 129.6, 128.7, 127.0 (ArC), 121.7 (ArCBr), 118.0 (d, $^2J_{C,F} = 23$ Hz, 2'-C), 115.5 (d, $^2J_{C,F} = 21.1$ Hz, 4'-C); **FTIR** ν_{max}/cm^{-1} (KBr): 3117, 3065, 2917, 2855, 2487(OH), 1895, 1687, 1613, 1583, 1566, 1496, 1479, 1442, 1378, 1338, 1285, 1250, 1204, 1183, 1070, 972, 866, 819, 807, 764, 573, 501; **HRMS** (ESI-TOF) m/z : $[M+H]^+$ Calcd for $C_{16}H_{11}^{79}BrFN_2O_2$ 360.9982, found 360.9987.

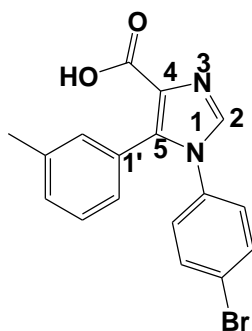
8.2.6.4. 1-(4-Bromophenyl)-5-(3-methoxyphenyl)-1*H*-imidazole-4-carboxylic acid **87c**



1-(4-Bromophenyl)-5-(3-methoxyphenyl)-1*H*-imidazole-4-carboxylic acid **87c** was successfully synthesized according to the general procedure using ethyl 1-(4-bromophenyl)-5-(3-

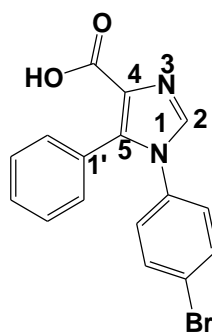
methoxyphenyl)-1*H*-imidazole-4-carboxylate **88c** (385 mg, 0.96 mmol) and NaOH (77 mg, 1.92 mmol) in MeOH (5 ml) and water (5 ml); **Physical characteristics**: pale yellow solid; **Yield**: 280 mg, 78%; **¹H NMR** (400 MHz, DMSO-*d*₆) δ 12.3 (1H, br, COOH), 8.05 (1H, s, 2-CH), 7.59 (2H, d, *J* = 8.0 Hz, ArH), 7.18 (2H, t, *J* = 6.6 Hz, ArH), 6.87 (2H, d, *J* = 10.0 Hz, ArH), 6.75 (2H, d, *J* = 7.6 Hz, ArH) 3.65 (3H, s, ArOCH₃); **¹³C NMR** (101 MHz, DMSO-*d*₆) δ 163.7 (C=O), 158.4 (ArCOCH₃), 138.1 (2-C), 136.9, 134.9, 132.2, 130.5, 129.8, 128.9, 128.3, 123.1, 121.6, 116.8, 144.0, (ArC), 55.0 (ArCOCH₃); **FTIR** $\nu_{\max}/\text{cm}^{-1}$ (KBr): 3117, 3061, 3004, 2969, 2830, 2565 (OH), 1909, 1704, 1674, 1909, 1704, 1674, 1601, 1548, 1496, 1465, 1421, 1355, 1343, 1254, 1217, 1172, 1040, 977, 852, 726, 539, 504; **H.RMS** (ESI-TOF) *m/z*: [M+H]⁺ Calcd for C₁₇H₁₄⁷⁹BrN₂O₃ 373.0182, Found 373.0201

8.2.6.5. 1-(4-Bromophenyl)-5-(3-methylphenyl)-1*H*-imidazole-4-carboxylic acid **87d**



1-(4-Bromophenyl)-5-(3-methylphenyl)-1*H*-imidazole-4-carboxylic acid **87d** was successfully synthesized according to the general procedure using ethyl 1-(4-bromophenyl)-5-(3-methylphenyl)-1*H*-imidazole-4-carboxylate **88d** (420 mg, 1.09 mmol) and NaOH (87 mg, 2.18 mmol) in MeOH (5 ml) and water (5 ml); **Physical characteristics**: white solid; **Yield**: 292 mg, 75%; **¹H NMR** (400 MHz, DMSO-*d*₆) δ 12.2 (1H, br, COOH), 8.04 (1H, s, 2-CH), 7.58 (2H, d, *J* = 8.4 Hz, ArH), 7.10-7.19 (5H, m, ArH), 6.97 (1H, d, *J* = 7.2 Hz, ArH), 2.22 (3H, s, ArCH₃); **¹³C NMR** (101 MHz, DMSO-*d*₆) δ 163.7 (C=O), 138.1 (2-C), 137.2, 136.8, 134.8, 132.2, 131.4, 130.5, 129.2, 128.5, 128.3, 127.8, 127.6, (ArC), 121.5 (ArCBr), 20.9 (ArCCH₃); **FTIR** $\nu_{\max}/\text{cm}^{-1}$ (KBr): 3134, 2923, 2848, 2498 (OH), 1895, 1705, 1613, 1591, 1547, 1495, 1351, 1261, 1218, 1184, 1066, 1026, 974, 852, 727, 539, 501; **HRMS** (ESI-TOF) *m/z*: [M+H]⁺ Calcd for C₁₇H₁₄⁷⁹BrN₂O₂ 357.0233, found 357.0244.

8.6.5.6.1-(4-Bromophenyl)-5-phenyl-1*H*-imidazole-4-carboxylic acid **87e**



1-(4-Bromophenyl)-5-phenyl-1*H*-imidazole-4-carboxylic acid **87e** was successfully synthesized according to the general procedure using ethyl 1-(4-bromophenyl)-5-phenyl-1*H*-imidazole-4-carboxylate **88e** (427 mg, 1.15 mmol) and NaOH (92 mg, 2.30 mmol) in MeOH (5 ml) and water (5 ml); **Physical characteristics**: white solid; **Yield**: 249 mg, 63%; **¹H NMR** (400 MHz, DMSO-*d*₆): δ 12.2 (1H, br, COOH), 8.06 (1H, s, 2-CH), 7.57 (2H, d, *J* = 8.0 Hz, ArH), 7.15-7.31 (7H, m, ArH); **¹³C NMR** (101 MHz, DMSO-*d*₆) δ 163.7 (C=O), 138.2 (2-C), 137.1, 134.8, 132.2, 130.8, 130.5, 125.9, 128.5, 128.3, 127.8 (ArC), 121.5 (ArCBr); **FTIR** ν_{\max} /cm⁻¹ (KBr): 3117, 3096, 2969, 2848, 2470 (OH), 1930, 1721, 1683, 1609, 1558, 1494, 1388, 1356, 1257, 1169, 1070, 1012, 975, 846, 780, 696, 521; **HRMS** (ESI-TOF) *m/z*: [M+H]⁺ Calcd for C₁₆H₁₂⁷⁹BrN₂O₂ 343.0077, found 343.0089.

8.3. Chapter 3 experimental procedures

8.3.1. . Synthesis of 5-aryl-1,3-oxazole

8.3.1.1. Microwave assisted van Leusen general synthetic procedure A

To a 10 ml microwave reaction vessel equipped with a magnetic stirrer bar was introduced aryl aldehyde (1 molar equivalent), TosMIC (1.1 molar equivalents) and K_2CO_3 (2 molar equivalents). An inert atmosphere was then created by degassing through evacuating and refilling with argon three times, followed by addition of anhydrous MeOH (10 ml). The resulting capped reaction mixture was then microwave irradiated at a set temperature of 90°C and a power of 120 Watts for 7 min (monitored by TLC and conditions maintained until consumption of the TosMIC reagent). Upon completion of the reaction, the solvent was evaporated *in vacuo*. The crude material was purified by flash column chromatography [elution with ethyl acetate and hexane ratio (1:4)] to afford 5-aryl-1,3-oxazole derivatives with R_f values of between 0.51-0.65.

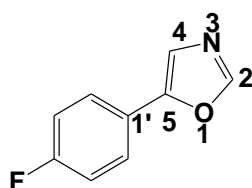
8.3.1.2. Microwave assisted van Leusen general synthetic procedure B

To a 10 ml microwave reaction vessel equipped with a magnetic stirrer bar was introduced aryl aldehyde (1 molar equivalent), TosMIC (1.1 molar equivalents) K_2CO_3 (2 molar equivalents). An inert atmosphere was then created by degassing through evacuating and refilling with argon three times, followed by introduction of anhydrous MeCN (5 ml). The resulting reaction mixture was capped and microwave irradiated at a set temperature of 90°C and a power of 120 Watts for 12 min. Upon completion of the reaction (monitored by TLC and conditions maintained until consumption of the TosMIC reagent), the solvent was then evaporated *in vacuo*. The crude material was then stirred at 0°C in a mixture containing MeOH (4 ml) and water (0.5 ml) until a precipitate formed. The precipitate was collected, washed with water and dried under high vacuum to give 5-aryl-4-tosyl-4,5-dihydro-1,3-oxazoles with R_f values between 0.64-0.72.

8.3.1.3. Aromatization general synthetic procedure C

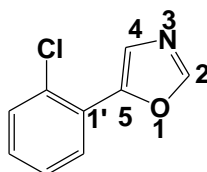
A mixture of 5-aryl-4-tosyl-4,5-dihydro-1,3-oxazole (1 molar equivalent) in toluene (5 ml) was refluxed for 1 hour. After completion of the reaction, toluene was concentrated *in vacuo* and the crude material was purified by column chromatography [eluting with hexane and ethyl acetate (4:1)] to furnish 5-aryl-1,3-oxazoles after drying under high vacuum (with R_f values of between 0.51-0.65).

8.3.1.4. 5-(4-Fluorophenyl)-1,3-oxazole 96a



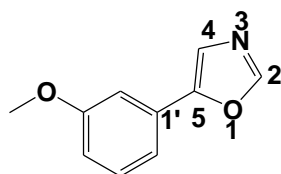
5-(4-Fluorophenyl)-1,3-oxazole **96a** was successfully synthesized from reaction of 4-fluorobenzaldehyde (166 mg, 1.34 mmol), TosMIC (287 mg, 1.47 mmol) and K_2CO_3 (370 mg, 2.68 mmol) in dry MeOH as described in synthetic procedure A; **Physical characteristics:** brown oil; **Yield:** 184 mg, 84%; **1H NMR** (400 MHz, $CDCl_3$) δ 7.89 (1H, s, 2-CH), 7.61-7.64 (2H, m, ArH), 7.29 (1H, s, 4-CH), 7.10 (2H, t, $J = 7.6$ Hz, ArH); **^{13}C NMR** (101 MHz, $CDCl_3$) δ 162.7 (d, $^1J_{C,F} = 249.9$ Hz, *para*-CF), 150.72 (5-C), 150.4 (2-C), 126.2 (d, $^3J_{C,F} = 8.1$ Hz, *ortho*-C), 124.0 (d, $^4J_{C,F} = 4.0$ Hz, 1-C), 121.1 (4-C), 116.1 (22.1 Hz, *meta*-C); **HRMS** (ESI-TOF) m/z : $[M+H]^+$ Calcd for C_9H_7FNO 164.0506, found 164.0508.

8.3.1.5. 5-(2-Chlorophenyl)-1,3-oxazole 96b



5-(2-Chlorophenyl)-1,3-oxazole **96b** was successfully synthesized from reaction of 2-chlorobenzaldehyde (170 mg, 1.21 mmol), TosMIC (260 mg, 1.33 mmol) and K_2CO_3 (333 mg, 2.41 mmol) in dry MeOH as described in synthetic procedure A; **Physical characteristics:** pale yellow solid; **Yield:** 161 mg, 74%; **Melting point:** 44-46°C (lit.²³³); **1H NMR** (400 MHz, $CDCl_3$) δ 7.87 (1H, s, 2-CH), 7.72 (1H, s, ArH), 7.71 (1H, s, 4-CH) 7.28-7.39 (1H, m, ArH), 7.24-7.25 (1H, m, ArH), 7.16-7.20 (1H, m, ArH); **^{13}C NMR** (101 MHz, $CDCl_3$) δ 150.3 (2-C), 148.0 (5-C), 130.7, 130.6, 129.1, 127.8, 127.0, 126.5 (ArC), 126.3 (4-C); **HRMS** (ESI-TOF) m/z : $[M+H]^+$ Calcd for C_9H_7ClNO 180.0211, found 180.0245.

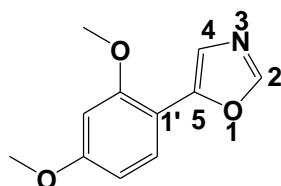
8.3.1.6. 5-(3-Methoxyphenyl)-1,3-oxazole 96c



5-(3-Methoxyphenyl)-1,3-oxazole **96c** was successfully synthesized from reaction of 3-methoxybenzaldehyde (163 mg, 1.20 mmol), TosMIC (258 mg, 1.32 mmol) and K_2CO_3 (330 mg,

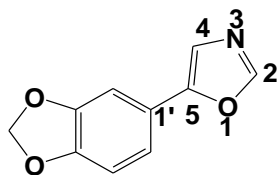
2.39 mmol) in dry MeOH as described in synthetic procedure A; **Physical characteristics:** pale yellow oil; **Yield:** 126 mg, 60%; **¹H NMR** (400 MHz, CDCl₃) δ 7.84 (1H, s, 2-CH), 7.55 (1H, dd, *J* = 4.8 Hz, 2 Hz, ArH), 7.21 (1H, s, 4-CH and 6.92 (2H, d, *J* = 8.8 Hz, ArH), 3.81 (3H, s, ArOCH₃); **¹³C NMR** (101 MHz, CDCl₃) δ 159.8 (ArCOCH₃), 151.5 (5-C), 149.8 (2-C), 125.8, 120.5, 119.8, 114.3 (ArC), 55.2 (ArCOCH₃); **HRMS** (ESI-TOF) *m/z*: [M+H]⁺ Calcd for C₁₀H₁₀NO₂ 176.0706, found 176.0736.

8.3.1.7. 5-(2,4-Dimethoxyphenyl)-1,3-oxazole 96d



5-(2,4-Dimethoxyphenyl)-1,3-oxazole **96d** was successfully synthesized from reaction of 2,4-dimethoxybenzaldehyde (160 mg, 0.96 mmol), TosMIC (207 mg, 1.06 mmol) and K₂CO₃ (267 mg, 1.93 mmol) in dry MeOH as described in general synthetic procedure A; **Physical characteristics:** pale yellow solid; **Yield:** 87 mg, 44%; **Melting point:** 104-106°C; **¹H NMR** (400 MHz, CDCl₃) δ 7.85 (1H, s, 2-CH), 7.66 (1H, *J* = 8.8 Hz, ArH), 7.42 (1H, s, 4-CH), 6.53-6.59 (2H, m, ArH), 3.83 and 3.92 (6H, 2 x s, 2 x ArOCH₃); **¹³C NMR** (101 MHz, CDCl₃) δ 160.9 and 156.9 (2 x ArCOCH₃), 148.9 (2-C), 148.0 (5-C), 126.9 (ArC), 123.5 (4-C), 110.3, 104.9, 98.5 (ArC), 55.4 and 55.8 (2 x ArCOCH₃); **HRMS** (ESI-TOF) *m/z*: [M+H]⁺ Calcd for C₁₁H₁₂NO₃ 206.0812, found 206.0839.

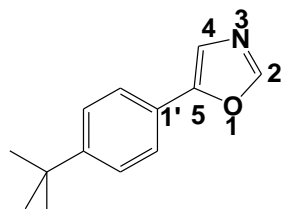
8.3.1.8. 5-(Benzo[*d*][1,3]dioxol-5-yl)-1,3-oxazole 96e



5-(Benzo[*d*][1,3]dioxol-5-yl)-1,3-oxazole **96e** was successfully synthesized from reaction of piperonal (140 mg, 0.93 mmol), TosMIC (199 mg, 1.02 mmol) and K₂CO₃ (257 mg, 1.86 mmol) in dry MeOH as described in a synthetic procedure A and from refluxing of (4*R*,5*R*)/(4*S*,5*S*)-5-(benzo[*d*][1,3]dioxol-5-yl)-4-tosyl-4,5-dihydrooxazole **97e** (200 mg, 0.60 mmol) in toluene as describe in a general synthetic procedure C; **Physical characteristics:** yellow solid; **Yield:** 470 mg, 76 mg, 43% for synthetic procedure A and 78 mg, 69% for synthetic procedure C; **Melting Point:** 44-46°C (lit³⁵²); **¹H NMR** (400 MHz, CDCl₃) δ 7.86 (1H, s, 2-CH), 7.21 (1H, s, 4-CH), 7.10-7.18 (2H, m, ArH), 6.85 (1H, d, *J* = 7.6 Hz, ArH), 6.00 (ArOCH₂O); **¹³C NMR** (101 MHz,

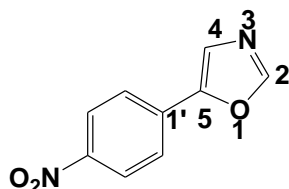
CDCl₃) δ 148.9 (2-C), 148.0 (5-C), 148.2 and 148.0 (2 x ArCOCH₂O), 132.5 (ArC), 121.9 (4-C), 118.6, 108.8, 105.0 (ArC), 101.4 (ArCOCH₂O); **HRMS** (ESI-TOF) m/z: [M+H]⁺ Calcd for C₁₀H₈NO₃ 190.0499, found 190.0528.

8.3.1.9. 5-(4-*tert*-Butylphenyl)-1,3-oxazole 96f



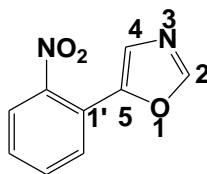
5-(4-*tert*-Butylphenyl)-1,3-oxazole **96f** was successfully synthesized from reaction of 4-*tert*-butylbenzaldehyde (149 mg, 0.92 mmol), TosMIC (197 mg, 1.01 mmol) and K₂CO₃ (254 mg, 1.84 mmol) in dry MeOH as described in synthetic procedure A; **Physical characteristics:** sticky brown material; **Yield:** 109 mg, 59%; **¹H NMR** (400 MHz, CDCl₃) δ 7.55 (1H, s, 2-CH), 7.58-7.60 (2H, d, *J* = 8.4 Hz, ArH), 7.44-7.47 (2H, d, *J* = 8.4 Hz, ArH), 7.31 (1H, s, 4-CH) 1.34 [9H, s, ArC(CH₃)₃]; **¹³C NMR** (101 MHz, CDCl₃) δ 151.9 (2-C), 150.2 (5-C), 134.6, 125.9, 125.0, 124.2 (ArC), 120.9 (4-C), 34.7 [ArC(CH₃)₃], 31.2, {ArC(CH₃)₃}; **HRMS** (ESI-TOF) m/z: [M+H]⁺ Calcd for C₁₃H₁₆NO 202.1242, found 202.1234.

8.3.1.10. 5-(4-Nitrophenyl)-1,3-oxazole 96g



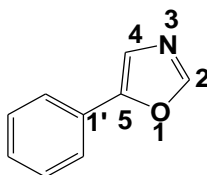
5-(4-Nitrophenyl)-1,3-oxazole **96g** was successfully synthesized from reaction of 4-nitrobenzaldehyde (165 mg, 1.09 mmol), TosMIC (234 mg, 1.2 mmol) and K₂CO₃ (301 mg, 2.18 mmol) in dry MeOH as described in synthetic procedure A; **Physical characteristics:** yellow solid; **Yield:** 207 mg, 73%; **Melting point:** 137-139 °C (lit.³⁵³), **¹H NMR** (400 MHz, CDCl₃) δ 8.28-8.31 (2H, m, ArH), 8.02 (1H, s, 2-CH), 7.80-7.83 (2H, m, ArH), 7.56 (1H, s, 4-CH); **¹³C NMR** (101 MHz, CDCl₃) δ 151.8 (2-C), 149.5 (5-C), 147.4 (ArCNO₂), 133.4, 124.8, 124.7 (ArC), 124.5 (4-C); **HRMS** (ESI-TOF) m/z: [M+H]⁺ Calcd for C₉H₇N₂O₃ 191.0451, found 191.0458.

8.3.1. 11. 5-(2-Nitrophenyl)-1,3-oxazole 96h



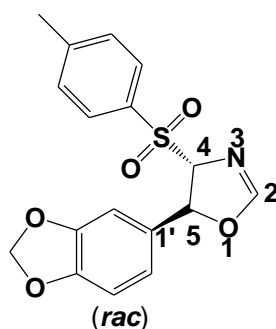
5-(2-Nitrophenyl)-1,3-oxazole **96h** was successfully synthesized from reaction of 2-nitrobenzaldehyde (177 mg, 1.17 mmol), TosMIC (252 mg, 1.29 mmol) and K_2CO_3 (254 mg, 1.84 mmol) in dry MeOH as described in general synthetic procedure A and from refluxing of 5-(2-nitrophenyl)-4-tosyl-4,5-dihydrooxazole **97h** (339 mg, 0.98 mmol) in toluene as described in general synthetic procedure C; **Physical characteristics**: pale yellow solid; **Yield**: 151 mg, 68% for synthetic procedure A and 117 mg, 63% for general synthetic procedure C; **Melting point**: 70-72°C (lit.³⁵⁴); **1H NMR** (400 MHz, $CDCl_3$) δ 7.97 (1H, s, 2-CH), 7.84-7.85 (1H, m, ArH), 7.64-7.72 (2H, m, ArH), 7.51-7.55 (1H, m, ArH), 7.39 (1H, s, 4-CH); **^{13}C NMR** (101 MHz, $CDCl_3$) δ 151.6 (2-C), 147.5 (5-C), 146.5 (ArCNO₂), 132.5, 129.8, 129.6, 125.8, 124.4 (ArC), 121.6 (4-C); **HRMS** (ESI-TOF) m/z : $[M+H]^+$ Calcd for $C_9H_7N_2O_3$, 191.0451, found 191.0475.

8.3.1.12. 5-Phenyl-1,3-oxazole 96i



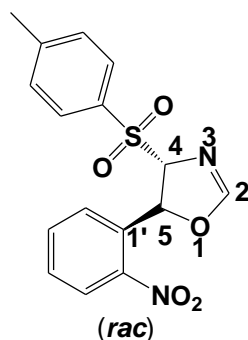
5-Phenyl-1,3-oxazole **96i** was successfully synthesized from refluxing of (4*R*,5*R*)/(4*S*,5*S*)-5-phenyl-4-tosyl-4,5-dihydrooxazole **97i** (319 mg, 1.06 mmol) in toluene as described in general synthetic procedure C; **Physical characteristics**: pale yellow solid; **Yield**: 105 mg, 68%; **Melting point**: 38-41°C (lit.²³¹); **1H NMR** (400 MHz, $CDCl_3$) δ 7.96 (1H, s, 2-CH), 7.66-7.70 (2H, m, ArH), 7.43-7.49 (2H, m, ArH), 7.38-7.40 (2H, m, 4-CH and ArH); **^{13}C NMR** (101 MHz, $CDCl_3$) δ 151.5 (2-C), 150.4 (5-C), 128.9, 128.6, 127.7, 124.3 (ArC), 121.3 (4-C); **HRMS** (ESI-TOF) m/z : $[M+H]^+$ Calcd for C_9H_7NO 145.0528, found 145.0521.

8.3.1.13. (4*R*,5*R*)/(4*S*,5*S*)-5-(Benzo[*d*][1,3]dioxol-5-yl)-4-tosyl-4,5-dihydrooxazole 97e



(4*R*,5*R*)/(4*S*,5*S*)-5-(Benzo[*d*][1,3]dioxol-5-yl)-4-tosyl-4,5-dihydrooxazole **97e** was successfully synthesized from reaction of piperonal (162 mg, 1.08 mmol), TosMIC (232 mg, 1.19 mmol) and K_2CO_3 (299 mg, 2.16 mmol) in MeCN as described in synthetic procedure B; **Physical characteristics**: white solid; **Yield**: 298 mg, 80%; **$^1\text{H NMR}$** (400 MHz, CDCl_3) δ 7.83(2H, d, $J = 8.8$ Hz, ArH), 7.37(2H, d, $J = 8.8$ Hz, ArH), 7.18 (1H, d, $J = 1.2$ Hz, 2-CH), 6.74-6.81 (3H, m, ArH), 5.97 (2H, s, ArOCH_2O), 5.94 (1H, d, $J = 6.0$ Hz, 5-CH), 4.99 (1H, dd, $J = 4.4$ Hz, 1.6 Hz, 4-CH), 2.45 (3H, s, ArCH_3); **$^{13}\text{C NMR}$** (101 MHz, CDCl_3) δ 159.3 (2-C), 148.4 and 148.3 (2 x ArCOCH_2O), 145.7, 133.1, 131.4, 129.9, 129.5, 119.5, 108.6, 105.6 (ArC), 101.4 (ArCOCH_2O), 92.4 (4-C), 79.4 (5-C), 21.7 (ArCCH_3); **FTIR** $\nu_{\text{max}}/\text{cm}^{-1}$ (KBr): 3314, 1675, 1596, 1503, 1447, 1303, 1257, 1141, 1062, 1039, 938, 816.

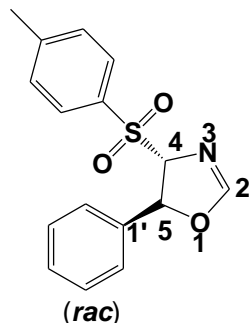
8.3.1.14. (4*R*,5*R*)/(4*S*,5*S*)-5-(2-Nitrophenyl)-4-tosyl-4,5-dihydrooxazole 97h



(4*R*,5*R*)/(4*S*,5*S*)-5-(2-Nitrophenyl)-4-tosyl-4,5-dihydrooxazole **97h** was successfully synthesized from reaction of 2-nitrobenzaldehyde (281 mg, 1.86 mmol), TosMIC (400 mg, 2.05 mmol) and K_2CO_3 (514 mg, 3.72 mmol) in dry MeCN as described in synthetic procedure B; **Physical characteristics**: orange solid; **Yield**: 419 mg, 65%; **$^1\text{H NMR}$** (400 MHz, CDCl_3) δ 7.90-7.93 (1H, m, ArH), 7.85 (2H, d, $J = 8.8$ Hz, ArH), 7.52-7.69 (3H, m, ArH and 2-CH), 7.38 (2H, d, $J = 8.8$ Hz, ArH), 6.39 (1H, d, $J = 7.2$ Hz, ArH), 5.32 (1H, $J = 6$ Hz, 5-CH), 5.30 (1H, $J = 2 \setminus 6.0$ Hz, 4-CH), 2.46 (3H, s, ArCH_3); **$^{13}\text{C NMR}$** (101 MHz, CDCl_3) δ 159.0 (2-C), 148.2, 145.9, 133.4, 132.9, 130.8, 130.4, 129.9, 129.7, 129.6, 125.2 (ArC), 91.8 (4-C), 77.03 (5-C), 21.8 (ArCCH_3); **FTIR**

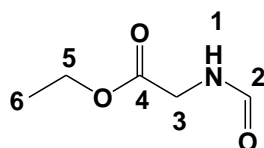
$\nu_{\max}/\text{cm}^{-1}$ (KBr): 2922, 2868, 1702, 1672, 1599, 1524, 1347, 1317, 1224, 1133, 1036, 1011, 855, 815, 687, 569.

8.3.1.15. (4*R*,5*R*)/(4*S*,5*S*)-5-Phenyl-4-tosyl-4,5-dihydrooxazole **97i**



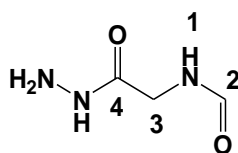
(4*R*,5*R*)/(4*S*,5*S*)-5-Phenyl-4-tosyl-4,5-dihydrooxazole **97i** was successfully synthesized from reaction of benzaldehyde (152 mg, 1.43 mmol), TosMIC (307 mg, 1.57 mmol) and K_2CO_3 (395 mg, 2.86 mmol) in MeCN as described in synthetic procedure B; **Physical characteristics:** white solid; **Yield:** 327 mg 76%; **$^1\text{H NMR}$** (400 MHz, CDCl_3) δ 7.84 (2H, d, $J = 8.8$ Hz, ArH), 7.32-7.43 (7H, m, ArH), 7.21 (1H, d, $J = 1.6$ Hz, 2-CH), 6.05 (1H, d, $J = 6.0$ Hz, 5-CH), 5.03 (1H, dd, $J = 2.6$ Hz, 4-CH), 2.46 (3H, s, ArCH_3); **$^{13}\text{C NMR}$** (101 MHz, CDCl_3) δ 159.4 (2-C), 145.7, 137.7, 133.2, 129.9, 129.5, 129.1, 129.0, 125.2 (ArC), 92.6 (4-CH), 76.4 (5-CH), 21.7 (ArCCH_3); **FTIR** $\nu_{\max}/\text{cm}^{-1}$ (KBr): 2894, 2875, 1622, 1316, 1304, 1148, 1102, 968, 814.

8.3.2. Synthesis of ethyl 2-formamidoacetate **104**



A mixture of ethyl glycine ester hydrochloride (10.00 g, 71.6 mmol), ethyl formate (31.0g, 418.4 mmol) and triethylamine (14.60 g, 144.3 mmol) was stirred at room temperature for 3 days. Upon completion, the precipitate was filtered off and the filtered solution was cooled with ice. The resulting precipitate was filtered off and the filtrate was concentrated *in vacuo* to give ethyl 2-formamidoacetate **104**; **Physical characteristics:** colourless oil; **Yield:** 7.61 g; 81%; **$^1\text{H NMR}$** (400 MHz, CDCl_3) δ 8.17 (1H, s, 2-CH), 7.38 (1H, s, NH), 4.14 (2H, q, $J = 7.6$ Hz, 5- CH_2), 3.98 (2H, d, $J = 5.6$ Hz, 3- CH_2), 1.20-1.24 (3H, t, $J = 7.6$ Hz, 6- CH_3); **$^{13}\text{C NMR}$** (101 MHz, CDCl_3) δ 169.4 (4-C), 161.4 (2-C), 61.5 (5-C), 39.8 (3-C), 13.9 (6-C).

8.3.3. Synthesis of *N*-(2-hydrazinyl-2-oxoethyl)formamide **103**



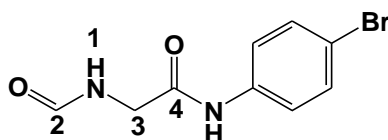
Hydrazine monohydrate (9.54 g, 190.5 mol) was added to a solution of ethyl 2-formamidoacetate (5.00 g, 38.1 mol) in MeOH (100 ml). The resulting reaction mixture was stirred at room temperature for 3 hours. The precipitate was filtered off and dried under high vacuum to afford *N*-(2-hydrazinyl-2-oxoethyl)formamide **103**; **Physical characteristics**: White solid; **Yield**: 3.17 g, 71%; **Melting Point**: 130-133°C (lit^{355,356}); **¹H NMR** (400 MHz, DMSO-*d*₆) δ 9.12 (1H, s, 1-NH), 8.25 (1H, s, NH₂NH), 8.08 (1H, s, 2-CH), 4.26 (2H, s, NH₂NH), 3.72 (2H, d, *J* = 5.6 Hz, 3-CH₂); **¹³C NMR** (101 MHz, DMSO-*d*₆) δ 167.9 (4-C), 161.6 (2-C), 40.2 (3-C).

8.3.4. Synthesis of *N*-aryl-2-formamidoacetamide

8.3.4.1. General synthetic procedure

To a solution of the *N*-(2-hydrazinyl-2-oxoethyl)formamide (1 molar equivalent) in 1M HCl (40 ml) was added dropwise a solution of NaNO₂ (1 molar equivalent) in H₂O (20 ml) at 0°C over a period of 15 minutes. After stirring for 20 minutes at the same temperature, the mixture was neutralized with saturated aqueous NaHCO₃ and then a solution of aniline (3 molar equivalents) in THF (40 ml) was added to the mixture at 0°C over a period of 20 minutes. After stirring for 5 hours at the same temperature, THF was evaporated *in vacuo*. The crude was separated by column chromatography [elution with ethyl acetate: hexane (1:7)], followed by ethyl acetate: hexane (1:1) afford pure *N*-aryl-2-formamidoacetamide derivatives. The *R_f* value = 0.5-1.0 in ethyl acetate: hexane (1:1).

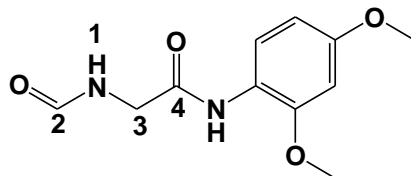
8.3.4.2. *N*-(4-Bromophenyl)-2-formamidoacetamide **102a**



N-(4-Bromophenyl)-2-formamidoacetamide **102a** was successfully synthesized according to the general procedure using *N*-(2-hydrazinyl-2-oxoethyl)formamide **103** (228 mg, 1.95 mmol), 4-bromoaniline (1.01 g, 5.86 mmol); **Physical characteristics**: white solid; **Yield**: 678 mg, 45%; **Melting point**: 189-192°C; **¹H NMR** (400 MHz, DMSO-*d*₆) δ 10.2 (1H, s, ArNH), 8.39 (1H, s, NHCHO), 8.16 (1H, s, 2-CHO), 7.59-7.61 (2H, dd, *J* = 5.2 Hz, 2.0 Hz, ArH), 7.52-7.54 (2H, m,

ArH), 3.97 (2H, d, $J = 6.0$ Hz, 3-CH₂); ¹³C NMR (101 MHz, DMSO-*d*₆) δ 168.4 (4-C), 162.5 (2-C), 139.1, 132.5, 123.6, 115.8 (ArC), 42.2 (3-C).

8.3.4.2. *N*-(2,4-Dimethoxyphenyl)-2-formamidoacetamides **102b**



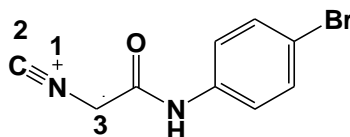
N-(2,4-Dimethoxyphenyl)-2-formamidoacetamide **102b** was successfully synthesized according to the general procedure using *N*-(2-hydrazinyl-2-oxoethyl)formamide (325 mg, 2.78 mmol), 2,4-dimethoxyaniline (1.26 mg, 8.34 mmol); **Physical characteristics**: light brown solid; **Yield**: 1.35 g, 68%; **Melting point**: 141-144°C; ¹H NMR (400 MHz, DMSO-*d*₆) δ 9.09 (1H, s, ArNH), 8.36 (1H, s, NHCHO), 8.16 (1H, s, 2-CHO), 7.75 (1H, d, $J = 8.4$ Hz, ArH), 6.65 (1H, s, ArH), 6.52 (1H, d, $J = 7.6$ Hz, ArH), 3.98 (2H, d, $J = 5.6$ Hz, NCH₂), 3.78 and 3.89 (6H, 2 x s, 2 x ArOCH₃); ¹³C NMR (101 MHz, DMSO-*d*₆) δ 167.9 (4-C), 162.5 (2-C), 157.7 and 152.0 (2 x ArCOCH₃), 124.0, 120.8, 105.0, 99.8 (ArC), 56.7 and 56.2 (2 x ArCOCH₃), 42.2 (3-C).

8.3.5. Synthesis of 2-isocyano-*N*-arylacetamide **101**

8.3.5.1. General procedure

To a suspension of *N*-aryl-2-formamidoacetamide (1 molar equivalent) and triethylamine (4 molar equivalents) in DCM (10 ml) was added dropwise phosphoryl chloride (2 molar equivalents) at 10-15°C over a period of 20 min. After stirring for 30 min at room temperature, 25 % aqueous Na₂CO₃ (15 ml) was added to the reaction mixture under ice cooling and the DCM layer was separated. The aqueous layer was extracted with DCM (3 x 15 ml). The combined organic layer was washed with H₂O, dried over MgSO₄, and then evaporated *in vacuo* to give crude product, which was then subjected to chromatography on silica gel eluting with ethyl acetate to give *N*-aryl-2-isocyanoacetamide

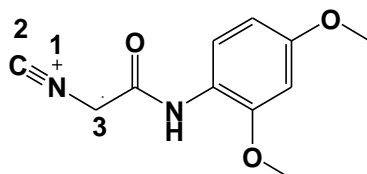
8.3.5.2. Synthesis of 2-isocyano-*N*-(4-bromophenyl)acetamide **101a**



2-Isocyano-*N*-(4-bromophenyl)acetamide **101a** was successfully synthesized from reaction of *N*-(4-bromophenyl)-2-formamidoacetamide **102a** (1.10 g, 4.28 mmol) Et₃N (1.73 g, 17.12 mmol) and POCl₃ (1.12 g, 9.64 mmol) in DCM as described in the general procedure; **Physical**

characteristics: white solid; **Yield:** 348 mg, 34%; **Melting point:** 204-207°C; **¹H NMR** (400 MHz, CDCl₃) δ 10.3 (1H, s, ArNH), 7.96 (2H, dd, *J* = 2.9 Hz, ArH), 7.68-7.57(1H, m, ArH), 4.32 (2H, s, 3-CH₂); **¹³C NMR** (101 MHz, CDCl₃) δ 162.1 (C=O), 159.3 (2-C), 137.8, 132.4, 131.5, 114.3 (ArC), 42.6 (4-C); **FTIR** $\nu_{\max}/\text{cm}^{-1}$ (KBr): 3340, 3250 (NH), 2883, 2736, 2675, 2160 (NC), 1702, 1652, 1592, 1536, 1412, 1378, 1275, 1223, 989, 829.

8.3.5.4. Synthesis of 2-isocyano-*N*-(2,4-dimethoxyphenyl)acetamide **101b**



2-Isocyano-*N*-(2,4-dimethoxyphenyl)acetamide **101b** was successfully synthesized from reaction of *N*-(2,4-dimethoxyphenyl)-2-formamidoacetamide **102b** (774 mg, 3.25 mmol), Et₃N (1.32 g, 13.00 mmol) and POCl₃ (757 mg, 6.50 mmol) in DCM as described in the general procedure; **Physical characteristics:** white solid; **Yield:** 659 mg, 92%; **Melting point:** 144-147°C; **¹H NMR** (400 MHz, CDCl₃) δ 8.50 (1H, s, ArNH), 8.12 (1H, d, *J* = 8.8 Hz, ArH), 6.45-6.50 (2H, m, ArH), 4.30 (2H, s, 3-CH₂), 3.83 (6H, 2 x s, 2 x ArOCH₃); **¹³C NMR** (101 MHz, CDCl₃) δ 162.8 (C=O), 159.4 (2-C), 157.3 and 149.7 (2 x ArCOCH₃), 120.7, 119.5, 103.7, 98.6 (ArC), 55.9 & 55.5 (2 x ArCOCH₃), 45.8 (3-C); **FTIR** $\nu_{\max}/\text{cm}^{-1}$ (KBr): 3291 (NH), 2959, 2929, 2880, 2157 (NC), 1728, 1549, 1464, 1282, 1209, 1126, 1072.

8.3.6. Attempted reaction of *N*-aryl-2-isocyanoacetamide with benzoyl chloride and benzaldehydes

8.3.6.1. General procedure A

N-(2,4-dimethoxyphenyl)-2-isocyanoacetamide (0.91 mmol) and triethylamine (1.18 mmol) in dry DCM (3 ml) were cooled to 0°C in an ice bath, followed by slow addition of a solution of benzoyl chloride (0.91 mmol) in dry DCM (2 ml). The resulting reaction mixture was stirred for 1 hour at 0°C and then allowed to warm to room temperature and further stirred for 24-48 hours. TLC analysis showed no product formation.

8.3.6.2. General procedure B

N-(2,4-dimethoxyphenyl)-2-isocyanoacetamide (1.23 mmol) and DBU (1.23 mmol) in dry DCM (3ml) were cooled to 0°C in an ice bath, followed by slow addition of a solution of benzoyl chloride (1.23 mmol) in dry DCM (2 ml). The reaction was stirred for 1 hour at 0°C and then

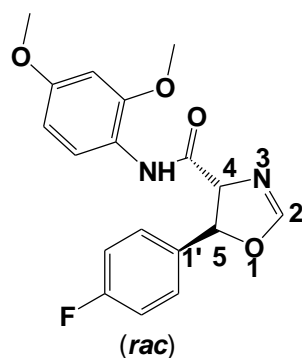
allowed to warm to room temperature and stirred for 48 hours. Once the reaction appeared complete by TLC analysis, the reaction mixture was poured into 10% aqueous NaHCO₃ solution and extracted with DCM (3 x 2 ml). The combined organic layers were washed again with the NaHCO₃ solution and brine then dried over MgSO₄, filtered and concentrated *in vacuo*. Crude material obtained was purified by silica gel column chromatography with a 1:10 to 1:1 ethyl acetate: hexane gradient solvent system to afford the starting material *N*-(2,4-dimethoxyphenyl)-2-isocyanoacetamide 249 mg, 85% recovered yield.

8.3.7. Reaction of *N*-aryl-2-isocyanoacetamide with benzaldehydes

8.3.7.1. General procedure

N-(2,4-dimethoxyphenyl)-2-isocyanoacetamide (1 molar equivalent) was added in one portion to a solution of benzaldehydes (1 molar equivalent), DBU (1 molar equivalent) in CH₂Cl₂ (5.0 ml) at 0°C. The mixture was allowed to warm to room temperature and stirred for 48 hours (monitored by TLC). The solvent was removed and then a saturated aqueous solution of NaHCO₃ (10 ml) was added and the resulting mixture was extracted with ethyl acetate (3 x 10 ml). The combined organic layers were dried (MgSO₄) and concentrated under reduced pressure. Products were purified by silica gel chromatography, elution with EtOAc/hexane (1:4) followed by 1.

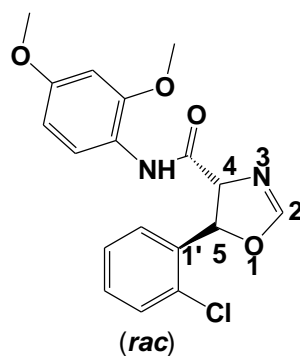
8.3.7.2. (4*R*,5*R*/4*S*,5*S*)-*N*-(2,4-Dimethoxyphenyl)-5-(4-fluorophenyl)-4,5-dihydrooxazole-4-carboxamide **107a**



(4*R*,5*R*/4*S*,5*S*)-*N*-(2,4-Dimethoxyphenyl)-5-(4-fluorophenyl)-4,5-dihydrooxazole-4-carboxamide **107a** was successfully synthesized according to the general procedure using *N*-(2,4-dimethoxyphenyl)-2-isocyanoacetamide **101b** (145 mg, 0.66 mmol), 4-fluorobenzaldehyde (82 mg, 0.66 mmol) and DBU (100 mg, 0.66 mmol) in DCM; **Physical characteristics**: light yellow solid; **Yield**: 159 mg, 70%; **Melting point**: 187-189°C; **¹H NMR** (400 MHz, CDCl₃) δ 8.72 (1H, s, NH), 8.27 (1H, d, *J* = 8.8 Hz, ArH), 7.42-7.46 (2H, m, ArH), 7.07-7.10 (2H, m, ArH), 7.18 (1H, s, 2-CH), 6.46-6.49 (2H, m, ArH), 5.72 (1H, d, *J* = 7.6 Hz, 5-CH), 4.62 (1H, d, *J* = 7.6 Hz, 4-CH), 3.80 and 3.87 (6H, 2 x s, ArOCH₃); **¹³C NMR** (101 MHz, CDCl₃) δ 167.9 (C=O), 162.6

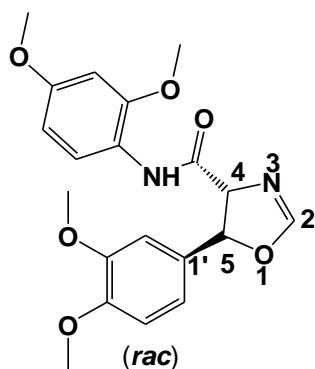
(d, $^1J_{CF}$ = 247 Hz, *para*-CF), 156.8 and 149.7 (2x ArCOCH₃), 135.6 (ArC), 127.3 (d, $^4J_{CF}$ = 3 Hz, 1'-C), 121.1 (ArC), 120.3 (d, $^3J_{CF}$ = 8.1 Hz, *ortho*-C), 115.8 (d, $^4J_{CF}$ = 22.1 Hz, *meta*-C), 114.3, 103.7, 98.7 (ArC), 82.1 (4-C), 71.3 (5-C), 55.7 and 55.5 (2 x ArCOCH₃);

8.3.7.3. (4*R*,5*R*/4*S*,5*S*)-*N*-(2,4-Dimethoxyphenyl)-5-(2-chlorophenyl)-4,5-dihydrooxazole-4-carboxamide **107b**



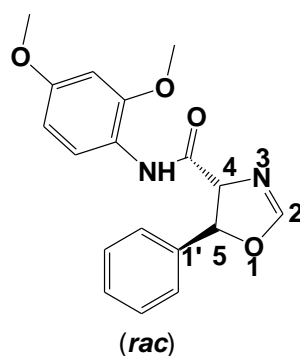
((4*R*,5*R*/4*S*,5*S*)-*N*-(2,4-Dimethoxyphenyl)-5-(2-chlorophenyl)-4,5-dihydrooxazole-4-carboxamide **107b** was successfully synthesized according to the general procedure using *N*-(2,4-dimethoxyphenyl)-2-isocyanoacetamide **101b** (308 mg, 1.40 mmol), 2-chlorobenzaldehyde (197 mg, 1.40 mmol) and DBU (213 mg, 1.40 mmol) in DCM; **Physical characteristics**: light yellow solid; **Yield**: 303 mg, 60%; **Melting point**: 189-191°C; **¹H NMR** (400 MHz, CDCl₃) δ 8.62 (1H, s, NH), 8.25 (1H, d, *J* = 8.8 Hz, ArH), 7.42-7.44 (4H, m, ArH), 7.16 (1H, s, 2-CH), 6.44-6.49 (2H, m, ArH), 6.07 (1H, d, *J* = 8.4 Hz, 5-CH), 4.80-4.82 (1H, d, *J* = 8.4 Hz, 4-CH), 3.87 and 3.79 (6H, 2 x s, 2 x ArOCH₃); **¹³C NMR** (101 MHz, CDCl₃) δ 168.2 (C=O), 161.6 (2-C), 157.0 and 149.8 (ArCOCH₃), 136.1, 131.5, 130.1, 129.5, 128.7, 126.9, 120.6, 115.4, 103.7, 98.6 (ArC), 80.7 (4-C), 75.2 (5-C), 55.8 and 55.5 (2 x ArCOCH₃).

8.3.7.4. (4*R*,5*R*,4*S*,5*S*)-*N*-(2,4-Dimethoxyphenyl)-5-(3,4-dimethoxyphenyl)-4,5-dihydrooxazole-4-carboxamide **107c**



(4*R*,5*R*/4*S*,5*S*)-*N*-(2,4-Dimethoxyphenyl)-5-(3,4-dimethoxyphenyl)-4,5-dihydrooxazole-4-carboxamide **107c** was successfully synthesized according to the general procedure using *N*-(2,4-dimethoxyphenyl)-2-isocyanoacetamide **101b** (275 mg, 1.36 mmol), 3-methoxybenzaldehyde (226 mg, 1.36 mmol) and DBU (207 mg, 1.36 mmol) in DCM; **Physical characteristics**: light yellow solid; **Yield**: 289 mg, 55%; **Melting point**: 182 -185°C; **¹H NMR** (400 MHz, CDCl₃) δ 8.61 (1H, s, NH), 8.18 (1H, d, *J* = 8.4 Hz, ArH), 7.15-7.20 (2H, m, ArH), 6.36-6.54 (3H, m, ArH), 6.99 (1H, d, *J* = 1.6 Hz, 2-CH), 5.69 (1H, d, *J* = 8.4 Hz, 5-CH), 4.71-4.73 (1H, dd, *J* = 3 Hz, 4-CH), 3.71, 3.75, 3.79 and 3.80 (12H, 4 x s, 4 x ArOCH₃); **¹³C NMR** (101 MHz, CDCl₃) δ 168.7 (C=O), 161.7 (2-C), 156.5, 156.2, 152.5 and 149.6 (4 x ArCOCH₃), 135.5, 130.0, 128.1, 124.6, 120.8, 105.9, 104.3, 98.6 (ArC); (4-C), 75.2 (5-C), 55.6, 55.8, 59.5 and 59.6 (4 x ArCOCH₃).

8.3.7.5. (4*R*,5*R*/4*S*,5*S*)-*N*-(2,4-Dimethoxyphenyl)-5-phenyl-4,5-dihydrooxazole-4-carboxamide **107d**



(4*R*,5*R*/4*S*,5*S*)-*N*-(2,4-Dimethoxyphenyl)-5-phenyl-4,5-dihydrooxazole-4-carboxamide **107d** was successfully synthesized according to the general procedure using *N*-(2,4-dimethoxyphenyl)-2-isocyanoacetamide **101b** (115 mg, 0.57 mmol), benzaldehyde (61 mg, 0.57 mmol) and DBU (87 mg, 0.57 mmol) in DCM; **Physical characteristics**: light yellow solid; **Yield**: 134 mg, 72%; **Melting point**: 156-159°C; **¹H NMR** (400 MHz, CDCl₃) δ 8.72 (1H, s, NH), 8.27 (1H, d, *J* = 8.8 Hz, ArH), 7.34-7.47 (4H, m, ArH), 7.18 (1H, s, 2-CH), 6.46-6.49 (3H, m, ArH), 5.76 (1H, d, *J* = 8.0 Hz, 5-CH), 4.80-4.82 (1H, d, *J* = 7.4 Hz, 4-CH), 3.87 and 3.80 (6H, 2 x s, 2 x ArOCH₃); **¹³C NMR** (101 MHz, CDCl₃) δ 168.1 (C=O), 156.8 (2-C), 156.6 and 149.7 (2 x ArCOCH₃), 139.9, 132.4, 128.8, 128.4, 125.4, 120.5, 103.6, 98.7 (ArC), 82.6 (4-C), 60.4 (5-C), 55.7 and 55.5 (2 x ArCOCH₃).

8.3.8. Attempted oxidation of 4,5-aryl-4,5-dihydro-*N*-(3,5-dimethoxyphenyl)oxazole-4-carboxamides

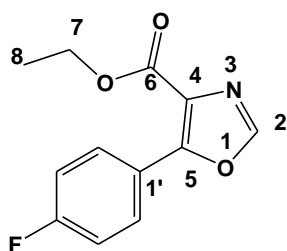
(4*R*,5*R*/4*S*,5*S*)-5-Aryl-4,5-dihydro-*N*-(3,5-dimethoxyphenyl)oxazole-4-carboxamides (0.5 mmol) was dissolved in 5 ml of dry DCM and cool in an ice bath. DBU (1.4 mmol) was then added followed by slow addition of bromotrichloromethane (1.4 mmol). The reaction was stirred for 1 hour and then allowed to warm to room temperature and was stirred for a further 24-48 hours. Unfortunately no desired products were obtained.

8.3.9. Synthesis of ethy-5-aryl-1,3-oxazole-4-carboxylates

8.3.9.1. General procedure

To a solution of ethyl 2-isocyanoacetate (1 molar equivalent) and triethylamine (3 molar equivalents) in THF (20 ml) was added a solution of benzoyl chloride (1 molar equivalent) in THF (4 ml) slowly at 0 °C. After stirring for 40 minutes at 0 °C, the reaction mixture was warmed to room temperature. After stirring for 48 hours, water was added to the reaction mixture (30 ml). The aqueous layer was extracted with EtOAc (2 x 20 ml) and the combined organic layer was washed with 1N HCl (2 x 10 ml), water (15 ml), then dried over MgSO₄ and then filtered. The solvent was then evaporated under reduced pressure to obtain brown oily crude material which was purified by flash column chromatography [eluting with hexane: EtOAc (6:1) followed by (4:1) and then (1:1)] to afford the desired ethy-5-aryl-1,3-oxazole-4-carboxylates

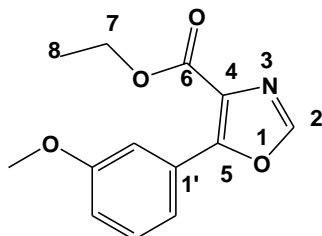
8.3.9.2. Ethyl 5-(4-fluorophenyl)oxazole-4-carboxylate **109a**



Ethyl 5-(4-fluorophenyl)oxazole-4-carboxylate **109a** was successfully synthesized using ethyl 2-isocyanoacetate (1.08 g, 9.57 mmol), Et₃N (2.90 g, 28.7 mmol) and 4-fluorobenzoyl chloride (1.52 g, 9.57 mmol in THF (20 ml) as described in the general procedure; **Physical characteristics**: pale yellow solids; **Yield**: 1.62 g, 72%; **¹H NMR** (400 MHz, CDCl₃) δ 8.08 (2H, dd, *J* = 5.2 Hz, 2.6 Hz, ArH), 7.90 (1H, s, 2-CH), 7.13 (2H, t, *J* = 8.8 Hz, ArH), 3.38 (2H, q, *J* = 7.2 Hz, OCH₂CH₃), 1.38-1.42 (3H, t, *J* = 7.2 Hz, OCH₂CH₃); **¹³C NMR** (101 MHz, CDCl₃) δ

163.8 (d, $^1J_{C,F} = 252$ Hz, *para*-CF), 161.9 (C=O), 154.7 (5-C), 148.8 (2-C), 130.7 (d, $^3J_{C,F} = 8$ Hz, *ortho*-C), 126.3 (4-C), 122.9 (d, $^4J_{C,F} = 4$ Hz, 1'-C), 115.6 (d, $^2J_{C,F} = 21$ Hz, *meta*-C), 61.5 (7-C), 14.2 (8-C).

8.3.9.3. Ethyl 5-(3-methoxyphenyl)oxazole-4-carboxylate **109c**



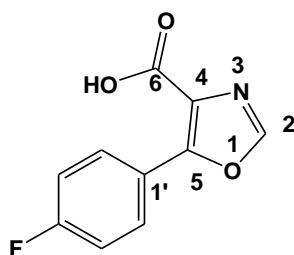
Ethyl 5-(3-methoxyphenyl)oxazole-4-carboxylate **109c** was synthesized from ethyl 2-isocynoacetate (967 mg, 8.55 mmol), Et₃N (2.60 g, 25.7 mmol) and 3-methoxybenzoyl chloride (1.46 g, 8.55 mmol) in THF (20 ml) as described in general procedure; **Physical characteristics:** yellow solids; **Yield:** 1.42 g, 67%; **¹H NMR** (400 MHz, CDCl₃) δ 7.89 (1H, s, 2-CH), 7.62 (1H, d, $J = 8.4$ Hz, ArH), 7.34 (1H, t, $J = 8.4$ Hz, ArH), 7.01 (1H, d, $J = 8.4$ Hz, ArH), 6.97-6.99 (1H, m, ArH), 4.37 (2H, q, $J = 7.2$ Hz, OCH₂CH₃), 3.85 (3H, s, ArOCH₃), 1.37-1.41 (3H, t, $J = 7.2$ Hz, OCH₂CH₃); **¹³C NMR** (101 MHz, CDCl₃) δ 161.8 (C=O), 159.4 (ArCOCH₃), 155.2 (5-C), 148.8 (2-C), 129.4, 127.7 (ArC), 126.7 (4-C), 120.7, 116.5, 113.6 (ArC), 61.4 (7-C), 55.3 (ArCOCH₃), 14.2 (8-C).

8.3.10. Hydrolysis of ethyl 1,5-diaryl-oxazole-4-carboxylates

8.3.10.1. General synthetic procedure

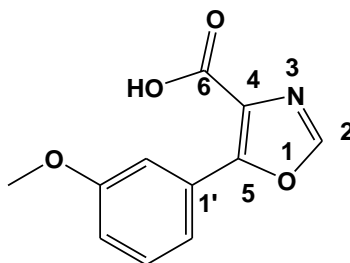
NaOH (1.5 molar equivalent) was added to a solution of ethyl 5-aryl-1,3-oxazole-4-carboxylate (1 molar equivalent) in MeOH (5 ml) and H₂O (5 ml). The resulting reaction solution was refluxed until disappearance of the starting material (observed by TLC). Volatile methanol was removed *in vacuo* and the remaining aqueous crude material was slowly neutralized with 1M HCl. The product was then extracted with EtOAc, washed with brine and dried over MgSO₄ to give the 1,5-diaryl-oxazole-carboxylic acids.

8.3.10.2. 5-(4-Fluorophenyl)oxazole-4-carboxylic acid **108a**



5-(4-Fluorophenyl)oxazole-4-carboxylic acid **3.13a** was successfully synthesized from ethyl 5-(4-fluorophenyl)oxazole-4-carboxylate **109a** (442 mg, 1.88 mmol) and NaOH (113 mg, 2.82 mmol) as described in the general procedure; **Physical characteristics:** pale yellow solids; **Yield:** 347 mg, 89%; **Melting Point:** 168-171 °C; **¹H NMR** (400 MHz, DMSO-*d*₆) δ 13.2 (1H, s, COOH), 8.52 (1H, s, 2-CH), 8.03 (2H, dd, *J* = 5.6 Hz, 3.2 Hz, ArH), 7.33 (2H, t, *J* = 8.8 Hz, ArH); **¹³C NMR** (101 MHz, DMSO-*d*₆) δ 163.0 (d, ¹*J*_{C,F} = 250 Hz, *para*-CF), 162.9 (C=O), 153.1 (5-C), 150.7 (2-C), 130.9 (d, ³*J*_{C,F} = 9 Hz, *ortho*-C), 126.7 (4-C), 123.4 (d, ⁴*J*_{C,F} = 3 Hz, 1'-C), 115.6 (d, ²*J*_{C,F} = 22 Hz, *meta*-C); **FTIR** ν_{\max} /cm⁻¹ (KBr): 3047, 2917, 2856, 2461 (OH), 1727, 1608, 1506, 1243, 1165, 833, 799, 622, 504.

8.3.10.3. 5-(3-Methoxyphenyl)oxazole-4-carboxylic acid **108c**



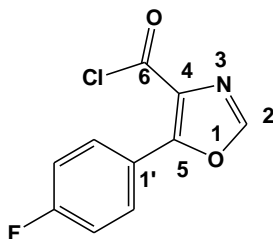
5-(3-Methoxyphenyl)oxazole-4-carboxylic acid **108c** was successfully synthesized from ethyl 5-(3-methoxyphenyl)oxazole-4-carboxylate **109c** (2.00 g, 8.09 mmol) and NaOH (484 mg, 12.1 mmol) as described in the general synthetic procedure; **Physical characteristics:** yellow solid; **Yield:** 1.45 g, 82%; **Melting point:** 115-118°C; **¹H NMR** (400 MHz, DMSO-*d*₆) δ 13.2 (1H, s, COOH), 8.53 (1H, s, 2-CH), 7.65 (1H, s, ArH), 7.55 (1H, d, *J* = 8.0 Hz, ArH), 7.44 (1H, t, *J* = 8.2 Hz, ArH), 7.07 (1H, dd, *J* = 6.0 Hz, 2.0 Hz, ArH), 3.82 (3H, s, ArOCH₃); **¹³C NMR** (101 MHz, DMSO-*d*₆) δ 163.0 (C=O), 159.3 (ArCOCH₃), 153.5 (5-C), 150.6 (2-C), 129.7, 127.9, 127.1 (4-C), 120.4, 115.9, 113.9 (ArC), 55.3 (ArCOCH₃); **FTIR** ν_{\max} /cm⁻¹ (KBr): 2913, 2878, 2569 (OH), 1709, 1596, 1570, 1495, 1296, 1214, 1189, 848, 747.

8.3.11. Preparation of 5-aryloxazole-4-carbonyl chloride

8.3.11.1 General synthetic procedure

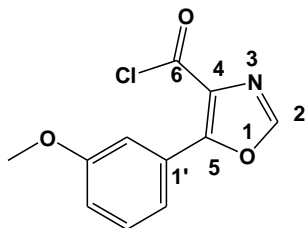
A mixture 5-aryloxazole-4-carboxylic acid (1 molar equivalent) and thionyl chloride (6 molar equivalents) was refluxed for 8 hours. Upon reaction completion, the excess thionyl chloride was removed by co-evaporation with toluene to afford 5-aryloxazole-4-carbonyl chloride after drying under high vacuum.

8.3.11.2. 5-(4-Fluorophenyl)oxazole-4-carbonyl chloride 112a



5-(4-Fluorophenyl)oxazole-4-carbonyl chloride **112a** was successfully synthesized by refluxing of 5-(4-fluorophenyl)oxazole-4-carboxylic acid **108a** (218 g, 1.05 mmol) and SOCl_2 (6.30 mmol) as described by the general procedure; **Physical characteristics:** yellow solid; **Yield:** 211 mg, 89%; **$^1\text{H NMR}$** (400 MHz, CDCl_3) δ 8.03 (2H, dd, $J = 5.6$ Hz, 2.0 Hz, ArH), 7.94 (1H, s, 2-CH), 7.17 (2H, t, $J = 8.4$ Hz, ArH); **$^{13}\text{C NMR}$** (101 MHz, CDCl_3) δ 164.1 (d, $^1J_{\text{C,F}} = 255$ Hz, *para*-CF), 163.1 (C=O), 156.0 (5-C), 148.6 (2-C), 130.8 (d, $^3J_{\text{C,F}} = 9$ Hz, *ortho*-C), 128.8 (C-4), 121.7 (d, $^4J_{\text{C,F}} = 3.0$ Hz, 1'-C), 116.1 (d, $^2J_{\text{C,F}} = 22$ Hz, *meta*-C).

8.3.11.3. 5-(3-Methoxyphenyl)oxazole-4-carbonyl chloride 112c



5-(3-Methoxyphenyl)oxazole-4-carbonyl chloride **112c** was successfully synthesized by refluxing of 5-(3-methoxyphenyl)oxazole-4-carboxylic acid **108c** (340 mg, 1.55 mmol) and SOCl_2 (9.30 mmol) as described by the general procedure; **Physical characteristics:** yellow solid; **Yield:** 302 mg, 82%; **$^1\text{H NMR}$** (400 MHz, CDCl_3) 7.92 (1H, s, 2-CH), 7.62 (2H, overlapping doublet and singlet, $J = 8.4$ Hz, ArH), 7.35 (1H, t, $J = 8.4$ Hz, ArH), 7.34 (1H, d, $J = 8.4$ Hz, ArH), 3.81 (3H, s, ArOCH_3); **$^{13}\text{C NMR}$** (101 MHz, DMSO-d_6): δ 162.9 (C=O), 159.5 (ArCOCH_3), 156.6 (5-C), 148.5 (2-C), 129.7, 128.9, 126.4, 120.6, 118.1, 113.1 (ArC), 55.3 (ArCOCH_3);

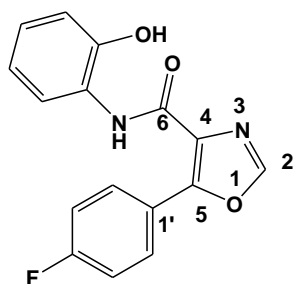
8.3.12. Synthesis of *N*,5-diaryl-4-carboxamide-1,3-oxazole

8.3.12.1 General synthetic procedure

To a mixture of aniline (1 molar equivalent) and 5-aryloxazole-4-carbonyl chloride (1 molar equivalent) in ethyl acetate (7 ml) was added triethylamine (1.3 molar equivalents) at 0°C with stirring. The resulting mixture was stirred for 48 hours at room temperature. Upon completion, 1M HCl was added and the mixture was extracted with EtOAc (2 x 5 ml). The combined

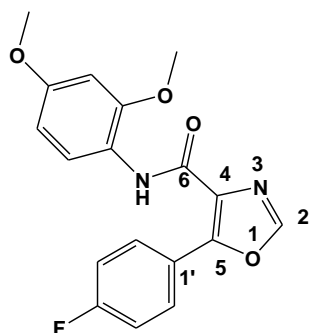
organic layer was washed with water (5 ml), dried over MgSO₄, filtered and solvent was concentrated *in vacuo*. The resulting crude material was purified by column chromatography on silica gel, [elution with hexane: EtOAc ratio of (7:1), followed by (1:1)] to furnish the *N*,5-diaryl-4-carboxamide-1,3-oxazole **100a-e** and **100g-i**, whereas in the cases where product containing a carboxylic acid, the crude material was crystallized from DCM to afford the desired products **100f**, **100j** and **100k**.

8.3.12.2. 5-(4-Fluorophenyl)-*N*-(2-hydroxyphenyl)oxazole-4-carboxamide **100a**



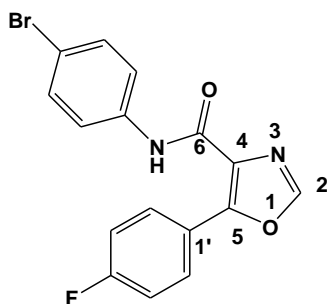
5-(4-Fluorophenyl)-*N*-(2-hydroxyphenyl)oxazole-4-carboxamide **100a** was successfully synthesized from 2-hydroxyaniline (48 mg, 0.45 mmol), 5-(4-fluorophenyl)oxazole-4-carbonyl chloride **112a** (12 mg, 0.45 mmol) and Et₃N (60 mg, 0.59 mmol) in EtOAc as described by the general procedure; **Physical characteristics**: brownish yellow solid; **Yield**: 113 mg, 84%; **Melting point**: 89-92°C; **¹H NMR** (400 MHz, CDCl₃) δ 9.26 (1H, s, NH), 8.19 (2H, dd, *J* = 6.0 Hz, 2.8 ArH), 7.80 (1H, s, 2-CH), 6.80-7.22 (7H, overlapping signals, OH and ArH); **¹³C NMR** (101 MHz, CDCl₃) δ 163.9 (d, ¹*J*_{C,F} = 252 Hz, *para*-CF), 160.1 (C=O), 153.4 (5-C), 148.5 (2-C), 148.0 (ArCOH), 130.8 (d, ³*J*_{C,F} = 8 Hz, *ortho*-C), 127.4 (4-C), 127.0, 125.3 (ArC), 122.7 (d, ⁴*J*_{C,F} = 3 Hz, 1'-C), 122.3, 120.5, 119.4, 115.7 (d, ²*J*_{C,F} = 22 Hz, *meta*-C); **FTIR** *v*_{max}/cm⁻¹ (KBr): 3352, 3126, 1669, 1604, 1533, 1456, 1361, 1282, 1234, 965, 761; **HRMS** (ESI-TOF) *m/z*: [M+H]⁺ Calcd for C₁₆H₁₂FN₂O₃ 299.0826, found 299.0841.

8.3.12.3. 5-(4-Fluorophenyl)-*N*-(2,4-dimethoxyphenyl)oxazole-4-carboxamide **100b**



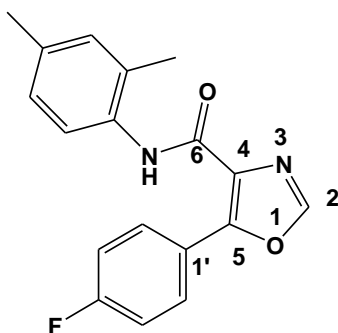
5-(4-Fluorophenyl)-N-(2,4-dimethoxyphenyl)oxazole-4-carboxamide **100b** was successfully synthesized from 2,4-dimethoxyaniline (110 mg, 0.72 mmol), 5-(4-fluorophenyl)oxazole-4-carbonyl chloride **112a** (162 mg, 0.72 mmol) and Et₃N (95 mg, 0.94 mmol) in EtOAc as described by the general procedure; **Physical characteristics**: brown crystals; **Yield**: 168 mg, 68%; **Melting point**: 154-157°C; **¹H NMR** (400 MHz, CDCl₃) δ 9.50 (1H, s, NH), 8.33-8.39 (3H, m, ArH), 7.86 (1H, s, 2-CH), 7.14 (2H, t, *J* = 8.8 Hz, ArH), 6.52 (1H, s, ArH), 6.49 (1H, d, *J* = 8.8 Hz, ArH), 3.91 and 3.80 (6H, 2 x s, 2 x ArOCH₃); **¹³C NMR** (101 MHz, CDCl₃) δ 163.6 (d, ¹*J*_{C,F} = 252 Hz, *para*-CF), 158.4 (C=O), 156.6 (ArCOCH₃), 152.2 (5-C), 149.8 (ArCOCH₃), 147.7 (2-C), 130.6 (d, ³*J*_{C,F} = 9 Hz, *ortho*-C), 129.0 (4-C), 123.3 (d, ⁴*J*_{C,F} = 3 Hz, 1'-C), 121.0, 120.6 (ArC), 115.5 (d, ²*J*_{C,F} = 22 Hz, *meta*-C), 103.7, 98.6 (ArC), 55.5 and 55.8 (2 x ArCOCH₃); **FTIR** $\nu_{\max}/\text{cm}^{-1}$ (KBr): 3367, 3128, 3034, 3013, 2956, 2921, 2834, 1666, 1606, 1548, 1454, 1417, 1280, 1208, 1158, 1128, 1067, 1036, 920, 882, 834, 818, 787, 691, 636, 513; **HRMS** (ESI-TOF) *m/z*: [M+H]⁺ Calcd for C₁₆H₁₆FN₂O₄, 343.1089 found 343.1116.

8.3.12.3. 5-(4-Fluorophenyl)-N-(4-bromophenyl)oxazole-4-carboxamide **100c**



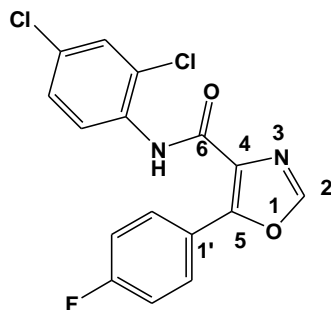
5-(4-Fluorophenyl)-N-(4-bromophenyl)oxazole-4-carboxamide **100c** was successfully synthesized from 4-bromoaniline (138 mg, 0.80 mmol), 5-(4-fluorophenyl)oxazole-4-carbonyl chloride **112a** (181 mg, 0.80 mmol) and Et₃N (105 mg, 1.04 mmol) in EtOAc as described by the general procedure; **Physical characteristics**: pale yellow solid; **Yield**: 211 mg, 73%; **Melting point**: 176-179 °C; **¹H NMR** (400 MHz, DMSO-d₆): δ 9.09 (1H, s, NH), 8.32 (2H, dd, *J* = 6.0 Hz, 2.8 Hz ArH), 7.87 (1H, s, 2-CH), 7.58-7.60 (2H, d, *J* = 8.8 Hz, ArH), 7.46 (2H, d, *J* = 8.4 Hz, ArH), 7.15 (2H, dd, *J* = 8.8 Hz, ArH); **¹³C NMR** (101 MHz, DMSO-d₆): δ 163.8 (d, ¹*J*_{C,F} = 250.4 Hz, *para*-CF), 158.9 (C=O), 153.0 (5-C), 147.7 (2-C), 136.8, 132.0, 130.6 (d, C-6', ³*J*_{C,F} = 9.0 Hz, *ortho*-C), 127.4 (ArC), 122.7 (d, ⁴*J*_{C,F} = 3.1 Hz, 1'-C), 121.4 (4-C), 117.03 (ArC), 115.7 (d, ³*J*_{C,F} = 22.1 Hz, *meta*-C); **FTIR** $\nu_{\max}/\text{cm}^{-1}$ (KBr): 3370, 3136, 2924, 2857, 1673, 1609, 1336, 1371, 1245, 1120, 1064, 873, 835, 629, 499; **HRMS** (ESI-TOF) *m/z*: [M+H]⁺ Calcd for C₁₆H₁₁⁷⁹BrFN₂O₂ 360.9982, found 361.0004.

8.3.12.4. 5-(4-Fluorophenyl)-*N*-(2,4-dimethylphenyl)oxazole-4-carboxamide 100d



5-(4-Fluorophenyl)-*N*-(2,4-dimethylphenyl)oxazole-4-carboxamide **100d** was successfully synthesized from 2,4-dimethylaniline (93 mg, 0.77 mmol), 5-(4-fluorophenyl)oxazole-4-carbonyl chloride **112a** (174 mg, 0.77 mmol) and Et₃N (101 mg, 1.00 mmol) in EtOAc as described by the general procedure; **Physical characteristics:** pale yellow crystals; **Yield** 167 mg, 70%; **Melting point:** 141-143 °C; **¹H NMR** (400 MHz, CDCl₃) δ 9.02 (1H, s, NH), 8.37 (2H, dd, *J* = 5.6 Hz, 3.2 Hz, ArH), 7.94 (1H, d, *J* = 8.4 Hz, ArH), 7.87 (1H, s, 2-CH), 7.14 (2H, t, *J* = 8.8 Hz, ArH), 7.05 (1H, overlapping singlet and doublet, *J* = 10.8 Hz, ArH), 7.05 (1H, s, ArH), 2.32 and 2.34 (6H, 2 x s, 2x ArCH₃); **¹³C NMR** (101 MHz, CDCl₃) δ 163.7 (d, ¹*J*_{C,F} = 255 Hz, *para*-CF), 158.9 (C=O), 152.5 (5-C), 147.7 (2-C), 136.8 (ArC), 134.6 and 132.9 (2 x ArCCH₃), 131.1, 130.6 (d, ³*J*_{C,F} = 9 Hz, *ortho*-C), 128.8, 128.6 (4-C), 127.3 (ArC), 123.1 (d, ⁴*J*_{C,F} = 3 Hz, 1-C), 122.1 (4-C), 115.4 (d, ²*J*_{C,F} = 22 Hz, *meta*-C), 20.9 and 17.6 (2 x ArCCH₃); **FTIR** ν_{\max} /cm⁻¹ (KBr): 3397, 3130, 3017, 2919, 1680, 1614, 1536, 1443, 1299, 1231, 1160, 1111, 1068, 938, 873, 832, 763, 624, 553, 515; **HRMS** (ESI-TOF) *m/z*: [M+H]⁺ Calcd for C₁₈H₁₀FN₂O₂ 311.1186, found 311.1190.

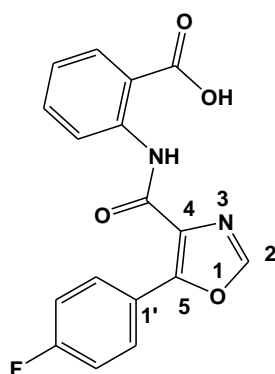
8.3.12.5. (2,4-Dichlorophenyl)-5-(4-fluorophenyl)oxazole-4-carboxamide 100e



(2,4-Dichlorophenyl)-5-(4-fluorophenyl)oxazole-4-carboxamide **100e** was successfully synthesized from 2,4-dichloroaniline (105 mg, 0.65 mmol), 5-(4-fluorophenyl)oxazole-4-carbonyl chloride **112a** (147 mg, 0.65 mmol) and Et₃N (86 mg, 0.85 mmol) in EtOAc as described by the general procedure; **Physical characteristics:** white solid; **Yield:** 64 mg, 72%; **Melting point:**

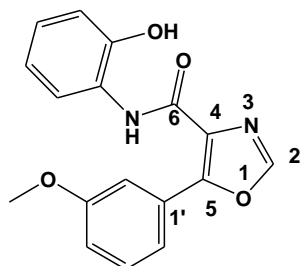
218-221 °C; **¹H NMR** (400 MHz, DMSO-*d*₆): δ 9.71 (1H, s, NH), 8.61 (1H, s, 2-CH), 8.93 (1H, t, *J* = 5.6 Hz, ArH), 7.85 (1H, s, ArH), 7.26 (1H, d, *J* = 8.4 Hz, ArH), 7.19 (1H, s, ArH), 7.11 (2H, t, *J* = 8.4 Hz, ArH), 6.97 (1H, d, *J* = 8.4 Hz, ArH); **¹³C NMR** (101 MHz, DMSO-*d*₆): δ 163.6 (d, ¹*J*_{C,F} = 252 Hz, *para*-CF), 158.9 (C=O), 153.4 (2-C), 147.9 (ArC), 152.2 (5-C), 147.9, 133.6, 130.7 (d, ³*J*_{C,F} = 9 Hz, *ortho*-C), 129.8 (ArC), 124.6 (d, ⁴*J*_{C,F} = 3 Hz, 1'-C), 124.6, 122.5, 120.1 (ArC), 115.8 (d, ²*J*_{C,F} = 22 Hz, *meta*-C); **FTIR** ν_{\max} /cm⁻¹ (KBr): 3331, 3124, 2926, 2847, 1682, 1587, 1525, 1412, 1241, 1168, 843, 804, 682, 636, 513; **HRMS** (ESI-TOF) *m/z*: [M+H]⁺ Calcd for C₁₆H₁₀Cl₂FN₂O₂ 351.0098, found 351.0095.

282-(5-(4-Fluorophenyl)oxazole-4-carboxamido)benzoic acid **100f**



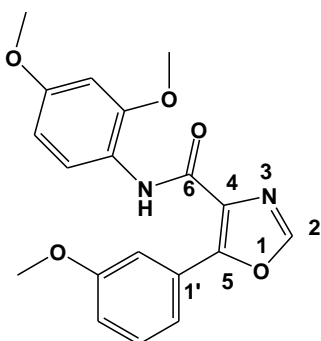
2-(5-(4-Fluorophenyl)oxazole-4-carboxamido)benzoic acid **100f** was successfully synthesized from 2-aminobenzoic acid (82 mg, 0.60 mmol), 5-(4-fluorophenyl)oxazole-4-carbonyl chloride **112a** (135 mg, 0.60 mmol) and Et₃N (78 mg, 0.78 mmol) in EtOAc as described by the general procedure; **Physical characteristics**: pale yellow solid; **Yield**: 125 mg, 64%; **Melting point**: 180-183 °C; **¹H NMR** (400 MHz, DMSO-*d*₆) δ 13.6 (1H, s, COOH), 12.5 (1H, s, NH), 8.78 (2H, d, *J* = 8.4 Hz, ArH), 8.66 (1H, s, 2-CH), 8.28 (2H, t, *J* = 7.2 Hz, ArH), 8.06 (2H, d, *J* = 8.4 Hz, ArH), 7.62 (2H, d, *J* = 8.4 Hz, ArH); **¹³C NMR** (101 MHz, DMSO-*d*₆) δ 169.0 (COOH), 163.0 (d, ¹*J*_{C,F} = 250.2 Hz, *para*-CF), 159.4 (CONH), 151.3 (2-C), 150.3 (5-C), 140.4, 134.0, 131.3 (ArC), 130.7 (d, ³*J*_{C,F} = 8.1 Hz, *ortho*-C), 128.6 (ArC), 123.7 (d, ⁴*J*_{C,F} = 3.0 Hz, 1'-C), 123.0, 120.0, 116.8 (ArC), 115.6 (d, ²*J*_{C,F} = 22.1 Hz, *meta*-C); **FTIR** ν_{\max} /cm⁻¹ (KBr): 3092, 3008, 2456, 2255, 1672, 1608, 1584, 1504, 1451, 1408, 1303, 1243, 1164, 984, 842, 762, 659, 643, 540; **HRMS** (ESI-TOF) *m/z*: [M+H]⁺ Calcd for C₁₇H₁₂FN₂O₄ 327.0781, found 327.0795.

8.3.12.6. 5-(3-Methoxyphenyl)-*N*-(2-hydroxyphenyl)oxazole-4-carboxamide 100g



5-(3-Methoxyphenyl)-*N*-(2-hydroxyphenyl)oxazole-4-carboxamide **100g** was successfully synthesized from 2-hydroxyaniline (101 mg, 0.93 mmol), 5-(3-methoxyphenyl)oxazole-4-carbonyl chloride **112c** (221 mg, 0.93 mmol) and Et₃N (122 mg, 1.21 mmol) in EtOAc as described by the general procedure; **Physical characteristics**: yellow solid; **Yield**: 150 mg, 52%; **Melting point**: 99-1102°C; **¹H NMR** (400 MHz, CDCl₃) δ 9.36 (1H, s, NH), 9.06 (1H, s, ArOH), 8.02 (1H, s, ArH), 7.92 (1H, s, 2-CH), 7.79 (1H, d, *J* = 8.4 Hz, ArH), 7.37 (1H, t, *J* = 8.4 Hz, ArH), 7.14-7.20 (2H, m, ArH), 7.01-7.07 (2H, m, ArH), 6.90 (1H, t, *J* = 8.4 Hz, ArH), 3.88 (1H, s, ArOCH₃); **¹³C NMR** (101 MHz, CDCl₃) δ 160.3 (C=O), 159.5 (ArCOH), 154.2 (5-C), 148.9 (ArCOCH₃), 148.9 (2-C), 148.0, 129.5, 127.7, 127.5, 125.3, 122.5, 120.6, 120.5, 119.9, 117.2, 113.4 (ArC), 55.4 (ArOCH₃); **FTIR** ν_{\max} /cm⁻¹ (KBr): 3609, 3443, 3357, 3134, 1730, 1660, 1570, 1535, 1493, 1456, 1331, 1235, 1057, 1013, 880, 828, 742, 641, 610; **HRMS** (ESI-TOF) *m/z*: [M+H]⁺ Calcd for C₁₉H₁₅N₂O₅ 311.1026, found 311.1036.

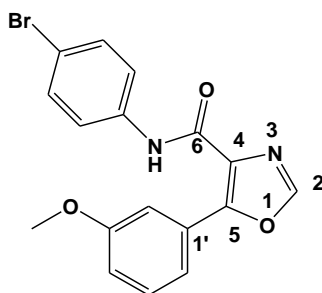
8.3.12.7. 5-(3-Methoxyphenyl)-*N*-(2,4-dimethoxyphenyl)oxazole-4-carboxamide 100h



5-(3-Methoxyphenyl)-*N*-(2-hydroxyphenyl)oxazole-4-carboxamide **100h** was successfully synthesized from 2,4-dimethoxyaniline (124 mg, 0.81 mmol), 5-(3-methoxyphenyl)oxazole-4-carbonyl chloride **112c** (193 mg, 0.81 mmol) and Et₃N (111 mg, 1.10 mmol) in EtOAc as described by the general procedure; **Physical characteristics**: brownish white solid; **Yield**: 207 mg, 72%; **Melting point**: 169-172°C; **¹H NMR** (400 MHz, CDCl₃) δ 9.45 (1H, s, NH), 8.33-8.39

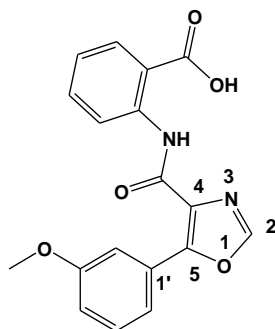
(3H, m, ArH), 7.86 (1H, s, 2-CH), 7.14 (2H, t, $J = 8.8$ Hz, ArH), 6.52 (1H, s, ArH), 6.49 (1H, d, $J = 8.8$ Hz, ArH), 3.91, 3.88 & 3.80 (9H, 3 x s, 3 x ArOCH₃); ¹³C NMR (101 MHz, CDCl₃) δ 159.5 (C=O), 158.4, 156.5 and 152.9 (3 x ArCOCH₃), 149.8, 147.8, 129.6, 129.4, 128.1, 1212.2, 120.6, 120.4, 116.4, 113.3, 103.7, 98.6 (ArC), 55.8, 55.5 and 55.4 (3 x ArCO_CH₃); FTIR $\nu_{\max}/\text{cm}^{-1}$ (KBr): 3371, 3117, 3078, 2925, 2830, 1662, 1536, 1498, 1368, 1296, 1249, 1212, 1161, 1127, 1030, 788, 698, 637; HRMS (ESI-TOF) m/z : [M+H]⁺ Calcd for C₁₉H₁₉N₂O₅ 355.1288, found 355.1309.

8.3.12.8. 5-(3-Methoxyphenyl)-*N*-(4-bromophenyl)oxazole-4-carboxamide 100i



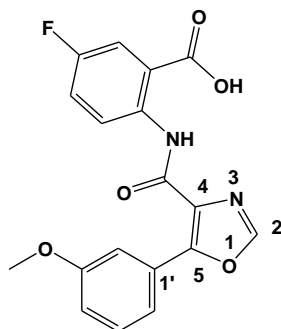
5-(3-Methoxyphenyl)-*N*-(4-bromophenyl)oxazole-4-carboxamide **100i** was successfully synthesized from 4-bromoaniline (146 mg, 0.85 mmol), 5-(3-methoxyphenyl)oxazole-4-carbonyl chloride **112c** (202 mg, 0.85 mmol) and Et₃N (112 mg, 1.11 mmol) in EtOAc as described by the general procedure; **Physical characteristics**: pale yellow crystals; **Yield**: 266 mg, 84%; **Melting point**: 167-169 °C; ¹H NMR (400 MHz, CDCl₃) δ 9.12 (1H, s, NH), 8.00 (1H, s, ArH), 7.86 (2H, overlapping singlet and doublet, $J = 8.8$ Hz, ArH and 2-CH), 7.61 (2H, d, $J = 8.8$ Hz, ArH), 7.46 (2H, d, $J = 8.4$ Hz, ArH), 7.38 (1H, t, $J = 8.4$ Hz, ArH), 7.00 (1H, dd, $J = 6.4$ Hz, 2 Hz, ArH), 3.90 (3H, s, ArOCH₃); ¹³C NMR (101 MHz, CDCl₃) δ 159.5 (C=O), 158.8 (ArCOCH₃), 153.6 (5-C), 147.7 (2-C), 136.8, 132.0, 129.5, 128.7 (ArC), 127.8 (C-4), 121.4, 120.6, 117.0, 116.7, 113.4 (ArC), 55.4 (ArCOCH₃); FTIR $\nu_{\max}/\text{cm}^{-1}$ (KBr): 3360, 3133, 3004, 2952, 2834, 1678, 1586, 1530, 1456, 1396, 1246, 1120, 1059, 826, 635, 508; HRMS (ESI-TOF) m/z : [M+H]⁺ Calcd for C₁₇H₁₄⁷⁹BrN₂O₃ 373.0182, found 373.0200

8.3.12.9. 2-(5-(3-Methoxyphenyl)oxazole-4-carboxamido)benzoic acid 100j



2-(5-(3-Methoxyphenyl)oxazole-4-carboxamido)benzoic acid **100j** was successfully synthesized from 2-aminobenzoic acid (130 mg, 0.95 mmol), 5-(3-methoxyphenyl)oxazole-4-carbonyl chloride (226 mg, 0.95 mmol) and Et₃N (126 mg, 1.24 mmol) in EtOAc as described by the general procedure; **Physical characteristics**: pale yellow solid; **Yield**: 167 mg, 52%; **Melting point**: 187-190°C; **¹H NMR**(400 MHz, DMSO-*d*₆): δ 13.54 (1H, br, COOH), 12.50 (1H, s, NH), 8.77 (1H, d, *J* = 8.4 Hz, ArH), 8.66 (1H, s, 2-CH), 8.04 (1H, d, *J* = 8.4 Hz, ArH), 7.93 (1H, s, ArH), 7.74 (1H, d, *J* = 8.4 Hz, ArH), 7.62 (1H, t, *J* = 7.6 Hz, ArH), 7.43(1H, t, *J* = 7.6 Hz, ArH), 7.18 (1H, t, *J* = 7.2 Hz, ArH), 7.07-7.10 (1H, m, ArH), 3.83 (3H, s, ArOCH₃); **¹³C NMR** (101 MHz, DMSO-*d*₆): δ 169.0 (COOH), 159.5 (CONH), 159.1 (ArCOCH₃), 152.5 (5-C), 150.3 (2-C), 140.4, 134.1, 131.3, 129.7 (ArC), 129.0 (4-C), 127.8, 123.0, 120.3, 120.0, 116.8, 116.0, 113.7 (ArC), 55.3 (ArCOCH₃); **FTIR** ν_{\max} /cm⁻¹ (KBr): 3252, 3130, 2830, 2634, 1678, 1586, 1560, 1448, 1404, 1262, 1012, 877, 827, 757, 663, 639; **HRMS** (ESI-TOF) *m/z*: [M+H]⁺ Calcd For C₁₈H₁₅N₂O₅ 399.0975, found 399.0977.

8.3.12.10. 2-(5-(4-Methoxyphenyl)oxazole-4-carboxamido)-4-fluorobenzoic acid **100k**



2-(5-(4-Methoxyphenyl)oxazole-4-carboxamido)-4-fluorobenzoic acid **100k** was successfully synthesized from 2-amino-5-fluorobenzoic acid (154 mg, 0.99 mmol), 5-(3-methoxyphenyl)oxazole-4-carbonyl chloride **112c** (235 mg, 0.99 mmol) and Et₃N(131 mg, 1.29 mmol) in EtOAc as described by the general procedure; **Physical characteristics**: yellow solid; **Yield**: 212 mg, 60%; **Melting point**: 191-194 °C; **¹H NMR** (400 MHz, DMSO-*d*₆) δ 13.8 (1H, br, COOH), 12.7 (1H, s, NH), 8.60-8.73 (2H, m, ArH), 8.57 (1H, s, 2-CH), 7.60-7. 8.18 (2H, m,

ArH), 7.07-7.16 (1H, s, ArH), 7.07-7.53 (2H, m, ArH), 3.86 (3H, s, ArOCH₃); ¹³C NMR (101 MHz, DMSO-*d*₆) δ 168.7 (COOH), 163.6 (d, ¹J_{C,F} = 252 Hz, CF), 159.8 (CONH), 159.1 (ArCOCH₃), 152.9 (5-C), 150.4 (2-C), 140.4, 133.9, 129.7, 128.6, 127.6, 120.3, 116.1, 113.7, 113.2, 110.1, 106.4 (ArC), 55.3 (ArCOCH₃); FTIR ν_{max}/cm⁻¹ (KBr): 3200, 3133, 2843, 2656, 1673, 1591, 1523, 1409, 1257, 1178, 1012, 876, 778, 641; HRMS (ESI-TOF) m/z: [M+H]⁺ Calcd. for C₁₈H₁₄N₂O₅ 357.0881; found 357.0906.

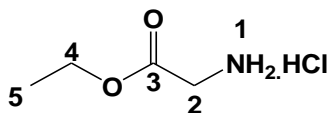
8.4. Chapter 4 experimental procedures

8.4.1. Synthesis of ethyl 2-amino hydrochloride salts

8.4.1.1. General synthetic procedure

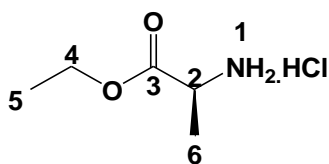
Thionyl chloride (1.2 molar equivalents) was added slowly to a mixture containing amino acid (1 molar equivalent) in ethanol (100 ml) at 0°C. After removal of the ice bath, the mixture was stirred for 5 hours under reflux. After cooling to room temperature, the excess ethanol and thionyl chloride were removed under reduce pressure. The resultant white solid was combined twice with ethanol and this was again removed under reduce pressure to remove adhering thionyl chloride completely. The product was then recrystallized from ethanol and dried under high vacuum.

8.4.1.2. Ethyl glycinate hydrochloride 105a



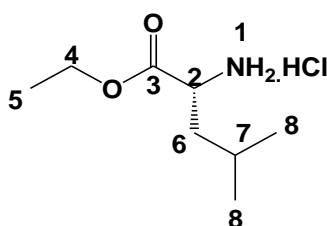
Ethyl glycinate hydrochloride **105a** was successfully synthesized using glycine (9.98 g, 133 mmol) and thionyl chloride (19.04 g, 160 mmol) in ethanol (100 ml) according to the general procedure; **Physical characteristics:** white solid; **Yield:** 16.71 g, 90%; **Melting point:** 144-147°C (lit.^{263,266}); ¹H NMR (400 MHz, CD₃OD) 4.36 (2H, q, *J* = 7.2 Hz, OCH₂CH₃), 3.87 (2H, s, NH₂), 1.37 (3H, t, *J* = 7.1, OCH₂CH₃); ¹³C NMR (101 MHz, CD₃OD) 168.5 (C=O), 63.4 (4-C), 41.1 (2-C), 14.39 (5-C).

8.4.1.3. *L*-Ethyl 2-aminopropanoate hydrochloride 105b



L-Ethyl 2-aminopropanoate hydrochloride **105b** was successfully synthesized using *L*-alanine (12.03 g, 135 mmol) and thionyl chloride (24.89 g, 162 mmol) in ethanol (100 ml) according to the general procedure; **Physical characteristics**: white solid; **Yield**: 20.53 g, 99%; **Melting point**: 76-78 °C (lit.^{270,271}); $^1\text{H NMR}$ (400 MHz, D₂O) 4.10 (2H, q, $J = 7.2$ Hz, OCH₂CH₃), 3.45 (2H, q, $J = 7.2$ Hz, 2-CH₂CH₃), 1.62 (2H, s, NH₂), 1.19 (3H, d, $J = 7.6$ Hz, CHCH₃), 1.16 (3H, t, $J = 7.6$ Hz, OCH₂CH₃); $^{13}\text{C NMR}$ (101 MHz, D₂O) δ 170.2 (C=O), 60.5 (4-C), 49.4 (2-C), 19.9 (6-C), 14.0 (5-C).

8.4.1.4. *D*-Ethyl 2-amino-4-methylpentanoate hydrochloride **105c**



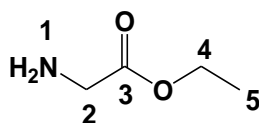
D-Ethyl 2-amino-4-methylpentanoate hydrochloride **105c** was successfully synthesized using *D*-leucine (13.77 g, 105 mmol) and thionyl chloride (14.99 g, 126 mmol) in ethanol (100 ml) according to the general procedure; **Physical characteristics**: white solid; **Yield**: 19.52 g, 95%; **Melting point**: 133-135°C (lit.³⁵⁷); $^1\text{H NMR}$ (400 MHz, CD₃OD) δ 4.12 (2H, q, $J = 7.2$ Hz, OCH₂CH₃), 3.45 [1H, d, $J = 7.4$ Hz, NHCH], 1.82 (2H, s, NH₂), 1.64-1.77 [1H, m, CHCH₂CH(CH₃)₂], 1.46-1.56 [1H, m, CHCH₂CH(CH₃)₂], 1.18 (3H, t, $J = 7.4$ Hz, OCH₂CH₃), 1.03 [1H, d, $J = 7.2$ Hz, CHCH₂CH(CH₃)₂]; $^{13}\text{C NMR}$ (101 MHz, CD₃OD) δ 176.5 (C=O), 60.5 (4-C), 52.6 (2-C), 43.3 (7-C), 24.8 (6-C) 22.9 and 21.7(2 x 8-C), 13.4 (5-C).

8.4.2. Synthesis of ethyl 2-aminoacylates

8.4.2.1. General synthetic procedure

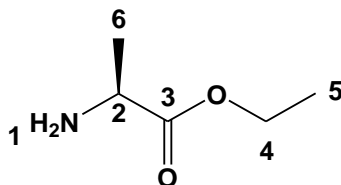
To a suspension of amino acid ethyl ester hydrochloride (1 molar equivalent) in chloroform (15 ml) was added a dropwise solution of triethylamine (1 molar equivalent) in chloroform (10 ml) at room temperature. The resulting reaction mixture was stirred at the same temperature for 6 hours, followed by refluxing for 1 hour. The mixture was allowed to cool to room temperature and solvent was concentrated *in vacuo* under reduced pressure to afford a white solid. The product was extracted with diethyl ether (3 x 25 ml) and then filtered. The filtrates were washed with ether (2 x 10 ml). The filtered solution was concentrated *in vacuo* under reduced pressure to afford pure ethyl -2-aminoacylates.

8.4.2.2. Ethyl 2-aminoacetate **115a**



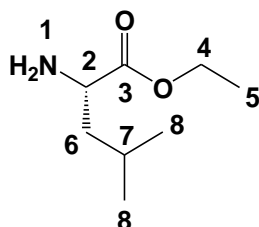
Glycine ethyl ester **115a** was successfully synthesized from glycine ethyl ester hydrochloride salts (10.00 g, 71.6 mmol) and Et₃N (7.25 g, 71.6 mmol) in CHCl₃ as described by the general synthetic procedure; **Physical characteristics**: yellow oil; **Yield**: 7.09 g, 96%; **Melting point**: 145-148°C (lit³⁵⁸); **¹H NMR** (400 MHz, CDCl₃) δ 4.14 (2H, q, *J* = 7.2 Hz, OCH₂CH₃), 3.40 (2H, s, CH₂CO), 1.67 (2H, s, NH₂), 1.23 (3H, t, *J* = 7.2 Hz, OCH₂CH₃); **¹³C NMR** (101 MHz, CDCl₃) δ 174.2 (C=O), 60.8 (4-C) 43.9 (2-C), 14.2 (5-C).

8.4.2.3. *L*-Alanine ethyl ester **115b**



L-Alanine ethyl ester **115b** was successful synthesized from *L*-ethyl 2-aminopropanoate hydrochloride (10.85 g, 70.6 mmol) and Et₃N (8.40 g, 70.6 mmol) in CHCl₃ as described by the general synthetic procedure; **Physical characteristics**: yellow oil; **Yield**: 8.11 g, 98%; **¹H NMR** (400 MHz, CDCl₃) δ 4.01 (2H, q, *J* = 7.2 Hz, OCH₂CH₃), 3.43 (2H, q, *J* = 7.2 Hz, 2-CHCH₃), 1.59 (2H, s, NH₂), 1.19 (3H, d, *J* = 7.4 Hz, CHCH₃), 1.13 (3H, t, *J* = 7.2 Hz, OCH₂CH₃); **¹³C NMR** (101 MHz, CDCl₃) δ 176.3 (C=O), 60.5 (4-C), 49.8 (2-C), 20.4 (6-C), 13.9 (5-C).

8.4.2.4. *D*-leucine ethyl ester **115c**



D-leucine ethyl ester **115c** as was successful synthesized from *D*-ethyl 2-amino-4-methylpentanoate hydrochloride (16.05 g, 82.0 mmol) and Et₃N (8.30 g, 82.0 mmol) in CHCl₃ as described by the general synthetic procedure; **Physical characteristics**: yellow oil; **Yield**: 13.06 g, 98%; **¹H NMR** (400 MHz, CDCl₃) δ 4.05 (2H, d, *J* = 7.4 Hz, OCH₂CH₃), 3.36 (1H, d, *J* = 7.2 Hz, NH₂CH₂), 1.80 (2H, s, NH₂), 1.65-1.72 [2H, m, CHCH₂CH(CH₃)₂], 1.44-1.51 [1H, m,

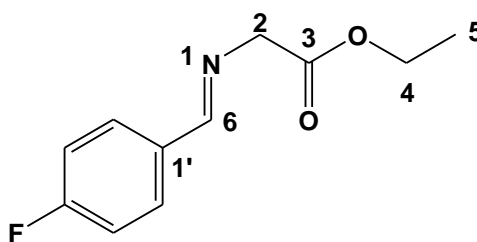
CHCH₂CH(CH₃)₂], 1.17 (3H, t, *J* = 7.4 Hz, OCH₂CH₃), 1.14 [6H, *J* = 7.4 Hz, CHCH₂CH(CH₃)₂]; ¹³C NMR (101 MHz, CDCl₃) δ 176.3 (C=O), 60.5 (4-C), 52.6 (2-C), 43.8 (7-C), 24.5 (6-C), 22.7 and 21.6 (2 x 8-C), 13.9 (5-C).

8.4.3. Preparation of ethyl 2-arylideneamino acyl intermediates

8.4.3.1. General procedure

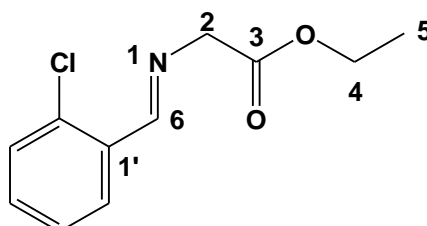
A solution of free amino acid ethyl ester (2 molar equivalents), aryl aldehyde (1 molar equivalent) and dried magnesium sulphate (0.5 g) was stirred in dry dichloromethane (15 ml) at room temperature for 16 hours. Upon completion, the magnesium sulphate was filtered off and washed with DCM. The combined organic layer was concentrated *in vacuo* and resulting products were kept at 80°C for 1 hour under reduced pressure in a rotavapor and dried under high vacuum to give pure ethyl 2-arylideneamino acyl intermediates..

8.4.3.2. (*E*)-Ethyl 2-(4-fluorobenzylideneamino)acetate 116a



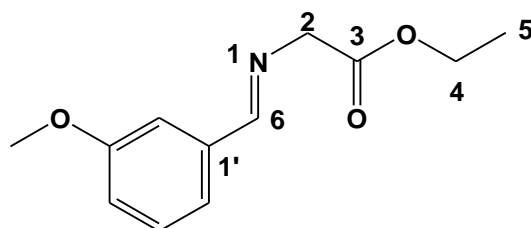
(*E*)-Ethyl 2-(4-fluorobenzylideneamino)acetate **116a** was successfully synthesized from 4-fluorobenzaldehyde (1.69 g, 13.60 mmol), ethyl 2-aminoacetate **115a** (2.80 g, 27.20 mmol) and MgSO₄ in DCM as described by the general procedure; **Physical characteristics:** light yellow oil; Yield: 2.59 g, 91%; ¹H NMR (400 MHz, CDCl₃) δ 8.20 (1H, s, N=CH), 7.71-7.74 (2H, m, ArH), 7.03-7.07 (2H, m, ArH), 4.33 (2H, s, 2-CH₂), 4.15 (2H, q, *J* = 7.4 Hz, OCH₂CH₃), 1.23 (3H, t, *J* = 7.2 Hz, OCH₂CH₃); ¹³C NMR (101 MHz, CDCl₃) δ 170.0 (C=O), 164.5 (d, *J*_{C,F} = 247 Hz, *para*-CF), 163.8 (N=CH), 131.3 (d, ⁴*J*_{CF} = 3 Hz, 1'-C), 115.7 (d, ³*J*_{CF} = 9.0 Hz, *ortho*-C), 115.5 (d, ²*J*_{CF} = 22 Hz, *meta*-C), 61.7 (4-C), 60.9 (2-C), 14.0 (5-C).

8.4.3.3. (*E*)-Ethyl 2-(2-chlorobenzylideneamino)acetate 116b



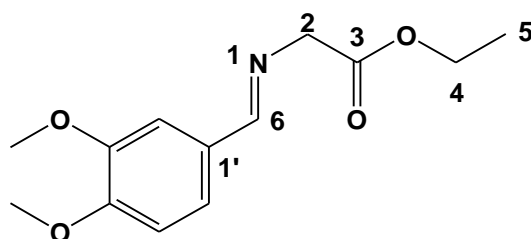
(*E*)-Ethyl 2-(3-methoxybenzylideneamino)acetate **116b** was successfully synthesized from 2-chlorobenzaldehyde (938 mg, 6.67 mmol), ethyl 2-aminoacetate **115a** (1.37 g, 13.34 mmol) and MgSO₄ in DCM as described by the general procedure; **Physical characteristics**: pale yellow oil; **Yield**: 1.31 g, 87%; **¹H NMR** (400MHz, CDCl₃) δ 8.18 (1H, s, N=CH), 7.55 (1H, J = 8.4 Hz, ArH), 7.27-7.30 (3H, m, ArH), 4.52 (2H, s, 2-CH₂), 4.12 (2H, J = 7.4 Hz, OCH₂CH₃), 1.17 (3H, t, J = 7.0 Hz, OCH₂CH₃); **¹³C NMR** (101 MHz, CDCl₃) δ 170.2 (C=O), 163.5 (N=CH), 139.6, 134.9, 131.8, 129.8, 127.1 (ArC), 61.6 (2-C), 61.0 (4-C), 14.1 (5-C).

8.4.3.4. (*E*)-Ethyl 2-(3-methoxybenzylideneamino)acetate **116c**



(*E*)-Ethyl 2-(3-methoxybenzylideneamino)acetate **116c** was successfully synthesized from 3-methoxybenzaldehyde (688 mg, 5.03 mmol), ethyl 2-aminoacetate **115a** (10.06 mmol) and MgSO₄ in DCM as described by the general procedure; **Physical characteristics**: pale yellow oil; **Yield**: 1.00 g, 90%; **¹H NMR** (400 MHz, CDCl₃) δ 8.24 (1H, s, N=CH), 7.38 (1H, s, ArH), 6.98-7.33 (3H, m, ArH), 4.39 (2H, s, 2-CH₂), 4.20 (2H, q, J = 7.2 Hz, OCH₂CH₃), 3.83 (3H, s, ArOCH₃), 1.27 (3H, t, J = 7.2 Hz, OCH₂CH₃); **¹³C NMR** (101 MHz, CDCl₃) δ 170.0 (C=O), 165.3 (N=CH), 159.7 (ArCOCH₃), 136.9, 129.4, 121.8, 118.0, 111.5 (ArC), 61.8 (4-C), 61.0 (2-C), 55.2 (ArCOCH₃), 14.1 (5-C).

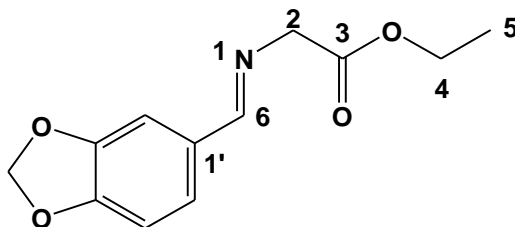
8.4.3.5. (*E*)-Ethyl 2-(3,4-dimethoxybenzylideneamino)acetate **116d**



(*E*)-Ethyl 2-(3,4-dimethoxybenzylideneamino)acetate **116d** was successfully synthesized from 3,4-dimethoxybenzaldehyde (1.40 g, 8.41 mmol), ethyl 2-aminoacetate **115a** (1.73 g, 16.82 mmol) and MgSO₄ in DCM as described by the general procedure; **Physical characteristics**: pale yellow oil; **Yield**: 1.97 g, 93%; **¹H NMR** (400 MHz, CDCl₃) δ 8.15 (1H, s, N=CH), 7.42 (1H, s, ArH), 7.13 (1H, dd, J = 6.4 Hz, 1.6 Hz, ArH), 7.13 (1H, d, J = 8.4 Hz, ArH), 4.33 (2H, s, 2-CH₂), 4.15 (2H, q, J = 7.4 Hz, OCH₂CH₃), 3.87 and 3.89 (6H, 2 x s, 2 x ArOCH₃), 1.24 (3H, t, J = 7.4 Hz,

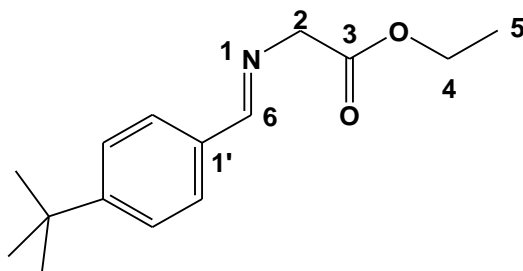
OCH₂CH₃); ¹³C NMR (101 MHz, CDCl₃) δ 170.2 (C=O), 164.8 (N=CH), 151.7 and 149.2 (2 x ArCOCH₃), 128.8, 123.7, 110.2, 108.7 (ArC), 61.9 (4-C), 60.9 (2-C), 55.8 and 55.9 (2 x ArCOCH₃), 14.1 (5-C).

8.4.3.6. (*E*)-Ethyl 2-((benzo[*d*][1,3]dioxol-6-yl)methyleneamino)acetate **116e**



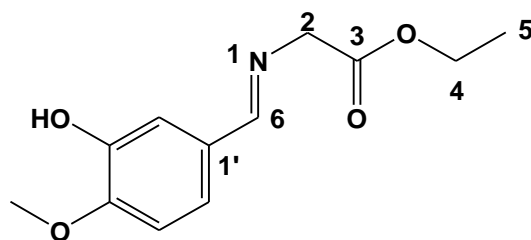
(*E*)-Ethyl 2-((benzo[*d*][1,3]dioxol-6-yl)methyleneamino)acetate **116e** was successfully synthesized from piperonal (1.22 g, 8.10 mmol), ethyl 2-aminoacetate **115a** (1.67 g, 16.2 mmol) and MgSO₄ in DCM as described by the general procedure; **Physical characteristics**: pale yellow oil; **Yield**: 1.73 g, 91%; ¹H NMR (400MHz; CDCl₃) δ 8.24 (1H, s, N=CH), 7.38 (1H, s, ArH), 6.98-7.33 (2H, m, ArH), 4.62 (2H, s, ArOCH₂O-); 4.39 (2H, s, 2-CH₂), 4.20 (2H, *J* = 7.2 Hz, OCH₂CH₃); 1.27 (3H, q, t, *J* = 7.2 Hz, OCH₂CH₃); ¹³C NMR (101 MHz, CDCl₃) δ 170.0 (C=O), 165.3 (N=CH), 159.7 and 149.8 (ArCOCH₂O), 136.9, 129.4, 121.8, 118.0 (ArC), 101.5 (ArCOCH₂O), 61.8 (4-C), 61.0 (2-C), 14.1 (5-C).

8.4.3.7. (*E*)-Ethyl 2-(4-*tert*-butylbenzylideneamino)acetate **116f**



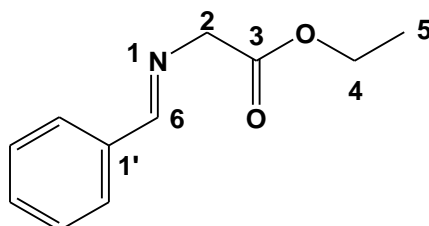
(*E*)-Ethyl 2-(4-*tert*-butylbenzylideneamino)acetate **116f** was successfully synthesized from 4-*tert*-butylbenzaldehyde (1.21 g, 7.45 mmol), ethyl 2-aminoacetate **115a** (1.54 g, 14.90 mmol) and MgSO₄ in DCM as described by the general procedure; **Physical characteristics**: yellow oil; **Yield**: 1.62 g, 88%; ¹H NMR (400MHz, CDCl₃) δ 8.25 (1H, s, N=CH), 7.69 (2H, d, *J* = 8.4 Hz, ArH), 7.42 (2H, q, *J* = 8.4 Hz, ArH), 4.38 (2H, s, 2-CH₂), 4.19 (2H, *J* = 7.4 Hz, OCH₂CH₃), 1.32 [9H, s, C(CH₃)₃], 1.27 (3H, t, *J* = 7.0 Hz, OCH₂CH₃); ¹³C NMR (101 MHz; CDCl₃) δ 170.2 (C=O), 165.2 (N=CH), 154.6, 132.9, 128.2, 125.5 (ArC), 62.1 (4-C), 60.9 (2-C), 34.9 [ArC(CH₃)₃], 31.3 [ArC(CH₃)₃], 14.1 (5-C).

8.4.3.8. (*E*)-Ethyl 2-(3-hydroxy-4-methoxybenzylideneamino)acetate **116g**



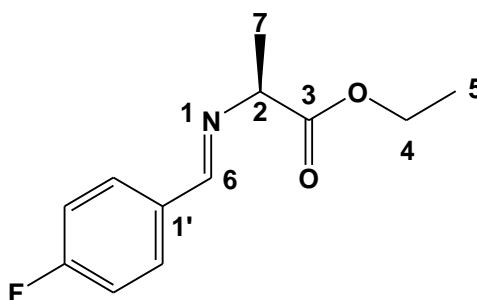
(*E*)-Ethyl 2-(3-hydroxy-4-methoxybenzylideneamino)acetate **116g** was successfully synthesized from 3-hydroxy-4-methoxybenzaldehyde (1.21 g, 7.92 mmol), ethyl 2-aminoacetate **115a** (1.63 g, 15.84 mmol) and MgSO_4 in DCM as described by the general procedure; **Physical characteristics**: orange oil; **Yield**: 1.62 g, 86%; **$^1\text{H NMR}$** (400 MHz, CDCl_3) δ 8.16 (1H, s, $\text{N}=\text{CH}$), 7.47 (1H, s, ArH), 7.09 (2H, d, $J = 8.4$ Hz, ArH), 5.29 (OH), 4.35 (2H, s, 2- CH_2), 4.20 (2H, q, $J = 7.2$ Hz, OCH_2CH_3), 3.89 (3H, s, ArOCH_3), 1.27 (3H, t, $J = 7.2$ Hz, OCH_2CH_3); **$^{13}\text{C NMR}$** (101 MHz, CDCl_3) δ 170.0 ($\text{C}=\text{O}$), 165.3 ($\text{N}=\text{CH}$), 159.7 (ArCOCH_3), 149.8 (ArCOH), 136.9, 118.0, 111.5, 98.0 (ArC), 61.8 (2-C), 61.0 (4-C), 55.2 (ArCOCH_3), 14.1 (5-C).

8.4.3.9. (*E*)-Ethyl 2-(benzylideneamino)acetate **116h**



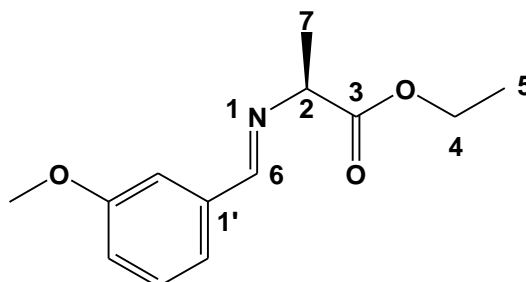
(*E*)-Ethyl 2-(benzylideneamino)acetate **116h** was successfully synthesized from benzaldehyde (647 mg, 6.10 mmol), ethyl 2-aminoacetate (1.26 g, 12.2 mmol) and MgSO_4 in DCM as described by the general procedure; **Physical characteristics**: colourless oil; **Yield**: 1.12 g, 96%; **$^1\text{H NMR}$** (400 MHz, CDCl_3) δ 8.26 (1H, s, $\text{N}=\text{CH}$), 7.38-7.76 (5H, m, ArH), 4.37 (2H, s, 2- CH_2), 4.18 (2H, q, $J = 7.2$ Hz, OCH_2CH_3), 1.25- (3H, t, $J = 7.2$ Hz, OCH_2CH_3); **$^{13}\text{C NMR}$** (101 MHz, CDCl_3) δ 170.0 ($\text{C}=\text{O}$), 165.8 ($\text{N}=\text{CH}$), 135.4, 131.7, 128.5, 128.3 (ArC), 61.9 (2-C), 60.9 (4-C), 14.1 (5-C).

8.4.3.10. (*S, E*)-Ethyl 2-(4-fluorobenzylideneamino)propanoate **117a**



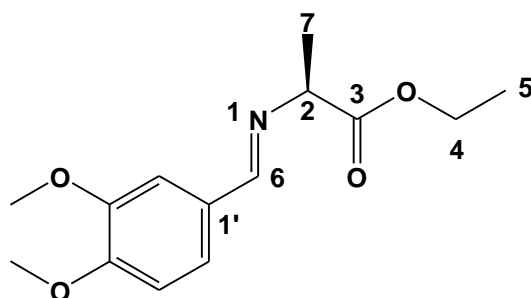
(*S, E*)-Ethyl 2-(4-fluorobenzylideneamino)propanoate **117a** was successfully synthesized from 4-fluorobenzaldehyde (826 mg, 6.66 mmol), *L*-alanine ethyl ester **115b** (1.56 g, 13.3 mmol) and MgSO_4 in DCM as described by the general procedure; **Physical characteristics**: pale yellow oil; **Yield**: 1.35 g, 91%; $^1\text{H NMR}$ (400 MHz, CDCl_3) δ 8.29 (1H, s, $\text{N}=\text{CH}$), 7.74-7.76 (2H, m, ArH), 7.38 (2H, t, $J = 8.4$ Hz, ArH), 4.11-4.21 (3H, m, 2- CHCH_3 and OCH_2CH_3), 1.50 (3H, q, $J = 7.2$ Hz, CHCH_3), 1.23 (3H, t, $J = 7.2$ Hz, OCH_2CH_3); $^{13}\text{C NMR}$ (101 MHz, CDCl_3) δ 170.0 ($\text{C}=\text{O}$), 164.4 (d, $^1J_{\text{C,F}} = 247$ Hz, *para*-CF), 163.8 ($\text{N}=\text{CH}$), 131.4 (d, $^4J_{\text{C,F}} = 3$ Hz, 1'-C), 126.4 (d, $^3J_{\text{C,F}} = 9$ Hz, *ortho*-C), 115.5 (d, $^2J_{\text{C,F}} = 22$ Hz, *meta*-C), 66.8 (2-C), 61.7 (4-C), 18.3 (7-C), 14.0 (5-C).

8.4.3.11. (*S, E*)-Ethyl 2-(3-methoxybenzylideneamino)propanoate **117b**



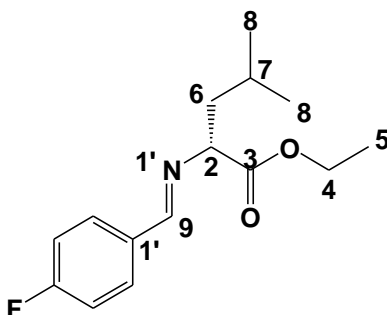
(*S, E*)-Ethyl 2-(3-methoxybenzylideneamino)propanoate **117b** was successfully synthesized from 3-methoxybenzaldehyde (905 mg, 6.65 mmol), *L*-alanine ethyl ester **115b** (1.56 g, 13.30 mmol) and MgSO_4 in DCM as described by the general procedure; **Physical characteristics**: light yellow oil; **Yield**: 1.13 g, 72%; $^1\text{H NMR}$ (400 MHz, CDCl_3) δ 8.20 (1H, s, $\text{N}=\text{CH}$), 7.30 (1H, s, ArH), 7.19-7.24 (2H, m, ArH), 6.89-6.92 (1H, m, ArH), 4.05-4.16 (3H, m, 2- CHCH_3 and OCH_2CH_3), 3.78 (3H, s, ArOCH_3), 1.44 (3H, q, $J = 7.4$ Hz, CHCH_3), 1.18 (3H, t, $J = 7.0$ Hz, OCH_2CH_3); $^{13}\text{C NMR}$ (101 MHz, CDCl_3) δ 172.5 ($\text{C}=\text{O}$), 162.7 ($\text{N}=\text{CH}$), 159.8 (ArCOCH_3), 137.1, 129.5, 121.8, 117.8, 111.7 (ArC), 67.9 (2-C), 61.0 (4-C), 55.3 (ArCOCH_3), 19.3 (7-C), 14.1 (5-C).

8.4.3.12. (*S,E*)-Ethyl 2-(3,4-dimethoxybenzylideneamino)propanoate **117c**



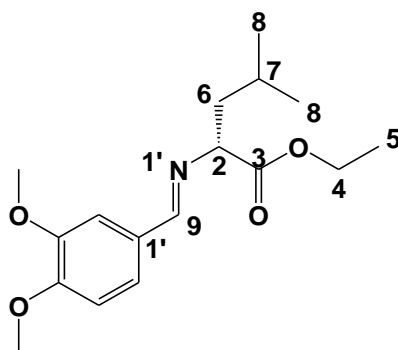
(*S,E*)-Ethyl 2-(3,4-dimethoxybenzylideneamino)propanoate **117c** was successfully synthesized from 3,4-dimethoxybenzaldehyde (1.16 g, 6.98 mmol), *L*-alanine ethyl ester (1.64 g, 13.96 mmol) and MgSO_4 in DCM as described by the general procedure; **Physical characteristics:** pale yellow oil; **Yield:** 1.54 g, 83%; **$^1\text{H NMR}$** (400 MHz, CDCl_3) δ 8.17 (1H, s, $\text{N}=\text{CH}$), 7.41 (1H, s, ArH), 7.14 (1H, d, $J = 8.4$ Hz, ArH), 6.82 (1H, d, $J = 8.4$ Hz, ArH), 4.05-4.18 (3H, m, 2- CHCH_3 and OCH_2CH_3), 3.86 and 3.89 (6H, 2 x s, 2 x ArOCH_3), 1.46 (3H, $J = 7.4$ Hz, CHCH_3), 1.21 (3H, t, $J = 7.2$ Hz, OCH_2CH_3); **$^{13}\text{C NMR}$** (101 MHz, CDCl_3) δ 172.6 ($\text{C}=\text{O}$), 162.2 ($\text{N}=\text{CH}$), 151.5 and 149.1 (2 x ArCOCH_3), 128.9, 123.5, 110.1, 108.8 (ArC), 67.7 (2-C), 60.8 (4-C), 55.9 and 55.8 (2 x ArCOCH_3), 19.3 (7-C), 14.0 (5-C).

8.4.3.13. (*R,E*)-Ethyl-5-(4-Fluorobenzylideneamino)-7-methyloctan-4-one **118a**



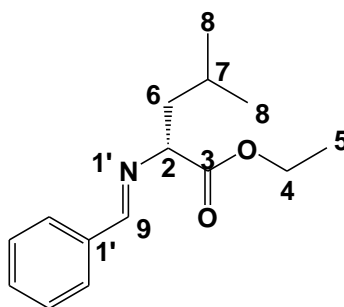
(*R,E*)-Ethyl 2-(4-fluorobenzylideneamino)-4-methylpentanoate **117a** was successfully synthesized from 4-fluorobenzaldehyde (943 mg, 7.60 mmol), *D*-leucine ethyl ester **115c** (2.42 g, 15.20 mmol) and MgSO_4 in DCM as described by the general procedure; **Physical characteristics:** pale yellow oil; **Yield:** 1.77 g, 88%; **$^1\text{H NMR}$** (400 MHz, CDCl_3) δ 8.25 (1H, s, $\text{N}=\text{CH}$), 7.76-7.79 (2H, m, ArH), 7.06-7.11 (2H, m, ArH), 4.03-4.23 (3H, m, 2- CH and OCH_2CH_3), 1.80-1.85 (2H, m, 6- CH_2), 1.54-1.59 (1H, m, 7- CH), 1.27 (3H, t, $J = 7.2$ Hz, OCH_2CH_3), 0.84 (6H, 2 x d, $J = 6.4$ Hz each, 2 x 8- CH_3); **$^{13}\text{C NMR}$** (101 MHz, CDCl_3) δ 172.4 ($\text{C}=\text{O}$), 164.0 (d, $J_{\text{CF}} = 250.9$ Hz, *para*-CF), 161.4 ($\text{N}=\text{CH}$), 132.0 (d, $^4J_{\text{CF}} = 3.0$ Hz, 1'-C), 130.4 (d, $^3J_{\text{CF}} = 10.1$ Hz, *ortho*-C), 115.6 (d, $^2J_{\text{CF}} = 22.1$ Hz, *meta*-C), 71.5 (2-C), 61.0 (4-C), 42.0 (6-C), 24.4 (7-C), 23.0 and 21.5 (2x 8-C), 14.1 (5-C).

8.4.3.14 (*R,E*)-Ethyl 2-(3,4-dimethoxybenzylideneamino)-4-methylpentanoate 117c



(*R,E*)-Ethyl 2-(3,4-dimethoxybenzylideneamino)-4-methylpentanoate **118c** was successfully synthesized from 3,4-dimethoxybenzaldehyde (961 mg, 5.78 mmol), D-leucine ethyl ester (1.84 g, 11.56 mmol) and MgSO_4 in DCM as described by the general procedure; **Physical characteristics**: pale yellow oil; **Yield**: 1.53 g, 86%; $^1\text{H NMR}$ (400 MHz, CDCl_3) δ 8.17 (1H, s, $\text{N}=\text{CH}$), 7.41 (1H, s, ArH), 7.14 (1H, d, $J = 8.4$ Hz, ArH), 6.82 (1H, d, $J = 8.4$ Hz, ArH), 4.05-4.18 (3H, m, 2- CHCH_3 and OCH_2CH_3), 3.86 and 3.89 (6H, 2 x s, 2 x ArOCH_3), 1.46 (3H, 1.80-1.85 (2H, m, 6- CH_2), 1.54-1.59 (1H, m, 7-CH), 1.27 (3H, t, $J = 7.2$ Hz, OCH_2CH_3), 0.84 (6H, 2 x d, $J = 6.4$ Hz each, 2 x 8- CH_3); $^{13}\text{C NMR}$ (101 MHz, CDCl_3) δ 172.6 ($\text{C}=\text{O}$), 162.2 ($\text{N}=\text{CH}$), 151.5 and 149.1 (2 x ArCOCH_3), 128.9, 123.5, 110.1, 108.8 (ArC), 67.7 (2-C), 60.8 (4-C), 3 (7-C), 14.0 (5-C), 71.5 (2-C), 61.0 (4-C), 55.9 and 55.8 (2 x ArCOCH_3), 42.0 (6-C), 24.4 (7-C), 23.0 and 21.5 (2 x 8-C), 14.1 (5-C).

8.4.3.15. (*R,E*)-Ethyl 2-(benzylideneamino)-4-methylpentanoate 118c



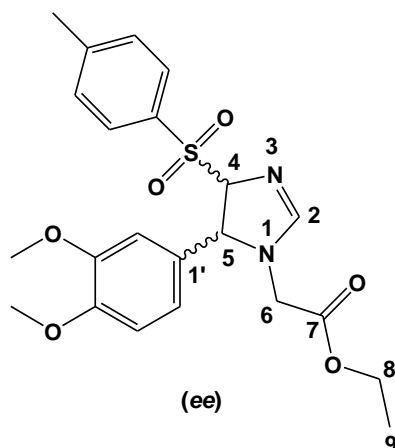
(*R,E*)-Ethyl 2-(benzylideneamino)-4-methylpentanoate **118c** was successfully synthesized from benzaldehyde (653 mg, 6.15 mmol), D-leucine ethyl ester **115c** (1.96 g, 12.30 mmol) and MgSO_4 in DCM as described by the general procedure; **Physical characteristics**: colourless oil; **Yield**: 1.23 g, 81%; $^1\text{H NMR}$ (400 MHz, CDCl_3) δ 8.26 (1H, s, $\text{N}=\text{CH}$), 7.38-7.76 (5H, m, ArH), 4.37 (2H, s, 2- CH_2), 1.46 (3H, 1.80-1.85 (2H, m, 6- CH_2), 1.54-1.59 (1H, m, 7-CH), 1.27 (3H, t, $J = 7.2$ Hz, OCH_2CH_3), 0.84 (6H, dd, $J = 6.4$, 2 x 8- CH_3); $^{13}\text{C NMR}$ (101 MHz, CDCl_3) δ 170.0 ($\text{C}=\text{O}$),

165.8 (N=CH), 135.4, 131.7, 128.5, 128.3 (ArC), 42.0 71.5 (2-C), 61.0 (4-C), 4.20 (6-C), 24.4 (7-C), 23.0 and 21.5 (2 x 8-C), 14.1 (5-C).

8.4.4. Synthesis of ethyl 2-(5-aryl-1*H*-imidazol-1-yl)acyl derivatives

8.4.4.1. Synthesis of ethyl 2-[5-(3,4-dimethoxyphenyl)-4-tosyl-4,5-dihydro-1*H*-imidazol-1-yl]acetate

To a stirred solution of ethyl-2-(3,4-dimethoxybenzylideneamino)acetate **116d** (451 mg, 2.04 mmol), TosMIC (398 mg, 2.04 mmol) in DCM (8 ml) was added dropwise a solution of DBU (311 mg, 2.04 mmol) in DCM (2 ml) at room temperature. Upon completion of addition, the resulted mixture was stirred at same temperature for 24 hours (monitored by TLC). After consumption of TosMIC, the solvent was concentrated in *vacuo* afforded crude brown oil. The crude product was separated by column chromatography elution with ethyl acetate: hexane ratio (1:1) afforded a diastereomeric mixture of (*cis*- and *trans*-ethyl 2-[5-(3,4-dimethoxyphenyl)-4-tosyl-4,5-dihydro-1*H*-imidazol-1-yl]acetate **119**.



Physical characteristics: brown oil; **Yield:** 501 mg, 55%; *cis*- and *trans*-ethyl 2-[5-(3,4-dimethoxyphenyl)-4-tosyl-4,5-dihydro-1*H*-imidazol-1-yl]acetate **119**: $^1\text{H NMR}$ (400MHz, CDCl_3) δ 8.15_{trans} (0.3H, s, 2-CH), 7.83 (2H, d, $J = 7.2$ Hz, ArH), 7.33 (2H, d, $J = 7.2$ Hz, ArH), 7.14_{cis} (0.7H, s, 2-CH), 6.78-6.93 (3H, m, ArH), 5.25_{cis} (0.7H, d, $J = 6.4$ Hz, 5-CH), 5.05_{cis} (0.7H, d, $J = 6.4$ Hz, 4-CH), 4.77_{trans} (0.6H s, 4- and 5-CH), 4.17- 4.23 (2H, m, OCH_2CH_3), 3.84-3.91 (6H, m, 2 x OCH_3 and CH_2CO), 2.42_{cis} (2H, s, ArCH_3), 2.04_{trans} (1H, s, ArCH_3), 1.22-1.27 (3H, m, OCH_2CH_3).

8.4.4.2. Synthesis of ethyl 2-[5-(3,4-dimethoxyphenyl)-1*H*-imidazol-1-yl]acetate

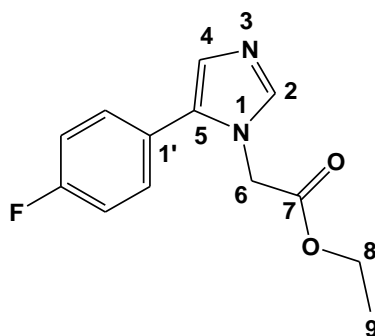
A diastereomeric mixture of ethyl 2-[5-(3,4-dimethoxyphenyl)-4-tosyl-4,5-dihydro-1*H*-imidazol-1-yl]acetate **119** (500 mg, 1.12 mmol) was dissolved in toluene (10 ml) and transferred into a 35 ml microwave vessel equipped with magnetic stirrer bar and then capped. The resulting solution

was microwave irradiated at a set temperature of 115°C and a set time of 10 minutes. After the resulting solution cooled down, the solvent was concentrated *in vacuo* to afford a dark brown oil which was separated by flash column chromatography (first elution with 100% ethyl acetate followed by 2% MeOH in ethyl acetate) to give pure ethyl 2-[5-(3,4-dimethoxyphenyl)-1*H*-imidazol-1-yl]acetate **120d** after drying under high vacuum, **Physical characteristics:** yellow solid; **Yield:** 167 mg, 60%.

8.4.4.3. Synthetic procedure

To a stirred solution of ethyl 2-(arylideneamino)acetate (1 molar equivalent), TosMIC (1 molar equivalent) in DCM (8 ml) was added dropwise a solution of DBU (1 molar equivalent) in DCM (2 ml) at room temperature. Upon completion of addition, the resulting mixture was stirred at the same temperature for 24 hours (monitored by TLC). After consumption of TosMIC, the solvent was concentrated *in vacuo* afforded brown oily crude material. The crude material was re-dissolved in toluene (10 ml) and transferred into a 35ml microwave vessel equipped with magnetic stirred bar and then capped. The resulting solution was microwave irradiated at a set temperature of 115°C and a set time of 10 minutes. After the solution cooled down, the solvent was concentrated *in vacuo* afforded dark brown oily crude material which was separated by flash column chromatography [first elution with (2:1) hexane: ethyl acetate followed by 1% MeOH in ethyl acetate] to give pure product after drying under high vacuum.

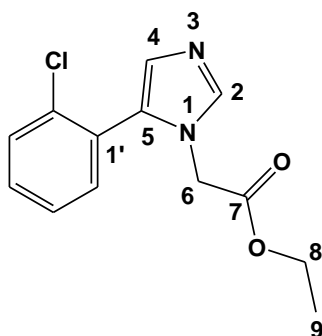
8.4.4.4. Ethyl 2-[5-(4-fluorophenyl)-1*H*-imidazol-1-yl]acetate **120a**



Ethyl 2-[5-(4-fluorophenyl)-1*H*-imidazol-1-yl]acetate **120a** was successfully synthesized from ethyl 2-(4-fluorobenzylideneamino)acetate **116a** (2.59 g, 12.4 mmol), TosMIC (2.42 mg, 12.4 mmol) and DBU (1.89 g, 12.4 mmol) as described by the general procedure; **Physical characteristics:** brown oil; **Yield:** 1.60 g, 52%; **¹H NMR** (400 MHz, CDCl₃) δ 7.51 (1H, s, 2-CH), 7.20-7.24 (2H, m, ArH), 7.02 (2H, t, *J* = 8.6 Hz, ArH), 6.98 (1H, s, 4-CH), 4.56 (2H, s, NCH₂), 4.08 (2H, q, *J* = 7.2 Hz, OCH₂CH₃), 1.13 (3H, t, *J* = 7.2 Hz, OCH₂CH₃); **¹³C NMR** (101 MHz, CDCl₃) δ 167.6 (C=O), 163.7 (d, ¹*J*_{C,F} = 249 Hz, *para*-CF), 138.9 (2-C), 132.4 (5-C), 130.8

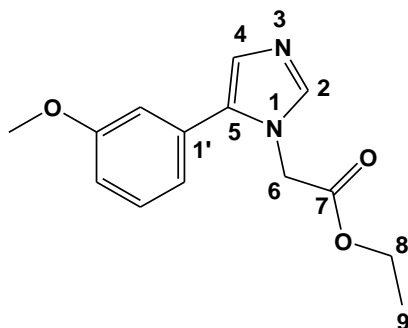
(d, $^3J_{\text{C,F}} = 8$ Hz, *ortho*-C), 127.9 (4-C), 125.1 (d, $^4J_{\text{C,F}} = 3$ Hz, 1'-C), 115.7 (d, $^2J_{\text{C,F}} = 22.1$ Hz, *meta*-C), 62.0 (8-C), 46.2 (6-C), 13.9 (9-C); **FTIR** $\nu_{\text{max}}/\text{cm}^{-1}$ (KBr): 3104, 3026, 1747, 1568, 1496, 1380, 1478, 1278, 1163, 854, 824, 698, 694, 543; **HRMS** (ESI-TOF) m/z : $[\text{M}+\text{H}]^+$ Calcd for $\text{C}_{13}\text{H}_{14}\text{FN}_2\text{O}_2$ 249.1034, found 249.1027.

8.4.4.5. Ethyl 2-(5-(2-chlorophenyl)-1*H*-imidazol-1-yl)acetate **120b**



Ethyl 2-(5-(2-chlorophenyl)-1*H*-imidazol-1-yl)acetate **120b** was successfully synthesized from ethyl 2-(2-chlorobenzylideneamino)acetate **116b** (824 mg, 3.65 mmol) TosMIC (713 mg, 3.65 mmol) and DBU (556 mg, 3.65 mmol) as described by the general procedure; **Physical characteristics**: brown oil; **Yield**: 237 g, 26%; **$^1\text{H NMR}$** (400 MHz, CDCl_3) δ 7.88 (1H, s, 2-CH), 7.38-7.50 (2H, m, ArH), 7.32-7.33 (2H, m, ArH), 7.10 (1H, s 4-CH), 4.62 (2H, s, NCH_2), 4.16 (2H, q, $J = 7.2$ Hz, OCH_2CH_3), 1.21 (3H, t, $J = 7.2$ Hz, OCH_2CH_3); **$^{13}\text{C NMR}$** (101 MHz, CDCl_3) δ 167.7 (C=O), 138.5 (2-C), 134.8, 133.2, 130.9, 130.4, 129.7 (ArC), 127.5 (4-C), 127.1 (ArC), 62.2 (8-C), 46.4 (6-C), 14.1 (9-C); **FTIR** $\nu_{\text{max}}/\text{cm}^{-1}$ (KBr): 2955, 2930, 1748, 1617, 1566, 1503, 1435, 1356, 1217, 1143, 1039, 759, 665, 513; **HRMS (ESI-TOF)** m/z : $[\text{M}+\text{H}]^+$ Calcd. for $\text{C}_{13}\text{H}_{14}\text{N}_2\text{O}_2\text{Cl}^+$ 265.0738; Found 265.0738.

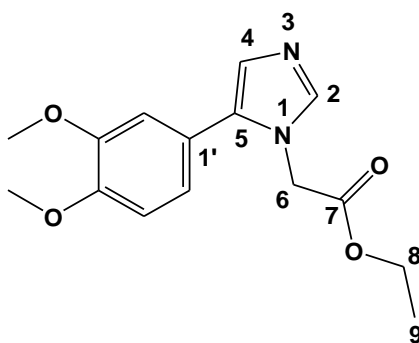
8.4.4.6. Ethyl 2-[5-(3-methoxyphenyl)-1*H*-imidazol-1-yl]acetate **120c**



Ethyl 2-[5-(3-methoxyphenyl)-1*H*-imidazol-1-yl]acetate **120c** was successfully synthesized from ethyl 2-(3-methoxybenzylideneamino)acetate **116c** (1.05 g, 4.76 mmol) TosMIC (929 mg, 4.76 mmol) and DBU (725 mg, 4.76 mmol) as described by the general procedure; **Physical**

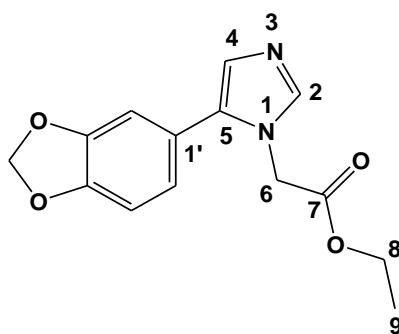
characteristics: brownish yellow oil; **Yield:** 471 mg, 38%; **¹H NMR** (400 MHz, CDCl₃) δ 7.57 (1H, s, 2-CH), 7.29-7.33 (1H, m, ArH), 7.08 (1H, s, 4-CH), 6.84-6.92 (3H, m, ArH), 4.66 (2H, s, NCH₂), 4.15 (2H, q, *J* = 7.2 Hz, OCH₂CH₃), 3.79 (3H, s, ArOCH₃), 1.19 (3H, t, *J* = 7.2 Hz, OCH₂CH₃); **¹³C NMR** (101 MHz, CDCl₃) δ 167.7 (C=O), 159.8 (ArCOCH₃), 139.0 (2-C), 133.2 (5-C), 130.3, 129.8, 127.8 (ArC), 121.01 (4-C), 114.3, 113.9 (ArC), 62.0 (8-C), 46.4 (6-C), 13.9 (9-C); **FTIR** $\nu_{\max}/\text{cm}^{-1}$ (KBr): 3126, 2887, 1745, 1604, 1591, 1536, 1453, 1425, 1379, 1326, 1292, 1225, 1027, 928, 800, 699, 516; **HRMS (ESI-TOF)** *m/z*: [M+H]⁺ Calcd for C₁₄H₁₇N₂O₃ 261.1234, found 261.1232.

8.4.4.7. Ethyl 2-[5-(3,4-dimethoxyphenyl)-1*H*-imidazol-1-yl]acetate **120d**



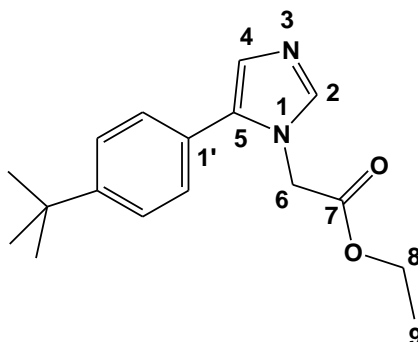
Ethyl 2-[5-(3,4-dimethoxyphenyl)-1*H*-imidazol-1-yl]acetate **120d** was successfully synthesized from ethyl 2-(2,4-dimethoxybenzylideneamino)acetate **116d** (837 mg, 3.33 mmol) TosMIC (650 mg, 3.33 mmol) and DBU (507 mg, 3.33 mmol) as described by the general procedure; **Physical characteristics:** yellow solid; **Yield:** 715 mg, 74%; **Melting point:** 67-70°C; **¹H NMR** (400MHz, CDCl₃) δ 7.56 (1H, s, 2-CH), 7.01 (1H, s, 4-CH), 6.81-6.88 (3H, m, ArH), 4.61 (2H, s, NCH₂), 4.13 (2H, q, *J* = 7.2 Hz, OCH₂CH₃) 3.83 and 3.87 (6H, 2 x s, 2 x ArOCH₃), 1.18 (3H, t, *J* = 7.2 Hz, OCH₂CH₃); **¹³C NMR** (101 MHz, CDCl₃) δ 167.8 (C=O), 149.2 and 148.9 (2 x ArCOCH₃), 138.5 (2-C), 133.3 (5-C), 127.3, 121.6, (ArC), 121.5 (4-C), 112.3, 111.2 (ArC), 61.9 (8-C), 55.81 and 55.78 (2 x ArCOCH₃), 46.3 (6-C), 13.9 (9-C); **FTIR** $\nu_{\max}/\text{cm}^{-1}$ (KBr): 2955, 2930, 1748, 1617, 1566, 1503, 1435, 1356, 1217, 1143, 1039, 759, 665, 513; **HRMS (ESI-TOF)** *m/z*: [M+H]⁺ Calcd for C₁₅H₂₁N₂O₄ 291.1339, found 291.1332

8.4.4.8. Ethyl 2-(5-(benzo[*d*][1,3]dioxol-6-yl)-1*H*-imidazol-1-yl)acetate **120e**



Ethyl 2-(5-(benzo[*d*][1,3]dioxol-6-yl)-1*H*-imidazol-1-yl)acetate **120e** was successfully synthesized from ethyl 2-((benzo[*d*][1,3]dioxol-6-yl)methyleneamino)acetate **116e** (838 mg, 3.56 mmol), TosMIC (695 mg, 3.56 mmol) and DBU (542 mg, 3.56 mmol) as described by the general synthetic procedure C; **Physical characteristics**: pale yellow solid; **Yield**: 439 mg, 45%; **Melting point**: 83-86°C; **¹H NMR** (400MHz, CDCl₃) δ 7.52 (1H, s, 2-CH), 6.97 (1H, s, 4-CH), 6.79 (1H, d, *J* = 7.4 Hz, ArH), 6.71-6.72 (2H, overlapping singlet and doublet, ArH), 5.95 (2H, s, ArOCH₂O), 4.60 (2H, s, NCH₂), 4.13 (3H, q, *J* = 7.2 Hz, OCH₂CH₃), 1.18 (3H, t, *J* = 7.2 Hz, OCH₂CH₃); **¹³C NMR** (101 MHz, CDCl₃) δ 167.7 (C=O), 147.8 and 148.7 (2 x ArCOCH₂O), 138.6 (2-C), 133.0 (5-C), 127.4, (ArC), 122.8 (4-C), 122.5, 109.4, 108.5 (ArC), 101.2 (ArCOCH₂O), 61.9 (8-C), 46.2 (6-C), 13.9 (9-C); **FTIR** ν_{\max} /cm⁻¹ (KBr): 3097, 2986, 2908, 2782, 1741, 1504, 1479, 1336, 1243, 1213, 1104, 1041, 921, 887, 813; **HRMS** (ESI-TOF) *m/z*: [M+H]⁺ Calcd for C₁₃H₁₃N₂O₄ 261.1183, found 261.1186.

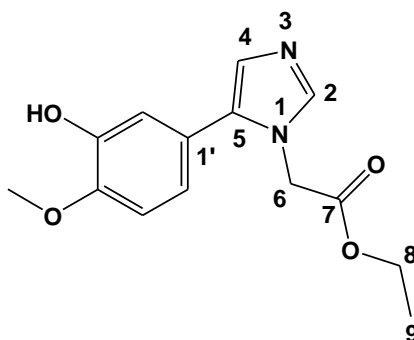
8.4.4.9. Ethyl 2-(5-(4-*tert*-butylphenyl)-1*H*-imidazol-1-yl)acetate **120f**



Ethyl 2-(5-(4-*tert*-butylphenyl)-1*H*-imidazol-1-yl)acetate **120f** was successfully synthesized from ethyl 2-(4-*tert*-butylbenzylideneamino)acetate **116f** (1.06 g, 4.30 mmol) TosMIC (839 mg, 4.30 mmol) and DBU (656 mg, 4.30 mmol) as described by the general procedure C; **Physical characteristics**: brown oil; **Yield**: 431 mg, 35%; **¹H NMR** (400 MHz, CDCl₃) δ 7.64 (1H, s, 2-CH), 7.45 (2H, d, *J* = 8.4 Hz, ArH), 7.28 (2H, d, *J* = 8.4 Hz, ArH), 7.10 (1H, s, 4-CH), 4.70 (2H, s, NCH₂), 4.19 (2H, q, *J* = 7.2 Hz, OCH₂CH₃), 1.37 [9H, s, C(CH₃)₃], 1.21 (3H, t, *J* = 7.2 Hz,

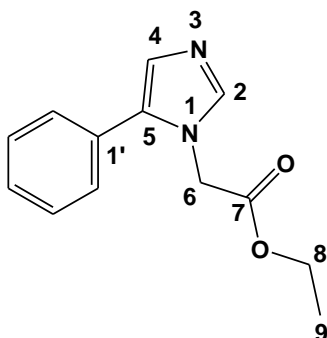
OCH₂CH₃); ¹³C NMR (101 MHz, CDCl₃) δ 167.8 (C=O), 151.5 [ArCC(CH₃)₃], 138.8 (2-C), 133.4, 128.6, 127.5, 126.1, 125.7 (ArC), 62.0 (8-C), 46.4 (6-C), 34.6 [ArCC(CH₃)₃], 31.2 [ArCC(CH₃)₃], 14.0 (9-C); FTIR ν_{max}/cm⁻¹ (KBr): 2966, 2904, 2870, 1755, 1480, 1363, 1265, 1219, 1113, 1011, 913, 840, 656, 565; HRMS (ESI-TOF) m/z: [M+H]⁺ Calcd for C₁₇H₂₃N₂O₂ 287.1754, found 287.1764.

8.4.4.10. Ethyl 2-(5-(3-hydroxy-4-methoxyphenyl)-1*H*-imidazol-1-yl)acetate 120g



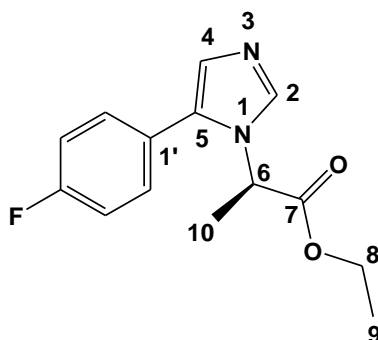
Ethyl 2-(5-(3-hydroxy-4-methoxyphenyl)-1*H*-imidazol-1-yl)acetate **120g** was successfully synthesized from ethyl 2-(3-hydrozyl-4-methoxybenzylideneamino)acetate **116g** (1.26 g, 5.32 mmol), TosMIC (1.04 g, 5.32 mmol) and DBU (810 mg, 5.32 mmol) as described by the general procedure; **Physical characteristics:** yellow solid; **Yield:** 750 mg, 51%; **Melting point:** 137-140°C; ¹H NMR (400 MHz, CDCl₃) δ 7.76 (1H, s, 2-CH), 7.06 (1H, s, 4-CH), 6.95-6.97 (1H, d, *J* = 8.4 Hz, ArH), 6.76-6.81 (2H, m, ArH), 5.24 (1H, brs, ArOH), 4.67 (2H, s, NCH₂), 4.16 (2H, q, *J* = 7.2 Hz, OCH₂CH₃), 3.87 (3H, s, ArOCH₃), 1.21 (3H, t, *J* = 7.2 Hz, OCH₂CH₃); ¹³C NMR (101 MHz, CDCl₃) δ 167.8 (C=O), 147.0 and 146.7 (ArCOCH₃ and ArCOH), 138.2 (2-C), 133.8 (5-C), 126.0, 122.5 (ArC), 120.1 (4-C), 115.0, 112.2 (ArC), 62.2 (8-C), 56.0 (ArCOCH₃), 46.5 (6-C), 14.1 (9-C); FTIR ν_{max}/cm⁻¹ (KBr): 2974, 2929, 2608, 1748, 1596, 1552, 1501, 1494, 1474, 1334, 1213, 1112, 1026, 956, 813, 616; HRMS (ESI-TOF) m/z: [M+H]⁺ Calcd for C₁₄H₁₇N₂O₄ 277.1183, found 277.1184.

8.4.4.11. Ethyl 2-[(5-phenyl)-1*H*-imidazol-1-yl]acetate 120h



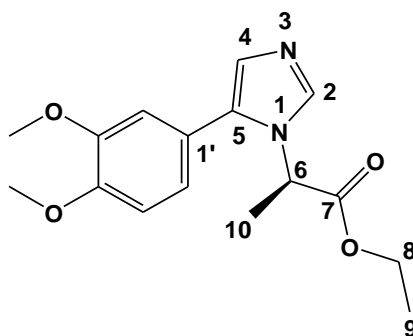
Ethyl 2-[(5-phenyl)-1*H*-imidazol-1-yl]acetate **120h** was successfully synthesized from ethyl 2-(benzylideneamino)acetate **116h** (996 mg, 5.21 mmol) TosMIC (1.02 g, 5.21 mmol) and DBU (793 mg, 5.21 mmol) as described by the general procedure C; **Physical characteristics**: pale yellow solid; **Yield**: 396 mg, 33%; **Melting point**: 144-147°C; **¹H NMR** (400MHz; CDCl₃) δ 7.58 (1H, s, 2-CH), 7.29-7.41 (5H, m, ArH), 7.08 (1H, s, 4-CH), 4.66 (2H, s, NCH₂), 4.14 (2H, q, *J* = 7.2 Hz, OCH₂CH₃), 1.18 (3H, t, *J* = 7.2 Hz, OCH₂CH₃); **¹³C NMR** (101 MHz, CDCl₃) δ 167.7 (C=O), 139.0 (2-C), 133.4 (5-C), 129.1, 128.9, 128.8, 128.3 (ArC), 127.8 (4-C), 62.0 (8-C), 46.4 (6-C), 13.9 (9-C); **FTIR** $\nu_{\max}/\text{cm}^{-1}$ (KBr): 3122, 2936, 2954, 1736, 1602, 1484, 1444, 1376, 1321, 1216, 1160, 1118, 1080, 978, 852, 824, 768, 700, 660; **HRMS** (ESI-TOF) *m/z*: [M+H]⁺ Calcd for C₁₃H₁₅N₂O₂ 231.1128, found 231.1126.

8.4.4.12. (*R*)-Ethyl 2-(5-(4-fluorophenyl)-1*H*-imidazol-1-yl)propanoate **121a**



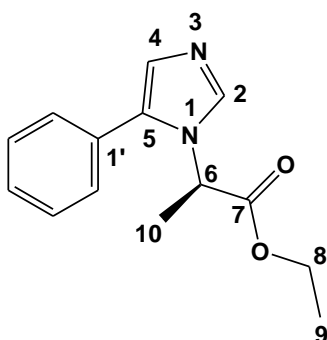
(*R*)-Ethyl 2-(5-(4-fluorophenyl)-1*H*-imidazol-1-yl)propanoate **121a** was successfully synthesized from (*R, E*)-ethyl 2-(4-fluorobenzylideneamino)propanoate **117a** (299 mg, 1.34 mmol), TosMIC (262 mg, 1.34 mmol) and DBU (204 mg, 1.34 mmol) as described by the general synthetic procedure C; **Physical characteristics**: pale yellow oil; **Yield**: 39 mg, 11%; **¹H NMR** (400 MHz, CDCl₃) δ 7.52 (1H, s, 2-CH), 7.20-7.24 (2H, m, ArH), 7.02 (2H, t, *J* = 8.8 Hz, ArH), 6.97 (1H, s, 4-CH), 4.56 (2H, s, NCH₂), 4.81 (1H, q, *J* = 7.2 Hz, CHCH₃), 4.17-4.25 (2H, q, *J* = 7 Hz, OCH₂CH₃), 1.65-1.72 (3H, d, *J* = 8 Hz, CHCH₃), 1.14 (3H, t, *J* = 7.2 Hz, OCH₂CH₃); **¹³C NMR** (101 MHz, CDCl₃) δ 167.3 (C=O), 163.2 (d, ¹*J*_{C,F} = 249 Hz, *para*-CF), 138.97 (2-C), 132.4 (5-C), 130.8 (d, ³*J*_{C,F} = 8 Hz, *ortho*-C), 127.9 (4-C), 125.1 (d, ⁴*J*_{C,F} = 3.0 Hz, 1'-C), 115.7 (d, ²*J*_{C,F} = 22 Hz, *meta*-C), 62.0 (8-C), 50.6 (6-C), 18.6 (10-C), 13.9 (9-C).; **FTIR** $\nu_{\max}/\text{cm}^{-1}$ (KBr): 2955, 2930, 1748, 1617, 1566, 1503, 1435, 1356, 1217, 1143, 1039, 759, 665, 513; **HRMS** (ESI-TOF) *m/z*: [M+H]⁺ Calcd for C₁₄H₁₆FN₂O₂ 263.1173, found 263.1190.

8.4.4.13. (*R*)-Ethyl 2-(5-(3,4-dimethoxyphenyl)-1*H*-imidazol-1-yl)propanoate **121b**



(*R*)-Ethyl 2-(5-(3,4-dimethoxyphenyl)-1*H*-imidazol-1-yl)propanoate **121b** was successfully synthesized from (*R, E*)-ethyl 2-(2,4-dimethoxybenzylideneamino)propanoate **117c** (483 mg, 1.82 mmol), TosMIC (355 mg, 1.82 mmol) and DBU (277 mg, 1.82 mmol) as described by the general synthetic procedure C; **Physical characteristics**: yellow solid; **Yield**: 127 mg, 23%; **¹H NMR** (400 MHz, CDCl₃) δ 7.69 (1H, s, 2-CH), 6.96 (1H, s, 4-CH), 6.78-6.88 (3H, m, ArH), 4.78 (1H, q, *J* = 8.4 Hz, CHCH₃), 4.10 (2H, q, *J* = 7.2 Hz, 2 x OCH₂CH₃), 3.82 and 3.86 (6H, 2 x s, ArOCH₃), 1.66 (3H, d, *J* = 7.2 Hz, CHCH₃), 1.16-1.20 (3H, t, *J* = 7.2 Hz, OCH₂CH₃); **¹³C NMR** (101 MHz, CDCl₃) δ 167.4 (C=O), 149.15 and 148.9 (2 x ArCOCH₃), 135.7 (2-C), 130.7 (5-C), 127.5, 127.7, 127.6, 112.6, 111.2 (ArC), 61.8 (8-C), 55.7 (6-C), 55.7 and 55.8 (2 x ArCOCH₃), 18.8 (10-C), 13.9 (9-C); **FTIR** ν_{\max} /cm⁻¹ (KBr): 3635, 2954, 2896, 2783, 1750, 1668, 1479, 1440, 1378, 1306, 1225, 1108, 1038, 933, 880, 815, 726, 668, 579; **HRMS** (ESI-TOF) *m/z*: [M+H]⁺ Calcd for C₁₆H₂₁N₂O₄ 305.1476, found 305.1503.

8.4.4.14. (*R*)-Ethyl 2-(5-phenyl-1*H*-imidazol-1-yl)propanoate **121d**



(*R*)-Ethyl 2-(5-(phenyl)-1*H*-imidazol-1-yl)propanoate **121d** was successfully synthesized from (*R, E*)-ethyl 2-(benzylideneamino)propanoate **117h** (372 mg, 1.81 mmol) TosMIC (353 mg, 1.81 mmol) and DBU (276 mg, 1.81 mmol) as described by the general synthetic procedure C; **Physical characteristics**: yellow solid; **Yield**: 88 mg, 20%; **¹H NMR** (400 MHz, CDCl₃) δ 7.76 (1H, s, 2-CH), 7.37-7.41 (3H, m, ArH), 7.27-7.29 (2H, m, ArH), 7.03 (1H, s, 4-CH), 4.80 (1H, q, *J* = 8.4 Hz, CHCH₃), 4.12 (2H, q, *J* = 7.2 Hz, OCH₂CH₃), 1.70 (3H, d, *J* = 7.2 Hz, CHCH₃), 1.17

(3H, t, $J = 7.2$ Hz, OCH_2CH_3); ^{13}C NMR (101 MHz, CDCl_3) δ 170.3 (C=O), 136.0 (2-C), 133.1 (5-C), 129.3, 129.2, 128.7, 128.3, 127.2 (ArC), 61.9 (8-C), 52.9 (6-C), 18.8 (10-C), 13.9 (9-C); HRMS (ESI-TOF) m/z : $[\text{M}+\text{H}]^+$ Calcd for $\text{C}_{14}\text{H}_{17}\text{N}_2\text{O}_2$ 245.1258; found 245.1279.

8.4.5. Synthesis of 2-(5-aryl)-1H-imidazol-1-yl)acetic acid derivatives

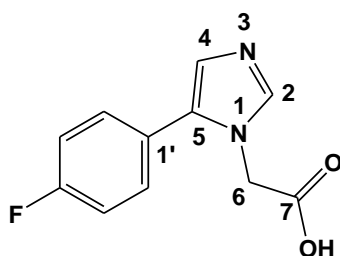
8.4.5.1 Synthetic procedure A

NaOH (3 molar equivalents) was added to a solution of ethyl 2-(5-aryl-1H-imidazol-1-yl)acetate (1 molar equivalent) in 15 ml of 1:1 MeOH: H_2O , and the solution was refluxed until disappearance of the starting material (observed by TLC). Volatile methanol was removed *in vacuo* and the remaining aqueous crude material was slowly neutralized with 1M HCl. Unfortunately, attempts to extract with ethyl acetate the product with ethyl acetate were unsuccessful.

8.4.5.2. Synthetic procedure B

In a 10 ml microwave vessels equipped with a magnetic stirrer bar, was added ethyl 2-(5-aryl-1H-imidazol-1-yl)acetate **120** (1 molar equivalent) and water (5 ml). The cap was placed and the resulting mixture was microwave irradiated at a set power of 200 Watts and a temperature of 105°C for 3 hours. After completion of the reaction, mixture was transferred into separating funnel, water (5 ml) was added, followed by the wash with ethyl acetate (3 x 10 ml). The water layer was evaporated *in vacuo* and dried under high vacuum to afford the desired pure 2-(5-aryl)-1H-imidazol-1-yl)acetic acids.

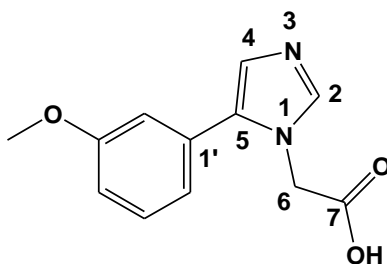
8.4.5.3. 2-[5-(4-Fluorophenyl)-1H-imidazol-1-yl]acetic acid **123a**



2-[5-(4-Fluorophenyl)-1H-imidazol-1-yl]acetic acid **123a** was successfully synthesized by microwave irradiation of ethyl 2-[5-(4-fluorophenyl)-1H-imidazol-1-yl]acetate **120a** (186 mg, 0.75 mmol) in water according to the general procedure B; **Physical characteristics:** pale yellow solid; **Yield:** 119 mg, 72%; **Melting point:** 189-192°C; ^1H NMR (400 MHz, $\text{DMSO}-d_6$) δ 7.89 (1H, s, 2-CH), 7.45-7.49 (2H, m, ArH), 7.31-7.35 (2H, m, ArH), 7.11 (1H, s, 4-CH), 6.61 (1H, broad s, OH), 4.88 (2H, s, NCH_2); ^{13}C NMR (101 MHz, $\text{DMSO}-d_6$) δ 170.7 (C=O), 162.3 (d, $J_{\text{C,F}}$

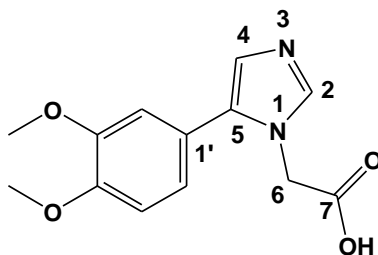
= 246 Hz, *para*-CF), 140.8 (2-C), 132.8 (5-C), 131.3 (d, $^3J_{C,F}$ = 8 Hz, *ortho*-C), 127.6 (4-C), 126.8 (d, $^4J_{C,F}$ = 3 Hz, 1'-C), 116.8 (d, $^2J_{C,F}$ = 22 Hz, *meta*-C), 47.4 (6-C); **FTIR** $\nu_{\max}/\text{cm}^{-1}$ (KBr): 3105, 3032, 2434, 1645, 1540, 1496, 1380, 1290, 1226, 1165, 1110, 544, 823, 767, 697, 693, 544; **HRMS** (ESI-TOF) m/z : $[M+H]^+$ Calcd for $C_{11}H_{10}FN_2O_2$ 221.0721, found 221.0720.

8.4.5.4. 2-[5-(3-Methoxyphenyl)-1*H*-imidazol-1-yl]acetic acid **123c**



2-[5-(3-Methoxyphenyl)-1*H*-imidazol-1-yl]acetic acid **123c** was successfully synthesized by microwave irradiation of ethyl 2-[5-(3-methoxyphenyl)-1*H*-imidazol-1-yl]acetate **120c** (250 mg, 0.96 mmol) in water according to the general procedure B; **Physical characteristics**: yellow solid; **Yield**: 125 mg, 56%; **$^1\text{H NMR}$** (400 MHz, $\text{DMSO-}d_6$) δ 7.87 (1H, s, 2-CH), 7.37-7.41 (1H, m, ArH), 7.13 (1H, s, 4-CH), 6.97-7.00 (3H, m, ArH), 6.51 (1H, brs, OH), 4.85 (2H, s, NCH_2), 3.80 (3H, s, ArOCH_3); **$^{13}\text{C NMR}$** (101 MHz, $\text{DMSO-}d_6$) δ 171.0 (C=O), 160.4 (ArCOCH_3), 140.9 (2-C), 133.6 (5-C), 130.9, 131.6, 127.6 (ArC), 121.2 (4-C), 114.6, 114.3 (ArC), 56.1 (ArCOCH_3), 47.9 (6-C); **FTIR** $\nu_{\max}/\text{cm}^{-1}$ (KBr): 3126, 2946, 2450, 1696, 1609, 1578, 1487, 1394, 1300, 1207, 1168, 1028, 854, 777, 693; **HRMS** (ESI-TOF) m/z : $[M+H]^+$ Calcd for $C_{12}H_{13}N_2O_3$ 233.0921, found 233.0922.

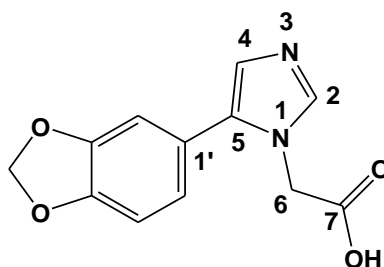
8.4.5.5. 2-[5-(3,4-Dimethoxyphenyl)-1*H*-imidazol-1-yl]acetic acid **123d**



2-[5-(3,4-Dimethoxyphenyl)-1*H*-imidazol-1-yl]acetic acid **123d** was successfully synthesized by microwave irradiation of ethyl 2-[5-(3,4-dimethoxyphenyl)-1*H*-imidazol-1-yl]acetate **120d** (139 mg, 0.48 mmol) in water according to the general procedure B; **Physical characteristics**: yellow solid; **Yield**: 89 mg, 71%; **Melting point**: 124-127°C; **$^1\text{H NMR}$** (400 MHz, $\text{DMSO-}d_6$) δ 7.82 (1H, s, 2-CH), 7.06 (1H, s, ArH), 6.92-7.04 (3H, m, ArH), 6.01 (1H, brs, OH), 4.78 (2H, s, NCH_2), 3.79 and 3.81 (6H, 2 x s, 2 x ArOCH_3); **$^{13}\text{C NMR}$** (101 MHz, $\text{DMSO-}d_6$) δ 171.2 (C=O),

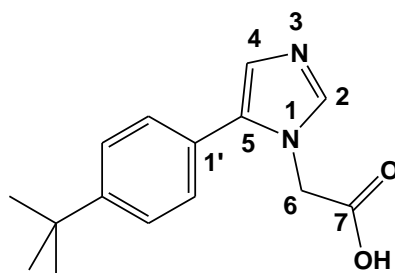
149.6 and 149.6 (2 x ArCOCH₃), 140.3 (2-C), 133.8 (5-C), 126.8, 122.8 (ArC), 121.6 (4-C), 112.9, 111.8 (ArC), 56.4 and 56.5 (2 x ArCOCH₃), 47.8 (6-C); **FTIR** $\nu_{\max}/\text{cm}^{-1}$ (KBr): 3126, 3050, 2970, 2841, 2604, 1612, 1512, 1471, 1447, 1380, 1324, 1256, 1224, 1181, 1146, 1021, 826, 806, 695, 676; **HRMS** (ESI-TOF) m/z : [M+H]⁺ Calcd for C₁₃H₁₅N₂O₄ 263.1040, Found 263.1017.

8.4.5.6. 2-(5-(Benzo[d][1,3]dioxol-6-yl)-1*H*-imidazol-1-yl)acetic acid **123e**



2-(5-(Benzo[d][1,3]dioxol-6-yl)-1*H*-imidazol-1-yl)acetic **123e** was successfully synthesized by microwave irradiation of ethyl 2-(5-(benzo[d][1,3]dioxol-6-yl)-1*H*-imidazol-1-yl)acetate **120e** (304 mg, 1.11 mmol) in water according to the general procedure B; **Physical characteristics**: yellow solid; **Yield**: 186 mg, 68% ; **Melting point**: 233-236°C; **¹H NMR** (400 MHz, DMSO-*d*₆) δ 7.82(1H, s, 2-CH), 7.00 (1H, d, $J = 8.0$ Hz, ArH), 6.97 (1H, s, 4-CH), 6.85 (2H, d, $J = 8.0$ Hz, ArH), 6.09 (2H, s, ArOCH₂O), 4.81 (2H, s, NCH₂); **¹³C NMR** (101 MHz, DMSO-*d*₆) δ 170 (C=O), 148.5 and 148.1 (ArCOCH₂O), 140.4 (2-C), 133.5 (5-C), 127.1, 124.0, 123.0, 109.6 (ArC), 102 (ArCOCH₂O), 47.6 (6-C); **FTIR** $\nu_{\max}/\text{cm}^{-1}$ (KBr): 3435, 3152, 3096, 2500, 1652, 1604, 1504, 1474, 1388, 1313, 1257, 1226, 1035, 882, 691; **HRMS** (ESI-TOF) m/z : [M+H]⁺ Calcd for C₁₂H₁₁N₂O₄ 247.0713, found 247.0702.

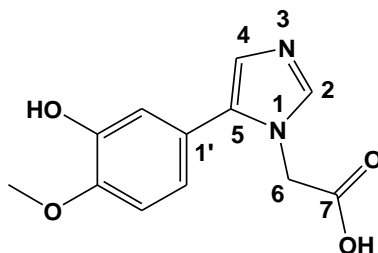
8.4.5.7. 2-(5-(4-*tert*-Butylphenyl)-1*H*-imidazol-1-yl)acetic acid **123f**



2-(5-(4-*tert*-Butylphenyl)-1*H*-imidazol-1-yl)acetic acid **123f** was successfully synthesized by microwave irradiation of ethyl 2-(5-(4-*tert*-butylphenyl)-1*H*-imidazol-1-yl)acetate (189 mg, 0.66 mmol) in water according to the general procedure B; **Physical characteristics**: yellow solid; **Yield**: 96 mg, 56% ; **Melting point**: 170-173°C; **¹H NMR** (400 MHz, DMSO-*d*₆) δ 7.84 (1H, s, 2-CH), 7.47 (2H, d, $J = 7.6$ Hz, ArH), 7.32 (2H, d, $J = 7.6$ Hz, ArH), 7.06 (1H, s, 4-CH), 4.70 (2H, s, NCH₂), 1.37 [9H, s, C(CH₃)₃]; **¹³C NMR** (101 MHz, DMSO-*d*₆) δ 167.8 (C=O), 151.5

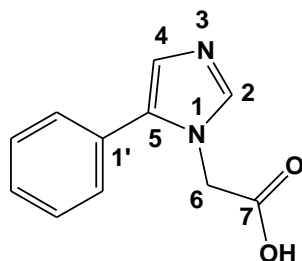
[ArCC(CH₃)₃], 138.8 (2-C), 133.4, 128.6, 127.5, 126.1, 125.7 (ArC), 46.4 (6-C), 34.6 [ArCC(CH₃)₃], 31.2 [ArCC(CH₃)₃]; **FTIR** $\nu_{\max}/\text{cm}^{-1}$ (KBr): 3132, 3035, 2961, 2905, 2868, 2509, 1722, 1678, 1625, 1463, 1378, 1335, 1269, 1233, 1112, 1035, 1010, 841, 677; **HRMS** (ESI-TOF) m/z : [M+H]⁺ Calcd for C₁₅H₁₉N₂O₂⁺ 259.1441, Found 259.1440.

8.4.5.8. 2-(5-(3-Hydroxy-4-methoxyphenyl)-1*H*-imidazol-1-yl)acetic acid **123g**



2-(5-(3-Hydroxy-4-methoxyphenyl)-1*H*-imidazol-1-yl)acetic acid **123g** was successfully synthesized from microwave irradiation of ethyl 2-(5-(3-hydroxy-4-methoxyphenyl)-1*H*-imidazol-1-yl)acetate **120g** (251 mg, 0.91 mmol) in water according to the general procedure B; **Physical characteristics**: yellow solid; **Yield**: 131 mg, 58%; **Melting point**: 211-214°C; **¹H NMR** (400 MHz, DMSO-*d*₆) δ 7.80 (1H, s, 2-CH), 6.97 (1H, s, 4-CH), 6.83 (1H, d, $J = 8.0$ Hz, ArH), 6.75 (2H, d, $J = 8.0$, ArH), 5.24 (1H, br, ArOH), 4.69 (2H, s, NCH₂), 3.75 (3H, s, ArOCH₃); **¹³C NMR** (101 MHz, DMSO-*d*₆) δ 170.3 (C=O), 147.6 and 146.7 (ArCOCH₃ and ArCOH), 139.0 (2-C), 133.2 (5-C), 125.1(ArC), 121.2 (4-C), 120.2, 115.8, 112.4 (ArC), 55.6 (ArCOCH₃), 47.1 (6-C); **FTIR** $\nu_{\max}/\text{cm}^{-1}$ (KBr): 2973, 2930, 2600, 1748, 1604, 1552, 1514, 1358, 1312, 1280, 1214, 1139, 1109, 1026, 865, 822; **HRMS** (ESI-TOF) m/z : [M+H]⁺ Calcd for C₁₂H₁₃N₂O₄ 249.2421, found 249.2438.

8.4.5.9. 2-(5-Phenyl-1*H*-imidazol-1-yl)acetic acid **123h**



2-(5-Phenyl)-1*H*-imidazol-1-yl)acetic acid **123h** was successfully synthesized by microwave irradiation of ethyl 2-[5-phenyl-1*H*-imidazol-1-yl]acetate **120h** (200 mg, 0.87 mmol) in water according to the general procedure B; **Physical characteristics**: pale yellow solid; **Yield**: 120 mg, 68%; **Melting point**: 175-178°C; **¹H NMR** (400 MHz, CDCl₃) δ 10.0 (1H, s, OH), 8.54 (1H, s, 2-CH), 7.2 (5H, m, ArH), 7.01 (1H, s, 4-CH), 4.55 (2H, s, NCH₂); **¹³C NMR** (101 MHz,

CDCl₃) δ 170.9 (C=O), 137.5 (2-C), 134.3 (5-C), 129.4, 129.2, 129.2 (ArC), 128.9 (C-4), 118.9 (ArC), 49.2 (6-C); **FTIR** $\nu_{\text{max}}/\text{cm}^{-1}$ (KBr): 3139, 2957, 2900, 2861, 2517, 1730, 1691, 1626, 1378, 1270, 1113, 766, 687; **HRMS** (ESI-TOF) m/z : [M+H]⁺ Calcd for C₁₁H₁₁N₂O₂ 203.0815; found 203.0807.

8.4.6. Synthesis of 2-(5-aryl-1*H*-imidazol-1-yl)acetohydrazide

8.4.6.1. General synthetic procedure A

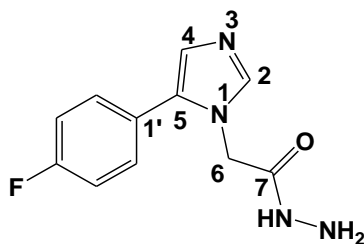
A mixture of ethyl 5-aryl-1*H*-imidazol-1-yl acylate (1 molar equivalent) and hydrazine monohydrate (3 molar equivalents), 64% in water) in MeOH (5 ml) was stirred for 24 hours at room temperature. Upon completion of reaction, the solvent was removed and DCM was added to generate a precipitate which was then filtered and dried to afford 2-(5-aryl-1*H*-imidazol-1-yl)acetohydrazides.

8.4.6.2. General synthetic procedure B

Ethyl 5-aryl-1*H*-imidazol-1-yl acylate (1 equivalent) and hydrazine monohydrate (3 equivalents) and MeOH (4 ml) were placed in a 10 ml microwave vessel equipped with a magnetic stirrer bar. The capped was then fitted and the resulting mixture was microwave irradiated at a set temperature of 75°C for 30 minutes. After completion of the reaction, the solvent was removed and DCM was added to generate precipitate which was then filtered and dried to afford 2-(5-aryl-1*H*-imidazol-1-yl)acetohydrazides.

(**NB:** ¹H and ¹³C NMR spectra reported below are for major rotamer only)

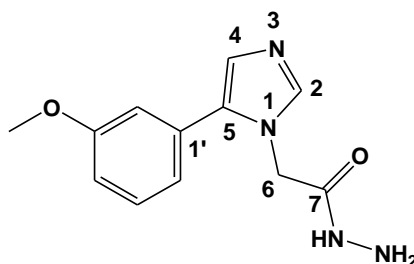
8.4.6.3. 2-[5-(4-Fluorophenyl)-1*H*-imidazol-1-yl]acetohydrazide **125a**



2-[5-(4-Fluorophenyl)-1*H*-imidazol-1-yl]acetohydrazide **125a** was successfully synthesized according to the general procedure A {ethyl 2-[5-(4-fluorophenyl)-1*H*-imidazol-1-yl]acetate **120a** (223 mg, 0.90 mmol) and hydrazine monohydrate (135 mg, 2.70 mmol)} and procedure B {ethyl 2-[5-(4-fluorophenyl)-1*H*-imidazol-1-yl]acetate **120a** (186 mg, 0.75 mmol) and hydrazine monohydrate (113 mg, 2.25 mmol)}; **Physical characteristics:** white solid; **Yields:** 181 mg, 86%

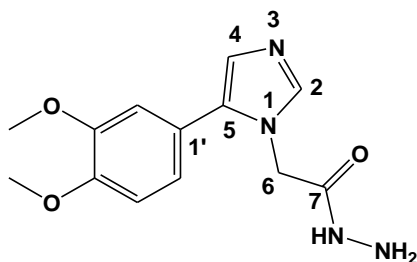
for procedure A and 162 mg, 92%; **Melting point:** 178-180°C; **¹H NMR** (400 MHz, DMSO-*d*₆) δ 9.35 (1H, s, NHNH₂), 7.23 (1H, s, 2-CH), 7.29-7.49 (4H, m, ArH), 7.03 (1H, s, 4-CH), 4.63 (2H, s, NCH₂), 3.40 (2H, s, NHNH₂); **¹³C NMR** (101 MHz, DMSO-*d*₆) δ 167.4 (C=O), 162.7 (d, ¹J_{C,F} = 243 Hz, *para*-CF), 140.9 (2-C), 132.7 (5-C), 131.4 (d, ³J_{C,F} = 8 Hz, *ortho*-C), 128.2 (4-C), 127.0 (d, ⁴J_{C,F} = 3 Hz, 1'-C), 116.6 (d, ²J_{C,F} = 22 Hz, *meta*-C), 46.78 (6-C); **FTIR** ν_{\max} /cm⁻¹ (KBr): 3104, 3026, 2417, 1747, 1495, 1380, 1223, 1163, 1110, 928, 824, 698, 674, 544, **HRMS** (ESI-TOF) *m/z*: [M+H]⁺ Calcd for C₁₁H₁₂FN₄O 235.0990, found 235.0995.

8.4.6.4. 2-[5-(3-Methoxyphenyl)-1*H*-imidazol-1-yl]acetohydrazide **125c**



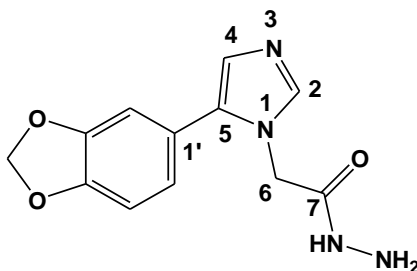
2-[5-(3-Methoxyphenyl)-1*H*-imidazol-1-yl]acetohydrazide **125c** was successfully synthesized according to the general procedure A {ethyl 2-[5-(3-methoxyphenyl)-1*H*-imidazol-1-yl]acetate **120c** (172 mg, 0.66 mmol) and hydrazine monohydrate (99 mg, 1.98 mmol)} and procedure B {ethyl 2-[5-(3-methoxyphenyl)-1*H*-imidazol-1-yl]acetate **120c** (122 mg, 0.47 mmol) and hydrazine hydrate (71 mg, 1.41 mmol)}; **Physical characteristics:** white solid; **Yields:** 117 mg, 72% for procedure A and 100 mg, 86%; **Melting point:** 152-154°C; **¹H NMR** (400 MHz, DMSO-*d*₆) δ 9.39 (1H, s, NHNH₂), 7.23 (1H, s, 2-CH), 7.36-7.40 (1H, m, ArH), 7.06 (1H, s, 4-CH), 6.95-7.00 (3H, m, ArH), 4.67 (2H, s, NCH₂), 4.35 (2H, s, NHNH₂) 3.81 (3H, s, ArOCH₃); **¹³C NMR** (101 MHz, DMSO-*d*₆) δ 167.5 (C=O), 160.3 (ArCOCH₃), 141.1 (2-C), 133.6 (5-C), 131.7, 130.9 (ArC), 128.2 (4-C), 121.3, 114.6, 114.2 (ArC), 56.1 (ArCOCH₃), 46.8 (6-C); **FTIR** ν_{\max} /cm⁻¹ (KBr): 3320, 3198, 3012, 2954, 1677, 1606, 1589, 1563, 1493, 1482, 1473, 1425, 1319, 1293, 1250, 1218, 1118, 1113, 1030, 1008, 866, 849, 818, 797, 722, 700, 650, 574; **HRMS** (ESI-TOF) *m/z*: [M+H]⁺ Calcd for C₁₂H₁₅N₄O₂ 247.1195, found 247.1208 .

8.5.4.5. 2-[5-(3,5-Dimethoxyphenyl)-1*H*-imidazol-1-yl]acetohydrazide **125d**



2-[5-(3,5-Dimethoxyphenyl)-1*H*-imidazol-1-yl]acetohydrazide **125d** was successfully synthesized according to the general procedure A {ethyl 2-[5-(3,4-dimethoxyphenyl)-1*H*-imidazol-1-yl]acetate **120d** (247 mg, 0.85 mmol) and hydrazine monohydrate (128 mg, 2.55 mmol)} and procedure B {ethyl 2-[5-(3,4-dimethoxyphenyl)-1*H*-imidazol-1-yl]acetate **120d** (238 mg, 0.82 mmol) and hydrazine monohydrate (123 mg, 2.46 mmol)}; **Physical characteristics:** yellow solid; **Yields:** 204 mg, 87% for procedure A and 213 mg, 94%; **Melting point:** 89-91°C; **¹H NMR** (400 MHz, DMSO-*d*₆) δ 9.38 (1H, s, NHNH₂), 7.69 (1H, s, 2-CH), 6.92-7.05 (4H, overlapping multiplets, ArH and 4-CH), 4.62 (2H, s, NCH₂), 3.80 and 3.82 (6H, 2 x s, 2 x ArOCH₃), 3.41 (2H, s, NHNH₂); **¹³C NMR** (101 MHz, DMSO-*d*₆) δ 167.6 (C=O), 149.5 & 149.6 (2 x ArCOCH₃), 140.5 (2-C), 133.7 (5-C), 127.5 (4-C), 122.9, 121.8, 112.8, 112.8 (ArC), 563 and 56.5 (2 x ArCOCH₃), 46.7 (6-C); **FTIR** $\nu_{\max}/\text{cm}^{-1}$ (KBr): 3565, 3209, 2938, 2838, 1693, 1586, 1557, 1511, 1463, 1418, 1321, 1254, 1168, 1142, 1112, 1024, 868, 815, 766, 656, 628, 601, 534; **HRMS** (ESI-TOF) *m/z*: [M+H]⁺ Calcd for C₁₃H₁₇N₄O₃ 277.1295, found 277.1260.

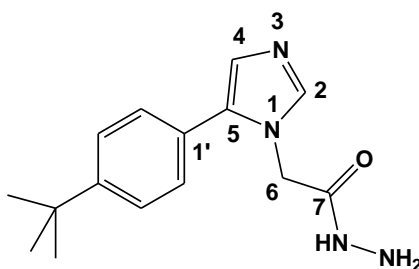
8.4.6.5. 2-(5-(Benzo[*d*][1,3]dioxol-6-yl)-1*H*-imidazol-1-yl)acetohydrazide **125e**



2-(5-(Benzo[*d*][1,3]dioxol-6-yl)-1*H*-imidazol-1-yl)acetohydrazide **125e** was successfully synthesized according to the general procedure A {ethyl 2-(5-(benzo[*d*][1,3]dioxol-6-yl)-1*H*-imidazol-1-yl)acetate **120e** (263 mg, 0.96 mmol) and hydrazine monohydrate (144 mg, 2.88 mmol)} and procedure B {ethyl 2-(5-(benzo[*d*][1,3]dioxol-6-yl)-1*H*-imidazol-1-yl)acetate **120e** (200 mg, 0.73 mmol) and hydrazine monohydrate (110 mg, 2.19 mmol)}; **Physical characteristics:** pale yellow solid; **Yields:** 215 mg, 86% for procedure A and 171 mg, 90% for synthetic procedure B); **Melting point:** 169-171°C; **¹H NMR** (400 MHz, DMSO-*d*₆) δ 9.33 (1H, s, NHNH₂), 7.65 (1H, s, 2-CH), 6.98 (1H, s, 4-CH), 6.92 (1H, d, *J* = 7.2 Hz, ArH), 6.84 (2H, d, *J* = 1.2 Hz, ArH), 6.06 (2H, s, ArOCH₂O), 4.58 (2H, s, NCH₂), 3.42 (2H, s, NHNH₂); **¹³C NMR** (101 MHz, DMSO-*d*₆) δ 170.9 (C=O), 147.5 and 147.1 (2 x ArCOCH₂O), 139.6 (2-C), 132.7 (5-

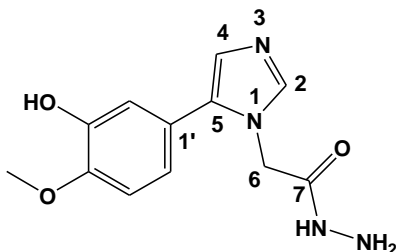
C), 127.2 (4-C), 126.7, 123.2, 122.0, 108.8 (ArC), 101.3 (ArCOCH₂O), 45.7 (6-C); **FTIR** $\nu_{\max}/\text{cm}^{-1}$ (KBr): 3318, 3210, 3104, 2994, 2929, 1655, 1619, 1561, 1500, 1428, 1344, 1321, 1292, 1231, 1121, 1142, 1040, 968, 934, 918, 880, 874, 841, 833, 809, 759, 665, 642, 579; **HRMS** (ESI-TOF) m/z : $[\text{M}+\text{H}]^+$ Calcd. for C₁₂H₁₃N₄O₃ 261.0982, found 261.0992.

8.4.6.7. 2-[5-(4-*tert*-Butylphenyl)-1*H*-imidazol-1-yl]acetohydrazide **125f**



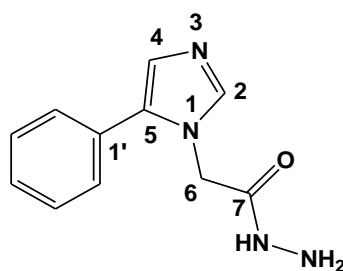
2-[5-(4-*tert*-Butylphenyl)-1*H*-imidazol-1-yl]acetohydrazide **125f** was successfully synthesized according to the general procedure A {ethyl 2-(5-(4-*tert*-butylphenyl)-1*H*-imidazol-1-yl)acetate (229 mg, 0.80 mmol) and hydrazine monohydrate (120 mg, 2.40 mmol)} and synthetic procedure B {ethyl 2-(5-(4-*tert*-butylphenyl)-1*H*-imidazol-1-yl)acetate (238 mg, 0.83 mmol) and hydrazine monohydrate (125 mg, 2.49 mmol)}; **Physical characteristics**: pale yellow solid; **Yields**: 174 mg, 80% for procedure A and 210 mg, 93% for synthetic procedure B; **Melting point**: 178-180°C; **¹H NMR** (400 MHz, DMSO-*d*₆) δ 9.28 (1H, s, NHNH₂), 7.69 (1H, s, 2-CH), 7.47 (2H, d, $J = 8.0$ Hz, ArH), 7.35 (2H, d, $J = 8.0$ Hz, ArH), 6.99 (1H, s, 4-CH), 4.63 (2H, s, NCH₂), 4.46 (2H, brs, NHNH₂), 1.34 [9H, s, C(CH₃)₃]; **¹³C NMR** (101 MHz, DMSO-*d*₆) δ 166.6 (C=O), 150.2 [ArCC(CH₃)₃], 140.2 (2-C), 132.8, 127.9, 127.0, 126.7, 125.6 (ArC), 45.8 (6-C), 34.4 [ArCC(CH₃)₃], 31.1 [ArCC(CH₃)₃]; **FTIR** $\nu_{\max}/\text{cm}^{-1}$ (KBr): 3335, 3220, 3062, 2957, 2865, 1663, 1603, 1589, 1501, 1478, 1382, 1362, 1296, 1274, 1228, 1116, 992, 964, 913, 842, 828, 783, 740, 648, 585, 564; **HRMS** (ESI-TOF) m/z : $[\text{M}+\text{H}]^+$ Calcd for C₁₅H₂₁N₄O 273.1710, found 273.1727.

8.4.6.8. 2-(5-(3-Hydroxy-4-methoxyphenyl)-1*H*-imidazol-1-yl)acetohydrazide **125g**



2-(5-(3-Hydroxy-4-methoxyphenyl)-1*H*-imidazol-1-yl)acetohydrazide **125g** was successfully according to the general procedure B using ethyl 2-(5-(3-hydroxy-4-methoxyphenyl)-1*H*-imidazol-1-yl)acetate **120g** (301 mg, 1.09 mmol) and hydrazine monohydrate (166 mg, 3.25 mmol) in MeOH; **Physical characteristics**: pale yellow solid; **Yield**: 269 mg, 94%; **Melting point**: 217-219°C; **¹H NMR** (400 MHz, DMSO-*d*₆) δ 9.28 (1H, s, *NHNH*₂), 7.76 (1H, s, 2-*CH*), 7.06 (1H, s, 4-*CH*), 6.95 (1H, d, *J* = 8.4 Hz, ArH), 6.76-6.81 (2H, m, ArH), 5.24 (1H, br, ArOH), 4.67 (2H, s, *NCH*₂), 3.87 (3H, s, ArOCH₃), 4.42 (2H, brs, *NHNH*₂); **¹³C NMR** (101 MHz, DMSO-*d*₆) δ 167.8 (C=O), 147.0 and 146.7 (ArCOCH₃ and ArCOH), 138.2 (2-*C*), 133.8 (5-*C*), 126.0, 122.5 (ArC), 120.1 (4-*C*), 115.0, 112.2 (ArC), 56.0 (ArCOCH₃), 46.5 (6-*C*); **FTIR** $\nu_{\max}/\text{cm}^{-1}$ (KBr): 3146, 3120, 3051, 2994, 2603, 1614, 1574, 1523, 1460, 1387, 1331, 1318, 1289, 1247, 1219, 1182, 1155, 1132, 1032, 857, 782, 673; **HRMS** (ESI-TOF) *m/z*: [M+H]⁺ Calcd for C₁₂H₁₅N₄O₃ 263.1139, found 263.1145.

8.4.6.9. 2-(5-Phenyl-1*H*-imidazol-1-yl)acetohydrazide **125h**



2-(5-Phenyl-1*H*-imidazol-1-yl)acetohydrazide **125h** was successfully synthesized according to the general procedure A {ethyl 2-(5-phenyl-1*H*-imidazol-1-yl)acetate (219 mg, 0.95 mmol) and hydrazine monohydrate **120h** (143 mg, 2.85 mmol)} and procedure B {ethyl 2-(5-phenyl-1*H*-imidazol-1-yl)acetate **120h** (115 mg, 0.50 mmol) and hydrazine monohydrate (75 mg, 1.50 mmol)}; **Physical characteristics**: pale yellow solid; **Yields**: 152 mg, 74% for procedure A and 97 mg, 90% for synthetic procedure B; **Melting point**: 172-174°C; **¹H NMR** (400 MHz, DMSO-*d*₆) δ 9.36 (1H, s, *NHNH*₂), 7.73 (1H, s, 2-*CH*), 7.41-7.48 (5H, m, ArH), 7.05 (1H, s, 4-*CH*), 4.66 (2H, s, *NCH*₂), 3.41 (2H, s, *NHNH*₂); **¹³C NMR** (101 MHz, DMSO-*d*₆) δ 167.5 (C=O), 141.1 (2-*C*), 133.2 (5-*C*), 130.5, 129.7, 129.1, 128.7, 128.1 (ArC), 128.1 (4-*C*), 46.8 (6-*C*); **FTIR** $\nu_{\max}/\text{cm}^{-1}$ (KBr): 3321, 3197, 3119, 3026, 2950, 1676, 1638, 1608, 1553, 1489, 1425, 1298, 1285, 1229, 1112, 1006, 927, 909, 820, 767, 718, 703, 678, 647, 581, 534; **HRMS** (ESI (ESI-TOF) *m/z*: [M+H]⁺ Calcd for C₁₁H₁₃N₄O 217.1084, found 217.1082.

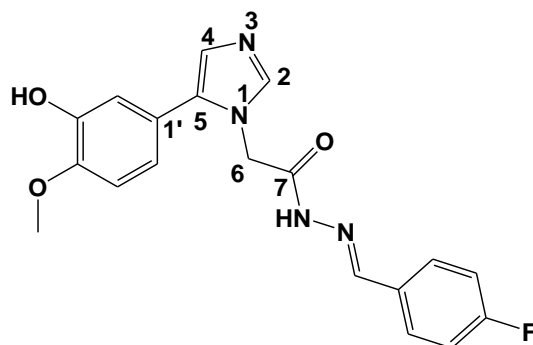
8.4.7. Synthesis of (*E*)-*N'*-arylidene-2-(5-aryl-1*H*-imidazol-1-yl)acetohydrazide

8.4.7.1. General synthetic procedure

2-(5-Aryl-1*H*-imidazol-1-yl)acetohydrazide (1 molar equivalent) was dissolved in anhydrous methanol (20 mL). To this solution was added aryl aldehyde (1.3 molar equivalents) slowly at room temperature. After addition, the mixture was refluxed for 16 hours until reaction completion, as monitored by TLC. The solvent was evaporated and the product purified by recrystallization from 75% EtOH and followed by drying under high vacuum.

N.B: Only proton NMR signals of the major rotamer are presented and assigned, while ^{13}C data is not assigned due to multiplicity of signals arising from rotamers at 30°C. Furthermore, the ^{13}C NMR spectra of fluorinated compounds were further complicated by additional signals as a result of fluorine splitting.

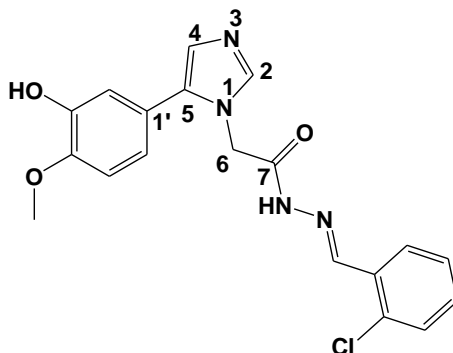
8.4.7.2. (*E*)-*N'*-(4-Fluorobenzylidene)-2-(5-(3-hydroxy-4-methoxyphenyl)-1*H*-imidazol-1-yl)acetohydrazide **127a**



(*E*)-*N'*-(4-Fluorobenzylidene)-2-(5-(3-hydroxy-4-methoxyphenyl)-1*H*-imidazol-1-yl)acetohydrazide **127a** was successfully synthesized from reaction of 2-(5-(3-hydroxy-4-methoxyphenyl)-1*H*-imidazol-1-yl)acetohydrazide **125g** (214 mg, 0.82 mmol) and 4-fluorobenzaldehyde (135 mg, 1.09 mmol) in MeOH according to the general procedure; **Physical characteristics:** white solid; **Yield:** 202 mg, 73%; **^1H NMR** (400 MHz, DMSO- d_6) δ 11.7 (1H, s, NH), 9.24 (1H, brs, OH), 7.99 (1H, s, N=CH), 7.23-7.75 (3H, m, ArH and 2-CH), 7.25-7.27 (2H, m, ArH), 6.95 (1H, s, 4-CH), 6.90 (1H, s, ArH), 6.77 (2H, d, $J = 6.0$ Hz, ArH), 5.24 (2H, s, NCH $_2$), 3.71 (3H, s, ArOCH $_3$); **^{13}C NMR** (101 MHz, DMSO- d_6) δ 169.1, 164.31, 164.0, 161.9, 147.6, 146.6, 146.5, 146.3, 143.1, 139.6, 133.19, 132.4, 132.3, 130.5, 129.4, 129.3, 129.2, 129.1, 126.2, 126.1, 121.3, 121.1, 120.6, 120.3, 116.5, 116.3, 115.9, 115.8, 115.7, 112.4, 112.2, 55.4, 45.9, 40.2; **FTIR** ν_{max} /cm $^{-1}$ (KBr): 3072, 2974, 2836, 1672, 1613, 1600, 1518, 1503,

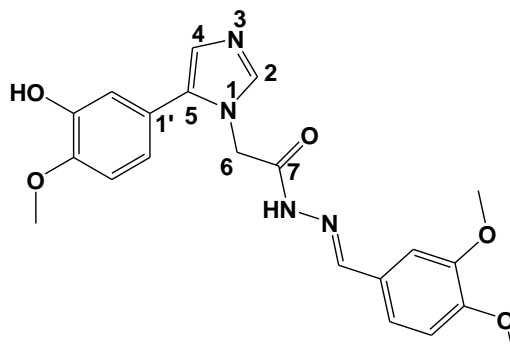
1491, 1433, 1413, 1306, 1290, 1256, 1155, 1106, 1033, 837, 812, 786, 661, 519; **HRMS** (ESI-TOF) m/z : Calcd for $C_{19}H_{18}FN_4O_3$, 369.1357, found 369.1366.

8.4.7.3. (*E*)-*N'*-(2-Chlorobenzylidene)-2-(5-(3-hydroxy-4-methoxyphenyl)-1*H*-imidazol-1-yl)acetohydrazide **127b**



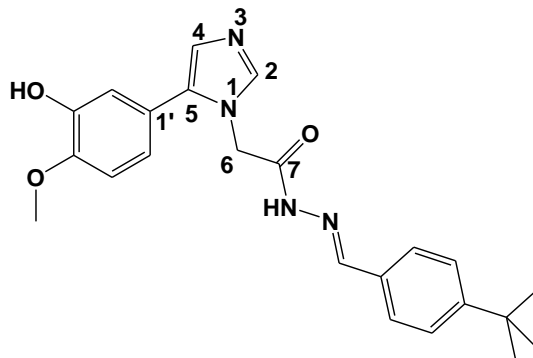
(*E*)-*N'*-(2-Chlorobenzylidene)-2-(5-(3-hydroxy-4-methoxyphenyl)-1*H*-imidazol-1-yl)acetohydrazide **127b** was successfully synthesized from reaction of 2-(5-(3-hydroxy-4-methoxyphenyl)-1*H*-imidazol-1-yl)acetohydrazide **125g** (315 mg, 1.20 mmol) and 2-chlorobenzaldehyde (219 mg, 1.56 mmol) in MeOH according to the general procedure; **Physical characteristics**: yellow solid; **Yield**: 296 mg, 64%; **¹H NMR** (400 MHz, DMSO-*d*₆) δ 11.9 (1H, s, NH), 9.23 (1H, brs, OH), 8.37 (1H, s, N=CH), 7.72 (1H, s, 2-CH), 7.37-7.44 (3H, m, ArH), 7.50 (1H, d, $J = 8.4$ Hz, ArH), 6.89 (1H, s, 4-CH), 6.90 (1H, s, ArH), 6.76-6.781 (2H, m, ArH), 5.27 (2H, s, NCH₂), 3.72 (3H, s, ArOCH₃); **¹³C NMR** (101 MHz, DMSO-*d*₆) δ 169.2, 164.2, 147.6, 146.5, 143.4, 140.2, 139.6, 133.2, 133.0, 131.5, 131.1, 131.0, 130.7, 130.6, 129.9, 127.6, 127.2, 127.6.9, 126.2, 121.3, 121.0, 120.6, 120.3, 115.7, 112.4, 112.2, 55.4, 45.6, 40.2; **FTIR** $\nu_{\max}/\text{cm}^{-1}$ (KBr): 3116, 3002, 2964, 2843, 1691, 1604, 1556, 1509, 1416, 1399, 1273, 1212, 1050, 1030, 965, 876, 773, 656, 561; **HRMS** (ESI-TOF) m/z : Calcd for $C_{19}H_{18}ClN_4O_3$, 385.1062, found 385.1062.

8.4.7.4. (*E*)-*N'*-(3,4-Dimethoxybenzylidene)-2-(5-(3-hydroxy-4-methoxyphenyl)-1*H*-imidazol-1-yl)acetohydrazide **127c**



(*E*)-*N'*-(3,4-Dimethoxybenzylidene)-2-(5-(3-hydroxy-4-methoxyphenyl)-1*H*-imidazol-1-yl)acetohydrazide **127c** was successfully synthesized from reaction of 2-(5-(3-hydroxy-4-methoxyphenyl)-1*H*-imidazol-1-yl)acetohydrazide **125g** (354 mg, 1.35 mmol) and 3,4-dimethoxybenzaldehyde (293 mg, 1.76 mmol) in MeOH according to the general procedure; **Physical characteristics**: yellow solid; **Yield**: 416 mg, 75%; **¹H NMR** (400 MHz, DMSO-*d*₆) δ 11.9 (1H, s, NH), 9.23 (1H, brs, OH), 8.37 (1H, s, N=CH), 7.72 (1H, s, 2-CH), 7.37-7.44 (4H, m, ArH), 7.50 (1H, d, *J* = 8.4 Hz, ArH), 6.89 (1H, s, 4-CH), 6.90 (1H, s, ArH), 6.76-6.78 (2H, m, ArH), 5.27 (2H, s, NCH₂), 3.72 (3H, s ArOCH₃); **¹³C NMR** (101 MHz, DMSO-*d*₆) δ 168.8, 161.7, 158.4, 158.3, 158.1, 158.0, 149.6, 149.5, 149.2, 149.0, 146.0, 130.4, 129.7, 129.2, 128.3, 127.1, 126.0, 125.7, 122.9, 109.5, 108.6, 101.2, 55.7, 55.6, 55.0, 55.4, 55.39, 55.2; 45.7, 40.1; **FTIR** $\nu_{\text{max}}/\text{cm}^{-1}$ (KBr): 3539, 3100, 3065, 2940, 2839, 1682, 1600, 1578, 1568, 1498, 1435, 1421, 1375, 1286, 1262, 1236, 1202, 1140, 1128, 1025, 864, 784, 753, 613, 578 ; **HRMS** (ESI-TOF) *m/z*: Calcd for C₂₁H₂₃N₄O₅ 411.1663, Found 411.1674.

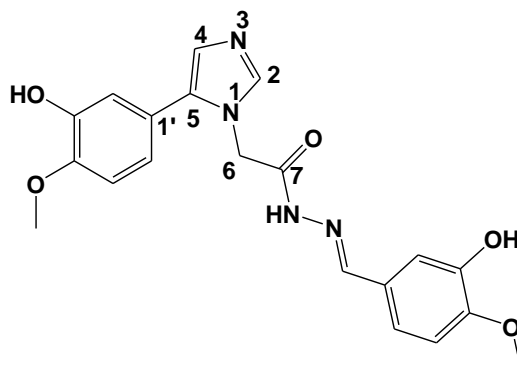
8.4.7.5. (*E*)-*N'*-(4-*tert*-Butylbenzylidene)-2-(5-(3-hydroxy-4-methoxyphenyl)-1*H*-imidazol-1-yl)acetohydrazide **127d**



(*E*)-*N'*-(4-*tert*-Butylbenzylidene)-2-(5-(3-hydroxy-4-methoxyphenyl)-1*H*-imidazol-1-yl)acetohydrazide **127d** was successfully synthesized from reaction of 2-(5-(3-hydroxy-4-

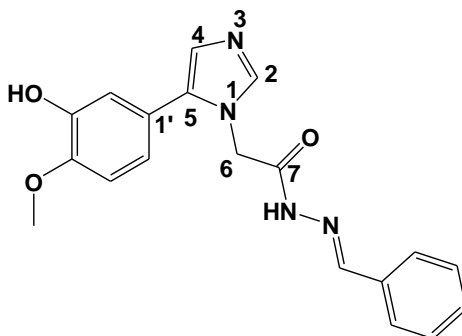
methoxyphenyl)-1*H*-imidazol-1-yl)acetohydrazide **125g** (218 mg, 0.83 mmol) and 4-*tert*-butylbenzaldehyde (217 mg, 1.08 mmol) in MeOH according to the general procedure; **Physical characteristics**: pale yellow solid; **Yield**: 236 mg, 70%; **¹H NMR** (400 MHz, DMSO-*d*₆) δ 11.7 (1H, s, NH), 9.17 (1H, brs, OH), 7.97 (1H, s, N=CH), 7.76 (1H, s, 2-CH), 7.57-7.59 (2H, d, *J* = 8 Hz, ArH), 7.41 (1H, d, *J* = 8.4 Hz, ArH), 6.97 (1H, s, 4-CH), 6.90 (1H, s, ArH), 6.78-6.82 (2H, m, ArH), 5.23 (2H, s, NCH₂), 3.72 (3H, s, ArOCH₃), 1.26 [9H, s, C(CH₃)₃]; **¹³C NMR** (101 MHz, DMSO-*d*₆) δ 168.9, 167.4, 163.9, 153.1, 152.9, 147.6, 147.5, 146.7, 146.6, 144.3, 139.7, 133.3, 131.3, 131.1, 126.5, 129.2, 128.2, 127.0, 126.8, 126.0, 125.9, 125.6, 125.4, 121.3, 121.1, 120.6, 115.8, 112.5, 112.2, 55.4, 45.9, 40.2; **FTIR** ν_{\max} /cm⁻¹ (KBr): 3096, 2965, 2900, 2865, 2730, 2596, 1694, 1587, 1517, 1482, 1393, 1277, 1239, 1213, 1113, 1023, 1004, 826, 809, 583, 570, 530; **HRMS** (ESI-TOF) *m/z*: Calcd for C₂₃H₂₇N₄O₃ 407.2078, found 407.2083.

8.4.7.6. (*E*)-*N*'-(3-Hydroxy-4-methoxybenzylidene)-2-(5-(3-hydroxy-4-methoxyphenyl)-1*H*-imidazol-1-yl)acetohydrazide **127e**



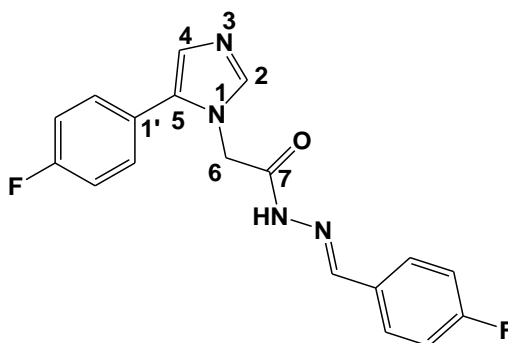
(*E*)-*N*'-(3-Hydroxy-4-methoxybenzylidene)-2-(5-(3-hydroxy-4-methoxyphenyl)-1*H*-imidazol-1-yl)acetohydrazide **127e** was successfully synthesized from reaction of 2-(5-(3-hydroxy-4-methoxyphenyl)-1*H*-imidazol-1-yl)acetohydrazide **125g** (326 mg, 1.24 mmol) and 3-hydroxy-4-methoxybenzaldehyde (227 mg, 1.49 mmol) in MeOH according to the general procedure; **Physical characteristics**: orange solid; **Yield**: 374 mg, 76%; **¹H NMR** (400 MHz, DMSO-*d*₆) δ 11.60 (1H, s, NH), 9.19 and 9.52 (2H, 2 x brs, OH), 7.86 (1H, s, N=CH), 7.73 (1H, s, 2-CH), 7.76 (1H, s, 4-CH), 7.38 (1H, d, *J* = 8.4 Hz, ArH), 7.25 (1H, s, ArH), 7.23 (1H, s, ArH), 6.75-6.82 (3H, m, ArH), 5.22 (2H, s, NCH₂), 3.71 and 3.77 (6H, 2 x s, 2 x ArOCH₃); **¹³C NMR** (101 MHz, DMSO-*d*₆) δ 168.4, 161.3, 158.4, 158.29, 158.2, 158.1, 149.4, 149.36, 149.33, 149.1, 146.8, 130.1, 130.0, 129.5, 128.7, 127.0, 125.5, 125.4, 1131.2, 110.0, 108.5, 101.3, 55.8, 55.5, 55.0; 45.5, 40.3; **FTIR** ν_{\max} /cm⁻¹ (KBr): (**KBr**): 3216, 3073, 2947, 2838, 1682, 1598, 1514, 1464, 1428, 1390, 1282, 1213, 1165, 1124, 1031, 957, 861, 817, 782, 565; **HRMS** (ESI-TOF) *m/z*: Calcd. for C₂₀H₂₁N₄O₅ 397.1506, found 397.1510.

8.4.7.7. (*E*)-*N'*-Benzylidene-2-(5-(3-hydroxy-4-methoxyphenyl)-1*H*-imidazol-1-yl)acetohydrazide **127f**



(*E*)-*N'*-Benzylidene-2-(5-(3-hydroxy-4-methoxyphenyl)-1*H*-imidazol-1-yl)acetohydrazide **127f** was successfully synthesized from reaction of 2-(5-(3-hydroxy-4-methoxyphenyl)-1*H*-imidazol-1-yl)acetohydrazide **125g** (213 mg, 0.81 mmol) and benzaldehyde (112 mg, .06 mmol) in MeOH according to the general procedure; **Physical characteristics**: white solid; **Yield**: 374 mg, 63%; **¹H NMR** (400 MHz, DMSO-*d*₆) δ 11.7 (1H, s, NH), 9.28 (1H, br, OH), 8.00 (1H, s, N=CH), 7.73 (1H, s, 2-CH), 7.68 -7.41 (5H, m, ArH), 6.95 (1H, s, 4-CH), 7.91 (1H, s, ArH), 6.77-6.82 (2H, m, ArH), 5.26 (2H, s, NCH₂), 3.72 (3H, s, ArOCH₃); **¹³C NMR** (101 MHz, DMSO-*d*₆) δ 169.1, 164.0, 147.5, 147.4, 146.6, 146.4, 144., 139.6, 39.5, 136.2, 134.6, 133.9, 133.8, 133.2, 130.2, 130.0, 129.4, 129.1, 127.7, 127.1, 126.9, 126.1, 121.3, 121.0, 120.6, 120.3, 115.7, 112.4, 112.2, 55.4, 46.3, 45.8; **FTIR** $\nu_{\max}/\text{cm}^{-1}$ (KBr): 3361, 3404, 3126, 3078, 3026, 2969, 2895, 2821, 2556, 1696, 1590, 1517, 1494, 1404, 1276, 1232, 1211, 1117, 1025, 960, 936, 821, 704; **HRMS** (ESI-TOF) *m/z*: Calcd for C₁₉H₁₉N₄O₃ 351.1452, found 351.1455.

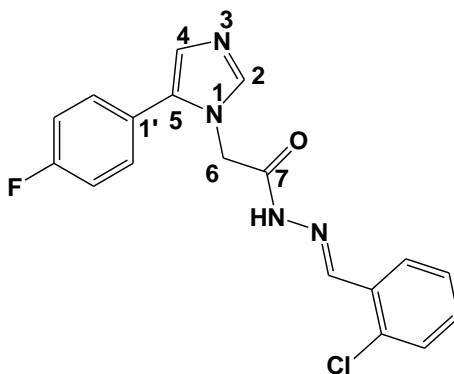
8.4.7.8. (*E*)-*N'*-(4-Fluorobenzylidene)-2-(5-(4-fluorophenyl)-1*H*-imidazol-1-yl)acetohydrazide **127g**



(*E*)-*N'*-(4-Fluorobenzylidene)-2-(5-(4-fluorophenyl)-1*H*-imidazol-1-yl)acetohydrazide **127g** was successfully synthesized from reaction of 2-(5-(4-fluorophenyl)-1*H*-imidazol-1-yl)acetohydrazide **125a** (353 mg, 1.51 mmol) and 4-fluorobenzaldehyde (225 mg, 1.96 mmol) in MeOH according to the general procedure; **Physical characteristics**: white solid; **Yield**: 278 mg, 54%; **¹H NMR**

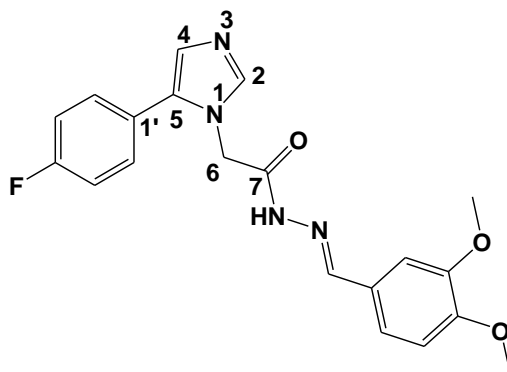
(400 MHz, DMSO- d_6) δ 11.7 (1H, s, NH), 7.99 (1H, s, N=CH), 7.81 (1H, s, 2-CH), 7.74 -7.79 (2H, m, ArH), 7.42-7.44 (2H, m, ArH), 7.24-7.28 (4H, m, ArH), 7.04 (1H, s, 4-CH), 5.29 (2H, s, NCH₂); ¹³C NMR (101 MHz, DMSO- d_6) δ 165.2, 164.4, 163.7, 163.1, 163.0, 162.7, 162.0, 160.9, 160.7, 160.6, 160.5, 146.4, 143.3, 140.4, 140.2, 132.1, 130.6, 130.5, 130.4, 130.3, 130.2, 129.4, 129.1, 127.3, 127.2, 126.3, 126.2, 126.0, 116.2, 116.0, 115.9, 115.8, 115.7, 115.6, 115.5, 46.4, 46.0; FTIR $\nu_{\max}/\text{cm}^{-1}$ (KBr): 3182, 3084, 2957, 2835, 1683, 1619, 1600, 1556, 1504, 1409, 1367, 1304, 1275, 1231, 1157, 1119, 961, 913, 841, 828, 786, 660, 529, 514; HRMS (ESI-TOF) m/z : Calcd for C₁₈H₁₅F₂N₄O⁺ 341.1208, Found 341.1217.

7.4.7.9. (*E*)-*N'*-(2-Chlorobenzylidene)-2-(5-(4-fluorophenyl)-1*H*-imidazol-1-yl)acetohydrazide **127h**



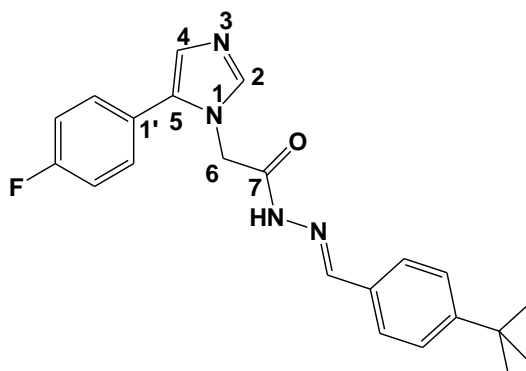
(*E*)-*N'*-(2-Chlorobenzylidene)-2-(5-(4-fluorophenyl)-1*H*-imidazol-1-yl)acetohydrazide **127h** was successfully synthesized from reaction of 2-(5-(4-fluorophenyl)-1*H*-imidazol-1-yl)acetohydrazide **125a** (478 mg, 2.04 mmol) and 2-chlorobenzaldehyde (287 mg, 2.65 mmol) in MeOH according to the general procedure; **Physical characteristics**: pale yellow solid; **Yield**: 495 mg, 68%; ¹H NMR (400 MHz, DMSO- d_6) δ 11.8 (1H, s, NH), 8.37 (1H, s, N=CH), 7.95 (1H, d, J = 8.0 Hz, ArH), 7.81 (1H, s, 2-CH), 7.37 -7.51 (6H, m, ArH), 7.21-7.26 (2H, m, ArH), 7.03 (1H, s, 4-CH), 5.31 (2H, s, NCH₂); ¹³C NMR (101 MHz, DMSO- d_6) δ 168.8, 163.8, 162.9, 160.5, 158.2, 143.4, 140.3, 134.7, 133.1, 133.0, 132.5, 132.0, 131.6, 131.1, 130.8, 130.6, 130.5, 130.3, 130.1, 129.8, 128.2, 127.6, 127.5, 127.2, 127.1, 127.0, 126.2, 115.8, 115.6, 46.4, 45.9; FTIR $\nu_{\max}/\text{cm}^{-1}$ (KBr): 3068, 3001, 2892, 2794, 1693, 1601, 1561, 1482, 1504, 1411, 1364, 1351, 1271, 1232, 1157, 1114, 1049, 1032, 954, 924, 846, 816, 759, 660, 594, 531; HRMS (ESI-TOF) m/z : Calcd for C₁₈H₁₅FCIN₄O 357.0913, Found 357.0918.

8.4.7.10. (*E*)-*N'*-(3,4-Dimethoxybenzylidene)-2-(5-(4-fluorophenyl)-1*H*-imidazol-1-yl)acetohydrazide **127i**



E-*N'*-(3,4-Dimethoxybenzylidene)-2-(5-(4-fluorophenyl)-1*H*-imidazol-1-yl)acetohydrazide **127i** was successfully synthesized from reaction of 2-(5-(4-fluorophenyl)-1*H*-imidazol-1-yl)acetohydrazide **125a** (461 mg, 1.97 mmol) and 3,4-dimethoxybenzaldehyde (393 mg, 2.56 mmol) in MeOH according to the general procedure; **Physical characteristics**: white solid; **Yield**: 495 mg, 68%; **¹H NMR** (400 MHz, DMSO-*d*₆) δ 11.6 (1H, s, NH), 8.64 (1H, s, N=CH), 7.90 (1H, s, ArH), 7.78 (1H, s, 2-CH), 7.48 (1H, s, ArH), 7.36-7.38 (2H, m, ArH), 7.15 (1H, d, *J* = 8.0 Hz, ArH), 6.97-7.08 (3H, m, ArH and 4-CH), 5.27 (2H, s, NCH₂), 3.78 and 3.82 (6H, 2 x s, ArOCH₃); **¹³C NMR** (101 MHz, DMSO-*d*₆) δ 168.5, 163.3, 162.9, 160.7, 160.5, 151.6, 150.8, 150.6, 150.7, 149.0, 147.6, 144.3, 140.1, 131.9, 130.5, 130.3, 130.2, 130.1, 127.3, 126.7, 126.5, 126.4, 123.5, 121.5, 115.8, 111.5, 111.4, 109.1, 108.5, 108.3, 55.6, 55.5, 55.4, 55.4, 46.5, 40.4; **FTIR** ν_{max} /cm⁻¹ (KBr): 3304, 3182, 3092, 2978, 2939, 2847, 1681, 1599, 1573, 1502, 1464, 1442, 1420, 1287, 1239, 1267, 1218, 116, 1141, 1027, 921, 851, 620, 534; **HRMS** (ESI-TOF) *m/z*: Calcd for C₂₀H₂₀FN₄O₃⁺ 383.1514, Found 383.1521.

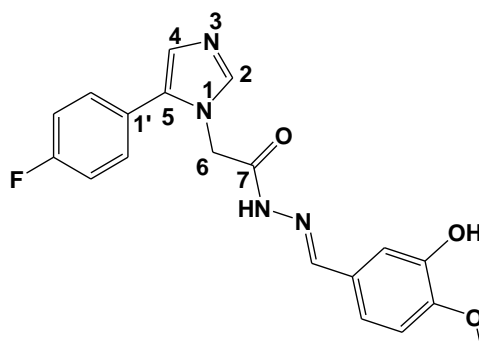
8.4.7.11. (*E*)-*N'*-(4-*tert*-Butylbenzylidene)-2-(5-(4-fluorophenyl)-1*H*-imidazol-1-yl)acetohydrazide **127j**



E-*N'*-(4-*tert*-Butylbenzylidene)-2-(5-(4-fluorophenyl)-1*H*-imidazol-1-yl)acetohydrazide **127j** was successfully synthesized from reaction of 2-(5-(4-fluorophenyl)-1*H*-imidazol-1-yl)acetohydrazide

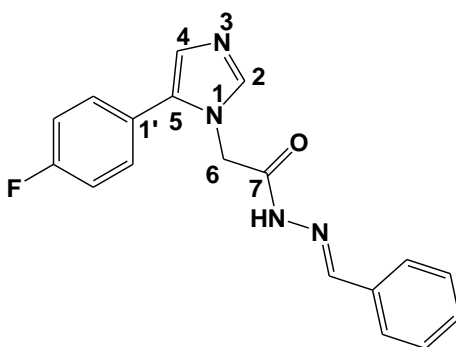
125a (285 mg, 1.22 mmol) and 4-*tert*-butylbenzaldehyde (257 mg, 1.59 mmol) in MeOH according to the general procedure; **Physical characteristics**: yellow solid; **Yield**: 268 mg, 58%; **¹H NMR** (400 MHz, DMSO-*d*₆) δ 11.7 (1H, s, NH), 7.98 (1H, s, N=CH), 7.81 (1H, s, 2-CH), 7.58-7.60 (2H, d, *J* = 8.0 Hz, ArH), 7.42-7.50 (6H, m, ArH), 7.23-7.25 (2H, d, *J* = 8.0 Hz, ArH), 7.04 (1H, s, 4-CH), 5.27 (2H, s, NCH₂), 1.26 [9H, 2 x s, C(CH₃)₃]; **¹³C NMR** (101 MHz, DMSO-*d*₆) δ 168.6, 166.4, 163.5, 163.6, 160.6, 153.1, 152.9, 152.9, 147.5, 144.3, 140.3, 140.2, 139.9, 132.0, 131.9, 131.8, 131.2, 131.1, 130.5, 130.5, 130.2, 129.2, 128.2, 127.2, 127.0, 126.8, 126.3, 126.0, 125.5, 125.3, 124.9, 115.8, 115.5, 56.1, 46.4, 45.9, 45.8, 38.9, 34.5, 31.0, 30.9, 18.5; **FTIR** ν_{\max} /cm⁻¹ (KBr): 3211, 3069, 2962, 2904, 2868, 1698, 1608, 1564, 1503, 1394, 1365, 1315, 1268, 1226, 1175, 1159, 1108, 833, 711, 607, 560; **HRMS** (ESI-TOF) *m/z*: Calcd for C₂₂H₂₄FN₄O 379.1929, found 379.1933.

8.4.7.12. (*E*)-*N'*-(3-Hydroxy-4-methoxybenzylidene)-2-(5-(4-fluorophenyl)-1*H*-imidazol-1-yl)acetohydrazide **128k**



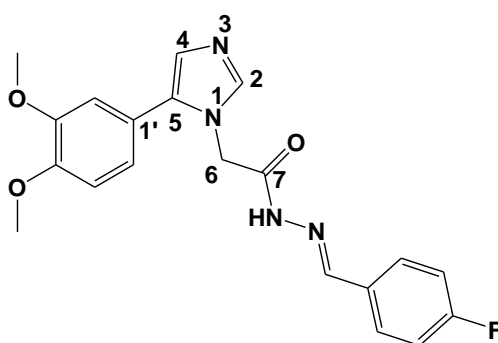
(*E*)-*N'*-(3-Hydroxy-4-methoxybenzylidene)-2-(5-(4-fluorophenyl)-1*H*-imidazol-1-yl)acetohydrazide **128k** was successfully synthesized from reaction of 2-(5-(4-fluorophenyl)-1*H*-imidazol-1-yl)acetohydrazide **120a** (586 mg, 2.50 mmol) and 3-hydroxy-4-methoxybenzaldehyde (494 mg, 3.25 mmol) in MeOH according to the general procedure; **Physical characteristics**: white solid; **Yield**: 699 mg, 76%; **¹H NMR** (400 MHz, DMSO-*d*₆) δ 11.5 (1H, s, NH), 9.61 (1H, brs, OH), 7.87 (1H, s, N=CH), 7.79 (1H, s, 2-CH), 7.41-7.46 (2H, m, ArH), 7.24-7.28 (3H, m, ArH), 7.05 (1H, d, *J* = 8.0 Hz, ArH), 7.03 (1H, s, 4-CH), 6.80 (1H, d, *J* = 8.0 Hz, ArH), 5.26 (2H, s, NCH₂), 3.80 (3H, s, ArOCH₃); **¹³C NMR** (101 MHz, DMSO-*d*₆) δ 168.5, 163.3, 163.0, 160.6, 149.2, 148.9, 148.0, 144.7, 140.4, 140.2, 132.0, 130.5, 130.4, 130.3, 130.2, 127.3, 127.2, 126.4, 126, 124.3, 122.2, 121.6, 115.90, 115.85, 115.7, 115.5, 115.4, 109.5, 109.14, 55.6, 48.6, 46.1, 40.1; **FTIR** ν_{\max} /cm⁻¹ (KBr): 3674, 3519, 3072, 2938, 1698, 1590, 1564, 1469, 1492, 1436, 1409, 1367, 1289, 1219, 1200, 1169, 1113, 1125, 1036, 950, 933, 857, 849, 812, 666, 615, 530; **HRMS** (ESI-TOF) *m/z*: Calcd for C₁₉H₁₈FN₄O₃ 369.1357, found 369.1363.

8.4.7.13. (*E*)-*N'*-Benzylidene-2-(5-(4-fluorophenyl)-1*H*-imidazol-1-yl)acetohydrazide **127l**



(*E*)-*N'*-Benzylidene-2-(5-(4-fluorophenyl)-1*H*-imidazol-1-yl)acetohydrazide **127l** was successfully synthesized from reaction of 2-(5-(4-fluorophenyl)-1*H*-imidazol-1-yl)acetohydrazide **125a** (360 mg, 1.54 mmol) and benzaldehyde (254 mg, 2.39 mmol) in MeOH according to the general procedure; **Physical characteristics**: pale yellow solid; **Yield**: 387 mg, 78%; **¹H NMR** (400 MHz, DMSO-*d*₆) δ 11.7 (1H, s, NH), 8.00 (1H, s, N=CH), 7.80 (1H, s, 2-CH), 7.67-7.72 (2H, d, *J* = 4 Hz, ArCH), 7.41-7.45 (5H, m, ArH), 7.21-7.30 (2H, m, ArH), 7.04 (1H, s, 4-CH), 5.29 (2H, s, NCH₂); **¹³C NMR** (101 MHz, DMSO-*d*₆) δ 168.7, 163.7, 162.9, 16.4, 160.6, 147.5, 144.3, 133.9, 133.8, 132.0, 130.5, 130.4, 130.3, 130.3, 130.2, 130.0, 128.9, 128.8, 127.2, 127.1, 126.9, 126.3, 126.2, 115.8, 115.8, 115.6, 115.5, 46.3, 45.9; **FTIR** ν_{\max} /cm⁻¹ (KBr): 3661, 3404, 3126, 3078, 3026, 2969, 2895, 2821, 1696, 1590, 1560, 1517, 1494, 1404, 1276, 1232, 1211, 1117, 1025, 960, 938, 821, 704; **HRMS** (ESI-TOF) *m/z*: Calcd for C₁₈H₁₆FN₄O 323.1303, found 323.1304.

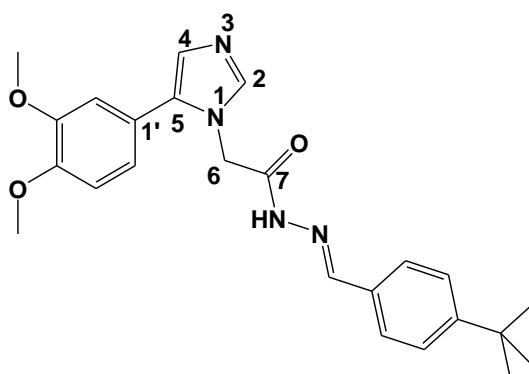
8.4.7.14. (*E*)-*N'*-(4-Fluorobenzylidene)-2-(5-(3,4-dimethoxyphenyl)-1*H*-imidazol-1-yl)acetohydrazide **127m**



(*E*)-*N'*-(4-Fluorobenzylidene)-2-(5-(3,4-dimethoxyphenyl)-1*H*-imidazol-1-yl)acetohydrazide **127m** was successfully synthesized from reaction of 2-(5-(3,4-dimethoxyphenyl)-1*H*-imidazol-1-yl)acetohydrazide **125d** (503 mg, 1.82 mmol) and 4-fluorobenzaldehyde (297 mg, 2.39 mmol) in MeOH according to the general procedure; **Physical characteristics**: pale yellow solid; **Yield**: 578 mg, 83%; **¹H NMR** (400 MHz, DMSO-*d*₆) δ 11.8 (1H, s, NH), 8.73 (1H, s, N=CH), 8.23 (1H, s, 2-CH), 8.00 (2H, d, *J* = 11.8 Hz, ArH), 7.41-7.47.28-7.34 (2H, m, ArH), 6.91-7.01 (4H, m,

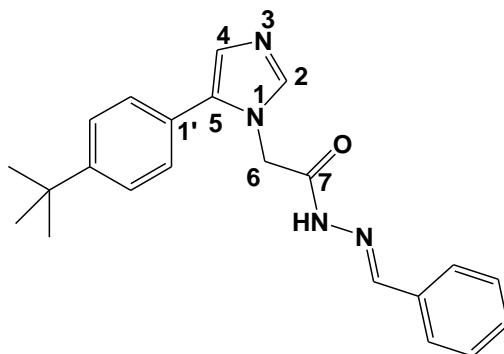
ArH and 4-CH), 5.30 (2H, s, NCH₂), 3.74 and 3.75 (6H, 2 x s, 2 x ArOCH₃); ¹³C NMR (101 MHz, DMSO-*d*₆) δ 168.6, 163.4, 162.8, 160.7, 160.5, 151.8, 151.0, 150.7, 150.5, 149.1, 147.7, 144.4, 140.0, 132.0, 132.1, 131.2, 130.8, 130.5, 127.9, 126.4, 126.0, 123.3, 121.5, 115.8, 111.5, 111.9, 109.5, 108.7, 108.6, 55.7, 55.5, 55.4, 55.3, 46.2, 40.1; **FTIR** ν_{\max} /cm⁻¹ (KBr): 3661, 3404, 3126, 3078, 3026, 2969, 2895, 2821, 1696, 1590, 1560, 1517, 1494, 1404, 1276, 1232, 1211, 1117, 1025, 960, 938, 821, 704; **HRMS** (ESI-TOF) *m/z*: Calcd for C₂₀H₂₀FN₄O₃ 383.1514, found 383.1522.

8.4.7.15. (*E*)-*N'*-(4-*tert*-Butylbenzylidene)-2-(5-(3,4-dimethoxyphenyl)-1*H*-imidazol-1-yl)acetohydrazide **127n**



(*E*)-*N'*-(4-*tert*-Butylbenzylidene)-2-(5-(3,4-dimethoxyphenyl)-1*H*-imidazol-1-yl)acetohydrazide **127n** was successfully synthesized from reaction of 2-(5-(3,4-dimethoxyphenyl)-1*H*-imidazol-1-yl)acetohydrazide **125d** (1.33 mmol) and 4-*tert*-butylbenzaldehyde (1.73 mmol) in MeOH according to the general procedure; **Physical characteristics**: yellow solid; **Yield**: 397 mg, 71%; **¹H NMR** (400 MHz, DMSO-*d*₆) δ 10.8 (1H, s, NH), 7.95 (1H, s, N=CH), 7.88 (1H, s, 2-CH), 7.51 (2H, d, *J* = 8.4 Hz, ArH), 7.39 (2H, d, *J* = 8.4 Hz, ArH), 7.30 (1H, s, ArH), 7.13 (1H, s, 4-CH), 6.86 (2H, d, *J* = 8.8 Hz, ArH), 5.18 (2H, s, NCH₂), 3.84 and 3.86 (6H, 2 x s, ArOCH₃), 1.34 [9H, s, C(CH₃)₃]; ¹³C NMR (101 MHz, DMSO-*d*₆) δ 168.9, 167.4, 152.8, 150.8, 150.6, 149.4, 147.4, 147.0, 146.8, 146.5, 144.0, 140, 133.3, 131.2, 131.0, 126.2, 128.6, 127.3, 126.7, 125.9, 125.9, 125.6, 125.1, 121.4, 115.9, 113.1, 112.8, 55.6, 55.4, 55.3, 45.9, 45.8, 45.7, 45.6; 38.8, 34.6, 31.0, 30.9, 18.5; **FTIR** ν_{\max} /cm⁻¹ (KBr): 3661, 3404, 3126, 3078, 3026, 2969, 2895, 2821, 1696, 1590, 1560, 1517, 1494, 1404, 1276, 1232, 1211, 1117, 1025, 960, 938, 821, 704; **HRMS** (ESI-TOF) *m/z*: Calcd for C₂₀H₂₀FN₄O₃ 421.2234, found 421.2238.

8.4.7.16. (*E*)-2-(5-(4-*tert*-Butylphenyl)-1*H*-imidazol-1-yl)-*N*'-benzylideneacetohydrazide
4.12o



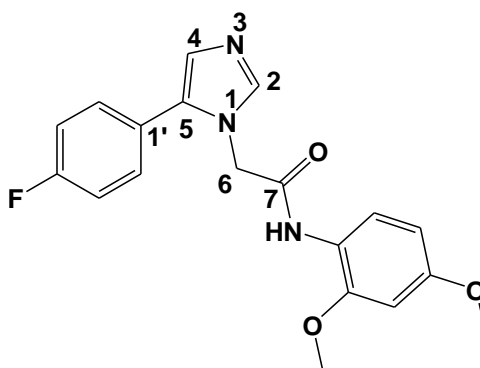
(*E*)-2-(5-(4-*tert*-Butylphenyl)-1*H*-imidazol-1-yl)-*N*'-benzylideneacetohydrazide **127o** was successfully synthesized from reaction of 2-(5-(4-*tert*-butylphenyl)-1*H*-imidazol-1-yl)acetohydrazide **125f** (253 mg, 0.93 mmol) and benzaldehyde (128 mg, 1.21 mmol) in MeOH according to the general procedure; **Physical characteristics**: yellow solid; **Yield**: 272 mg, 81%; **¹H NMR** (400 MHz, DMSO-*d*₆) δ 11.7 (1H, s, NH), 8.00 (1H, s, N=CH), 7.80 (1H, s, 2-CH), 7.67 (2H, d, *J* = 3.6 Hz, ArH), 7.41-7.45 (5H, m, ArH), 7.21-7.30 (2H, m, ArH), 7.04 (1H, s, 4-CH), 5.29 (2H, s, NCH₂); **¹³C NMR** (101 MHz, DMSO-*d*₆) δ 168.9, 161.5, 149.7, 149.6, 146.2, 146.0, 138.9, 138.5, 133.6, 131.2, 130.5, 128.2, 126.9, 125.8, 125.6, 125.5, 122.4, 122.3, 109.4, 108.5, 45.9, 45.7, 38.6, 34.7, 31.0, 30.9; **FTIR** ν_{\max} /cm⁻¹ (KBr): 3661, 3404, 3126, 3078, 3026, 2969, 2895, 2821, 1696, 1590, 1560, 1517, 1494, 1404, 1276, 1232, 1211, 1117, 1025, 960, 938, 821, 704; **HRMS** (ESI-TOF) *m/z*: Calcd for C₂₂H₂₅N₄O 361.2023, found 361.2025.

8.4.8. Synthesis of *N*-aryl-2-(5-aryl-1*H*-imidazol-1-yl)acetamide

8.4.8.1. General synthetic procedure

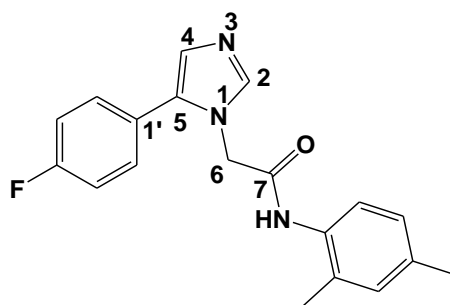
To a solution of the 2-(5-(4-fluorophenyl)-1*H*-imidazol-1-yl)acetohydrazide (1 molar equivalent) in 1M HCl (40 ml) was added dropwise a solution of NaNO₂ (1 molar equivalent) in H₂O (20 ml) at 0°C over a period of 15 minutes. After stirring for 20 minutes at the same temperature, the mixture was neutralized with saturated aqueous NaHCO₃ and then an aniline derivative (3 molar equivalents) in THF (40 ml) was added to the mixture at 0°C over a period of 20 minutes. After stirring for 3 hours at the same temperature, THF was evaporated *in vacuo*. The crude material was separated by column chromatography [elution with ethyl acetate: hexane (1:7), followed by 100% ethyl acetate: hexane] to afford pure products with *R_f* value of 0.5-1.0 in ethyl acetate: hexane (1:1).

8.4.8.2. 2-(5-(4-Fluorophenyl)-1H-imidazol-1-yl)-N-(2,4-dimethoxyphenyl)acetamide 128a



2-(5-(4-Fluorophenyl)-1H-imidazol-1-yl)-N-(2,4-dimethoxyphenyl)acetamide **128a** was successfully synthesized using 2-(5-(4-fluorophenyl)-1H-imidazol-1-yl)acetohydrazide **125a** (343 mg, 1.38 mmol) and 2,4-dimethoxyaniline (634 mg, 4.14 mmol) as described by the general procedure; **Physical characteristics:** light brown solid; **Yield:** 309 g, 63%; **¹H NMR** (400 MHz, CDCl₃) δ 8.02 (1H, d, *J* = 8.8 Hz, ArH), 8.01 (1H, s, NH), 7.76 (1H, s, 2-CH), 7.31-7.35 (2H, m, ArH), 7.16 (1H, s, ArH), 6.98 (2H, t, *J* = 8.8 Hz, ArH), 6.43 (2H, d, *J* = 8.0 Hz, ArH), 4.74 (2H, s, NCH₂), 3.72 and 3.78 (6H, 2 x s, 2 x ArOCH₃); **¹³C NMR** (101 MHz, CDCl₃) δ 164.2 (C=O), 162.9 (d, ¹*J*_{CF} = 253 Hz, *para*-CF), 157.2 and 149.6 (2 x ArCOCH₃), 138.9 (2-C), 132.5 (5-C), 130.9 (d, ³*J*_{CF} = 8 Hz, *ortho*-C), 128.1 (ArC), 124.5 (d, ⁴*J*_{CF} = 4 Hz, 1'-C), 121.1, 119.5 (ArC), 115.9 (d, ²*J*_{CF} = 22 Hz, *meta*-C), 103.7, 98.6 (ArC), 55.7 and 55.5 (2 x ArCOCH₃), 48.8 (6-C);

8.4.8.3. 2-(5-(4-Fluorophenyl)-1H-imidazol-1-yl)-N-(2,4-dimethylphenyl)acetamide 128b



2-(5-(4-Fluorophenyl)-1H-imidazol-1-yl)-N-(2,4-dimethylphenyl)acetamide **128b** was successfully synthesized using 2-(5-(4-fluorophenyl)-1H-imidazol-1-yl)acetohydrazide **125a** (335 mg, 1.35 mmol) and 2,4-dimethylaniline (491 mg, 4.05 mmol) as described by the general procedure; **Physical characteristics:** brown solid; **Yield:** 253 mg, 58%; **¹H NMR** (400 MHz, CDCl₃) δ 8.03 (1H, s, NH), 7.69 (1H, s, 2-CH), 7.34-7.40 (3H, m, ArH), 7.09-7.15 (3H, m, ArH), 6.92 (2H, s, ArH), 4.88 (2H, s, NCH₂), 2.24 and 1.97 (6H, 2 x s, 2 x ArCH₃); **¹³C NMR** (101 MHz, CDCl₃) δ 164.9 (C=O), 163.1 (d, ¹*J*_{CF} = 250 Hz, *para*-CF), 138.8 (2-C), 136.0 (ArC) 131.6 (5-C), 131.09,

130.9 (d, ${}^3J_{\text{CF}} = 8 \text{ Hz}$, *ortho*-C), 130.1, 128.8, 127.3, 127.1 (ArC), 123.5 (d, ${}^4J_{\text{CF}} = 4 \text{ Hz}$, 1²-C), 116.4 (ArC), 115.9 (d, ${}^2J_{\text{CF}} = 22 \text{ Hz}$, *meta*-C), 48.9 (6-C), 20.8 and 17.4 (2 x ArCCH₃).

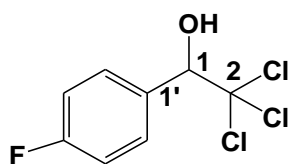
8.5. Chapter 5 experimental procedures

8.5.1. Synthesis of 2,2,2-trichloro-1-arylethanol

8.5.1.1. General synthetic procedure

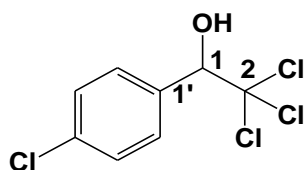
To mixture of benzaldehyde (1 molar equivalent) and chloroform (3 molar equivalent) was added dropwise DBU (1 molar equivalent) under argon. The reaction was stirred for 4-48 hours and then diluted with chloroform (40 mL) and washed with 2M HCl (3 x 10 ml). The organic phase was then dried over MgSO₄ and evaporated to produce 2,2,2-trichloro-1-arylethanone derivatives as enantiomer.

8.5.1.2. 2,2,2-Trichloro-1-(4-fluorophenyl)ethanol **132a**



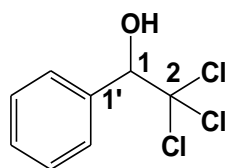
2,2,2-Trichloro-1-(4-fluorophenyl)ethanol **132a** was successfully synthesized from 4-fluorobenzaldehyde (770 mg, 6.20 mmol) and chloroform (1.5 ml, 18.60 mmol) according to the general procedure; **Physical characteristics:** brown oil; **Yield:** 1.42 g, 94%; **¹H NMR** (400 MHz, CDCl₃): δ 7.12 (2H, m, Hz, ArH), 7.02 (2H, t, *J* = 8.8 Hz, ArH), 5.24 (1H, s, 1-CH), 3.44 (1H, s, OH); **¹³C NMR** (101 MHz, CDCl₃): δ 163.9 (d, ¹*J*_{CF} = 250 Hz, *para*-CF), 132.6 (d, ⁴*J*_{CF} = 3 Hz, 1'-C), 129.5 (d, ³*J*_{CF} = 9 Hz, *ortho*-C) 115.7 (d, ²*J*_{CF} = 22 Hz, *meta*-C), 103.6 (2-C), 84.8 (1-C); **FTIR** *v*_{max}/cm⁻¹ (KBr): 3447 (OH), 3117, 3082, 1700, 1605, 1510, 1378, 1228, 1160, 1069, 827, 647, 564.

8.5.1.3. 2,2,2-Trichloro-1-(4-chlorophenyl)ethanol **132b**



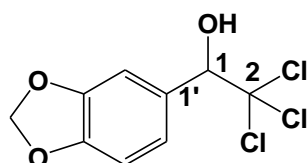
2,2,2-Trichloro-1-(4-chlorophenyl)ethanol **132b** was successfully synthesized from 4-chlorobenzaldehyde (486 mg, 3.46 mmol) and chloroform (0.85 ml, 10.38 mmol) according to the general procedure; **Physical characteristics:** colourless oil; **Yield:** 792 mg, 88%; **¹H NMR** (400 MHz, CDCl₃) δ 7.61-7.64 (2H, m, ArH), 7.38-7.42 (2H, m, ArH), 5.21 (1H, s, 1-CH), 3.45 (1H, s, OH); **¹³C NMR** (101 MHz, CDCl₃) δ 134.8 (ArCCl), 129.4, 129.1, 127.8, 120.5 (ArC), 103.0 (2-C), 84.4 (1-C); **FTIR** *v*_{max}/cm⁻¹ (KBr): 3326 (OH), 3073, 2930, 1717, 1604, 1473, 1440, 1186, 1075, 1049, 1037, 754, 642, 547.

8.7.5.1.4. 2,2,2-Trichloro-1-phenylethanol **132c**



2,2,2-Trichloro-1-phenylethanol **132c** was successfully synthesized from benzaldehyde (533 mg, 5.02 mmol) and chloroform (1.20 ml, 15.06 mmol) according to the general procedure; **Physical characteristics:** colourless oil; **Yield:** 1.05 g, 93%; **Melting point:** 34-37°C (lit.³⁵⁹); **¹H NMR** (400 MHz, CDCl₃) δ 7.61-7.64 (2H, m, ArH), 7.38-7.42 (3H, m, ArH), 5.21 (1H, s, 1-CH), 3.45 (1H, s, OH); **¹³C NMR** (101 MHz, CDCl₃) δ 134.8, 129.4, 129.1, 120.6 (ArC), 103.0 (2-C), 84.4 (1-C); **FTIR** $\nu_{\max}/\text{cm}^{-1}$ (KBr): 3426 (OH), 3065, 3034, 1701, 1595, 1586, 1494, 1454, 1388, 1091, 1194, 778, 644, 523.

8.5.1.5. 1-(Benzo[*d*][1,3]dioxol-6-yl)-2,2,2-trichloroethanol **132d**



1-(Benzo[*d*][1,3]dioxol-6-yl)-2,2,2-trichloroethanol **132d** was successfully synthesized from piperonal (800 mg, 5.33 mmol) and chloroform (1.30 ml, 15.99 mmol) according to the general procedure; **Physical characteristics:** pale yellow oil; **Yield:** 1.38 g, 96%; **¹H NMR** (400 MHz, CDCl₃) δ 7.19 (1H, d, s, ArH), 7.05 (1H, d, *J* = 8.0 Hz, ArH), 6.80 (1H, d, *J* = 8.0 Hz, ArH), 5.98 (2H, s, ArOCH₂O-), 5.13 (1H, s, 1-CH), 3.40 (1H, s, OH); **¹³C NMR** (101 MHz, CDCl₃) δ 148.5 and 147.2 (ArCOCH₂O), 128.5, 123.5, 109.2, 107.5, (ArC), 103.3 (2-C), 101.3 (ArCOCH₂O), 84.2 (1-C); **FTIR** $\nu_{\max}/\text{cm}^{-1}$ (KBr): 3500 (OH), 3304, 2899, 1607, 1503, 1489, 1445, 1260, 1039, 870, 919, 755, 654, 547.

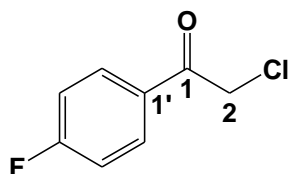
8.5.2. Synthesis of 2-chloro-1-arylethanone by oxidation

8.5.2.1. General synthetic procedure

In a three-necked flame dried round bottomed flask equipped with a refluxing condenser was created an oxygen free environment by degassing through evacuating and refilling with argon three times. The flask was charged with 2,2,2-trichloro-1-arylethanone (1 molar equivalent), CuCl (2 molar equivalents) and dry 1,2-dichloroethane (DCE) (10 ml). The resulting reaction mixture was stirred with a magnetic stirrer bar and a solution of 2,2'-bipyridine (2 molar equivalents) in DCE (10 ml) was added. The reaction mixture was heated at reflux for 8 hours (the progress of

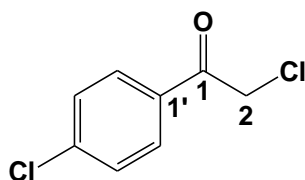
the reaction was monitored by TLC). The reaction mixture was then cooled and filtered through a celite pad and the filtrate was evaporated under reduced pressure. The crude product was purified by flash column chromatography on a short silica gel column using a mixture of ethyl acetate and hexane as the solvent for elution to afford 2-chloro-1-aryl-ethanones.

8.5.2.2. 2-Chloro-1-(4-fluorophenyl)ethanone **133a**



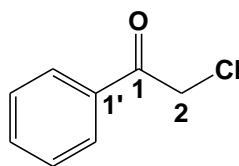
2-Chloro-1-(4-fluorophenyl)ethanone **133a** was successfully synthesized from (*R*)-2,2,2-trichloro-1-(4-fluorophenyl)ethanol **132a** (170 mg, 0.70 mmol), CuCl (188 mg, 1.40 mmol) and bipyridine (219 mg, 1.40 mmol) in DCE (10 ml) according to the general procedure; **Physical characteristics**: white solid; **Yield**: 112 mg, 66%; **Melting point**: 47-49°C (lit.³⁶⁰); **¹H NMR** (400 MHz, CDCl₃) δ 7.12-7.68 (2H, m, ArH), 7.02-7.09 (2H, t, *J* = 8.8 Hz, ArH), 4.56 (2H, s, 2-CH); **¹³C NMR** (101 MHz, CDCl₃) δ 164.1 (d, ¹*J*_{CF} = 250 Hz, *para*-CF), 159.1 (C=O) 132.6 (d, ⁴*J*_{CF} = 3 Hz, 1'-C), 129.8 (d, ³*J*_{CF} = 9 Hz, *ortho*-C) 115.5 (d, ²*J*_{CF} = 22 Hz, *meta*-C); **FTIR** ν_{\max} /cm⁻¹ (KBr): 3366, 29995, 2947, 1706 (C=O), 1697, 1593, 1507, 1413, 1212, 1159, 1101, 1003, 830, 817, 790, 590, 557.

8.5.2.3. 2-Chloro-1-(4-chlorophenyl)ethanone **133b**



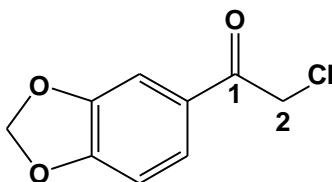
2-Chloro-1-(4-chlorophenyl)ethanone **133b** was successfully synthesized from (*R*)-2,2,2-trichloro-1-(4-chlorophenyl)ethanol **132b** (164 mg, 0.63 mmol), CuCl (169 mg, 1.26 mmol) and bipyridine (187 mg, 1.26 mmol) in DCE according to the general procedure; **Physical characteristics**: white solid; **Yield**: 98 mg, 60%; **Melting point**: 100-103°C (lit.^{361,362}); **¹H NMR** (400 MHz, CDCl₃) δ 7.84 (2H, m, ArH), 7.45-7.48 (2H, m, ArH), 4.66 (2H, s, 2-CH₂); **¹³C NMR** (101 MHz, CDCl₃) δ 189.0 (C=O), 140.5, 132.4, 129.9, 129.2 (ArC), 45.6 (2-C); **FTIR** ν_{\max} /cm⁻¹ (KBr): 3360, 3066, 2954, 1736 (C=O), 1693, 1590, 1483, 1396, 1313, 1213, 1034, 1000, 782, 526.

8.5.2.4. 2-Chloro-1-phenylethanone 133c



2,2,2-Chloro-1-(4-chlorophenyl)ethanone **133c** was successfully synthesized from (*R*)-2,2,2-trichloro-1-phenylethanol (717 mg, 3.18 mmol), CuCl (855 mg, 6.36 mmol) and bipyridine 993 mg, (6.36 mmol) in DCE (15 ml) according to the general procedure; **Physical characteristics:** pale yellow solid; **Yield:** 384 mg, 54%; **Melting point:** 55-58°C (lit.³⁶³); **¹H NMR** (400 MHz, CDCl₃) δ 7.90-7.96 (2H, m, ArH), 7.59-7.64 (1H, m, ArH), 7.48-7.751 (2H, m, ArH), 4.72 (2H, s, 2-CH₂); **¹³C NMR** (101 MHz, CDCl₃) δ 191.0 (C=O), 133.9, 133.2, 128.9, 128.5 (ArC), 46.0 (2-C); **FTIR** $\nu_{\max}/\text{cm}^{-1}$ (KBr): 33373, 3036, 2994, 1701 (C=O), 1596, 1581, 1449, 1399, 1329, 1212, 1099, 1000, 905, 789, 758, 686, 559.

8.5.2.5. 1-(Benzo[*d*][1,3]dioxol-6-yl)-2-chloroethanone 133d



1-(Benzo[*d*][1,3]dioxol-6-yl)-2-chloroethanone **133d** was successfully synthesized from (*R*)-1-(benzo[*d*][1,3]dioxol-6-yl)-2,2,2-trichloroethanol (2.27 g, 7.66 mmol), CuCl (2.06 g, 15.32 mmol) and bipyridine (2.39 g, 15.3 mmol) in DCE (30 ml) according to the general procedure; **Physical characteristics:** pale yellow solid; **Yield:** 365 mg, 24%; **Melting point:** 88-90°C (lit.³⁶⁴); **¹H NMR** (400 MHz, CDCl₃): δ 7.19 (1H, s, ArH), 7.05 (1H, d, *J* = 8.4 Hz, ArH), 6.80 (1H, d, *J* = 8.4 Hz, ArH), 5.98 (2H, s, ArOCH₂O-), 4.72 (2H, s, 2-CH₂); **¹³C NMR** (101 MHz, CDCl₃) δ 148.5 and 147.2 (ArCOCH₂O), 134.8, 129.4, 129.1, 127.8 (ArC), 101.4 (ArCOCH₂O-), 46.0 (2-C); **FTIR** $\nu_{\max}/\text{cm}^{-1}$ (KBr): 3356, 3065, 2900, 2791, 1686 (C=O), 1503, 1488, 1448, 1401, 1355, 1283, 1261, 1209, 1098, 1037, 927, 810, 784, 688, 643, 558.

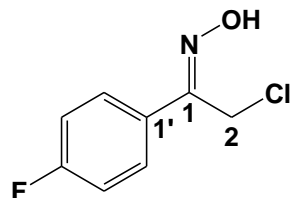
8.5.3. Synthesis of 2-chloro-1-arylethanone oxime

8.5.3.1. General synthetic procedure

To a solution of 2-chloro-1-arylethanone (1 molar equivalent) in methanol (20 ml) and water (5 ml) was added NH₂OH.HCl (3 molar equivalents) at room temperature. The homogenous clear solution was allowed to stir for 12 hours prior to concentration *in vacuo*. The resulting solids were dissolved in water (3 ml) and extracted with CHCl₃ (3 x 10 ml), the organic layer was dried over

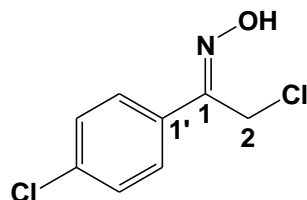
MgSO₄ and concentrated *in vacuo*. The resulting solids were washed with hexanes (3 x 5 ml) and dried under high vacuum to yield (*E*) - and (*Z*) isomers of 2-chloro-1-aryl-ethanone oximes.

8.5.3.2. (*E/Z*)-2-Chloro-1-(4-fluorophenyl)ethanone oxime **129a**



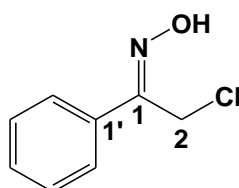
(*E/Z*)-2-Chloro-1-(4-fluorophenyl)ethanone oxime **129a** was successfully synthesized from 2-chloro-1-(4-fluorophenyl)ethanone **133a** (1.86 g, 7.70 mmol) and NH₂OH.HCl (1.61 g, 23.10 mmol) in MeOH (30 ml) and water (4 ml) according to the general procedure; **Physical characteristics**: pale yellow solid; **Yield**: 1.86 g, 94%; **¹H NMR** (400 MHz, CDCl₃) δ 9.25 and 8.95 (1H, s, OH), 7.99-8.02 and 7.66-7.69 (2H, m, ArH), 7.62-7.64 and 7.09-7.60 (2H, m, ArH), 4.60 and 4.45 (2H, s, 2-CH₂); **¹³C NMR** (101 MHz, CDCl₃) δ 162.6 & 162.0 (d, ¹J_{CF} = 250 Hz, *para*-CF), 130.7 and 131.4_r (d, ⁴J_{CF} = 3 Hz, 1'-C), 129.3 and 128.2 (d, ³J_{CF} = 9 Hz, *ortho*-C), 115.7 and 115.5 (d, ¹J_{CF} = 22 Hz, *meta*-C), 44.6 and 32.2 (2-C); **FTIR** ν_{max}/cm⁻¹ (KBr): 3295 (OH), 3082, 2986, 2986, 1701 (C=O), 1686, 1571, 1508, 1413, 1401, 1314, 1284, 1209, 1159, 836, 589.

8.5.3.3. (*E/Z*)-2-Chloro-1-(4-chlorophenyl)ethanone oxime **129b**



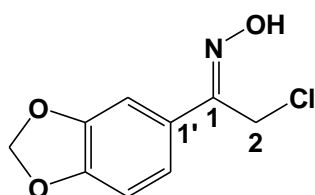
(*E/Z*)-2-Chloro-1-(4-chlorophenyl)ethanone oxime **129b** was successfully synthesized from 2-chloro-1-(4-chlorophenyl)ethanone **133b** (2.77 g, 10.70 mmol) and NH₂OH.HCl (2.23 g, 32.10 mmol) in MeOH (18 ml) and water (2.5 ml) according to the general procedure; **Physical characteristics**: yellow solid; **Yield**: 2.72 g, 93%; **¹H NMR** (400 MHz, CDCl₃): δ 9.41 and 9.11 (1H, s, OH), 7.89-7.91 and 7.61 (2H, d, *J* = 8.4 Hz each, ArH), 7.55-7.57 and 7.38-7.41 (2H, m, ArH), 4.59 and 4.44 (2H, s, 2-CH₂); **¹³C NMR** (101 MHz, CDCl₃) δ 153.5 and 152.9 (C=NOH), 136.1, 136.6, 129.9, 129.0, 127.5, 128.72, 122.6, 122.7 (ArC), 44.5 and 32.1 (2-C); **FTIR** ν_{max}/cm⁻¹ (KBr): 3360 (OH), 3000, 2947, 1686, 1589, 1570, 1448, 1489, 1314, 1297, 1211, 1093, 1013, 833, 818, 766, 588.

8.5.3.4. (*E/Z*)-2-Chloro-1-phenylethanone oxime **129c**



(*E/Z*)-2-Chloro-1-phenylethanone oxime **129c** was successfully synthesized from 2-chloro-1-(4-chlorophenyl)ethanone (1.77 g, 7.93 mmol) and $\text{NH}_2\text{OH}\cdot\text{HCl}$ (1.65 g, 23.79 mmol) in MeOH (20 ml) and water (3 ml) according to the general procedure; **Physical characteristics**: pale yellow solid; **Yield**: 1.66 g, 88%; **Melting point**: 78-79 °C; **$^1\text{H NMR}$** (400 MHz, CDCl_3) δ 8.26 (1H, br, OH), 7.96-7.98 and 7.69-7.71 (2H, m, ArH), 7.58-7.60 and 7.43-7.47 (3H, m, ArH), 4.63 and 4.46 (2H, s, 2- CH_2); **$^{13}\text{C NMR}$** (101 MHz, CDCl_3) δ 154.3 & 153.9 ($\text{C}=\text{NOH}$), 134.0, 133.2, 130.3, 130.0, 128.8, 128.7, 128.3, 126.2 (ArC), 44.7 and 32.3 (2-C); **FTIR** $\nu_{\text{max}}/\text{cm}^{-1}$ (KBr): 3226 (OH), 3060, 2986, 2917, 1700, 1604, 1569, 1449, 1326, 1314, 1264, 960, 917, 766, 692, 527.

8.3.5.5. (*E/Z*)-1-(Benzo[*d*][1,3]dioxol-6-yl)-2-chloroethanone oxime **129d**



(*E/Z*)-1-(Benzo[*d*][1,3]dioxol-6-yl)-2-chloroethanone oxime **129d** was successfully synthesized from 2-chloro-1-(4-chlorophenyl)ethanone (238 mg, 0.89 mmol) and $\text{NH}_2\text{OH}\cdot\text{HCl}$ (186 mg, 2.67 mmol) in MeOH (1.5 ml) and water (0.2 ml) according to the general procedure; **Physical characteristics**: white solid; **Yield**: 236 mg, 94%; **$^1\text{H NMR}$** (400 MHz, $\text{DMSO}-d_6$): δ 11.9, 11.8 (1H, s, OH), 7.19-7.23 (2H, m, ArH), 6.95-6.97 (1H, m, ArH), 6.06 and 6.05 (2H, s, ArOCH_2O), 4.67 and 4.61 (2H, s, 2- CH_2); **$^{13}\text{C NMR}$** (101 MHz, $\text{DMSO}-d_6$): δ 151 ($\text{C}=\text{NOH}$), 148.2 and 147.7 (2 x ArCOCH_2O), 127.7, 120.3, 108.2, 105.6 (ArC), 101.4 (ArCOCH_2O), 32.0 (2-C); **FTIR** $\nu_{\text{max}}/\text{cm}^{-1}$ (KBr): 3269 (OH), 3008, 2908, 1717, 1604, 1501, 1455, 1308, 1270, 1252, 1231, 1037, 953, 818, 569.

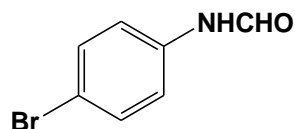
8.5.4. Synthesis of *N*-aryl formamide

8.5.4.1. General synthetic procedure

A mixture of an aniline (1 molar equivalent) and formic acid (10 molar equivalents) was placed in a 35 ml microwave vessel and then capped. This mixture was irradiated using standard method at 110°C for 1 hour. TLC monitored the progress of the reaction. After completion of the reaction,

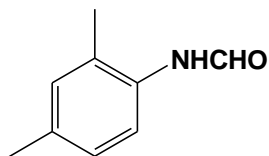
ethyl acetate (10 ml) was added and mixture was washed with water (3 x 5 ml) and the organic layer dried over anhydrous MgSO_4 and then filtered. The ethyl acetate was evaporated under vacuum to afford *N*-formylated aryl amines. The presence of rotamers was evident from the ^1H and ^{13}C NMR spectra.

8.5.4.2. *N*-(4-Bromophenyl)formamide **139a**



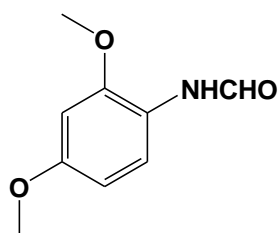
N-(4-Bromophenyl)formamide **139a** was successfully synthesized from 4-bromoaniline (433 mg, 2.52 mmol) and formic acid (0.85 ml, 25.20 mmol) according to the general procedure; **Physical characteristics:** pale yellow solid; **Yield:** 464 mg, 92%; **Melting point:** 118-120°C (lit.³⁶⁵); **^1H NMR** (400 MHz, CDCl_3) δ 8.68_{major} (0.7H, s, CHO), 8.36_{minor} (0.3H, s, CHO), 7.96_{minor} (0.3H, br, NH), 7.95_{minor} (0.3H, d, $J=2.4$ Hz, ArH), 7.047_{major} (0.7H, br, NH), 7.011-7.32 (3.7H, m, ArH); **^{13}C NMR** (101 MHz, CDCl_3): δ 162.6_{major} and 159.2_{minor} (CHO), 134.1, 133.7, 132.8, 132.1, 121.6, 120.3, 118.9, 117.7 (ArC *both major and minor*).

7.5.4.3. *N*-(2,4-Dimethylphenyl)formamide **139b**



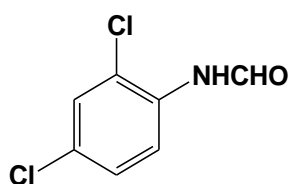
N-(2,4-Dimethylphenyl)formamide **139b** was successfully synthesized from 2,4-dimethylaniline (2.07 g, 48.50 mmol) and formic acid (18 ml, 485.00 mmol) according to the general procedure; **Physical characteristics:** pale yellow solid; **Yield:** 5.72 g, 79%; **Melting point:** 115-117 °C (lit.³⁶⁶); **^1H NMR** (400 MHz, CDCl_3) δ 8.54_{major} (0.6H, d, $J= 11.6$ Hz, CHO), 8.39_{minor} (0.4 H, s, CHO), 7.96_{major} (0.6H, br, NH), 7.95_{minor} (0.4H, d, $J=2.4$ Hz, ArH), 7.17_{minor} (0.4H, br, NH), 7.011-7.32_{overlapping major and minor} (2.6H, m, ArH), 2.30 & 2.26_{major} and 2.29 & 2.23_{minor} (2 x ArCH₃); **^{13}C NMR** (101 MHz, CDCl_3) δ 163.5_{major} and 159.2_{minor} (2-CHO), 135.9, 135.3, 132.4, 131.9, 131.8, 131.2, 130.0, 129.9, 127.5, 20.8, 20.7 (ArC *both major and minor*), 20.8, 20.7, 17.6, 17.5 (ArCCH₃ *both major and minor*);

8.5.4.4. *N*-(2,4-Dimethoxyphenyl)formamide **139c**



N-(2,4-Dimethoxyphenyl)formamide **139c** was successfully synthesized from 2,4-dimethoxyaniline (5.33 g, 34.8 mmol) and formic acid (13 ml, 348.00 mmol) according to the general procedure; **Physical characteristics:** pale yellow solid; **Yield:** 4.67 g, 74%; **¹H NMR** (400 MHz, CDCl₃) δ 8.54_{major} (0.3H, dd, *J*= 11.8 Hz, CHO), 8.39_{minor} (0.7H, d, *J*= 11.8 Hz, CHO), 8.24_{major} (0.7H, d, *J*= 8.4 Hz, ArH), 7.62_{minor} (0.7H, br, NH), 7.45_{major} (0.3H, br, NH), 7.08_{minor} (1.3H, d, *J*= 8.8 Hz, ArH) 6.45-6.51_{overlapping major and minor signals} (2H, m, ArH), 2.30 & 2.26_{major} and 2.29 & 2.23_{minor} (6H, 2 x s, ArOCH₃); **¹³C NMR** (101 MHz, CDCl₃) δ 162.1_{major} and 158.4_{minor} (CHO), 158.1, 156.7, 150.9 and 149.1 (ArCOCH₃ both major and minor), 121.2, 120.3, 119.3, 119.2, 104.1, 103.7, 99.5, 98.7 (ArC both major and minor), 55.7, 55.5 and 55.1 (ArCOCH₃ for both major and minor).

8.5.4.5. *N*-(2,4-Dichlorophenyl)formamide **139d**



N-(2,4-Dichlorophenyl)formamide **139d** was successfully synthesized from 2,4-dichloroaniline (5.70 g, 35.20 mmol) and formic acid (13 ml, 353.00 mmol) according to the general procedure; **Physical characteristics:** pale yellow solid; **Melting point:** 157-158°C (lit.³⁶⁷); **Yield:** 5.55 g, 83%; **¹H NMR** (400 MHz, CDCl₃) δ 8.73_{major} (0.2H, dd, *J*= 11.6 Hz, NH), 8.51_{major and minor} (2H, s, CHO and ArH), 7.74_{minor} (0.8, br, NH), 7.07-7.03_{overlapping major and minor signals} (2H, m, ArH); **¹³C NMR** (101 MHz, CDCl₃) δ 160.9_{major} and 158.7_{cis} (CHO), 134.4, 133.7, 131.1, 129.7, 125.7, 125.1, 122.1, 121.7, 120.5, 118.3 (ArC both major and minor).

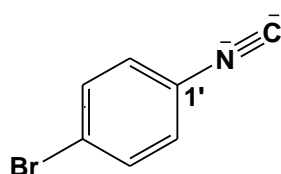
8.5.5. Dehydration of *N*-arylformamide

8.5.5.1. General synthetic procedure

To a suspension of *N*-formylated aryl formamide (1 molar equivalent) and triethylamine (3 molar equivalents) in DCM (10 ml) was added dropwise phosphoryl chloride (1.2 molar equivalents) at 5-10°C over a period of 30 min. After stirring for 2 hours at room temperature, 25 % aqueous Na₂CO₃ (80 ml) was added to the reaction mixture under ice cooling and the DCM layer was

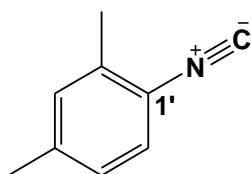
separated. The aqueous layer was extracted with DCM. The combined organic layer was washed with water, dried over MgSO_4 , and then evaporated *in vacuo* to obtain crude product, which was subjected to column chromatography [eluting with hexane and EtOAc (1:1)] to furnish pure aryl isocyanide.

8.5.5.2. 1-Isocyano-4-bromobenzene **130a**



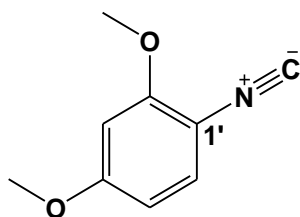
1-Isocyano-4-bromobenzene **130a** was successfully synthesized from *N*-(4-bromophenyl)formamide **139a** (1.50 g, 7.50 mmol); triethylamine (2.28 g, 22.5 mmol) and phosphoryl chloride (1.08 g, 9.00 mmol) in DCM (20 ml) according to the general procedure; **Physical characteristics**: pale yellow solid; **Yield**: 1.28 g, 94%; **Melting point**: 96-98°C (lit.³⁶⁸); **¹H NMR** (400 MHz, CDCl_3): δ 7.16 (2H, d, J = 8.8 Hz, ArH); 6.34 (2H, d, J = 8.8 Hz, ArH), **¹³C NMR** (101 MHz, CDCl_3): δ 165.7 (NC), 133.1, 131.6, 16.8, 124.5 (ArC).

8.5.5.3. 1-Isocyano-2,4-dimethylbenzene **130b**



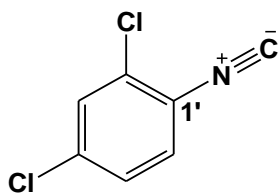
1-Isocyano-2,4-dimethylbenzene **130b** was successfully synthesized from *N*-(2,4-dimethylphenyl)formamide **139b** (701 mg, 4.70 mmol); triethylamine (1.43 g, 14.10 mmol) and phosphoryl chloride (657 mg, 5.64 mmol) in DCM (10 ml) according to the general procedure; **Physical characteristics**: Pale yellow solid; **Yield**: 573 mg, 93%; **Melting point**: 55-58°C (lit.³⁶⁹); **¹H NMR** (400 MHz, CDCl_3) δ 7.19 (1H, d, J = 8.4 Hz, ArH), 7.06 (1H, s, ArH), 6.99 (2H, d, J = 8.4 Hz, ArH), 2.37 and 2.33 (3H, 2 x s, 2 x ArCH₃); **¹³C NMR** (101 MHz, CDCl_3) δ 164.8 (t, J = 6 Hz, NC), 139.4, 134.5, 131.0, 127.2, 126.1 (ArC), 123.9 (t, J = 13 Hz, 1'-C), 21.1 and 18.3 (2 x ArCCH₃).

8.5.5.4. 1-Isocyano-2,4-dimethoxybenzene **130c**



1-Isocyano-2,4-dimethoxybenzene **130c** was successfully synthesized from *N*-(2,4-dimethoxyphenyl)formamide **139c** (1.12 g, 6.20 mmol); triethylamine (1.88 g, 18.60 mmol) and phosphoryl chloride (866 mg, 7.44 mmol) in DCM (15 ml) according to the general procedure; **Physical characteristics:** pink solid; **Yield:** 890 mg, 88%; **Melting point:** 67-69°C (lit.³⁷⁰); **¹H NMR** (400 MHz, CDCl₃): δ 7.25 (1H, d, *J* = 8.8 Hz, ArH), 6.39-6.46 (2H, overlapping doublet and singlet, ArH), 3.88 and 3.81 (6H, 2 x s, 2 x ArOCH₃); **¹³C NMR** (101 MHz, CDCl₃) δ 165.72 (NC), 161.1 and 156.1 (2 x ArCOCH₃), 128.3, 109.5, 104.5 (ArC), 55.9 and 55.6 (2 x ArCOCH₃).

8.5.5.5. 1-Isocyano-2,4-dichlorobenzene **130d**



1-Isocyano-2,4-dichlorobenzene **130d** was successfully synthesized from *N*-(2,4-dichlorophenyl)formamide **133d** (437 mg, 2.30 mmol); triethylamine (698 mg, 6.90 mmol) and phosphoryl chloride (320 mg, 2.75 mmol) in DCM according to the general procedure; **Physical characteristics:** pale yellow solid; **Yield:** 371 mg, 94%; **¹H NMR** (400 MHz, CDCl₃): δ 7.33 (1H, s, ArH), 7.48 (2H, m, ArH); **¹³C NMR** (101 MHz, CDCl₃) δ 164.8 (t, *J* = 6 Hz, NC), 139.4, 134.5, 131.0, 127.2, 126.1, 123.9 (t, *J* = 13 Hz, 1'-C).

8.5.6. Synthesis of 3-aryl-*N*-substituted-isoxazol-5-amine derivatives

8.5.6.1. General synthetic procedure: method A

To a solution of 1-chloro-1-arylethanone oxime intermediates (1 molar equivalent) in dry CH₂Cl₂ (10 ml) was added the isocyanide (2 molar equivalents). The reaction mixture was stirred at room temperature for 24 hours (monitored by TLC). Upon completion, water was added and the crude material was extracted with CH₂Cl₂ (2 x 10ml). The combine organic layers were dried over MgSO₄ and concentrated *in vacuo* and the product separated by column chromatography.

8.5.6.2. General synthetic procedure: method B

To a solution of 1-chloro-1-arylethanone oxime intermediates (1 molar equivalent) in dry CH_2Cl_2 (10 ml) was added the isocyanide (2 molar equivalents) and Na_2CO_3 (4 molar equivalent). The reaction mixture was stirred at room temperature for 24 hours (monitored by TLC). Upon completion, water was added and the crude material was extracted with CH_2Cl_2 (2 x 10ml). The combine organic layers were dried over MgSO_4 and concentrated *in vacuo* and the product separated by column chromatography

8.5.6.3. General synthetic procedure: method C

To a solution of 1-chloro-1-aryl-ethanone oxime intermediates (1 molar equivalent) in dry CH_2Cl_2 (10 ml) was added the isocyanide (2 molar equivalents) and $\text{NaOAc}\cdot\text{H}_2\text{O}$ (4 molar equivalents). The reaction mixture was stirred at room temperature for 7 days (monitored by TLC). Upon completion, water was added and the crude material was extracted with CH_2Cl_2 (2 x 10ml). The combine organic layers were dried over MgSO_4 and concentrated *in vacuo* and the product separated by column chromatography

8.5.6.4. General synthetic procedure: method D

To a solution of 1-chloro-1-aryl-ethanone oxime intermediates (1 molar equivalent) in dry CH_2Cl_2 (10 ml) was added the isocyanide (2 molar equivalents) and K_2CO_3 (4 molar equivalents). The reaction mixture was stirred at room temperature for 5 days (monitored by TLC). Upon completion, water was added and the crude material was extracted with CH_2Cl_2 (2 x 10ml). The combine organic layers were dried over MgSO_4 and concentrated *in vacuo* and the product separated by column chromatography.

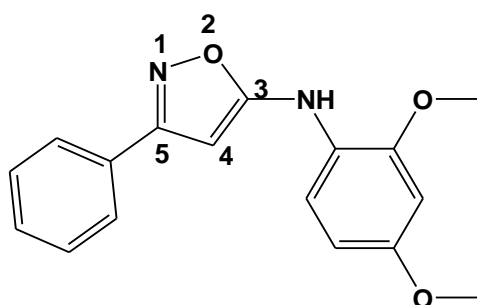
8.5.6.5. General synthetic procedure: method E

To a solution of -chloro-1-aryl-ethanone oxime intermediates (1 molar equivalent) in dry CH_2Cl_2 (10 ml) was added the isocyanide (2 molar equivalents) and Cs_2CO_3 (4 molar equivalents). The reaction mixture was stirred at room temperature for 1 hour (monitored by TLC). Upon completion, water was added and the crude material was extracted with CH_2Cl_2 (2 x 10ml). The combine organic layer was dried over MgSO_4 and concentrated *in vacuo* and the product separated by column chromatography

8.5.6.6. General synthetic procedure: method F

A solution of 1-chloro-1-arylethanone oxime intermediates (1 molar equivalent) in dry CH_2Cl_2 (10 ml) was cooled to -10°C , followed by addition of the isocyanide (2 molar equivalent) and Na_2CO_3 (4 molar equivalent). The reaction mixture was stirred at THE same temperate for 2 hours, followed by additional stirring at room temperature for 24 hours (monitored by TLC plate). Upon completion, water was added and the crude material was extracted with CH_2Cl_2 (2 x 10ml). Combine organic layer was dried over MgSO_4 and concentrated *in vacuo* and the product was separated by column chromatography

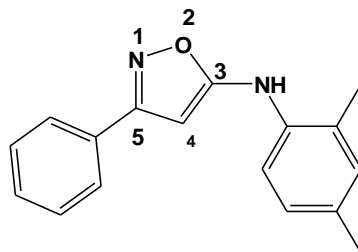
8.5.6.7. N-(2,4-Dimethoxyphenyl)-3-phenylisoxazol-5-amine 131a



N-(2,4-Dimethoxyphenyl)-3-phenylisoxazol-5-amine **131a** was successfully synthesized as described by the general procedure **B** {2-chloro-1-phenylethanone oxime **129c** (562 mg, 1.18 mmol), 1-isocyano-2,4-dimethoxybenzene **130c** (385 mg, 2.36 mmol) and Na_2CO_3 (500 g, 4.72 mmol) in DCM (10 ml)}; synthetic procedure **C** {2-chloro-1-phenylethanone oxime **129c** (215 mg, 0.90 mmol), 1-isocyano-2,4-dimethoxybenzene **130c** (292 mg, 1.79 mmol) and $\text{NaOAc}\cdot\text{H}_2\text{O}$ (3.58 mmol) in DCM }; synthetic procedure **D** {2-chloro-1-phenylethanone oxime **129c** (141 mg, 0.59 mmol), 1-isocyano-2,4-dimethoxybenzene **130c** (193 mg, 1.18 mmol) and K_2CO_3 (326 mg, 2.36 mmol) in DCM (10 ml)}; synthetic procedure **E** {2-chloro-1-phenylethanone oxime **129c** (146 mg, 0.61 mmol), 1-isocyano-2,4-dimethoxybenzene **130c** (197 mg, 1.21 mmol) and Cs_2CO_3 (792 mg, 2.43 mmol) in DCM (10 ml)} and synthetic procedure **F** {2-chloro-1-phenylethanone oxime **129c** (162 mg, 0.68 mmol), 1-isocyano-2,4-dimethoxybenzene **130c** (222 mg, 1.36 mmol) and Na_2CO_3 (287 mg, 2.71 mmol) in DCM at -10°C }; **Physical characteristics:** brown oil; **Yield:** 42 mg, 12% for procedure **B**; 35 mg, 13% for procedure **C**; 19 mg, 11% for procedure **D**; 20 mg, 11% for procedure **E**; 24 mg, 12% for procedure **F**; **$^1\text{H NMR}$** (400 MHz, CDCl_3) δ 7.78 (1H, m, ArH), 7.32-7.45 (5H, m, ArH), 6.93 (1H, s, NH), 6.45-6.54 (2H, m, ArH), 5.8- (1H, s, 4-CH), 3.88 and 3.81 (6H, 2 x s, 2 x ArOCH_3); **$^{13}\text{C NMR}$** (101 MHz, CDCl_3) δ 166.4 (5-C), 163.5 (3-C), 155.7 and 149.4 (2 x ArCOCH_3), 129.7, 128.6, 126.6, 122.4, 120.5, 117.2, 103.9, 99.3 (ArC), 78.3 (4-C), 55.8 and 55.6 (2 x ArCOCH_3); **FTIR** $\nu_{\text{max}}/\text{cm}^{-1}$ (KBr): 3314

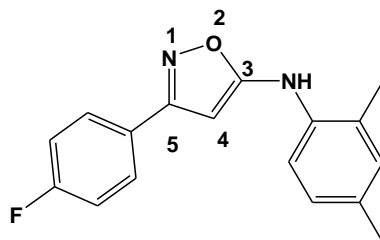
(NH), 3001, 2936, 2836, 1747, 1686, 1621, 1586, 1531, 1464, 1418, 1285, 1208, 1182, 1158, 1071, 1033, 948, 832, 730, 695.

8.5.6.8. *N*-(2,4-Dimethylphenyl)-3-phenylisoxazol-5-amine **131b**



N-(2,4-Dimethylphenyl)-3-phenylisoxazol-5-amine **131b** was successfully synthesized from 2-chloro-1-phenylethanone oxime **129c** (909 mg, 3.81 mmol), 1-isocyano-2,4-dimethylbenzene **130b** (1.00 g, 7.62 mmol) and Na₂CO₃ (1.62 g, 15.24 mmol) in DCM (15) according to the general procedure B; **Physical characteristics**: pale yellow solid; **Yield**: 201 mg, 20%; **¹H NMR** (400 MHz, CDCl₃) δ 7.68 (2H, d, *J* = 7.6 Hz, ArH), 7.35 (3H, m, ArH), 7.19 (1H, d, *J* = 8.4 Hz, ArH), 6.98 (2H, d, *J* = 7.2 Hz, ArH), 6.56 (1H, s, NH), 5.83 (1H, s, 4-CH), 2.55 and 2.50 (2 x ArCH₃); **¹³C NMR** (101 MHz, CDCl₃) δ 167.1 (5-C), 163.6 (3-C), 134.9, 133.9, 131.7, 129.7, 129.6, 128.7, 128.6, 127.6, 126.6, 120.1, 116.1 (ArC), 78.4 (4-C), 20.7 and 17.5 (ArCCH₃); **FTIR** $\nu_{\max}/\text{cm}^{-1}$ (KBr): 3268 (NH), 3143, 3021, 1632, 1612, 1581, 1525, 1487, 1416, 1292, 1263, 1219, 958, 811, 736, 692, 625.

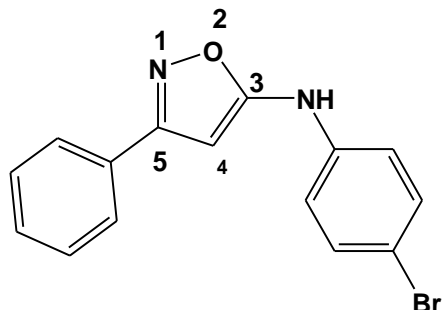
8.5.6.9. 3-(4-Fluorophenyl)-*N*-(2,4-dimethylphenyl)isoxazol-5-amine **131c**



3-(4-Fluorophenyl)-*N*-(2,4-dimethylphenyl)isoxazol-5-amine **13c** was successfully synthesized from 2-chloro-1-(4-fluorophenyl)ethanone oxime **129a** (1.58 g, 6.16 mmol), 1-isocyano-2,4-dimethylbenzene **130b** (1.62 g, 12.32 mmol) and Na₂CO₃ (2.61 g, 24.64 mmol) in DCM (20 ml) according to the general procedure B; **Physical characteristics**: pale yellow solid; **Yield**: 156 mg, 9%; **¹H NMR** (400 MHz, CDCl₃) δ 7.60 (2H, m, ArH), 7.12 (1H, *J* = 8.4 Hz, ArH), 6.92-7.00 (4H, m, ArH), 6.35 (1H, s, NH), 5.43 (1H, s, 4-CH), 2.21 and 2.15 (2 x ArCH₃); **¹³C NMR** (101 MHz, CDCl₃) δ 167.4 (5-C), 163.6 (d, ¹*J*_{CF} = 249 Hz, *para*-CF), 162.7 (3-C), 134.7, 131.7, 129.0, 128.4, 127.6, 125.8, 120.31, 120.5, 115.6 (ArC), 78.1 (4-C), 20.7 and 17.5 (2 x ArCCH₃);

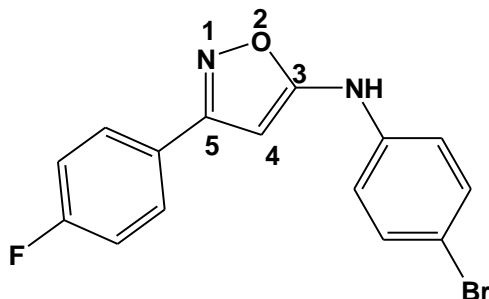
FTIR $\nu_{\max}/\text{cm}^{-1}$ (KBr): 3267 (NH), 3077, 2921, 1620, 1586, 1549, 1448, 1391, 1307, 1266, 1219, 1157, 1012, 952, 844, 827, 742, 609.

8.5.6.10. *N*-(4-Bromophenyl)-3-phenylisoxazol-5-amine **131d**



N-(4-Bromophenyl)-3-phenylisoxazol-5-amine **131d** was successfully synthesized from 2-chloro-1-phenylethanone oxime **129c** (157 mg, 0.66 mmol), 1-isocyano-4-bromobenzene **130a** (240 mg, 1.32 mmol) and Na_2CO_3 (278 mg, 2.64 mmol) in DCM (5 ml) according to the general procedure B; **Physical characteristics**: pale yellow solid; **Yield**: 23 mg, 11%; **$^1\text{H NMR}$** (400 MHz, $\text{DMSO}-d_6$) δ 10.2 (1H, s, NH), 7.85-7.88 (2H, m, ArH), 7.48-7.51 (5H, m, ArH), 7.21-7.23 (2H, m, ArH), 6.29 (1H, s, 4-CH); **$^{13}\text{C NMR}$** (101 MHz, $\text{DMSO}-d_6$) 155.4 (5-C), 162.7 (3-C), 139.2, 132.1, 129.9, 129.2, 128.9, 126.4, 118.5, 112.7 (ArC), 79.5 (4-C); **FTIR** $\nu_{\max}/\text{cm}^{-1}$ (KBr): 3391 (NH), 3208, 3158, 3103, 1652, 1598, 1576, 1492, 1475, 1426, 1395, 1306, 1284, 1232, 1183, 1074, 1007, 819, 767, 741, 706, 696, 499.

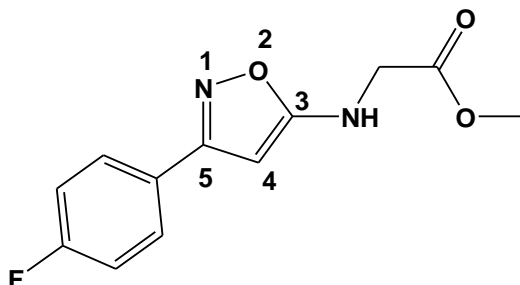
8.5.6.11. *N*-(4-Bromophenyl)-3-(4-fluorophenyl)isoxazol-5-amine **131e**



N-(4-Bromophenyl)-3-(4-fluorophenyl)isoxazol-5-amine **131e** was successfully synthesized from 2-chloro-1-(4-fluorophenyl)ethanone oxime **129a** (216 mg, 0.84 mmol), 1-isocyano-4-bromobenzene **130a** (606 mg, 1.68 mmol) and Na_2CO_3 (356 mg, 3.36 mmol) in DCM (10 ml) according to the general procedure B; **Physical characteristics**: pale yellow solid; **Yield**: 25 mg, 9%; **$^1\text{H NMR}$** (400 MHz, CDCl_3): δ 10.2 (1H, s, NH), 7.90-7.94 (2H, m, ArH), 7.51 (2H, d, $J = 8.8$ Hz, ArH), 7.30 (2H, d, $J = 8.4$ Hz, ArH), 7.21 (2H, d, $J = 8.8$ Hz, ArH), 6.30 (1H, s, 4-CH); **$^{13}\text{C NMR}$** (101 MHz, CDCl_3) δ 165.5 (5-C), 164.3 (d, $^1J = 249$ Hz, *para*-CF), 161.9 (3-C), 139.2,

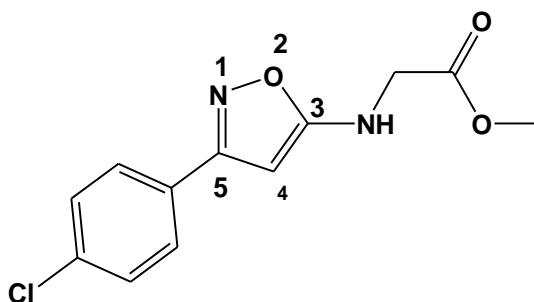
132.1, 128.8, 118.5, 116.0, 115.8, 112.8 (ArC), 79.5 (4-C); **FTIR** $\nu_{\max}/\text{cm}^{-1}$ (KBr): 3281 (NH), 3208, 3137, 3090, 2923, 2855, 1650, 1530, 1466, 1439, 1388, 1301, 1233, 1159, 1098, 1011, 953, 847, 746, 719, 603, 528, 499.

8.5.6.12. Methyl 2-(3-(4-fluorophenyl)isoxazol-5-ylamino)acetate **141a**



Methyl 2-(3-(4-fluorophenyl)isoxazol-5-ylamino)acetate **141a** was successfully synthesized from 2-chloro-1-(4-fluorophenyl)ethanone oxime **129a** (1.59 g, 6.21 mmol), methyl isocyanoacetate (1.23 g, 12.42 mmol) and Na_2CO_3 (2.60 g, 24.48 mmol) in DCM (30 ml) according to the general procedure B; **Physical characteristics**: pale yellow solid; **Yield**: 544 mg, 35%; **$^1\text{H NMR}$** (400 MHz, CDCl_3): δ 7.68-7.71 (2H, m, ArH), 7.06-7.11 (2H, m, ArH), 5.34 (1H, t, $J = 5.0$ Hz, NH), 5.28 (1H, s, 4-CH), 4.00 (2H, d, $J = 5.5$ Hz, NHCH_2), 3.79 (3H, s, OCH_3); **$^{13}\text{C NMR}$** (101 MHz, CDCl_3) δ 170.1 (C=O), 169.3 (5-C), 163.6 (d, $1J = 249$ Hz, *para*-CF), 162.7 (3-C), 128 (d, $^3J = 8$ Hz, *ortho*-C), 125.8 (d, $^4J = 3$ Hz, 1'-C), 115.7 (d, $^2J = 21$ Hz, ArC), 77.3 (4-C), 52.5 (OCH_3), 45.3 (NHCH_2); **FTIR** $\nu_{\max}/\text{cm}^{-1}$ (KBr): 3407 (NH), 3123, 2958, 2924, 2852, 1742, 1619, 1597, 1506, 1445, 1396, 1246, 1222, 1161, 1017, 980, 950, 887, 841, 757, 596, 514.

8.5.6.13. Methyl 2-(3-(4-chlorophenyl)isoxazol-5-ylamino)acetate **141b**



Methyl 2-(3-(4-chlorophenyl)isoxazol-5-ylamino)acetate **141b** was successfully synthesized from 2-chloro-1-(4-chlorophenyl)ethanone oxime **129b** (622 mg, 2.28 mmol), methyl isocyanoacetate (452 mg, 4.56 mmol) and Na_2CO_3 (697 mg, 9.12 mmol) in DCM (10 ml) according to the general procedure B; **Physical characteristics**: pale yellow solid; **Yield**: 274

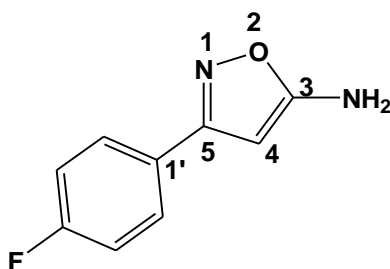
mg, 45%; $^1\text{H NMR}$ (400 MHz, CDCl_3): δ 9.10 (1H, s, NH), 7.74 (2H, d, $J = 8.4$ Hz, ArH), 7.42 (2H, d, $J = 8.4$ Hz, ArH), 6.75 (1H, s, 4-CH), 4.27 (2H, s, NHCH_2), 3.85 (3H, s, OCH_3); $^{13}\text{C NMR}$ (101 MHz, CDCl_3) δ 170.4 (C=O), 162.8 (5-C), 162.2 (3-C), 154.6, 136.4, 128.1, 127.2 (ArC), 77.6 (4-C), 55.3 (OCH_3), 42.2 (NHCH_2); **FTIR** $\nu_{\text{max}}/\text{cm}^{-1}$ (KBr): 3381 (NH), 3113, 2982, 2917, 2860, 1743, 1630, 1572, 1514, 1441, 1225, 1330, 1016, 953, 835, 756, 504.

8.5.7. Synthesis of 3-aryl-isoxazol-5-amine derivatives

8.5.7.1 General synthetic procedure

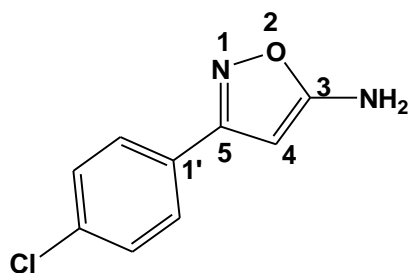
To a suspension of KCN (1.2 molar equivalent) in MeOH (10 ml) was added dropwise a solution of 2-chloro-aryl-ethanone oximes (1 molar equivalent) in MeOH (10 ml) at room temperature. The mixture was stirred for 30 min, followed by removal of KCl by filtration. Evaporation of the solvent in the filtrate gave a residue, which was chromatographed on silica gel using a mixture of EtOAc and hexane (2: 1) as an eluent to afford 3-aryl-isoxazol-5-amine derivatives

8.5.7.2. 3-(4-Fluorophenyl)isoxazol-5-amine 144a



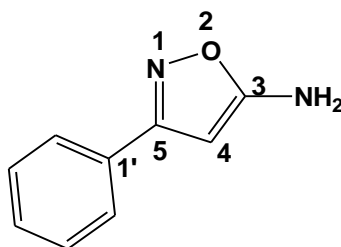
3-(4-Fluorophenyl)isoxazol-5-amine **144a** was successfully synthesized from 2-chloro-1-(4-fluorophenyl)ethanone oxime **129a** (1.28 g, 5.00 mmol), KCN (378 mg, 6.00 mmol) in MeOH (10 ml) according to the general procedure; **Physical characteristics**: brown oil; **Yield**: 606 mg, 68%; $^1\text{H NMR}$ (400 MHz, CDCl_3) δ 7.67 (2H, m, ArH), 7.06 (2H, t, $J = 8.4$ Hz, ArH), 5.37 (1H, s, 4-CH), 4.70 (1H, s, NH_2); $^{13}\text{C NMR}$ (101 MHz, CDCl_3) δ 169.1 (5-C), 163.6 (d, $^1J_{\text{CF}} = 248.5$ Hz, *para*-CF), 162.9 (3-C), 128.4 (d, $^3J_{\text{CF}} = 8$ Hz, *ortho*-C), 125.8 (d, $^4J_{\text{CF}} = 3$ Hz, 1'-C), 115.7 (d, $^2J_{\text{CF}} = 21$ Hz, *meta*-C), 78.0 (4-C); **FTIR** $\nu_{\text{max}}/\text{cm}^{-1}$ (KBr): 3454 (NH_2), 3285, 3224, 3133, 1639, 1610, 1579, 1529, 1480, 1334, 1222, 1156, 954, 899, 843, 746, 589, 529.

8.5.7.3. 3-(4-Chlorophenyl)isoxazol-5-amine 144b



3-(4-Chlorophenyl)isoxazol-5-amine **144b** was successfully synthesized from 2-chloro-1-(4-chlorophenyl)ethanone oxime **129b** (3.36 g, 12.31 mmol), KCN (962 mg, .77 mmol) in MeOH (20 ml) according to the general procedure; **Physical characteristics**: pal orange solid; **Yield**: 1.51 g, 63%; **Melting point**: 164-166°C (lit.³⁷¹); **¹H NMR** (400 MHz, CDCl₃): δ 7.67 (2H, d, *J* = 8.4 Hz, ArH), 7.06 (2H, d, *J* = 8.4 Hz, ArH), 5.37 (1H, s, 4-CH), 4.70 (1H, s, NH₂); **¹³C NMR** (101 MHz, CDCl₃): δ 169.1 (5-C), 162.9 (3-C), 136.1, 129.9, 127.5, 128.72 (ArC), 78.0 (4-C); **FTIR** $\nu_{\max}/\text{cm}^{-1}$ (KBr): 3433 (NH₂), 3301, 3243, 3189, 1642, 1595, 1569, 1569, 1476, 1442, 1088, 1012, 952, 891, 836, 750, 499.

8.5.7.4. 3-Phenylisoxazol-5-amine 144c



3-Phenylisoxazol-5-amine **144c** successfully synthesized from 2-chloro-1-(4-chlorophenyl)ethanone oxime **129c** (5.68 g, 23.8 mmol), KCN (1.86 g, 28.5 mmol) in MeOH (20 ml) according to the general procedure; **Physical characteristics**: pale yellow solid; **Yield**: 2.02 g, 53%; **Melting point**: 109-111°C (lit.³⁷²); **¹H NMR** (400 MHz, CDCl₃): δ 7.71 (2H, m, ArH), 7.40 (3H, m, ArH), 5.42 (1H, s, 4-CH), 4.50 (1H, s, NH₂); **¹³C NMR** (101 MHz, CDCl₃): δ 168.9 (5-C), 163.8 (3-C), 129.7, 129.6, 128.7, 126.5 (ArC), 78.2 (4-C); **FTIR** $\nu_{\max}/\text{cm}^{-1}$ (KBr): 3321 (NH₂), 3175, 1644, 1578, 1485, 1430, 1340, 1308, 1286, 1213, 1025, 849, 821, 736, 695, 654.

APPENDIX: A: Virtual screening of pepMMsMIMIC 3-dimensional database using BST-2-Vpu interaction

The main aim of virtual screening of the MMsINC® database (<http://mms.dsfarm.unipd.it/pepMMsMIMIC>)³⁷³ is to suggest possible peptidomimetic molecules as a starting point, whose essential pharmacophoric group is able to inhibit the BST-2-Vpu interaction. The workflow diagram (*Figure A*) below illustrates the basic procedure followed by PepMMsMIMIC, a web-oriented tool. A pdb file of BST-2 (ID. 2LK9) was used as a template for querying the MMsINC® database.

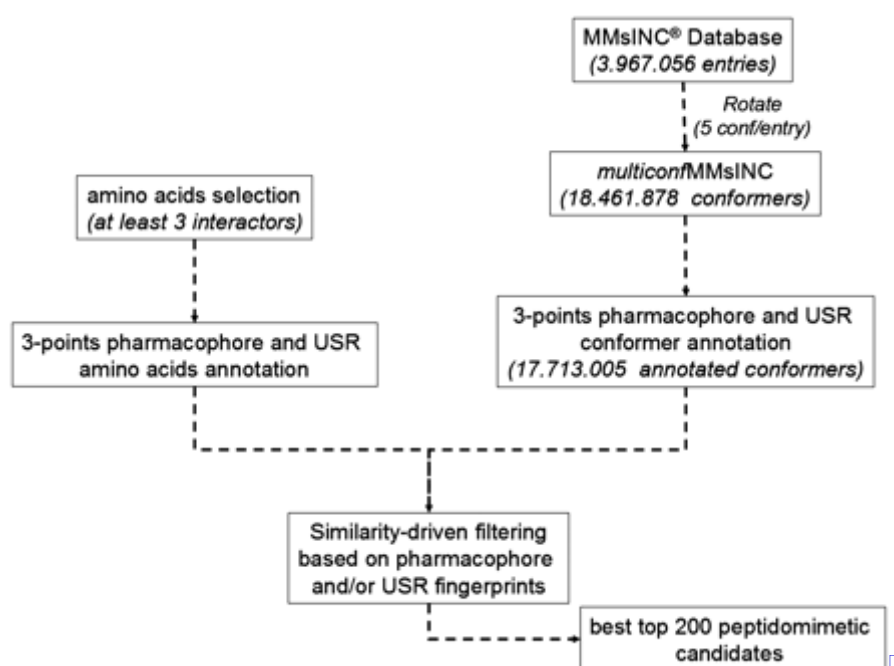


Figure A: pepMMsMIMIC's workflow

In all cases the pharmacophore is generated by the web-tool using BST-2 residues Ile34, Ile37 and Lue41. The following scoring functions were used to rank the compounds in the database; namely: 1) hybrid scoring function { 60% of pharmacophore finger similarity based on weighted similarity coefficient and 40% of shape score similarity based on the ultra-shape recognition}; 2) fingerprint based filtering of shape similarity; 3) based only on the pharmacophoric similarity {"Pharmacophoric fingerprint similarity method, based on weighted Tversky coefficient (wTv).}" and 4) based only on shape similarity. The pepMMsMIMIC search returned with the best 200 peptidomimetic compounds per scoring method. A selection of the top molecules per scoring method are shown in the *Figure B* below.

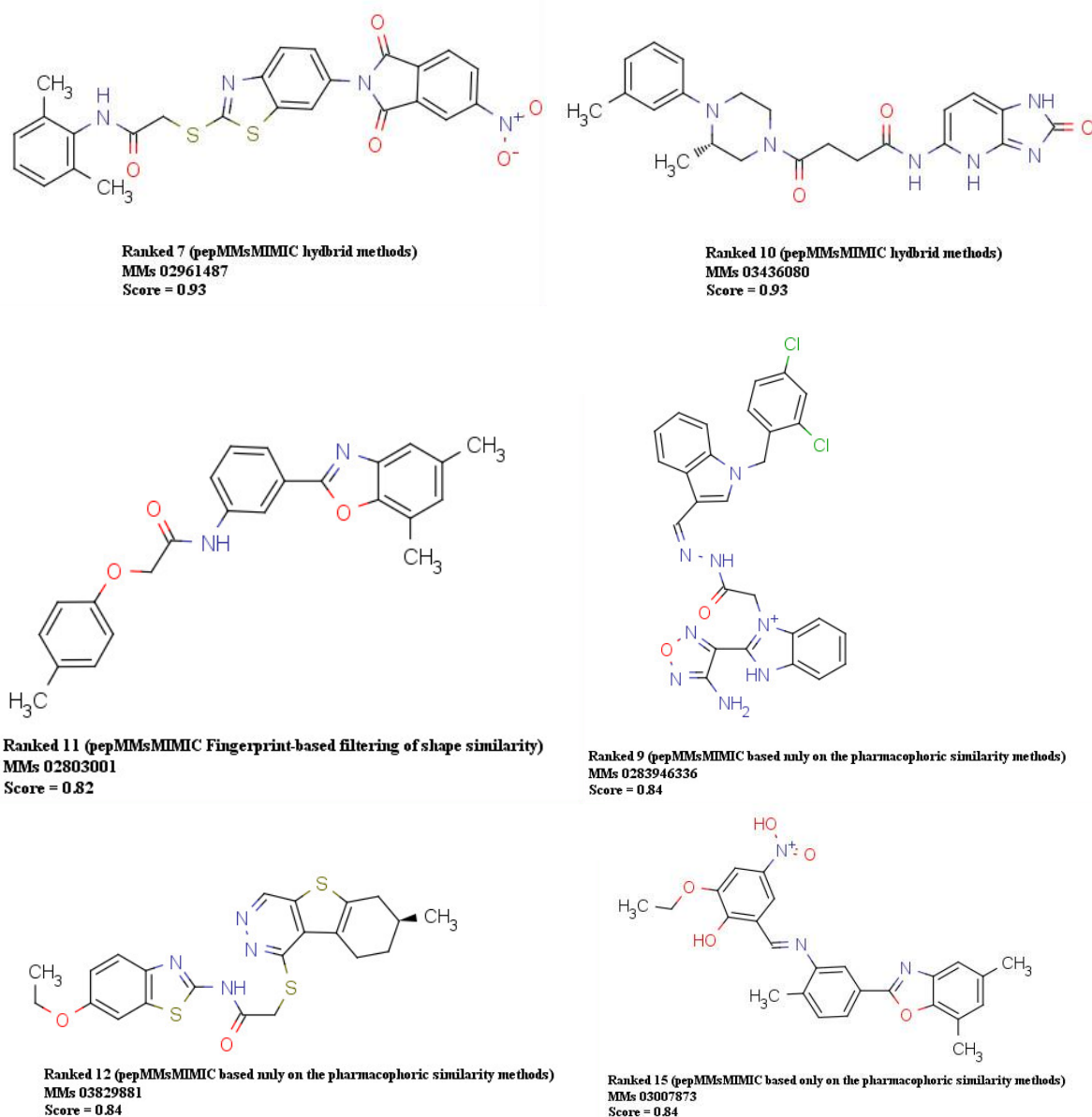


Figure B: A selection of high-ranked *in silico* identified peptidomimetic compounds

Recurring heterocyclic scaffolds from the virtual screening can be highlighted, namely: benzimidazole, benzothiazole, benzoxazole, imidazopyridine, pyrimidinone, tetrahydrobenzothiophene and piperazine. These nitrogen containing heterocyclic systems have the potential to be developed into new series of compounds by varying the substituents R1, R2 and R3 (Figure C).

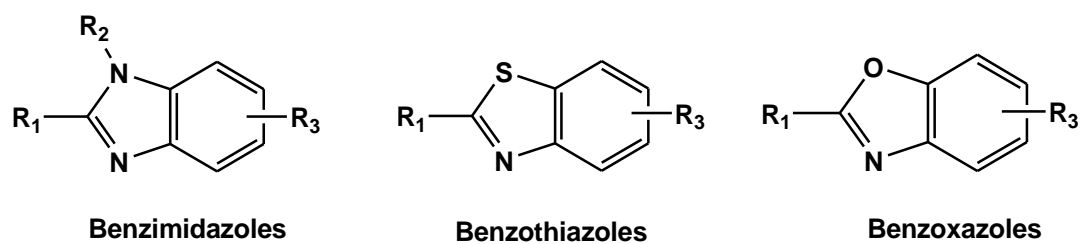
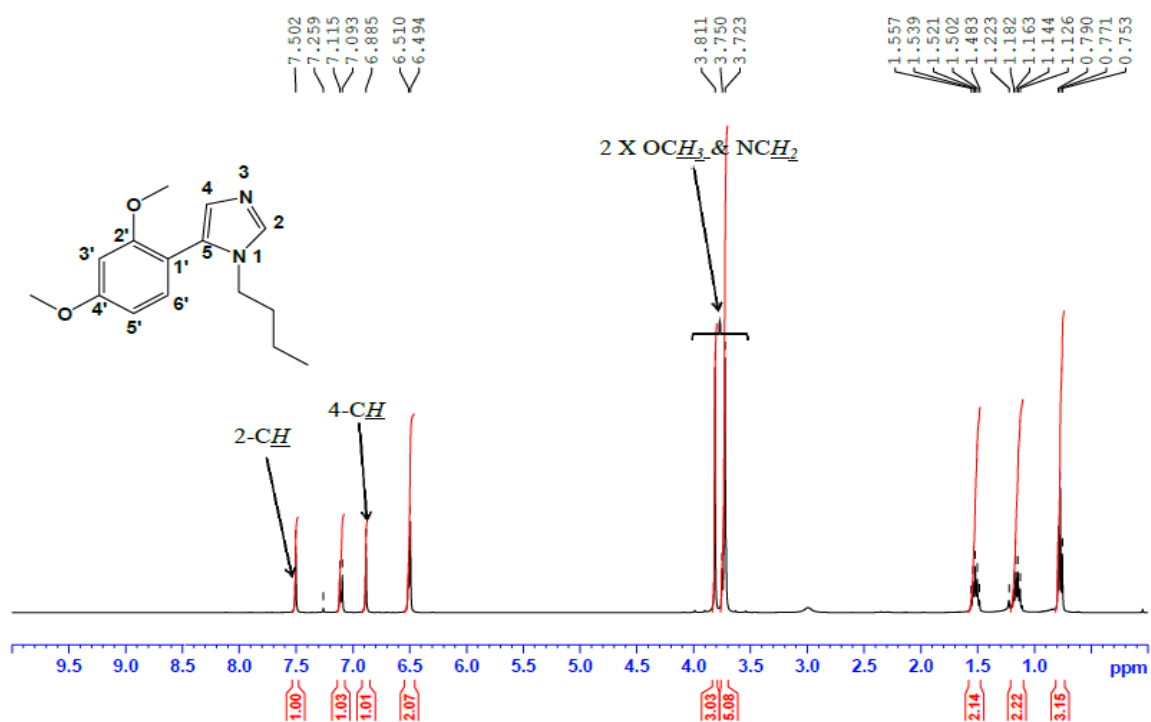


Figure 8: Nitrogen heterocyclic scaffolds of interest

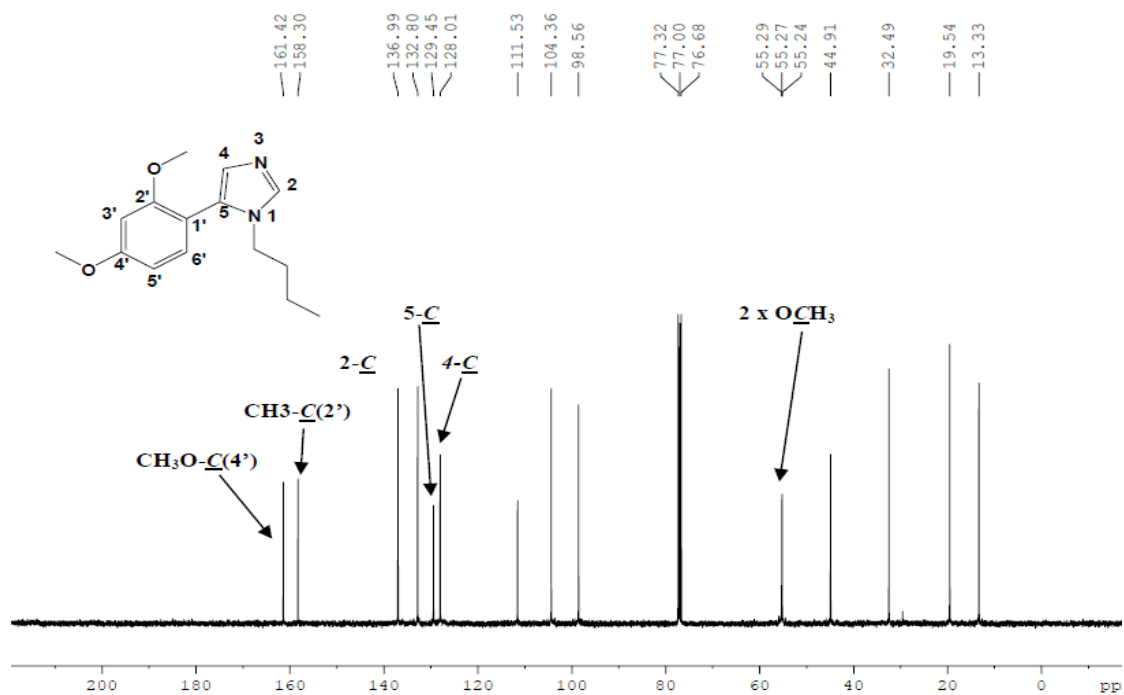
Figure C: Highlighted recurring heterocyclic scaffolds from the virtual screening.

APPENDIX B: Selected spectra

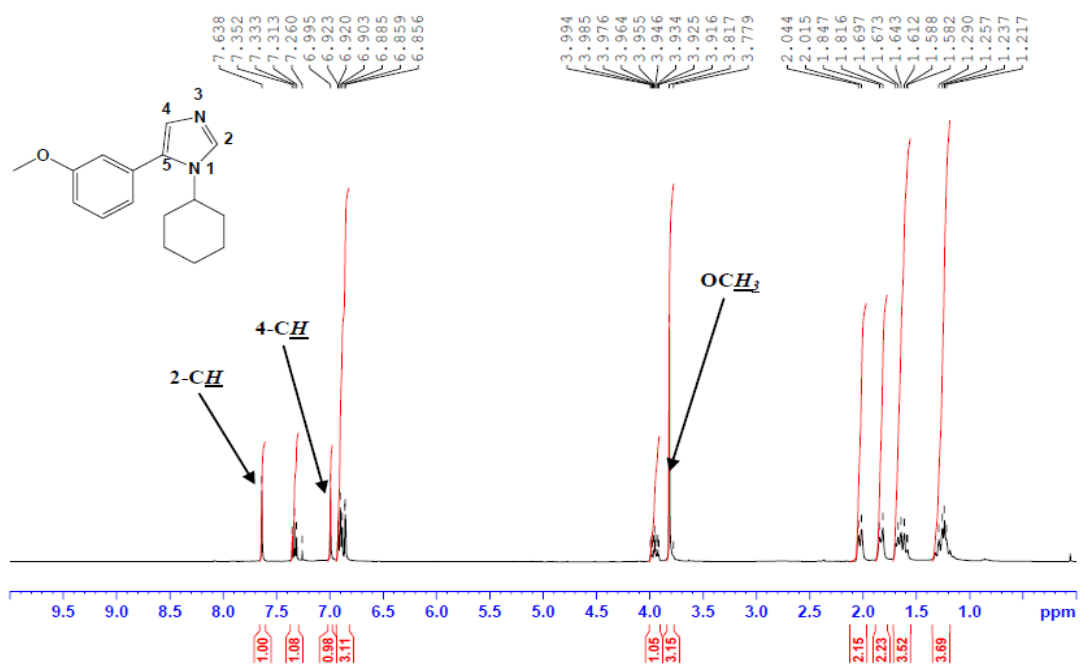
^1H NMR spectrum of compound 79d



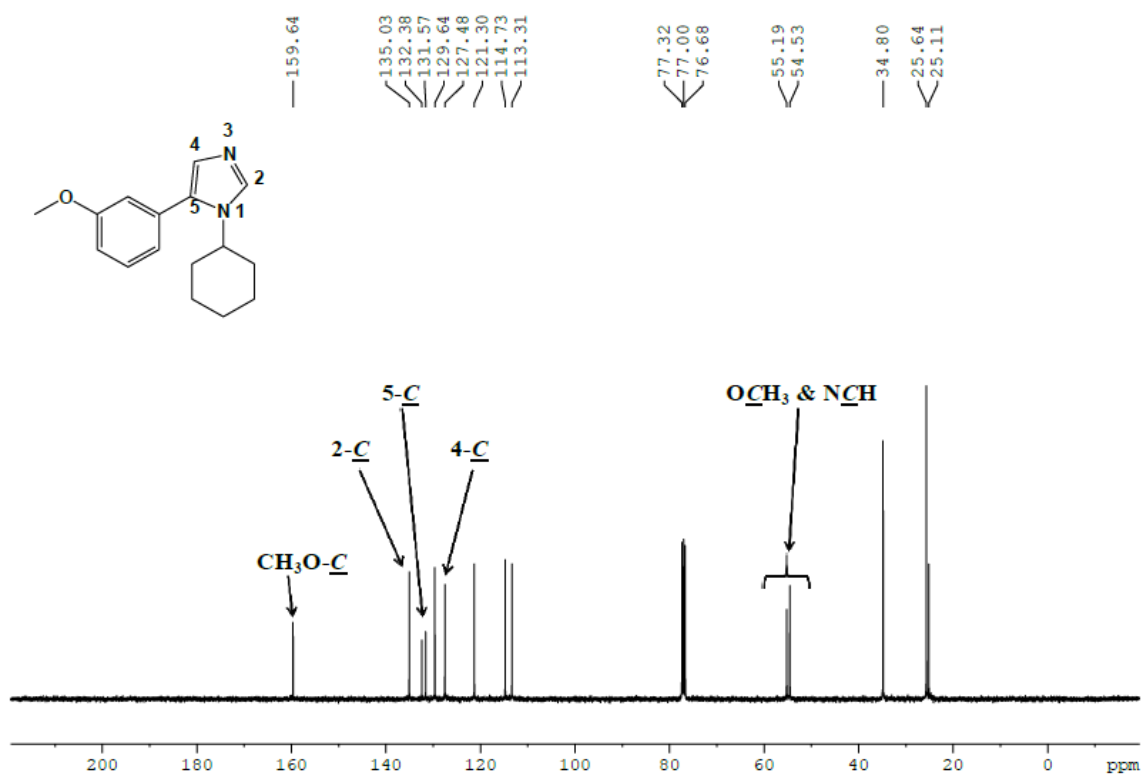
^{13}C NMR spectrum of compound 79d



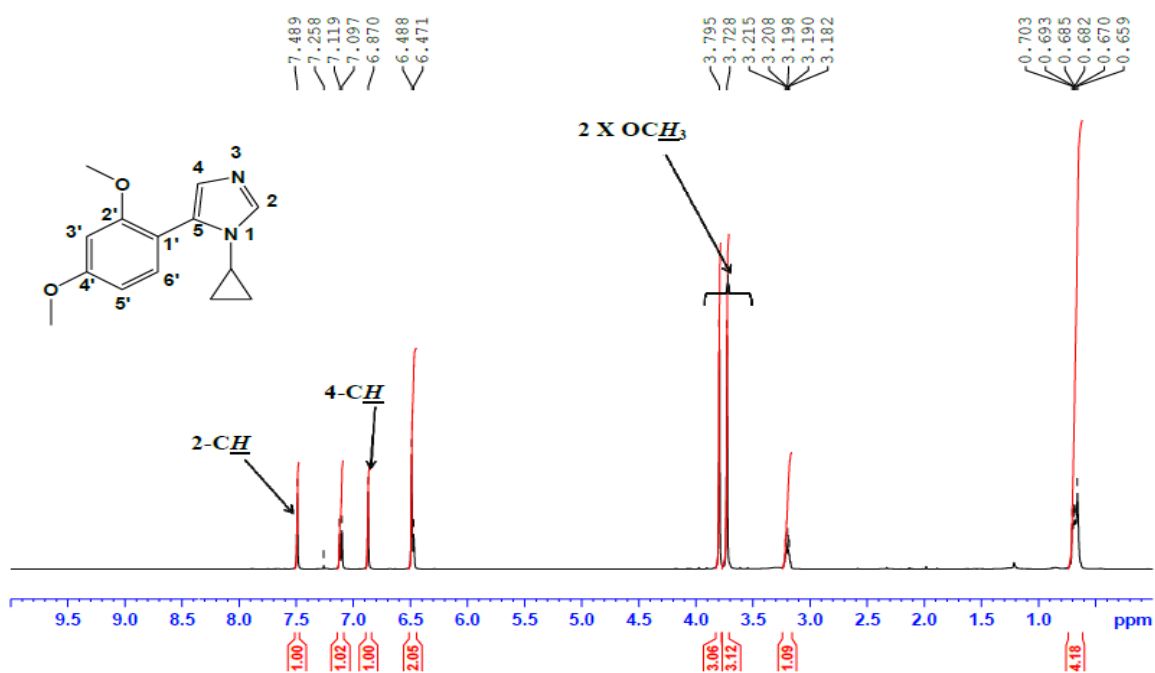
¹H NMR spectrum of compound 80c



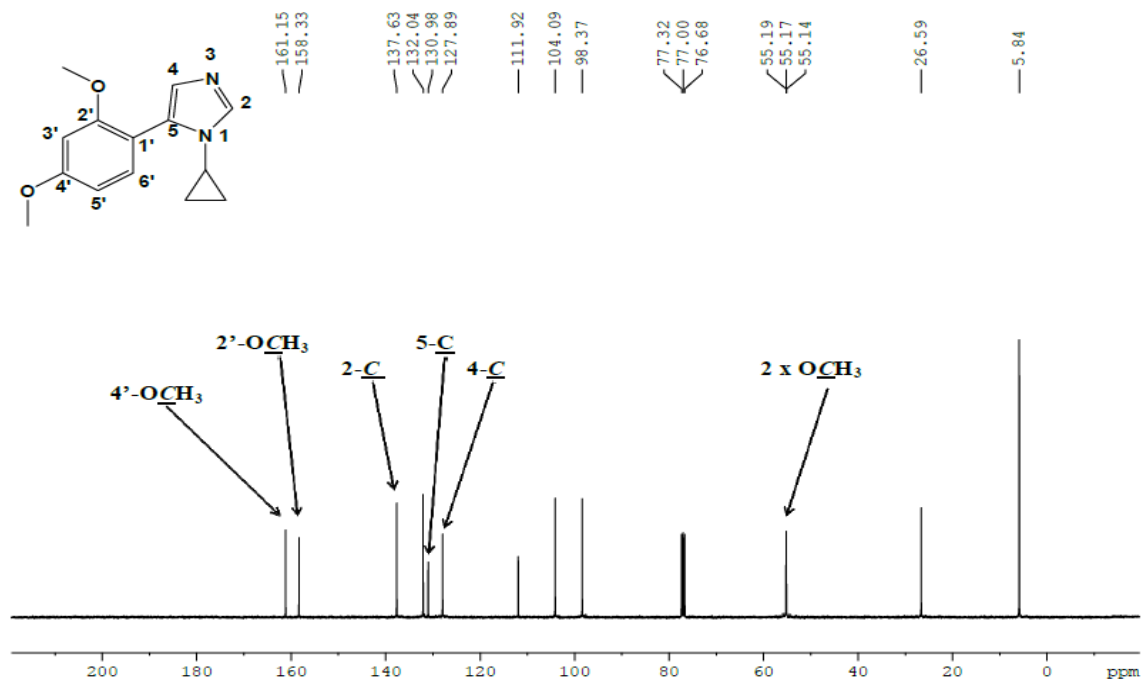
¹³C NMR spectrum of compound 80c



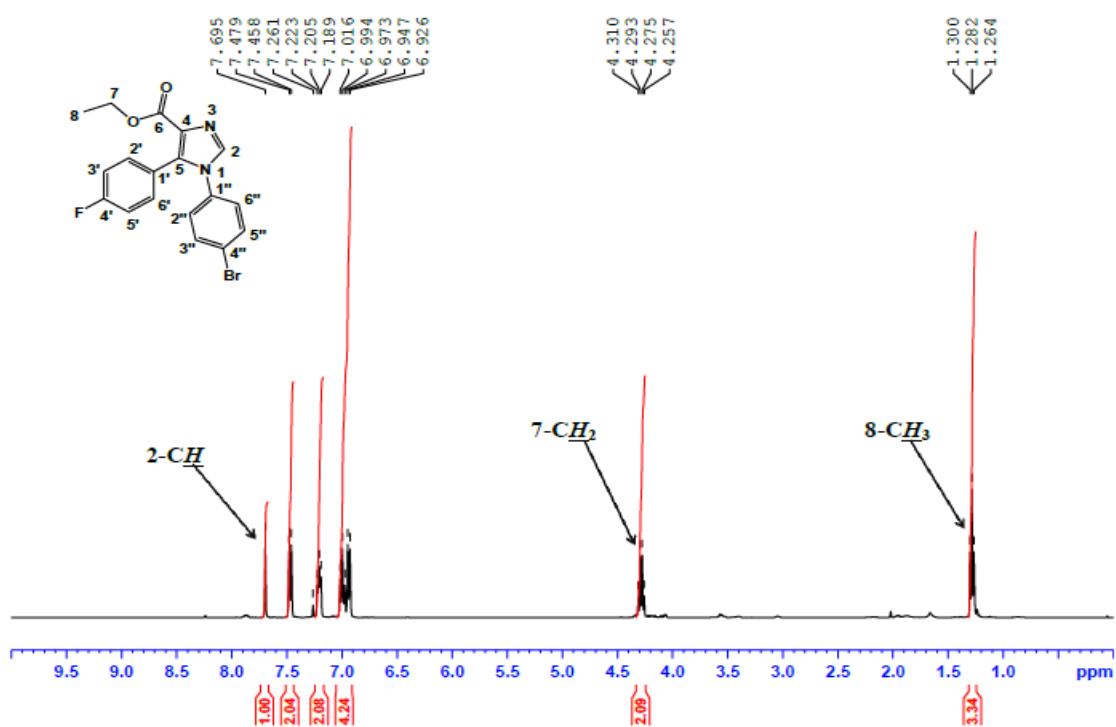
^1H NMR spectrum of compound 81d



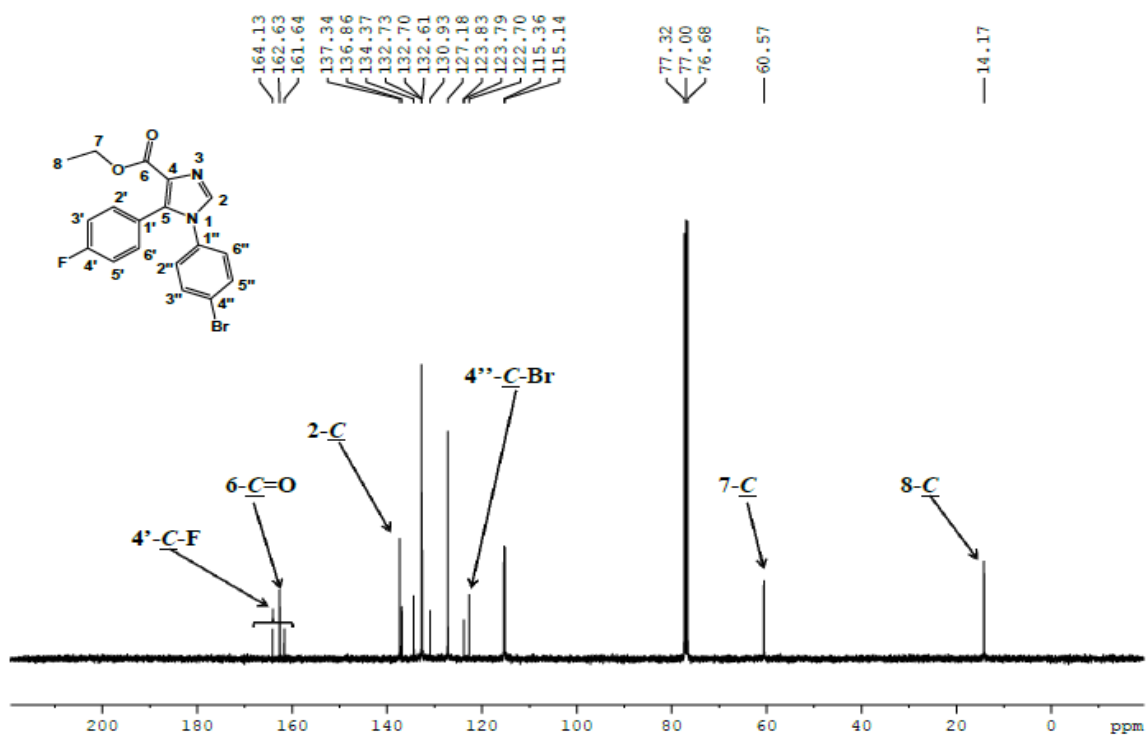
^{13}C NMR spectrum of compound 81d



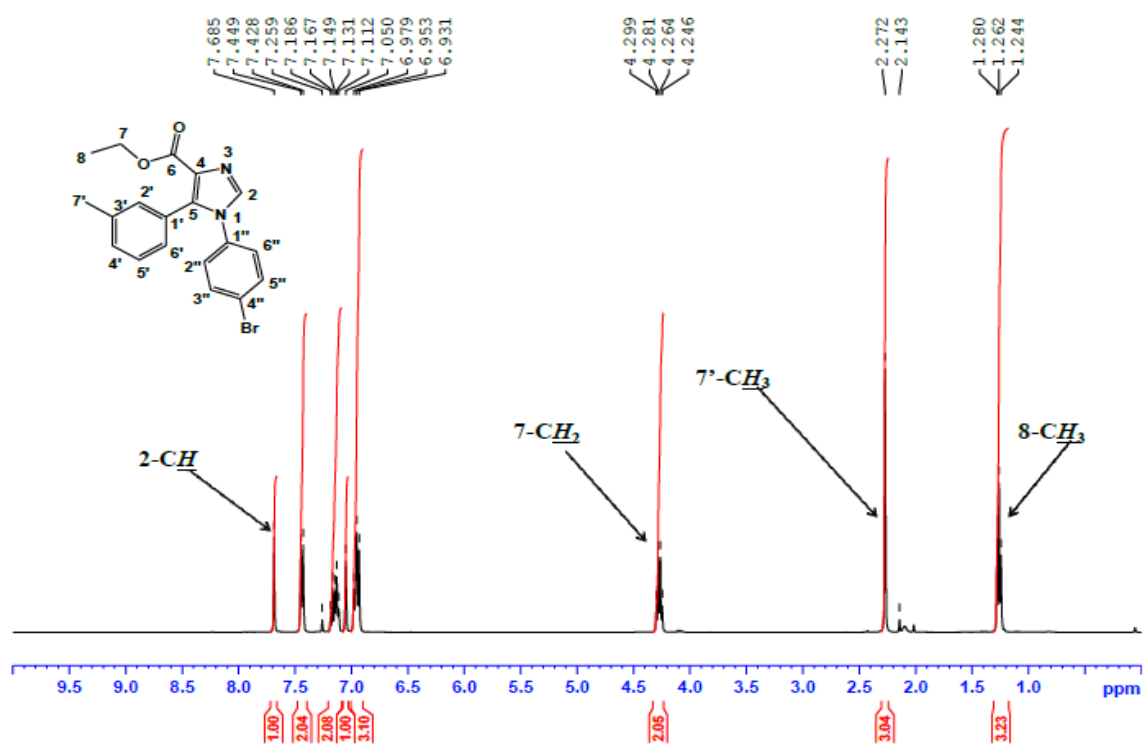
¹H NMR spectrum of compound 88a



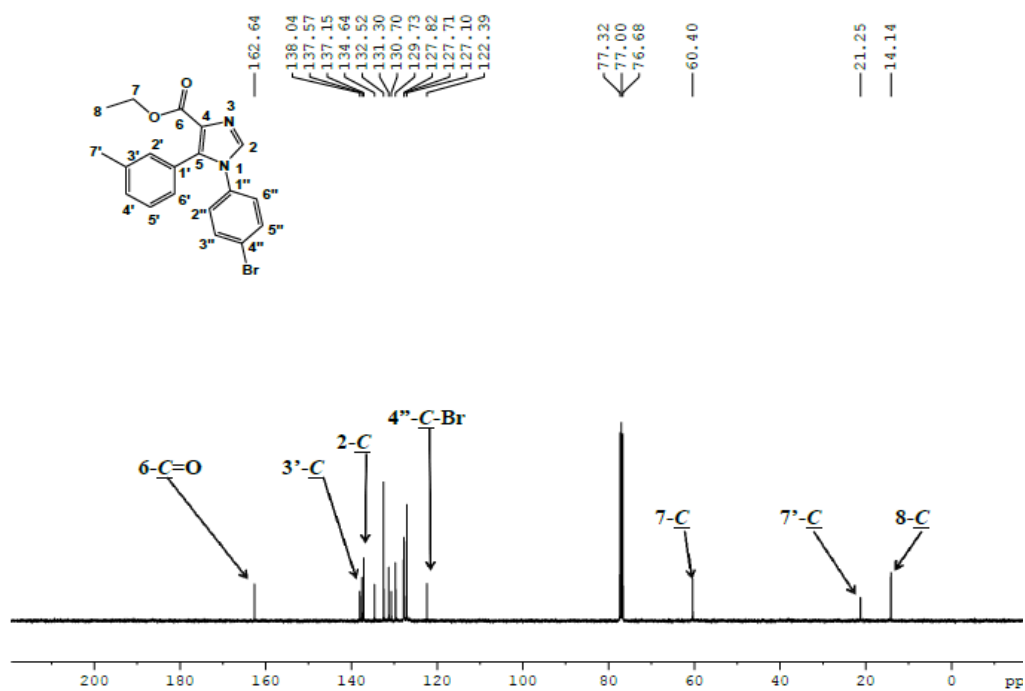
¹³C NMR spectrum of compound 88a



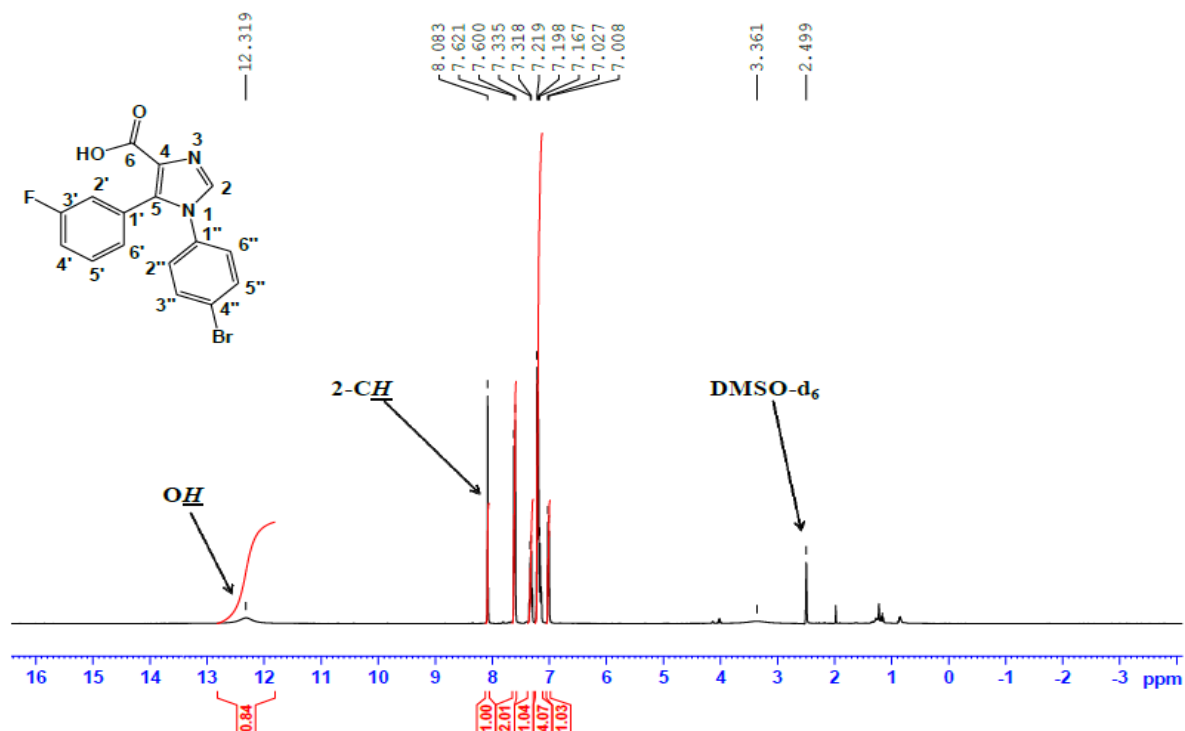
^1H NMR of compound 88d



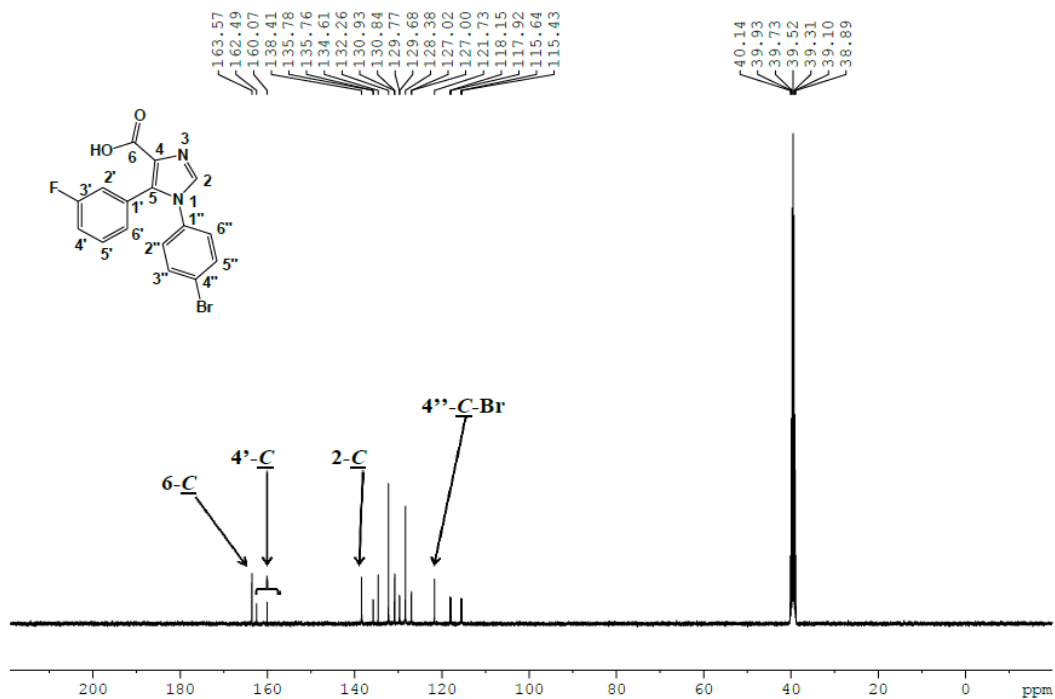
^{13}C NMR spectrum of compound 88a



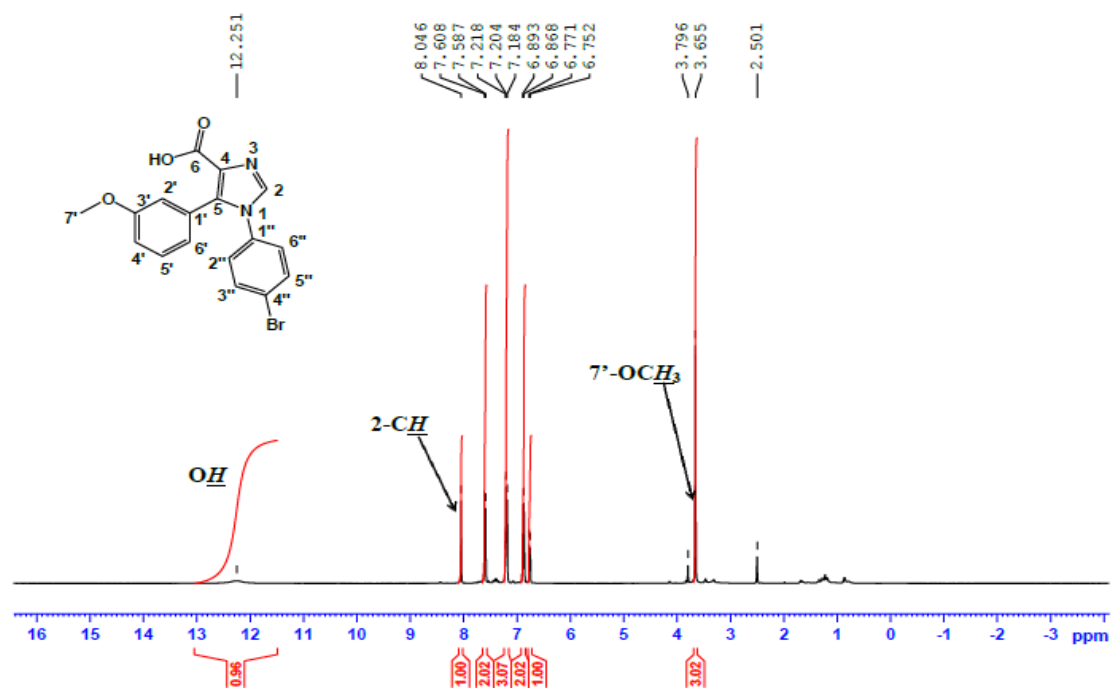
¹H NMR spectrum of compound 87b



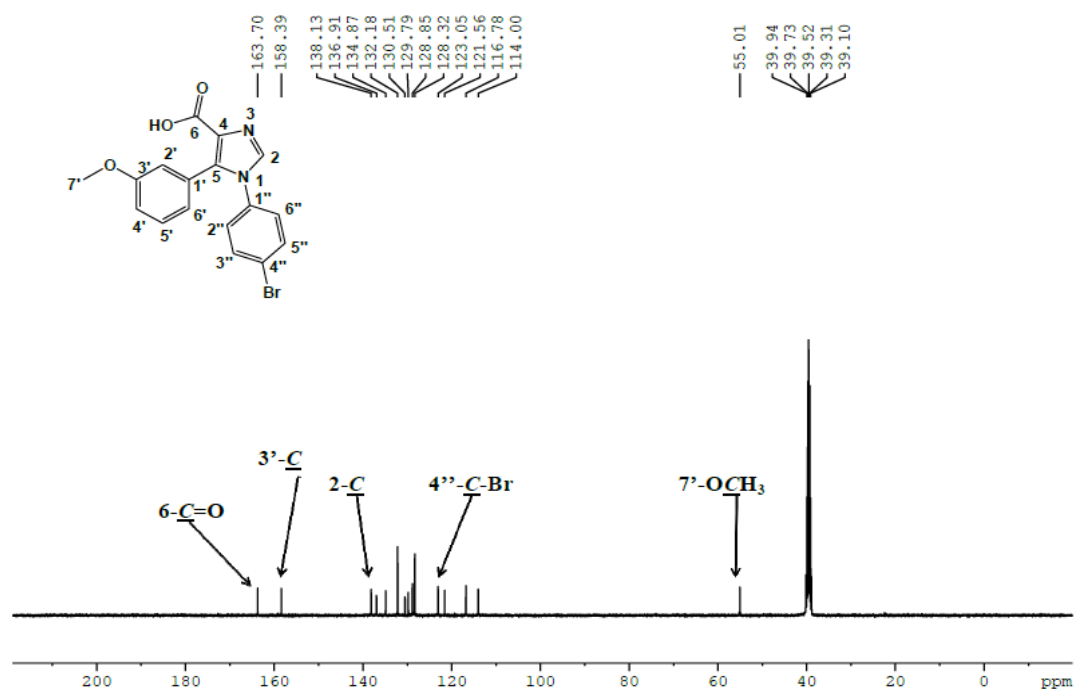
¹³C NMR spectrum of compound 87b



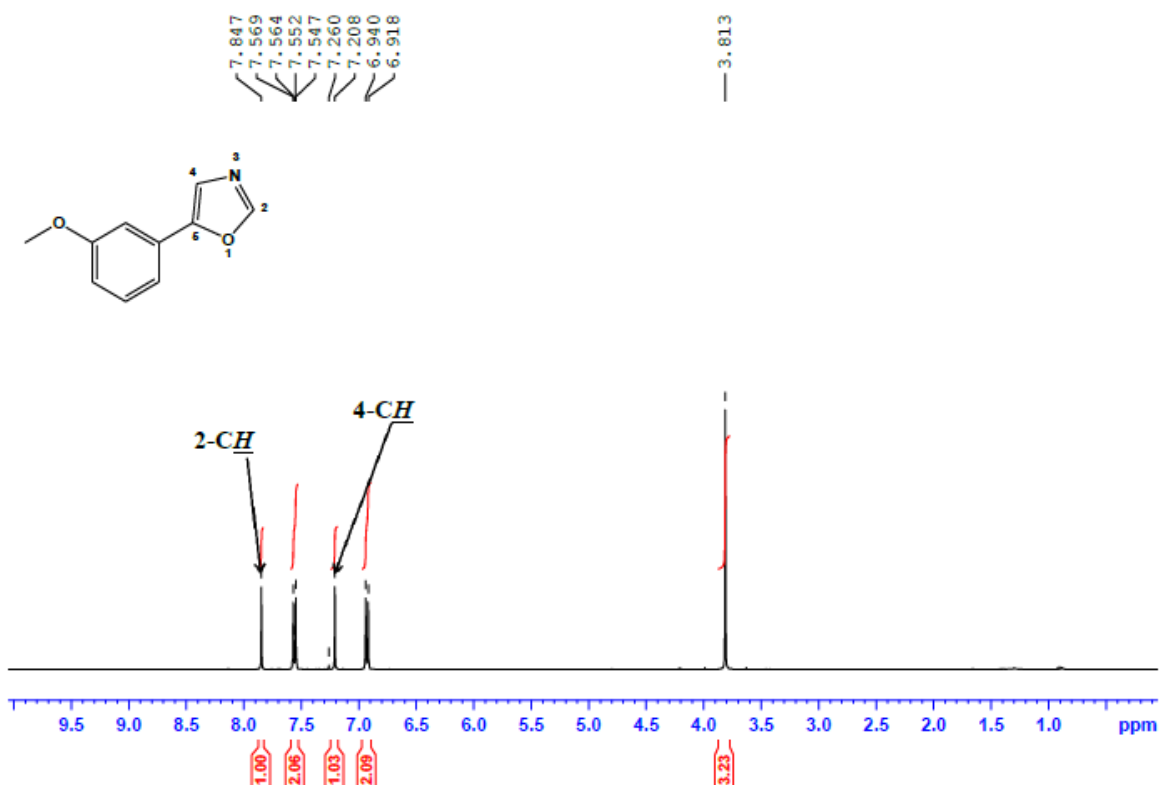
¹H NMR spectrum of compound 87c



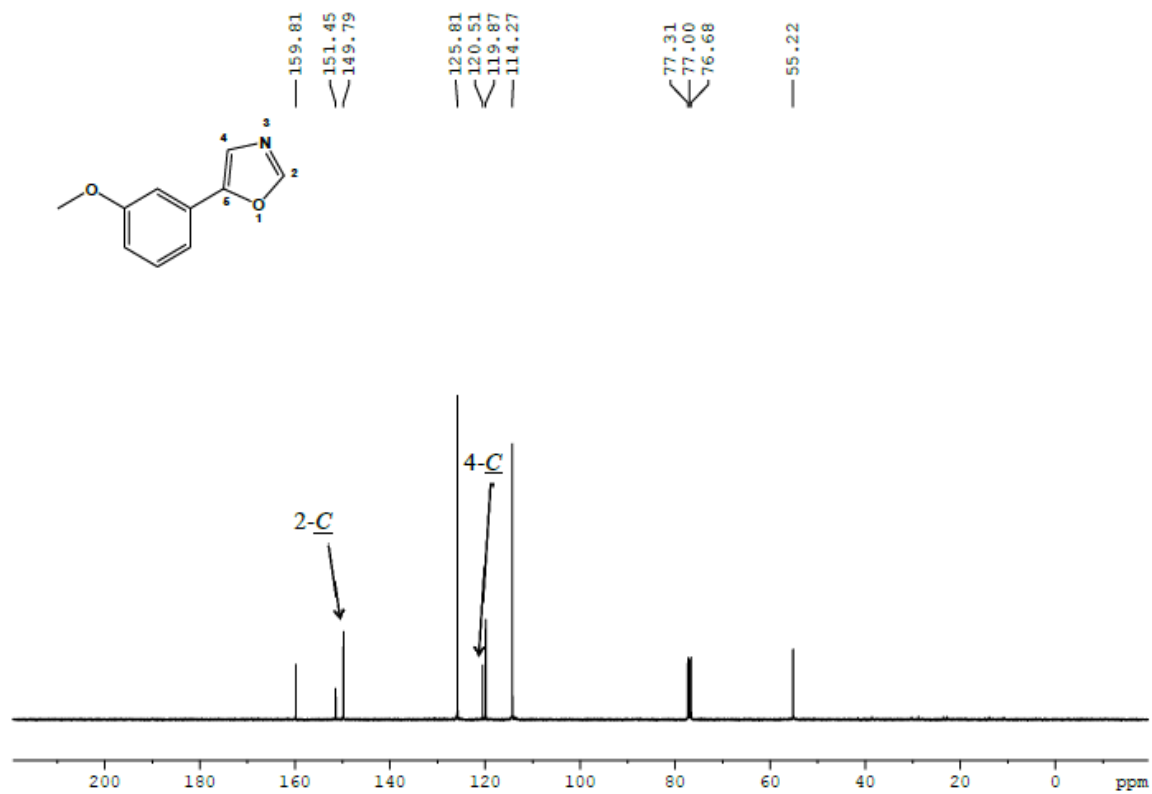
¹³C NMR spectrum of compound 87c



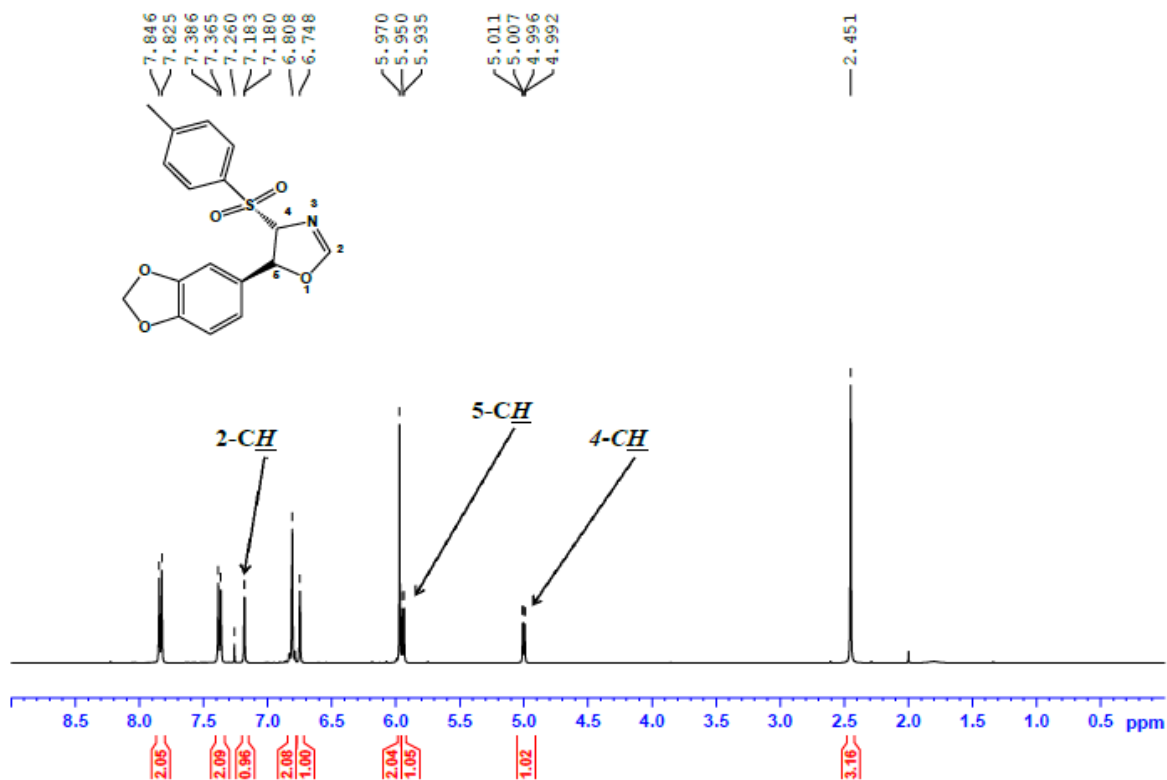
^1H NMR spectrum of compound 96c



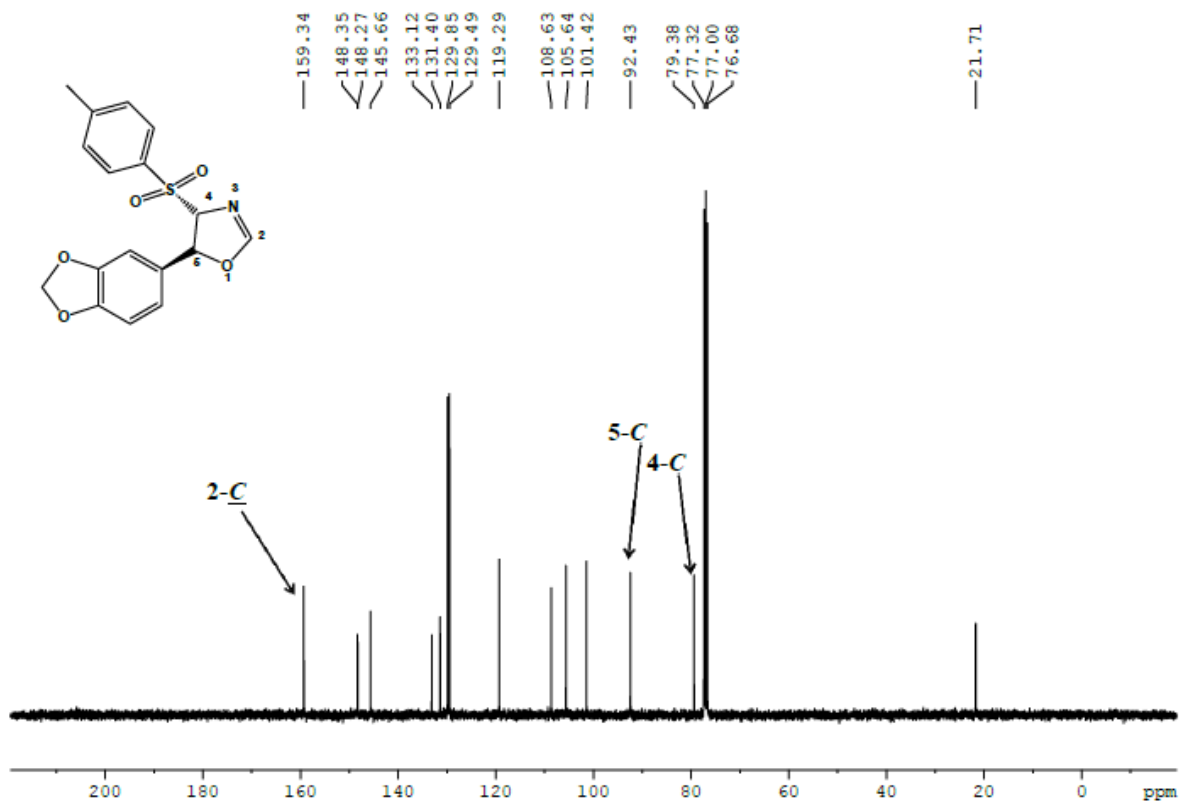
^{13}C NMR spectrum of compound 96c



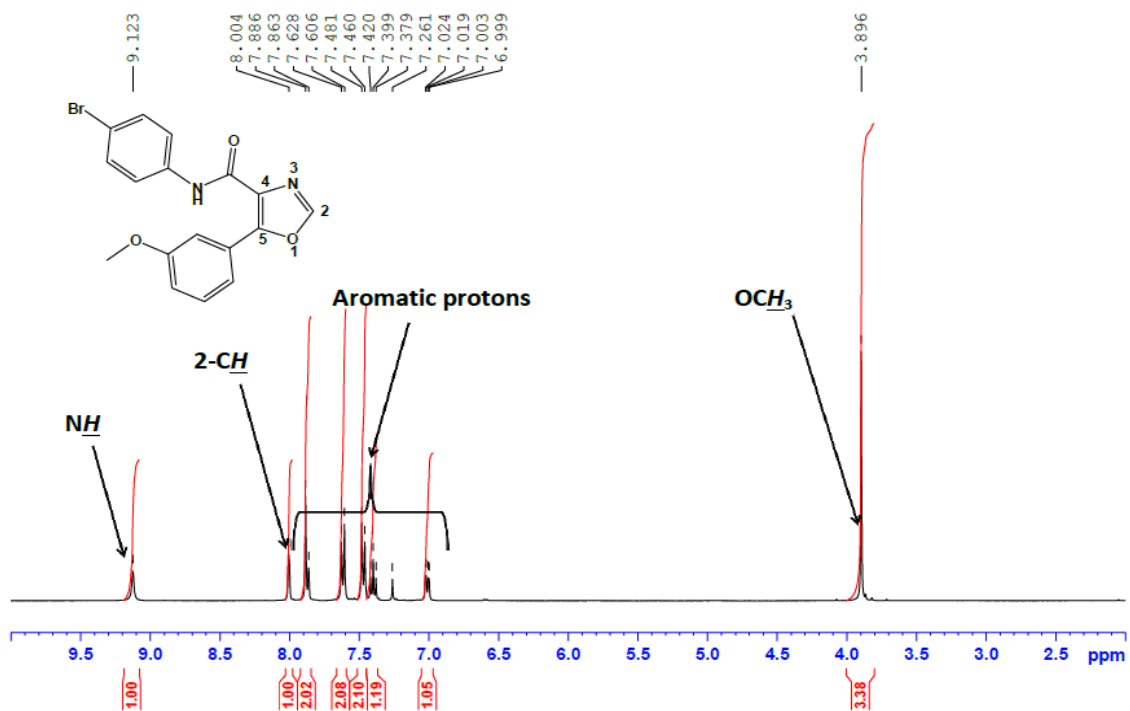
¹H NMR spectrum of compound 97e



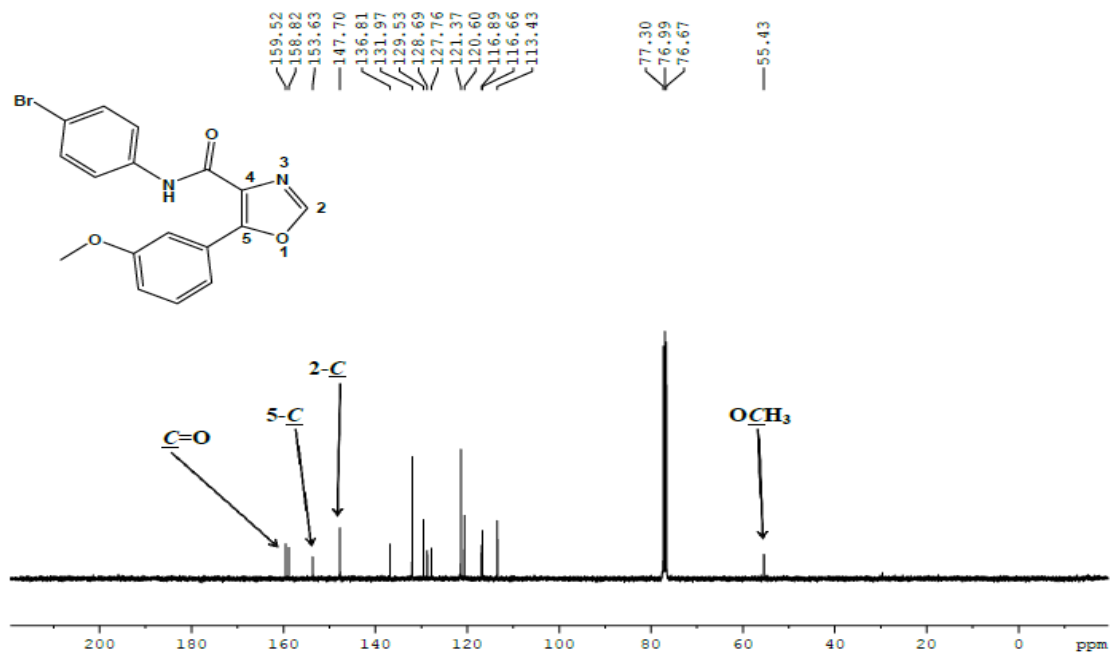
¹³C NMR spectrum of compound 97e



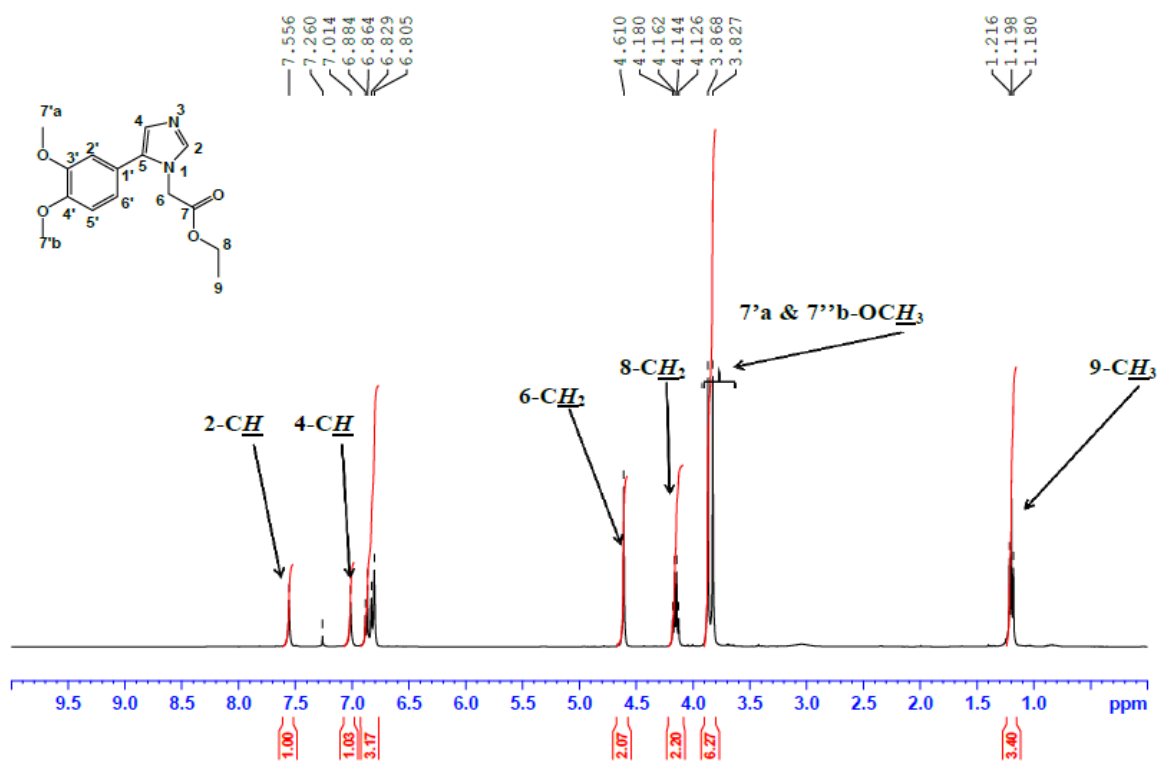
¹H NMR spectrum of compound 100i



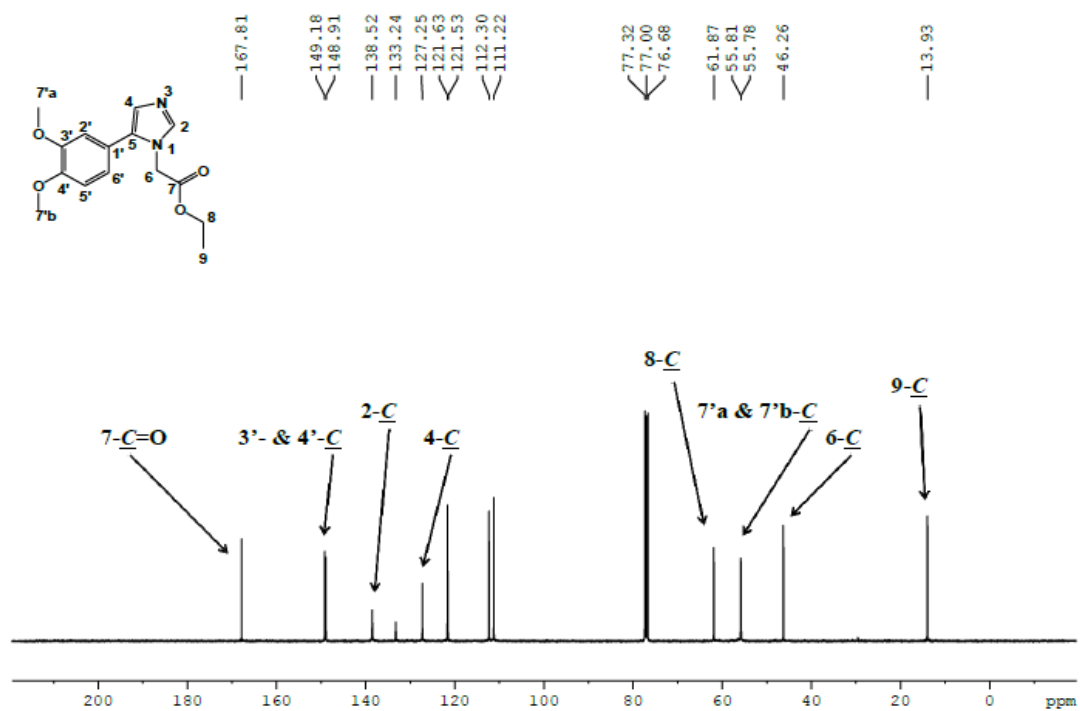
¹³C NMR spectrum of compound 100i



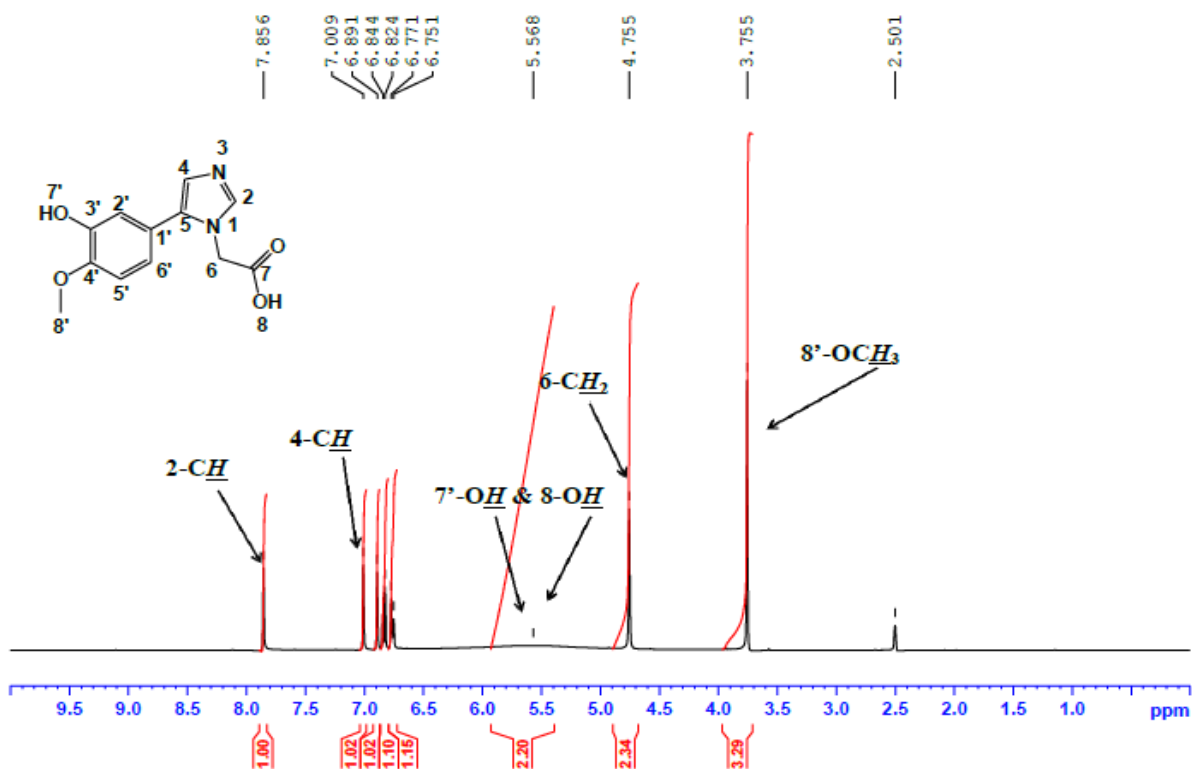
¹H NMR spectrum of compound 120d



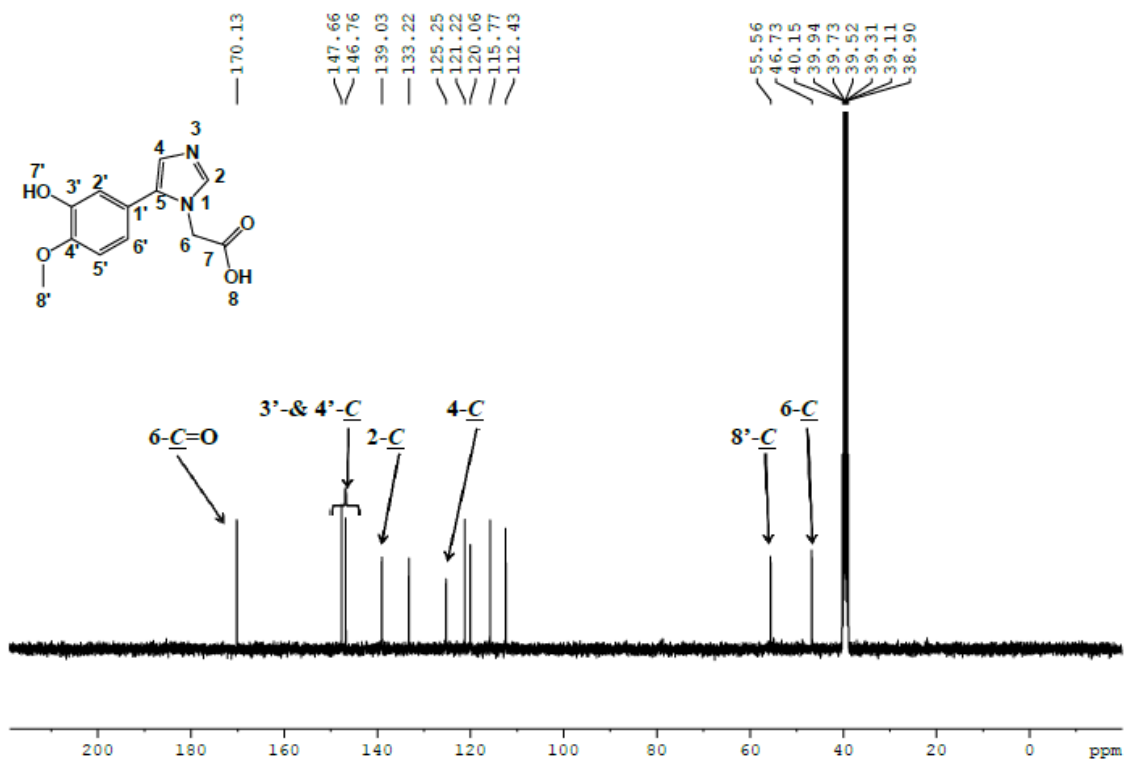
¹³C NMR spectrum of compound 120d



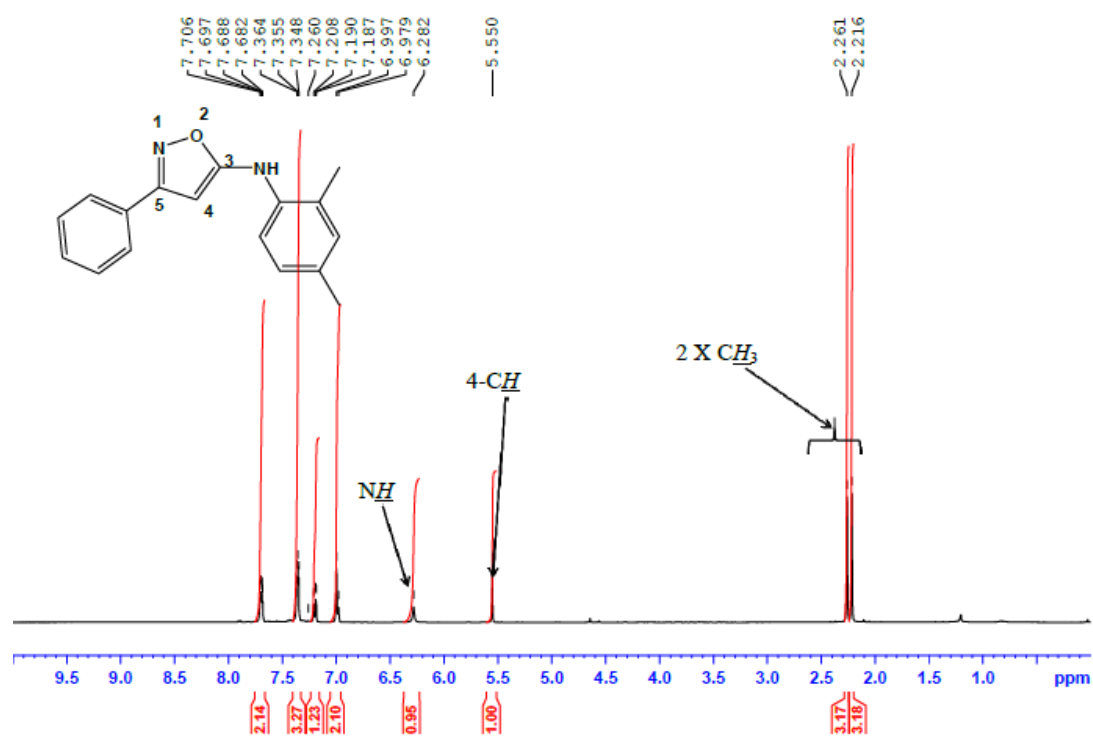
¹H NMR spectrum of compound 123g



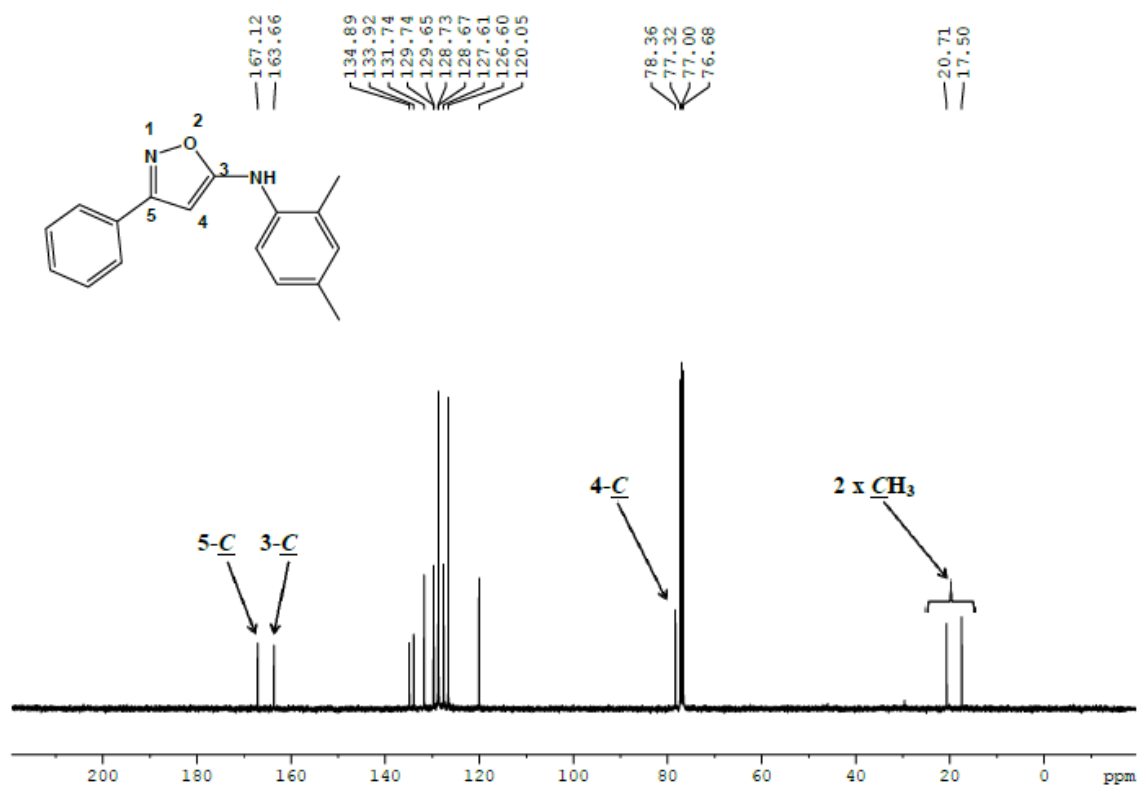
¹³C NMR spectrum of compound 123g



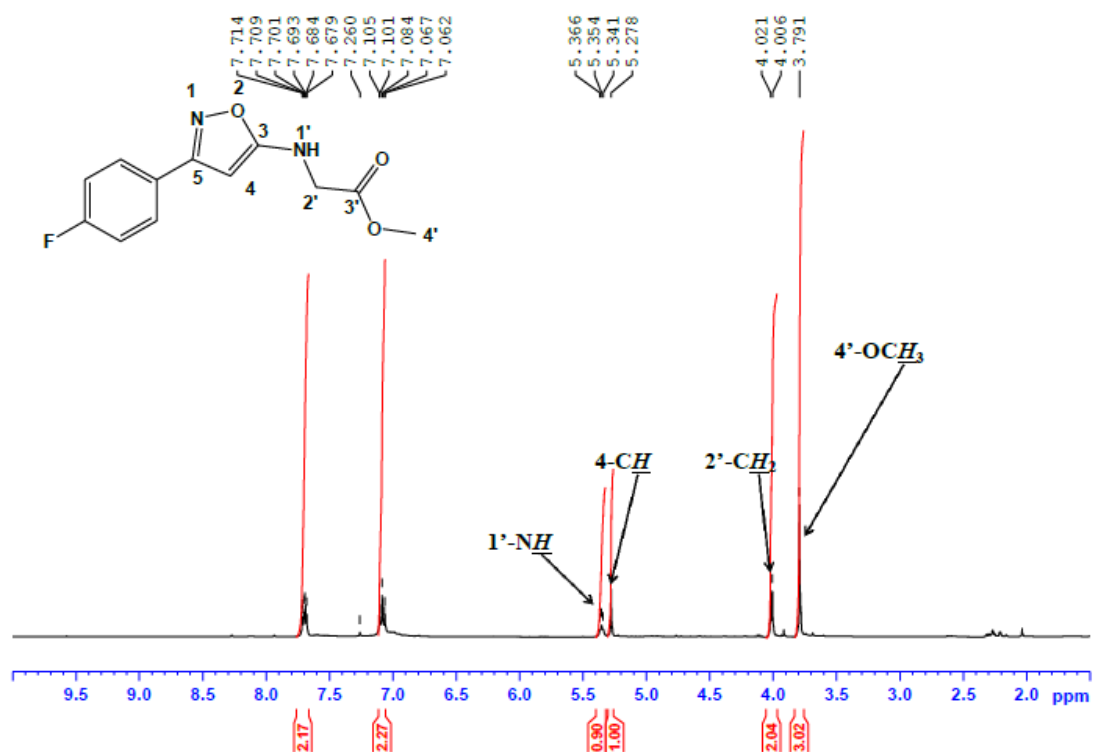
¹H NMR spectrum of compound 131b



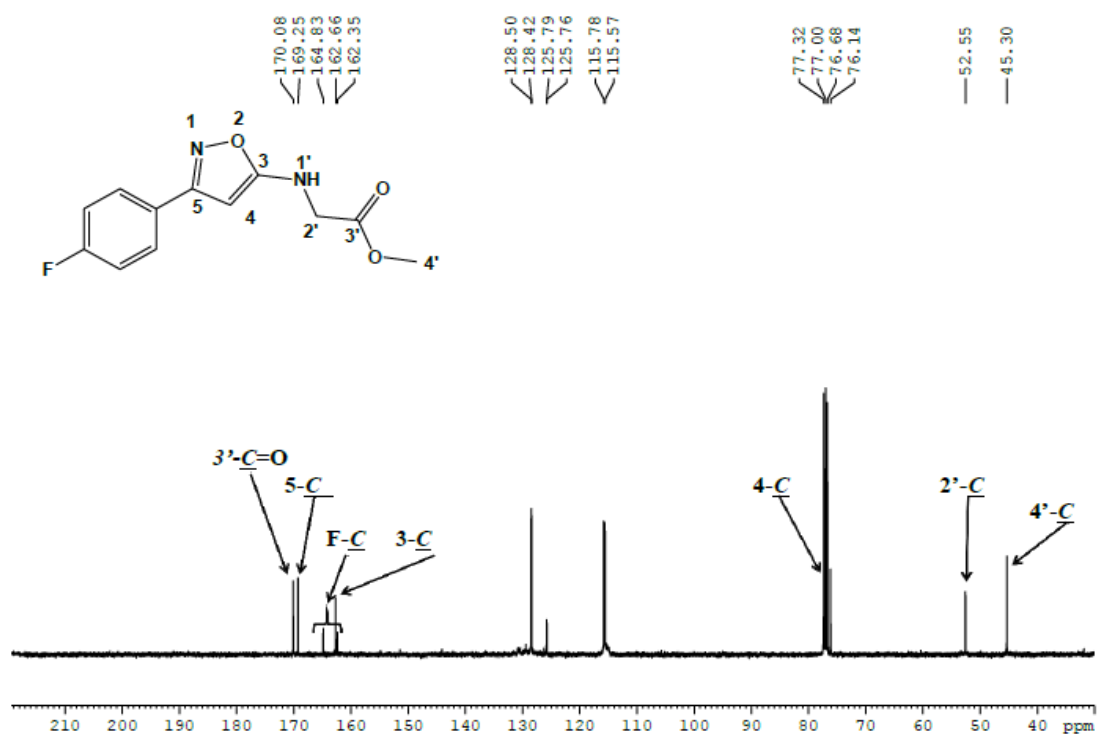
¹³C NMR spectrum of compound 131b



¹H NMR spectrum of compound 141a



¹³C NMR spectrum of compound 141a



References

1. Rick, N. G. **2009**. *From Discovery to Approval*. 2nd ed. Hoboken, New Jersey.
2. Chorghade, M. S. **2007**. *Drug Discovery and Development*. Volume 7. Hoboken New Jersey.
3. UNAIDS., **2015**., *Fact sheet: 2014 statistics*.
4. Maurice, J. *The Lancet.*, **2014**, *383 (9928)*, 1535-1536.
5. Cohen, M. S; Chen, Y. Q.; McCauley, M.; Gamble, T.; Hosseinipour, M. C.; Kumarasamy N.; Hakim, J. G.; Kumwenda, J.; Grinsztejn, B.; Pilotto, J. H.; Godbole, S. V.; Mehendale, S.; Chariyalertsak, S.; Santos, B. R.; Mayer, K. H.; Hoffman, I. F.; Eshleman, S. H.; Piwowar-Manning, E.; Wang, L.; Makhema, J.; Mills, L. A.; de Bruyn, G.; Sanne, I.; Eron, J.; Gallant J.; Havlir, D.; Swindells, S.; Ribaud, H.; Elharrar, V.; Burns, D.; Taha, T. E.; Nielsen-Saines, K.; Celentano, D.; Essex, M.; Fleming, T. R. N. *Engl. J. Med.*, **2011**, *365*, 493-505.
6. Brechtel, J. R.; Breitbart, W.; Galietta, M.; Krivo, S.; Rosenfeld, B. J. *Pain. Symptom. Manage.*, **2001**, *21 (10)*, 41-51.
7. Branich, R.; Crowley, S.; Victoria, M.; Lo, Y. R.; Souteyrand, Y.; Dye, C.; Gilks, C.; Guerma, T.; De Cock, K. M.; William, B. J. *Int. AIDS. Soc.*, **2010**, *13*, 1-8.
8. Weiss, R. A. *in Retroviridae*, 2nd Ed, Levi, J. A. (Eds), plenum press, New York, **1992**, 1-108
9. Kwong, P. D.; Wyatt, R.; Robison, J.; Sweet, R.W.; Sodroski, J.; Hendrickson, W. A. *Nature.*, **1998**, *393*, 648-659.
10. Chan, D. C., Fass, D., Berger, J.M., Kim, P.S., *Cell.*, **1997**, *89*, 263-273.
11. Weissenhorn, W.; Dessen, A.; Harrison, S. C.; Skehel, J. J.; Wiley, D. C. *Nature.*, **1997**, *387*, 426-430.
12. Tilton, J. C.; Doms, R. W. *Antiviral. Res.*, **2010**, *85*, 91-100.
13. Gauser, B. K.; Li, S.; Klinsko, V. Y.; Flinch, J. T.; Sundquist, W. I. *Science.*, **1999**, *283*, 80-83.
14. Li, S.; Hill, C. P.; Sundquist, W. I.; Flinch, J. T. *Nature.*, **2000**, *407*, 409-413.
15. Briggs, J. A. G.; H.; Wilk, T.; Welker, R.; **Kräusslich**, H., G.; Fuller, S. D. *EMBO J.*, **2003**, *22*, 1707-1715.
16. Fouchier, R. A.; Malim, M. H. *Adv. Virus Res.*, **1999**, *52*, 275-299.
17. Galloway, P.; Hope, T.; Chin, D.; Trono, D.; *Proc. Natl. Acad. Sci. U. S. A.* **1997**, *94*, 9825-9830.
18. Engelman, A.; cherepanov, P. *Nature Rev. Microbiol.*, **2012**, *10*, 279-290.
19. Bar-Margen, T.; Donahue, D. A.; McDonough, E. I.; Kuhl, B. D.; Faltenbacher, V. H.; Xu, H.; Michaud, V.; Sloan, R. D.; Wainberg, M. A. *AIDS.*, **2010**, *24*, 2171-2179.
20. Vandegraaff, N.; Engelman, A. *Expert Rev. Mol. Med.*, **2009**, *9*, 1-19.

-
21. Miller, M.; Farnet, C.; Bushman, F. J. *Virology*, **1997**, *71*, 5382-5390.
 22. Serrao, E.; Odde, S.; Ramkumar, K.; Neamati, N. *Retrovirology*, **2009**, *6* (25), 1-14.
 23. Dow, D. E.; Barlett, J. A. *Infect. Dis. Ther.*, **2014**, *3*, 83-102.
 24. Hightower, K. E.; Wang, R.; Deanda, F.; Johns, B. A.; Waever, K.; Shen, Y.; Tomberlin, G. H.; Carter (III), L.; Broderick, T.; Sigethy, S.; Seki, T.; Kobayshi, M.; Underwood, M. R. *Antimicrob. Agents. Chemother.*, **2011**, *55* (10), 4552-4559.
 25. Bartholomeeusen, K.; Christ, F.; Hendrix, J.; Rain, J. C.; Emiliani, S.; Benarous, R.; Debyser, Z.; Gijssbers, R.; De Rijck, J. *J. Biol. Chem.*, **2008**, *284*, 11467-11477.
 26. Bartholomeeusen, K., De Rijck, J., Busschots, K., Desender, L., Gijssbers, R., Emiliani, S., Benarous, R., Debyser, Z., Christ, F. *J. Mol. Biol.*, **2007**, *372*, 407-421.
 27. Harrison, A.T. MSc thesis., Witwatersrand University, **2014**
 28. Pierre, L. B.; Proudfoot, J. *Boehringer Ingelheim Pharmaceuticals Inc.*; pp1-6.
 29. Brik, A.; Wong, C. *Org. Biomol.Chem.*, **2003**, *1*, 5-14.
 30. Turner, B. G.; Summers, M. F.; *J. Mol. Biol.*, **1996**, *272*, 872-877.
 31. Ratner, L.; *Prosp. Drug Discov. Des.*, **1993**, *1*, 2-22.
 32. Magadán, J. G.; Bonifacino, J. S. *J. Virology*, **2012**, *86*, 757-772.
 33. Schubert, U.; Bour, S.; Ferrer-Montiel, A. V.; Montal, M.; Maldarell, F. *J. Virology*, **1996**, *70*, 809-819.
 34. Deora, A.; Ratner, L. *J. Virology*, **2001**, *75*, 714-6718.
 35. Strebel, K. **1996**. In G. Myers, B. T. Korber, B. Foley, K.-T. Jeong, J. W. Mellors, and S. Wain-Hobson (ed.), *Human retroviruses and AIDS: a compilation and analysis of nucleic acid and amino acid sequences.*, Los Alamos National Laboratory, Los Alamos, N.Mex.
 36. Andrew, A.; Strebel, K. *Mol Aspects Med.*, **2010**, *31* (5), 407-417.
 37. Arias, J. F.; Iwabu, Y.; Tokunaga, K. *Frontier of Microbiology.*, **2011**, *250*, 1-9.
 38. Ishikawa, J.; Kaisho, T.; Tomizawa, H.; Lee, B. O.; Kobune, Y.; Inazawa, J.; Oritani, K.; Itoh, M.; Ochi, T.; Ishihara, K.; Hirano, T. *Genomics.*, **1995**, *26*, 527-534.
 39. Kupzig, S.; Korolchuk, V.; Rollason, R.; Sugden, A.; Wilde, A; Banting, G. *Traffic.*, **2003**, *4*, 694-709.
 40. Iwabu, Y.; Fujita H.; Kinomoto, M.; Kaneko, K.; Ishizaka, Y.; Tanaka, Y.; Sata, T.; Tokunaga, K. *J. Biol. Chem.*, **2009**, *284*, 35060-35072.
 41. Gupta, R. K.; Hué, S.; Schaller, T.; Verschoor, E.; Pillay, D.; Towers, G. J. *PLoS Pathog.*, **2009**, *5* (5), 1-9.
 42. McNatt, M. W.; Zang, T.; Hatzioannou, T.; Bartlett, M.; Fofana, I. B.; Johnson, W. E.; Neil, S. J. D.; Bieniasz, P. D. *PLoS Pathog.*, **2009**, *5*, 5 (2), 1-12.

-
43. Sato, K.; Gee, P.; Koyanagi, Y. *Frontiers Microbiol.*, **2012**, *3* (131), 1-9.
44. Arias, J. F.; Iwabu, Y.; Tokunaga, K. *Curr. HIV Res.*, **2012**, *10*, 283-291.
45. Skasko, M.; Wang, Y.; Tain, Y.; Tokarev, A.; Munguia, J.; Ruiz, A.; Stephens, E. B.; Opella, S. J.; Guatelli, J. *J. Biol. Chem.*, **2012**, *287* (1), 58-67.
46. Park, S. H.; De Angelis, A. A.; Nevzorov, A. A.; Wu, C. H. Opella, S. J. *J. Biophys.*, **2006**, *91*, 3032-3042.
47. Zhou, J.; Zhang, Z.; Mi, Z.; Wang, X.; Zhang Q.; Li, X.; Liang, C.; Cen, S. *Biochem.*, **2012**, *51*, 1288-1296.
48. Kobayashi, T.; Ode, H.; Yoshida, T.; Sato, K.; Gee, P.; Yamamoto, S. P.; Ebina, I.; Strebel, K.; Sato, H.; Koyanagi, Y. *J. Virol.*, **2011**, *85* (2), 932-945.
49. Shimura, K.; Kodama, E.; Sakagami, Y.; Matsuzaki, Y.; Watanabe, W.; Yamataka, K., Watanabe, Y.; Ohata, Y.; Doi, S, Sato, M.; Kano, M.; Ikeda, S.; Mastuoka, M. *J. Virol.*, **2008**, *82* (2), 764-774.
50. Walmsley, S. L.; Antela, A.; Clumeck, N.; Duiculescu, D.; Eberhard, A.; Gutiérrez, F.; Hocqueloux, L.; Maggiolo, F.; Sandkovsky, U.; Granier, C.; Pappa, K.; Wynne, B.; Min, S.; Nichols, G. *New Eng. J. Med.*, **2013**, *369* (19), 1807-1818.
51. Summa, V.; Petrocchi, A.; Bonelli, F.; Crescenzi, B.; Donghi, M.; Ferrara, M.; Fiore, F., Gardelli, C.; Gonzalez Paz, O.; Hazuda, D. J.; Jones, P.; Kinzel, O.; Laufer, R.; Monteagudo, E.; Muraglia, E.; Nizi, E.; Orvieto, F.; Pace, P.; Pescatore, G.; Scarpelli, R.; Stillmock, K.; Witmer, M.V.; Rowley, M. *J. Med. Chem.*, **2008**, *51* (18), 5843-5855.
52. Savarino, A. *Expert Opin Investig Drugs.*, **2006**, *15* (12), 1507-1522.
53. Christ, F.; Shaw, S.; Demeulemeeste, J.; Sesimmie, B. A.; Marchand, A.; Butler, S.; Smets, W.; Chaltin, P.; Westby, M.; Debyser, Z.; Pickford, C. *Antimicrob. Agents Chemother.*, **2012**, *56* (8), 4365-4374.
54. Christ, F.; Voet, A.; Marchand, A.; Nicolet, S.; Desimmie, B. A.; Marchand, D.; Bardiot, D.; Van der Veken, N. J.; Van Remoortel, B.; Strelkov, S. V.; De Maeyer, M. Chaltin, P.; Debyser, Z. *Nat. Chem. Biol.* **2010**, *6* (6), 442-448.
55. Du, L. Zhao, Y.; Chen, J.; Yang, L.; Zheng, Y.; Tang, Y.; Shen, X.; Jiang, H. *Biochem. Biophysic. Res. Comm.* **2008**, *375*, 139-144.
56. Hou, Y.; McGuinness, D. E.; Prongay, A. J.; Feld, B.; Ingravallo, P.; Ogert, R. A.; Lunn, C. A.; Howe, J. A. *J. Biomol. Screen.*, **2008**, *13* (5), 406-414.
57. De Luca, L.; Gitto, R.; Christ, F.; Ferro, S.; De Grazia, S.; Morreale, F.; Debyser, Z.; Chimirri, A. *Antiviral Res.*, **2011**, *92* (1), 102-107.

-
58. Ferro, S.; De Luca, L.; Agharbaou, E. F.; Christ, F.; Debuser, Z.; Gitto, R. *Bioorg. Med. Chem.*, **2015**, *23*, 3208-3214.
59. Agharbaoui, F. E.; Hoyte, A. C.; Ferro, S.; Gitto, R.; Buemi, M. R.; Fuchus, J. R.; Kvaratskhelia, M.; De Luca, L. *Eur. J. Med. Chem.*; **2016**, *123*, 673-683
60. Sharma, A.; Slaughter, A.; Jena, N.; Feng, L.; Kessler, J. J.; Fadel, H. J.; Malani, N.; Male, F.; Wus, L.; Poeschla, E.; Bushman, F. D.; Fuch, J. R.; Kvaratskheli, M. *PLoS Pathog.*, **2014**, *10* (5), e1004171.
61. Tintori, C.; Demeulemeester, J.; Franchi, L.; Massa, S.; Debyser, Z.; Christ, F.; Botta, M. *Bioorg. Med. Chem. Lett.*, **2012**, *22*, 3109-3114.
62. Khoury, G.; Ewart, G.; Luscombe, C.; Miller, M.; Wilkinson, J. *Antimicrob. Agents Chemother.*, **2010**, *54* (2), 834-845.
63. Zhang, Q.; Mi, Z.; Huang, Y.; Ma, L.; Ding, J.; Wang, J.; Zhang, Y.; Chen, Y.; Zhou, J.; Guo, F.; Li, X.; Cen, S. *Retrovirology.*; **2016**, *2* (13), 13.
64. Mi, Z.; Ding, J.; Zhang, Q.; Zhou, J.; Ma, L.; Yu, H.; Liu, Z.; Shan, G.; Li, X.; Zhou, J.; Wei, T.; Zhang, L.; Guo, F.; Liang, C.; Cen, S. *Sci. Rep.*, **2015**, *6* (5), 18499.
65. Erlanson, D. A. *Top. Curr. Chem.*, **2011**, *317*, 1-32.
66. Folkers, G.; Jahnke, W.; Erlanson, D. A.; Mannhold, R.; Kubinyi, H. **2006**. *Fragment-based Approaches in Drug Discovery (Methods and Principles in Medicinal Chemistry)*. Weinheim: Wiley-VCH. ISBN 3-527-31291-9.
67. McCarthy, D. J.; Campbell, A. J.; Kern, G.; Moustakas, D. *J. Chem. Inf. Model.*, **2014**, *54* (3), 693-704
68. Chessari, G.; Woodhead, A. J. *Drug Discov. Today.*, **2009**, *14*, 668-675.
69. Congreve, M.; Carr, R.; Murray, C.; Jhoti, H. A. *Drug Discov. Today.* **2003**, *8*, 876-877.
70. Wielens, J.; Headey, S. J.; Deadman, J. J.; Rhodes, D. I.; Parker, M. W.; Chalmers, D. K.; Scanlon, M. J. *Chem. Med. Chem.*, **2011**, *6*, 258-261.
71. Verlinde, C. L.; Fan, E.; Shibata, S.; Zhang, Z.; Sun, Z.; Deng, W.; Ross, J.; Kim, J.; Xiao, L.; Arakaki, T. L.; Bosch, J.; Caruthers, J. M.; Larson, E. T.; Letrong, I.; Napuli, A.; Kelly, A.; Mueller, N.; Zucker, F.; Van Voorhis, W. C.; Buckner, F. S.; Merritt, E. A.; Hol, W. G., *Curr. Top Med. Chem.*, **2009**, *9* (18), 1678-1687.
72. Shuker, S. B.; Hajduk, P. J.; Meadows, R. P.; Fesik, S. W., *Science.*, **1996**, *274* (5292), 1531-1534.
73. Harner, M. J.; Frank, A. O.; Fesik, S. W. *J. Biomol. NMR.*, **2013**, *56* (2), 65-75.

-
74. Friberg, A.; Vigil, D.; Zhao, B.; Daniels, R. N.; Burke, J. P.; Garcia-Barrantes, P. M.; Camper, D.; Chauder, B. A.; Lee, T.; Olejniczak, E. T., Olejniczak, E. T.; Fesik, S. W. *J. Med. Chem.*, **2013**, *56*, 15-30.
75. Hajduk, P. J.; Augeri, D. J.; Mack, J.; Mendoza, R.; Yang, J.; Betz, S. F.; Fesik, S. W. *J. Am. Chem. Soc.*, **2000**, *122*, 7898-7904.
76. Bollag, G.; Hirth, P.; Tsai, J.; Zhang, J.; Ibrahim, P. N.; Cho, H.; Spevak, W.; Zhang, C.; Zhang Y.; Habets, G.; Burton, E. A.; Wong, B.; Tsang, G.; West, B. L.; Powell, B.; Sheloe, R.; Marimuthu, A.; Nguyen, H.; Artis, D. R.; Schessinger, J.; Su, F.; Higgins, B.; Lyer, R.; Andrea, K. D.; Koehler, A.; Stumm, M.; Lin, P. S.; Lee, R. J.; Grippo, J.; Puzanov, I.; Kim, K. B.; Ribas, A.; McArthur, G. A.; Sosman, J. A.; Chapman, P. B.; Flaherty, K. T.; Xu, X.; Nathanson, K. L.; Nolop, K. *Nature.*, **2010**, *467*, 596-599.
77. Spencer, R. *Biotechnol. Bioeng. Com. Chem.*, **1998**, *61*, 61-67.
78. Pereira, D. A.; Williams, J. A. *Br. J. Pharmacol.*, **2007**, *161*, 53-61.
79. Blundell, T. L. *Nature.*, **1996**, *384*, 23-26
80. Wermuth, C. G. **2006.**, *Analogues as means of discovering new drugs. In: Fischer, J., Ganellin, C.R. (Eds.), Analog Based Drug Discovery.* John Wiley-VCH.
81. Pollack, S. J.; Beyer, K. S.; Lock, C.; Müller, I.; Sheppard, D.; Lipkin, M.; Hardick, D.; Blurton, P.; Leonard, P. M.; Hubbard, P. A.; Todd, D.; Richardson, C. M.; Ahrens, T.; Baader, M.; Hafenbradl, D. O.; Hilyard, K.; Bürli, R. W. *J. Comput. Aided. Mol. Des.* **2011**, *25* (7), 677-687
82. Hann, M. M.; Leach, A. R.; Harper, G. J. *Chem. Inf. Comput. Sci.*; **2001**, *41*, 856-864.
83. Hopkins, A. L.; Groom, C. R. *Nat. Rev. Drug. Discov.*, **2002**; *1*, 727-730.
84. Hopkins, A. L.; Mason, J. S.; Overington, J. P. *Curr. Opin. Struct. Biol.*, **2006**, *16*, 127-136.
85. Shepherd, C. A.; Hopkins, L. A.; Navratilova, I. *Prog. Biophys. Mol. Biol.*, **2014**, *116*, 113-123.
86. Lipinski, C. A.; Lombardo, F.; Dominy, B. W.; Feeney, P. J. *Adv. Drug. Deliv. Rev.* **2001**, *46*, 3-26.
87. Shuker, S. B.; Hajduk, P. J.; Meadows, R. P.; Fesik, S. W. *Science.*, **1996**, *274*, 1531-1534.
88. Zartlet, E. D.; Mo, H. *Curr. Top. Med. Chem.*, **2007**, *7*, 1592-1599.
89. Mayer, M.; Meyer, B. *Angew. Chem. Int. Ed.*, **1999**, *38* (12), 1784-1788.
90. Pierce, M. M.; Raman, C. S.; Nall, B. T. *Methods.*, **1999**, *19*, 213-221.
91. Ladbury, J. E.; Klebe, G.; Freire, E. *Nat. Rev. Drug Discov.*, **2010**, *9*, 23-27.
92. Ferguson, F. M.; Fedorov, O.; Cahikuad, A.; Philpott, M.; Muniz, J. R. C.; Felletar, I.; Von Delft, F.; Heightman, T.; Knapp, S.; Abell, C.; Ciulli, A. *J. Med. Chem.*, **2013**, *56*, 10183-10187.

-
93. Serrao, E.; Debnath, B.; Otake, H.; Kuang, Y.; Christ, F.; Debysier, Z.; Neamti, N. *J. Med. Chem.*, **2013**, *56* (6), 2311-2322.
94. Beaudet, L.; Be'dard, J.; Breton, B.; Mercuri, R. J.; Budarf, M. L. *Genome Res.*, **2001**, *11*, 600-608.
95. Wigle, T. J.; Herold, J. M.; Senisterra, G. A.; Vedadi, M.; Kireev, D. B.; Arrowsmith, C. H.; Frye, S.V.; Janzen, W. P.; *J. Biomol. Screen.*, **2010**, *15*, 62-71.
96. Green, N. M. *Methods Enzymol.*, **1990**, *184*, 51-67.
97. Van Leusen, A. M.; Van Leusen, D. *Encyclopaedia of reagents for organic chemistry.*, New York,, Papuette, L. A., Ed. Wiley:, **1995**, *7*, 4973-4979.
98. Van Leusen, D. Van Leusen, A. M. *Org. React.*, **2004**, *57* (3), 417-666.
99. Van Leusen, D.; Oldenziel, O. H.; Van Leusen, A. M. *J. Org. Chem.*, **1977**, *42* (19), 3114-3118
100. Van Leusen, A. M.; Strating, J. *Q. Rep. Sulfur Chem.*, **1970**, *5*, 67-78.
101. www.sigmaaldrich.com/catalog/product/aldrich/188204.
102. Olijnsma, T.; Engberts, J. B. F. N.; Strating, J. *Recl. Trav. Chim. Pays-Bas.*, **1972**, *91*(2), 209-212.
103. Lujan-Montelongo, A.; Estevez, A. O.; Fleming, F. F. *Eur. J. Org. Chem.*, **2015**, *9*, 1602-1605.
104. Hoogenboom, B. E.; Oldenziel, O. H.; van Leusen, A.M. *Org. Syn.*, **1977**, *57*, 102.
105. Van Leusen, A. M.; Bourma, R. J.; Possel, O. *Tetrahedron Lett.*, **1975**, *16* (40), 3487-3488.
106. Yadav, J. S.; Ready, P. S.; Joshi, B. V. *Tetrahedron Lett.*, **1988**, *44* (23), 7243-7254.
107. Johnson, D. W. *Chem. Phys. Lipids.*, **1990**, *1*, 65-71.
108. Sisko, J.; Mellinger, M.; Sheldrake, P. W.; Baine, N. H. *Tetrahedron Lett.*, **1996**, *37*, 8113-8114
109. Lygin, A. V.; de Meijere, A. *Angew. Chem. Int. Ed.*, **2010**, *49*, 9094-9097.
110. Van Leusen, A. M.; Wildeman, J.; Oldenziel, O. H. *J. Org. Chem.*, **1977**, *42* (7), 1153-1158.
111. Sisko, J.; Kassick, A.; Mellinger, M.; Filan, J. J.; Allen, A.; Olsen, M. A. *J. Org. Chem.*, **2000**, *65*, 1516-1524.
112. Hao, W.; Jiang, Y.; Cai, M. *J. Org. Chem.*, **2014**, *79*, 3634-3640.
113. Bunev, A. S.; Vasiliev, M. A.; Statsyuk, V. E.; Ostapenko, G. I.; Peregudov, A. S. *J. Fluorine Chem.*, **2014**, *163*, 34-37.
114. Yugandar, S.; Acharya, A.; Ila, H. *J. Org. Chem.*, **2013**, *78* (8), 3948-3960.
115. Van Leusen, D.; van Echten, E.; Van Leusen, A. M. *J. Org. Chem.*, **1992**, *57* (8), 2245-2249.
116. Arnold, D. P.; Brown, R. F. C.; Nitschinsk, L. J.; Perlmutter, P.; Tope, H. K. *Aust. J. Chem.*, **1994**, *47*, 975-978.
117. Barton, D. H. R.; Kervagoret, J.; Zard, S. Z. *Tetrahedron.*, **1990**, *46* (21), 7587-7598
118. Chen, W.; Shao, J.; Li, Z.; Giulianotti, M. A.; Yu, Y. *Can. J. Chem.*, **2012**, *90*, 214-221.

-
119. Zhou, F.; Liu, J.; Ding, k.; Liu, J.; Cai, Q. *J. Org. Chem.*, **2011**, *76*, 5346-5353.
120. Ni, L.; Li, Z.; Wu, F.; Xu, J. Wu, X.; Kong, L. Yao, H. *Tetrahedron Lett.*, **2012**, *53*, 1271-1274.
121. Coppola, A.; Alonso, P. S.; Sucunza, D.; Burgos, C.; Alaja'rn, R.; Billa, J. A.; Mosquera, M. E. G.; Vaquore, J. J. *Org. Lett.*, **2013**, *15*, 3388-3391.
122. Garima, Srivastava V. P. Yadav, D. S. L. *Tetrahedron Lett.*, **2011**, *52*, 4622-4626.
123. Kristna, P. R.; Dayaker, G.; Reddy, P. V. N. *Tetrahedron Lett.*, **2006**, *47*, 5977-5980.
124. Van Cutsem, J. *Am. J. Med.*, **1983**, *74* (1), 29-15.
125. Van Den Bossche, H.; Willemsens, G.; Cools, W.; Cornelissen, F.; Lauwers, W. F.; Van Cutsem, J. M. *Antimicrob. Agents Chemother.*, **1980**, *17* (6), 922-928.
126. Sahlin, K.; Kumar, P.; Kumar, N. *Der Chemica Sinica.*, **2010**, *1* (3), 36-47.
127. Sharma, D.; Narasimhan, B.; Kumar, P.; Judge, V.; Narang, R.; De Clercq, E.; Balzarini, J. *Eur. J. Med. Chem.*, **2009**, *44*, 2347-2353.
128. Jawaharmala; Narwal, S.; Singh, G.; Saini, D. R. A. *Indo. J. Pharm. Sci.*, **2012**, *2* (3), 305-312.
129. Menozzi, G.; Merello, L.; Fossa, P.; Schenone, S.; Ranise, A.; Mosti, L.; Bondavalli, F.; Loddo, R.; Murgioni, C.; Mascia, V.; La Collab, P.; Tamburini, E. *Bioorg. Med. Chem.*, **2004**, *12*, 5465-5483.
130. Baviskar, A. T.; Madaan, C.; Preet, R.; Mohapatra, P.; Jain, V.; Agarwal, A.; Guchhait, S. K.; Kundu, C. N.; Banerjee, U. C.; Bharatam, P. V. *J. Med. Chem.*, **2011**, *54* (14), 5013-5030.
131. Baroniya, S.; Anwar, Z. Sharma, P. K.; Dudhe, R.; Kumar, N. *Der. Pharmacia. Sinica.*, **2010**, *1* (3), 172-182.
132. Benincori, T.; Brenna, E.; Sannicolo, F. *J. Chem. Soc. Perkin Trans. 1.*, **1993**, *6*, 675-679.
133. Elderfield, R. C.; Shriner, R. L. *Science.*, **1957**, *125* (3259), 1206-1207.
134. Debus, H. *Annalen der Chemie und Pharmacie.*, **1858**, *107* (2), 199 -208.
135. Elderfield C., R. *5- membered heterocycles combining two heteroatoms & their benzo derivatives, heterocyclic compound*, **1957**, *5*, 744.
136. Shamsuzzaman; Khan, M. S.; Alam, M.; Tabassum, Z.; Ahmad, A.; Khan, A. U. *Eur. J. Med. Chem.* **2010**; *45*, 1094-1097.
137. Kovačević, S. Z.; Kuzmanović, S. O. P.; Jevrić, L.R.; Kalajđžija, N. A. *APTEFF.* **2013**, *44*, 1-321.
138. Praveena, C. H. L.; Rani, V. E.; Spoorthy, Y. N.; Ravindranath, L. K. *Der. Pharma. Chemica.*, **2013**, *5* (4), 58-70.
139. Reddy, A. B.; Hymavathi, R.V.; Swamy. G. N. *J. Chem. Sci.*, **2013**, *125* (3),. 495-509.
140. Moorkoth, S.; Srinivasan, K. K; Bukka, D. *Elixir Pharmacy*, **2013**, *54*, 12315-12318.

-
141. Kim, S. H.; Markovitz, B.; Trovato, R.; Murphy, B. R.; Austin, H.; Willardsen, A. J.; Baichwal, V.; Morham, S.; Bajji, A. *Bioorg. Med. Chem. Lett.*, **2013**, *23*, 2888-2892.
142. Zhou, X.; Zhang, M.; Sun, W.; Yang, X.; Wang, G.; Sui, D.; Yu, X.; Qu, S. *Biol. Pharm. Bull.*, **2009**, *32(12)*, 1986-1990.
143. Robinson, R. *J. Chem. Soc.*, **1909**, *95*, 2167.
144. Keni, M.; Tepe, J. J. *J. Org. Chem.* **2005**, *70*, 4211-4213.
145. Wasserman, H. H.; Vinick, F. J. *J. Org. Chem.*, **1973**, *38 (13)*, 2407-2408.
146. Wiley, R. H. *Chem. Rev.*, **1945**, *37*, 401.
147. Cornforth, J. W.; Cornforth, R. H. *J. Chem. Soc.*, **1949**, 1028-1030.
148. Bellur, E.; Freifeld, I.; Langer, P. *Tetrahedron Lett.* **2005**, *47*, 2151-2154.
149. Daidone, G.; Maggio, B.; Schillaci, D. *Pharmazie.*, **1990**, *45*, 441-442.
150. Demir, A. S.; Akhmedov, I. M.; Sesenoglu, O. *Tetrahedron.*, **2002**, *58*, 9793-9799.
151. Meshram, H. M.; Prasad B. R. V.; Kumar, D. A. *Tetrahedron Lett.*, **2010**, *51*, 3477-3480.
152. Davis, F. A.; Bowen, K.; Xu, H.; Velvadapu, V.; Ballard, C. *Tetrahedron.*, **2008**, *64*, 4174-4182.
153. Adib, M.; Mohammadi, B.; Sheikhi, E.; Bijanzadeh, H. R. *Chin. Chem. Lett.*, **2011**, *22*, 314-317.
154. Ugi, I., *Isonitrile Chemistry*, Academic. **1971**, Ed.; Press: New York.
155. Nenajdenko, V. G., *Isocyanide Chemistry*; **2012**, Ed.; Wiley-VCH: Weinheim.
156. Barybin, M. V. *Coord. Chem. Rev.*, **2010**, *254*, 1240-1252.
157. Meier, M.; Mueller, B.; Ruechardt, C. *J. Org. Chem.*, **1987**, *52 (4)*, 648-652.
158. Malatesta, L. *Prog. Inorg. Chem.* **1959**, *1*, 283-379.
159. Ugi, I.; Meyr, R. *Angew. Chem.*, **1958**, *70*, 702-703.
160. Hofmann, A. W. *Ann. Chem. Pharm.* **1867**, *144*, 114-120.
161. Pornet, J.; Maginiac, L. *Tetrahedron Lett.*, **1971**, *15*, 967-970.
162. Ugi, I.; Fetzer, U.; Eholzer, U.; Knupfer, H.; Offermann, K. *Angew. Chem., Int. Ed. Engl.* **1965**, *4*, 472.
163. Weber, W. P.; Gokel, G. W.; Ugi, I. K. *Angew. Chem.*, **1972**, *11*, 530-531.
164. Buron, C.; Kaim, L.EI.; Uslu, A. *Tetrahedron. Lett.*, **1997**, *38 (46)*, 8027-8030.
165. Reitz, D. B.; Isakson, P. C. *Curr. Pharm. Des.*, **1995**, *1*, 211-220.
166. Chavatte, P.; You, S.; Marot, C.; Baurin, N.; Lesieur, D. *J. Med. Chem.*, **2001**, *44*, 3223-3230.
167. Erdélyi, P.; Fodor, T.; Varga, A. K.; Czugler, M.; Gere, A.; Fischer, J. *Bioorg. Med. Chem.*, **2008**, *16 (9)*, 5322-5330.

-
168. Shin, K. D.; Lee, M. Y.; Shin, D. S.; Lee, S.; Son, K. H.; Koh, S.; Paik, Y. K.; Kwon, B. M.; Han, D. C. *J. Biol. Chem.*, **2005**, *280*, 41439-41448.
169. Yong, J. P.; Lu, C. Z.; Wu, X. *Anticancer Agents Med. Chem.*, **2015**, *15* (1), 131-136.
170. Rouchaud, J., Gustin, F. ; Moulard, C. *Bull. Soc. Chim. Belg.*, **1993**, *102* (8), 543-555.
171. Wakefield, B. J. *Sci. Synth.*, **2001**, *11*, 229-288.
172. Zhou, Y.; Chen, Y.; Miao, W.; Qu, J. J. *Heterocycl. Chem.*, **2010**, *47*, 1310- 1316.
173. Liu, X. H.; Cui, P.; Song, B. A.; Bhadury, P. S.; Zhu, H. L.; Wang, S. F. *Bioorg. Med. Chem.*, **2008**, *16*, 4075-4082.
174. Becker, A.; Grecksch, G.; Bernstein, H.G.; Höllt, V.; Bogerts, B. *Psychopharmacology.*, **1999**, *144* (4), 333-3338.
175. Praveen, C.; Kalyanasundaram, A.; Perumal, P. T.; *Synlett.*, **2010**, 777-781.
176. Crossley, J. A.; Browne, D. L. *J. Org. Chem.*, **2010**, *75*, 5414-5416.
177. Fujiwara, T.; Sato, A.; El-Farrash, M.; Miki, S.; Abe, K.; Isaka, Y.; Kodama, M.; Wu, Y.; Chen, L. B.; Harada, H.; Sugimoto, H.; Hatanaka, M.; Hinumana, Y. *Antimicrob. Agents Chemother.*, **1998**, *42*, 1340-1345.
178. Silvestri, R.; Artico, M.; Massa, S.; Marceddu, T.; De Montis, F.; La Colla, L. *Bioorg. Med. Chem. Lett.*, **2000**, *10*, 253-256.
179. Silvestri, R.; Artico, M.; De Martino, G.; Ragno, R.; Massa, S.; Lodda, R.; Mugioni, A.; GiluliaLoi, A.; La Colaa, P. Pani, A. *Med. Chem.*, 2002, *45*, 1567-1576.
180. Serrao, E.; Xu, Z. -L.; Debnath, B.; Christ, F.; Debyser, Z.; Long, Y. -Q.; Neamati, N. *Bioorg. Med. Chem.*, **2013**, *21*, 5963-5972
181. Kempf, D. J.; Marsh, K. C.; Kumar, G.; Rodrigues, A. D.; Denissen, J. F.; McDonald, E.; Kukulka, M. J.; Hsu, A.; Granneman, G. .; Baroldi, P. A.; Sun, E.; Pizzuti, D.; Plattner, J. J.; Norbeck, D. W.; Leonard, J. M.; *Antimicrob. Agents Chemother.*, **1997**, *41* (3), 654-660.
182. Loh, B.; Vozzolo, L.; Mok, B. J.; Lee, C. C.; Fitzmaurice, R. J.; Caddick, S.; Fassati, A. *Chem. Biol. Drug Des.*, **2010**; *75*, 461-474.
183. Burkhard, P.; Hommel, U.; Sanner. M.; Walkinshaw, M.D. *J.Mol Biol.*, **1999**; *287*, 853-858.
184. Shoichet, B. K. *Nature.*, **2004**; *432*, 862-865.
185. See Rashamuse, T.J. PhD Chemistry Proposal (Witwatersrand University, June **2013**).
186. Houwing, A.; Wildeman, J.; van Leusen, A. M. *Tetrahedron Lett.*, **1976**, *2*, 143-146.
187. Hernández-Molina, R.; Mederos A. "Acyclic and Macrocyclic Schiff Base Ligands" in *Comprehensive Coordination Chemistry II.*, **2003**, 411-446.
188. Yang, Z.; Sun, P. *Molbank.*, **2006**, *M514*, 1-3.
189. Xu, J.; Zhuang, R.; Bao, L.; Tang, G.; Zhao, Y. *Green Chem.*, **2012**, *14*, 2384-2387.

-
190. Liu, L.; Zhang, S.; Fu, X.; Yan, C. H. *Chem. Commun.*, **2011**, 47, 10148-10150.
191. Van Driessche, B.; Van Brabant, W.; D'Hooghe, M.; Dejaegher, Y.; De Kimpe, N. *Tetrahedron.*, **2006**, 62 (29), 6882-6892.
192. Albert, J.; Cadena, M.; Granell, J.; Solans, X.; Font-Bardia, M. *J. Organomet. Chem.*, **2004**, 689, 4889-4896.
193. Pfefferkorn, J. A.; Song, Y.; Sun, K. L.; Miller, S. R.; Trivedi, B. K.; Choi, C.; Sorenson, R. J.; Bratton, L. D.; Unangst, P. C.; Larsen, S. D.; Poel, T. J.; Cheng, X. M.; Lee, C.; Erasga, N.; Auerbach, B.; Askew, V.; Dillon, L.; Hanselman, J. C.; Lin, Z.; Lu, G.; Robertson, A.; Olsen, K.; Mertz, T.; Sekerke, C.; Pavlovsky, A.; Harris, M. S.; Bainbridge, G.; Caspers, N.; Chen, H.; Eberstadt, M. *Bioorg. Med. Chem. Lett.*, **2007**, 17 (16), 4538-4544.
194. Beck, J. F.; Neshat, A.; Schmidt, J. A. R. *Eur. J. Inorg. Chem.*, **2010**, 32, 5146-5155.
195. Selvakumar, K.; Vancheesan, S. *Polyhedron.*, **1996**, 15 (22), 3979-3986.
196. Varma, R. S. *Green. Chem.*, **1999**, 15, 43-55.
197. Loupy, A.; Petit, A.; Hamelin, J.; Texier-Boullet, F.; Françoise, P.; Mathe, D. *Synthesis.*, **1998**, 1213-1234.
198. Lidstron, P.; Tierney, J.; Wathey, B.; Westman, J. *Tetrahedron.*, **2001**, 57, 9225-9283.
199. Andrade, C. K. Z.; Takada, S. C. S.; Alves, L. M.; Rodrigues, J. P.; Juliana, P.; Suarez, P. A. Z.; Brando, R. F.; Soares, V. C. D. *Synlett.*, **2004**, 12, 2135-2138.
200. Jiang, L.; Jin, L.; Tian, H.; Xuegin, Y.; Yu, X.; Xu, Q. *Chem. Commun. (United Kingdom).*, **2011**, 47 (38), 10833-10835.
201. Reichert, S.; Breit, B. *Org. Lett.*, **2007**, 9 (5), 899-902.
202. Flipping, L. A.; Muchonski, J. M. Carter, D. S. *J. Org. Chem.*, **1993**, 58 (9), 2463-2467.
203. Mosterio, R.; Perille, E.; Fernandez, A.; Lopez-Torres, M.; Vila, J. M.; Suarez, A. *Appl. Organomet. Chem.*, **2000**, 14 (10), 634-639.
204. Mueller, W.; Nozulak, J.; Roy, B. L. *Patent No. 2005118535* (15 December **2005**)
205. Beaudet, L.; Rodriguez-Suarez, R.; Venne, M.-H.; Caron, M.; Bédard, J.; Brechler, V.; Parent, S.; Bielefeld-Sévigny, M. *Nature*, **2008**, Methods 5.
206. Christ, F.; Voet, A.; Marchand, A.; Nicolet, S.; Desimmie, B. A.; Marchand, D.; Bardiot, D.; Van der Veken, N. J.; Van Remoortel, B.; Strelkov, S. V.; De Maeyer, M. Chaltin, P.; Debysers, Z. *Nat. Chem. Biol.*, **2010**, 6(6), 442-448.
207. Du, L. Zhao, Y.; Chen, J.; Yang, L.; Zheng, Y.; Tang, Y.; Shen, X.; Jiang, H. *Biochem. Biophysic. Res. Comm.*, **2008**, 375, 139-144.

-
208. Slaughter, A.; Jurado, K. A.; Deng, N.; Feng, L.; Kessl, J. J.; Shkriabai, N.; Larue, R. C.; Fadel, H. J.; Patel, P. A.; Jena, N.; Fuchs, J. R.; Poeschla, E.; Levy, R. M.; Engelman, A.; Kvaratskhelia, M. *Retrovirology*, **2014**, *11*, 1-14.
209. Xue, W. Liu, H.; Yao, X. *PLoS ONE*, **2014**, *9* (3), e90799
210. Corey, E. J. *Angew. Chem. Int. Ed. Engl.*, **1991**, *30* (5), 455-465.
211. Satoshi, U. Hideko, N. *J. Org. Chem.*, **2009**, *74* (11), 4272-4277
212. Ge, G. C.; Ding, C. H.; Hou, X. L. *Org. Chem. Front.*, **2014**, *1*, 382-385.
213. Srivastava, A. K.; Bahel, S. C.; *Agric. Biol. Chem*, **1976**, *40* (4), 801-803.
214. Cheng, C. J.; Sun, G.; Jieping, W.; Sun, C.; *Synlett.*, **2009**, *16*, 2663-2668
215. John, J. M.; Loorthuraja, R.; Antoniuk, E.; Bergens, S. H. *Catal. Sci. Technol.*, **2015**, *5* (2), 1181-1186.
216. Vigorita, M. G.; Saporito, G.; Previtera, T.; Pizzimenti, F. C. J. Bisiignano, G. *Farmaco.*, **1986**, *41* (2), 168-174.
217. Van Dijk, T.; Burck, S.; Rong, M. K.; Rosenthal, A. J.; Nieger, M.; Slootweg, J. C.; Lammertsma, K. *Angew. Chem. Int. Ed.*, **2014**, *53* (34), 9068-9071.
218. Liu, X.; Wu, P.; Li, J.; Cui, C. *J. Org. Chem.*, **2015**, *80* (8), 3737-3744.
219. Aguilar, A.; Zhou, H.; Chen, J.; Liu, L.; Bai, L.; McEachern, D.; Yang, C.-Y.; Meagher, J.; Stuckey, J.; Wang, S. *J. Med. Chem.* **2013**, *56*, 3048-3067.
220. Yang, J.; Teng, Y.; Ara, S.; Rallapalli, S.; Cook, J. M. *Synthesis (Stuttg)*. **2009**, *40*, nihpa145687.
221. Feng, B. Y.; Shelat, A.; Doman, T. N. Guy, R. K.; Shoichet, B. K. *Nature. Chem. Biol.*, **2005**, *1*, 146-148.
222. Card, G. L.; Blasdel, L.; England, B. P.; Zhang, C.; Suzuki, Y.; Gillette, S.; Fong, D.; Ibrahim, P. N.; Artis, D. R.; Bollag, G.; Milburn, M. V.; Kim, S. H.; Schlessinger, J.; Zhang, K. Y., *Nat. Biotechnol.*, **2005**, *23* (2), 201-207.
223. Hughes, S. J.; Millan, D. S.; Kilty, I. C.; Lewthwaite, R. A.; Mathias, J. P.; O'Reilly, M. A.; Pannifer, A.; Phelan, A.; Stuhmeier, F.; Baldock, D. A.; Brown, D. G. *Bioorg. Med. Chem. Lett.*, **2011**, *21* (21), 6586-6590.
224. Godemann, R.; Madden, J.; Kramer, J.; Smith, M.; Fritz, U.; Hesterkamp, T.; Barker, J.; Hoppner, S.; Hallett, D.; Cesura, A.; Ebneith, A.; Kemp, J. *Biochemistry*, **2009**, *48* (45), 10743-10751.
225. Kumar, A.; Voet, A.; Zhang, K. Y. J. *Curr. Med. Chem.*, **2012**, *19*, 5128-5147.
226. De Luca, L.; Gitto, R.; Christ, F.; Ferro, S.; De Grazia, S.; Morreale, F.; Debysen, Z.; Chimirri, A. *Antiviral Res.*, **2011**, *92* (1), 102-107.

-
227. Sharma, A.; Slaughter, A.; Jena, N.; Feng, L.; Kessler, J. J.; Fadel, H. J.; Malani, N.; Male, F.; Wus, L.; Poeschla, E.; Bushman, F. D.; Fuch, J. R.; Kvaratskheli, M. *PLoS Pathog.*, **2014**, *10* (5), e100417.
228. Zhang, F. -H.; Debnath, B.; Xu, Z. -L.; Yang, L. -M., Song, L. -R.; Zheng, Y.; -T.; Neamati, N., Lon, Y. -Q. *Eur. J. Med. Chem.*, **2017**, *125*, 1051-1063.
229. Cherepanov, P.; Ambrosio, A. L. B.; Rahman, S.; Ellenberger, T.; Engelman, A. *Proc. Natl. Acad. Sci. U. S. A.* **2005**, *102*, 17308-17313.
230. Van Leusen, A. M.; Hoogenboom, B. E.; Sierius, H. *Tetrahedron Lett.*, **1972**, *13*, 3114-3118.
231. Van Leusen, D.; Van Leusen, Albert M. *Organic Reactions* (Hoboken, NJ, United States), **2001**, *57*, 433
232. Companyo, X.; Moyano, A.; Rios, R. *Lett. Org. Chem.*, **2009**, *6*, 293-296.
233. Flegeau, E. F.; Popkin, M. E.; Greaney, M. F. *Org. Lett.*, **2008**, *10* (13), 2717-2720.
234. Mayuko, N.; Koji, H.; Tetsuya, S.; Masahiro, M. *Angew. Chem. Int. Ed.* **2012**, *51* (28), 6993-6997.
235. Cavalluzzo, C.; Voet, A.; Christ, F.; Singh, B. K.; Sharma, A.; Debyser, Z.; De Maeyer, M.; Van der Eycken, E. *RSC Advances*, **2012**, *2*, 974-984.
236. Momin, M. I. K.; Ramjugernath, D.; Mosa, R. A.; Opoku, A. R.; Koobanally, N. A. *Med. Chem. Res.*, **2015**, *24*, 2075-2084.
237. Svajger, U.; Horvat, Ž.; Knez, D.; Rožman, P.; Turk, S.; Gobec, S. *Med. Chem. Res.*, **2015**, *24*, 362-371.
238. Matsumoto, K.; Suzuki, M.; Nunami, K.; Yoneda, N.; Takiguchi, K. *Bull. Inst. Chem. Res., Kyoto Univ.* **1983**, *61* (2), 79-88.
239. Matsuo, T.; Hayashi, A.; Abe, M.; Matsuda, T.; Hisaeda, Y.; Hayashi, T. *J. Am. Chem. Soc.*, **2009**, *131* (42), 15124-15125.
240. Giustiniano, M. V.; Cassese, H.; Maro, S. D.; Galli, U.; Novellino, E.; Tron, G. C. *J. Org. Chem.*, **2014**, *79*, 6006-6014.
241. Sladojevich, F.; Trachocchi, A.; Guarna, A.; Dixon, D.J. *J. Am. Chem. Soc.*, **2011**, *133* (6), 1710-1713.
242. Moraski, G. C.; Chang, M.; Estrada, A. V.; Franzblau, S. G.; Möllmann, U.; Miller, M. J. *Eur. J. Med. Chem.*, **2010**, *45*, 1703-1716.
243. Schöllkopf, U.; Schroder, R. *Angew. Chem.*, **1971**, *83* (10), 358-359.
244. Suzuki, M.; Iwasaki, T.; Matsumoto, K.; Okumura, K. *Syn. Commun.*, **1972**, *2*, 237-242.

-
245. Ozaki, Y.; Maeda, S.; Iwasaki, T.; Matumoto, K.; Odawara, A.; Sasaki, Y.; Morita, T. *Chem. Pharma. Bull.*, **1983**, *31* (12), 4417-4424.
246. Strazzolini, P.; Misuri, N.; Polese, P. *Tetrahedron Lett.*, **2005**, *46* (12), 2075-2078.
247. Barbayanni, E.; Fotakopoulou, I.; Schmidt, M.; Constantinou-Kokotou, V.; Bornscheuer, U. T.; Kokotos, G. *J. Org. Chem.*, **2005**, *70* (22), 8730-8733.
248. Zhang, Q.; Zhao, B.; Song, Y.; Hua, C.; Gou, X.; Chen, B.; Zhao, J. *Heteroatom Chemistry.*, **2015**, *26* (5), 348-354.
249. Coban, G.; Kose F. .A.; K; Kirmizibayra, P. B.; Pabuccuoglu, V. *Med. Chem. Res.*, **2015**, *24* (10), 3710-3729.
250. Schneider, T. L.; Halloran, K. T.; Hillner, J. A.; Conry, R. R.; Linton, B. R. *Chem.-Eur. J.*, **2013**, *19* (45), 15101-15104.
251. Ueda, S.; Nagasawa, H. *J. Org. Chem.*, **2009**, *74* (11), 4272-4277.
252. Feng, B. Y.; Shelat, A.; Doman, T. N. Guy, R. K.; Shoichet, B. K. *Nat. Chem. Biol.*, **2005**, *1*, 146-148.
253. Hughes, S. J.; Millan, D. S.; Kilty, I. C.; Lewthwaite, R. A.; Mathias, J. P.; O'Reilly, M. A.; Pannifer, A.; Phelan, A.; Stuhmeier, F.; Baldock, D. A.; Brown, D. G. *Bioorg. Med. Chem. Lett.*, 2011, *21* (21), 6586-6590.
254. Godemann, R.; Madden, J.; Kramer, J.; Smith, M.; Fritz, U.; Hesterkamp, T.; Barker, J.; Hoppner, S.; Hallett, D.; Cesura, A.; Ebneith, A.; Kemp, J. *Biochemistry.*, **2009**, *48* (45), 10743-10751.
255. Kumar, A.; Voet, A.; Zhang, K. Y. J. *Curr. Med. Chem.*, **2012**, *19*, 5128-5147.
256. De Las Rivas J, Fontanillo C. *PLoS Comp. Biol.*, **2010**, *6* (6), e1000807
257. Williams, R.M. *Synthesis of Optically Active Amino Acids*, Pergamon Press: Oxford, **1989**
258. Barrett, G. C. *Chemistry and biochemistry of the amino acids*, CHAPMAN AND HALL LONDON, **1985**.
259. Hasegawa, S.; Ichiyama, T.; Sonaka, I.; Ohsaki, A.; Okada, S.; Wakiguchi, H.; Kudo, K.; Kittaka, M.; Hra, M.; Furukawa, S. *Clin. Exp. Immunol.*; **2012**, *167*, 269-274.
260. De Clercq, E. *Int. J. Antimicrob.*, **2009**, *33*, 307-32.
261. Hruby, V. J., *Nat. Rev.*, **2002**, *1*, 847-858.
262. Liu, W.; Zhang, L.; Zhou, H.; Yang, C.; Miao, Z.; Zhao, Y. *Nucleosides, Nucleotides & Nucleic Acids.*, **2013**, *32*(4), 161-173.
263. Sun, C.; Zhu, J.; Wang, H.; Jin, J.; Xing, J.; Yang, D. *Eur. J. Med. Chem.*, **2011**, *46*(1), 11-20.
264. Lewer, P.; Graupner, P. R.; Hahn, D. R.; Karr, L. L. *J. Nat. Prod.*, **2006**, *66*, 1506-1510.
265. Hover, J. A.; Bock, C. W.; Bhat, K. L. *Heterocycles*, **2003**, *60*(4), 791-798.

-
266. Lassiano, L.; Pavan, M. V.; Bert, F.; Kokotos, G.; Markids, T.; Mennuni, L.; Makovec, F.; Varnava, A.; *Bioorg. Med. Chem.*, **2009**, *17* (96), 2336-2350.
267. Sera, A.; Itoh, K.; Yamada, H.; Aoki, R. *Bull. Chem. Soc. Jpn.*, **1981**, *54* (11), 3453-3455.
268. Brun, P.; Dean, A.; Marco, V.; Surajit, P.; Castagliuolo, I.; Carta, D.; Ferlin, M. G. *Eur. J. Med. Chem.*, **2013**, *32*, 486-497.
269. Smith, D. G.; Law, G. L.; Murray, B. S.; Pal, R.; Parker, D.; Wong, K. L. *Chem. Commun.*, **2011**, *47* (26), 7347-7349.
270. Chambers, R. W.; Carpenter, F. H. *J. Am. Chem. Soc.*, **1955**, *77*, 1522-1526.
271. Lee, S. J.; Kim, E.; Seo, M. L.; Do, Y.; Lee, Y. A.; Sim, S.; Jung, J. H.; Kohiso, M.; Simizu, T. *Tetrahedron.*, **2008**, *7*, 1522-1526.
272. McKerrow, J. D.; Al-Rawi, J. M. A.; Brooks, P. *Synth. Commun.*, **2010**, *40* (8), 1161-1179.
273. Chen, H.; He, M.; Wang, Y.; Zhai, L.; Cui, Y.; Li, Y.; Li, Y.; Zhou, H.; Hong, X.; Deng, Z. *Green Chemistry.*, **2011**, *13* (10), 2723-2726.
274. Cabrera, S.; Arrayás R. G.; Carretero, J. C. *J. Am. Chem. Soc.*, **2005**, *127* (47), 16394-16395.
275. Li, G.; Liang, Y.; Antilla, J. C. *J. Am. Chem. Soc.*, **2007**, *129*(18), 5830-5831.
276. Walton, M. C.; Yang, Y. F.; Hong, X.; Houk, K. N.; Overman, L. E. *Org. Lett.*, **2015**, *17* (24), 6166-6169.
277. Van Loon, A. A.; Holton, M. K.; Downey, C. R.; White, T. M.; Rolph, C. E.; Bruening, S. R.; Li, Guanqun; D., Katherine M.; Pelkey, S. J.; Pelkey, E. T. *J. Org. Chem.*, **2014**, *79* (17), 8049-8058.
278. Sommer, K.; Williams, R. M. *Tetrahedron.*, **2008**, *64* (30), 7106-7111.
279. Walton, M. C.; Yang, Y. F.; Hong, X.; Houk, K. N.; Overman, L. E. *Org. Lett.*, **2015**, *17* (24), 6166-6169.
280. López-Pérez, A.; Adrio, J.; Carretero, J. C. *J. Am. Chem. Soc.*, **2008**, *130*, 10084-10085.
281. Yang, Q. L.; Xie, M. S.; Xia C.; Sun, H. L.; Zhang, D. J.; Huang, K. X.; Guo, Z.; Qu, G. R.; Guo, H. M. *Chem. Commun.*, **2014**, *50*, 14809-14812.
282. Sladojevich, F.; Trachocchi, A.; Guarna, A.; Dixon, D.J. *J. Am. Chem. Soc.*, **2011**, *133* (6), 1710-1713.
283. Zhou, H.; Aguilar, A.; Chen, J.; Bai, L.; Liu, L.; Meagher, J. L.; Yang, C. Y.; McEachern, D.; Cong, X.; Stuckey, J. A.; Wang, S. *J. Med. Chem.*, **2012**, *55*, 6149-6161.
284. Nazari, S.; Iravani, N.; Ahmady, A. Z.; Nezhad, M. V.; Keshavarz, M. *Curr. Organocat.*, **2014**, *1* (1), 1-6.
285. Polshettiwar, V.; Varma, R. S. *Chem. Soc. Rev.*, **2008**, *37*, 1546-1557.
286. Kim, Y. J.; Streitwieser, A.; Chow, A.; Fraenkel, G. *Org. Lett.*, **1999**, *13*, 2069-2071.

-
287. Kemnitz, C. R. Loewen, M. J. *J. Am. Chem. Soc.*, **2007**, *129* (9), 2521-2528.
288. Zhang, F. -H.; Debnath, B.; Xu, Z. -L.; Yang, L. -M., Song, L. -R.; Zheng, Y.; -T.; Neamati, N., Lon, Y. -Q. *Eur. J. Med. Chem.*, **2017**, *125*, 1051-1063.
289. Cheng, A.; Merz, K. M. *J. Med. Chem.*, **2003**, *46* (17), 3572-3580.
290. Egan, W. J.; Merz, K. M., Jr.; Baldwin, J. J., *J. Med. Chem.*, **2000**, *43*, 3867-3877.
291. Xue, W.; Liu, H.; Yao, X. *PLoS ONE.*, **2014**, *9* (3), e90799.
292. Tintori, C.; Demeulemeester, J.; Franchi, L.; Massa, S.; Debyser, Z., Christ, F.; Botta, M. *Bioorg. Med. Chem. Lett.*, **2012**, *22*, 3109-3114.
293. Sanchez, T. W.; Debnath, B.; Christ, F.; Otake, H., Debyser, Z.; Neamat, N. *Bioorg. Med. Chem.*, **2013**, *21*, 957-963.
294. Yang, L.; Wang, P.; Wu, J. F.; Yang, L. M.; Wang, R. R., Pang, W.; Li, Y. G.; Shen, Y. M.; Zheng, Y. T.; Li, X. *Bioorg. Med. Chem.*; **2016**, *24*, 2125-2136.
295. Lipinski, C. A.; Lombardo, F.; Dominy, B. W.; Feeney, P. J. *Adv. Drug. Delivery. Rev.*, **1997**, *23*, 325.
296. Reitz, D. B.; Isakson, P. C. *Curr. Pharm. Des.*, **1995**, *1*, 211-220.
297. Erdélyi, P.; Fodor, T.; Varga, A. K.; Czugler, M.; Gere, A.; Fischer, J. *Bioorg. Med. Chem.*, **2008**, *16* (9), 5322-5330.
298. Shin, K. D.; Lee, M. Y.; Shin, D. S.; Lee, S.; Son, K. H.; Koh, S.; Paik, Y. K.; Kwon, B. M.; Han, D. C. *J. Biol. Chem.*, **2005**, *280*, 41439-41448
299. Rouchaud, J., Gustin, F. ; Moulard, C. *Bull. Soc. Chim. Belg.*, **1993**, *102/8*, 543-555.
300. Wakefield, B. J. *Sci. Synth.*, **2001**, *11*, 229-288
301. Liu, X. H.; Cui, P.; Song, B. A.; Bhadury, P. S.; Zhu, H. L.; Wang, S. F. *Bioorg. Med. Chem.*, **2008**, *16*, 4075-4082
302. Wyvratt, J. M.; Hazen, G.; Weinstock, L. M.; *J. Org. Chem.*, **1987**, *52*, 944-945.
303. Wang, P.; Tao, W.-J.; Sun, X.-L.; Liao, S.; Tang, Y.; *J. Am. Chem. Soc.*, **2013**, *135*, 16849-16852.
304. Aggarwal, V. K. Mereu, A. *J. Org. Chem.*, **2000**, *65*, 7211-7212.
305. Ram N. R.; Manoj T. P. *J. Org. Chem.*, **2008**, *73*, 5633-5635.
306. Zhang, Y.; Stephens, D.; Hernandez, G.; Mendoza, R.; Larionov, O. V. *Chem. -Eur. J.*, **2012**, *18* (52), 16612-16615.
307. Crowther, A. L.; Holt, G. *J. Chem. Soc.*, **1963**, 2818-2821.
308. Sheehan, H. C.; Yang, D. D. H. *J. Am. Chem. Soc.*, **1958**, *80* (5), 1154-1158
309. Strazzoline, P.; Giumanini, A. G.; Cauci, S. *Tetrahedron.*, **1990**, *46*, 1081-1118.
310. Habibi, D.; Rahmani, P.; Akbaripناه, H. *J. Chem.*, **2013**, 1-6.

-
311. Hosseini, Sarvari, M.; Sharghi, H. *J. Org. Chem.*, **2006**, *71* (17), 6652-6654.
312. Bandgar, B. P.; Kinkar, S. N.; Chobe, S. S.; Mandawad, G. G.; Yemul, O. S.; Dawane, B. S. *Arch. Appl. Sci. Res.*, **2011**, *3* (3), 246-25.
313. Reddy, P. G.; Kumar, G. D. K.; Baskaram S. *Tetrahedron.*, **2000**, *41*, 9149-9151.
314. Dhake, K. P.; Tambade, P. J.; Singhal, R. S.; Bhanage, B. M. *Green Chem. Lett. Rev.*, 2011, *4* (2), 151-157.
315. Kamble, V. T.; Bondle, G. M.; Pisal, P. M. *Arab. J. Chem.*, **2013**: [doi:10.1016/j.arabjc.2013.09.007](https://doi.org/10.1016/j.arabjc.2013.09.007)
316. Kamijo, S.; Jin, T.; Yamamoto, Y. *Angew. Chem. Int. Edit.*, **2002**, *41* (10), 1780-1782.
317. Polisar, J. G. Norton, J. R. *Tetrahedron.*, **2012**, *68* (49), 10236-10240.
318. Wang, Y.; Wang, H.; Peng, J.; Zhu, Q. *Org. Lett.*, **2011**, *13* (17), 4604-4607.
319. Guirado, A; Zapata, A.; Gomez, J. L.; Travalon, L.; Golvez, J. G. *Tetrahedron.*, **1999**, *55*, 9631-9640.
320. Morishima, I; Mizuno, A.; Yonezawa, T.; Goto, K. *J. Chem. Soc. D*, **1970**, 1321-1322.
321. Kong, Y. C.; Kim, K.; Park, Y. J. *Heterocycles.*, **2001**, *55* (1), 75-89.
322. Rossolini, G. M.; Arena, F.; Pecile, P.; Pollini, S. *Clin. Opin. Pharmacol.*, **2014**, *18*, 56-60.
323. Golkar, Z.; Bagazra, O.; Pace, D. G.; *J. Infect. Dev. Ctries.*; **2014** *8*(2), 129-136.
324. Phillips, R. S. *Clini. Microbiol. Rev.*; **2001**, *14*, 208-226.
325. McLuckie, A., ed. **2009**. *Respiratory disease and its management*. New York: Springer. p 51. ISBN 978-1-84882-094-4.
326. Pommerville, J. C. 9th ed. **2010**. *Alcama's Fundamentals of Microbiology* . Sudbury MA: Jones and Bartlett. P 323. ISBN 0-7637-6258-X.
327. Badri, M.; Wilson, D.; Wood, R. *Lancet.*; **2002**, *359* (9323), 2059-2064.
328. Bristow, C. C.; Larson, E., Vilakazi-Nhlapo, A. K.; Wilson, M.; Klausner J. D.; *Int. J. Tuberc. Lung. Dis.*, **2012**, *16* (8), 1020-1022.
329. Fischer, J.; Ganellin, C. R. **2006**. *Analogue-based Drug Discovery*. John Wiley & Sons. p490. ISBN 9783527607495
330. Jukes, T. H. *Rev. Infect. Diseases.*, **1985**, *7* (5), 702-707.
331. Elks, J. **2014**, *The Dictionary of Drugs: Chemical Data: Chemical Data, Structures and Bibliographies*. Springer. p356. ISBN 978-1-4757-2085-3.
332. Morton; I.K.; Hall. Judith M. **2012**. *Concise Dictionary of Pharmacological Agents: Properties and Synonyms*. Springer Science & Business Media. p92. ISBN 978-94-011-4439-1.
333. Zhanel, G. G.; Fontaine, S; Adam, H; Schurek, K; Mayer, M; Noreddin, A. M.; Gin, A. S.; Rubinstein, E; Hoban, D. J. *Treat. Resp. Med.*, **2006**, *5* (6), 437-465.

-
334. Gootz, T. D.; Larrenll, J. F.; Sutcliffe, J. A. *Antimicrob. Agents Chemother.*, **1990**, *34* (1), 8-16.
335. Stork, C. M. **2006**. "Antibiotics, antifungals, and antivirals". In Nelson LH, Flomenbaum N, Goldfrank LR, Hoffman RL, Howland MD, Lewin NA. *Goldfrank's toxicologic emergencies*. New York: McGraw-Hill. p847. ISBN 0-07-143763-0.
336. WHO report, Global tuberculosis control, Geneva, **2011**.
337. Takechi, M.; Matsuo, M.; Ziba, C.; MacHeso, A.; Butao, D.; Zungu, I. L.; Chakanika, I.; Bustos, M. D.; *Trop. Med. Int. Health.*, **2001**, *6*, 429-434.
338. Roper, C.; Pearce, R.; Bredenkamp, B.; Gumedde, J.; Drakeley, C.; Mosha, F.; Chandramohan, D.; Sharp, B. *Lancet.*, **2003**, *361*, 1174-1181.
339. Hussain, A; Das, S. R.; Tanwar, C, Jameel, S. *Virology J.*, **2007**, *4*, 81-91.
340. Le Noury, D. A. PhD thesis, Title: *Comparison of HIV-1 Vpu interaction with CD4 and CD74.*, University of Witwatersrand, **2016**.
341. Van Vuuren, S. F.; Kamatou, G. P.; Viljoen, A. M. ; *S. Afr. J. Bot.*, **2010**, *76*, 686-691.
342. Eloff, J. *Planta Medica.*, **1998**, *64*, 711-713
343. Traut, T. PhD thesis, Title; *Design, synthesis and biological activity of novel HIV integrase inhibitors*, University of Johannesburg, **2012**
344. Yoakim, C., Amad, M., Bailey, M., Bethell, R., Bos, M., Cordingley, M., Coulombe, R., Duan, J., Edwards, P., Fader, L., Faucher, A., Garneau, M., Jakalian, A., Kawai, S., Lamarte, L., LaPlante, S., Luo, L., Mason, S., Paupart, M., Rioux, N., Simoneau, B., Tsantrizos, Y., Witvrouw, M., Fenwick, C., **2011**. *Preclinical Profile of BI 224436, a Novel HIV-1 Non-Catalytic Site Integrase Inhibitor*.
345. Reichert, S.; Briet, B. *Org. Lett.* **2007**, *9* (5), 899-902.
346. Baddar, F.G., Iskander, Z. *J. Chem. Soc.*, **1954**, 209-213.
347. Ziegler, F. E.; Fowler, K.W.; *J. Org. Chem.*, 1976, *41* (9), 1564-1566.
348. Strumberg, D.; Pommer, Y. Paull, K.; Jayaramna, M.; Nagafuji, P.; Pamela, C. M. *J. Med. Chem.*, **1999**, *42* (3), 446-457.
349. Sun, G.; Wang, J.; Sun, C. *Synlett.*, **2009**, *16*, 2663-2668.
350. Lee, C. K.; Yu, J. S.; Ji, Y. R. *J. Heterocycl. Chem.*; **2002**, *39* (6), 1219-1227.
351. Vigorita, M. G.; Saporito, G.; Previtiera, T.; Pizzimenti, F. C.; Bisignano, G. *Farmaco, Edizione Scientifica*, **1986**, *41*(2), 168-174.
352. Besselièvre, F.; Mahuteau-Betzer, F.; Grierson, D. S.; Piguel, S. *J. Org. Chem.*, **2008**, *73* (8), 3278-3280.
353. Vinay Kumar, K. S.; Swaroop, T. R.; Rajeev, N.; Vinayaka, A. C.; Lingaraju, G. S.; Rangappa, K. S.; Sadashiva, M. P. *Synlett.*, **2016**, *27* (9), 1363-1366.

-
354. Akula, M.; Thigulla, Y.; Davis, C.; Jha, M.; Bhattacharya, A. *Org. Biomol. Chem.*, **2015**, *13*(9), 2600-2605.
355. King, F. E.; Clark-Lewis, J. W.; Kidd, D. A. A.; Smith, G. R. *J. Chem. Soc.*, **1954**, 1039-1043.
356. Takiguchi, K.; Yamada, K.; Suzuki, M.; Nunami, K.; Hayashi, K.; Matsumoto, K. *Agric. Biol. Chem.*, **1989**, *56* (1), 69-76.
357. Kopple, K. D.; Katz, J. J. *J. Am. Chem. Soc.*, **1956**, *78*, 6199-6205.
358. Bender, M. L.; Turnquest, B. W. *J. Am. Chem. Soc.*, **1957**, *79*, 1889-1893
359. Chattaway, F. D.; Muir, R. J. K. *J. Chem. Soc.*, **1934**, 701-703.
360. Wei, Q. -L.; Zhang, S. -S.; Gao, J.; Li, W. -H.; Xu, L. Z.; Yu, Z. -G.; *Bioorg. Med. Chem.*, **2006**, *14* (21), 7146-7153.
361. Levin, N.; Hartung, W. H. *J. Org. Chem.*, **1942**, *7*, 408-415.
362. Bergmann, F.; Kalmus, A.; Breuer, E.; *J. Am. Chem. Soc.*, **1957**, *79*, 4178-4181.
363. Truce, W. E.; Sack, B. H. *J. Am. Chem. Soc.*, **1948**, *70* (11), 395-3959.
364. Antunes, H.; Fardelone, L. C.; Rodrigues, J. A. R.; Moran, P. J. S. *Tetrahedron: Asymmetry.*, **2004**, *15* (17), 2615-2620.
365. Dyadchenko, V. P.; Belov, N. M.; Lemenovskii, D. A.; Antipin, M. Y.; Lyssenko, K. A.; Bruce, A. E.; Bruce, M. R. M. *J. Organomet. Chem.*, **2009**, *695* (2), 304-309.
366. Marion, L.; Oldfield, C. W. *Can. J. Res. Section B: Chemical Sciences*; **1947**, *25B*, 1-13.
367. Das, B.; Krishnaiah, M.; Balasubramanyam, P.; Veeranjanyulu, B.; Kumar, D. N. *Tetrahedron Lett.*, **2008**, *49* (11), 2225-2227.
368. Janza, B.; Studer, A.; *Org. Lett.*, **2006**, *8* (9), 1875-1878
369. Ugi, I.; Fetzer, U.; Eholzer, U.; Knupfer, H.; Offerman, K. *Angew. Chem.*, **1965**, *77* (11), 492-504.
370. Costa, S. P. G.; Maria, H. L. S.; Pereira-Lima, S. M. M. A. *Org. Biomol. Chem.*, **2003**, *1* (9), 1475-1479
371. Nenajdenko, V. G.; Golubinskii, I. V.; Lenkova, O. N.; Shastin, A. V.; Balenkova, E. S. *Russ. Chem. Bul.*, **2005**, *54* (7), 1728-1732.
372. Bourbeau, M. P.; Rider, J. T. *Org. Lett.*, **2006**, *8* (17), 3679-3680.
373. Floris M., Masciocchi J., Fanton M., and Moro S. *Nucl. Acids Res.*, **2011**, 1-9.